Univerzita Karlova
1. lékařská fakulta

Studijní program: Biologie a patologie buňky
Studijní obor: Biologie a patologie buňky

Mgr. Karolína Strnadová

Fenotyp melanocytů za fyziologických a patologických podmínek

Phenotype of melanocytes under physiological and pathological conditions

Disertační práce

Školitel: MUDr. Lukáš Lacina, Ph.D.

Praha, 2022

Prohlášení:

Prohlašuji, že jsem závěrečnou práci zpracovala samostatně a že jsem řádně uvedla a citovala všechny použité prameny a literaturu. Současně prohlašuji, že práce nebyla využita k získání jiného nebo stejného titulu.

Souhlasím s trvalým uložením elektronické verze mé práce v databázi systému meziuniverzitního projektu Theses.cz za účelem soustavné kontroly podobnosti kvalifikačních prací.

V Praze, 1.7.2022

Karolína Strnadová

Podpis

Identifikační záznam:

STRNADOVÁ, Karolína. *Fenotyp melanocytů za fyziologických a patologických podmínek. [Phenotype of melanocytes under physiological and pathological conditions]*. Praha, 2022. Počet stran 112, bez příloh. Disertační práce (Ph.D.). Univerzita Karlova, 1. lékařská fakulta, Anatomický ústav. Školitel Lacina, Lukáš.

Abstrakt

Neopomenutelnými reprezentanty buněčných populací kůže, kromě dominantních keratinocytů a fibroblastů, jsou také melanocyty. Melanocyty jsou pigmentové buňky, jejichž primární funkcí je produkce pigmentu melaninu, který je důležitý pro ochranu keratinocytů před škodlivým ultrafialovým zářením. Nadměrné vystavení tomuto záření je rizikovým faktorem pro vznik kožních nádorů včetně maligního melanomu kůže, při kterém dochází k patologické transformaci melanocytů v buňky melanomu. Předložená disertační práce pojednává o studiu melanocytů a zaměřuje se na 4 tematické okruhy spojené zejména s jejich patologiemi. V prvním tematickém okruhu je do souvislostí dána zvyšující se incidence maligního melanomu kůže se stárnutím populace. Jednou z příčin se zdá být častější výskyt prozánětlivého ladění tkání ve stárnoucím organismu. Toto ladění připravuje vhodné prostředí pro vývoj nádoru. Druhý tematický okruh se orientuje na nové přístupy, které by mohly rozšířit škálu diagnostických metod pro časnou detekci maligního melanomu. První metodicky využívá detekci prozánětlivých molekul v těle pacienta, např. v době diagnózy. Bylo zjištěno, že vyšší sérové hladiny IL-6 nebo IL-8 korelují s nepříznivou prognózou pacienta. Druhý přístup se opírá o možnosti detekce nádorových buněk a možnosti jejich odlišení od buněk zdravých s využitím metod, jako je povrchem zesílená Ramanova spektroskopie rozšířená o metody umělé inteligence využívající konvolučních neuronových sítí. *In silico* se toto spojení vyznačuje vysokou senzitivitou. Práce třetího tematického okruhu se snaží různými metodami o modelování mikroprostředí melanomu ve 3D, a to jak v *in vitro* podmínkách, tak *in ovo* na chorioalantoidní membráně kuřete. Čtvrtý tematický okruh se zaměřuje na mezibuněčnou komunikaci mezi maligními buňkami melanomu a buňkami mikroprostředí, převážně nádorově-asociovanými fibroblasty. V tomto okruhu je kladen důraz na komunikaci zprostředkovanou extracelulárními váčky – exosomy. Z dosažených dat vyplývá, že exosomy produkované melanomem podporují nádorově-asociované fibroblasty a ty změnou svých vlastností dále podporují progresi nádoru.

Klíčová slova

Melanocyty, maligní melanom, stárnutí, zánět, mikroprostředí, nádorově-asociované fibroblasty, sféroidy, IL-6, exosomy

Abstract

In addition to the dominant keratinocytes and fibroblasts, melanocytes are also indispensable representatives of skin cell populations. Melanocytes are pigment cells whose primary function is to produce the pigment melanin, which is important for protecting keratinocytes from harmful ultraviolet radiation. Excessive exposure to this radiation is a risk factor for the development of skin tumours, including malignant melanoma of the skin, in which pathological transformation of melanocytes into melanoma cells occurs. The presented thesis focuses on 4 thematic areas associated mainly with malignant melanoma. In the first thematic area, the increasing incidence of malignant skin melanoma is associated with the ageing of the population. One of the reasons seems to be the more frequent occurrence of proinflammatory setting in the ageing organism. It prepares a suitable environment for tumour development. The second thematic area focuses on new approaches that could expand the range of diagnostic methods for the early detection of malignant melanoma. The first approach methodically uses the detection of proinflammatory molecules in the patient´s serum. Higher serum levels of IL-6 and IL-8 correlate with an unfavourable patient prognosis. The second approach is based on the possibility of detecting a tumour cell and the possibility of distinguishing it from a healthy cell using methods such as surface-enhanced Raman spectroscopy extended by artificial intelligence methods using convolutional neural networks. *In silico* it seems to be highly sensitive. In the third thematic area there are described various methods to model the melanoma microenvironment in 3D, *in vitro* or *in ovo* using the chorioallantoic membrane of the chicken. The fourth thematic area focuses on intercellular communication between malignant melanoma cells and cells of the tumour microenvironment, predominantly cancer-associated fibroblasts. In this area, emphasis is placed on communication through extracellular vesicles – the exosomes. The data showed that exosomes produced by melanoma change the biological properties of cancer-associated fibroblasts to promote tumour progression.

Key words

Melanocytes, malignant melanoma, ageing, inflammation, microenvironment, cancer-associated fibroblasts, spheroids, IL-6, exosomes

Poděkování

Na tomto místě bych ráda poděkovala svému školiteli MUDr. Lukáši Lacinovi, Ph.D. za odborné vedení, cenné rady při psaní disertační práce a trpělivost. Ráda bych také vyjádřila upřímný vděk za jeho podporu a čas, který mi v průběhu celého doktorského studia věnoval.

Dále bych ráda poděkovala vedoucímu naší výzkumné skupiny a bývalému přednostovi Anatomického ústavu 1. LF UK, prof. MUDr. Karlu Smetanovi Jr., DrSc., za neocenitelné rady, motivaci, přečtení této práce a jeho připomínky.

Vřele děkuji také RNDr. Barboře Dvořánkové, Ph.D., která mi předala spoustu praktických rad v oblasti tkáňové kultivace a byla mi oporou a člověkem, na kterého se mohu vždy obrátit.

Děkuji také všem kolegům, se kterými jsem mohla spolupracovat. Bez nich by tato disertační práce nevznikla. Speciálně děkuji mým nejbližším kolegům, jmenovitě: RNDr. Pavlu Szabovi, Ph.D., MUDr. Aleši-Janu Pavlíčkovi, MUDr. Michalu Špankovi, MUDr. Lence Peterkové, MUDr. Michaele Tesařové, MUDr. Veronice Bandúrové, MUDr. Štěpánu Novákovi, MUDr. Ondřeji Kodetovi, Ph.D., MUDr. Janu Kučerovi, Ph.D., Heleně Stýblové, Ing. Michalu Kolářovi, Ph.D. a celému jeho týmu a v neposlední řadě Ing. Elišce Drobné Krejčí, Ph.D., která laskavě přečetla rukopis této práce a poskytla mi cennou zpětnou vazbu.

Dík patří také celému kolektivu Anatomického ústavu 1. LF UK, který je místem, kde je radost pracovat.

Na závěr bych chtěla z celého srdce poděkovat mé rodině za celoživotní podporu a lásku. Děkuji tátovi Pavlovi, mámě Olze a bratru Vojtěchovi. Upřímně děkuji také mému partnerovi a mým nejbližším přátelům za jejich pochopení, důvěru a povzbudivá slova.

Seznam zkratek a jazykové poznámky

Ortografická norma předkládané disertační práce se zejména v případě odborné terminologie odvolává na ustálené formy tak, jak je zachycuje lexikon VOKURKA, Martin, HUGO, Jan a kol. *Velký lékařský slovník*. 10. aktualizované vydání. Praha: Maxdorf, [2015]. Jessenius. ISBN 978-80-7345-456-2. V obecných aspektech sleduje celý text českou jazykovou normu shrnutou v online publikaci *Internetová jazyková příručka* [online] (2008–2021). Praha: Ústav pro jazyk český AV ČR, v. v. i. Cit. 1. 4. 2022. <*https://prirucka.ujc.cas.cz/*>. (Práce používá data, která poskytuje výzkumná infrastruktura LINDAT/CLARIAH-CZ (https://lindat.cz) podporovaná Ministerstvem školství, mládeže a tělovýchovy České republiky (projekt č. LM2018101).)

S ohledem na dominantní podíl zejména anglicky psaných literárních zdrojů, ze kterých tato práce vychází, jsou některá v odborné komunitě běžně užívaná slovní spojení ponechána v originálních formách bez pokusu o jejich doslovný převod do češtiny (často násilný a ve výsledku neobvyklý). Cizojazyčný termín takto užitý je odlišen v textu *kurzívou.*

Zkratka	**Anglicky**	**Česky (je-li běžně užíván název)**
AJCC	*American Joint Committee on Cancer*	Americký výbor proti rakovině
AKT	*Protein Kinase B*	Proteinkináza B
α-MSH	*α-Melanocyte Stimulating Hormone*	α-melanocyty stimulující hormon
αSMA	α-*Smooth Muscle Actin*	α-hladkosvalový aktin
APC	*Antigen Presenting Cells*	Antigen prezentující buňky
ARF6	*Adenosine diphosphate-Ribosylation Factor 6*	
Bak	*BCL2 Antagonist/Killer*	
Bax	*BCL2 Associated X, Apoptosis regulator*	
Bcl-2	*B-cell lymphoma-2*	
Bcl-xL	*B-cell lymphoma-extra large*	

BRAF	*B-Raf Proto-Oncogene*	
CAF	*Cancer-associated fibroblasts*	Nádorově-asociované fibroblasty
CAM	*Chorioallantoic membrane*	Chorioalantoidní membrána
CDK4	*Cyclin Dependent Kinase 4*	
CDKN2A, též ARF nebo $p16^{INK4A}$ nebo CDK4 inhibitor	*Cyclin Dependent Kinase Inhibitor 2A*	
c-Fos	*Fos Proto-Oncogene*	
c-Jun	*Jun Proto-Oncogene*	
c-Myc	*MYC Proto-Oncogene*	
COL1A1	*Collagen Type I Alpha 1 Chain*	
COL1A2	*Collagen Type I Alpha 2 Chain*	
COL3A1	*Collagen Type III Alpha 1 Chain*	
CREB	*CAMP Responsive Element Binding Protein 1*	
CXCL1	*C-X-C Motif Chemokine Ligand 1*	
CXCL8 (též IL-8)	*C-X-C Motif Chemokine Ligand 8 (Interleukin 8)*	
CXCR1	*C-X-C Motif Chemokine Receptor 1*	
CTLA-4	*Cytotoxic T-lymphocyte Antigen 4*	
DCT, též TYRP2	*Dopachrome Tautomerase*	Dopachrom tautomeráza
DHI	*5,6-dihydroxyindole*	5,6-dihydroxyindol
DHICA	*5,6-dihydroxyindole-2-carboxylic acid*	5,6-dihydroxyindol-2-karboxylová kyselina
DNA	*Deoxyribonucleic Acid*	Deoxyribonukleová kyselina
ECM	*Extracelullar Matrix*	Extracelulární matrix
EGF	*Epidermal Growth Factor*	Epidermální růstový faktor
ELK1	*ETS-Like Gene 1*	
EMT	*Epithelial-Mesenchymal Transition*	Epitelo-mezenchymový přechod

ESCRT	*Endosomal Sorting Complex Required for Transport*	Komplex endosomálního třídění potřebného pro transport
FAP	*Fibroblast Activation Protein*	Fibroblastový aktivační protein
FBS	*Foetal Bovine Serum*	Fetální bovinní sérum
FGF2	*Fibroblast Growth Factor 2*	Fibroblastový růstový faktor 2
GDP	*Guanosindifosfát*	
GEF	*Guanosine Exchange Factor*	
GM-CSF	*Granulocyte-Macrophage Colony-Stimulating Factor*	
GNA11	*G protein Subunit Alpha 11*	
GNAQ	*G protein Subunit Alpha Q*	
Gp130	*Membrane Glycoprotein 130*	
GPER	*G protein-coupled Estrogen Receptor*	
GRB2	*Growth Factor Receptor-Bound protein 2*	
HDF	*Human Dermal Fibroblasts*	Lidské dermální fibroblasty
HGF	*Hepatocyte Growth Factor*	Hepatocytární růstový faktor
HIF	*Hypoxia-Inducible Factor*	Transkripční faktor indukovaný hypoxií
HLA	*Human Leukocyte Antigen*	
HMGB1	*High Mobility Group Box-1*	
ID1	*Inhibitor of Differentiation 1*	
IF	*Impact Factor*	Impakt faktor
IFNα2b	*Interferon-α-2b*	
IFN-γ	*Interferon-γ*	
IL-1	*Interleukin-1*	
IL-1α	*Interleukin-1α*	
IL1RA	*Interleukin 1 Receptor Antagonist*	
IL-2	*Interleukin-2*	

IL-6	*Interleukin-6*	
IL-10	*Interleukin-10*	
IL-13	*Interleukin-13*	
IL-17	*Interleukin-17*	
IL-18	*Interleukin-18*	
IL-33	*Interleukin-33*	
JAK2/STAT3	*Janus Kinase 2/Signal Transducer and Activator of Transcription 3*	
JDF	*Juvenile Dermal Fibroblasts*	Juvenilní dermální fibroblasty (z neozářené části kůže dítěte)
Ki-67	*Marker of Proliferation Ki-67*	
KIT, též c-Kit nebo CD117	*KIT Proto-Oncogene, Receptor Tyrosine kinase*	
KSR1	*Kinase Suppressor Of Ras 1*	
LDH	*Lactate Dehydrogenase*	Laktátdehydrogenáza
L-DOPA	*3,4-dihydroxyphenylalanine*	3,4-dihydroxyfenylalanin
LIF	*Leukemia Inhibitory Factor*	
MALAT1	*Metastasis Associated Lung Adenocarcinoma Transcript*	
MAPK/ERK	*Mitogen-Activated Protein Kinase/Extracelullar signal-Regulated Kinase*	Mitogenem aktivovaná proteinkináza/Extracelulárním signálem regulovaná proteinkináza
MC1R	*Melanocortin 1 Receptor*	
mCAF	*Cancer-associated fibroblasts isolated from malignant melanoma*	Nádorově-asociované fibroblasty izolované z maligního melanomu
MEK	*Mitogen-Activated Protein Kinase Kinase*	Mitogenem aktivovaná proteinkináza kináza
Melan-A (MART-1)	*Melanoma Antigen Recognized by T-Cells 1*	

MHC	*Major Histocompatibility Complex*	Hlavní histokompatibilní komplex
MIP-1ß	*C-C Motif Chemokine Ligand 4*	
miRNA, též miR	*MicroRNA*	
MITF	*Melanocyte Inducing Transcription Factor*	
MMP	*Matrix Metalloproteinase*	Matrix metaloproteináza
MTT		3-(4,5-dimethylthiazolyl-2)-2,5-diphenyltetrazolium bromid
MVB	*Multivesicular body*	Multivesikulární tělísko
NEAT1	*Nuclear Enriched Abundant Transcript 1*	
NF-1	*Neurofibromin 1*	
NK	*Natural Killer cells*	Přirození zabíječi
NKG2D	*Killer Cell Lectin Receptor K1*	
NRAS	*Neuroblastoma RAS viral oncogene homolog*	
$p21^{Waf1}$	*Cyclin Dependent Kinase Inhibitor 1A*	
$p27^{kip1}$	*Cyclin Dependent Kinase Inhibitor 1B*	
p53	*Tumour protein P53*	
PAX3	*Paired Box 3*	
PBS	*Phosphate-Buffered Saline*	Pufrovaný fyziologický roztok
PD-1	*Programmed Cell Death 1*	
PDF	*Photo-damaged Dermal Fibroblasts*	Dermální fibroblasty z fotoexponované kůže (seniorního dárce)
PD-L1	*Programmed Cell Death-1 Ligand 1*	

PD-L2	*Programmed Cell Death 1 Ligand 2*	
PGE2	*Prostaglandin E2*	
PGF2	*Prostaglandin F2*	
PI3K	*Phosphoinositol-3-Kinase*	Fosfoinositol-3-kináza
Pmel17, též gp100 nebo HMB-45	*Premelanosome Protein*	
PTEN	*Phosphatase and Tensin homolog*	
RAC1	*Ras-related C3 botulinum toxin substrate 1*	
RAL	*Ras-like protein*	
RANTES	*C-C Motif Chemokine Ligand 5*	
RAS	*Rat Sarcoma gene*	
RASSF1	*Ras association domain family 1*	Reaktivní formy kyslíku
RTK	*Tyrosine Kinase Receptor*	Tyrosinkinázový receptor
S100A	*S100 Calcium Binding Protein A*	
S100B	*S100 Calcium Binding Protein B*	
SASP	*Senescent-Associated Secretory Phenotype*	Sekreční fenotyp sdružený se senescencí
SCF	*Stem Cell Factor*	
SCID	*Severe Combined Immunodeficiency*	Těžká kombinovaná imunodeficience
SERS	*Surface Enhanced Raman Spectroscopy*	Povrchem zesílená Ramanova spektroskopie
Snail 2	*Snail Family Transcriptional Repressor 2*	
SOD2	*Superoxide Dismutase 2*	Superoxid dismutáza 2
SOS	*Son Of Sevenless*	
SOX10	*SRY-Box Transcription Factor 10*	
SPF	*Sun Protection Factor*	Ochranný faktor proti slunci
TCR	*T-cell Receptor*	T-buněčný receptor
TEX	*Tumor-derived Exosomes*	Nádorově asociované exosomy

TGFß	*Transforming Growth Factor* ß	
TIMP	*Tissue Inhibitor of Matrix Metalloproteinase*	Tkáňové inhibitory matrix metaloproteináz
TNF	*Tumor Necrosis Factor*	
TRAIL	*Tumour Necrosis Factor-Related Apoptosis-Inducing Ligand*	
TYR	*Tyrosinase*	Tyrosináza
TYRP1	*Tyrosinase-Related Protein 1*	Tyrosináze příbuzný protein 1
UV	*Ultraviolet (light)*	Ultrafialové (světlo)
ÚZIS		Ústav zdravotnických informací a statistiky
VEGF-A	*Vascular Endothelial Growth Factor A*	Vaskulární endotelový růstový faktor A
VEGFR1	*Vascular Endothelial Growth Factor Receptor 1*	Receptor 1 pro vaskulární endotelový růstový faktor
xCT	*Cystine/Glutamate Transporter*	Cystin-glutamátový transporter
ZEB2	*Zinc Finger E-Box Binding Homeobox 2*	

Seznam obrázků a tabulek

Obsah

1 Úvod

Kůže představuje jeden z největších orgánů lidského těla a plní různorodé fyziologické funkce. Současně může být postižena i početnými patologickými stavy. Studium biologie lidské kůže přineslo již v předchozích dekádách velmi detailní poznatky, z nichž mnohé mají dokonce svůj translační potenciál a nalezly i klinické uplatnění. Kromě základních populací lidské kůže, epidermálních keratinocytů a dermálních fibroblastů, kůži spoluvytvářejí další, takzvané minoritní, buněčné populace. Jednou z nich jsou i melanocyty, jejichž biologie je náplní předkládané disertační práce.

Melanocyty jsou buňky vývojově vycházející z buněk neurální lišty. Za embryonálního vývoje jejich prekurzory migrují do míst svého určení, např. epidermis kůže. Fyziologicky zde pak zajišťují tvorbu pigmentu melaninu, která je realizována v organelách zvaných melanosomy. Tento pigment následně předávají svými výběžky okolním keratinocytům, a vytvářejí tak funkční jednotku (tzv. *Epidermal Melanin Unit*). Melanocyt tak předávaným melaninem přispívá k ochraně jejich jádra před nadměrnou expozicí ultrafialovému záření a následnému poškození integrity genetické informace DNA. Nadměrné ozáření totiž představuje základní rizikový faktor pro neoplastickou transformaci epidermálních keratinocytů a vznik epidermálních karcinomů, velmi běžných zhoubných nádorů, které postihují lidskou populaci. Mimo to ale ultrafialové záření může poškozovat i samu populaci melanocytů, a zvyšuje tak riziko vzniku kožního nádoru – maligního melanomu. Toto maligní onemocnění představuje jeden z nejagresivnějších kožních nádorů, jehož incidence v populaci stoupá. Časná detekce primárního ložiska maligního melanomu může být pro pacienta zásadní, protože umožňuje dosažení plně kurativního efektu prostřednictvím chirurgické léčby. Problém nadále ale představuje často rychlá progrese nádorového onemocnění, kdy nádorové buňky invadují lokálně a posléze pak i migrují do vzdálenějších míst krevním či lymfatickým řečištěm, což vede k tvorbě metastáz.

Klíčovým faktorem podílejícím se na regulaci invazivního chování nádoru je nádorové mikroprostředí. Pro buňky a struktury spoluvytvářející nádor, ale odlišné od maligně transformované nádorové populace, se historicky vžil v patologii termín stroma. Stromatu byly přisuzovány v starších dobách spíše jen podpůrné a nutritivní funkce. V novějším konceptu je přiznáván stromatu významný podíl na formování právě komplexního mikroprostředí, které může významně ovlivnit i maligní populaci.

Jednou z hlavních buněčných populací tohoto nádorového mikroprostředí jsou nádorově-asociované fibroblasty, které jsou důležitými producenty složek extracelulární matrix a mnoha biologicky aktivních, zejména prozánětlivých, faktorů. Interakce a mezibuněčná komunikace mezi nádorovými a stromálními buňkami je pak zásadní pro vývoj nádoru. Proto byly právě mechanismy mikroprostředí a jejich vliv na melanocyty klíčovým přístupem a objektem zájmu při výzkumné práci vedoucí k sepsání předkládané disertační práce.

2 Literární přehled

2.1 Kůže, struktura a vývoj

Kůže, *integumentum commune*, je krycím orgánem tvořící rozhraní mezi vnitřním prostředím těla a vnějším prostředím; působí tedy primárně jako ochrana těla před nežádoucími vlivy z okolí (Roger et al. 2019). Kromě vytváření mechanické ochranné bariéry se kůže účastní i termoregulace, a to prostřednictvím činnosti ekrinních potních žláz a regulací průtoku krve v kožním cévním řečišti (Rittié and Fisher 2015). Za zmínku stojí i její další funkce, např. metabolické jako je tvorba vitaminu D (Mostafa and Hegazy 2013), sekreční a exkreční funkce, nebo kožní čití. Významný je obecně i její estetický a psychosociální aspekt.

Kůže je v užším slova smyslu tvořena dvěma hlavními vrstvami – epidermis a dermis. Tyto hlavní vrstvy kůže volněji doplňuje ještě hlouběji uložené podkožní tukové vazivo (tzv. hypodermis) (Obr. 1).

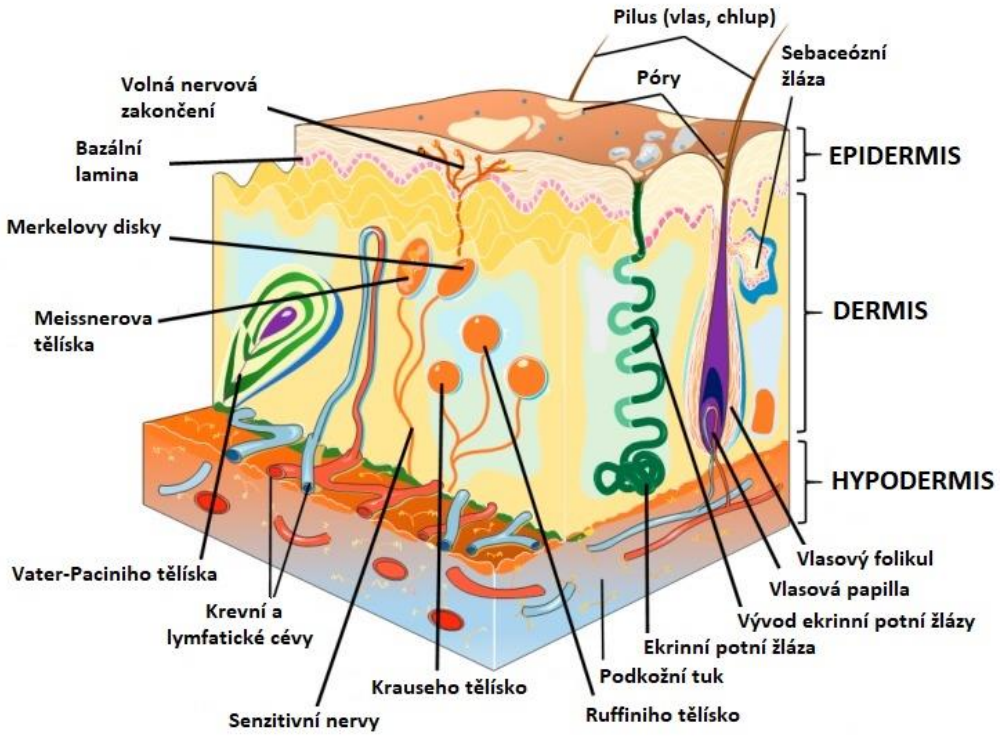

Obr. 1 Schématické znázornění řezu kůží. Kůže se skládá ze tří vrstev: epidermis, dermis a hypodermis. Kůže obsahuje různé typy buněk (zejména keratinocyty, fibroblasty, melanocyty, buňky imunitního systému), rozdílné senzorické receptory a kožní adnexa (např. vlasy, mazové a potní žlázy). Epidermis působí jako ochranná bariéra před vnějšími nežádoucími vlivy. Dermis představuje podpůrnou vrstvu kvůli bohaté extracelulární matrix a zajišťuje také výživu díky přítomným krevním a lymfatickým cévám (převzato a upraveno dle Chamcheu et al. 2019).

Epidermis, pokožka, je povrchovou vrstvou obsahující převážně keratinocyty, které ve vrstvách epidermis postupně dosahují různých stádií diferenciace (Brettmann and de Guzman Strong 2018). Epidermis je ektodermového původu. Kromě převažujících keratinocytů pak nalezneme v pokožce i pigmentové buňky melanocyty (viz kapitola 2.2), antigen prezentující Langerhansovy buňky nebo Merkelovy buňky (Tobin 2017). Tyto minoritní populace ale vznikají v jiných zárodečných listech a strukturách a do epidermis se dostávají až sekundárně. Histologicky představuje epidermis rohovějící mnohovrstevný dlaždicový epitel. Ten se dělí podle stratifikace na nejhlouběji při bazální membráně uložené *stratum basale*, nad ním směrem k povrchu následuje *stratum spinosum*, *stratum granulosum* a plně keratinizované *stratum corneum* (Obr. 2). S*tratum lucidum* je patrno jen na tlustém typu kůže (tj. akrálně) a nachází se na hranici *stratum granulosum* a *stratum corneum* (Sadler 2011).

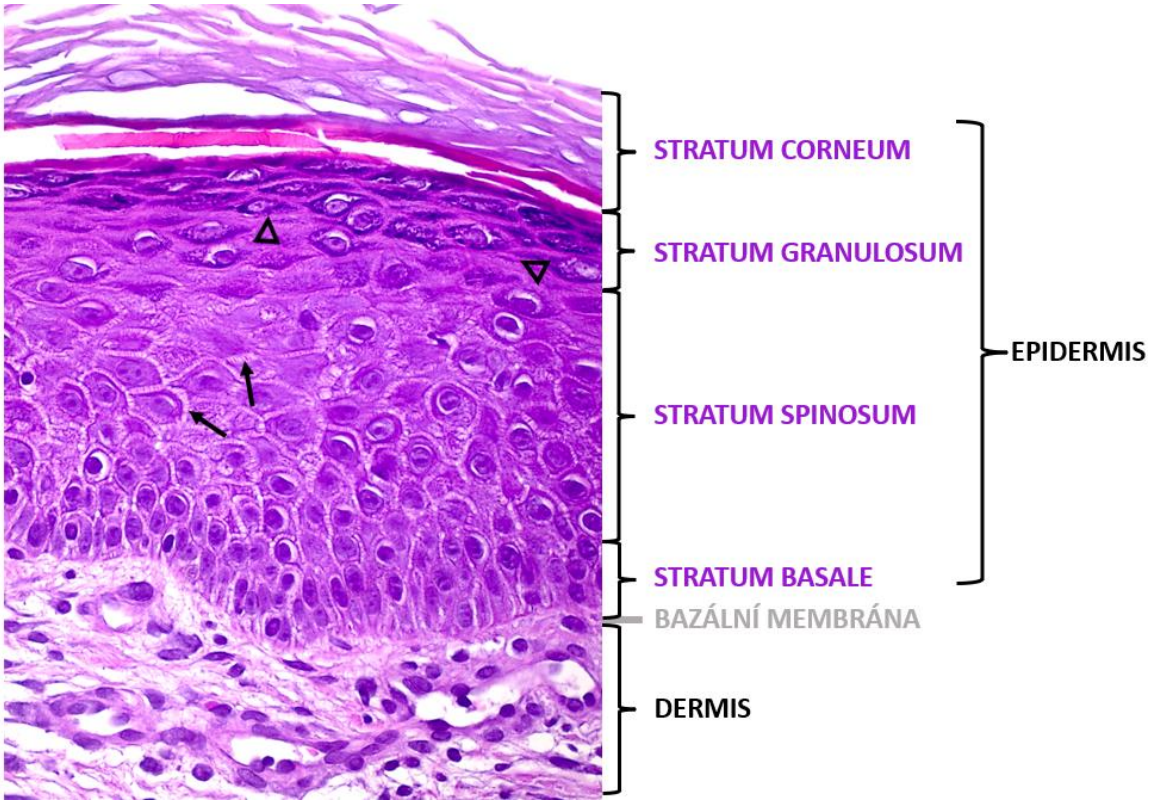

Obr. 2 Stratifikace epidermis na histologickém preparátu. Epidermis je histologicky rohovějícím mnohovrstevným dlaždicovým epitelem, který je dělen na *stratum basale*, *stratum spinosum*, *stratum granulosum* a *stratum corneum*. Fotografie byla poskytnuta Dermatovenerologickou klinikou 1. LF UK a VFN. Šipka – adhezní buněčné spoje desmozomy mezi polygonálními keratinocyty ve *stratum spinosum*; prázdný trojúhelník – keratohyalinová granula keratinocytů ve *stratum granulosum*.

Dermis je definována jako podpůrná vazivová vrstva kůže nacházející se pod bazální membránou epidermis. Z pohledu embryonálního vývoje má mezenchym formující

budoucí dermis v různých částech těla odlišný původ. V oblasti zad je dermis derivátem dermatomů somitů, v přední a boční oblasti trupu nebo na končetinách pochází dermis z laterální ploténky mezodermu a v oblasti hlavy je původem z buněk neurální lišty (Sadler 2011).

Podle struktury lze dermis rovněž dělit do vrstev. Její povrchová vrstva (*stratum papillare*) vybíhá proti epidermis v papilách, zatímco její hlubší a kompaktnější vrstva (*stratum reticulare*) dává kůži mechanickou podporu (Obr. 3) (Cole et al. 2018). Dermis je složená z acelulárních kolagenních a elastických fibril a dále pak z buněk – zejména fibroblastů, v menším rozsahu ale i z rezidentních, či migrujících buněk imunitního systému (např. histiocyty, makrofágy, CD4+ a CD8+ T lymfocyty).

Fibroblasty dynamicky syntetizují, organizují, ale i odbourávají extracelulární matrix (anglicky: *Extracelullar Matrix*; ECM). Účastní se nejen fyziologických procesů, jako je kontinuální obnova struktury dermis, ale i reparace po ztrátovém zranění, tedy hojení ran. Fibroblasty jsou přímo zdrojem, či se alespoň spoluúčastní některých patologických procesů, jakými jsou abnormální hojení (např. hypertrofické jizvy), fibrotizující onemocnění (např. sklerodermie) či nádory, kde v mikroprostředí nádoru fungují jako nádorově-asociované fibroblasty (anglicky: *Cancer-associated fibroblasts*; CAF) (Wlaschek et al. 2021).

V kontextu struktury kůže je nutno zmínit také adnexální struktury, jako jsou potní žlázy a pilosebaceózní jednotky. V dermis jsou přítomné i krevní a lymfatické cévy, nervová zakončení a specializovaná tělíska (Tobin 2017; Chambers and Vukmanovic-Stejic 2020).

Kůže se v průběhu nejen prenatálního, ale i postnatálního vývoje dramaticky mění. Stárnutí kůže není jen chronologický fenomén. Jde o komplexní proces, při němž hrají roli intrinsické (endogenní) i extrinsické (exogenní) faktory, které podněcují zhoršenou fyziologickou funkci a kompromitují i strukturní integritu kůže. Právě morfologické a funkční aspekty stárnutí se velmi významně dotýkají tématu předkládané doktorské teze.

2.1.1 Endogenní faktory ovlivňující stárnutí kůže

Ve stárnoucí kůži dochází strukturálně jednak k numerickému úbytku buněk, ale také ke ztrátám objemu ECM v důsledku snížení jejich biosyntetické výkonnosti. To je dále akcentováno i relativním nárůstem aktivity ECM degradujících enzymů (Robert et al. 2009). Navíc se častěji objevuje zmenšování podílu elastinu, fragmentace vláknité struktury ECM, což ztěžuje rozprostření fibroblastů (Cole et al. 2018). U stárnoucí kůže

dochází nejen ke ztenčování vrstev, především epidermis, v důsledku numerické atrofie keratinocytů, ale typicky dochází k zmenšené hydrataci, tedy k poklesu podílu vody v epidermis. Kůže je xerotická, změněné mechanické vlastnosti se vyznačují i změnou textury a povrchového reliéfu (tj. četnějšími vráskami) (Chambers and Vukmanovic-Stejic 2020).

Stárnutí kůže je funkčně také významně spjato i s buněčnou senescencí. Před více než půlstoletím byl v buněčné biologii etablován pojem „buněčná senescence“ pro stav, ve kterém se buňka ocitá, když již nemá kapacitu se dále dělit (Narita and Lowe 2005). Tento limitovaný replikační potenciál byl prvně popsán *in vitro* na primárních lidských fibroblastech v podmínkách tkáňových kultur a bývá tedy uváděn s odkazem na svého objevitele a popularizátora této problematiky také jako Hayflickův limit (Hayflick and Moorhead 1961). Buněčná senescence pozorovaná Hayflickem a Moorheadem (1961) byla později vysvětlena mechanisticky jako důsledek dramatického zkrácení, či úplné ztráty chromozomálních telomer při nedostatečné (či zcela chybějící) endogenní telomerázové aktivitě (Muñoz-Espín and Serrano 2014). Tento model lze s určitou nadsázkou interpretovat jako interní časomíru buňky.

V dnešní době je ale již známo, že fenomén buněčné senescence může být navozen i několika dalšími intrinsickými mechanismy. Mezi ně patří blokáda buněčného cyklu prostřednictvím inhibitorů cyklin dependentních kináz a známých tumor-supresorových genů jako je např. $p16^{INK4A}$ (*Cyclin Dependent Kinase Inhibitor 2A; viz CDKN2A*), $p21^{Waf1}$ (*Cyclin Dependent Kinase Inhibitor 1A)* a $p27^{kip1}$ (*Cyclin Dependent Kinase Inhibitor 1B*). Dalším zodpovědným faktorem může být produkce prozánětlivých či jiných tkáň degradujících faktorů navazujících na poškození tkáně (Muñoz-Espín and Serrano 2014; Vicente et al. 2016). Senescence tedy v těchto případech sehrává roli určitého obecného funkčního modulu chování, který je aktivován v kontextu abnormální situace vedoucí k poškození buňky. Toto chování dává buňkám šanci dokončit reparativní procesy, a zajistit tak integritu zejména dědičné informace. Pokud ale reparace není možná, bude buňka eliminována apoptózou, nebo alespoň vyřazena z proliferace navozenou senescencí. Nebude tak docházet ke kumulativnímu zvyšování mutační zátěže ve tkáni. V epidermis a dalších rychle se obnovujících strukturách jsou poškozené buňky kontinuálně odstraňovány při procesu diferenciace. Selhání takové eliminace může zásadně usnadnit rozvoj některých patologií včetně maligních nádorů.

Bez ohledu na konkrétní proces vedoucí buňky do senescence je jejich výsledné biologické chování v obecných rysech obdobné. Navozené komplexní změny tohoto typu

je optimální popisovat více parametry. Velkou výpovědní hodnotu pro účely komparace má komplexní analýza sekretomu buněk za normálních podmínek a po dosažení či navození senescence. Ustanovený specifický sekretom senescentní buňky bývá označován jako sekreční fenotyp asociovaný se senescencí (anglicky: *Senescent-Associated Secretory Phenotype*; SASP) (Campisi 2005).

Dosažení senescence neovlivňuje pouze samotnou senescentní buňku, ale bude mít dopad i na celou tkáň, ve které k této změně dochází. SASP umožňuje buňkám parakrinními prostředky komunikovat s okolím, a ovlivňovat tak funkčně sousedící buňky. Za určitých podmínek může jeden buněčný typ navodit senescenci v sousedních buňkách prostřednictvím sekrece cytokinů, chemokinů a růstových faktorů (Acosta et al. 2013).

Senescenci podléhají obě majoritní buněčné populace kůže, keratinocyty a fibroblasty, což vede k morfologicky nápadným změnám. Velmi akcentované změny na kůži jsou pak přítomny u vzácných syndromů akcelerovaného stárnutí, jako je progerie (syndrom Hutchinson-Gilford) (Dreesen 2020). Senescence ale postihuje i minoritní buněčné typy včetně melanocytů, které pak exprimují $p16^{INK4A}$, mají dysfunkční telomery a snižuje se u nich HMGB1 (*High Mobility Group Box-1*), jehož nízká hladina je považována za další znak buněčné senescence. Kromě toho senescentní melanocyty ovlivňují svým SASP i sousedící keratinocyty a způsobují i u nich dysfunkci telomer vedoucí k nízké proliferaci a posléze k atrofii epidermis (Victorelli et al. 2019). Wang et al. (2014) popisuje, že senescenci u lidských melanocytů může navodit také IFN-γ (*Interferon-γ*), což je mechanisticky vysvětleno následně zvýšenou expresí proteinu p21. Navíc melanocyty po dlouhodobém vystavení IFN-γ také masivně produkují cytokin IL-6 (*Interleukin-6*), který je jedním z klíčových faktorů SASP (Wang et al. 2014).

Proces stárnutí kůže bývá ovlivněn i nerovnováhou mezi endogenním vznikem a inaktivací reaktivních forem kyslíku (anglicky: *Reactive Oxygen Species*; ROS) a jiných volných radikálů vznikajících při základním oxidativně-fosforylačním metabolismu každé buňky. K tomu může docházet zvýšenou měrou u mitochondriálního oxidativního stresu, který se objevuje zejména u lidí ve věku nad 60 let (Lu et al. 1999). Antioxidační enzymy jsou zodpovědné za bezpečné odstraňování ROS i zmírnění jejich škodlivých účinků. Jedním z hlavních antioxidačních enzymů je superoxid dismutáza 2 (anglicky: *Superoxide Dismutase 2*; SOD2). Nepřítomnost SOD2 u myšího modelu způsobila sníženou aktivitu mitochondriálního komplexu II vedoucí k poškození jaderné DNA a

následně i k navození senescence. Apoptóza přitom v epidermis nebyla indukována. Toto pozorování ilustruje, jak se mitochondriální oxidativní stres spolu s buněčnou senescencí podílí na stárnutí kůže (Velarde et al. 2012).

V tomto případě spolehlivé odlišení podílu vlivu endogenně vznikajících a exogenně přicházejících ROS není snadné, tudíž v biologických systémech není lehko stanovitelná hranice mezi vlivy exogenními a endogenními.

2.1.2 Exogenní faktory ovlivňující stárnutí kůže

Za změnami ve struktuře a fyziologických funkcích kůže stojí i celá řada exogenních faktorů. Zpravidla se uvádí vlivy fyzikální, pocházející ze zevního prostředí (např. různé typy záření), vlivy chemické jako jsou reaktivní kyslíkové radikály či chemické environmentální polutanty, ale i některé vlivy biologické. Při analýze je pak nutno zohlednit i klinicky relevantní vlivy behaviorální, např. kouření, alimentární návyky a nezdravá životospráva (Strnadova et al. 2019; publikace II).

Pro karcinogenezi v kontextu kůže je ale zcela zásadním faktorem ultrafialové (anglicky: *Ultraviolet*; UV) záření. Právě tento faktor je epidemiologicky nejvýznamnější příčinou pro vznik kožních malignit včetně maligního melanomu kůže (blíže kapitola 2.3), a proto bude tato kapitola zaměřena zejména na faktor UV záření.

UV záření se dělí na spektrální pásma dle vlnových délek, a sice na UVA (315–400 nm), UVB (280–315 nm) a UVC (100–280 nm). Sluneční záření dopadající na zemský povrch sestává dominantně z UVA (90–95 %) a UVB paprsků (5–10 %), zatímco přirozené UVC je z velké části absorbováno ozónovou vrstvou atmosféry (Obr. 3) (Amaro-Ortiz et al. 2014; Sample and He 2018). UV paprsky dopadají na kůži v průběhu celého života jednotlivce, byť kumulace dávky nepodléhá lineárnímu modelu (Karagas et al. 2007). Při excesivní expozici ale může dojít k urychlení stárnutí a tento výsledný strukturální a funkční efekt označujeme jako *photoageing* (Yaar and Gilchrest 2007).

Přirozené i akcentované stárnutí způsobené UV zářením ovlivňuje tedy nejen povrchovou epidermis, ale také hlubší vrstvu dermis. Tyto dva aspekty od sebe nelze oddělit a v průběhu jednotlivých kroků vedoucích ke vzniku zhoubného nádoru sehrává aktinické poškození určitou roli.

UVB může způsobit přímé poškození deoxyribonukleové kyseliny (anglicky: *Deoxyribonucleic Acid*; DNA) v buňkách epidermis. UVA penetruje hlouběji až do dermis a zvyšuje zde ROS, které nepřímo mohou také vyvolávat DNA mutagenezi,

zároveň v dermis dochází i ke strukturálnímu poškození vedoucímu například až k solární elastolýze elastinových vláken (Amaro-Ortiz et al. 2014).

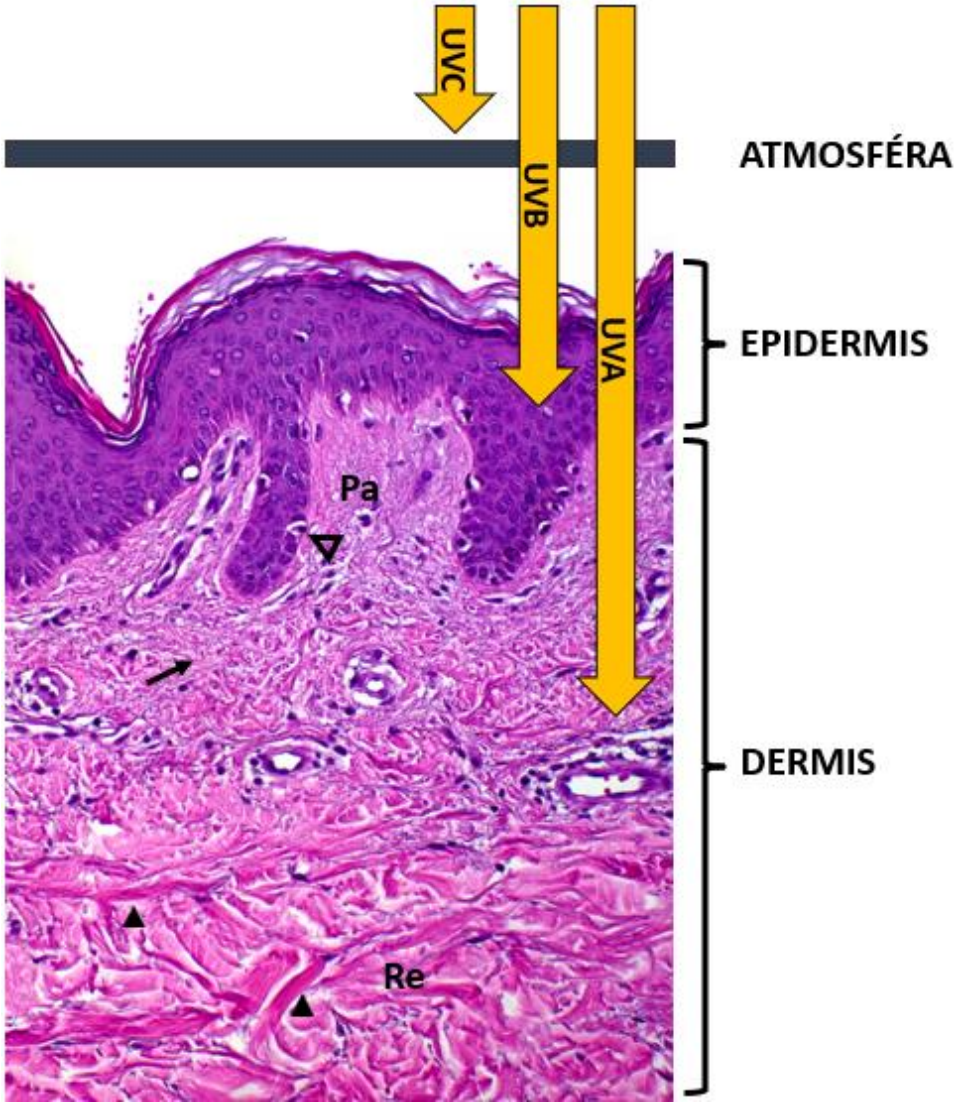

Obr. 3 Vliv UV záření na kůži. UV záření dopadající na kůži je převážně složeno ze spektrálních oblastí UVA a UVB. UVC je absorbováno ozonovou vrstvou atmosféry. UVB dosahuje hlavně epidermis kůže. Rizikem při nadměrném vystavení UVB je spálení kůže a následné přímé poškození DNA. UVA penetruje až do dermis, zvyšuje riziko ROS a oxidativního stresu vedoucí k DNA mutagenezi a předčasnému stárnutí kůže (Amaro-Ortiz et al. 2014). Fotografie byla poskytnuta Dermatovenerologickou klinikou 1. LF UK a VFN. Pa – *stratum papillare*; Re – *stratum reticulare*; prázdný trojúhelník – melanocyt; šipka – jemná extracelulární matrix ve *stratum papillare*; plný trojúhelník – hrubé kolagenní snopce ve *stratum reticulare.*

V dermis dochází k degradaci kolagenu a jiných proteinů ECM vyvolané zvýšenou aktivitou matrix metaloproteináz (anglicky: *Matrix Metalloproteinase*; MMP) (Quan et al. 2009). Zdá se, že aktivita tkáňových inhibitorů matrix metaloproteináz (anglicky: *Tissue Inhibitor of Matrix Metalloproteinase*; TIMP) je ve stárnoucí kůži nižší, jako bylo objeveno v případě TIMP1 (Hornebeck 2003). Recentně provedená genová analýza potvrdila, že vystavení lidských dermálních fibroblastů UVB záření navozuje sníženou

expresi genů pro kolagen *COL1A1 (Collagen Type I Alpha 1 Chain)*, *COL1A2 (Collagen Type I Alpha 2 Chain)*, *COL3A1 (Collagen Type III Alpha 1 Chain)* a zvýšenou expresi MMP (např. *MMP9*, *MMP10* nebo *MMP3*), nicméně aktivita TIMP vykazovala nejednotné trendy. Exprimovaný *TIMP3* byl zde downregulován, naopak geny *TIMP1*, *TIMP2* a *TIMP4* byly upregulovány. Těmito extrinsickými vlivy inspirovaný model stárnutí naznačuje, že TIMP reagovaly spíše na zvyšující se aktivitu MMP než na UVB záření (Lago and Puzzi 2019).

Souhrnně vzato, vlivy prostředí jako je právě UV záření, ROS, chemické polutanty a další škodliviny způsobují funkční vyčerpání ochranných mechanismů daných správnou funkcí antioxidačních enzymů. To vede ve výsledku také k poškození DNA a následně i k tkáňové reakci spojené se sekrecí prozánětlivých faktorů produkovaných buňkami kůže (jako je tomu u SASP). Zánětlivé prostředí stimuluje translaci dalších proteinů, např. různých MMP způsobujících degradaci ECM (Pillai et al. 2005).

Je tedy zřejmé, že exogenně zapříčiněné poškození kůže vyvolává změny reflektované na endogenní úrovni, a jak již bylo zmíněno, nelze tak tyto faktory od sebe jednoduše v biologických systémech oddělit.

2.2 Melanocyty za fyziologických podmínek

2.2.1 Vývoj melanocytů

U obratlovců existuje velké množství různých typů buněk produkujících pigmenty (Schartl et al. 2016). Pro potřeby humánní morfologie a fyziologie je ale klíčovým buněčným představitelem tohoto typu melanocyt. Melanocyty jsou pigmentové buňky, které se nachází v pokožce ve *stratum basale*. Pigmentové buňky nalézáme ale i v *tunica vasculosa* oka, vnitřním uchu, mozkových obalech nebo srdci. Pro vývojové biology představuje vývoj melanocytů zajímavý model, který vysvětluje pozoruhodně širokou distribuci tohoto buněčného typu v lidském těle.

U savců pochází melanocyty z multipotentních kmenových buněk neurální lišty. Nejprve se bipotentní progenitor melanoblastů a gliových buněk vyznačuje pozitivitou pro SOX10 (*SRY-Box Transcription Factor 10*) (Mort et al. 2015). Po uzavření neurální trubice (spojením neurálních valů) tato progenitorová populace projde nejprve epitelově-mezenchymovým přechodem (anglicky: *Epithelial-Mesenchymal Transition*; EMT), čímž se uvolní z neurálních valů, a posléze migruje vyvíjejícím se embryem. V oblasti hlavy dochází k EMT ještě před uzavřením neurální trubice. Při migraci odlišujeme dva

směry. Po migraci ventrální cestou dává progenitorová populace vzniknout například některým složkám periferního nervového systému. Druhou možností je pak migrace dorzolaterální cestou vedoucí ke vzniku melanoblastů (Silver and Pavan 2006). V kůži tyto buňky pronikají dermis, osidlují *stratum basale* epidermis a tvoří prekurzory melanocytů (Qiu et al. 2019).

Některé melanocyty si zachovávají v cílové tkáni také svůj charakter nízce diferencovaných kmenových buněk, ty se nalézají v rozšířeném segmentu zevní kořenové epitelové pochvy vlasového folikulu označované jako „*bulge*“. Zde přítomná populace kmenových buněk melanocytů (anglicky: *Melanocyte Stem Cells*; MelSC) vytváří rezervu schopnou sebeobnovy, která je čerpána ve fázi anagenu růstového cyklu vlasových folikulů. Tyto melanocyty jsou pak zodpovědné za barvu vlasů a ochlupení (Joshi et al. 2019). Stárnutím ztrácí MelSC svojí schopnost sebeobnovy a vlasy postupně šediví (Wang et al. 2016). Zatímco MelSC ve vlasovém folikulu vykazují značnou plasticitu – v případě ztrátového poškození epidermis může z vlasových folikulů docházet i k repopulaci epidermis a následné repigmentaci (Obr. 4), např. při vitiligu (Cui et al. 1991; Yardman-Frank and Fisher 2021) – melanocyty v epidermis jsou vysoce diferencovanou populací buněk, které v případě jednotlivě se vyskytujících buněk ve *stratum basale* proliferují pouze výjimečně, a jsou tak stabilními dlouho žijícími buňkami (Cichorek et al. 2013; Casalou et al. 2022).

Nicméně existuje i studie popisující možnou diferenciaci melanocytů z dermálních prekurzorů, konkrétně dermálních kmenových buněk izolovaných z novorozeneckých předkožek a kultivovaných v nediferencovaném stavu. Tyto buňky exprimovaly znaky buněk neurální lišty (např. nestin). *In vitro* vykazovaly dermální kmenové buňky multipotentní charakter, které bylo možno diferencovat v jiné buněčné typy, např. buňky hladké svaloviny, adipocyty nebo právě melanocyty. V kontextu rekonstrukce kůže se tyto melanocyty usídlily při bazální membráně, byly pigmentované a exprimovaly následně i typické znaky pro melanocyty. To naznačuje, že by mohl existovat i jiný zdroj pro epidermální melanocyty, než jsou MelSC ve vlasových folikulech (Li et al. 2010).

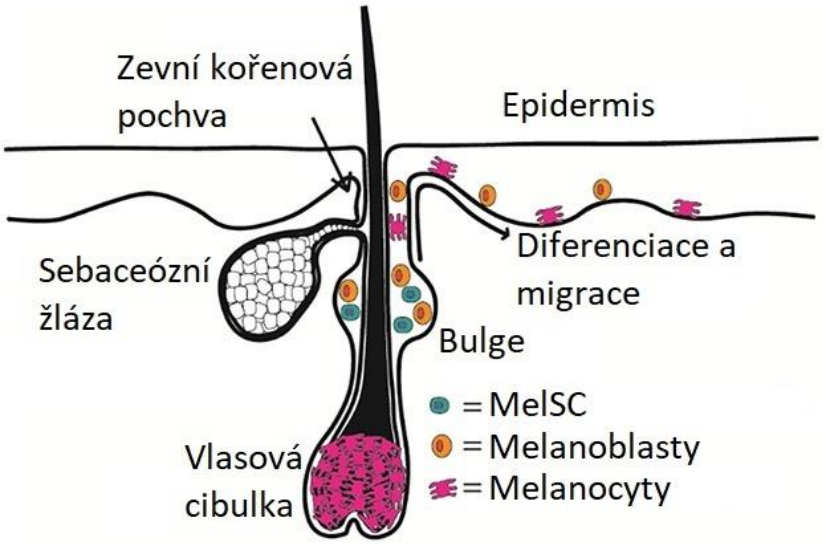

Obr. 4 Rezervoár kmenových buněk melanocytů v kůži. MelSC osidlují rozšířený segment zevní kořenové pochvy vlasového folikulu zvaný bulge. V případě potřeby perifolikulární repigmentace, např. v důsledku ztrátového poškození epidermis nebo při vitiligu, se část klidových MelSC a melanoblastů v bulge aktivuje a migruje do oblasti nad tento segment. V tomto místě dochází k další diferenciaci a migraci směrem do periferní epidermis, kde následně dochází k repigmentaci (převzato a upraveno dle Yardman-Frank and Fisher (2021).

Popsaná velká schopnost tohoto buněčného typu udržovat si kmenové charakteristiky spojované s nízkým stupněm diferenciace a dále pozoruhodná schopnost migrovat, mohou být důvodem, proč se melanocyty po neoplastické transformaci v buňky maligního melanomu chovají tak agresivně, jsou schopny odolávat terapii a také snadno metastazují (Mort et al. 2015).

2.2.2 Melanogeneze

Melanocyty tvoří přibližně 4 % buněčné populace v bazální vrstvě epidermis a svými dendritickými výběžky dosahují do úrovně *stratum spinosum*. Jeden melanocyt je obklopen zhruba 36 keratinocyty a dohromady tvoří epidermální melaninovou jednotku (Fitzpatrick and Breathnach 1963; Quevedo 1972; Seiberg 2001; Nordlund 2007). Svými výběžky předávají keratinocytům pigment melanin ve formě zralých melanosomů, které v cytoplazmě jako štít chrání jádra keratinocytů a pohlcují energii dopadajících fotonů UV záření (Obr. 5) (Seiberg 2001).

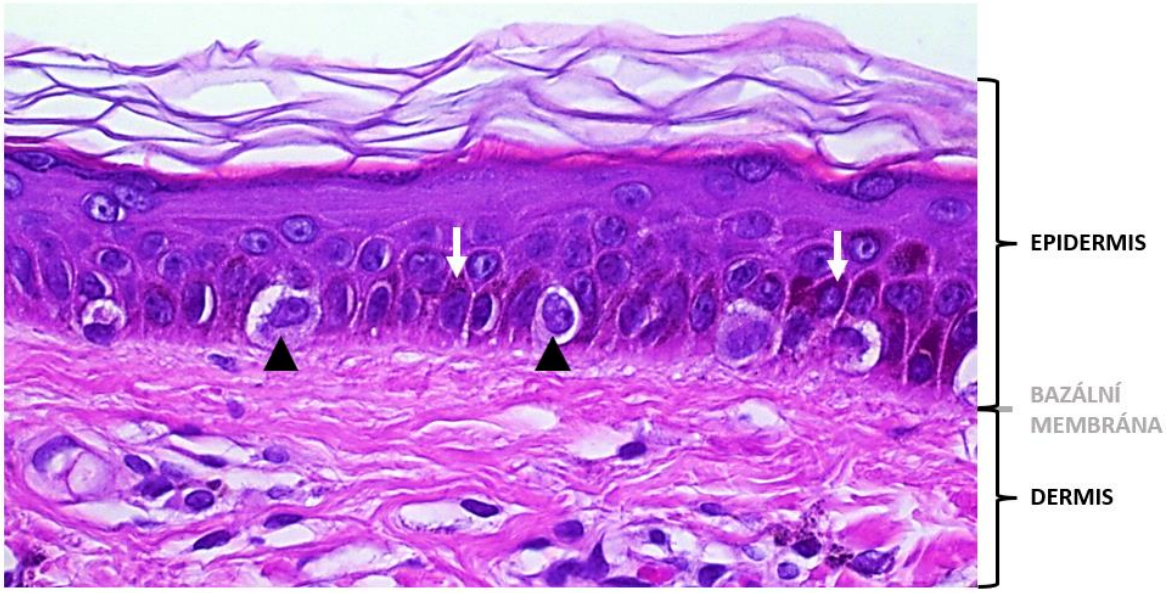

Obr. 5 Pigmentové buňky kůže. Na hranici mezi epidermis a dermis se nachází bazální membrána, na kterou nasedají pigmentové buňky kůže – melanocyty. Melanocyty předávají okolním keratinocytům v epidermis pigment melanin, který chrání jejich jádra před UV zářením. Fotografie byla poskytnuta Dermatovenerologickou klinikou 1. LF UK a VFN. Bílá šipka – pigment melanin chránící jádro keratinocytu; plný trojúhelník – melanocyt.

Melanin se u člověka v kůži přirozeně vyskytuje v několika formách – hnědočerný eumelanin, žlutočervený feomelanin či smíšený melanin. V lidském těle je dále přítomen i chemicky příbuzný pigment, neuromelanin, syntetizovaný v *substantia nigra* středního mozku (mesencephalon), který je ale funkčně velmi odlišný (Mort et al. 2015; Slominski et al. 2004; Zecca et al. 2001). U lidí se v kůži nejčastěji vyskytuje eumelanin, proto bude s ohledem na jeho funkční význam popsána melanogeneze právě této formy melaninu.

Průběh melanogeneze je možné dělit podle fází tvorby organel melanosomů, ve kterých je pigment uložen (Obr. 6). Tyto váčky se do jisté míry podobají lysozomům. První fázi (I) vzniku eumelanosomů představují membránou ohraničené vezikuly zatím postrádající pigment, ale obsahující již v lumen základy proteinových fibril. Tyto proteinové fibrily jsou zcela dotvořeny ve stádiu II a melanosom se pak vyznačuje elipsoidním tvarem. V této fázi začíná také syntéza eumelaninu. Ve stádiu III a IV se eumelanosom obohacuje o elektrondenzní melanin, který se postupně ukládá na fibrilách až do úplného zaplnění lumen organely (Raposo and Marks 2007; D'Alba and Shawkey 2019). Hlavní strukturální složkou fibril je protein Pmel17 (*Premelanosome Protein*; též gp100), který obsahuje opakující se sekvence aminokyselin prolinu/serinu/threoninu, tzv. RPT doménu (Bissig et al. 2016). Delece této domény vede k neschopnosti tvořit fibrily a zamezuje rozpoznání Pmel17 monoklonální protilátkou užívanou při běžné diagnostice pod označením HMB45 (Hoashi et al. 2010). Další kriticky významný protein pro

strukturní zrání melanosomů je vedle Pmel17 i Melan-A (označovaný také jako MART-1 - *Melanoma Antigen Recognized by T-Cells 1)* (Yamaguchi et al. 2007).

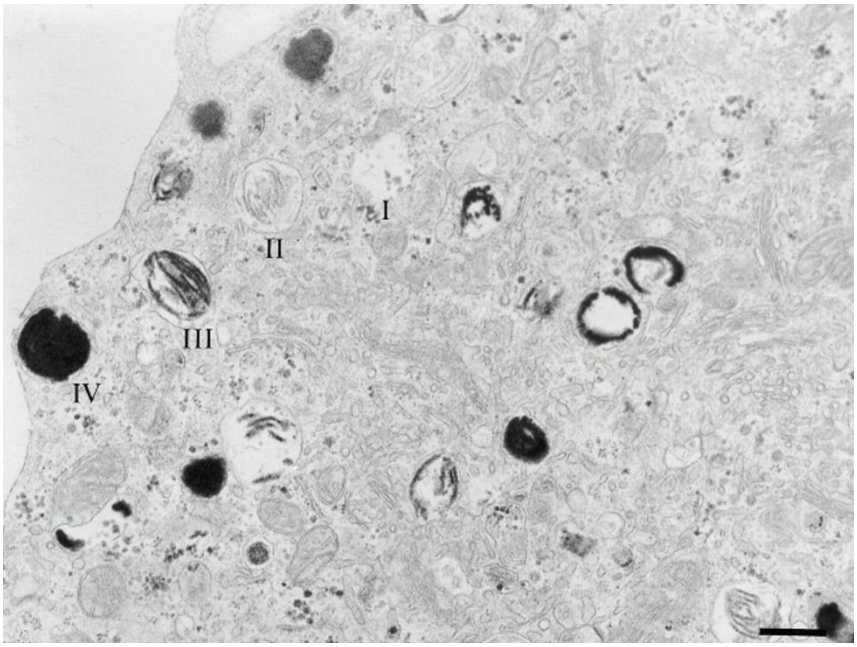

Obr. 6 Zrání melanosomů. Obrázek z imunoelektronové mikroskopie odhaluje stádia zrání melanosomů. Ve stádiu I se v membránově ohraničených váčcích objevují základy proteinových fibril dominantně tvořených z Pmel17. Ve stádiu II proteinové fibrily dorůstají. Ve stádiu III a IV dochází k syntéze melaninu, který postupně vyplňuje lumen melanosomu (převzato a upraveno dle Raposo et al. 2001).

Biochemická syntéza eumelaninu je několikastupňový proces a začíná přeměnou L-tyrosinu na dopachinon prostřednictvím enzymu tyrosinázy (anglicky: *Tyrosinase*; TYR). Mezistupněm této přeměny je 3,4-dihydroxyfenylalanin (anglicky: *3,4-dihydroxyphenylalanine*; L-DOPA). Dopachinon je následně přeměněn na leukodopachrom, poté na dopachrom a v důsledku oxidačně-redukčních reakcí na meziprodukty 5,6-dihydroxyindol (anglicky: *5,6-dihydroxyindole;* DHI) a 5,6-dihydroxyindol-2-karboxylovou kyselinu (anglicky: *5,6-dihydroxyindole-2-carboxylic acid;* DHICA). DHI a DHICA polymerizují a vytváří hnědočerný eumelanin. Kromě TYR hrají důležitou roli v tomto procesu i další dva enzymy: tyrosináze příbuzný protein 1 (anglicky: *Tyrosinase-Related Protein 1*; TYRP1) a dopachrom tautomeráza (anglicky: *Dopachrome Tautomerase*; DCT nebo TYRP2) (Obr. 7) (Hearing and Jiménez 1987; Slominski et al. 2004; Yamaguchi et al. 2010). Přítomnost těchto proteinů je velmi specifická pro melanocyty a může tedy být chápána jako jejich velmi specifický fenotypový znak využitelný i diagnosticky.

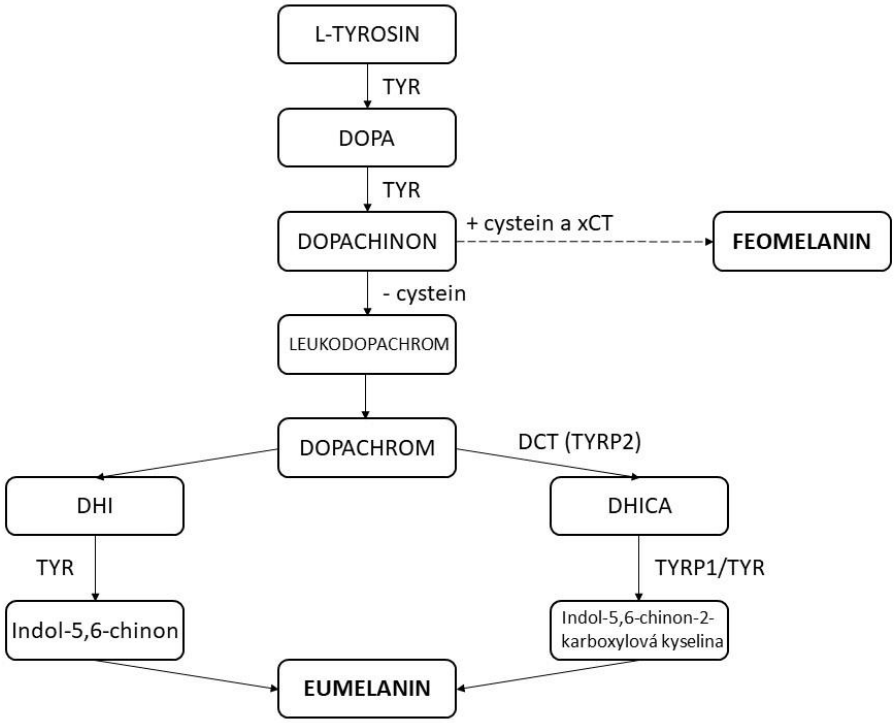

Obr. 7 Syntéza eumelaninu. Schéma znázorňuje několikastupňový proces přeměny L-tyrosinu na hnědočerný pigment eumelanin. V případě, že je přítomen cystein a cystin-glutamátový transporter (anglicky: *Cystine/Glutamate Transporter*; xCT), z dopachinonu může vzniknout přes benzothiazinové meziprodukty žlutočervený feomelanin (převzato a upraveno dle Zhang et al. 2018).

Biogeneze melanosomů a syntéza melaninu je klíčově regulována transkripčním faktorem MITF (*Melanocyte Inducing Transcription Factor*) (Vachtenheim and Borovanský 2010). Kromě toho svou roli v produkci melaninu hraje i hodnota pH. Bylo dokázáno, že neutrální pH je optimální pro efektivní melanogenezi a naopak nízké kyselé pH snižuje aktivitu enzymu TYR, a tudíž i produkci melaninu (Ancans et al. 2001). Dalšími klinicky relevantními stimuly ovlivňujícími pigmentaci mohou být například extrinsický faktor UV záření nebo intrinsický faktor, jako je probíhající zánět (Videira et al. 2013).

UV záření je důležitým regulačním faktorem melanogeneze a následně získané pigmentace. UVB záření zahajuje soubor dějů vedoucí k „zpožděnému/nepřímému“ opálení (z anglického *delayed tanning*), které trvá dny až týdny (Yardman-Frank and Fisher 2021). Na tomto procesu se podílí onkogen *p53* (*Tumour protein P53*), jehož aktivita je v důsledku UVB záření zvýšená, a to přímo vede k transkripci genu proopiomelanokortinu v keratinocytech (Cui et al. 2007; Park et al. 2009). Jedním z možných aktivních produktů tohoto polypeptidu je po sestřihu α-melanocyty stimulující hormon (anglicky: α-*Melanocyte Stimulating Hormone*; α-MSH), který zintenzivňuje syntézu melaninu (Yamaguchi et al. 2007; Videira et al. 2013). Bylo zjištěno, že při

inaktivaci tumor-supresorového genu *p53* u myši nedochází k opálení kůže (Cui et al. 2007), které je považováno za adaptivní odpověď kůže na DNA poškození způsobené UV zářením (Videira et al. 2013). U starších jedinců může, v důsledku kumulativního působení dávek UVB záření, docházet k fokální hyperpigmentaci způsobené akumulací melaninu v cytoplazmě keratinocytů v podobě tzv. *lentigo solaris* (Imokawa 2019).

I krátkodobá nadlimitní expozice UVB záření může způsobit spálení kůže, klinicky odpovídající *dermatitis solaris*. Akutní poškození kůže se projevuje zčervenáním, bolestí, někdy až tvorbou puchýřů, či dokonce nekrózou keratinocytů. Klinicky tedy naplňuje Celsovy[1] znaky zánětu (Scott et al. 2004). Dochází při ní skutečně k akumulaci imunitních buněk, které produkují celou řadu zánětlivých proteinů a způsobují kožní zánět (Hossain et al. 2021; Ansary et al. 2021). V kůži vystavené nadměrné solární radiaci vznikají ve velkém množství také ROS (Mittal et al. 2014), které aktivují signální kaskády v keratinocytech a fibroblastech vedoucí také ke zvýšené expresi zánětlivých molekul, např. cytokinů (Ansary et al. 2021). Parakrinní produkce těchto proteinů dvěma hlavními buněčnými populacemi kůže je dalším faktorem ovlivňujícím melanogenezi v melanocytech (Obr. 8) (Fu et al. 2020). Zvýšená hladina ROS a tedy ve výsledku buněčného stresu může být také spouštěčem některých kožních autoimunitních onemocnění, např. vitiliga, které se vyznačuje autoimunitně podmíněnou ztrátou melanocytů a následnou depigmentací postižené části kůže (Bergqvist and Ezzedine 2020). Bylo zjištěno, že právě u vitiliga dochází k elevaci hladin cytokinů IL-6, IL-17 (*Interleukin-17*) nebo TNF (*Tumor Necrosis Factor*) (Yang et al. 2018). Tyto faktory lze monitorovat i v periferní krvi (Tomaszewska et al. 2020). Škála relevantních molekul ovlivňujících pigmentaci kůže je ale velmi široká (review Fu et al. 2020).

[1]Aulus Cornelius Celsus (25 př. n. l. – 50 n. l.)

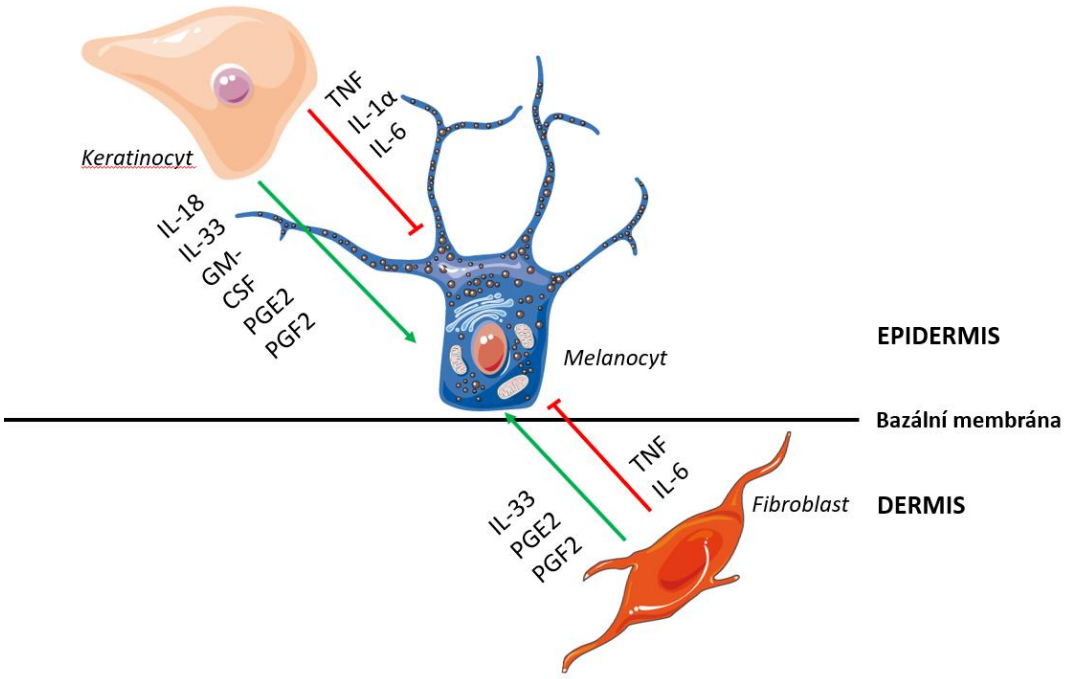

Obr. 8 Zánětlivé faktory ovlivňující melanogenezi. Faktory produkované dvěma největšími buněčnými populacemi kůže – keratinocyty v epidermis a fibroblasty v dermis – parakrinně ovlivňují melanogenezi v melanocytech. Keratinocyty stimulují melanogenezi sekrecí proteinů, jako jsou IL-18 (*Interleukin-18*), IL-33 (*Interleukin-33*), GM-CSF (*Granulocyte-Macrophage Colony Stimulating Factor*), PGE2 (*Prostaglandin E2*) a PGF2 (*Prostaglandin F2*), naopak ji inhibují produkcí TNF, IL-1α *(Interleukin-1α)* a IL-6. Fibroblasty podporují melanogenezi sekrecí IL-33, PGE2 a PGF2. Inhibice melanogeneze je stimulována, ze strany fibroblastů, produkcí TNF a IL-6. Obrázky byly staženy z obrázkové banky Servier Medical Art image bank zdarma dostupné na smart.servier.com. Servier Medical Art podléhá licenci Creative Commons Attribution 3.0 Unported License. Schéma vychází z review Fu et al. (2020) a je upraveno pro potřeby této doktorské práce autorkou.

2.2.3 Identifikace melanocytů in situ na molekulární úrovni

Identifikace melanocytu na úrovni světelné mikroskopie v základním histologickém barvení technikou hematoxylin-eosin na tkáňovém řezu je jistě možná, ale pro potřeby patologické diagnostiky a dále i pro potřeby výzkumné práce je taková detekce nedostatečně spolehlivá. Významné rozšíření možností studia melanocytů a melanocytárních patologií přineslo rutinní využívání imunohistochemie a v pozdější době i molekulárních metod jako například *in situ* hybridizace.

Na molekulární úrovni jsou melanocyty v epidermis identifikovány dle několika znaků (Tab. 1). Tyto geny a jejich proteinové produkty se objevují primárně při vývoji melanocytů nebo jejich melanogenezi. Bohužel, ani tyto pokročilé techniky zpravidla neumožní identifikaci melanocytu či jeho prekurzorů založenou na jediném markeru. Pro udržení dostatečné senzitivity a specificity bývá tedy pro diagnostické aplikace často užívána paralelně kombinace několika (často 2–3) protilátek.

Pozitivní znaky pro melanocyty epidermis (v abecedním pořadí)
Bcl-2
DOPA
KIT (seu c-Kit nebo CD117)
Melan-A (seu MART-1)
MITF-M
Pmel17 (seu gp100 nebo HMB-45)
S100 protein
SOX10
TYR
TYRP1
TYRP2 (DCT)

Tab. 1 Specifické antigeny melanocytů epidermis. Tabulka shrnuje abecedně seřazené proteiny, pro které jsou melanocyty v epidermis pozitivní. Na jejich základě lze melanocyty identifikovat na molekulární úrovni, a rozeznat je tak od jiných populací buněk (převzato a upraveno dle Passeron et al. 2007).

Genová rodina Bcl-2 (*B-cell lymphoma-2*) je obecně schopna regulovat propustnost vnější mitochondriální membrány. Tvoří ji jak proapoptické tak antiapoptické proteiny. Proapoptické faktory, např. Bax (*BCL2 Associated X, Apoptosis regulator*), Bak (*BCL2 Antagonist/Killer*), zvyšují propustnost mitochondriální membrány vedoucí k vyloučení cytochromu C z mitochondrie, což je prvotní krok v průběhu programované buněčné smrti. Cytochrom C utváří multiproteinový komplex apoptosom (Eberle and Hossini 2008). Oproti tomu antiapoptické proteiny jako jsou Bcl-2 nebo Bcl-xL (*B-cell lymphoma-extra large*), inhibují proapoptické faktory a v případě melanocytů regulují jejich přežití (Opferman and Kothari 2018), jak bylo zjištěno i na experimentech s *Bcl2* null myší, které vykazovaly ztrátu pigmentace a dramatickou redukci kmenové populace melanocytů (Mak et al. 2006). Podobně bylo pozorováno i vymizení folikulárních melanocytů u *bcl-2*$^{-/-}$ myší, u kterých byla biochemicky detekována ztráta 60–70 % melaninu v druhém vlasovém cyklu po depilaci (Yamamura et al. 1996).

Proto-onkogen KIT (*KIT Proto-Oncogene, Receptor Tyrosine kinase, též CD117 nebo c-Kit*) kóduje tyrosinkinázový receptor. Ligand, který se na tento receptor váže, je SCF (*Stem Cell Factor*). Po navázání tohoto cytokinu na KIT dochází k fosforylaci mnoha intracelulárních proteinů, které hrají roli v proliferaci, diferenciaci, migraci nebo

v hematopoéze a melanogenezi (Pham et al. 2020). Interakce KIT a SCF je potřebná pro přežití melanocytů při migraci v dermis, ale i v zevní epitelové pochvě vlasového folikulu (Yoshida et al. 2001). Exon 10 u *Kit* kóduje transmembránovou doménu tohoto proteinu. Vyřazení tohoto exonu, s využitím inducibilního knock-out systému Cre-*loxP* (Kim et al. 2018), se u myši fenotypově projevuje bílými skvrnami na srsti a redukcí počtu melanoblastů v raném vývoji (Aoki et al. 2015).

S100 proteiny zahrnují širokou škálu nízkomolekulárních Ca^{2+} vázajících proteinů s rozmanitou funkcí, jako jsou regulace proliferace, diferenciace, transkripce, apoptózy, Ca^{2+} homeostázi aj. (Eckert et al. 2004; Donato et al. 2012). Konkrétně zástupce této rodiny, S100B (*S100 Calcium Binding Protein B*), je pozitivním znakem pro melanocyty a je diagnostickým markerem i pro kožní melanom (Shrestha et al. 1998). Podobně i S100A (*S100 Calcium Binding Protein A*) je znakem s vysokou senzitivitou pro melanocyty a buňky maligního melanomu, ale jeho použití při diagnostice je značně nespecifické (Xia et al. 2016). Nutno zmínit, že S100 protein je přítomen i u další epidermální buněčné populace a sice Langerhansových buněk; navíc se nachází i u mnoha jiných buněčných typů zejména původem z buněk neurální lišty jako u Schwannových buněk a astrocytů nebo v oblasti hlavy a krku u chondrocytů či adipocytů (Böni et al. 1997; Donato et al. 2012). Právě s astrocyty se pojí výzkum na myších, u nichž je vyřazen gen pro S100B, který naznačuje, že normální hladiny tohoto proteinu snižují riziko epileptických záchvatů (Dyck et al. 2002). Při chemickém podráždění kůže, např. hydrochinonem a kyselinou retinovou (látky používající se klinicky pro léčbu hyperpigmentací), se zvyšuje intracelulární i extracelulární hladina S100B. Částečné potlačení (tzv. *knock-down*) aktivity tohoto genu u kultivovaných melanocytů vede k jejich apoptóze. Výsledky naznačují, že by zvýšená exprese S100B mohla být kompenzační reakcí pro ochranu melanocytů před cytotoxicitou (Cheong et al. 2014).

S100 je jedním z běžně užívaných znaků při diagnostice melanomu. Oceňována je zejména vysoká senzitivita dostupných protilátek. Při hodnocení 60 cytologických vzorků od 58 pacientů s metastatickým maligním melanomem byl protein S100 pozitivní v 87 % případů. Dokonce i při absenci dvou dalších typických znaků pro melanocyty a maligní melanom – Pmel17 (HMB-45) a Melan-A (MART-1) – byl S100 přítomný v 73 % případů. S100 se tak dá považovat za vysoce užitečný diagnostický marker maligního melanomu (Erdag et al. 2013), zejména je-li užíván v kombinaci s dalšími znaky.

DOPA, TYR, TYRP1, TYRP2, Pmel17 a Melan-A jsou proteiny již zmíněné při melanogenezi a zrání melanosomů. Knock-out genu *Tyrp2* u myší snižuje obsah melaninu

v chlupech a barva srsti je nevýrazná, nicméně viabilita primárních melanocytů je zachována a nebyly zaznamenány změny v distribuci TYR nebo TYRP1 (Guyonneau et al. 2004). Inaktivace genu *Pmel17* (*Pmel*$^{-/-}$) u myší nenarušuje viabilitu ani fertilitu, ale dochází u nich ke snížení eumelaninu v chlupech oproti *wild-type* myším a zároveň melanocyty obsahují více sférické melanosomy. Pmel17 je tak důležitým faktorem pro epidermální pigmentaci (Hellström et al. 2011). Obdobné výsledky jsou pozorovány u myši s vyřazeným genem pro Melan-A. Myši s touto deficiencí mají deformované melanosomy a dochází u nich opět ke ztrátě pigmentu v kůži a srsti (Aydin et al. 2012).

MITF reguluje transkripci tří hlavních enzymů melanogeneze – TYR, TYRP1 a TYRP2 (D'Mello et al. 2016) a objevuje se v několika isoformách s různým tkáňovým expresním profilem. Jeho M-isoforma (*MITF-M*) je exprimována výhradně u melanocytů (Fuse et al. 1996; Nguyen and Fisher 2019) a je zásadním regulátorem nejen vývoje, proliferace a přežití melanocytů, ale i produkce melaninu (Vachtenheim and Borovanský 2010). Mutace v tomto genu způsobuje jednu z forem Waardenburgova syndromu projevujícího se ztrátou sluchu a defektem v pigmentaci (Tassabehji et al. 1994). Bylo zjištěno, že exprese *MITF* je přímo ovlivňována navázáním SOX10 a PAX3 *(Paired Box 3)* na jeho promotor (Bondurand et al. 2000).

2.3 Maligní melanom kůže a jeho fenotyp

2.3.1 Charakteristika a etiopatogeneze

Maligní melanom je jedno z nejzhoubnějších nádorových onemocnění, které vzniká neoplastickou proliferací transformovaných melanocytů. Všeobecně známým rizikovým faktorem pro vznik melanomu je expozice UV záření a zejména pak četnost spálení kůže v průběhu dětství a dospívání (Gandini et al. 2005; Leonardi et al. 2018). Předpokládá se totiž, že kumulace dávky záření v tomto ohledu není plně lineární (Karagas et al. 2007). UV záření tak nadále zůstává nejrizikovějším mutagenem i s odstupem dekád po proběhlé expozici.

Na UV záření poškozující DNA odpovídají kožní keratinocyty produkcí α-MSH. Tento hormon je vázán na receptor MC1R (*Melanocortin 1 Receptor*) na melanocytech, což vyvolává uvolnění melaninu, který tvoří ochranný štít před dalším poškozením buněčných jader. Nedostatečné reparační mechanismy a genotoxický efekt UV záření mohou způsobit nekontrolovatelný růst a dělení buněk, které vyústí až ve vývoj melanomu.

Rizikové faktory u maligního melanomu zohledňované v klinické dermatoonkologii jsou fototyp kůže, genetická predispozice, stav imunitního systému, rodinná anamnéza, počet atypických melanocytárních névů a samozřejmě zvyšující se věk (Marks 2000; Abdel-Malek et al. 2000; Hawkes et al. 2016; Leonardi et al. 2018).

Podle Ústavu zdravotnických informací a statistiky (ÚZIS) byl v poslední hodnocené dekádě, tj. období 2009–2018, pozorován nejvýraznější vzestup celkové incidence onkologických diagnóz právě u zhoubného melanomu kůže, u kterého byla zaznamenána průměrná roční procentuální změna jako nárůst o 3,5 %[2]. I přestože incidence maligního melanomu v České republice (Obr. 9) i celosvětově stále stoupá, mortalita zůstává přibližně stabilní (Obr. 9).

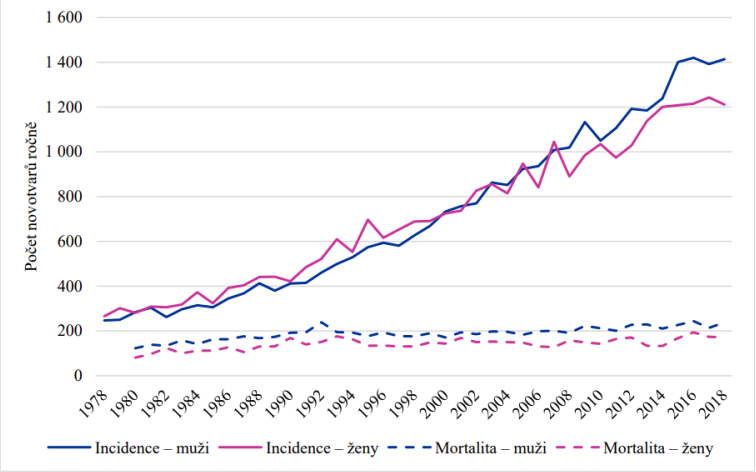

Obr. 9 Graf pro vývoj incidence a mortality[3] zhoubného melanomu kůže dle pohlaví (absolutní počty). Data zveřejněná Ústavem zdravotnických informací a statistiky (ÚZIS) za období 2009–2018.

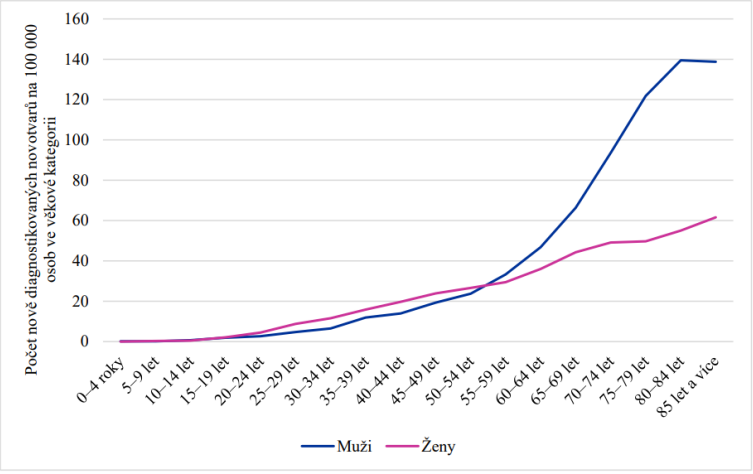

Obr. 10 Graf věkově specifické incidence zhoubného melanomu kůže. Data zveřejněná Ústavem zdravotnických informací a statistiky (ÚZIS) za období 2014–2018.

[2]https://www.uzis.cz/res/f/008352/novotvary2018
[3]Zdroj dat mortality: od roku 1994 Český statistický úřad

Výrazný je počet nově diagnostikovaných novotvarů u mužské populace nad 70 let, kdy křivka nabírá strmě rostoucí tendenci (Obr. 10). Důvodů může být několik. Historickou příčinou mohlo být častější vystavení těchto pacientů slunci při práci ve venkovním prostředí, ale i ve volnočasových aktivitách, a to v období, kdy nebyla propagována účinná fotoprotekce. Fotoprotekce se stala předmětem medicínsky relevantní osvěty teprve přibližně na přelomu 80. a 90. let minulého století (Ma and Yoo 2021). V současné době se jeví i nadále jako primární důvod nižší ochota mužské populace používat fotoprotektivně působící dermokosmetiku, tedy s ochranným faktorem proti slunci (anglicky: *Sun Protection Factor;* SPF) a nebo podstupovat pravidelné preventivní prohlídky u dermatologů (Smalley 2018; Raimondi et al. 2020).

Dalším důvodem odlišnosti postižení pacientů podle pohlaví může být z fyziologického hlediska i nižší hladina hormonu estrogenu, než se vyskytuje u žen. Autoři studie z roku 2018 (Natale et al. 2018) totiž poukázali na fakt, že receptor GPER (*G protein-coupled Estrogen Receptor*) na buňkách melanomu je aktivován právě estrogenem, který spouští signalizaci prostřednictvím protein kinázy A. Přes další komponenty signální dráhy jako je CREB (*CAMP Responsive Element Binding Protein 1*) a MITF dochází k aktivaci genů důležitých pro diferenciaci melanocytů, zvýšenou produkci melaninu, sníženou proliferační aktivitu nebo depleci c-Myc (*MYC Proto-Oncogene*). Deplece tohoto proteinu má na svědomí další významné děje v buňce: hypofosforylaci RB (*Retinoblastoma*) proteinu (pozastavení buněčného cyklu a transkripce), zvýšenou expresi HLA (*Human Leukocyte Antigen*) proteinů a snížený výskyt PD-L1 (*Programmed Cell Death-1 Ligand 1*). To všechno následně zlepšuje odpověď pacienta s maligním melanomem na léčbu (Natale et al. 2018). GPER a „klasické“ estrogenové receptory α a ß byly hodnoceny také u melanomu vyskytujícím se v těhotenství oproti melanomu u netěhotných žen a mužů. Bylo zjištěno, že při pozitivním nálezu GPER je v 95 % případů pozitivně detekován i estrogenový receptor ß. Tato dvojí pozitivní exprese je spojena s příznivější prognózou – nižší bývá hodnota Breslowa (viz kapitola 2.3.2) a mitotická aktivita, naopak vyšší bývá zánětlivá celulizace, tedy infiltrace peritumorálních lymfocytů (Fábián et al. 2017). Snížená exprese estrogenového receptoru ß je nalezena u progresivnějších melanomů invadujících hlouběji do dermis (Schmidt et al. 2006).

2.3.2 Klasifikace a diagnostika

Maligní melanom je možno v humánní patologii dále rozdělit dle umístění primárního ložiska na kožní maligní melanom (zastoupený dále několika klinickými variantami), slizniční melanom a uveální melanom (Rabbie et al. 2019). V rámci této disertační práce bude pozornost věnována malignímu melanomu kůže, okulární a slizniční forma vykazuje klinicky i biologicky totiž v mnoha aspektech velmi odlišnou problematiku.

V dermatologii používaná klinická klasifikace (Štork et al. 2013) kožního maligního melanomu utilitárně umožňuje popisovat 4 základní klinické varianty:

1) lentigo maligna melanom,
2) superficiálně se šířící melanom,
3) nodulární melanom,
4) akrolentiginózní melanom.

Klinicky poněkud vzácnější variantou melanomu je lentigo maligna melanom vznikající v ložisku lentigo maligna. Tato léze složená z dysplastických melanocytů je chápána jako jeho prekanceróza (Iznardo et al. 2020). Lentigo maligna je klinicky nepravidelné pigmentované makulózní ložisko různé velikosti, které se nachází hlavně na sluncem exponovaných částech kůže, jakými jsou obličej a krk (Ward et al. 2017). Typicky se vyskytuje zejména v séniu a pomalu progreduje v čase. Tato varianta tedy umožňuje nahlížet na melanom prizmatem klasické vícekrokové postupné karcinogeneze.

Dvě další, klinicky nejčastější, varianty, představují spíše než zcela svébytné jednotky dvě možné morfologické fáze růstu maligního melanomu. Tyto varianty mohou vznikat tzv. *de novo* na kůži bez předchozí léze typu prekancerózy, ale mohou vycházet i z transformace pigmentových névů, ať již kongenitálních, tak získaných. Právě toto téma malignizace melanocytárního névu je klinicky velmi ožehavým problémem, se kterým se pojí možnosti včasné detekce suspektních lézí pomocí epiluminiscenční dermatoskopie (Argenyi 1997). Přes nepopiratelný pokrok a zejména digitalizaci a automatizaci těchto diagnostických prostředků zůstává i nadále definitivní diagnostika melanomu na úrovni histologické.

Superficiálně se šířící melanom představuje iniciálně tenkou lézi. Ve fázi horizontálního (synonymum: radiálního) růstu dochází nejprve v epidermis (tedy *in situ*) k proliferaci atypických melanocytů tvořících atypická hnízda. Maligní melanocyty mohou migrovat do vyšších vrstev epidermis (tzv. pagetoidní šíření (Masterpol et al.

2013)) a do dermálních struktur vzdálených od místa primárního výskytu melanocytů při bazální membráně. Pro klinické posouzení a odlišení suspektních lézí vyžadujících další verifikaci se klinicky používá algoritmus označovaný akronymem ABCDE (složený z počátečních písmen jednotlivých kategorií – anglicky: *Asymmetry, Border, Color, Diameter, Evolving*) (Friedman et al. 1985; Abbasi et al. 2004).

U některých nádorů zaznamenáváme zejména fázi vertikálního růstu, melanocyty rychle invadují do dermis, kde se dále množí. Vznikající nádor tak časně klinicky nabývá charakter nodulární, tedy vyvýšené léze (Štork et al. 2013; Ward et al. 2017). U některých melanomů je dokumentována i velmi dlouhá předpokládaná doba pozvolné horizontální doby růstu (i roky), po které teprve dojde k nástupu vertikální růstové aktivity. Takové léze pak bývají označovány jako tzv. sekundárně nodulární (Krajsová 2018). Striktní odlišování těchto dvou variant tedy není biologicky opodstatněné, ale má nepopiratelnou klinickou hodnotu. Až vyklenování nad povrch okolní kůže upoutává pozornost a ve výsledku může tedy zkreslovat anamnestickou informaci o celkovém trvání procesu.

Poslední varianta, tzv. akrolentiginózní melanom, má vyšší incidenci na akrech, postihuje převážně plosky, dlaně a subunguální (podnehtové) partie. Tato kategorie je definována spíše distribučně, tedy anatomickou lokalizací. Klinicky a biologicky se ale také poněkud odlišuje od předchozích variant, nezřídka zcela pozbývá schopnost produkovat melanin a jeví se tedy jako tzv. amelanotický melanom (Štork et al. 2013; Basurto-Lozada et al. 2021).

Na histopatologické úrovni existuje velké množství variant maligního melanomu. K histologickému popisu rozsahu invaze melanomu byla využívána Clarkova klasifikace (Tab. 2), která morfologicky hodnotí prorůstání nádoru vrstvami kůže (Clark 1967; Clark et al. 1969). Tento přístup je možno dosti dobře aplikovat i na rutinně barveném tkáňovém řezu a historicky byl velmi cenným pokusem o určování prognózy na základě pokročilosti nádoru. Nicméně je tento utilitární přístup zatížen určitou mírou subjektivního hodnocení struktur patologem, dále je pak tuto diskrétně definovanou stratifikaci obtížné statisticky hodnotit, např. pro potřeby analýzy přežívání pacientů.

Z toho důvodu byl o něco později navržen metricky hodnocený parametr (index) metodicky popsaný Breslowem. Tato hodnota (tzv. Breslow; vyjádřena v milimetrech, s přesností na desetinu mm) znamená perpendikulárně určenou vzdálenost nejhlouběji uložené nádorové struktury od *stratum granulosum* (Breslow 1970). Tento údaj se klinicky velmi dobře osvědčil jako jednoduchý a současně i spolehlivý prognostický biomarker, jehož vyšší hodnota odráží riziko biologicky nepříznivého vývoje onemocnění

(Štork et al. 2013). Nicméně v praxi je doposud Clarkova klasifikace často uváděna společně s hodnotou podle Breslowa, čímž je možné pro klinika zvýšit komplementárně vypovídací hodnotu těchto parametrů a invazi dát do vztahu ke struktuře okolní kůže.

Klasifikace dle Clarka	**Stádium**
Intraepidermální výskyt	I
Výskyt ve *stratum papillare* dermis	II
Nádor zasahuje k papilárně-retikulárnímu přechodu	III
Výskyt ve *stratum reticulare* dermis	IV
Výskyt v podkožní tukové tkáni	V

Tab. 2 Klasifikace maligního melanomu dle Clarka. Tabulka popisuje histologickou klasifikaci melanomu dle hloubky invaze vrstvami kůže (převzato a upraveno dle Hasney et al. 2008).

Americký výbor proti rakovině (anglicky: *American Joint Committee on Cancer*; AJCC) v poslední publikované tzv. TNM klasifikaci pro popis melanomu doporučuje tzv. základní popisnou charakteristiku nádorů (Balch et al. 2009, 7. vydání; Gershenwald et al. 2017, 8. vydání; Keung and Gershenwald 2018, přehled důležitých změn v 8. vydání oproti 7. vydání). V tomto konceptu parametr T popisuje velikost nádoru a stav povrchové ulcerace, parametr N postižení uzlin a parametr M přítomnost vzdálených metastáz a hladinu laktátdehydrogenázy (anglicky: *Lactate Dehydrogenase*; LDH) v séru (Keung and Gershenwald 2018). Tato klasifikace rozděluje melanomy do 4 klinicko-patologických stádií, kdy lze stručně říct, že stádia I a II popisují různě pokročilé fáze lokalizovaného onemocnění, stádium III označuje postižení lymfatických uzlin a stádium IV znamená výskyt vzdálených metastáz. Stádium 0 označuje melanom *in situ* (Clark I) (Štork et al. 2013; Gershenwald et al. 2017).

Pro potřeby rutinní klinické onkologie jsou však zmíněné klinicko-patologické klasifikace často nedostačující (Yang et al. 2020). Vyžadovány jsou stále se zpřesňující indikátory, biomarkery, které mohou v klinické praxi identifikovat například více ohrožené pacienty, či pacienty reagující příznivě na některou léčebnou modalitu. Zavedení těchto biomarkerů do praxe by umožnilo zlepšit prognózu pacientů.

Jedním z příkladů takovýchto postupů aplikovaných v současnosti může být včasné určení genetického profilu melanomu a jeho molekulárně cílená léčba. Předpokladem takovéto stratifikace pacientů je znalost spektra mutací, které se u maligního melanomu vyskytují. Nejčastěji jsou mutace na velkých souborech pacientů identifikovány v genech

BRAF (*B-Raf Proto-Oncogene*), *NF-1* (*Neurofibromin 1*) a genové rodině *RAS* (*Rat Sarcoma gene*) – zde je nejčastější mutace v genu *NRAS* (*Neuroblastoma RAS viral oncogene homolog*). Čtvrtou skupinu představuje tzv. triple-wild type, u kterých jsou nalezeny *wildtype* (nemutované) formy genů *BRAF*, *NRAS* a *KIT* (Rebecca et al. 2020).

Za zmínku stojí i fakt, že geny s vysokou penetrancí a predispozicí pro vznik melanomu významně kontrolují buněčný cyklus. Jsou jimi *CDKN2A* (*Cyclin Dependent Kinase Inhibitor 2A*) a *ARF* na stejné chromozomálním oblasti 9p21, ale lišící se v prvním exonu, nebo *CDK4* (*Cyclin Dependent Kinase 4*) (Pho et al. 2006).

Je zajímavé, že přestože morfologicky patologie typizuje například nádory vycházející z oka a z kůže do jedné kategorie souhrnně uváděné jako „melanom“, je při mutační analýze zjevné, že molekulárně jsou tato onemocnění diametrálně odlišná. Uveální melanom totiž vykazuje somatické mutace nejčastěji v genech *GNAQ* (*G protein Subunit Alpha Q*) a *GNA11* (*G protein Subunit Alpha 11*) (Tang et al. 2016). Některé mechanismy ale slizniční melanomy a kožní melanomy přesto sdílejí. Klinicko-patologická studie naznačuje, že zvýšená exprese c-KIT se objevuje u pacientek s melanomem vulvy a mohlo by se jednat o prognostický faktor tohoto typu melanomu (Heinzelmann-Schwarz et al. 2014).

Další možné genové mutace, které stojí za rizikem vzniku maligního melanomu, shrnuje obrázek 11 (Bertrand et al. 2020).

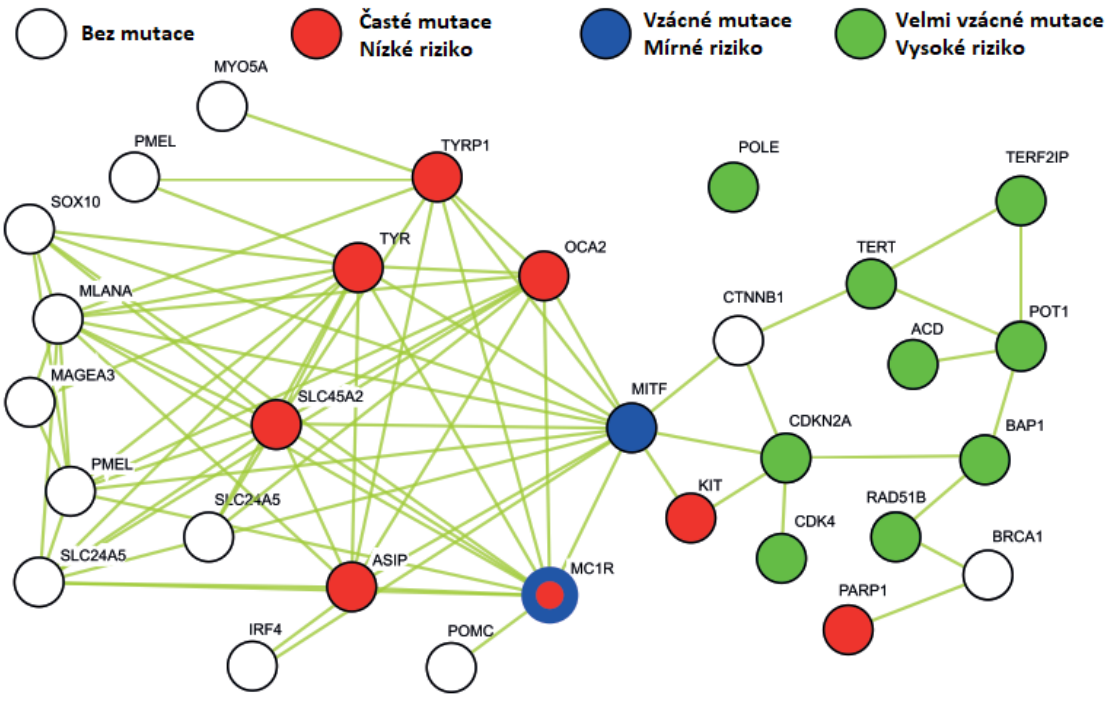

Obr. 11 Mapa interakcí mezi geny vyskytující se v biologii melanocytů, které jsou spjaté s rizikem vzniku maligního melanomu. Každý kruh reprezentuje jeden gen a každá čára pak přímou (fyzickou) nebo nepřímou (funkční) vazbu mezi proteiny, které jsou kódovány těmito geny. *Zeleně:* geny s velmi vzácnými mutačními variantami spojenými s vysokým rizikem vzniku maligního melanomu; *modře:* geny se vzácnými variantami spjaté s mírným rizikem vzniku maligního melanomu; *červeně:* geny s častými variantami asociované s nízkým rizikem vzniku maligního melanomu; *bíle:* geny zapojené v biologii melanocytů, které nevykazují známou mutační variantu asociovanou s maligním melanomem. Za zmínku stojí, že levý klastr shromažďuje hlavně geny melanogeneze, a pravý klastr pak geny buněčného cyklu, kontrolního mechanismu délky telomer a geny pro opravy DNA (převzato a upraveno dle Bertrand et al. 2020).

2.3.3 Deregulace hlavních signálních drah vedoucí k vývoji maligního melanomu

Maligní melanom vzniká většinou na podkladě mnoha získaných somatických genetických změn. Hereditární faktory mohou v tomto procesu sehrávat roli, ale klinický význam tohoto aspektu je v současnosti omezený. Zpravidla jsou poškozeny geny základních buněčných procesů, jako je proliferace, růst a metabolismus, apoptóza, kontrola buněčného cyklu nebo replikace. Tyto genové mutace vedou u melanomu k aberantní aktivaci dvou hlavních signálních drah: mitogenem aktivované proteinkinázy/extracelulárním signálem regulované proteinkinázy (anglicky: *Mitogen-Activated Protein Kinase/Extracelullar signal-Regulated Kinase*; MAPK/ERK) a fosfoinositol-3-kinázy (anglicky: *Phosphoinositol-3-Kinase*; PI3K) (Leonardi et al. 2018).

MAPK/ERK signální dráha (Obr. 12) je aktivována růstovými a stresovými faktory, hormony nebo cytokiny, které se váží s membránovým tyrosinkinázovým receptorem (anglicky: *Tyrosine Kinase Receptor*; RTK). Po vazbě dojde k přenesení signálu na adaptorový protein GRB2 (*Growth factor Receptor-Bound protein 2*) interagující s faktory GEF (*Guanosine Exchange Factor*), převážně s faktorem SOS (*Son Of Sevenless*). Tím je zajištěna aktivace malé GTPázy RAS navázané na cytoplazmatické membráně (Buday and Downward 1993; Aronheim et al. 1994). Ta následně aktivuje protein z proteinové rodiny RAF (např. BRAF). RAF fosforyluje mitogenem aktivovanou proteinkinázu kinázu (anglicky: *Mitogen-Activated Protein Kinase Kinase*; MEK) na serinových zbytcích. Fosforylovaný MEK aktivuje serin/threoninovou kinázu ERK fosforylací motivu threonin-kyselina glutamová-tyrosin. Fosforylovaná ERK působí v cytoplazmě nebo proniká do jádra a reguluje genovou expresi více jak 50 genů převážně zodpovědných za buněčný růst, dělení a diferenciaci. Tento mechanistický diagram má některé klinicky relevantní implikace. Příkladem změny v MAPK signální dráze je *BRAF*

mutace, kdy je nejčastěji valin (V) substituován za kyselinu glutamovou (E) na kodonu 600 – *BRAF*^{V600E}. Méně časté jsou substituce za lysin (*BRAF*^{V600K}) nebo arginin (*BRAF*^{V600R}). Takto mutovaný *BRAF* významně zvyšuje aktivitu BRAF kinázy a nekontrolovaně spouští další kroky této dráhy, což vede k nadměrné proliferaci neoplastických buněk a k progresi nádoru (Eroglu and Ribas 2016; Aasen et al. 2019; Czarnecka et al. 2020). Vysoká aktivita BRAF se zdála být tedy vhodným terapeutickým cílem u vhodně mutovaného maligního melanomu. Zlomem v léčbě melanomu bylo zavedení BRAF, posléze i MEK inhibitorů a jejich kombinace (viz kapitola 2.3.4.3). Tato léčiva o malé molekule vykazovala klinicky signifikantní efekt, nicméně až 20 % melanomů získá k této léčbě rezistenci, a to buď reaktivací MAPK dráhy nebo aktivací jiných signálních drah zahrnující např. PTEN (*Phosphatase and Tensin homolog*), NF-1 nebo RAS (Czarnecka et al. 2020).

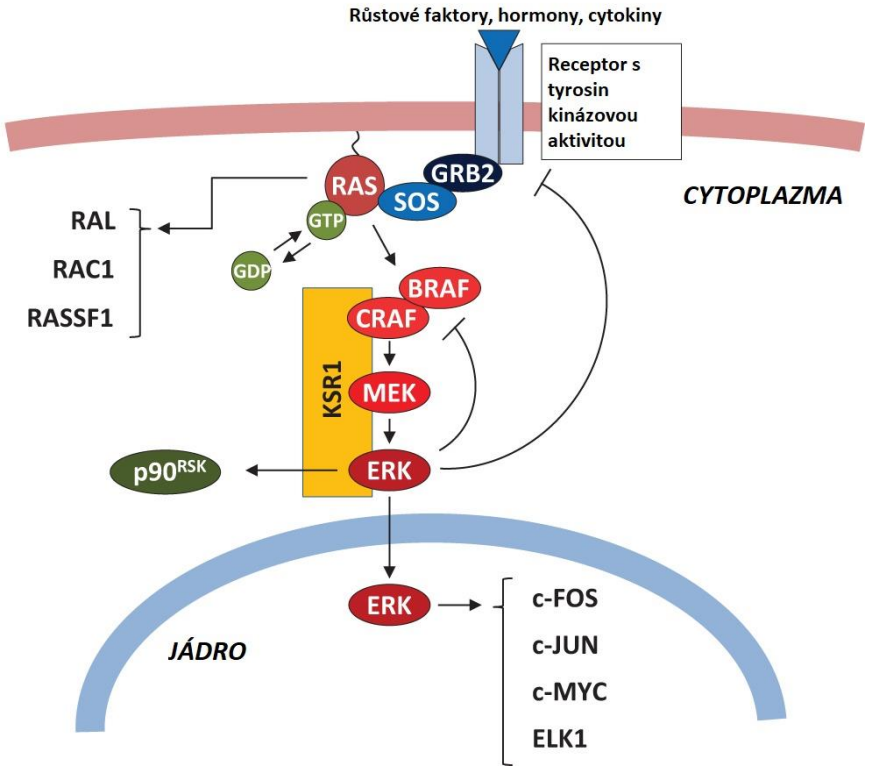

Obr. 12 Přehled MAPK/ERK signální dráhy. Po navázání ligandu na RTK je signál přenesen přes proteiny GRB2 a SOS na protein RAS. Po navázání GTP (*Guanosintrifosfát*) na RAS dochází k aktivaci dalších kináz v kaskádě (RAF – MEK – ERK). Fosforylovaná ERK působí v cytoplazmě, nebo je translokována do jádra. Následně je schopna stimulovat transkripční faktory, a ovlivnit tak transkripci genů pro různé buněčné procesy. c-Fos – *Fos Proto-Oncogene*, c-Jun – *Jun Proto-Oncogene*, c-Myc – *Myc Proto-Oncogene*, ELK1 – *ETS-Like Gene 1*, GDP – *Guanosindifosfát*, KSR1 – *Kinase Suppressor Of Ras 1*, RAC1 – *Ras-related C3 botulinum toxin substrate 1*, RAL – *Ras-like protein*, RASSF1 - *Ras association domain family 1* (převzato a upraveno dle Zaballos and Santisteban 2017).

PI3K/AKT signální dráha začíná opět vazbou ligandu na RTK, která aktivuje PI3K. Ta fosforylací fosfatidylinositol-4,5-bisfosfátu na fosfatidylinostiol-3,4,5-trisfosfát aktivuje proteinkinázu B (anglicky: *Protein Kinase B*; AKT). *PTEN* je tumor-supresorový gen a jeho proteinový produkt se chová jako fosfatáza, která defosforyluje fosfatidylinostiol-3,4,5-trisfosfát, což vede k inhibici PI3K/AKT signální dráhy, a tím k blokaci buněčné proliferace. Ztráta funkčního PTEN je pozorována ve více jak 10 % všech případů melanomu a vede k aktivaci PI3K/AKT signální dráhy (Paraiso et al. 2011). V důsledku toho je nekontrolovatelně stimulováno přežití buněk, což je zároveň podporováno inhibicí apoptózy (Davies 2012; Aasen et al. 2019; Czarnecka et al. 2020). Studie z roku 2019 (Yoo et al. 2019) popisuje, že u maligního melanomu může důležitou roli pro dráhu PI3K/AKT hrát i malá GTPáza ARF6 (*Adenosine diphosphate-Ribosylation Factor 6*). ARF6 je potřebná pro aktivaci PI3K a AKT a podporuje vznik metastáz a zvýšenou progresi nádoru (Yoo et al. 2019).

2.3.4 Současné léčebné modality

Základní modalitou v léčbě časného stadia melanomu zůstává chirurgie, tedy radikální operace včasně detekovaného primárního ložiska se zachováním dostatečného lemu zdravé kůže. U melanomů s tloušťkou nad 1 mm Breslowovy škály je pacient podroben i resekci sentinelové uzliny (Bajčiová 2016), byť tento výkon je spíše diagnostický a neovlivňuje ve výsledku přežívání pacienta. I v pokročilejších stádiích melanomu má chirurgická excize nálezu svůj význam, nicméně v případě metastazujícího melanomu vynětí primárního ložiska, popřípadě resekce spádové lymfatické oblasti (exenterace), nestačí, a je nutno u pacienta zvážit systémovou léčbu. Vzhledem ke značné radio- a chemorezistenci melanomu byly tyto konvenční metody spojeny s relativně nízkým kurativním efektem, dodnes ale například dakarbazin či kombinovaná chemoterapie s využitím platinových derivátů mají své místo v onkologických schématech. Do popředí se tak v léčbě maligního melanomu dostávaly od 80. let imunoterapeutika, zejména látky jako IFNα2b (*Interferon-α-2b*) a IL-2 (*Interleukin-2*) (Gupta et al. 2017). V poslední dekádě pak nabyla imunoterapie zacilující kontrolní body imunity (checkpoints) značného významu, a stala se tak vedle cílené terapie také metodou volby v klinické praxi. Možnosti současné schválené léčby maligního melanomu shrnuje tabulka 3 (Khair et al. 2019).

Existuje nepřeberné množství experimentálních farmakologických přístupů léčby maligního melanomu, které jsou v různých fázích preklinického a klinického testování. S ohledem na téma předkládané disertační práce a aktuálnosti tohoto tématu je možno zmínit, že terapeutický potenciál vykazují i umělá analoga estrogenů – bazedoxifen a raloxifen. Tyto selektivní modulátory estrogenových receptorů jsou schváleny a klinicky využívány u žen po menopauze k léčbě osteoporózy (Pickar and Komm 2015). Dále se uvádí, že vedlejší mechanismus jejich působení zahrnuje i blokádu interakce IL-6 a jeho receptoru gp130 (*Membrane Glycoprotein 130*). Tento mechanismus by mohl mít v medicíně využití ať již v onkologii, tak i v jiných odvětvích medicíny jako je revmatologie či při léčbě infekcí. Navozená blokáda by mohla nejen omezit šíření nádoru, ale omezit i rozvoj kachexie u onkologického pacienta. Mohly by tak zmírnit komplikace u nádorových (Yadav et al. 2017) nebo virem postižených pacientů, např. s onemocněním COVID-19, u kterých se rozvíjí cytokinová bouře (Smetana et al. 2020; Smetana and Brábek 2020).

Lék	Cíl	Mechanismus	Indikace	Rok schválení
Monoterapie monoklonálními protilátkami				
Ipilimumab	CTLA-4	Blokace lidskou IgG1 monoklonální protilátkou	Neresekabilní pokročilý metastazující melanom	2011
Nivolumab	PD-1	Blokace lidskou IgG4 monoklonální protilátkou	Pokročilý metastazující melanom; refraktorní na ipilimumab	2014* *2017 schválen jako adjuvantní léčba melanomu s postižením lymfatických uzlin nebo u pacientů s metastatickým onemocněním, kteří podstoupili kompletní resekci
Pembrolizumab	PD-1	Blokace humanizovanou IgG4 monoklonální protilátkou	Neresekabilní melanom – stádium III/IV	2014
Kombinovaná terapie monoklonálními protilátkami				
Ipilimumab + nivolumab	CTLA-4 + PD-1	Blokace monoklonálními protilátkami	Neresekabilní melanom – stádium III/IV; PD-L1 negativní	2015
Cílená léčba – monoterapie inhibitory tyrosinkináz				
Vemurafenib	BRAF	BRAF inhibitor způsobující apoptózu v důsledku přerušení MAPK signální dráhy	Neresekabilní melanom s mutací $BRAF^{V600}$	2011
Dabrafenib	BRAF	BRAF inhibitor způsobující apoptózu v důsledku přerušení MAPK signální dráhy	Neresekabilní melanom s mutací $BRAF^{V600}$ (není indikován pro *wild-type* BRAF melanom (Abraham and Stenger 2014))	2013

Trametinib	MEK	MEK1 a MEK2 inhibitor způsobující buněčnou smrt v důsledku přerušení MAPK signální dráhy	Neresekabilní melanom s mutací $BRAF^{V600E/K}$ (nesmí být použit po BRAF inhibitoru)	2013
Cílená léčba – kombinovaná terapie inhibitory tyrosinkináz				
Dabrafenib + trametinib	BRAF + MEK	BRAF+MEK inhibice	Neresekabilní melanom s mutací $BRAF^{V600E/K}$	2013
Vemurafenib + cobimetinib	BRAF + MEK	BRAF+MEK inhibice	Melanom s mutací $BRAF^{V600}$	2015** **2018 schválen jako adjuvantní léčba u pacientů s melanomem s postižením lymfatických uzlin, kteří podstoupili kompletní resekci
Další možnosti cílené léčby a imunoterapie				
Interferon	IFNα2b	Imunostimulační účinky jako zvýšení nádorové infiltrace lymfocyty, snížení cirkulujících T-reg a modulace rovnováhy STAT1/STAT3	Adjuvantní terapie pro stádium III (bez melanomu, ale s vysokým rizikem rekurence); adjuvantní léčba pro stádium IIB nebo IIC s primární lézí melanomu; tloušťka > 4mm	1995
Aldesleukin	IL-2	Proliferace T lymfocytů a stimulace cytotoxicity CD8 + NK	Metastatický melanom	1998
T-VEC	Onkolytický herpes simplex virus	Lokální a přímá infekce a smrt nádorových buněk	Neresekabilní melanom stádia IIIB, IIIC nebo IV	2015

Tab. 3 Možnosti léčby maligního melanomu. Tabulka shrnuje možnosti schválené cílené léčby, imunoterapie a další kombinované terapie v léčbě maligního melanomu (převzato a upraveno dle Khair et al. 2019).

2.3.4.1 Chemoterapie a radioterapie

Od 70. let 20. století byla primární léčbou metastatického melanomu chemoterapie v čele s alkylačním cytostatikem dakarbazinem, která vykazovala léčebnou odpověď pacientů mezi 15–25 % (Gogas et al. 2007). Pro zlepšení pacientovy odpovědi na léčbu melanomu byly prováděny studie s kombinovanými chemoterapeutickými režimy, tj. s kombinací různých chemoterapeutik v pravidelně opakované sekvenci, příkladem je trojkombinace cytostatik cisplatiny, vinblastinu a dakarbazinu (tzv. CVD režim), která vykazovala léčebnou odpověď kolem 40 % (Legha et al. 1989).

Radioterapie je u melanomu využívána především v adjuvantní léčbě, např. po vyjmutí primárního ložiska nebo sentinelových uzlin. Zároveň je hojně využívána v paliativní léčbě pro redukci symptomů nemoci a pro zlepšení kvality života (Strojan 2010). Jako forma lokální léčby může být použita v případě nedostatečné resekce u lentigo maligna nebo u metastatického melanomu, kde je problematické chirurgické odstranění metastáz, především v mozku (Bajčiová 2016).

2.3.4.2 Imunoterapie cílená na kontrolní body imunity (checkpoints)

Přítomnost buněk imunitního systému v maligním melanomu byla na histologické úrovni známa již dlouho. Přestože tato infiltrace je u maligního melanomu poměrně nápadná, nebylo klinicky zřejmé, že by imunitní systém udržoval zhoubný nádor pod kontrolou. Velký význam byl v tradiční představě připisován T cytotoxickým lymfocytům a očekávalo se, že nádorová progrese je důsledkem jejich nedostatečné funkce.

Aktivace T lymfocytů je složitý několika krokový proces vyžadující specifické navázání T-buněčného receptoru (anglicky: *T-cell Receptor*; TCR) na hlavní histokompatibilní komplex (anglicky: *Major Histocompatibility Complex*; MHC) na cytoplazmatické membráně víceméně všech buněk lidského organismu (MHC typ I). MHC (typ II) má význačnou roli v prezentování antigenních peptidů vzniklých uvnitř patogenem napadené nebo neoplastické buňky nebo na antigen prezentujících buňkách (anglicky: *Antigen Presenting Cells*; APC). Kromě toho musí být k úplné aktivaci přítomen kostimulační signál, čímž je zpravidla vazba CD28 molekuly na povrchu T lymfocytů s molekulami CD80 a CD86 (oba patří do imunoglobulinové rodiny B7) na povrchu APC (Obr. 13) (Buchbinder and Desai 2016).

Ochranu organismu před nadměrnou aktivací T lymfocytů a celého imunitního systému zajišťují kontrolní body imunity, tzv. checkpointy, které tak brání vzniku autoimunitních nemocí. Druhou stranou mince tohoto mechanismu je ale umožnění navození nádorové tolerance, což ve výsledku nádorovým buňkám usnadňuje únik před T lymfocyty. Blokáda imunitních kontrolních bodů umožňuje obnovit proliferaci T lymfocytů a prodloužit jejich aktivaci, čímž je zesílena T lymfocytární imunitní reakce a imunitní dozor (Krajsová 2015). Mezi takové nejznámější imunitní kontrolní body patří CTLA-4 (*Cytotoxic T-lymphocyte Antigen 4*) a receptor PD-1 (*Programmed Cell Death 1*) s ligandem PD-L1 (Obr. 13) (Ott et al. 2013). Jelikož kontrolní body imunity fungují

na principu interakce receptor-ligand, mohou být snadno blokovány protilátkami nebo modulovány rekombinantními formami těchto receptorů/ligandů (Pardoll 2012).

Dokladem klinické aplikovatelnosti tohoto terapeutického konceptu je terapeutická blokáda CTLA-4. CTLA-4 je inhibiční molekulou, která se váže s vyšší afinitou k molekulám CD80 a CD86 na APC než kostimulační CD28, takže nedochází k tvorbě aktivačního signálu, naopak dochází k potlačení T lymfocytární aktivity (Sobhani et al. 2021). Přesný mechanismus této inhibice nebyl ještě popsán, ale navrhovanými možnostmi jsou např. přímá inhibice TCR (Schneider et al. 2006) nebo odstranění ligandů CD80 a CD86 z APC trans-endocytózou (Qureshi et al. 2011). CTLA-4 reguluje proliferaci T lymfocytů v rané fázi imunitní odpovědi, primárně v lymfatických uzlinách nebo slezině (Buchbinder and Desai 2016).

Monoklonální protilátka proti CTLA-4 na T lymfocytech byla prvním schváleným lékem v oblasti imunoterapie maligního melanomu (Pardoll 2012; Buchbinder and Desai 2016; Carlino and Long 2016). Klinická studie hodnotící účinnost tohoto inhibitoru CTLA-4 s dakarbazinem vůči dakarbazinu s placebem odhalila, že monoklonální protilátka proti CTLA-4 zlepšila medián celkového přežití pacientů na 11,2 měsíce oproti 9,1 měsícům u kontroly (Robert et al. 2011).

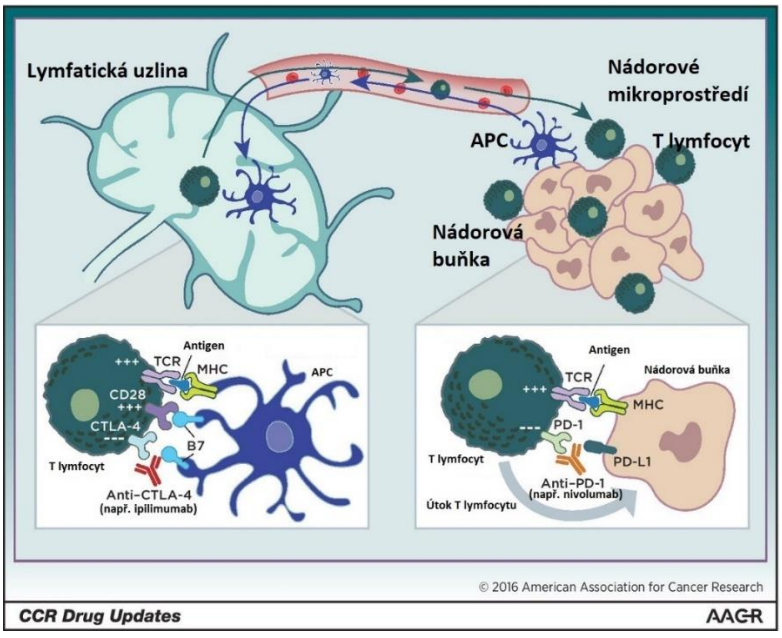

Obr. 13 Aktivace T lymfocytu s využitím monoklonálních protilátek proti CTLA-4 a PD-1. Komplexní proces aktivace T lymfocytu zahrnuje vazbu TCR a MHC s navázaným antigenem a kostimulační vazba CD28 s molekulami z rodiny B7 (např. CD80 a CD86). Mimo to se na povrchu T lymfocytů vyskytují imunitní kontrolní body (CTLA-4, PD-1), které chrání organismus před nadměrnou aktivací imunitního systému. V případě anergie imunitního systému u onkologických pacientů byly vyvinuty inhibitory imunitních kontrolních bodů (např. ipilimumab, nivolumab) uplatňující se v protinádorové léčbě (Carlino and Long 2016).

PD-1 je dalším z imunitních checkpointů patřících do stejné imunoglobulinové rodiny jako CD28 a CTLA-4. Oproti CTLA-4 potlačuje T lymfocytární imunitní odpověď během efektorové fáze v periferních tkáních včetně nádorového mikroprostředí (Ott et al. 2013; Buchbinder and Desai 2016). Receptor PD-1 využívá, pro svou správnou funkci, dvou přirozeně se vyskytujících ligandů – PD-L1 a PD-L2 (*Programmed Cell Death 1 Ligand 2*). Dráha PD-1/PD-L1 podporuje apoptózu T lymfocytů (Zatloukalová et al. 2016). Vzhledem k účinnosti jsou v současné době anti PD-1 monoklonální protilátky preferovány jako standardní postup v první linii léčby. Klinická studie, v které byla hodnocena účinnost kombinace inhibitoru PD-1/PD-L1 s inhibitorem CTLA-4, prokázala zlepšení přežití bez progrese na 11,5 měsíce oproti monoterapiím (inhibitorem CTLA-4 – 2,9 měsíce; inhibitorem PD-1/PD-L1 – 6,9 měsíce) (Larkin et al. 2015).

2.3.4.3 Cílená léčba

Odhalení mutací stojících za vznikem maligního melanomu v MAPK signální dráze vedla k vývoji BRAF inhibitorů, jako jsou vemurafenib a dabrafenib, jejichž cílem je hyperaktivovaná BRAF kináza, nebo MEK inhibitorů působících níže (*downstream*) v signální dráze, jako jsou trametinib a cobimetinib (Faghfuri et al. 2018). Nepříznivým aspektem jednotlivých inhibičních preparátů při léčbě melanomu je získaná rezistence s následnou progresí léčiv (Eroglu and Ribas 2016). Z toho důvodu byly klinicky zkoumány reakce pacientů na kombinaci BRAF a MEK inhibitorů (Ribas et al. 2014; Larkin et al. 2014; Ribas et al. 2020). Tyto studie ukázaly příznivý terapeutický přínos, a to i u pacientů, kteří v předchozí léčbě podstoupili monoterapii BRAF inhibitorem, jakožto jedinou dostupnou možnost léčby v dřívějších letech.

2.4 Nádorové mikroprostředí a jeho modelování

Nádorové mikroprostředí je důležitým faktorem ovlivňujícím chování nádoru a jeho biologické vlastnosti. Dominantní populaci nádorového mikroprostředí představují nádorově asociované fibroblasty (CAF). CAF produkují složky ECM a sekrecí cytokinů, chemokinů a jiných proteinů bioaktivní povahy stimulují progresi a šíření nádoru. Komplexní ekosystém nádoru doplňují ještě nejrůznější imunitní buňky, endotelové buňky, pericyty a z nich tvořené krevní a lymfatické cévy (Lacina et al. 2015; Lacina et al. 2018).

Chování buněk bývá běžně studováno v laboratorních dvojrozměrných kultivačních podmínkách, kdy buňky adherují na kultivační plastik. Jedná se o kultivaci v takzvaném monolayeru a je možné takto dosáhnout kultury jak primárních populací, tak spontánně vzniklých či cíleně imortalizovaných buněčných linií. Tyto podmínky však nepřinášejí věrný obraz fyziologie nádoru. Snahou je tak vytvářet trojrozměrné buněčné modely nebo organotypické kultury kůže simulující kromě nádoru i nádorové mikroprostředí a vzájemné buněčné interakce.

2.4.1 Jednoduché modely mikroprostředí ve 2D

Adherentní primární buněčné kultury nebo ustanovené buněčné linie kultivované ve dvojrozměrných kultivačních podmínkách konvenčním přístupem nejsou dostatečně věrným obrazem složitého nádorového ekosystému. Buňky monokultury v takto redukovaném prostředí ztrácejí možnosti interakce s jinými buněčnými typy, ale i interakce s nebuněčným prostředím, což jsou kritické aspekty pro regulaci jejich fyziologické funkce v každé tkáni (Xie et al. 2021). Snahou je tedy tyto planární buněčné modely modifikovat do té míry, aby lépe přiblížily prostředí a chování nádoru. Jednou z takových fyzikálně-chemických modifikací může být například modifikace kultivačního povrchu (například jeho tuhost, *stiffness*; povrchový reliéf, míra hydrofobicity, přítomnost adherovaných peptidů či proteinů), ale i nastavení fyzikálních parametrů kultivačního prostředí např. teploty, laminárního proudění média nebo hypoxie.

Zejména hypoxie pak pro studium nádorů představuje velmi významné téma. Jedná se o adaptaci solidních nádorů na nízký přísun kyslíku. V důsledku trvající intratumorální hypoxie je podpořena jejich agresivita a metastatický potenciál, dochází k novotvorbě cév, nádory vykazují nižší senzitivitu k radio- a chemoterapii a metabolicky se přepínají na využívání glukózy (Li et al. 2021). Při hypoxii v nádorové tkáni je snížena aktivita specifických prolyl hydroxyláz a naopak jsou aktivovány transkripční faktory indukované hypoxií (anglicky: *Hypoxia-Inducible Factor*; HIF) (Balamurugan 2016). Při vyřazení funkce genů (jejich umlčením, též silencingem, prostřednictvím různých genetických metod či chemických inhibitorů) pro HIF-1α a jednu z miRNA (*MicroRNA*; miR) – miR-210 – byla na základě měření mitochondriální aktivity, produkce ROS a metabolických změn pozorována apoptóza u melanomové linie A375 (Špaková et al. 2021). Spojitost HIF-1α a miR-210 byla ale pozorována, např. i u nádorů hlavy a krku (Huang et al. 2009).

Další možnou modifikací 2D kultivace, která zvyšuje komplexnost tohoto tradičního přístupu, může být vytvoření směsné kultury (tj. kokultivace). V tomto případě jeden typ buněk působí na typ druhý a dochází k velmi rozsáhlé interakci nejen fyzické (přímé), ale i prostřednictvím uvolňovaných biologicky aktivních molekul (tj. nepřímé, parakrinní). Tento prvek je v podstatě vždy přítomen u primárních buněčných kultur *in vitro*, kdy směs buněk putuje z kousků tkání zdravých či nádorových a ovlivňují se navzájem. V pozdějších vyšších pasážích ale často převládne jeden dominantní buněčný typ, což sníží výpovědní hodnotu experimentu.

Historicky velmi cenným pionýrským příkladem takové kokultivační techniky může být užití radiací nebo mitomycinem proliferačně inaktivovaných fibroblastů jako podpůrné vrstvy (tzv. feederu) pro pěstování humánních keratinocytů *in vitro* (Rheinwald and Green 1975). Metoda díky interakci dvou buněčných typů umožnila i přípravu materiálu pro klinické aplikace v popáleninové medicíně.

V podobně koncipovaném experimentálním modelu bylo využito nádorově asociovaných fibroblastů pro studium jejich vlivu na primární humánní keratinocyty. Bylo zjištěno, že kokultivace stromálních fibroblastů z bazocelulárního karcinomu a zdravých keratinocytů pozměňuje vlastnosti zdravých keratinocytů a posouvá je směrem k fenotypu, který se objevuje u keratinocytů bazaliomu, např. exprese některých jednoduchých keratinů (např. keratin 19) (Lacina et al. 2007).

Pro potřeby analýzy vlivu kokultivace je možno sledované populace od sebe fyzicky oddělit pomocí tzv. insertové techniky. Buňky tedy ztrácejí možnost přímého fyzického kontaktu, ale prostřednictvím propustných membrán insertů dochází při definované porozitě materiálu i nadále ke kontinuálnímu prostupování uvolňovaných malých molekul aktivních látek přes póry této membrány. Použití insertu tedy akcentuje mechanismy, které se účastní regulace ve tkáni v parakrinním módu. Využití této metody pro jednoduché modelování mikroprostředí bylo použito i v publikaci (I), která je součástí této disertační práce (Jobe et al. 2018). Při použití insertů s většími póry (obvykle 8 μm) lze tuto metodu přetvořit v tzv. *transwell migration assay* pro studium buněčné migrace či invazivity (Justus et al. 2014), což činí metodiku atraktivní například pro studium buněk melanomu nebo jimi ovlivněných buněčných typů (Zhou et al. 2018; Dong et al. 2021).

Systém, který může být vnímán jako pomezí 2D kultur i 3D modelů, je mikrofluidika (Coluccio et al. 2019). Jedná se o techniky, ve kterých jsou vytvářeny pro studium buněk struktury s komplexy kanálků a komůrek osídlených buňkami, méně často tkáněmi či

jejich explantáty. V kanálcích kontinuálně a orientovaně proudí kultivační médium (často je tok regulován na základě jednoduchých fyzikálních principů kapilárních sil). Tato zařízení umožňují přesnou kontrolu různých parametrů fyzikálních a chemických, např. koncentračních gradientů látek nebo tlaku (Mehling and Tay 2014). Mikrofluidní systémy umožňují i sledování interakcí v nádorovém mikroprostředí. Příkladem může být komunikace mezi imunitními splenocyty a buňkami melanomu oddělenými v komůrkách mikrofluidního zařízení, ale propojenými kanálky (Mattei et al. 2014). V tomto případě je výhodou kontinuální pomalý tok média a lze tedy na základě designu systému rozhodnout, která populace bude zdrojem a která cílem pro působení aktivních molekul.

2.4.2 Jednoduché modely mikroprostředí ve 3D

Nejjednodušším trojrozměrným modelem je přerůstání buněk z monolayeru do mnohovrstevné kultury, tzv. multilayeru (Benien and Swami 2014). V tomto případě nedochází zejména u nádorových imortalizovaných linií k zastavení mitotické aktivity kontaktní inhibicí. Fenomén proliferační zástavy v postkonfluentní fázi kultury buněk vzájemným kontaktem se uplatňuje ale spíše u buněk normálních, např. u fibroblastů. Vzniklá mnohovrstevná struktura pak může vykazovat velmi odlišné vlastnosti než klasické 2D kultury. V některých případech mohou vznikat u kultur ponechaných bez pasáže i sférické útvary uvolňované do média.

Dalším klasickým přístupem, který posouvá jednoduchý model k vyšší úrovni komplexnosti, je simulace extracelulární matrix pomocí hydrogelů ze zesítěných složek ECM. Kultivace buněk tak probíhá v přirozených, jednodruhových či komplexně definovaných hydrogelech (např. želatina, kolagen typu I, fibrin, laminin, kyselina hyaluronová, alginát, Matrigel®, atd.) (Vasile et al. 2020), nebo syntetických hydrogelech (např. polyethylenglykol a polyvinylalkohol) (Chen et al. 2018b; Bettahar et al. 2021; Zulkiflee and Fauzi 2021). Velmi populárním se stal při modelování 3D struktur Matrigel®, který je solubilizovanou matricí bazální membrány secernovanou buňkami myšího Engelbreth-Holm-Swarmova sarkomu. Tento produkt obsahuje převážně laminin, kolagen IV, heparan sulfátové proteoglykany a entaktin, tedy proteiny běžně se objevující v bazální membráně (Kleinman et al. 1982). Tyto modely umožňují například studium invaze nádorových buněk.

Hojně využívaným trojrozměrným modelem jsou sféroidy (Obr. 14). Jedná se o agregáty z buněk jednoho i více typů, vhodné pro simulaci převážně avaskulárních solidních nádorů a jejich mikroprostředí (Riffle and Hegde 2017).

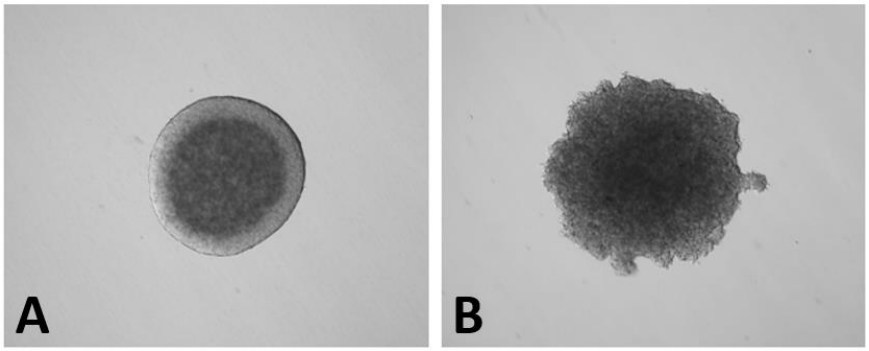

Obr. 14 Sféroidy. Sféroidy vytvořené po 48 hod. metodou visící kapky z 50 000 buněk **(A)** linie dlaždicobuněčného karcinomu hypofaryngu FaDu (ATCC HTB-43™) a **(B)** linie maligního melanomu G-361 (ATCC CRL-1424™).

Technicky mohou být vytvořeny např. kultivací v peletě za využití centrifugace (Achilli et al. 2012), na neadhezivních kultivačních nádobách (Redondo-Castro et al. 2018), metodou visící kapky (Obr. 15) (Raghavan et al. 2015; Schmid et al. 2016; Gupta et al. 2021), pomocí rotačních kultur a bioreaktorů (Phelan et al. 2019), na základě mikrofluidního systému (Aijian and Garrell 2015; Aref et al. 2018) nebo magnetickou levitací (Ryu et al. 2019; Urbanczyk et al. 2020; Gaitán-Salvatella et al. 2021; Kotze et al. 2021).

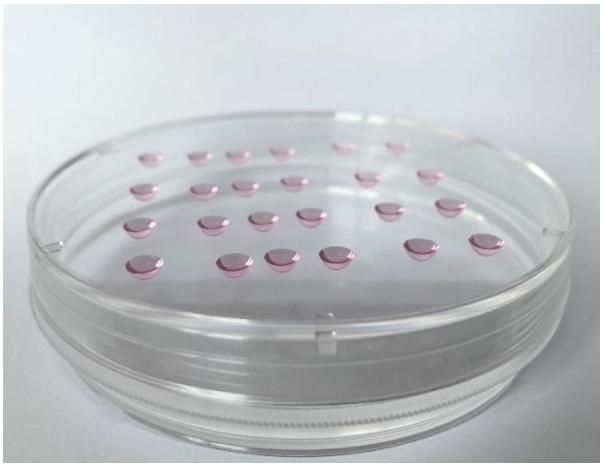

Obr. 15 Metoda visící kapky. Fotografie znázorňuje metodu visící kapky (z anglického *hanging drop method*). Tato metoda umožňuje vytvoření 3D modelu sféroidu (Obr. 14), čímž lze simulovat interakce různých buněčných typů v nádorovém mikroprostředí. Tato metoda byla využita v publikaci VIII, kde byly dva typy různě aktinicky poškozených fibroblastů jednotlivě smíchány s buňkami melanomové linie G-361 v poměru 1:1. Na spodní neadhezivní povrch víčka Petriho misky pak byly pomocí pipety umisťovány kapky o objemu 25 µl a počtu 50 000 buněk na kapku z dané buněčné suspenze. Dno misky bylo naplněno 15 ml pufrovaným fyziologickým roztokem (anglicky: *Phosphate-Buffered Saline*; PBS) pro zachování humidity. Miska byla přikryta víčkem s visícími kapkami (viz fotografie) a inkubována (37 °C, 5% CO_2) po dobu 60 hod. Zformované sféroidy byly následně přeneseny do kultivačního média v neadhezivní bakteriologické Petriho misce na dalších 48 hod. Podobně byla metoda visící kapky použita i v publikaci IX.

V současnosti se jako časově výhodná metoda pro tvorbu uniformních sféroidů jeví tzv. *bioprinting* (biotisk), kdy jsou jednotlivé buňky obalené v bioinkoustu extrudovány na kultivační plochu pomocí biotiskárny (Zhuang et al. 2021; Anada et al. 2019; De Moor et al. 2020; Swaminathan and Clyne 2020; Zhao et al. 2019; Williams et al. 2013). Schmidt *et al.*, (2019) použili buněčné linie maligního melanomu pro biotisk ve třech různých materiálech: Matrigelu® a dvou komerčně dostupných bioinkoustech s obsahem alginátu nebo metakrylované želatiny. Autoři zjistili, že buňky melanomu, v bioinkoustu vytvořeném na podkladě alginátu neproliferují, zatímco v metakrylátovém želatinovém bioinkoustu vytváří malé shluky buněk po 7 dnech kultivace. Kultivaci v Matrigelu®, který nejvěrněji napodobuje přirozené podmínky, tolerovaly melanomové linie dobře, proliferovaly rychle a buňky byly schopné migrovat a prostupovat materiálem (Schmidt et al. 2019).

Nicméně možnosti bioprintingu pro onkologický výzkum se nadále rozšiřují. Jelikož utvoření 3D buněčné formace v bioinkoustu trvá nějaký čas, Swaminathan *et al.*, (2019) se pokusili tisknout v bioinkoustu už přímo předem vytvořené sféroidy z lidské epitelové buněčné linie (karcinomu prsu). Sféroidy si zachovaly svůj tvar, funkci i životaschopnost. Na modelu byla následně testována účinnost chemoterapeutika paclitaxelu. Je velmi významné, že buňky ve sféroidu byly vůči působení paclitaxelu odolnější v porovnání s jednotlivými buňkami ve 2D kultuře. Další kvalitativní skok nastal tehdy, když byly sféroidy komponovány jako smíšeně buněčné, a kromě lidských epitelových maligních buněk obsahovaly i buňky endotelu. Jelikož paclitaxel je cytostatikem s anti-angiogenními účinky (Belotti et al. 1996; Schwartz 2009; Bocci et al. 2013), působil ve sféroidech smrt endotelových buněk, a došlo tak k dezintegraci struktury sféroidů a k rozptýlení viabilních epitelových buněk v bioinkoustu (Swaminathan et al. 2019).

Sféroidy mají obdobně jako nádory centrální oblast nedostatečně zásobenou kyslíkem a živinami (Obr. 16), jako to bylo popsáno např. u karcinomu prsu. Zpravidla se ve středu nalézá až nekrotická buněčná drť a málo aktivní buňky (Jimenez et al. 2001). Naproti tomu periferní zóna sestává hlavně z mitoticky aktivních buněk pozitivních na Ki-67 (*Marker of Proliferation Ki-67*) schopných proliferace a migrace ze sféroidu (Vörsmann et al. 2013). Sféroidy jsou sice vyráběny z relativně homogenní populace nádorových buněk, ale následná metoda kultivace ve 3D přináší diverzifikaci této populace, což dobře odpovídá heterogenitě vídané v tumorech. Chiew *et al.* (2017) analyzovali komunikaci mezi buňkami z karcinomu jater a endotelovými buňkami, které

tvořily komplexní kanály připomínající kapilární řečiště uvnitř hypoxického centra sféroidu. Na tomto modelu pak bylo možno hodnotit změněný cytotoxický efekt anti-angiogenních látek sorafenibu, sunitinibu a axitinibu. Bylo pak evidentní, že hypoxické jádro významně moduluje příjem léčiva, což ukazuje realističtější penetrační gradient ve srovnání s monolayerem (Chiew et al. 2017).

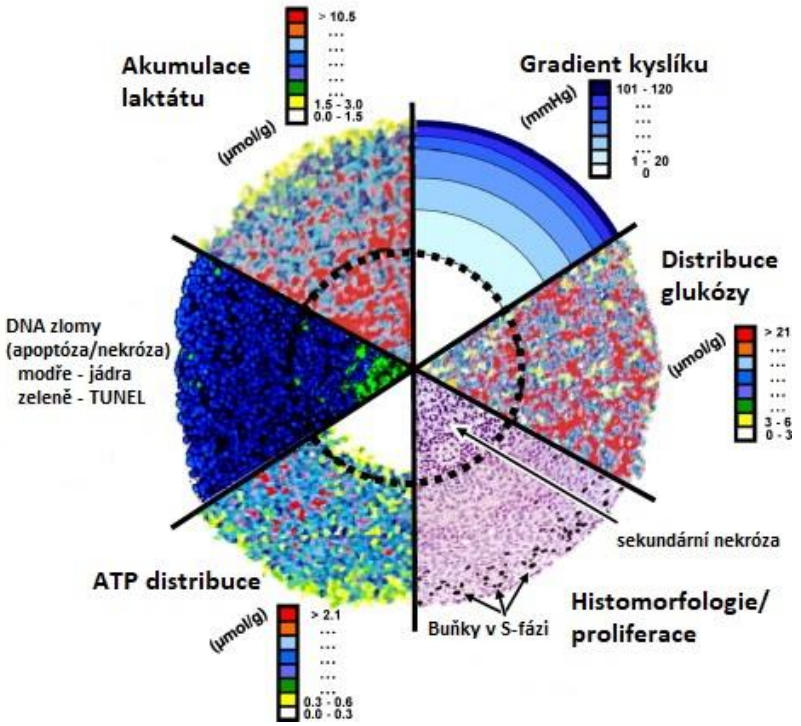

Obr. 16 Charakteristika sféroidu. Kombinací různých technik je vidět koncentrické uspořádání kyslíku, živin, proliferujících a viabilních buněk uvnitř sféroidu a směrem k jeho periferii (převzato a upraveno dle Hirschhaeuser et al. 2010). *TUNEL* – metoda pro detekci DNA zlomů značením 3´-hydroxylovaných konců ve dvouřetězcových DNA zlomech generovaných během apoptózy/nekrózy.

2.4.3 Organotypické modely kůže

Organotypické modely kůže představují pokusy o rekonstrukci kůže *in vitro* zapojením relevantních buněčných populací. V minimalistickém pokusu lze použít keratinocyty jako zdroj pro modelování epidermis a fibroblasty zalité v kolagenovém gelu jako jednoduchý model dermis. V širším pojetí lze pro zvýšení fyziologické relevance do modelu dosadit další buněčné typy nacházející se v kůži, např. melanocyty, Langerhansovy buňky, endotelové buňky nebo linie nádorové, a vytvořit tak komplexnější model (Oh et al. 2013). Výhodou je samozřejmě uniformita a reprodukovatelnost výsledků, zejména pokud je model založen na imortalizovaných buněčných liniích. To ale nutně vnáší do modelu také odchylky od standardních

fyziologických regulačních principů. Mnohem náročnější je využití primárních humánních buněčných populací s omezenou proliferační kapacitou. Tento přístup často vyžaduje pro udržení reprodukovatelnosti výsledků „poolování“ (tj. smíšení) primárních buněk od více dárců (Stoddart et al. 2012).

Trojrozměrné modelování se snaží více odrážet fyziologické prostředí a organotypické konstrukty strukturně odpovídají architektuře tkáně. Zároveň poskytují atraktivnější platformu pro studium nádorové senzitivity k léčivým přípravkům. V neposlední řadě je ale nutno vzít v úvahu, že v biomedicínském výzkumu je v poslední dekádě patrná snaha organotypické modely zařadit do rutinního testování s cílem významně nahradit či plně eliminovat modely zvířecí.

Význam hybridního modelu lze ilustrovat na melanomových sféroidech inkorporovaných do organotypického rekonstruktu kůže. Tento model prokázal významné rozdíly v terapeutickém výsledku při srovnání s konvenčními dvourozměrnými kulturami. Obě léčebné kombinace, TRAIL (*Tumour Necrosis Factor-Related Apoptosis-Inducing Ligand*) + cisplatina a TRAIL + UVB záření, efektivně omezovaly životnost buněk melanomu ve 2D kultuře, zatímco u komplexního 3D modelu byly usmrceny pouze při použití kombinace TRAIL + cisplatina (Vörsmann et al. 2013). Jinou metodou vytvořený hybridní model doplněný ještě o krevní a lymfatické cévy umožňuje například komunikaci mezi nádorem a mikroprostředím. Na tomto modelu byl jako léčivo studován BRAF inhibitor vemurafenib, který podle předpokladu ovlivnil proliferaci a apoptózu melanomových buněk. Překvapivě ale byly pozorovány buňky schopné další proliferace i po vystavení vemurafenibem. Tyto se vyskytovaly hlavně v blízkosti fibroblastů, což demonstruje jejich podpůrný a ochranný účinek (Bourland et al. 2018).

2.4.4 Zvířecí modely

Chování nádoru a jeho mikroprostředí je často studováno *in vivo* na zvířecích modelech, které poskytují ve srovnání s *in vitro* modely komplexnější obraz fyziologie a patologie, a jsou tedy předstupněm ke klinickým studiím. Oproti *in vitro* modelům se jedná ale o možnost eticky problematickou a cenově nejnáročnější.

Široce používanými modelovými organismy pro studium nádorové biologie jsou myši (*Mus musculus*), respektive jejich různě upravené kmeny (Szadvari et al. 2016; Poh et al. 2016; Kersten et al. 2017; Olson et al. 2018). Myš představuje výhodný savčí model, ale pro experimentální účely a pro jejich reprodukovatelnost je často nutno tohoto

živočicha výrazně modifikovat, například modifikovat jeho imunitní systém. Myš tak poskytuje relativně snadné možnosti tvorby vysoce definovaných imunologicky defektních kmenů, které zefektivňují xenotransplantace, např. humánních maligních buněčných linií (Morton et al. 2016). Limitem pro reprodukovatelnost výsledků je používání vysoce inbrední populace. S postupem doby ale bylo prokázáno, že lidský a myší imunitní systém nejsou plně funkčně identické (Mestas and Hughes 2004). Pro přiblížení lidským imunologickým procesům bylo nutno používat humanizované myší modely. Jedná se o imunodeficientní myši, které mají transplantované lidské geny, buňky či tkáně (Allen et al. 2019). Jedním z takových prvních modelů byla myš s geneticky podmíněnou těžkou kombinovanou imunodeficiencí (anglicky: *Severe Combined Immunodeficiency*; SCID) s transplantovaným lidským fetálním brzlíkem nebo lymfatickou uzlinou. U takto modifikovaných SCID myší byly nalezeny lidské T i B lymfocyty cirkulující v periferii (McCune et al. 1988). Nelze však zcela marginalizovat námitky (etické, genetické, bezpečnostní atd.) proti takovým úpravám.

Dalšími savčími modely, které nalézají své uplatnění v onkologickém výzkumu jsou například potkan (*Rattus norvegicus*) (Dennison et al. 2015), králík (*Oryctolagus cuniculus f. domesticus*) (Ioannidi et al. 2018; Bai et al. 2021) nebo prase *(Sus scrofa f. domestica*) (Bourneuf 2017; Horak et al. 2019; van der Weyden et al. 2020). Mimo savce lze použít i některé jiné živočišné druhy, které jsou však fyziologicky vzdálenější. V tomto kontextu je možno zmínit jako modelové organismy např. octomilku (*Drosophila melanogaster*) (Rudrapatna et al. 2012) nebo rybu dánio pruhované (*Danio rerio*) (Bootorabi et al. 2017).

V obecně společenském pohledu je používání zvířecích modelů k vědeckým účelům často vnímáno jako eticky problematické a v budoucnu je plánováno od testování na zvířatech upouštět a využívat ne-animální modely, jak proklamuje Evropská komise[4] a další zodpovědné instituce ve Spojených státech amerických[5] nebo Velké Británii[6]. Z těchto důvodů se zdá jako vhodný model – disponující již vysokou mírou komplexnosti a současně respektující panující etické koncepty – ptačí chorioalantoidní membrána (anglicky: *Chorioallantoic membrane*; CAM). Model založený na užití kuřecího embrya

[4]https://www.europarl.europa.eu/news/en/agenda/briefing/2021-09-13/7/ending-the-use-of-animals-in-research-and-testing
[5]https://www.science.org/content/article/us-epa-eliminate-all-mammal-testing-2035; https://www.epa.gov/sites/default/files/2019-09/documents/image2019-09-09-231249.pdf
[6]https://assets.publishing.service.gov.uk/government/uploads/system/uploads/attachment_data/file/417441/Delivery_Report_2015.pdf

je často považován za eticky přijatelný, jelikož etické komise považují kuřecí zárodek do 17. dne vývoje za bolest nepociťující organismus (Ribatti 2016).

CAM vzniká během ptačího vývoje spojením mezodermálních vrstev alantois a choria a představuje membránu se sítí krevních kapilár. Funkčně obstarává výměnu plynů přes póry skořápky a příjem živin z bílku či skořápky. Tento model je přirozeně vývojově imunopermisivní a umožňuje studovat např. tkáňové štěpy (Klingenberg et al. 2014), hojení ran (Ribatti et al. 1999), provádět toxikologické analýzy (Kue et al. 2014) nebo aplikovat molekuly stimulující či inhibující angiogenezi (Ribatti 2008; Ribatti 2016; Kennedy et al. 2021). Na CAM byl studován i růst různých typů nádorů (Avram et al. 2017; Schmitd et al. 2019; Sharrow et al. 2020; Pinto et al. 2021). Inokulace buněčné linie melanomu na CAM způsobila tvorbu primárních i sekundárních nádorových mas se silnou angiogenní reakcí už 3. den od aplikace (Avram et al. 2017). Obdobné výsledky jsme pozorovali i v rámci experimentů publikace (V) této disertační práce (Strnadová et al. 2020).

Dynamika změn chorioalantoidní membrány a vyvíjejícího se kuřete je precizně popsána klasickými morfologickými metodami a je detailně popsáno její fázování. Široce používán je koncept podle Hamburgera-Hamiltona, kteří v padesátých letech 20. století vytvořili soubor kreseb a fotografií zobrazujících 46 chronologických stádií vývoje kuřete od oplozeného vajíčka po plně vyvinuté kuře trvajícího 20–21 dní (Hamburger and Hamilton 1992). Koncept je možno ale dobře extrapolovat i na další ptáky, například kachnu (Li et al. 2019). Toto je velmi výhodné pro plánování časového rámce experimentů. Limitujícím faktorem pro tento model může být fyziologické trvání vývoje ptačího zárodku (Chu et al. 2022). Obtížnější na hodnocení může být i sledování vaskularizace a nádorového růstu na CAM, protože probíhá více směry a je obtížné žijící zárodek mechanicky stabilizovat bez omezení jeho vitality. I na tomto poli dochází k vývoji a rozvoji nových technologií. Velmi zajímavým technologickým zlepšením bylo zavedení ultrazvukového sledování skenerem *in ovo* (Eckrich et al. 2020), což obohatilo repertoár ultrazvukových metod. Již dříve bylo známo využití Dopplerovského principu s ultrazvukovým mikrovaskulárním zobrazením při studiu nádorové vaskularizace v ptačím embryu (Huang et al. 2019). Dále byly pro hodnocení modelů na CAM využity i metody jako magnetická rezonance (Kim et al. 2011) nebo výpočetní tomografie (CT) s použitím kontrastní látky při studiu morfogeneze ptačích embryí (Henning et al. 2011).

2.5 Exosomy jako nástroj mezibuněčné komunikace u maligního melanomu

Mezibuněčná komunikace je nezbytnou součástí fungování nádorového mikroprostředí. Tato komunikace byla dříve dichotomicky dělena na komunikaci na úrovni přímého kontaktu mezi buňkami anebo prostřednictvím chemických mediátorů na různou vzdálenost, tedy autokrinním, parakrinním či endokrinním způsobem. V posledních letech se kromě toho do popředí zájmu dostává i typ parakrinní mezibuněčné interakce zprostředkované nejrůznějšími extracelulárními váčky (vezikuly). Extracelulární vezikuly se dělí na několik typů. Při kategorizaci těchto tělísek se zohledňuje parametr jejich velikosti nebo původu.

Velikostně extracelulární vezikuly dělíme na apoptotická tělíska (50–5000 nm), mikrovezikuly (100–1000 nm) a nejmenší exosomy (30–150 nm). Apoptotická tělíska představují pozůstatky po apoptotickém rozpadu nepotřebných či jinak poškozených buněk v důsledku programované buněčné smrti. Mikrovezikuly, někdy též označované jako ektosomy, se uvolňují pučením z plazmatické membrány. Exosomy vznikají jako produkty aktivity endocytotické dráhy (Obr. 17) (Akers et al. 2013). Jejich sekreci do extracelulárního prostoru předchází vznik tzv. multivesikulárního tělíska (anglicky: *Multivesicular body*; MVB). To vzniká invaginací endosomální membrány do vlastního lumen endosomu, čímž dochází k tvorbě malých membránových intraluminálních váčků. Obsahem intraluminálních váčků jsou sekvestrované komponenty cytoplazmy původní buňky. Vzniklé MVB následně fúzuje s plazmatickou membránou, a buňka tak uvolňuje intraluminální váčky do mimobuněčného prostoru. Tento proces exocytózy je reflektován používanou nomenklaturou, kdy je zvykem, po dokončení exocytózy, intraluminální váčky nadále terminologicky označovat již jako exosomy (Van Niel et al. 2018). Kromě uvedené možnosti exocytózy může být alternativním osudem MVB jeho fúze s lysozomem a jeho následná degradace (Tancini et al. 2019).

Biogeneze exosomů je kontrolována různými molekulárními mechanismy, zpravidla závislými na tzv. komplexu endosomálního třídění potřebného pro transport (anglicky: *Endosomal Sorting Complex Required for Transport*; ESCRT) (Hurley 2010; Hurley and Hanson 2010). ESCRT je komplex proteinů, který napomáhá remodelovat membránu endosomu s cílem vytvořit intraluminální váčky s příslušným nákladem. Důležitou součástí exosomů jsou i membránové tetraspaniny, proteiny považované za charakteristické znaky exosomů a extracelulárních vezikul (Yáñez-Mó et al. 2015).

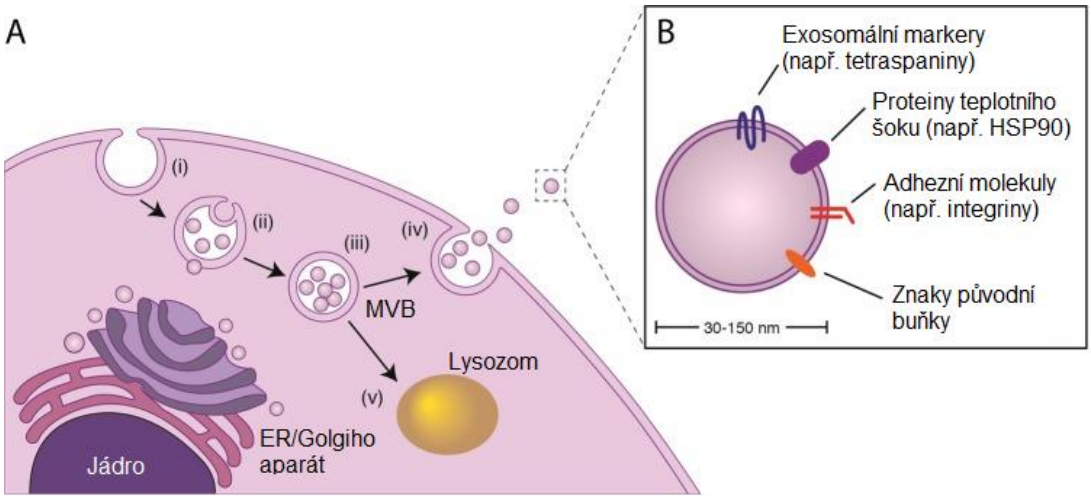

Obr. 17 Biogeneze exosomů. A) Exosomy vznikají na podkladě endocytotické dráhy. (i) Invaginace plazmatické membrány a vznik endosomu; (ii) Invaginace endosomální membrány se sekvestrovanými částmi cytoplazmy; (iii) Vznik multivesikulárního tělíska (MVB) s intraluminálními váčky; (iv) Fúze MVB s plazmatickou membránou a sekrece exosomů; (v) Degradace v lysozomu. **B)** Exosomy obsahují proteiny a jiné molekuly reflektující původní buňku. ER - endoplazmatické retikulum (převzato a upraveno dle de Couto, 2019).

Náklad exosomů (běžně je užíván anglický termín *cargo*) odráží fyziologický stav zdrojové buňky. Obecně se uvádí, že exosomy v sobě ukrývají části různých nukleových kyselin (DNA, RNA), různorodé proteiny a lipidy. Jako nosič informace se zdají velmi významné různé typy RNA, kromě klasických kódujících mRNA jsou to hlavně často zmiňované nekódující miRNA (Kalluri and LeBleu 2020). Mezi různými buňkami existují velmi podstatné rozdíly právě ve složení carga exosomů a tedy jeho analýza může dokonce poukazovat na původ či identitu zdroje. Dále je dokladováno, že exosomy v sobě střádají i metabolity nebo poškozenou DNA, a zbavují tak parentální buňku odpadních látek pro udržení stálosti jejího vnitřního prostředí (Takahashi et al. 2017). Exosomy mohou cirkulovat a být detekovány v extracelulárních tekutinách, jako jsou krev, moč, sliny. *In vitro* jsou uvolňovány do kultivačních médií. Z těchto důvodů jsou exosomy považovány za další významné zprostředkovatele mezibuněčného kontaktu (Javeed and Mukhopadhyay 2017). Běžně užívanou metodou pro izolaci exosomů z tělních tekutin nebo kultivačních médií je ultracentrifugace s hustotním gradientem, též gradientová ultracentrifugace. Pro získání čistých frakcí izolovaných exosomů se využívá hustotního gradientu o různé koncentraci z roztoku sacharózy nebo iodixanolu, např. OptiPrep (Alere Technologies AS, Oslo, Norsko), který byl použit i v publikaci IX. Tato technika poskytuje dobrou výslednou kvalitu izolovaných exosomů (Duong et al. 2019).

Pro svůj potenciál významného komunikačního nástroje jsou exosomy v posledních letech inkorporovány i do schématu fungování nádorového mikroprostředí. Exosomy

byly primárně považovány za prostředek využívaný buňkami nádoru při regulaci nádorového mikroprostředí. Uvádí se, že nádorově asociované exosomy (anglicky: *Tumor-derived Exosomes*; TEX) se aktivně podílí na stimulaci angiogeneze, imunosuprese nebo vzniku metastáz za účelem progrese nádorového onemocnění (Whiteside 2016). Ne jinak je tomu u agresivního onemocnění kůže, maligního melanomu.

Bylo zjištěno, že exosomy z melanomových linií zvyšují aerobní glykolýzu a snižují oxidativní fosforylaci u lidských dermálních fibroblastů. To vede k extracelulární acidifikaci, která je známým fyzikálně-chemickým faktorem uplatňujícím se u nádorového mikroprostředí. Tento poznatek dobře odpovídá dlouho v onkologii studovanému Warburgově efektu (Pascale et al. 2020; Vaupel and Multhoff 2021). Zaměřením se na exosomy byla potvrzena důležitost jimi přenášených miRNA v cargu. Konkrétně se jednalo o miR-155 a miR-210, které hrály zásadní roli při výše zmíněných metabolických změnách (La Shu et al. 2018).

Exosomy z melanomu jsou schopny navodit transformaci fibroblastů v nádorově-asociované fibroblasty (Zhou et al. 2018; Hu and Hu 2019). U takto reprogramovaných fibroblastů byla exosomální miR-155 určena i jako spouštěč exprese proangiogenních faktorů v důsledku aktivace JAK2/STAT3 (*Janus Kinase 2/Signal Transducer and Activator of Transcription 3*) signální dráhy, která podpořila produkci vaskulárního endotelového růstového faktoru A (anglicky: *Vascular Endothelial Growth Factor A;* VEGF-A), fibroblastového růstového faktoru 2 (anglicky: *Fibroblast Growth Factor 2;* FGF2) a MMP9 (Zhou et al. 2018).

S ohledem na mechanismus komunikace bylo významným zjištěním, že miR-21 byla horizontálním přenosem z buněk melanomu dopravena prostřednictvím exosomů a předána okolním fibroblastům, u kterých následně došlo k inhibici exprese TIMP3. Tím byla podpořena aktivita MMP účastnících se degradace ECM. To vysvětluje zvýšenou invazivitu fibroblastů a jejich putování v nádorovém mikroprostředí (Wang et al. 2020). Nádorově asociované fibroblasty často fungují jako navádějící buňky pro migraci nádorových maligních buněk.

Pro úspěšné zakládání metastáz je kromě invazivity buněk nádoru významná i jejich schopnost uchytit se ve vzdálených tkáních. Zdá se, že některé orgány umožňují tuto kolonizaci snadněji a spekuluje se o faktorech mikroprostředí, které pomáhají cirkulujícím nádorovým buňkám tuto kritickou etapu zvládnout. Předpokládá se, že rostoucí primární nádor může vykazovat systémový efekt, a ovlivňovat tak i vzdálené

tkáně a vytvářet tzv. pre-metastatická místa, tedy potenciální ložiska pro druhotné šíření nádoru při metastatické diseminaci. Kromě solubilních faktorů byla sledována i potenciální role exosomů. Metastatická diseminace byla podpořena exosomy z melanomu, ale i exosomy z progenitorových buněk kostní dřeně (Peinado et al. 2012).

Za důležitý znak invazivního chování nádorové buňky je považován i EMT. Tento děj je významný zejména u karcinomů, ale svou roli sehrává i u melanomu. Exosomy z melanomu dokázaly svým působením u primárních melanocytů snížit expresi E-cadherinu a naopak zvýšit expresi vimentinu. Vzhledem k tomu, že fenotyp melanocytů je odlišný od buněk karcinomů a že vimentin je jimi exprimován běžně, je podstatnější, že expozice exosomům dokázala významně zvýšit expresi klíčových regulátorů EMT – ZEB2 (*Zinc Finger E-Box Binding Homeobox 2*) a Snail 2 (*Snail Family Transcriptional Repressor 2*) (Xiao et al. 2016). Podobný výsledek dokladovala i další recentní studie, což naznačuje, že TEX a jejich miRNA (např. let-7i, miR-106b-5p) jsou schopny měnit fenotyp melanocytů (Xiao et al. 2016; Luan et al. 2021). Cargo TEX tak může přispívat k progresi maligního melanomu.

Exosomální miRNA z melanomu chrání nádor i před agresivní imunitní reakcí, a to prostřednictvím snížení aktivity cytotoxických T lymfocytů. Toto je vysvětlováno poklesem jejich sekrece cytokinů a granzymu B (Vignard et al. 2020). Serinová proteáza granzym B totiž tvoří důležitou součást granul cytotoxických T lymfocytů a spouští kaspázami iniciovanou programovanou buněčnou smrt (Velotti et al. 2020).

V plazmě pacientů trpících generalizovaným maligním melanomem byly detekovány exosomy bohaté i na imunosupresivně působící proteiny. Ty signifikantně snížily proliferaci CD8+ T lymfocytů nebo přímo indukovaly jejich apoptózu. Exosomy potlačovaly i expresi NKG2D (*Killer Cell Lectin Receptor K1*) (Sharma et al. 2020), povrchového proteinu převážně na cytotoxických imunitních buňkách jako jsou CD8+ T lymfocyty nebo přirození zabíječi (anglicky: *Natural Killer cells*; NK) (Wensveen et al. 2018).

Role mikroprostředí je ale mnohem komplexnější. Většinou byl dosud studován regulační vliv TEX na buňky mikroprostředí. Ovšem mikroprostředí velmi silně determinuje také vlastnosti maligního tumoru. Bylo tak dokladováno několik miRNA, jejichž exprese je u samotných buněk maligního melanomu nepatrná, ale při vystavení vlivu mikroprostředí (např. v nepermisivním mikroprostředí) dojde u maligních buněk k omezení EMT, migrace a jejich invazivity (Liu et al. 2012; Rang et al. 2016). Tato změna

je regulována právě miRNA exogenního (tj. nemelanomového) původu z nádorového mikroprostředí.

Exosomy nebo mechanismy jimi spouštěné, by tedy mohly být i klíčem k potenciálním novým terapeutickým přístupům, či by mohly příznivě modifikovat efektivitu terapeutických způsobů stávajících. Jak bylo uvedeno výše, imunoterapie představuje v současné době slibnou cestu v léčbě melanomu. Jedním z dominantně využívaných moderních terapeutických přístupů k léčbě melanomu je zacílení na PD-1/PD-L1. Právě zde ale exosomy sehrávají velmi pozoruhodnou roli. Exosomy z buněk melanomu nesou na svém povrchu ligand PD-L1, který se váže na receptor PD-1 vystavený na aktivovaných T lymfocytech. Tato vazba funkčně navozuje v mikroprostředí tumoru imunosupresi a buňky nádoru nejsou imunitním systémem eliminovány. Navíc bylo zjištěno, že IFN-γ, který je za normálních okolností produkován CD8+ T lymfocyty, pozitivně stimuluje i obsah exosomálního PD-L1, čímž je paradoxně ale potlačena právě funkce CD8+ T lymfocytů a ve výsledku je pak podpořen i růst nádoru. Současně bylo u pacientů s maligním melanomem zjištěno, že hladina cirkulujícího exosomálního PD-L1 pozitivně koreluje s hladinou IFN-γ, která však podléhá změnám v průběhu imunologické léčby anti-PD-1 (Chen et al. 2018a). Role exosomálního PD-L1 a současně IL-10 (*Interleukin-10*) při inhibici imunitní odpovědi CD8+ T lymfocytů byla potvrzena i v recentní studii (Shu et al. 2020). Potlačení této odpovědi je nezávislé na mutačním statutu genu *BRAF* u melanomových linií (Shu et al. 2020).

Lze tedy konstatovat, že buňky melanomu manipulují prostřednictvím exosomů s okolními buněčnými typy ve prospěch růstu a šíření nádoru. Potlačují odpověď imunitního systému, podporují novotvorbu cév pro dostatečné cévní zásobení nádoru nebo pro možnou invazi nádorových buněk (Kahlert and Kalluri 2013). Nepochybný je ale i vliv exosomů tvořených nemaligními populacemi nádorového mikroprostředí. Vědecké studie ohledně chování těchto malých extracelulárních vezikul tak dokladují jejich důležitost při mezibuněčné komunikaci v nádorovém mikroprostředí. Je zjevné, že zacílení exosomů a jejich carga by mohlo být potenciálně významným přístupem k léčbě širší skupiny pacientů.

3 Cíle práce

Ve své disertační práci jsem se zaměřila na tyto otázky:

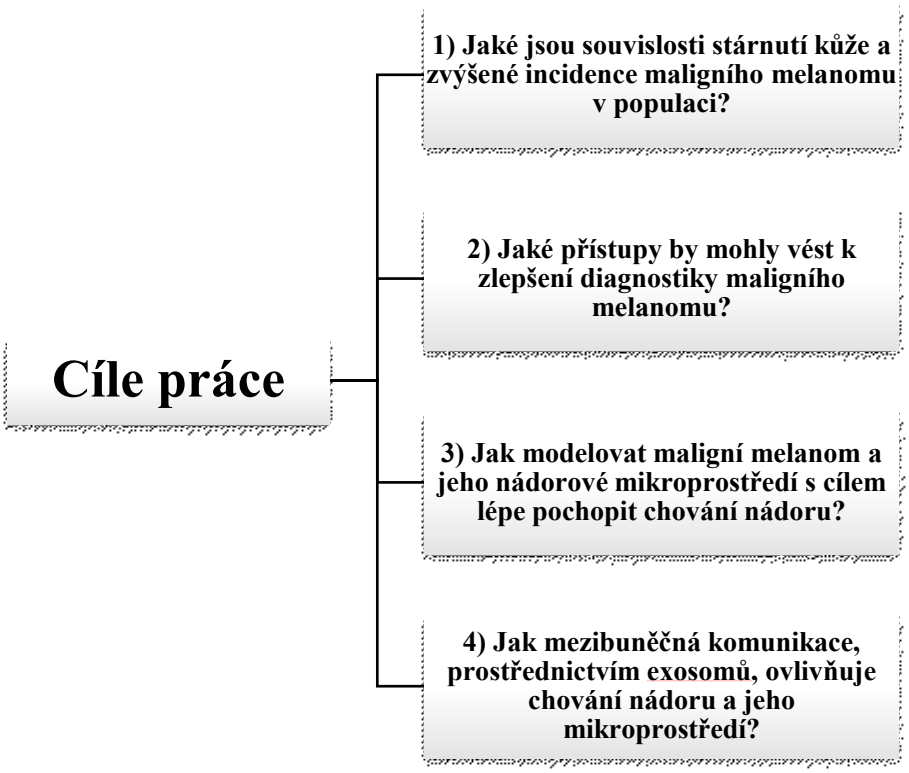

4 Seznam publikovaných prací autorky se vztahem k tématu disertace

Součástí této disertační práce jsou níže uvedené chronologicky řazené publikace autorky (v textu jsou označeny římskou číslicí). Disertační práce sestává ze 6 originálních a 3 přehledových článků. Hodnota impakt faktoru (anglicky: *Impact Factor*; IF) daného časopisu je uvedena v závorce a vztahuje se k příslušnému roku, kdy byla publikace vydána. Výsledky disertační práce a komentáře k publikacím se nachází v kapitole 6. Součástí kapitoly je i citační ohlas jednotlivých článků. Kopie publikací jsou zařazeny na konec této disertační práce a jsou její nedílnou součástí.

I. Jobe NP, Živicová V, Mifková A, Rösel D, Dvořánková B, Kodet O, Strnad H, Kolář M, Šedo A, Smetana K Jr, **Strnadová K**, Brábek J, Lacina L. Fibroblasts potentiate melanoma cells in vitro invasiveness induced by UV-irradiated keratinocytes. *Histochem Cell Biol.* 2018 May;149(5):503-516. **(IF: 2.640)**

II. **Strnadova K**, Sandera V, Dvorankova B, Kodet O, Duskova M, Smetana K, Lacina L. Skin aging: the dermal perspective. *Clin Dermatol*. 2019 Jul-Aug;37(4):326-335. **(IF: 2.458)**

III. Kučera J, **Strnadová K**, Dvořánková B, Lacina L, Krajsová I, Štork J, Kovářová H, Skalníková HK, Vodička P, Motlík J, Dundr P, Smetana K Jr, Kodet O. Serum proteomic analysis of melanoma patients with immunohistochemical profiling of primary melanomas and cultured cells: Pilot study. *Oncol Rep.* 2019 Nov;42(5):1793-1804. **(IF: 3.417)**

IV. Erzina M, Trelin A, Guselnikova O, Dvorankova B, **Strnadova K**, Perminova A, Ulbrich, P, Mares, D, Jerabek, V, Elashnikov, R, Svorcik, V, Lyutakov, O. Precise cancer detection via the combination of functionalized SERS surfaces and convolutional neural network with independent inputs. *Sensors and Actuators, B: Chemical*. 2020 Apr 1;308. 127660. **(IF: 7.335)**

V. **Strnadová K**, Španko M, Dvořánková B, Lacina L, Kodet O, Shbat A, Klepáček I, Smetana K Jr. Melanoma xenotransplant on the chicken chorioallantoic membrane: a complex biological model for the study of

cancer cell behaviour. *Histochem Cell Biol*. 2020 Aug;154(2):177-188. **(IF: 4.304)**

VI. Kodet O, Kučera J, **Strnadová K**, Dvořánková B, Štork J, Lacina L, Smetana K Jr. Cutaneous melanoma dissemination is dependent on the malignant cell properties and factors of intercellular crosstalk in the cancer microenvironment (Review). *Int J Oncol*. 2020 Sep;57(3):619-630. **(IF: 5.65)**

VII. Brábek J, Jakubek M, Vellieux F, Novotný J, Kolář M, Lacina L, Szabo P, **Strnadová K**, Rösel D, Dvořánková B, Smetana K Jr. Interleukin-6: Molecule in the Intersection of Cancer, Ageing and COVID-19. *Int J Mol Sci*. 2020 Oct 26;21(21):7937. **(IF: 5.923)**

VIII. Novotný J, **Strnadová K**, Dvořánková B, Kocourková Š, Jakša R, Dundr P, Pačes V, Smetana K Jr, Kolář M, Lacina L. Single-Cell RNA Sequencing Unravels Heterogeneity of the Stromal Niche in Cutaneous Melanoma Heterogeneous Spheroids. *Cancers* (Basel). 2020 Nov 10;12(11):3324. **(IF: 6.639)**

IX. **Strnadová K**, Pfeiferová L, Přikryl P, Dvořánková B, Vlčák E, Frýdlová J, Vokurka M, Novotný J, Šáchová J, Hradilová M, Brábek J, Šmigová J, Rösel D, Smetana K Jr., Kolář M, Lacina L. Exosomes produced by melanoma cells significantly influence the biological properties of normal and cancer-associated fibroblasts. *Histochem Cell Biol.* 2022;157(2):153–172. **(IF: 4.304)**

5 Materiál a metody

Veškerý biologický materiál byl pro řešení výzkumných prací získáván vždy s písemným informovaným souhlasem pacienta v souladu s etickými komisemi uvedených klinických pracovišť s plným respektem k Helsinské deklaraci z roku 1964. Biologický materiál, využitý v rámci této disertační práce, byl odebírán převážně na Dermatovenerologické klinice 1. LF UK a VFN, Klinice otorinolaryngologie a chirurgie hlavy a krku 1. LF UK a FN v Motole nebo Klinice plastické chirurgie FNKV.

V laboratořích Anatomického ústavu 1. LF UK byl biologický materiál následně zpracován pro histologickou analýzu, nebo byl využit jako zdroj pro kultivaci buněk a následné *in vitro* experimenty. Jednalo se hlavně o izolaci dermálních fibroblastů ze zdravých kontrolních tkání, nádorově-asociovaných fibroblastů z primárních nádorů či metastáz melanomu nebo buněk maligního melanomu z punktátů, např. z maligního ascitu pacienta. Keratinocyty byly izolovány z dodávané kůže a standardně kultivovány feederovou technikou na mitomycinem C ošetřených 3T3 myších fibroblastech (Rheinwald and Green 1975). Kromě toho byly v experimentech využívány i komerčně dostupné linie maligního melanomu (A2058, G-361). Melanomová linie BLM byla poskytnuta L. van Kempenem a J.H.J.M. van Kriekenem (Univerzita svatého Radbouda, Nijmegen, Nizozemské království). Kontrolou k buňkám maligního melanomu byly vysoce pigmentované melanocyty poskytnuté J. Vachtenheimem (Ústav lékařské biochemie a laboratorní diagnostiky 1. LF UK, Česká republika). Xenotransplantace buněk byly prováděny na embryích masných hybridů Ross 308 kura domácího (*Gallus gallus domestica*; Xaverov, Česká republika). Chorioalantoidní membrány kuřecích embryí byly využity i jako zdroj pro izolaci fibroblastů. Kontrolou byly fibroblasty izolované z kůže dospělých slepic.

Specifikace použitého materiálu a detailní popis metod a statistického hodnocení jsou uvedeny v jednotlivých článcích autorky, které jsou nedílnou součástí této disertační práce, proto nebudou v této kapitole blíže popsány.

Je však nutné zmínit, že některé metody uvedené v publikacích by nebylo možné provést bez spolupráce s jinými institucemi a jejich specializovanými pracovišti. Genomové metody a bioinformatická analýza (publikace I, VIII, IX) byly provedeny na Oddělení genomiky a bioinformatiky na Ústavu molekulární genetiky Akademie věd České republiky. Proteomické metody (např. Luminex xMAP® kuličková assay

v publikaci III) byly realizovány v Laboratoři aplikovaných proteomových analýz a výzkumného centra Pigmod na Ústavu živočišné fyziologie a genetiky Akademie věd České republiky. Metoda gradientové ultracentrifugace pro izolaci exosomů (publikace IX) byla prováděna v Laboratoři nefrologické proteomiky a extracelulárních vezikul na Ústavu patologické fyziologie 1. lékařské fakulty Univerzity Karlovy. Metody uvedené v publikaci IV (kromě přípravy biologického materiálu) byly provedeny na Ústavu inženýrství pevných látek VŠCHT v Praze a Katedře mikroelektroniky Fakulty elektrotechnické ČVUT v Praze. Intenzivní spolupráce (publikace I, VII, IX) probíhala také s Laboratoří invazivity nádorových buněk v BIOCEVu (Přírodovědecká fakulta Univerzity Karlovy).

6 Výsledky a diskuse publikovaných prací s citačním ohlasem

6.1 Tematický okruh: Stárnutí kůže a jeho vztah ke zvýšené incidenci melanomu

Autorská publikace II: **Strnadova K**, Sandera V, Dvorankova B, Kodet O, Duskova M, Smetana K, Lacina L. Skin aging: the dermal perspective. *Clin Dermatol*. 2019 Jul-Aug;37(4):326-335. **(IF: 2.458)**

Citační ohlas podle Web of Science (mimo autocitace): 8

Autorská publikace VII: Brábek J, Jakubek M, Vellieux F, Novotný J, Kolář M, Lacina L, Szabo P, **Strnadová K**, Rösel D, Dvořánková B, Smetana K Jr. Interleukin-6: Molecule in the Intersection of Cancer, Ageing and COVID-19. *Int J Mol Sci*. 2020 Oct 26;21(21):7937. **(IF: 5.923)**

Citační ohlas podle Web of Science (mimo autocitace): 14

Oba uvedené přehledové články II a VII detailně prezentují známá data shrnutá v kapitole 2.1. Kůže, struktura a vývoj v literárním přehledu předkládané disertační práce.

Přehledový článek II se tematicky věnuje v širším pohledu známým faktorům stárnutí kůže a jejich podílu na zvýšení incidence nádorových onemocněních jako maligní melanom, bazocelulární nebo spinocelulární karcinom u stárnoucí populace. Klinicky výrazným rysem je alterace struktury epidermis a dermis v průběhu stárnutí, což může vést i k chronické kožní fragilitě stárnoucí kůže zvané dermatoporóza. Při narušení struktury kůže exogenními a endogenními vlivy sehrává důležitou roli mimo jiné populace dermálních fibroblastů, která se mění také funkčně, tedy zejména změnou skladby svého sekretomu. V případě nádorové transformace pak spoluvytváří příhodné prostředí pro nádorový růst a invazi, toto umožňuje např. sekrecí prozánětlivých molekul. Publikace VII se soustředí na jednu z těchto prozánětlivých molekul v průběhu fyziologického stárnutí a s ním souvisejících patologií, na IL-6 (Obr. 18).

V přehledovém článku VII jsou shrnuty poznatky o fyziologické funkci IL-6, jeho signální dráze a její regulaci. IL-6 se ale uplatňuje i při stárnutí či patologických situacích, jako jsou chronické zánětlivé choroby a nádorová onemocnění. Recentní pandemie onemocnění COVID-19 rovněž postavila IL-6 do popředí výzkumného zájmu a lze

diskutovat o možnostech jeho terapeutického cílení, jak přímého, tak pomocí protilátek, např. bazedoxifenu nebo raloxifenu, které cílí na receptor pro IL-6. IL-6, důležitá molekula nádorového mikroprostředí, proto představuje cíl při léčbě různých onemocněních.

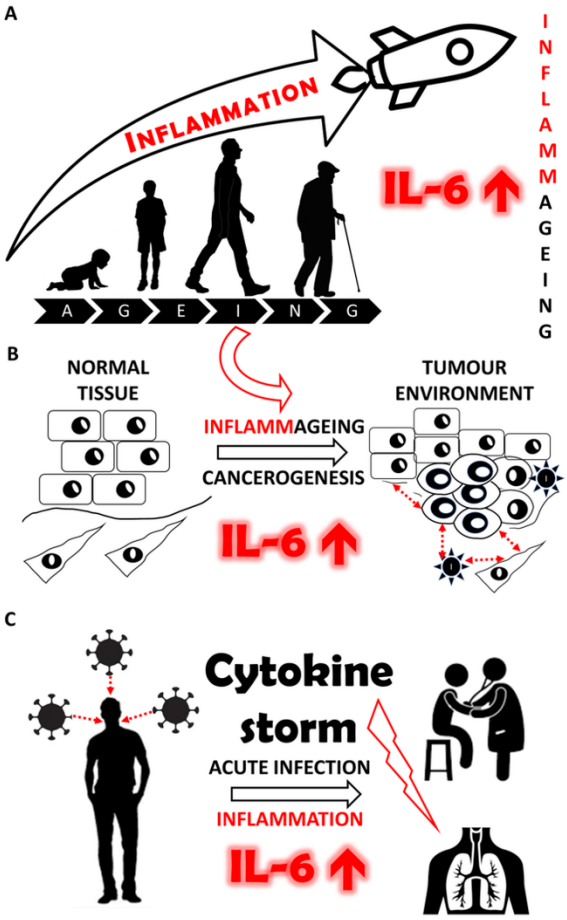

Obr. 18 Interleukin-6. IL-6 je cytokin s různorodými účinky, jehož zvýšená hladina souvisí se stárnutím a nastavením chronického zánětlivého prostředí u starších osob (A), které je vhodným prostředím pro vznik nádorů. Tento cytokin dále uplatňuje svou roli při komunikaci mezi rakovinnými buňkami a dalšími buněčnými sousedy v rámci nádorového mikroprostředí (B) a v neposlední řadě je základním faktorem cytokinové bouře u pacientů s akutní infekcí, např. s onemocněním COVID-19 (C). Tento grafický abstrakt je součástí publikace VII od Brábek et al. (2020).

I když stárnutí není možno vnímat jako nemoc, je senium obdobím, kdy narůstá deregulace biologických procesů v organismu, což následně usnadňuje nástup mnohých chorob. Jedním z významných faktorů tohoto životního období je i nástup chronického prozánětlivého stavu v těle, který podporuje mimo jiné i potenciální rozvoj malignit. Vzhledem k narůstajícímu počtu lidí seniorského věku v populaci tak dochází k nárůstu případů diagnostikovaného nádorového onemocnění, včetně maligního melanomu.

6.2 Tematický okruh: Zlepšení časné detekce maligního melanomu

Autorská publikace III: Kučera J, **Strnadová K**, Dvořánková B, Lacina L, Krajsová I, Štork J, Kovářová H, Skalníková HK, Vodička P, Motlík J, Dundr P, Smetana K Jr, Kodet O. Serum proteomic analysis of melanoma patients with immunohistochemical profiling of primary melanomas and cultured cells: Pilot study. *Oncol Rep.* 2019 Nov;42(5):1793-1804. **(IF: 3.417)**

Citační ohlas podle Web of Science (mimo autocitace): 3

Kožní melanom v pokročilém stádiu nadále představuje onemocnění s omezenými terapeutickými možnostmi a relativně špatnými léčebnými výsledky. V posledních letech došlo k výraznému pokroku především v imunoterapii melanomu (kapitola 2.3.4.2), ale je i nadále obtížné predikovat terapeutickou odpověď. Z toho důvodu je snahou hledat a identifikovat molekuly, biomarkery, které by zlepšily, usnadnily, či zpřesnily diagnostiku a umožnily selekci ohroženého pacienta, nebo pomohly zvolit optimální terapii a případně byly i prognostickými faktory. Tato pilotní studie je srovnávací analýzou 31 sérových proteinů, jako jsou cytokiny, chemokiny a růstové faktory, provedenou na pacientech trpících maligním melanomem a na zdravých kontrolách.

Sérologická analýza ukázala, že přítomnost primárního nádoru je spojena se sníženými hladinami IL-2, IL-13 (*Interleukin-13*), RANTES (*C-C Motif Chemokine Ligand 5*) a zvýšenými hladinami IL1RA (*Interleukin 1 Receptor Antagonist*), MIP-1ß (*C-C Motif Chemokine Ligand 4*) a epidermálního růstového faktoru (anglicky: *Epidermal Growth Factor;* EGF).

IL-2 aktivuje NK buňky i T lymfocyty a jako imunoterapeutický lék byl jeden z prvních použit v léčbě maligního melanomu (Rosenberg et al. 1998). Uvádí se, že snížená exprese tohoto interleukinu přispívá k nedostatečné indukci specificity cytotoxických T lymfocytů proti nádoru. Dalším důvodem se zdá být preferenční vazba IL-2 na receptory regulačních T lymfocytů (Sun et al. 2019). IL-13 je protizánětlivým cytokinem produkovaným CD4+ T lymfocyty nebo makrofágy a žírnými buňkami (Wynn 2003). U prozánětlivého chemokinu RANTES bylo zjištěno, že je jedním z chemokinů důležitým pro přilákání aktivovaných CD8+ T lymfocytů k metastázám melanomu (Harlin et al. 2009).

Další prozánětlivý chemokin MIP-1ß přitahuje monocyty do lokálního mikroprostředí nádoru, které tvoří důležitou komponentu stromatu regulující nádorový

růst (Nath et al. 2006). Vyšší sérové hladiny MIP-1ß a IL1RA u pacientů s melanomem korespondují s výsledky i z jiných studií (Paganelli et al. 2019; Wang et al. 2021). Zvýšení EGF v séru může pozitivně ovlivnit růst nádoru a podporovat vznik mikrometastáz v lymfatických uzlinách (Bracher et al. 2013). Tato data naznačují imunologickou deregulaci u pacientů s melanomem, která se odráží ve změnách sérové hladiny faktorů nezbytných pro stimulaci a inhibici růstu rakoviny.

Analýza séra dále ukázala, že hodnoty Breslowovy klasifikace naměřené v primárních nádorech pozitivně korelovaly se sérovými hladinami IL-6, CXCL8 (*C-X-C Motif Chemokine Ligand 8*; též IL-8), IL-13, VEGF-A (Obr. 19).

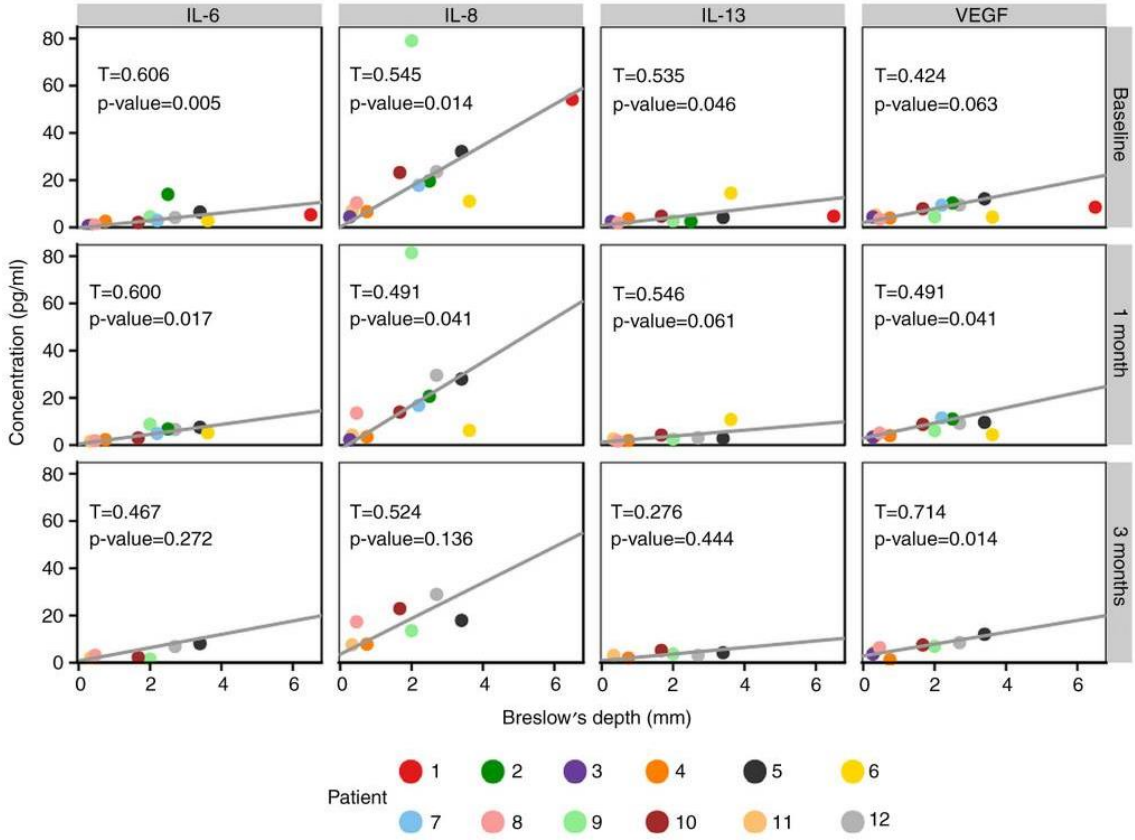

Obr. 19 Korelace hodnot Breslowa se sérovými hladinami vybraných proteinů. Analýza séra, ve třech časech odběru (před excizí primárního nádoru, měsíc nebo tři měsíce po excizi), ukázala zvyšující se naměřenou hladinu vybraných proteinů IL-6, IL-8, IL-13 a VEGF, čím vyšší byla hodnota Breslowa u primárního nádoru daného pacienta. Převzato a upraveno z publikace III od Kučera et al. (2019).

Vedle sérologické analýzy byla provedena imunohistochemická analýza primárních nádorů pacientů. Imunohistochemická analýza naznačuje značnou heterogenitu, ale lze souhrnně říci, že hepatocytární růstový faktor (anglicky: *Hepatocyte Growth Factor;* HGF), receptor 1 pro vaskulární endotelový růstový faktor (anglicky: *Vascular Endothelial Growth Factor Receptor 1;* VEGFR1*),* IL-6 a jeho receptor nebo receptor

pro IL-8, zvaný CXCR1 (*C-X-C Motif Chemokine Receptor 1*), jsou široce v nádorech exprimovány.

V této pilotní studii byla prokázána přítomnost širokého spektra zánětlivých molekul v séru pacientů. Současně však tato studie odhalila obrovský rozsah interindividuálních rozdílů mezi testovanými pacienty a také intraindividuální kolísání hodnot. Z výsledků je patrné, že výskyt některých faktorů koreluje s nepříznivými hodnotami Breslowovy klasifikace. Zvýšená hladina VEGFA pozorovaná v séru pacientů naznačuje, jak vitálně nádor potřebuje bohaté cévní zásobení. Imunohistochemická analýza byla provedena u primárních melanomů a také u několika melanomových buněčných linií a fibroblastů asociovaných s melanomem a výsledná data korelují s výsledky ze sérologické analýzy.

V současnosti používané markery, jako LDH a S100 proteiny, mají „stagingový" a prognostický význam, ale neodrážejí přesné chování organismu v době diagnózy nebo v průběhu progrese melanomu, takže strategie založená na kombinaci několika biomarkerů by mohla být v budoucnu přínosná a mohla by přispět k efektivnější detekci či terapii.

Autorská publikace IV: Erzina M, Trelin A, Guselnikova O, Dvorankova B, **Strnadova K**, Perminova A, Ulbrich, P, Mares, D, Jerabek, V, Elashnikov, R, Svorcik, V, Lyutakov, O. Precise cancer detection via the combination of functionalized SERS surfaces and convolutional neural network with independent inputs. *Sensors and Actuators, B: Chemical*. 2020 Apr 1;308. 127660. **(IF: 7.335)**

Citační ohlas podle Web of Science (mimo autocitace): 22

V této publikaci jsou prezentovány pokročilé technologické přístupy a je diskutován jejich potenciál k implementaci do laboratorní medicínské diagnostiky. Blíže jsme se zaměřili na možnou detekci změn ve složení kultivačního média vyplývajících z metabolické a sekreční aktivity nádorových a nenádorových buněk. Tento přístup kombinuje několik metod z oblasti nanotechnologie, povrchové chemie, plazmoniky a povrchem zesílené Ramanovy spektroskopie (anglicky: *Surface Enhanced Raman Spectroscopy*; SERS) a jejich spojení s metodami umělé inteligence (tzv. konvolučních neuronových sítí). Hlavním cílem této pilotní práce bylo testovat užitnou hodnotu těchto technologií při analýze komplexních biologických vzorků, které by mohly imitovat diagnostické vzorky získané od pacientů.

V experimentech byla použita, jako komplexní biologické směsi, kultivační média získaná z kultur buněk melanomu, nádorově asociovaných fibroblastů, ale i normálních buněk. Iniciálně metoda SERS umožnila charakterizaci molekulárních rozdílů jednotlivých kondiciovaných kultivačních médií od nádorových i nenádorových buněk. Pro každý použitý druh kondiciovaného média byla sestavena spektra specifická a zároveň dostatečně senzitivně indikující změny související s výskytem nádoru. V dalším kroku pak byly testovány neznámé vzorky obdobného typu. Lze konstatovat, že i ve fázi randomizovaného experimentu došlo ve 100 % případů k přesné identifikaci vzorku.

Tato studie demonstruje potenciál SERS a umělé inteligence konvolučních neuronových sítí pro budoucí klinické využití. Lze vyvozovat, že tato metodika by mohla být klíčem k rychlé detekci nádorů či monitoringu maligního onemocnění. Biologicky je ale nutno uvážit, že nádorové onemocnění je u každého pacienta do značné míry velmi individuální, a navíc se mění v čase vzhledem k tendenci mutovat v průběhu času. Přes úspěch dosažený v tomto experimentu nelze zaručit absolutní spolehlivost této metody a její užitnou hodnotu v klinické praxi. K etablování této metody na poli diagnostiky bude ještě nutno zvýšit počet různorodých vzorků pro ověření senzitivity a specificity tohoto postupu, a bude tedy i nadále potřeba rozsáhlé interdisciplinární spolupráce.

6.3 Tematický okruh: Modelování nádorového mikroprostředí

Autorská publikace I: Jobe NP, Živicová V, Mifková A, Rösel D, Dvořánková B, Kodet O, Strnad H, Kolář M, Šedo A, Smetana K Jr, **Strnadová K**, Brábek J, Lacina L. Fibroblasts potentiate melanoma cells in vitro invasiveness induced by UV-irradiated keratinocytes. *Histochem Cell Biol.* 2018 May;149(5):503-516. **(IF: 2.640)**
Citační ohlas podle Web of Science (mimo autocitace): 11

Jedním z největších rizikových faktorů pro vznik maligního melanomu je UV záření, jak bylo také popsáno v kapitole 2.3.1. V této publikaci je testován vliv UV radiace na normální keratinocyty a jejich následná interakce s normálními a nádorově-asociovanými fibroblasty z melanomu od různých donorů.

Expresní profily těchto fibroblastů ukázaly, že obecně se normální a nádorově-asociované fibroblasty z melanomu signifikantně liší řádově ve stovkách genů (průměrně ve 402 genech). Současně je třeba upozornit na velmi významnou interindividuální variabilitu této deregulace mezi jednotlivými donory. U všech nádorově-asociovaných

fibroblastů byla ale pozorována zvýšená exprese genů pro cytokin IL-6 a chemokiny CXCL8 a CXCL1 (*C-X-C Motif Chemokine Ligand 1*), tedy proteiny podporující invazní potenciál buněk nádoru. Imunocytochemická analýza prokázala, že všechny tyto nádorově asociované fibroblasty vykazovaly expresi běžných intermediárních filament (např. vimentinu, typického znaku pro mezenchymální buňky). Velmi variabilně ale tyto stromální fibroblasty na úrovni proteinu exprimovaly α-hladkosvalový aktin (anglicky: α-*Smooth Muscle Actin*; αSMA), který je typickým znakem pro nádorově-asociované fibroblasty. Jako teoretické východisko pro náš experiment jsme zvolili interakci epitelových buněk poškozených ultrafialovými paprsky s normálním či aktinicky změněným modelem dermis. Keratinocyty byly pro tyto účely ozářeny UVB, a to buď mírnějším frakcionovaným ozařováním simulujícím chronickou intermitentní expozici (3 x 10 mJ/cm^2) nebo subletální dávkou simulující akutní zátěž (100 mJ/cm^2).

Nádorové mikroprostředí bylo v této publikaci modelováno pomocí insertového systému UVB-ozářených keratinocytů a neozářených fibroblastů. Bioaktivní látky produkované do kultivačního média v důsledku této kokultivace vytvořily kondiciované médium, které obsahovalo mediátory reakce na proběhlé poškození. U modelů časných maligních melanomů musí být brána v potaz nejen dermální komponenta stromatu, ale poněkud atypicky je třeba vzít v úvahu i keratinocyty, které jsou v přímém sousedství maligních či malignizujících buněk melanocytárního původu. Takto kondiciované komplexní médium bylo následně použito k ovlivnění dvou buněčných linií maligního melanomu (A2058 a BLM) zalitých v podobě sféroidů do kolagenového gelu.

Výsledky ukázaly, že bioaktivní látky z kokultury UVB-ozářených keratinocytů a nádorově asociovaných fibroblastů z melanomu signifikantně podporují invazi melanomových linií. Méně výrazný účinek na invazi měla kokultivace s normálními dermálními fibroblasty nebo tehdy, kdy byly ke kondiciování média užity jen ozářené keratinocyty samotné. Obecně lze shrnout, že vysoká dávka UVB záření u keratinocytů způsobila následné zpomalení invaze buněk melanomu oproti frakcionovanému ozařování nižší dávkou (Obr. 20). Tento výsledek do značné míry dobře ilustruje význam intermitentní expozice UV paprskům známé z klinické onkologie.

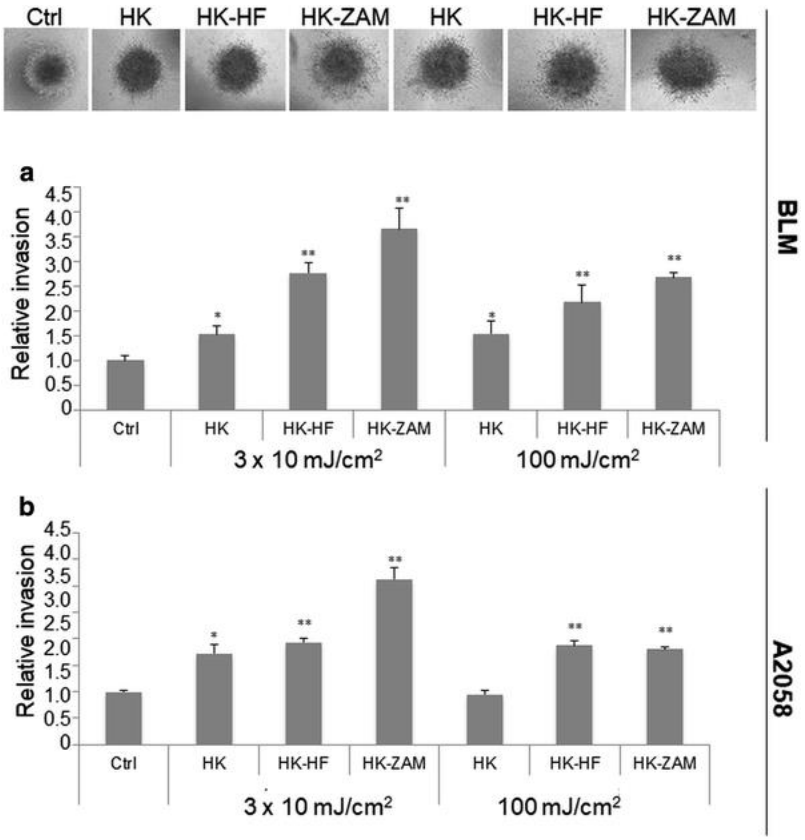

Obr. 20 Invaze buněk melanomových linií BLM a A2058. Bioaktivní látky kondiciovaných médií z kokultury UV-ozářených keratinocytů (HK) a nádorově-asociovaných fibroblastů (ZAM) nejvýrazněji podporují invazi buněk melanomu. Mírnější frakcionované ozařování HK (3 x 10 mJ/cm^2) je pro invazi buněk melanomu více účinné než jednorázová subletální dávka ozáření HK (100 mJ/cm^2). Převzato a upraveno z publikace I od Jobe et al. (2018).

Opakované ozáření nízkými dávkami UVB v této publikaci připomíná opakované vystavení nechráněné pokožky slunci. Životaschopnost keratinocytů je zachována, ale i tato nízká dávka působí DNA poškození. Fibroblasty v dermis kůže komunikují s takto poškozenými keratinocyty parakrinní produkcí bioaktivních látek a z výsledků je patrné, že v případě výskytu ložiska melanomu podporují jeho schopnost invadovat.

Autorská publikace V: **Strnadová K**, Španko M, Dvořánková B, Lacina L, Kodet O, Shbat A, Klepáček I, Smetana K Jr. Melanoma xenotransplant on the chicken chorioallantoic membrane: a complex biological model for the study of cancer cell behaviour. *Histochem Cell Biol*. 2020 Aug;154(2):177-188. **(IF: 3.57)**
Citační ohlas podle Web of Science (mimo autocitace): 2

Kuřecí chorioalantoidní membrána je ptačím homologem savčí placenty. Pro plnění své role při vývoji embrya je nutně vysoce vaskularizovanou tkání (blíže kapitola 2.4.4), což ji predisponuje k provádění některých typů biologických experimentů. Tato

publikace se zaměřuje na xenotransplantaci melanomových buněk na kuřecí CAM, jakožto komplexnější biologický model pro studium chování nádorových buněk.

V *in vitro* experimentech byly izolovány fibroblasty z CAM nebo kůže dospělých jedinců kura domácího a po jejich kultivaci bylo odebráno kondiciované médium. Následně byly studovány účinky těchto médií na růst a metabolismus buněk melanomových linií. Výsledky ukázaly, že bioaktivní látky produkované fibroblasty do média významně změnily kinetiku proliferace 3 sledovaných melanomových buněčných linií oproti kontrolnímu médiu. Toto pozorování zdůrazňuje závislost nádoru na jeho komunikaci s okolními buňkami mikroprostředí. Metabolická aktivita těchto buněk pak byla měřena a porovnána MTT (3-(4,5-dimethylthiazolyl-2)-2,5-diphenyltetrazolium bromid) testem. Před experimenty *in ovo* byla také provedena imunocytochemická analýza zaměřující se na možnosti spolehlivé detekce lidských melanomových buněk v kuřecí tkáni. Klíčem k řešení této otázky byla literárně udávaná a námi ověřená aplikace protilátky proti vimentinu, klon V9 (DAKO, Glostrup, Dánsko). Toto barvení bylo negativní u všech fibroblastů ptačího původu, ale spolehlivě značilo buňky obsahující vimentin lidského původu včetně buněk melanomu. Tento test se jevil jako spolehlivější než aplikace některých jiných melanomových markerů např. HMB-45 (Pmel17), který může být ovlivněn i kultivačními podmínkami.

Po xenotransplantaci melanomových buněk *in ovo* byly mikroskopicky pozorovány shluky těchto buněk na povrchu CAM. V pozdějších fázích experimentu, tj. po 6 dnech, byly tyto shluky viditelné i pouhým okem. Injekce modré pryskyřice (Mercox II Blue, Mercox-Japan Vilene, Tokyo, Japonsko) do cév embrya umožnila lepší optickou vizualizaci průběhu cév a vytváření vaskulárních struktur směřujících k shluku melanomových buněk. Dále bylo patrné, že cévy pouze masu buněk překrývaly, ale nepenetrovaly do ní.

Invaze nádorových buněk do stromatu CAM byla vzácná a histologicky byla potvrzena pouze u dvou vzorků ze 45. V těchto případech barvení vimentinem odhalilo rozptýlení melanomových buněk na povrchu CAM a také uvnitř stromatu. Jejich identita byla dále potvrzena barvením HMB-45 (Obr. 21).

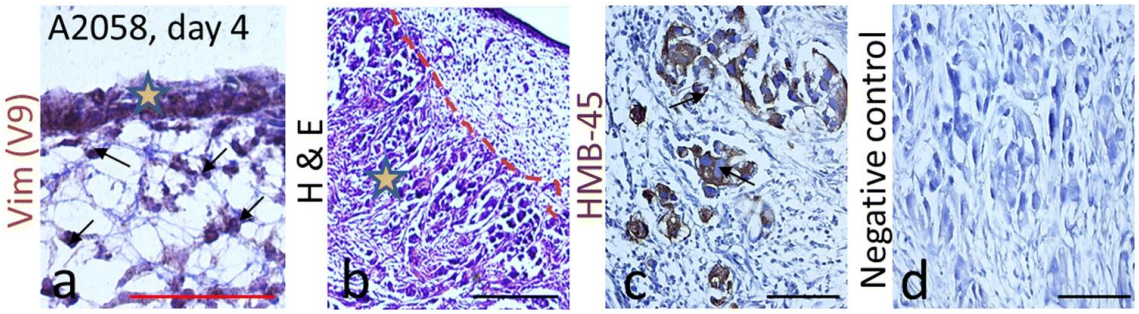

Obr. 21 Řez kuřecí chorioalantoidní membránou. Buňky melanomové linie A2058, značené vimentinem, jsou lokalizovány na povrchu CAM (hvězdička) s občasným výskytem ve stromatu CAM (šipky) (a). Pouze v jednom případě byla pozorována solidní masa melanomu ve stromatu (hvězdička) (b), tyto buňky byly barveny pozitivně na HMB-45 (c). Měřítko: 100, popř. 300 μm. Převzato a upraveno z publikace V od Strnadová et al. (2020).

Je zřejmé, že bioaktivní látky produkované fibroblasty do média stimulují proliferaci nádorových buněk, i když je jejich původ odlišný. *In ovo* tvoří transplantované buňky melanomu shluky na CAM, které následně stimulují dostředivý růst cév do místa přihojení. Vzhledem k těmto vlastnostem je CAM tradičně používána jako vhodný nástroj pro studium vaskularizace a angiogeneze (Ribatti 2008; Nowak-Sliwinska et al. 2014; Burggren and Antich 2020). Omezení invazního potenciálu melanomových buněk může být způsobeno časovou restrikcí experimentu vynucenou rychlostí vývoje embrya kuřete nebo nepermisivními biologickými vlastnostmi CAM. I přes tyto limitace CAM kuřecího embrya nabízí v některých aspektech i nadále atraktivní *in vivo* biologický model pro studium chování melanomových buněk.

Autorská publikace VIII: Novotný J, **Strnadová K**, Dvořánková B, Kocourková Š, Jakša R, Dundr P, Pačes V, Smetana K Jr, Kolář M, Lacina L. Single-Cell RNA Sequencing Unravels Heterogeneity of the Stromal Niche in Cutaneous Melanoma Heterogeneous Spheroids. *Cancers* (Basel). 2020 Nov 10;12(11):3324. **(IF: 6.639)**
Citační ohlas podle Web of Science (mimo autocitace): 5

Tento původní článek VIII je zaměřen na hodnocení funkční diverzity fibroblastů při interakcích s buňkami melanomu, a to na 3D modelu s využitím moderní metody single-cell RNA sekvenování.

Pro modelování diverzity dermálního mikroprostředí byly využity dva zdroje dermálních fibroblastů. Jednalo se o juvenilní fibroblasty z neozářené části kůže dítěte (anglicky: *Juvenile Dermal Fibroblasts*; JDF) a fibroblasty z fotoexponované kůže seniorního dárce (anglicky: *Photo-damaged Dermal Fibroblasts*; PDF). Heterogenní

sféroidy složené z buněk melanomu a z daného typu fibroblastů (v poměru 1:1) utvořené metodou visící kapky představovaly pak 3D model simulující ekosystém nádoru. Klíčovou metodou, která měla rozlišit chování různě aktinicky poškozených fibroblastů při vytváření mikroprostředí melanomu, byla single-cell RNA analýza.

3D model heterogenních sféroidů s typickou morfologií byl vytvářen metodou visící kapky (Obr. 15) a ačkoli k inokulaci byla použita směs obou buněčných typů, byla pozorována v rámci sféroidu prostorová segregace. Imunohistologické barvení řezů těchto sféroidů pak umožnilo vizualizovat zajímavou distribuci obou typů buněk. Fibroblasty detekované specifickou protilátkou TE-7 (Novus Biologicals, Centennial, CO, USA), se nacházely ve středu sféroidu, zatímco buňky melanomu značené protilátkami proti specifickým znakům melanocytů (HMB-45, S100 – obé DAKO, Glostrup, Dánsko) byly lokalizovány spíše na periferii.

Po disociaci sféroidů na suspenzi jednotlivých buněk byl model analyzován pomocí single-cell RNA sekvenování. Tento přístup ve spojení s biostatistickým přístupem umožnil od sebe rozdělit nejen dvě zdrojové populace, ale dále charakterizovat jejich případně vzniklou heterogenitu. Fibroblasty byly identifikovány podle exprese specifických genů, například genu pro fibroblastový aktivační protein (anglicky: *Fibroblast Activation Protein*; FAP). Naopak buňky melanomu byly od populace fibroblastů odlišeny genem pro Melan-A, který hraje roli při biogenezi melanosomů, a je tak typickým znakem melanocytů. Exprese těchto znaků byla potvrzena i na úrovni proteinu na histologických řezech.

Bioinformatická analýza primárních dermálních fibroblastů ze sféroidů ukázala, že oba typy fibroblastů lze shodně funkčně rozdělit do tří klastrů na základě jejich expresního profilu (Obr. 22). První skupina, označovaná jako ECM-, byla bohatá na expresi genů pro prozánětlivé faktory, jako jsou cytokiny a chemokiny. Zároveň postrádala přepsané geny zodpovědné za produkci extracelulární matrix. Druhá skupina ID+ obsahovala transkripty genů zodpovědných za diferenciační a dediferenciační procesy, které se objevují v signální kaskádě superrodiny TGFß (*Transforming Growth Factor* ß). Příkladem je gen ID1 (*Inhibitor of Differentiation 1*). Třetí skupina ECM+ představuje klasický náhled na fibroblasty jakožto producenty složek mezibuněčné hmoty. Tato skupina hojně transkribovala geny pro extracelulární matrix např. kolagen 1. Rozdělení na tři funkčně odlišné skupiny bylo zřetelnější u PDF, tedy fotoexponovaných fibroblastů ze staršího pacienta.

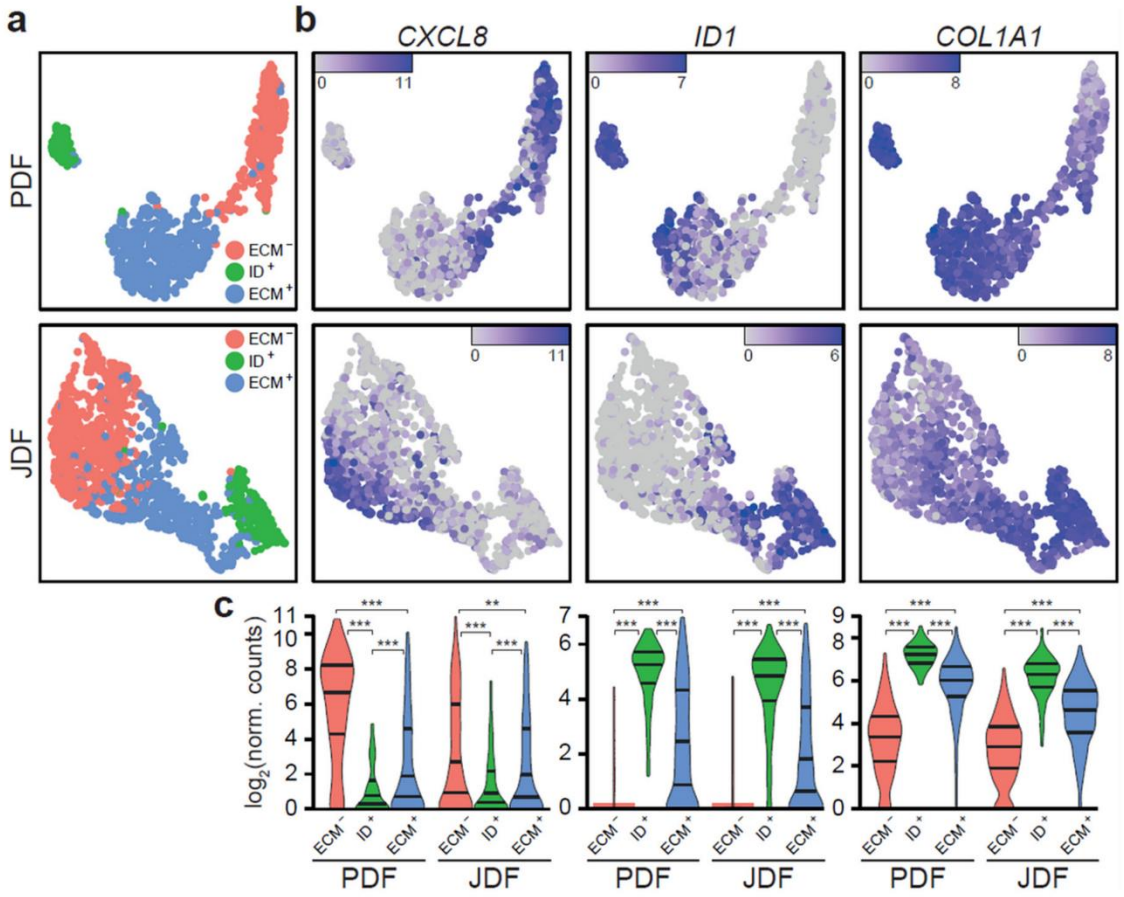

Obr. 22 Bioinformatická analýza JDF a PDF z heterogenních sféroidů. (a) Oba typy fibroblastů se v blízkosti buněk melanomu ve sféroidu rozčlenily na 3 fenotypově odlišné shluky na základě jejich genové exprese. (b) Skupina fibroblastů ECM- výrazně exprimuje prozánětlivé cytokiny a chemokiny, např. *CXCL8*. Buňky skupiny ID+ jsou identifikovány silnou expresí genů zodpovědných za diferenciační a dediferenciační procesy, např. *ID1*. ECM+ je třetí skupinou fibroblastů hojně exprimujících transkripty genů ECM. (c) Klastry jsou v JDF i PDF ekvivalentní a vykazují statisticky významné rozdíly v expresi jejich markerových genů (** $p < 0.01$; *** $p < 0.001$, Mann-Whitney U test). Převzato a upraveno z publikace VIII od Novotný et al. (2020).

Na podkladě biologické databáze KEGG (popisující vztahy mezi geny, potažmo jimi kódovanými proteiny, a propojující je funkčně do sítí) byly pozorovány významné rozdíly mezi klastry fibroblastové populace. Při srovnání skupiny ECM- vůči ID+ byla u obou typů fibroblastů odhalena snížená exprese genů asociovaných s fokální adhezí, dále s interakcí receptorů a extracelulární matrix a s TGFß signální dráhou. Specifické změny pro PDF ukazovaly zvýšenou expresi genů spjatých s interakcí cytokinů a jejich receptorů nebo se signálními drahami Nod-like a Toll-like receptorů. Ty jsou součástí vrozené imunitní odpovědi vedoucí k produkci cytokinů a chemokinů, např. IL-6, IL-1α, LIF (*Leukemia Inhibitory Factor)* nebo CXCL8 (Kawai and Akira 2011; Wicherska-pawłowska et al. 2021). Ustanovení chronického zánětlivého prostředí je jedním z hlavních aktivátorů nádorového růstu, čemuž podle těchto výsledků napomáhají hlavně

stárnoucí buňky stromatu. Zároveň byla u PDF detekována snížená exprese genů pro oxidativní fosforylaci, což bývá u buněk nádoru běžným jevem jdoucím ruku v ruce s aktivnější glykolýzou.

Při srovnání klastrů ECM- vůči ECM+ byla u obou typů fibroblastů pozorována opět snížená exprese genů spojená s TGFß signální kaskádou. U PDF lze nalézt sníženou expresi genů pro fokální adhezi a genů pro interakci receptorů s extracelulární matrix. Exprese genů pro export proteinů je naopak zvýšena.

Při posledním srovnání klastrů ID+ vůči ECM+ byly pozorovány pouze marginální rozdíly v aktivitě signálních drah. Z těchto výsledků vyplývá, že rozdíly u aktinicky poškozených stárnoucích fibroblastů PDF se koncentrují v klastru ECM-.

Bioinformatická analýza byla provedena i u buněk melanomu z rozvolněných sferoidů. Analýza ukázala rozdělení pouze do dvou klastrů bez ohledu na typ užitých fibroblastů. Jeden z těchto klastrů byl transkripčně více aktivní, což je reprezentováno zvýšenou expresí *NEAT1* (*Nuclear Enriched Abundant Transcript 1*) a *MALAT1* (*Metastasis Associated Lung Adenocarcinoma Transcript 1*), což jsou geny dlouhých nekódujících RNA. Dlouhé nekódující RNA byly popsány v mnoha fyziologických a patologických procesech. Zmíněné geny jsou důležité např. při stabilizaci jaderných tělísek a sestřihu pre-mRNA a uvádí se, že stimulují migraci kožního i uveálního melanomu (Xia et al. 2019; Wu et al. 2020). Jelikož byla detekována exprese prozánětlivých faktorů ve specifických klastrech fibroblastů, cílem bylo zjistit, zda k této expresi dochází i u buněk melanomu. Data naznačují, že CXCL1 je převážně produkován buňkami melanomu, zatímco IL-6 a LIF jsou exprimovány fibroblasty. CXCL8 byl transkribován u obou buněčných populací, tedy u melanomu i dermálních fibroblastů. Tyto molekuly regulují nádorový ekosystém a podporují invazivní chování nádoru v něm.

Invazní potenciál buněk ze sféroidu byl také testován v kolagenovém gelu modelující extracelulární prostředí. Migrovaly zde nejprve jednotlivé fibroblasty následované buňkami melanomu v protáhlých výběžcích. Přidáním exogenního IL-6 do kultivačního média byla invaze buněk zvýšena a buňky melanomu migrovaly v masivních prstovitých čepech. Farmakologická inhibice tocilizumabem, který cílí na receptor IL-6, potvrdila očekávanou blokaci buněčné migrace.

Heterogenní sféroidy tvořené z melanomových buněk a fibroblastů v kombinaci se single-cell RNA sekvenováním představují velmi standardní model, který lze použít pro studium interakce fibroblastů s buňkami melanomu doplněný o velmi robustní analytický genetický přístup. Tento 3D model umožňuje lépe pochopit chování nádorového

ekosystému než konvenční 2D buněčné kultury. Tato studie potvrdila, že dermální fibroblasty nejsou homogenní skupinou, ale místo toho obsahují několik samostatných subpopulací s rozdílným expresním profilem. Právě metoda single-cell RNAseq umožňuje zachytit i subtilnější či méně početné populace, které ale mohou mít velký regulační potenciál. Tyto minoritní populace by v konvenčním sekvenování (tzv. bulk-seq) mohly uniknout pozornosti.

Endogenně a exogenně poškozené dermální fibroblasty (tedy změněné jak vlivem stárnutí, tak i UV ozáření) přispívají větší měrou k prozánětlivému prostředí, a stávají se tak důležitou komponentou určující charakter nádorového mikroprostředí. Jelikož jsou fibroblasty všude přítomnými buňkami, terapeutické cílení na celou populaci se obecně jeví jako riskantní a nereálný cíl. Hlubší znalosti heterogenity fibroblastů mohou představovat důležitý přínos a mohou mít dopad na vývoj nových přístupů v léčbě nádoru s cílením na jeden z klastrů s pro-nádorovým chováním.

6.4 Tematický okruh: Mezibuněčná komunikace

Autorská publikace VI: Kodet O, Kučera J, **Strnadová K**, Dvořánková B, Štork J, Lacina L, Smetana K Jr. Cutaneous melanoma dissemination is dependent on the malignant cell properties and factors of intercellular crosstalk in the cancer microenvironment (Review). *Int J Oncol*. 2020 Sep;57(3):619-630. **(IF: 5.24)**
Citační ohlas podle Web of Science (mimo autocitace): 4

Jak bylo blíže ozřejměno v kapitole 2.3.1., incidence maligního melanomu kůže stoupá. Tento přehledový článek VI se zaměřuje na interpretaci známých dat týkajících se vzniku kožního maligního melanomu a jeho následné diseminace, tedy rozsevu nádorových buněk do tkání a orgánů pacienta v průběhu progrese onemocnění (Obr. 23). Maligní melanom kůže vzniká na podkladě genetické mutace spojené s deregulací signálních drah. Invazní potenciál nádoru je ale také významně ovlivněn nádorovým mikroprostředím. Diseminace nádoru začíná nejprve vstupem do lumen intratumorálních cév a následnou cirkulací buněk nádoru v těle pacienta. Kritickým momentem pro metastazaci je ale dosažení nového vhodného, tzv. permisivního, prostředí v nějakém orgánu. Predilekční lokalizací pro buňky maligního melanomu při zakládání metastáz jsou zejména lymfatické uzliny, plíce a mozek.

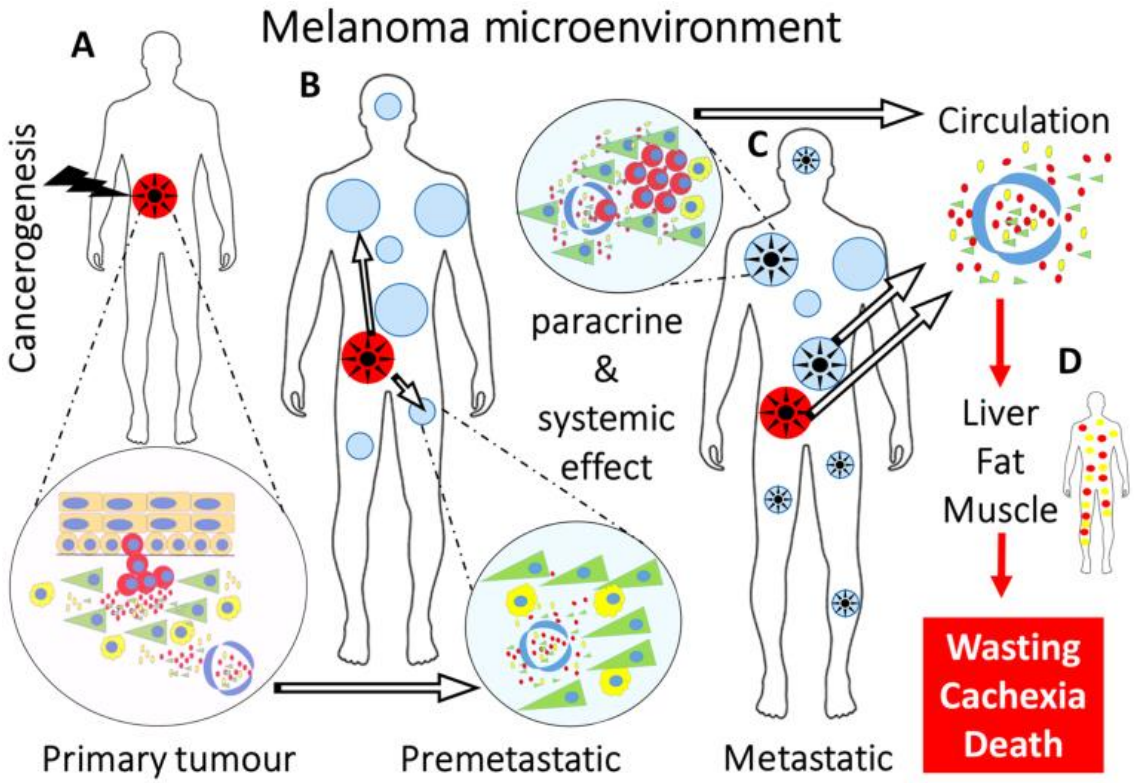

Obr. 23 Vznik, progrese a systémový efekt kožního maligního melanomu. (A) Vznik primárního nádoru ovlivňuje prostřednictvím parakrinní signalizace i okolní nerakovinné buňky (v růžovém kruhu je blíže znázorněno nádorové mikroprostředí). Tato parakrinní interakce stimuluje maligní potenciál nádoru. Signální molekuly následně difundují a unikají do krevního/lymfatického oběhu. (B) Cirkulace uvolněných cytokinů, chemokinů a růstových faktorů aktivuje normální vzdálené tkáně, které v nich formují vhodná premetastatická místa pro metastáze nádoru (detail v modře vyplněném kruhu). (C) V některých z těchto premetastatických nik se vytvoří sekundární (metastatické) nádory, což podmiňuje pozdější systémový efekt typický pro generalizované malignity. (D) Cirkulující bioaktivní látky vyvolávají fyzické a funkční orgánové změny vedoucí ke chřadnutí, nechutenství, a dokonce až k smrti pacienta. Převzato a upraveno z publikace VI od Kodet et al. (2020).

Důležitou součástí přehledového článku je shrnutí hlavních způsobů mezibuněčné komunikace v nádorovém mikroprostředí kožního maligního melanomu v průběhu jeho progrese.

Konkrétně je zaměřen na přímé mezibuněčné kontakty prostřednictvím kadherinů, dále na bioaktivní látky účastnící se parakrinní signalizace anebo na komunikaci využívající extracelulární tělíska – exosomy (kapitola 2.5). Tyto membránové váčky by neměly být v nádorové biologii opomíjeny, jelikož je stále lépe dokladováno, že hrají v mikroprostředí nádoru nezanedbatelnou roli (viz publikace IX).

V neposlední řadě je v této publikaci diskutováno, jak cirkulující bioaktivní látky jako cytokiny a chemokiny podporují vznik metastáz a jak navozují strukturální i funkční orgánové změny. Tento efekt se uplatňuje i na velké vzdálenosti a jde spíše již o systémový efekt. Takovéto působení na pacienta může vést ke kachexii, anorexii, celkovému strádání organismu a v nejhorším případě i k úmrtí. Přehledový článek také

zmiňuje význam možnosti cílené léčby v prevenci vzniku metastáz a reflektuje nový koncept léčiv – migrastatika (Gandalovičová et al. 2017). Migrastatika cílí terapeuticky totiž na invazivní schopnosti buněk. Kombinace migrastatik a tradičních onkologických léků by mohla být slibnou cestou v léčbě nádorových onemocnění.

Tento přehledový článek tedy shrnuje poznatky o vzniku kožního maligního melanomu, diskutuje jeho chování v prostředí nenádorových buněk, proces progrese a invaze nádoru až k jeho systémovému efektu na celý organismus.

Autorská publikace IX: **Strnadová K**, Pfeiferová L, Přikryl P, Dvořánková B, Vlčák E, Frýdlová J, Vokurka M, Novotný J, Šáchová J, Hradilová M, Brábek J, Šmigová J, Rösel D, Smetana K Jr., Kolář M, Lacina L. Exosomes produced by melanoma cells significantly influence the biological properties of normal and cancer-associated fibroblasts. *Histochem Cell Biol.* 2022;157(2):153–172. **(IF: 4.304)**
Citační ohlas podle Web of Science (mimo autocitace): 2

Exosomy představují nástroj pro jednu z mnoha možných forem mezibuněčné komunikace. Mohou tedy ovlivňovat i chování nádoru a jeho mikroprostředí. Naše studie byla zaměřena na sledování vlivu exosomů izolovaných z buněk melanomu na funkční a fenotypové vlastnosti normálních lidských dermálních fibroblastů (anglicky: *Human Dermal Fibroblasts*; HDF) a nádorově-asociovaných fibroblastů izolovaných z maligního melanomu (anglicky: *Cancer-associated fibroblasts isolated from malignant melanoma*; mCAF).

Z několika možných přístupů jsme pro dosažení optimálního výtěžku zvolili metodu ultracentrifugace s hustotním gradientem. Pro izolaci exosomů byly buňky melanomu ponechány v kultivačním médiu s 5% fetálním bovinním sérem (anglicky: *Foetal Bovine Serum*; FBS) zbaveného exosomů (A27208-01, Thermofisher Scientific, Waltham, MA, USA). Cílem tak bylo získat exosomy pouze od melanomových buněk. Kondiciované médium bylo stočeno v několika krocích s využitím roztoku pro hustotní gradient OptiPrep (Alere Technologies AS, Oslo, Norsko). Následně byl obsah zkumavky rozdělen na dvanáct mililitrových frakcí odshora dolů. Frakce 6, 7 a 8 obsahující purifikované exosomy byly spojeny dohromady, zředěny PBS a znovu odstředěny. Na závěr byly tyto koncentrované frakce resuspendovány v PBS a takto připravený vzorek byl použit pro další analýzu a experimenty.

Exosomy po izolaci gradientovou ultracentrifugací byly charakterizovány na základě velikosti a koncentrace částic (Obr. 24). Pro gradientovou ultracentrifugaci jako pro optimální izolační metodu svědčila i dokonalá morfologie potvrzená elektronovovou mikroskopií izolátu, která potvrdila vysokou puritu exosomů a absenci jiných elementů, například proteinových agregátů (Obr. 24). V neposlední řadě bylo ultracentifugací dosahováno i vysokého obsahu celkového proteinu, od kterého se odvozovalo použité množství exosomů při experimentech. Zjistili jsme, že proliferační aktivita obou typů studovaných fibroblastů závisí na použité proteinové koncentraci. Při zvyšující se koncentraci dochází k zpomalování buněčného množení. Podobně došlo i k zpomalení buněčné adheze (posuzované změnou impedance automatizovaného měřícího systému iCelligence).

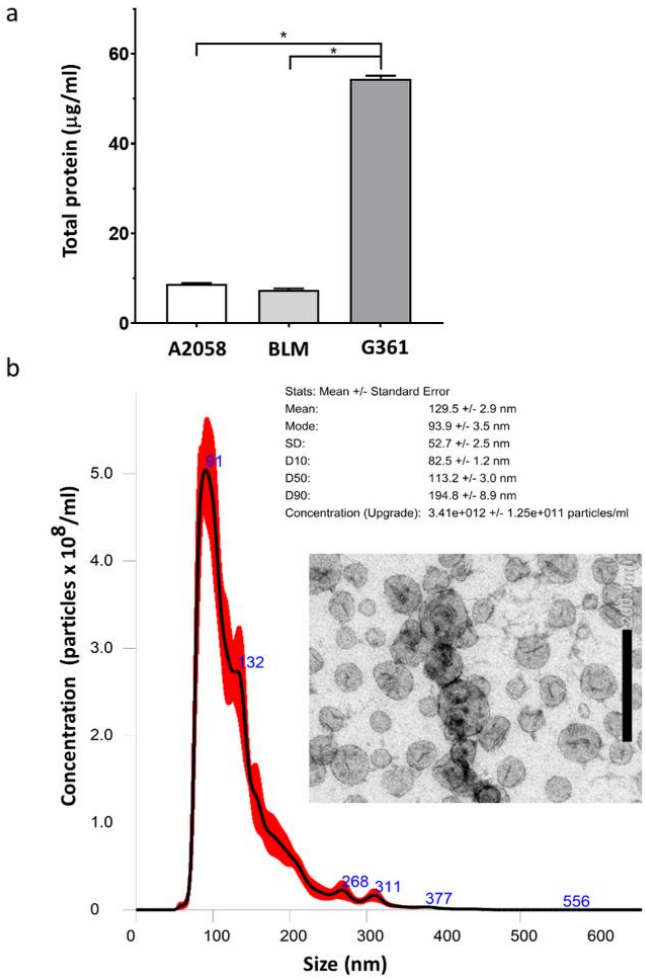

Obr. 24 Charakterizace exosomů izolovaných z melanomové linie G361. (a) Graf znázorňuje kvantifikaci celkového proteinu exosomů izolovaných z tří melanomových linií, kdy pouze G361 produkovaly exosomy v takovém množství, které bylo dostačující pro následné experimenty (chybové úsečky představují standardní odchylky pozorovaných hodnot; statistická významnost byla vypočtena neparametrickým Tukeyho testem významnosti ($p \leq 0.05$ byla považována za statisticky významnou). (b) Exosomy z G361 vykazovaly typickou charakteristiku exosomů vzhledem k morfologii (elektronový mikroskop) a velikosti (*Nanoparticle tracking analysis*). Převzato a upraveno z publikace IX od Strnadová et al. (2022).

Vliv exosomů na fibroblasty byl dále studován na trojrozměrném modelu mimikujícím dermis. Krátkodobá kultivace s exosomy v médiu ukázala zrychlení invaze kolagenovým gelem jak v případě nádorově-asociovaných fibroblastů, tak u normálních dermálních fibroblastů.

Ve 3D podmínkách byl efekt exosomů zkoumán i dlouhodoběji po dobu 7 dní. Kompozitní sféroidy vytvořené metodou visící kapky obsahovaly kromě fibroblastů i buňky melanomu a byly spolu s exosomy imobilizovány v kolagenovém gelu. Na snímcích z elektronového mikroskopu bylo pozorováno, že exosomy si uchovávají své strukturní vlastnosti mezi vlákny kolagenu. Invaze nádorových buněk pak ukázala, že model s nádorově asociovanými fibroblasty potencovaný přidanými exosomy zesiluje invazivní potenciál melanomových buněk signifikantně. V kontrolním případě s normálními fibroblasty však výsledky nedosáhly hranice pro signifikantní rozdíl.

Na molekulární úrovni byly fibroblasty hodnoceny na Ústavu molekulární genetiky Akademie věd České republiky. Po 72hodinové kultivaci obou typů fibroblastů s exosomy byla izolovaná jejich RNA. Transkriptomická analýza (Obr. 25) ukázala, že u obou typů fibroblastů dochází pod vlivem exosomů k reorganizaci genů pro extracelulární matrix, např. zvýšením exprese genů pro MMP. To koreluje s výsledky, kdy samotné fibroblasty zrychlují svou invazi kolagenovým gelem. Nádorově-asociované fibroblasty pod vlivem exosomů zvyšují expresi genů pro cytokiny a chemokiny, např. *IL-6* a *CXCL8*, čímž ustanovují prozánětlivý charakter nádorového mikroprostředí podporující progresi nádoru.

Zajímavým zjištěním byla rozdílná exprese dvou proteinů: IL1RA a thrombospondinu-1. IL1RA je receptorem pro IL-33 a je zvýšen pod vlivem exosomů u nádorově-asociovaných fibroblastů. Je znám pro svojí roli při nádorové progresi (Mantovani et al. 2018). Naopak thrombospondin-1 je u těchto fibroblastů pod vlivem exosomů snížen. Jiná data ukazují, že exprese tohoto proteinu u buněk melanomu inhibuje progresi nádoru. Na druhou stranu zvýšená exprese tohoto proteinu u stromálních buněk kožního melanomu je spjata se sníženým přežíváním (Trotter et al. 2003).

Hlavním výstupem této publikace tedy je, že exosomy hrají významnou roli v mezibuněčné komunikaci mezi nádorem a ostatními buňkami nádorového mikroprostředí. Bylo zjištěno, že tyto malé extracelulární váčky, izolované z buněk maligního melanomu, stimulují prozánětlivé chování nádorově-asociovaných fibroblastů a že změnou těchto vlastností podporují šíření nádoru. Publikace dále prokazuje, jak

dramaticky se mohou měnit biologické vlastnosti nádoru při použití 2D a 3D kultivačních technik.

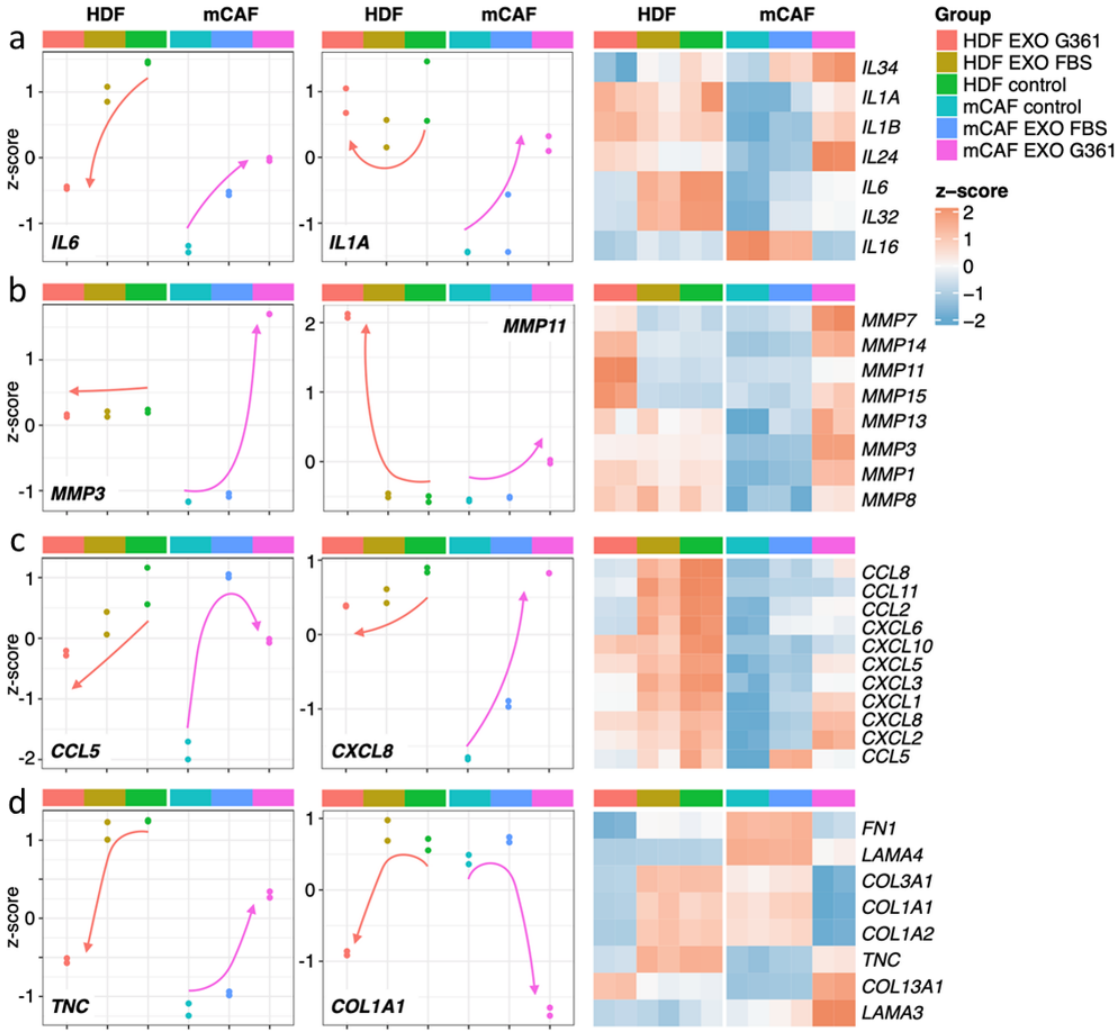

Obr. 25 Transkriptomická analýza HDF a mCAF pod vlivem exosomů. Grafy ukazují změny v genové expresi u HDF nebo mCAF, které byly stimulovány exosomy z G361 (EXO G361) nebo FBS (EXO FBS) po dobu 72 hod. Celkový trend je označen oranžovou (HDF) nebo růžovou (mCAF) šipkou. Panel (a) představuje genové změny s důrazem na interleukiny, kdy lze pozorovat např. nárůst exprese *IL6* u mCAF EXO G361. Panel (b) ukazuje změny v expresi matrix metaloproteináz. Převážně dochází ke zvýšené expresi u mCAF EXO G361, ale i u některých vybraných genů pro MMP lze pozorovat jejich zvýšenou expresi u HDF EXO G361. Panel (c) ukazuje změny v expresi chemokinů, jejichž zvýšená exprese je pozorována u stimulovaných mCAF. Panel (d) znázorňuje změny na úrovni mRNA pro molekuly extracelulární matrix. Opačný trend byl pozorován u genu pro *TNC* (*tenascin-C*), jehož protein je bohatou molekulou nádorového mikroprostředí mnoha nádorů. Převzato a upraveno z publikace IX od Strnadová et al. (2022).

7 Závěr a zhodnocení cílů

Tato disertační práce pojednává o fenotypu melanocytů za fyziologických a převážně patologických podmínek, které modelově představuje zhoubné onemocnění kůže – maligní melanom. O souvislostech změn kůže v průběhu stárnutí organismu a zvýšené incidenci maligního melanomu nebo obecně nádorů v populaci pojednávají dva přehledové články II a VII. V nich je diskutováno, jak je stárnutí zapříčiněno exogenními a endogenními vlivy, přičemž stárnutí kůže významně ovlivňuje zejména fyzikální faktor UV záření. Stárnutí organismu a dlouhodobé vystavení těmto radiačním vlivům je následně doprovázeno poškozením DNA, deregulací biologických pochodů v tkáních těla, přechodem buněk do senescence a zvýšeným prozánětlivým laděním mikroprostředí organismu. V souvislosti s produkcí prozánětlivých molekul, např. IL-6, je vytvářen chronický zánět, který v lidském těle usnadňuje vznik nádorových procesů. Nádor si pak ve tkáni dále průběžně dotváří své mikroprostředí. Dominantní roli v tomto mikroprostředí mají nádorově-asociované fibroblasty, které podporují nádorovou progresi. Kvalitní lékařská péče umožňuje přežití lidí do vyššího věku, než tomu bylo v minulosti. Na druhou stranu dochází čím dál častěji k rozvoji civilizačních chorob, které odrážejí negativní vlivy moderního životního stylu, vystavení dlouhodobému stresu či nedostatku fyzické aktivity. Jedním z takových civilizačních břemen jsou i maligní nádory. Lze tedy říct, že zvýšená incidence maligního melanomu, či obecně nádorových onemocnění, souvisí se stárnutím populace, které je doprovázeno u jednotlivců buněčnými a tkáňovými změnami, které usnadňují vznik nádorů.

Včasná detekce maligního melanomu představuje do současnosti zásadní krok zlepšující prognózu pacienta. V publikaci III byla analyzována séra pacientů trpících maligním melanomem a byly identifikovány některé cytokiny (např. IL-6), chemokiny (např. IL-8) a růstové faktory (např. VEGF), které reflektují změny na úrovni organismu v době diagnózy nebo v průběhu progrese onemocnění. Bohužel, konvenčně používané diagnostické screeningové metody (např. různé varianty sérologie) u maligního melanomu nejsou v současnosti považovány za významně přínosné. Důraz je tedy v onkologickém výzkumu nutno klást také na inovativní technologie a mezioborovou spolupráci. V publikaci IV byly proto experimentálně sledovány změny kondiciovaných médií připravených z kultur nádorových a nenádorových buněk. Kondiciovaná média můžeme pokládat za analogii komplexních biologických tekutin analyzovaných

v klinické medicíně. Tato média byla studována inovativní technologií, s uplatněním plazmoniky a SERS.

Identifikace vhodných sérových biomarkerů a nových přístupů, které jsme vyzkoušeli v publikaci III a IV, by mohly obohatit dosavadní úzkou škálu diagnostických, či screeningových metod a přispět k rychlejšímu a správnějšímu rozhodování při diagnostice a léčbě například právě maligního melanomu.

Výše zmíněná kondiciovaná média jsou tradičním přístupem k získávání materiálu zejména pro biochemickou analýzu z tkáňových kultur. Úspěšné modelování maligního melanomu ale vyžaduje komplexní přístup a zapojení jeho nádorového mikroprostředí. V současnosti je tedy patrná tendence k optimalizaci kultur hlavně ve 3D podmínkách, protože ty optimálně odráží biologické chování nádoru. Ve studii I byl demonstrován vliv látek secernovaných nádorově-asociovanými fibroblasty spolu s ozářenými keratinocyty na invazi buněk melanomu v *in vitro* podmínkách. Bylo potvrzeno, že dlouhodobější vystavení UV záření v menších dávkách a sekrece aktivních biomolekul buňkami kůže zvyšuje invazi nádorových buněk z 3D modelu melanomu v podobě homogenních sféroidů. V publikaci VIII byly obdobně využity heterogenní sféroidy pro modelování melanomu s důrazem na interakce nádorové populace s juvenilními neozářenými či aktinicky poškozenými fibroblasty mimikujícími mikroprostředí. Prostřednictvím single-cell RNA sekvenování a bioinformatické analýzy bylo zjištěno, že fibroblasty vytváří v modelu nádoru různě diferencované skupiny na základě svých vlastností a chovají se v prostředí nádoru jinak. Převážná část populace fibroblastů je zodpovědná za produkci extracelulární matrix, druhá skupina se vymezuje expresí genů pro TGFß signální kaskádu a třetí klastr fibroblastů je zajímavý pro svou expresi genů zánětu. Příkladem je produkce IL-6 podporující maligní chování nádoru.

V prostředí nádorových kultur může zvyšovat řízeně míru komplexity modelu jen do určité míry. Do současnosti platí, že z mnoha důvodů je pro mnoho experimentů kriticky významné jejich ověření na zvířecím modelu. V publikaci V bylo tedy nádorové mikroprostředí modelováno *in ovo* prostřednictvím CAM kuřete, na které byly transplantovány buňky melanomu. Výsledky naznačují, že komponenty CAM podporují nádor v růstu, ale jejich intravaskulární nebo intrastromální invazivní potenciál byl detekován pouze výjimečně. Důvodem může být krátkodobá kultivace z důvodu líhnutí kuřete nebo biologické vlastnosti CAM. Všechny tři uvedené modely napomáhají lépe pochopit chování nádoru, než je tomu u planárních kultivací *in vitro*.

Jestliže přehledový článek VI shrnuje poznatky o mezibuněčné komunikaci u kožního maligního melanomu a jeho diseminaci v těle pacienta, je na místě snažit se i o mechanistické sledování těchto dějů. V poslední publikaci zařazené do této disertační práce (publikace IX) jsme se tedy zaměřili na exosomy jako informační nosiče mezibuněčné komunikace. Exosomy vznikají exocytózou a umožňují předání informace z buňky zdrojové buňkám okolním. Exosomy mohou ale přecházet i do cirkulujících tělesných tekutin a ovlivňovat i struktury organismu značně vzdálené. Tato studie se zaměřila v kontextu této disertace zejména na rozdíly v chování zdravých fibroblastů a mCAF v přítomnosti exosomů z buněčné linie melanomu. mCAF se pod vlivem exosomů více aktivují a vzrůstá u nich exprese prozánětlivých molekul na úrovni mRNA.

Maligní melanom je jedno z nejagresivnějších maligních kožních onemocnění, které vzniká neoplastickou transformací a proliferací melanocytů. V této disertační práci byly sledovány souvislosti mezi stárnutím kůže a zvýšenou incidencí maligního melanomu. Solidní nádory vyžadují pro svůj růst a šíření specifické nádorové mikroprostředí, ve kterém dominantní roli sehrává populace nádorově-asociovaných fibroblastů. Mnoho z faktorů považovaných za typické rysy sekretomu v senescenci překvapivě sehrává významnou podpůrnou roli v nádorových procesech. Tento nádorový ekosystém jsme modelovali ve 3D podmínkách za použití různých fibroblastů a potvrdili jsme tak, jak značnou roli hraje exprese prozánětlivých molekul podporujících vhodné prostředí pro růst nádoru. Kromě této parakrinní komunikace solubilními molekulami je důležitou součástí informačního toku nádorového prostředí i komunikace prostřednictvím exosomů. Exosomy aktivují nádorově-asociované fibroblasty a napomáhají invazi nádorových buněk.

Diagnostika a léčba maligního melanomu je do současnosti považována klinickými onkology za mimořádně náročnou problematiku. Je tedy potřeba nacházet i nadále nové metody a přístupy, které by v tomto snažení napomohly. Některé tyto trendy by mohly mít východisko v publikacích prezentovaných v této disertační práci.

8 Souhrn

- Kůže je v průběhu života vystavována ultrafialovému záření a dalším fyzikálním, biologickým, či chemickým faktorům, které ji poškozují. Kumulativním působením těchto škodlivých vlivů dochází ke změnám na úrovni tkáně, buněk i

jejich genetické informace. Aktinické poškození kůže UV zářením je jednou z hlavních příčin pro vznik maligního melanomu. Důvodem, proč je populačně u starších jedinců větší riziko vzniku nádorového onemocnění včetně melanomu, je právě kumulace poškození tkáně v průběhu stárnutí. To vede navíc k chronicky prozánětlivému ladění tkáňového mikroprostředí, které rozvoj nádoru usnadňuje. S věkem také současně klesá i schopnost organismu se mutacím aktivně bránit jejich opravou.

- Sekretom UV ozářených keratinocytů a nádorově-asociovaných fibroblastů zvyšuje invazi buněk melanomu ze sféroidů v kolagenovém gelu. Tento model poukazuje na synergii vlivu nádorového mikroprostředí a UV radiace na progresi maligního melanomu.
- Model heterogenních sféroidů složených z buněk melanomu a rozdílně aktinicky zatížených fibroblastů byl podroben single-cell RNA sekvenování a bioinformatické analýze. Z té vyplývá, že fibroblasty se v přítomnosti nádorových buněk rozdělují do klastrů na základě své genové exprese. Fakt, že stárnutí a stres plynoucí z poškození buněk je důležitým faktorem pro vývoj maligního onemocnění včetně melanomu, dokladuje i nález, že jeden z klastrů aktinicky poškozených fibroblastů významně exprimuje geny prozánětlivých mediátorů.
- Chorioalantoidní membrána kuřete je vhodným komplexním modelem pro studium nádorové neovaskularizace, ale při studiu invazivního chování maligního melanomu má tento přístup své určité limity.
- Exosomy hrají významnou roli v mezibuněčné komunikaci mezi nádorem a ostatními buňkami nádorového mikroprostředí. Stimulují prozánětlivé chování nádorově-asociovaných fibroblastů, čímž podporují nádorový růst.
- Časná detekce maligního melanomu představuje lepší prognózu pacienta. Z analýzy sér pacientů s maligním melanomem vyplývá, že je přítomnost primárního nádoru významně spojena se sníženými hladinami IL-2, IL-13, RANTES a zvýšenými hladinami IL1RA, MIP-1ß a EGF. Progrese nádoru je stimulována IL-6 a IL-8, jejichž výskyt koreluje s nepříznivými hodnotami Breslowovy klasifikace.

9 Summary

- The skin is exposed to ultraviolet radiation and other physical, biological, or chemical factors during life. The cumulative effect of these harmful effects leads to changes in the level of tissue, cells, and their genetic information. Actinic damage to the skin by UV radiation is one of the main causes of malignant melanoma. The elderly people have a greater risk of developing cancer because of the cumulative tissue damage during ageing. This leads to chronically proinflammatory tuning of the tissue microenvironment. Furthermore, the ability of a body to resist mutations is decreasing with age.
- Secretome of UV-irradiated keratinocytes and cancer-associated fibroblasts increased the invasion of melanoma cells from spheroids in the collagen gel. This model showed the influence of the tumour microenvironment and UV radiation on the progression of malignant melanoma.
- A model of heterogeneous spheroids composed of melanoma cells and otherwise actinically damaged fibroblasts was subjected to single-cell RNA sequencing and bioinformatic analysis. The fibroblasts were distinguished into clusters based on their gene expression in the presence of a tumour. The claim that ageing and endogenous cell damage are the important factors in the adverse development of malignant melanoma is confirmed by the fact that one of the clusters of actinically damaged fibroblasts expressed genes for inflammation.
- The chicken chorioallantoic membrane is a suitable model for the study of neovascularization, but it found its limits in the study of the invasive behavior of malignant melanoma.
- Exosomes play an important role in intercellular communication between the tumour and other cells of the tumour microenviroment. They stimulated the proinflammatory behavior of cancer-associated fibroblasts, thereby promoting the tumour growth.
- Early detection of malignant melanoma represents a better prognosis of the patient. Analysis of sera from patients with malignant melanoma showed that the presence of the primary tumour was significantly associated with decreased levels of IL-2, IL-13, RANTES and increased levels of IL1RA, MIP-1ß and EGF. Tumour progression was stimulated by IL-6 and IL-8, the occurence of which correlated with unfavorable Breslow classification values.

10 Seznam použité literatury

Aasen S. N., Parajuli H., Hoang T., Feng Z., Stokke K., Wang J., Roy K., Bjerkvig R., Knappskog S., Thorsen F. (2019) Effective treatment of metastatic melanoma by combining mapk and pi3k signaling pathway inhibitors. *Int. J. Mol. Sci.* **20**, 1–19.

Abbasi N. R., Shaw H. M., Rigel D. S., Friedman R. J., McCarthy W. H., Osman I., Kopf A. W., Polsky D. (2004) Early Diagnosis of Cutaneous Melanoma Revisiting the ABCD Criteria. *JAMA* **292**, 2771–2776.

Abdel-Malek Z., Scott M. C., Suzuki I., Tada A., Im S., Lamoreux L., Ito S., Barsh G., Hearing V. J. (2000) The melanocortin-1 receptor is a key regulator of human cutaneous pigmentation. *Pigment Cell Res.* **13**, 156–162.

Abraham J., Stenger M. (2014) Dabrafenib in advanced melanoma with BRAF V600E mutation. *J. community Support. Oncol.* **12**, 48–49.

Achilli T. M., Meyer J., Morgan J. R. (2012) Advances in the formation, use and understanding of multi-cellular spheroids. *Expert Opin. Biol. Ther.* **12**, 1347–1360.

Acosta J. C., Banito A., Wuestefeld T., Georgilis A., Janich P., Morton J. P., Athineos D., Kang T., Lasitschka F., Andrulis M., Pascual G., Morris K. J., Khan S., Jin H., Dharmalingam G., Snijders A. P., Carroll T., Capper D., Pritchard C., Inman G. J., Longerich T., Sansom O. J., Benitah S. A., Zender L., Gil J. (2013) A complex secretory program orchestrated by the inflammasome controls paracrine senescence. *Nat. Cell Biol.* **15**, 978–990.

Aijian A. P., Garrell R. L. (2015) Digital Microfluidics for Automated Hanging Drop Cell Spheroid Culture. *SLAS Technol.* **20**, 283–295.

Akers J. C., Gonda D., Kim R., Carter B. S., Chen C. C. (2013) Biogenesis of extracellular vesicles (EV): exosomes, microvesicles, retrovirus-like vesicles, and apoptotic bodies. *J. Neurooncol.* **113**, 1–11.

Allen T. M., Brehm M. A., Bridges S., Ferguson S., Kumar P., Mirochnitchenko O., Palucka K., Pelanda R., Sanders-Beer B., Shultz L. D., Su L., PrabhuDas M. (2019) Humanized immune system mouse models: progress, challenges and opportunities. *Nat. Immunol.* **20**, 770–774.

Amaro-Ortiz A., Yan B., D'Orazio J. A. (2014) Ultraviolet radiation, aging and the skin: Prevention of damage by topical cAMP manipulation. *Molecules* **19**, 6202–6219.

Anada T., Pan C.-C., Stahl A., Mori S., Fukuda J., Suzuki O., Yang Y. (2019) Vascularized Bone-Mimetic Hydrogel Constructs by 3D Bioprinting to Promote Osteogenesis and Angiogenesis. *Int. J. Mol. Sci.* **20**, 1096.

Ancans J., Tobin D. J., Hoogduijn M. J., Smit N. P., Wakamatsu K., Thody A. J. (2001) Melanosomal pH controls rate of melanogenesis, eumelanin/phaeomelanin ratio and melanosome maturation in melanocytes and melanoma cells. *Exp. Cell Res.* **268**, 26–35.

Ansary T. M., Hossain M. R., Kamiya K., Komine M., Ohtsuki M. (2021) Inflammatory Molecules Associated with Ultraviolet Radiation-Mediated Skin Aging. *Int. J. Mol. Sci.* **22**, 3974.

Aoki H., Tomita H., Hara A., Kunisada T. (2015) Conditional deletion of kit in melanocytes: White spotting phenotype is cell autonomous. *J. Invest. Dermatol.* **135**, 1829–1838.

Aref A. R., Campisi M., Ivanova E., Portell A., Larios D., Piel B. P., Mathur N., Zhou C., Coakley R. V., Bartels A., Bowden M., Herbert Z., Hill S., Gilhooley S., Carter J., Cañadas I., Thai T. C., Kitajima S., Chiono V., Paweletz C. P., Barbie D. A., Kamm R. D., Jenkins R. W. (2018) 3D microfluidic ex vivo culture of organotypic tumor

spheroids to model immune checkpoint blockade. *Lab Chip* **18**, 3129–3143.
Argenyi Z. B. (1997) DERMOSCOPY (EPILUMINESCENCE MICROSCOPY) OF PIGMENTED SKIN LESIONS: Current Status and Evolving Trends. *Dermatol. Clin.* **15**, 79–95.
Aronheim A., Engelberg D., Li N., Al-Alawi N., Schlessinger J., Karin M. (1994) Membrane targeting of the nucleotide exchange factor Sos is sufficient for activating the Ras signaling pathway. *Cell* **78**, 949–961.
Avram S., Coricovac D. E., Pavel I. Z., Pinzaru I., Ghiulai R., Baderca F., Soica C., Muntean D., Branisteanu D. E., Spandidos D. A., Tsatsakis A. M., Dehelean C. A. (2017) Standardization of A375 human melanoma models on chicken embryo chorioallantoic membrane and Balb/c nude mice. *Oncol. Rep.* **38**, 89–99.
Aydin I. T., Hummler E., Smit N. P. M., Beermann F. (2012) Coat color dilution in mice because of inactivation of the melanoma antigen MART-1. *Pigment Cell Melanoma Res.* **25**, 37–46.
Bai L. P., Lv J. X., Kong L. W., Cao H. Y., Jin Y. (2021) Application of modified closed biopsy in rabbit model of VX2-transplanted bone tumor. *J. Orthop. Surg. Res.* **16**, 1–8.
Bajčiová V. (2016) Maligní melanom a nové možnosti jeho léčby. *Onkol. (Czech Republic)* **10**, 256–262.
Balamurugan K. (2016) HIF-1 at the crossroads of hypoxia, inflammation, and cancer. *Int. J. Cancer* **138**, 1058–1066.
Balch C. M., Gershenwald J. E., Soong S. J., Thompson J. F., Atkins M. B., Byrd D. R., Buzaid A. C., Cochran A. J., Coit D. G., Ding S., Eggermont A. M., Flaherty K. T., Gimotty P. A., Kirkwood J. M., McMasters K. M., Mihm M. C., Morton D. L., Ross M. I., Sober A. J., Sondak V. K. (2009) Final version of 2009 AJCC melanoma staging and classification. *J. Clin. Oncol.* **27**, 6199–6206.
Basurto-Lozada P., Molina-Aguilar C., Castaneda-Garcia C., Vázquez-Cruz M. E., Garcia-Salinas O. I., Álvarez-Cano A., Martínez-Said H., Roldán-Marín R., Adams D. J., Possik P. A., Robles-Espinoza C. D. (2021) Acral lentiginous melanoma: Basic facts, biological characteristics and research perspectives of an understudied disease. *Pigment Cell Melanoma Res.* **34**, 59–71.
Belotti D., Vergani V., Drudis T., Borsotti P., Pitelli M. R., Viale G., Giavazzi R., Taraboletti G. (1996) The microtubule-affecting drug paclitaxel has antiangiogenic activity. *Clin. Cancer Res.* **2**, 1843–9.
Benien P., Swami A. (2014) 3D tumor models: History, advances and future perspectives. *Futur. Oncol.* **10**, 1311–1327.
Bergqvist C., Ezzedine K. (2020) Vitiligo: A Review. *Dermatology* **236**, 571–592.
Bertrand J. U., Steingrimsson E., Jouenne F., Bressac-De Paillerets B., Larue L. (2020) Melanoma risk and melanocyte biology. *Acta Derm. Venereol.* **100**, 272–283.
Bettahar F., Bekkar F., Pérez-Álvarez L., Ferahi M. I., Meghabar R., Vilas-Vilela J. L., Ruiz-Rubio L. (2021) Tough Hydrogels Based on Maleic Anhydride, Bulk Properties Study and Microfiber Formation by Electrospinning. *Polymers (Basel).* **13**, 972.
Bissig C., Rochin L., Niel G. van (2016) PMEL Amyloid Fibril Formation: The Bright Steps of Pigmentation. *Int. J. Mol. Sci.* **17**, 1438.
Bocci G., Paolo A. Di, Danesi R. (2013) The pharmacological bases of the antiangiogenic activity of paclitaxel. *Angiogenesis* **16**, 481–492.
Bondurand N., Pingault V., Goerich D. E., Lemort N., Sock E., Caignec C. Le, Wegner M., Goossens M. (2000) Interaction among SOX10, PAX3 and MITF, three genes altered in Waardenburg syndrome. *Hum. Mol. Genet.* **9**, 1907–1917.

Böni R., Burg G., Doguoglu A., Ilg E. C., Schäfer B. W., Müller B., Heizmann C. W. (1997) Immunohistochemical localization of the Ca2+ binding S100 proteins in normal human skin and melanocytic lesions. *Br. J. Dermatol.* **137**, 39–43.

Bootorabi F., Manouchehri H., Changizi R., Barker H., Palazzo E., Saltari A., Parikka M., Pincelli C., Aspatwar A. (2017) Zebrafish as a model organism for the development of drugs for skin cancer. *Int. J. Mol. Sci.* **18**, 1–15.

Bourland J., Fradette J., Auger F. A. (2018) Tissue-engineered 3D melanoma model with blood and lymphatic capillaries for drug development. *Sci. Rep.* **8**, 1–13.

Bourneuf E. (2017) The MeLiM minipig: An original spontaneous model to explore cutaneous melanoma genetic basis. *Front. Genet.* **8**, 1–12.

Brábek J., Jakubek M., Vellieux F., Novotný J., Kolář M., Lacina L., Szabo P., Strnadová K., Rösel D., Dvořánková B., Smetana K. (2020) Interleukin-6: Molecule in the Intersection of Cancer, Ageing and COVID-19. *Int. J. Mol. Sci.* **21**, 7937.

Bracher A., Cardona A. S., Tauber S., Fink A. M., Steiner A., Pehamberger H., Niederleithner H., Petzelbauer P., Gröger M., Loewe R. (2013) Epidermal growth factor facilitates melanoma lymph node metastasis by influencing tumor lymphangiogenesis. *J. Invest. Dermatol.* **133**, 230–238.

Breslow A. (1970) Thickness, cross-sectional areas and depth of invasion in the prognosis of cutaneous melanoma. *Ann. Surg.* **172**, 902–908.

Brettmann E. A., Guzman Strong C. de (2018) Recent evolution of the human skin barrier. *Exp. Dermatol.* **27**, 859–866.

Buchbinder E. I., Desai A. (2016) CTLA-4 and PD-1 Pathways. *Am. J. Clin. Oncol.* **39**, 98–106.

Buday L., Downward J. (1993) Epidermal growth factor regulates p21ras through the formation of a complex of receptor, Grb2 adapter protein, and Sos nucleotide exchange factor. *Cell* **73**, 611–620.

Burggren W., Antich M. R. (2020) Angiogenesis in the avian embryo chorioallantoic membrane: A perspective on research trends and a case study on toxicant vascular effects. *J. Cardiovasc. Dev. Dis.* **7**, 1–18.

Campisi J. (2005) Senescent Cells, Tumor Suppression, and Organismal Aging: Good Citizens, Bad Neighbors. *Cell* **120**, 513–522.

Carlino M. S., Long G. V. (2016) Ipilimumab combined with nivolumab: A standard of care for the treatment of advanced melanoma? *Clin. Cancer Res.* **22**, 3992–3998.

Casalou C., Moreiras H., Mayatra J. M., Fabre A., Tobin D. J. (2022) Loss of 'Epidermal Melanin Unit' Integrity in Human Skin During Melanoma-Genesis. *Front. Oncol.* **12**, 1–14.

Chambers E. S., Vukmanovic-Stejic M. (2020) Skin barrier immunity and ageing. *Immunology* **160**, 116–125.

Chamcheu J. C., Roy T., Uddin M. B., Banang-mbeumi S., Chamcheu R. N., Walker A. L., Liu Y., Huang S. (2019) Role and Therapeutic Targeting of the PI3K / Akt / mTOR Signaling Pathway in Skin Cancer : Natural and Synthetic Agents Therapy. *Cells* **8**, 1–33.

Chen G., Huang A. C., Zhang W., Zhang G., Wu M., Xu W., Yu Z., Yang J., Wang B., Sun H., Xia H., Man Q., Zhong W., Antelo L. F., Wu B., Xiong X., Liu X., Guan L., Li T., Liu S., Yang R., Lu Y., Dong L., McGettigan S., Somasundaram R., Radhakrishnan R., Mills G., Lu Y., Kim J., Chen Y. H., Dong H., Zhao Y., Karakousis G. C., Mitchell T. C., Schuchter L. M., Herlyn M., Wherry E. J., Xu X., Guo W. (2018a) Exosomal PD-L1 contributes to immunosuppression and is associated with anti-PD-1 response. *Nature* **560**, 382–386.

Chen Y. N., Jiao C., Zhao Y., Zhang J., Wang H. (2018b) Self-Assembled Polyvinyl

Alcohol-Tannic Acid Hydrogels with Diverse Microstructures and Good Mechanical Properties. *ACS Omega* **3**, 11788–11795.
Cheong K. A., Noh M., Kim C. H., Lee A. Y. (2014) S100B as a potential biomarker for the detection of cytotoxicity of melanocytes. *Exp. Dermatol.* **23**, 165–171.
Chiew G. G. Y., Wei N., Sultania S., Lim S., Luo K. Q. (2017) Bioengineered three-dimensional co-culture of cancer cells and endothelial cells: A model system for dual analysis of tumor growth and angiogenesis. *Biotechnol. Bioeng.* **114**, 1865–1877.
Chu P.-Y., Koh A. P.-F., Antony J., Huang R. Y.-J. (2022) Applications of the Chick Chorioallantoic Membrane as an Alternative Model for Cancer Studies. *Cells Tissues Organs* **211**, 222–237.
Cichorek M., Wachulska M., Stasiewicz A., Tymińska A. (2013) Skin melanocytes: biology and development. *Adv. Dermatology Allergol.* **1**, 30–41.
Clark W. H. (1967) A classification of malignant melanoma in man correlated with histogenesis and clinical behavior. *Adv. Biol. Ski. Pigment. Syst.* **8**, 621–645.
Clark W. H., From L., Bernardino E. A., Mihm M. C. (1969) The Histogenesis and Biologic Behavior of Primary Human Malignant Melanomas of the Skin. *Cancer Res.* **29**, 705–727.
Cole M. A., Quan T., Voorhees J. J., Fisher G. J. (2018) Extracellular matrix regulation of fibroblast function: redefining our perspective on skin aging. *J. Cell Commun. Signal.* **12**, 35–43.
Coluccio M. L., Perozziello G., Malara N., Parrotta E., Zhang P., Gentile F., Limongi T., Raj P. M., Cuda G., Candeloro P., Fabrizio E. Di (2019) Microfluidic platforms for cell cultures and investigations. *Microelectron. Eng.* **208**, 14–28.
Couto G. de (2019) Macrophages in cardiac repair: Environmental cues and therapeutic strategies. *Exp. Mol. Med.* **51**, 1–10.
Cui J., Shen L.-Y., Wang G. (1991) Role of Hair Follicles in the Repigmentation of Vitiligo. *J. Invest. Dermatol.* **97**, 410–416.
Cui R., Widlund H. R., Feige E., Lin J. Y., Wilensky D. L., Igras V. E., D'Orazio J., Fung C. Y., Schanbacher C. F., Granter S. R., Fisher D. E. (2007) Central Role of p53 in the Suntan Response and Pathologic Hyperpigmentation. *Cell* **128**, 853–864.
Czarnecka A. M., Bartnik E., Fiedorowicz M., Rutkowski P. (2020) Targeted therapy in melanoma and mechanisms of resistance. *Int. J. Mol. Sci.* **21**, 1–21.
D'Alba L., Shawkey M. D. (2019) Melanosomes: Biogenesis, properties, and evolution of an ancient organelle. *Physiol. Rev.* **99**, 1–19.
D'Mello S. A. N., Finlay G. J., Baguley B. C., Askarian-Amiri M. E. (2016) Signaling pathways in melanogenesis. *Int. J. Mol. Sci.* **17**, 1–18.
Davies M. A. (2012) The Role of the PI3K-AKT Pathway in Melanoma. *Cancer J.* **18**, 142–147.
Dennison K. L., Samanas N. B., Harenda Q. E., Hickman M. P., Seiler N. L., Ding L., Shull J. D. (2015) Development and characterization of a novel rat model of estrogen-induced mammary cancer. *Endocr. Relat. Cancer* **22**, 239–248.
Donato R., R. Cannon B., Sorci G., Riuzzi F., Hsu K., J. Weber D., L. Geczy C. (2012) Functions of S100 Proteins. *Curr. Mol. Med.* **13**, 24–57.
Dong X., Wang Y., Qu Y., Liu J., Feng X., Xu X. (2021) MicroRNA-603 Promotes Progression of Cutaneous Melanoma by Regulating TBX5. *Comput. Math. Methods Med.* **2021**, 1–11.
Dreesen O. (2020) Towards delineating the chain of events that cause premature senescence in the accelerated aging syndrome Hutchinson–Gilford progeria (HGPS). *Biochem. Soc. Trans.* **48**, 981–991.
Duong P., Chung A., Bouchareychas L., Raffai R. L. (2019) Cushioned-Density Gradient

Ultracentrifugation (C-DGUC) improves the isolation efficiency of extracellular vesicles. *PLoS One* **14**, 1–16.

Dyck R. H., Bogoch I. I., Marks A., Melvin N. R., Teskey G. C. (2002) Enhanced epileptogenesis in S100B knockout mice. *Mol. Brain Res.* **106**, 22–29.

Eberle J., Hossini A. (2008) Expression and Function of Bcl-2 Proteins in Melanoma. *Curr. Genomics* **9**, 409–419.

Eckert R. L., Broome A. M., Ruse M., Robinson N., Ryan D., Lee K. (2004) S100 proteins in the epidermis. *J. Invest. Dermatol.* **123**, 23–33.

Eckrich J., Kugler P., Buhr C. R., Ernst B. P., Mendler S., Baumgart J., Brieger J., Wiesmann N. (2020) Monitoring of tumor growth and vascularization with repetitive ultrasonography in the chicken chorioallantoic-membrane-assay. *Sci. Rep.* **10**, 1–14.

Erdag G., Chowdhuri S. R., Fetsch P., Erickson D., Hughes M. S., Filie A. C. (2013) KBA.62 and S100 protein expression in cytologic samples of metastatic malignant melanoma. *Diagn. Cytopathol.* **176**, 847–851.

Eroglu Z., Ribas A. (2016) Combination therapy with BRAF and MEK inhibitors for melanoma: Latest evidence and place in therapy. *Ther. Adv. Med. Oncol.* **8**, 48–56.

Fábián M., Rencz F., Krenács T., Brodszky V., Hársing J., Németh K., Balogh P., Kárpáti S. (2017) Expression of G protein-coupled oestrogen receptor in melanoma and in pregnancy-associated melanoma. *J. Eur. Acad. Dermatology Venereol.* **31**, 1453–1461.

Faghfuri E., Nikfar S., Niaz K., Faramarzi M. A., Abdollahi M. (2018) Mitogen-activated protein kinase (MEK) inhibitors to treat melanoma alone or in combination with other kinase inhibitors. *Expert Opin. Drug Metab. Toxicol.* **14**, 317–330.

Fitzpatrick T. B., Breathnach A. S. (1963) [THE EPIDERMAL MELANIN UNIT SYSTEM]. *Dermatol. Wochenschr.* **147**, 481–489.

Friedman R. J., Rigel D. S., Kopf A. W. (1985) Early detection of malignant melanoma: the role of physician examination and self-examination of the skin. *CA. Cancer J. Clin.* **35**, 130–151.

Fu C., Chen J., Lu J., Yi L., Tong X., Kang L., Pei S., Ouyang Y., Jiang L., Ding Y., Zhao X., Li S., Yang Y., Huang J., Zeng Q. (2020) Roles of inflammation factors in melanogenesis (Review). *Mol. Med. Rep.* **21**, 1421–1430.

Fuse N., Yasumoto K. I., Suzuki H., Takahashi K., Shibahara S. (1996) Identification of a melanocyte-type promoter of the microphthalmia-associated transcription factor gene. *Biochem. Biophys. Res. Commun.* **219**, 702–707.

Gaitán-Salvatella I., López-Villegas E. O., González-Alva P., Susate-Olmos F., Álvarez-Pérez M. A. (2021) Case Report: Formation of 3D Osteoblast Spheroid Under Magnetic Levitation for Bone Tissue Engineering. *Front. Mol. Biosci.* **8**, 1–10.

Gandalovičová A., Rosel D., Fernandes M., Veselý P., Heneberg P., Čermák V., Petruželka L., Kumar S., Sanz-Moreno V., Brábek J. (2017) Migrastatics—Anti-metastatic and Anti-invasion Drugs: Promises and Challenges. *Trends in Cancer* **3**, 391–406.

Gandini S., Sera F., Cattaruzza M. S., Pasquini P., Picconi O., Boyle P., Melchi C. F. (2005) Meta-analysis of risk factors for cutaneous melanoma: II. Sun exposure. *Eur. J. Cancer* **41**, 45–60.

Gershenwald J. E., Scolyer R. A., Hess K. R., Sondak V. K., Long G. V., Ross M. I., Lazar A. J., Faries M. B., Kirkwood J. M., McArthur G. A., Haydu L. E., Eggermont A. M. M., Flaherty K. T., Balch C. M., Thompson J. F. (2017) Melanoma staging: Evidence-based changes in the American Joint Committee on Cancer eighth edition cancer staging manual. *CA. Cancer J. Clin.* **67**, 472–492.

Gogas H. J., Kirkwood J. M., Sondak V. K. (2007) Chemotherapy for metastatic melanoma: Time for a change? *Cancer* **109**, 455–464.
Gupta A., Gomes F., Lorigan P. (2017) The role for chemotherapy in the modern management of melanoma. *Melanoma Manag.* **4**, 125–136.
Gupta P., Kar S., Kumar A., Tseng F. G., Pradhan S., Mahapatra P. S., Santra T. S. (2021) Pulsed laser assisted high-Throughput intracellular delivery in hanging drop based three dimensional cancer spheroids. *Analyst* **146**, 4756–4766.
Guyonneau L., Murisier F., Rossier A., Moulin A., Beermann F. (2004) Melanocytes and Pigmentation Are Affected in Dopachrome Tautomerase Knockout Mice. *Mol. Cell. Biol.* **24**, 3396–3403.
Hamburger V., Hamilton H. L. (1992) A series of normal stages in the development of the chick embryo. *Dev. Dyn.* **195**, 231–272.
Harlin H., Meng Y., Peterson A. C., Zha Y., Tretiakova M., Slingluff C., McKee M., Gajewski T. F. (2009) Chemokine Expression in Melanoma Metastases Associated with CD8+ T-Cell Recruitment. *Cancer Res.* **69**, 3077–3085.
Hasney C., Butcher R. B., Amedee R. G. (2008) Malignant melanoma of the head and neck: A brief review of pathophysiology, current staging, and management. *Ochsner J.* **8**, 181–185.
Hawkes J. E., Truong A., Meyer L. J. (2016) Genetic predisposition to melanoma. *Semin. Oncol.* **43**, 591–597.
Hayflick L., Moorhead P. S. (1961) The serial cultivation of human diploid cell strains. *Exp. Cell Res.* **25**, 585–621.
Hearing V. J., Jiménez M. (1987) Mammalian tyrosinase-The critical regulatory control point in melanocyte pigmentation. *Int. J. Biochem.* **19**, 1141–1147.
Heinzelmann-Schwarz V. A., Nixdorf S., Valadan M., Diczbalis M., Olivier J., Otton G., Fedier A., Hacker N. F., Scurry J. P. (2014) A clinicopathological review of 33 patients with vulvar melanoma identifies c-KIT as a prognostic marker. *Int. J. Mol. Med.* **33**, 784–794.
Hellström A. R., Watt B., Fard S. S., Tenza D., Mannström P., Narfström K., Ekesten B., Ito S., Wakamatsu K., Larsson J., Ulfendahl M., Kullander K., Raposo G., Kerje S., Hallböök F., Marks M. S., Andersson L. (2011) Inactivation of Pmel Alters Melanosome Shape But Has Only a Subtle Effect on Visible Pigmentation. *PLoS Genet.* **7**, e1002285.
Henning A. L., Jiang M. X., Yalcin H. C., Butcher J. T. (2011) Quantitative three-dimensional imaging of live avian embryonic morphogenesis via micro-computed tomography. *Dev. Dyn.* **240**, 1949–1957.
Hirschhaeuser F., Menne H., Dittfeld C., West J., Mueller-Klieser W., Kunz-Schughart L. A. (2010) Multicellular tumor spheroids: An underestimated tool is catching up again. *J. Biotechnol.* **148**, 3–15.
Hoashi T., Tamaki K., Hearing V. J. (2010) The secreted form of a melanocyte membrane-bound glycoprotein (Pmel17/gp100) is released by ectodomain shedding. *FASEB J.* **24**, 916–930.
Horak V., Palanova A., Cizkova J., Miltrova V., Vodicka P., Kupcova Skalnikova H. (2019) Melanoma-Bearing Libechov Minipig (MeLiM): The Unique Swine Model of Hereditary Metastatic Melanoma. *Genes (Basel).* **10**, 915.
Hornebeck W. (2003) Down-regulation of tissue inhibitor of matrix metalloprotease-1 (TIMP-1) in aged human skin contributes to matrix degradation and impaired cell growth and survival. *Pathol. Biol.* **51**, 569–573.
Hossain M. R., Ansary T. M., Komine M., Ohtsuki M. (2021) Diversified stimuli-induced inflammatory pathways cause skin pigmentation. *Int. J. Mol. Sci.* **22**.

Hu T., Hu J. (2019) Melanoma-derived exosomes induce reprogramming fibroblasts into cancer-associated fibroblasts via Gm26809 delivery. *Cell Cycle* **18**, 3085–3094.
Huang C., Lowerison M. R., Lucien F., Gong P., Wang D., Song P., Chen S. (2019) Noninvasive Contrast-Free 3D Evaluation of Tumor Angiogenesis with Ultrasensitive Ultrasound Microvessel Imaging. *Sci. Rep.* **9**, 1–11.
Huang X., Ding L., Bennewith K. L., Tong R. T., Welford S. M., Ang K. K., Story M., Le Q.-T., Giaccia A. J. (2009) Hypoxia-Inducible mir-210 Regulates Normoxic Gene Expression Involved in Tumor Initiation. *Mol. Cell* **35**, 856–867.
Hurley J. H. (2010) The ESCRT complexes. *Crit. Rev. Biochem. Mol. Biol.* **45**, 463–487.
Hurley J. H., Hanson P. I. (2010) Membrane budding and scission by the ESCRT machinery: it's all in the neck. *Nat. Rev. Mol. Cell Biol.* **11**, 556–566.
Imokawa G. (2019) Melanocyte activation mechanisms and rational therapeutic treatments of solar lentigos. *Int. J. Mol. Sci.* **20**, 3666.
Ioannidi L., Seliniotakis K., Bontzos G., Sourvinos G., Haniotis V., Tsiapa I., Maris T. G., Detorakis E. T. (2018) Surface-Coil MRI for Small Peripheral Choroidal Melanoma: Imaging in a Rabbit Eye Model. *Ocul. Oncol. Pathol.* **4**, 364–369.
Iznardo H., Garcia-Melendo C., Yélamos O. (2020) Lentigo maligna: Clinical presentation and appropriate management. *Clin. Cosmet. Investig. Dermatol.* **13**, 837–855.
Javeed N., Mukhopadhyay D. (2017) Exosomes and their role in the micro-/macro-environment: A comprehensive review. *J. Biomed. Res.* **31**, 386–394.
Jimenez R. E., Wallis T., Visscher D. W. (2001) Centrally necrotizing carcinomas of the breast : A distinct histologic subtype with aggressive clinical behavior. *Am. J. Surg. Pathol.* **25**, 331–337.
Jobe N. P., Živicová V., Mifková A., Rösel D., Dvořánková B., Kodet O., Strnad H., Kolář M., Šedo A., Smetana K., Strnadová K., Brábek J., Lacina L. (2018) Fibroblasts potentiate melanoma cells in vitro invasiveness induced by UV-irradiated keratinocytes. *Histochem. Cell Biol.* **149**, 503–516.
Joshi S. S., Tandukar B., Pan L., Huang J. M., Livak F., Smith B. J., Hodges T., Mahurkar A. A., Hornyak T. J. (2019) CD34 defines melanocyte stem cell subpopulations with distinct regenerative properties. *PLoS Genet.* **15**, 1–25.
Justus C. R., Leffler N., Ruiz-Echevarria M., Yang L. V. (2014) In vitro Cell Migration and Invasion Assays. *J. Vis. Exp.* 88, 1–8.
Kahlert C., Kalluri R. (2013) Exosomes in tumor microenvironment influence cancer progression and metastasis. *J. Mol. Med.* **91**, 431–437.
Kalluri R., LeBleu V. S. (2020) The biology , function , and biomedical applications of exosomes. *Science.* **367**.
Karagas M. R., Zens M. S., Nelson H. H., Mabuchi K., Perry A. E., Stukel T. A., Mott L. A., Andrew A. S., Applebaum K. M., Linet M. (2007) Measures of cumulative exposure from a standardized sun exposure history questionnaire: A comparison with histologic assessment of solar skin damage. *Am. J. Epidemiol.* **165**, 719–726.
Kawai T., Akira S. (2011) Toll-like Receptors and Their Crosstalk with Other Innate Receptors in Infection and Immunity. *Immunity* **34**, 637–650.
Kennedy D. C., Coen B., Wheatley A. M., McCullagh K. J. A. (2021) Microvascular Experimentation in the Chick Chorioallantoic Membrane as a Model for Screening Angiogenic Agents including from Gene-Modified Cells. *Int. J. Mol. Sci.* **23**, 452.
Kersten K., Visser K. E., Miltenburg M. H., Jonkers J. (2017) Genetically engineered mouse models in oncology research and cancer medicine. *EMBO Mol. Med.* **9**, 137–153.
Keung E. Z., Gershenwald J. E. (2018) The eighth edition American Joint Committee on

Cancer (AJCC) melanoma staging system: implications for melanoma treatment and care. *Expert Rev. Anticancer Ther.* **18**, 775–784.

Khair D. O., Bax H. J., Mele S., Crescioli S., Pellizzari G., Khiabany A., Nakamura M., Harris R. J., French E., Hoffmann R. M., Williams I. P., Cheung A., Thair B., Beales C. T., Touizer E., Signell A. W., Tasnova N. L., Spicer J. F., Josephs D. H., Geh J. L., Ross A. M. K., Healy C., Papa S., Lacy K. E., Karagiannis S. N. (2019) Combining immune checkpoint inhibitors: Established and emerging targets and strategies to improve outcomes in melanoma. *Front. Immunol.* **10**, 1–20.

Kim H., Kim M., Im S.-K., Fang S. (2018) Mouse Cre-LoxP system: general principles to determine tissue-specific roles of target genes. *Lab. Anim. Res.* **34**, 147.

Kim J. S., Min J., Recknagel A. K., Riccio M., Butcher J. T. (2011) Quantitative Three-Dimensional Analysis of Embryonic Chick Morphogenesis Via Microcomputed Tomography. *Anat. Rec.* **294**, spc1–spc1.

Kleinman H. K., McGarvey M. L., Liotta L. A., Robey P. G., Tryggvason K., Martin G. R. (1982) Isolation and characterization of type IV procollagen, laminin, and heparan sulfate proteoglycan from the EHS sarcoma. *Biochemistry* **21**, 6188–6193.

Klingenberg M., Becker J., Eberth S., Kube D., Wilting J. (2014) The chick chorioallantoic membrane as an in vivo xenograft model for Burkitt lymphoma. *BMC Cancer* **14**, 339.

Kodet O., Kučera J., Strnadová K., Dvořánková B., Štork J., Lacina L., Smetana K. (2020) Cutaneous melanoma dissemination is dependent on the malignant cell properties and factors of intercellular crosstalk in the cancer microenvironment (Review). *Int J Oncol* **57**, 619–630.

Kotze L. A., Beltran C. G. G., Lang D., Loxton A. G., Cooper S., Meiring M., Koegelenberg C. F. N., Allwood B. W., Malherbe S. T., Hiemstra A. M., Glanzmann B., Kinnear C., Walzl G., Plessis N. du (2021) Establishment of a Patient-Derived, Magnetic Levitation-Based, Three-Dimensional Spheroid Granuloma Model for Human Tuberculosis. *mSphere* **6**, 1–21.

Krajsová I. (2015) Imunoterapie metastazujícího melanomu. *Onkologie* **9**, 183–187.

Krajsová I. (2018) Diagnostika melanomu a současná doporučení pro léčbu a sledování. *Čes-slov Derm* 1, 4–16.

Kučera J., Strnadová K., Dvořánková B., Lacina L., Krajsová I., Štork J., Kovářová H., Skalníková H. K., Vodička P., Motlík J., Dundr P., Smetana K., Kodet O. (2019) Serum proteomic analysis of melanoma patients with immunohistochemical profiling of primary melanomas and cultured cells: Pilot study. *Oncol. Rep.* **42**, 1793–1804.

Kue C. S., Tan K. Y., Lam M. L., Lee H. B. (2014) Chick embryo chorioallantoic membrane (CAM): An alternative predictive model in acute toxicological studies for anti-cancer drugs. *Exp. Anim.* **64**, 129–138.

Lacina L., Kodet O., Dvořánková B., Szabo P., Smetana K. (2018) Ecology of melanoma cell. *Histol. Histopathol.* **33**, 247–254.

Lacina L., Plzak J., Kodet O., Szabo P., Chovanec M., Dvorankova B., Smetana K. (2015) Cancer microenvironment: What can we learn from the stem cell niche. *Int. J. Mol. Sci.* **16**, 24094–24110.

Lacina L., Smetana K., Dvořánková B., Pytlík R., Kideryová L., Kučerová L., Plzáková Z., Štork J., Gabius H. J., André S. (2007) Stromal fibroblasts from basal cell carcinoma affect phenotype of normal keratinocytes. *Br. J. Dermatol.* **156**, 819–829.

Lago J. C., Puzzi M. B. (2019) The effect of aging in primary human dermal fibroblasts. *PLoS One* **14**, 1–14.

Larkin J., Ascierto P. A., Dréno B., Atkinson V., Liszkay G., Maio M., Mandalà M.,

Demidov L., Stroyakovskiy D., Thomas L., la Cruz-Merino L. de, Dutriaux C., Garbe C., Sovak M. A., Chang I., Choong N., Hack S. P., McArthur G. A., Ribas A. (2014) Combined Vemurafenib and Cobimetinib in BRAF -Mutated Melanoma . *N. Engl. J. Med.* **371**, 1867–1876.

Larkin J., Chiarion-Sileni V., Gonzalez R., Jacques Grob J., Lao C. D., Schadendorf D., Dummer R., Smylie M., Rutkowski P., Francesco Ferrucci P., Hill A., Wagstaff J., Carlino M. S., Wolchok J. D., Hodi S., Jdw D. (2015) Combined Nivolumab and Ipilimumab or Monotherapy in Previously Untreated Melanoma Corresponding authors. *N Engl J Med* **373**, 23–34.

Legha S. S., Ring S., Papadopoulos N., Plager C., Chawla S., Benjamin R. (1989) A prospective evaluation of a triple-drug regimen containing cisplatin, vinblastine, and dacarbazine (CVD) for metastatic melanoma. *Cancer* **64**, 2024–2029.

Leonardi G. C., Falzone L., Salemi R., Zanghì A., Spandidos D. A., Mccubrey J. A., Candido S., Libra M. (2018) Cutaneous melanoma: From pathogenesis to therapy (Review). *Int. J. Oncol.* **52**, 1071–1080.

Li N., Fukunaga-Kalabis M., Yu H., Xu X., Kong J., Lee J. T., Herlyn M. (2010) Human dermal stem cells differentiate into functional epidermal melanocytes. *J. Cell Sci.* **123**, 853–860.

Li S., Bai S., Qin X., Zhang J., Irwin D. M., Zhang S., Wang Z. (2019) Comparison of whole embryonic development in the duck (Anas platyrhynchos) and goose (Anser cygnoides) with the chicken (Gallus gallus). *Poult. Sci.* **98**, 3278–3291.

Li Y., Zhao L., Li X. F. (2021) Hypoxia and the Tumor Microenvironment. *Technol. Cancer Res. Treat.* **20**, 1–9.

Liu S., Kumar S. M., Lu H., Liu A., Yang R., Pushparajan A., Guo W., Xu X. (2012) MicroRNA-9 up-regulates E-cadherin through inhibition of NF-κB1-Snail1 pathway in melanoma. *J. Pathol.* **226**, 61–72.

Lu C. Y., Lee H. C., Fahn H. J., Wei Y. H. (1999) Oxidative damage elicited by imbalance of free radical scavenging enzymes is associated with large-scale mtDNA deletions in aging human skin. *Mutat. Res. - Fundam. Mol. Mech. Mutagen.* **423**, 11–21.

Luan W., Ding Y., Xi H., Ruan H., Lu F., Ma S., Wang J. (2021) Exosomal miR-106b-5p derived from melanoma cell promotes primary melanocytes epithelial-mesenchymal transition through targeting EphA4. *J. Exp. Clin. Cancer Res.* **40**, 1–15.

Ma Y., Yoo J. (2021) History of sunscreen: An updated view. *J. Cosmet. Dermatol.* **20**, 1044–1049.

Mak S. S., Moriyama M., Nishioka E., Osawa M., Nishikawa S. I. (2006) Indispensable role of Bcl2 in the development of the melanocyte stem cell. *Dev. Biol.* **291**, 144–153.

Mantovani A., Barajon I., Garlanda C. (2018) IL-1 and IL-1 regulatory pathways in cancer progression and therapy. *Immunol. Rev.* **281**, 57–61.

Marks R. (2000) Epidemiology of melanoma. *Clin. Exp. Dermatol.* **25**, 459–463.

Masterpol K. S., Primiani A., Duncan L. M. (2013) Benign Melanocytic Proliferations with Pagetoid Spread BT - Atlas of Essential Dermatopathology, eds. Masterpol K. S., Primiani A., Duncan L. M., pp. 98–99, Springer London, London.

Mattei F., Schiavoni G., Ninno A. De, Lucarini V., Sestili P., Sistigu A., Fragale A., Sanchez M., Spada M., Gerardino A., Belardelli F., Businaro L., Gabriele L. (2014) A multidisciplinary study using in vivo tumor models and microfluidic cell-on-chip approach to explore the cross-talk between cancer and immune cells. *J. Immunotoxicol.* **11**, 337–346.

McCune J., Namikawa R., Kaneshima H., Shultz L., Lieberman M., Weissman I. (1988)

The SCID-hu mouse: murine model for the analysis of human hematolymphoid differentiation and function. *Science (80-.).* **241**, 1632–1639.
Mehling M., Tay S. (2014) Microfluidic cell culture. *Curr. Opin. Biotechnol.* **25**, 95–102.
Mestas J., Hughes C. C. W. (2004) Of Mice and Not Men: Differences between Mouse and Human Immunology. *J. Immunol.* **172**, 2731–2738.
Mittal M., Siddiqui M. R., Tran K., Reddy S. P., Malik A. B. (2014) Reactive oxygen species in inflammation and tissue injury. *Antioxidants Redox Signal.* **20**, 1126–1167.
Moor L. De, Fernandez S., Vercruysse C., Tytgat L., Asadian M., Geyter N. De, Vlierberghe S. Van, Dubruel P., Declercq H. (2020) Hybrid Bioprinting of Chondrogenically Induced Human Mesenchymal Stem Cell Spheroids. *Front. Bioeng. Biotechnol.* **8**, 1–20.
Mort R. L., Jackson I. J., Patton E. E. (2015) The melanocyte lineage in development and disease. *Development* **142**, 620–632.
Morton J. J., Bird G., Refaeli Y., Jimeno A. (2016) Humanized Mouse Xenograft Models: Narrowing the Tumor–Microenvironment Gap. *Cancer Res.* **76**, 6153–6158.
Mostafa W. Z., Hegazy R. A. (2013) Vitamin D and the skin: Focus on a complex relationship: A review. *J. Adv. Res.* **6**, 793–804.
Muñoz-Espín D., Serrano M. (2014) Cellular senescence: From physiology to pathology. *Nat. Rev. Mol. Cell Biol.* **15**, 482–496.
Narita M., Lowe S. W. (2005) Senescence comes of age. *Nat. Med.* **11**, 920–922.
Natale C. A., Li J., Zhang J., Dahal A., Dentchev T., Stanger B. Z., Ridky T. W. (2018) Activation of G protein-coupled estrogen receptor signaling inhibits melanoma and improves response to immune checkpoint blockade. *Elife* **7**, 1–19.
Nath A., Chattopadhya S., Chattopadhyay U., Sharma N. K. (2006) Macrophage inflammatory protein (MIP)1α and MIP1β differentially regulate release of inflammatory cytokines and generation of tumoricidal monocytes in malignancy. *Cancer Immunol. Immunother.* **55**, 1534–1541.
Nguyen N. T., Fisher D. E. (2019) MITF and UV responses in skin: From pigmentation to addiction. *Pigment Cell Melanoma Res.* **32**, 224–236.
Niel G. Van, D'Angelo G., Raposo G. (2018) Shedding light on the cell biology of extracellular vesicles. *Nat. Rev. Mol. Cell Biol.* **19**, 213–228.
Nordlund J. J. (2007) The Melanocyte and the Epidermal Melanin Unit: An Expanded Concept. *Dermatol. Clin.* **25**, 271–281.
Novotný J., Strnadová K., Dvořánková B., Kocourková Š., Jakša R., Dundr P., Pačes V., Smetana K., Kolář M., Lacina L. (2020) Single-cell RNA sequencing unravels heterogeneity of the stromal niche in cutaneous melanoma heterogeneous spheroids. *Cancers (Basel).* **12**, 1–22.
Nowak-Sliwinska P., Segura T., Iruela-Arispe M. L. (2014) The chicken chorioallantoic membrane model in biology, medicine and bioengineering. *Angiogenesis* **17**, 779–804.
Oh J. W., Hsi T.-C., Guerrero-Juarez C. F., Ramos R., Plikus M. V. (2013) Organotypic Skin Culture. *J. Invest. Dermatol.* **133**, 1–4.
Olson B., Li Y., Lin Y., Liu E. T., Patnaik A. (2018) Mouse models for cancer immunotherapy research. *Cancer Discov.* **8**, 1358–1365.
Opferman J. T., Kothari A. (2018) Anti-apoptotic BCL-2 family members in development. *Cell Death Differ.* **25**, 37–45.
Ott P. A., Hodi F. S., Robert C. (2013) CTLA-4 and PD-1/PD-L1 blockade: New immunotherapeutic modalities with durable clinical benefit in melanoma patients. *Clin. Cancer Res.* **19**, 5300–5309.

Paganelli A., Garbarino F., Toto P., Martino G. Di, D'Urbano M., Auriemma M., Giovanni P. Di, Panarese F., Staniscia T., Amerio P., Paganelli R. (2019) Serological landscape of cytokines in cutaneous melanoma. *Cancer Biomarkers* **26**, 333–342.

Paraiso K. H. T., Xiang Y., Rebecca V. W., Abel E. V., Chen Y. A., Munko A. C., Wood E., Fedorenko I. V., Sondak V. K., Anderson A. R. A., Ribas A., Palma M. D., Nathanson K. L., Koomen J. M., Messina J. L., Smalley K. S. M. (2011) PTEN Loss Confers BRAF Inhibitor Resistance to Melanoma Cells through the Suppression of BIM Expression. *Cancer Res.* **71**, 2750–2760.

Pardoll D. M. (2012) The blockade of immune checkpoints in cancer immunotherapy. *Nat. Rev. Cancer* **12**, 252–264.

Park H. Y., Kosmadaki M., Yaar M., Gilchrest B. A. (2009) Cellular mechanisms regulating human melanogenesis. *Cell. Mol. Life Sci.* **66**, 1493–1506.

Pascale R. M., Calvisi D. F., Simile M. M., Feo C. F., Feo F. (2020) The Warburg Effect 97 Years after Its Discovery. *Cancers (Basel).* **12**, 2819.

Passeron T., Coelho S. G., Miyamura Y., Takahashi K., Hearing V. J. (2007) Immunohistochemistry and in situ hybridization in the study of human skin melanocytes. *Exp. Dermatol.* **16**, 162–170.

Peinado H., Alečković M., Lavotshkin S., Matei I., Costa-Silva B., Moreno-Bueno G., Hergueta-Redondo M., Williams C., García-Santos G., Ghajar C. M., Nitadori-Hoshino A., Hoffman C., Badal K., Garcia B. A., Callahan M. K., Yuan J., Martins V. R., Skog J., Kaplan R. N., Brady M. S., Wolchok J. D., Chapman P. B., Kang Y., Bromberg J., Lyden D. (2012) Melanoma exosomes educate bone marrow progenitor cells toward a pro-metastatic phenotype through MET. *Nat. Med.* **18**, 883–891.

Pham D. M., Guhan S., Tsao H. (2020) Kit and melanoma: Biological insights and clinical implications. *Yonsei Med. J.* **61**, 562–571.

Phelan M. A., Gianforcaro A. L., Gerstenhaber J. A., Lelkes P. I. (2019) An Air Bubble-Isolating Rotating Wall Vessel Bioreactor for Improved Spheroid/Organoid Formation. *Tissue Eng. - Part C Methods* **25**, 479–488.

Pho L., Grossman D., Leachman S. A. (2006) Melanoma genetics: A review of genetic factors and clinical phenotypes in familial melanoma. *Curr. Opin. Oncol.* **18**, 173–179.

Pickar J. H., Komm B. S. (2015) Selective estrogen receptor modulators and the combination therapy conjugated estrogens/bazedoxifene: A review of effects on the breast. *Post Reprod. Heal.* **21**, 112–121.

Pillai S., Oresajo C., Hayward J. (2005) Ultraviolet radiation and skin aging: Roles of reactive oxygen species, inflammation and protease activation, and strategies for prevention of inflammation-induced matrix degradation - A review. *Int. J. Cosmet. Sci.* **27**, 17–34.

Pinto M. T., Ribeiro A. S., Conde I., Carvalho R., Paredes J. (2021) The chick chorioallantoic membrane model: A new in vivo tool to evaluate breast cancer stem cell activity. *Int. J. Mol. Sci.* **22**, 1–15.

Poh A. R., O'Donoghue R. J. J., Ernst M., Putoczki T. L. (2016) Mouse models for gastric cancer: Matching models to biological questions. *J. Gastroenterol. Hepatol.* **31**, 1257–1272.

Qiu W., Chuong C., Lei M. (2019) Regulation of melanocyte stem cells in the pigmentation of skin and its appendages: Biological patterning and therapeutic potentials. *Exp. Dermatol.* **28**, 395–405.

Quan T., Qin Z., Xia W., Shao Y., Voorhees J. J., Fisher G. J. (2009) Matrix-degrading metalloproteinases in photoaging. *J. Investig. Dermatology Symp. Proc.* **14**, 20–24.

Quevedo W. C. (1972) Epidermal melanin units melanocyte-keratinocyte interactions. *Integr. Comp. Biol.* **12**, 35–41.

Qureshi O. S., Zheng Y., Nakamura K., Attridge K., Manzotti C., Schmidt E. M., Baker J., Jeffery L. E., Kaur S., Briggs Z., Hou T. Z., Futter C. E., Anderson G., Walker L. S. K., Sansom D. M. (2011) Trans-Endocytosis of CD80 and CD86: A Molecular Basis for the Cell-Extrinsic Function of CTLA-4. *Science (80-.).* **332**, 600–603.

Rabbie R., Ferguson P., Molina-Aguilar C., Adams D. J., Robles-Espinoza C. D. (2019) Melanoma subtypes: genomic profiles, prognostic molecular markers and therapeutic possibilities. *J. Pathol.* **247**, 539–551.

Raghavan S., Ward M. R., Rowley K. R., Wold R. M., Takayama S., Buckanovich R. J., Mehta G. (2015) Formation of stable small cell number three-dimensional ovarian cancer spheroids using hanging drop arrays for preclinical drug sensitivity assays. *Gynecol. Oncol.* **138**, 181–189.

Raimondi S., Suppa M., Gandini S. (2020) Melanoma epidemiology and sun exposure. *Acta Derm. Venereol.* **100**, 250–258.

Rang Z., Yang G., Wang Y. W., Cui F. (2016) MIR-542-3p suppresses invasion and metastasis by targeting the proto-oncogene serine/threonine protein kinase, PIM1, in melanoma. *Biochem. Biophys. Res. Commun.* **474**, 315–320.

Raposo G., Marks M. S. (2007) Melanosomes — dark organelles enlighten endosomal membrane transport. *Nat. Rev. Mol. Cell Biol.* **8**, 786–797.

Raposo G., Tenza D., Murphy D. M., Berson J. F., Marks M. S. (2001) Distinct protein sorting and localization to premelanosomes, melanosomes, and lysosomes in pigmented melanocytic cells. *J. Cell Biol.* **152**, 809–823.

Rebecca V. W., Somasundaram R., Herlyn M. (2020) Pre-clinical modeling of cutaneous melanoma. *Nat. Commun.* **11**, 1–9.

Redondo-Castro E., Cunningham C., Cain S., Allan S., Pinteaux E., Miller J. (2018) Generation of Human Mesenchymal Stem Cell 3D Spheroids Using Low-binding Plates. *Bio-Protocol* **8**, 1–10.

Rheinwald J. G., Green H. (1975) Serial cultivation of strains of human epidermal keratinocytes: the formation of keratinizing colonies from single cells. *Cell* **6**, 331–343.

Ribas A., Daud A., Pavlick A. C., Gonzalez R., Lewis K. D., Hamid O., Gajewski T. F., Puzanov I., Wongchenko M., Rooney I., Hsu J. J., Yan Y., Park E., McArthur G. A. (2020) Extended 5-Year Follow-up Results of a Phase Ib Study (BRIM7) of Vemurafenib and Cobimetinib in BRAF -Mutant Melanoma. *Clin. Cancer Res.* **26**, 46–53.

Ribas A., Gonzalez R., Pavlick A., Hamid O., Gajewski T. F., Daud A., Flaherty L., Logan T., Chmielowski B., Lewis K., Kee D., Boasberg P., Yin M., Chan I., Musib L., Choong N., Puzanov I., McArthur G. A. (2014) Combination of vemurafenib and cobimetinib in patients with advanced BRAFV600-mutated melanoma: A phase 1b study. *Lancet Oncol.* **15**, 954–965.

Ribatti D. (2008) The chick embryo chorioallantoic membrane in the study of tumor angiogenesis. *Rom. J. Morphol. Embryol.* **49**, 131–135.

Ribatti D. (2016) The chick embryo chorioallantoic membrane (CAM). A multifaceted experimental model. *Mech. Dev.* **141**, 70–77.

Ribatti D., Nico B., Vacca A., Roncali L., Presta M. (1999) Endogenous and exogenous fibroblast growth factor-2 modulate wound healing in the chick embryo chorioallantoic membrane. *Angiogenesis* **3**, 89–95.

Riffle S., Hegde R. S. (2017) Modeling tumor cell adaptations to hypoxia in multicellular tumor spheroids. *J. Exp. Clin. Cancer Res.* **36**, 1–10.

Rittié L., Fisher G. J. (2015) Natural and sun-induced aging of human skin. *Cold Spring Harb. Perspect. Med.* **5**, 1–14.

Robert C., Thomas L., Bondarenko I., O'Day S., Weber J., Garbe C., Lebbe C., Baurain J.-F., Testori A., Grob J.-J., Davidson N., Richards J., Maio M., Hauschild A., Miller W. H., Gascon P., Lotem M., Harmankaya K., Ibrahim R., Francis S., Chen T.-T., Humphrey R., Hoos A., Wolchok J. D. (2011) Ipilimumab plus Dacarbazine for Previously Untreated Metastatic Melanoma. *N. Engl. J. Med.* **364**, 2517–2526.

Robert L., Labat-Robert J., Robert A. M. (2009) Physiology of skin aging. *Pathol. Biol.* **57**, 336–341.

Roger M., Fullard N., Costello L., Bradbury S., Markiewicz E., O'Reilly S., Darling N., Ritchie P., Määttä A., Karakesisoglou I., Nelson G., Zglinicki T. von, Dicolandrea T., Isfort R., Bascom C., Przyborski S. (2019) Bioengineering the microanatomy of human skin. *J. Anat.* **234**, 438–455.

Rosenberg S. A., Yang J. C., White D. E., Steinberg S. M. (1998) Durability of complete responses in patients with metastatic cancer treated with high-dose interleukin-2: Identification of the antigens mediating response. *Ann. Surg.* **228**, 307–319.

Rudrapatna V. A., Cagan R. L., Das T. K. (2012) Drosophila cancer models. *Dev. Dyn.* **241**, 107–118.

Ryu N. E., Lee S. H., Park H. (2019) Spheroid Culture System Methods and Applications for Mesenchymal Stem Cells. *Cells* **8**, 1–13.

Sadler T. W. (2011) *Langmanova lékařská embryologie = [Orig.: Langman's medical embryology]*, (ed. Brabec J.). Grada, Praha.

Sample A., He Y.-Y. (2018) Mechanisms and prevention of UV-induced melanoma. *Photodermatol. Photoimmunol. Photomed.* **34**, 13–24.

Schartl M., Larue L., Goda M., Bosenberg M. W., Hashimoto H., Kelsh R. N. (2016) What is a vertebrate pigment cell? *Pigment Cell Melanoma Res.* **29**, 8–14.

Schmid Y. R. F., Bürgel S. C., Misun P. M., Hierlemann A., Frey O. (2016) Electrical Impedance Spectroscopy for Microtissue Spheroid Analysis in Hanging-Drop Networks. *ACS Sensors* **1**, 1028–1035.

Schmidt A. N., Nanney L. B., Boyd A. S., King L. E., Ellis D. L. (2006) Oestrogen receptor-β expression in melanocytic lesions. *Exp. Dermatol.* **15**, 971–980.

Schmidt S. K., Schmid R., Arkudas A., Kengelbach-Weigand A., Bosserhoff A. K. (2019) Tumor Cells Develop Defined Cellular Phenotypes After 3D-Bioprinting in Different Bioinks. *Cells* **8**, 1295.

Schmitd L. B., Liu M., Scanlon C. S., Banerjee R., D'Silva N. J. (2019) The Chick Chorioallantoic Membrane In Vivo Model to Assess Perineural Invasion in Head and Neck Cancer. *J. Vis. Exp.* **176**, 139–148.

Schneider H., Downey J., Smith A., Zinselmeyer B. H., Rush C., Brewer J. M., Wei B., Hogg N., Garside P., Rudd C. E. (2006) Reversal of the TCR Stop Signal by CTLA-4. *Science (80-.).* **313**, 1972–1975.

Schwartz E. L. (2009) Antivascular actions of microtubule-binding drugs. *Clin. Cancer Res.* **15**, 2594–2601.

Scott A., Khan K. M., Cook J. L., Duronio V. (2004) What is "inflammation"? Are we ready to move beyond Celsus? *Br. J. Sports Med.* **38**, 248–249.

Seiberg M. (2001) Keratinocyte-Melanocyte Interactions During Melanosome Transfer. *Pigment Cell Res.* **14**, 236–242.

Sharma P., Diergaarde B., Ferrone S., Kirkwood J. M., Whiteside T. L. (2020) Melanoma cell-derived exosomes in plasma of melanoma patients suppress functions of immune effector cells. *Sci. Rep.* **10**, 1–11.

Sharrow A. C., Ishihara M., Hu J., Kim I. H., Wu L. (2020) Using the Chicken

Chorioallantoic Membrane In Vivo Model to Study Gynecological and Urological Cancers. *J. Vis. Exp.* **176**, 139–148.
Shrestha P., Muramatsu Y., Kudeken W., Mori M., Takai Y., Ilg E. C., Schafer B. W., Heizmann C. W. (1998) Localization of Ca2+-binding S100 proteins in epithelial tumours of the skin. *Virchows Arch.* **432**, 53–59.
Shu S. La, Matsuzaki J., Want M. Y., Conway A., Benjamin-Davalos S., Allen C. L., Koroleva M., Battaglia S., Odunsi A., Minderman H., Ernstoff M. S. (2020) An Immunosuppressive Effect of Melanoma-derived Exosomes on NY-ESO-1 Antigen-specific Human CD8 + T Cells is Dependent on IL-10 and Independent of BRAF V600E Mutation in Melanoma Cell Lines. *Immunol. Invest.* **49**, 744–757.
Shu S. La, Yang Y., Allen C. L., Maguire O., Minderman H., Sen A., Ciesielski M. J., Collins K. A., Bush P. J., Singh P., Wang X., Morgan M., Qu J., Bankert R. B., Whiteside T. L., Wu Y., Ernstoff M. S. (2018) Metabolic reprogramming of stromal fibroblasts by melanoma exosome microRNA favours a pre-metastatic microenvironment. *Sci. Rep.* **8**, 1–14.
Silver D. L., Pavan W. J. (2006) The origin and development of neural crest-derived melanocytes. *From Melanocytes to Melanoma Progress. to Malig.*, 3–26.
Slominski A., Tobin D. J., Shibahara S., Wortsman J. (2004) Melanin pigmentation in mammalian skin and its hormonal regulation. *Physiol. Rev.* **84**, 1155–1228.
Smalley K. S. (2018) Why do women with melanoma do better than men? *Elife* **7**, 1–3.
Smetana K., Brábek J. (2020) Role of Interleukin-6 in Lung Complications in Patients With COVID-19: Therapeutic Implications. *In Vivo (Brooklyn).* **34**, 1589–1592.
Smetana K., Rösel D., Brábek J. (2020) Raloxifene and Bazedoxifene Could Be Promising Candidates for Preventing the COVID-19 Related Cytokine Storm, ARDS and Mortality. *In Vivo (Brooklyn).* **34**, 3027–3028.
Sobhani N., Tardiel-Cyril D. R., Davtyan A., Generali D., Roudi R., Li Y. (2021) CTLA-4 in regulatory T cells for cancer immunotherapy. *Cancers (Basel).* **13**, 1–18.
Špaková I., Rabajdová M., Mičková H., Graier W. F., Mareková M. (2021) Effect of hypoxia factors gene silencing on ROS production and metabolic status of A375 malignant melanoma cells. *Sci. Rep.* **11**, 1–14.
Stoddart M., Richards R., Alini M. (2012) In vitro experiments with primary mammalian cells: To Pool or not to Pool? *Eur. Cells Mater.* **24**, i–ii.
Štork J., Arenberger P., Pizinger K., Semrádová V., Vosmík F. (2013) *Dermatovenerologie*. Galén, Praha.
Strnadová K., Pfeiferová L., Přikryl P., Dvořánková B., Vlčák E., Frýdlová J., Vokurka M., Novotný J., Šáchová J., Hradilová M., Brábek J., Šmigová J., Rösel D., Smetana K., Kolář M., Lacina L. (2022) Exosomes produced by melanoma cells significantly influence the biological properties of normal and cancer-associated fibroblasts. *Histochem. Cell Biol.* **157**, 153–172.
Strnadova K., Sandera V., Dvorankova B., Kodet O., Duskova M., Smetana K., Lacina L. (2019) Skin aging: the dermal perspective. *Clin. Dermatol.* **37**.
Strnadová K., Španko M., Dvořánková B., Lacina L., Kodet O., Shbat A., Klepáček I., Smetana K. (2020) Melanoma xenotransplant on the chicken chorioallantoic membrane: a complex biological model for the study of cancer cell behaviour. *Histochem. Cell Biol.* **154**, 177–188.
Strojan P. (2010) Role of radiotherapy in melanoma management. *Radiol. Oncol.* **44**, 1–12.
Sun Z., Ren Z., Yang K., Liu Z., Cao S., Deng S., Xu L., Liang Y., Guo J., Bian Y., Xu H., Shi J., Wang F., Fu Y.-X., Peng H. (2019) A next-generation tumor-targeting IL-2 preferentially promotes tumor-infiltrating CD8+ T-cell response and effective

tumor control. *Nat. Commun.* **10**, 3874.
Swaminathan S., Clyne A. M. (2020) Direct Bioprinting of 3D Multicellular Breast Spheroids onto Endothelial Networks. *J. Vis. Exp.* **176**, 139–148.
Swaminathan S., Hamid Q., Sun W., Clyne A. M. (2019) Bioprinting of 3D breast epithelial spheroids for human cancer models. *Biofabrication* **11**, 025003.
Szadvari I., Krizanova O., Babula P. (2016) Athymic nude mice as an experimental model for cancer treatment. *Physiol. Res.* **65**, S441–S453.
Takahashi A., Okada R., Nagao K., Kawamata Y., Hanyu A., Yoshimoto S., Takasugi M., Watanabe S., Kanemaki M. T., Obuse C., Hara E. (2017) Exosomes maintain cellular homeostasis by excreting harmful DNA from cells. *Nat. Commun.* **8**, 15287.
Tancini B., Buratta S., Sagini K., Costanzi E., Delo F., Urbanelli L., Emiliani C. (2019) Insight into the role of extracellular vesicles in lysosomal storage disorders. *Genes (Basel).* **10**, 1–21.
Tang T., Eldabaje R., Yang L. (2016) Current status of biological therapies for the treatment of metastatic melanoma. *Anticancer Res.* **36**, 3229–3241.
Tassabehji M., Newton V. E., Read A. P. (1994) Waardenburg syndrome type 2 caused by mutations in the human microphthalmia (MITF) gene. *Nat. Genet.* **8**, 251–255.
Tobin D. J. (2017) Introduction to skin aging. *J. Tissue Viability* **26**, 37–46.
Tomaszewska K., Kozłowska M., Kaszuba A., Lesiak A., Narbutt J., Zalewska-Janowska A. (2020) Increased Serum Levels of IFN- γ , IL-1 β , and IL-6 in Patients with Alopecia Areata and Nonsegmental Vitiligo. *Oxid. Med. Cell. Longev.* **2020**, 1–5.
Trotter M. J., Colwell R., Tron V. A. (2003) Thrombospondin-1 and cutaneous melanoma. *J. Cutan. Med. Surg.* **7**, 136–141.
Urbanczyk M., Zbinden A., Layland S. L., Duffy G., Schenke-Layland K. (2020) Controlled heterotypic pseudo-islet assembly of human β-cells and human umbilical vein endothelial cells using magnetic levitation. *Tissue Eng. - Part A* **26**, 387–399.
Vachtenheim J., Borovanský J. (2010) "Transcription physiology" of pigment formation in melanocytes: Central role of MITF. *Exp. Dermatol.* **19**, 617–627.
Vasile C., Pamfil D., Stoleru E., Baican M. (2020) New developments in medical applications of hybrid hydrogels containing natural polymers. *Molecules* **25**, 1539.
Vaupel P., Multhoff G. (2021) Revisiting the Warburg effect: historical dogma versus current understanding. *J. Physiol.* **599**, 1745–1757.
Velarde M. C., Flynn J. M., Day N. U., Melov S., Campisi J. (2012) Mitochondrial oxidative stress caused by Sod2 deficiency promotes cellular senescence and aging phenotypes in the skin. *Aging (Albany. NY).* **4**, 3–12.
Velotti F., Barchetta I., Cimini F. A., Cavallo M. G. (2020) Granzyme B in Inflammatory Diseases: Apoptosis, Inflammation, Extracellular Matrix Remodeling, Epithelial-to-Mesenchymal Transition and Fibrosis. *Front. Immunol.* **11**, 1–9.
Vicente R., Mausset-Bonnefont A. L., Jorgensen C., Louis-Plence P., Brondello J. M. (2016) Cellular senescence impact on immune cell fate and function. *Aging Cell* **15**, 400–406.
Victorelli S., Lagnado A., Halim J., Moore W., Talbot D., Barrett K., Chapman J., Birch J., Ogrodnik M., Meves A., Pawlikowski J. S., Jurk D., Adams P. D., Heemst D., Beekman M., Slagboom P. E., Gunn D. A., Passos J. F. (2019) Senescent human melanocytes drive skin ageing via paracrine telomere dysfunction. *EMBO J.* **38**, 1–18.
Videira I. F. dos S., Moura D. F. L., Magina S. (2013) Mechanisms regulating melanogenesis*. *An. Bras. Dermatol.* **88**, 76–83.
Vignard V., Labbe M., Marec N., Andre-Gregoire G., Jouand N., Fonteneau J. F., Labarriere N., Fradin D. (2020) MicroRNAs in tumor exosomes drive immune

escape in melanoma. *Cancer Immunol. Res.* **8**, 255–267.
Vörsmann H., Groeber F., Walles H., Busch S., Beissert S., Walczak H., Kulms D. (2013) Development of a human three-dimensional organotypic skin-melanoma spheroid model for in vitro drug testing. *Cell Death Dis.* **4**, e719.
Wang C., Wang Y., Chang X., Ba X., Hu N., Liu Q., Fang L., Wang Z. (2020) Melanoma-derived exosomes endow fibroblasts with an invasive potential via mir-21 target signaling pathway. *Cancer Manag. Res.* **12**, 12965–12974.
Wang J. X., Fukunaga-Kalabis M., Herlyn M. (2016) Crosstalk in skin: melanocytes, keratinocytes, stem cells, and melanoma. *J. Cell Commun. Signal.* **10**, 191–196.
Wang S., Zhou M., Lin F., Liu D., Hong W., Lu L., Zhu Y., Xu A. (2014) Interferon-γ induces senescence in normal human melanocytes. *PLoS One* **9**, 1–9.
Wang X., Montoyo-Pujol Y. G., Bermudez S., Corpas G., Martin A., Almazan F., Cabrera T., López-Nevot M. A. (2021) Serum Cytokine Profiles of Melanoma Patients and Their Association with Tumor Progression and Metastasis. *J. Oncol.* **2021**, 1–9.
Ward W. H., Lambreton F., Goel N., Yu J. Q., Farma J. M. (2017) Clinical Presentation and Staging of Melanoma. In: *Cutan. Melanoma Etiol. Ther.*, eds. Ward W. H., Farma J. M., Vol. 6, pp. 79–89, Codon Publications.
Wensveen F. M., Jelenčić V., Polić B. (2018) NKG2D: A master regulator of immune cell responsiveness. *Front. Immunol.* **9**.
Weyden L. van der, Brenn T., Patton E. E., Wood G. A., Adams D. J. (2020) Spontaneously occurring melanoma in animals and their relevance to human melanoma. *J. Pathol.* **252**, 4–21.
Whiteside T. L. (2016) Tumor-Derived Exosomes and Their Role in Cancer Progression. In: *Physiol. Behav.*, Vol. 176, pp. 103–141.
Wicherska-pawłowska K., Wróbel T., Rybka J. (2021) Toll-like receptors (Tlrs), nod-like receptors (nlrs) and rig-i-like receptors (rlrs) in innate immunity. tlrs, nlrs and rlrs ligands as immunotherapeutic agents for hematopoietic diseases. *Int. J. Mol. Sci.* **22**, 13397.
Williams S. K., Touroo J. S., Church K. H., Hoying J. B. (2013) Encapsulation of Adipose Stromal Vascular Fraction Cells in Alginate Hydrogel Spheroids Using a Direct-Write Three-Dimensional Printing System. *Biores. Open Access* **2**, 448–454.
Wlaschek M., Maity P., Makrantonaki E., Scharffetter-Kochanek K. (2021) Connective Tissue and Fibroblast Senescence in Skin Aging. *J. Invest. Dermatol.* **141**, 985–992.
Wu S., Chen H., Zuo L., Jiang H., Yan H. (2020) Suppression of long noncoding RNA MALAT1 inhibits the development of uveal melanoma via microRNA-608-mediated inhibition of HOXC4. *Am. J. Physiol. - Cell Physiol.* **318**, C903–C912.
Wynn T. A. (2003) IL-13 effector functions. *Annu. Rev. Immunol.* **21**, 425–456.
Xia J., Wang Y., Li F., Wang J., Mu Y., Mei X., Li X., Zhu W., Jin X., Yu K. (2016) Expression of microphthalmia transcription factor, s100 protein, and HMB-45 in malignant melanoma and pigmented nevi. *Biomed. Reports* **5**, 327–331.
Xia Y., Zhou Y., Han H., Li P., Wei W., Lin N. (2019) lncRNA NEAT1 facilitates melanoma cell proliferation, migration, and invasion via regulating miR-495-3p and E2F3. *J. Cell. Physiol.* **234**, 19592–19601.
Xiao D., Barry S., Kmetz D., Egger M., Pan J., Rai S. N., Qu J., McMasters K. M., Hao H. (2016) Melanoma cell–derived exosomes promote epithelial–mesenchymal transition in primary melanocytes through paracrine/autocrine signaling in the tumor microenvironment. *Cancer Lett.* **376**, 318–327.
Xie H., Appelt J. W., Jenkins R. W. (2021) Going with the flow: Modeling the tumor microenvironment using microfluidic technology. *Cancers (Basel).* **13**, 1–26.
Yaar M., Gilchrest B. A. (2007) Photoageing: Mechanism, prevention and therapy. *Br. J.*

Dermatol. **157**, 874–887.
Yadav A., Kumar B., Teknos T. N., Kumar P. (2017) Bazedoxifene enhances the anti-tumor effects of cisplatin and radiation treatment by blocking IL-6 signaling in head and neck cancer. *Oncotarget* **8**, 66912–66924.
Yamaguchi Y., Brenner M., Hearing V. J. (2007) The regulation of skin pigmentation. *J. Biol. Chem.* **282**, 27557–27561.
Yamaguchi Y., Hearing V. J., Maeda A., Morita A. (2010) NADPH:Quinone oxidoreductase-1 as a new regulatory enzyme that increases melanin synthesis. *J. Invest. Dermatol.* **130**, 645–647.
Yamamura K., Kamada S., Ito S., Nakagawa K., Ichihashi M., Tsujimoto Y. (1996) Accelerated disappearance of melanocytes in bcl-2-deficient mice. *Cancer Res.* **56**, 3546–3550.
Yáñez-Mó M., Siljander P. R. M., Andreu Z., Zavec A. B., Borràs F. E., Buzas E. I., Buzas K., Casal E., Cappello F., Carvalho J., Colás E., Cordeiro-Da Silva A., Fais S., Falcon-Perez J. M., Ghobrial I. M., Giebel B., Gimona M., Graner M., Gursel I., Gursel M., Heegaard N. H. H., Hendrix A., Kierulf P., Kokubun K., Kosanovic M., Kralj-Iglic V., Krämer-Albers E. M., Laitinen S., Lässer C., Lener T., Ligeti E., Line A., Lipps G., Llorente A., Lötvall J., Manček-Keber M., Marcilla A., Mittelbrunn M., Nazarenko I., Nolte-'t Hoen E. N. M., Nyman T. A., O'Driscoll L., Olivan M., Oliveira C., Pállinger É., Portillo H. A. Del, Reventós J., Rigau M., Rohde E., Sammar M., Sánchez-Madrid F., Santarém N., Schallmoser K., Ostenfeld M. S., Stoorvogel W., Stukelj R., Grein S. G. Van Der, Helena Vasconcelos M., Wauben M. H. M., Wever O. De (2015) Biological properties of extracellular vesicles and their physiological functions. *J. Extracell. Vesicles* **4**, 1–60.
Yang K., Oak A. S. W., Slominski R. M., Brożyna A. A., Slominski A. T. (2020) Current molecular markers of melanoma and treatment targets. *Int. J. Mol. Sci.* **21**, 3535.
Yang X., Yan L., Ha D., Qu L., Liu L., Tao Y. (2018) Changes in sICAM-1 and GM-CSF levels in skin tissue fluid and expression of IL-6, IL-17 and TNF-α in blood of patients with vitiligo. *Exp. Ther. Med.* **17**, 408–412.
Yardman-Frank J. M., Fisher D. E. (2021) Skin pigmentation and its control: From ultraviolet radiation to stem cells. *Exp. Dermatol.* **30**, 560–571.
Yoo J. H., Brady S. W., Acosta-Alvarez L., Rogers A., Peng J., Sorensen L. K., Wolff R. K., Mleynek T., Shin D., Rich C. P., Kircher D. A., Bild A., Odelberg S. J., Li D. Y., Holmen S. L., Grossmann A. H. (2019) The Small GTPase ARF6 Activates PI3K in Melanoma to Induce a Prometastatic State. *Cancer Res.* **79**, 2892–2908.
Yoshida H., Grimm T., Nishimura E. K., Nishioka E., Nishikawa S.-I., Kunisada T. (2001) Review: Melanocyte Migration and Survival Controlled by SCF/c-kit Expression. *J. Investig. Dermatology Symp. Proc.* **6**, 1–5.
Zaballos M. A., Santisteban P. (2017) Key signaling pathways in thyroid cancer. *J. Endocrinol.* **235**, R43–R61.
Zatloukalová P., Pjechová M., Babčanová S., Hupp T. R., Vojtěšek B. (2016) The Role of PD-1/PD-L1 Signaling Pathway in Antitumor Immune Response. *Klin. Onkol.* **29**, 4S72-4S77.
Zecca L., Tampellini D., Gerlach M., Riederer P., Fariello R. G., Sulzer D. (2001) Substantia nigra neuromelanin: Structure, synthesis, and molecular behaviour. *J. Clin. Pathol. - Mol. Pathol.* **54**, 414–418.
Zhang X. T., Wei K. J., Chen Y. Y., Shi Z. C., Liu L. K., Li J., Zhang G. R., Ji W. (2018) Molecular cloning and expression analysis of tyr and tyrp1 genes in normal and albino yellow catfish Tachysurus fulvidraco. *J. Fish Biol.* **92**, 979–998.
Zhao L., Xiu J., Liu Y., Zhang T., Pan W., Zheng X., Zhang X. (2019) A 3D Printed

Hanging Drop Dripper for Tumor Spheroids Analysis Without Recovery. *Sci. Rep.* **9**, 1–14.

Zhou X., Yan T., Huang C., Xu Z., Wang L., Jiang E., Wang H., Chen Y., Liu K., Shao Z., Shang Z. (2018) Melanoma cell-secreted exosomal miR-155-5p induce proangiogenic switch of cancer-associated fibroblasts via SOCS1/JAK2/STAT3 signaling pathway. *J. Exp. Clin. Cancer Res.* **37**, 1–15.

Zhuang P., Chiang Y. H., Fernanda M. S., He M. (2021) Using Spheroids as Building Blocks Towards 3D Bioprinting of Tumor Microenvironment. *Int. J. Bioprinting* **7**, 1–26.

Zulkiflee I., Fauzi M. B. (2021) Gelatin-polyvinyl alcohol film for tissue engineering: A concise review. *Biomedicines* **9**, 979.

Webové odkazy:

- *Internetová jazyková příručka* [online] (2008–2021). Praha: Ústav pro jazyk český AV ČR, [cit. 1. 4. 2022]. Dostupné z: *https://prirucka.ujc.cas.cz/*
- *Ústav zdravotnických informací a statistiky ČR* [online] (2018). Národní zdravotnický informační systém (NZIS), [cit. 9. 1. 2022]. Dostupné z: https://www.uzis.cz/res/f/008352/novotvary2018
- *Ending the use of animals in research and testing* [online] (2021). European Parliament [cit. 12. 3. 2022]. Dostupné z: https://www.europarl.europa.eu/news/en/agenda/briefing/2021-09-13/7/ending-the-use-of-animals-in-research-and-testing
- *U.S. EPA to eliminate all mammal testing by 2035* [online] (2019). Science [cit. 12. 3. 2022]. Dostupné z: https://www.science.org/content/article/us-epa-eliminate-all-mammal-testing-2035
- *Memorandum. Directive to Prioritize Efforts to Reduce Animal Testing* [online] (2019). United States Environmental Protection Agency [cit. 12. 3. 2022]. Dostupné z: https://www.epa.gov/sites/default/files/2019-09/documents/image2019-09-09-231249.pdf
- *Working to reduce the use of animals in scientific research. Delivery report* [online] (2015). [cit. 12. 3. 2022]. Dostupné z: https://assets.publishing.service.gov.uk/government/uploads/system/uploads/attachment_data/file/417441/Delivery_Report_2015.pdf

11 Soubor publikovaných prací autorky

PUBLIKACE I

Jobe NP, Živicová V, Mifková A, Rösel D, Dvořánková B, Kodet O, Strnad H, Kolář M, Šedo A, Smetana K Jr, **Strnadová K**, Brábek J, Lacina L. Fibroblasts potentiate melanoma cells in vitro invasiveness induced by UV-irradiated keratinocytes. *Histochem Cell Biol.* 2018 May;149(5):503-516. **(IF: 2.640)**

Histochemistry and Cell Biology (2018) 149:503–516
https://doi.org/10.1007/s00418-018-1650-4

ORIGINAL PAPER

Fibroblasts potentiate melanoma cells in vitro invasiveness induced by UV-irradiated keratinocytes

Njainday Pulo Jobe[1,2,8] · Veronika Živicová[3,4] · Alžběta Mifková[3,4] · Daniel Rösel[1,2] · Barbora Dvořánková[2,3] · Ondřej Kodet[2,3,5] · Hynek Strnad[6] · Michal Kolář[6] · Aleksi Šedo[7] · Karel Smetana Jr.[2,3] · Karolina Strnadová[2,3] · Jan Brábek[1,2] · Lukáš Lacina[2,3,5]

Accepted: 6 February 2018 / Published online: 12 February 2018

Abstract
Melanoma represents a malignant disease with steadily increasing incidence. UV-irradiation is a recognized key factor in melanoma initiation. Therefore, the efficient prevention of UV tissue damage bears a critical potential for melanoma prevention. In this study, we tested the effect of UV irradiation of normal keratinocytes and their consequent interaction with normal and cancer-associated fibroblasts isolated from melanoma, respectively. Using this model of UV influenced microenvironment, we measured melanoma cell migration in 3-D collagen gels. These interactions were studied using DNA microarray technology, immunofluorescence staining, single cell electrophoresis assay, viability (dead/life) cell detection methods, and migration analysis. We observed that three 10 mJ/cm^2 fractions at equal intervals over 72 h applied on keratinocytes lead to a 50% increase ($p < 0.05$) in in vitro invasion of melanoma cells. The introduction cancer-associated fibroblasts to such model further significantly stimulated melanoma cells in vitro invasiveness to a higher extent than normal fibroblasts. A panel of candidate gene products responsible for facilitation of melanoma cells invasion was defined with emphasis on IL-6, IL-8, and CXCL-1. In conclusion, this study demonstrates a synergistic effect between cancer microenvironment and UV irradiation in melanoma invasiveness under in vitro condition.

Keywords Cancer-associated fibroblasts · Keratinocytes · Cancer microenvironment · Cytokine · Chemokine · Melanoma

Introduction

The incidence of malignant melanoma is increasing globally. Despite the remarkable progress in melanoma research, the options of treatment in advanced stages of the disease are still very limited (Rastrelli et al. 2014). This can be linked to either primary resistance or to the frequently occurring phenomenon of acquired resistance to the therapy. Extensive UV light exposure is considered to be the most critical risk factors in cutaneous melanoma initiation due to the acquisition of mutations (D´Orazio

Njainday Pulo Jobe and Veronika Živicová contributed equally.

✉ Lukáš Lacina
lukas.lacina@lf1.cuni.cz

[1] Department of Cell Biology, Faculty of Sciences, Charles University in Prague, Viničná 7, 120 00 Prague 2, Czech Republic

[2] Biotechnology and Biomedicine Center of the Academy of Sciences and Charles University in Vestec (BIOCEV), Průmyslová 595, Vestec u Prahy, Prague, Czech Republic

[3] Institute of Anatomy, 1st Faculty of Medicine, Charles University, U Nemocnice 3, Prague 2, Czech Republic

[4] Department of Otorhinolaryngology, Head and Neck Surgery, 1st Faculty of Medicine, Charles University, V Úvalu 5, Prague 5, Czech Republic

[5] Department of Dermatovenereology, 1st Faculty of Medicine, Charles University, U Nemocnice 2, Prague 2, Czech Republic

[6] Institute of Molecular Genetics, Academy of Sciences of the Czech Republic vvi, Vídeňská 1083, Prague 4, Czech Republic

[7] Institute of Biochemistry and Experimental Oncology, 1st Faculty of Medicine, Charles University, U Nemocnice 5, Prague 2, Czech Republic

[8] Present Address: Cell and Experimental Pathology, Department of Translational Medicine, Lund University, Clinical Research Centre, Skåne University Hospital, Jan Waldenströms gata 35, 21421 Malmö, Sweden

et al. 2013; Lo and Fisher 2014; Brash 2015; Rünger 2016). The skin in childhood seems to be more vulnerable to UV. However, the incidence of malignant melanoma is rare. Therefore, the childhood represents a susceptible life stage for adult-onset UV radiation late effects. UV exposure leads to accumulation of resulting irreversible DNA alterations in the skin which can be manifested after several decades (Volkmer and Greinert 2011). On the other hand, the occurrence of melanoma in sun-protected sites such as mucosal or subungual regions indicates that previous extensive sun exposition is not always a necessary condition for the formation of this type of a tumour (Merkel and Gerami 2017).

Similarly, to other types of tumours, the microenvironment is a very important factor for malignant melanoma progression and spreading (Lacina et al. 2015, 2017; Wang et al. 2016; Dvořánková et al. 2017). Cancer-associated fibroblasts isolated from melanoma (mCAFs) significantly influence not only the phenotype of melanoma cells per se but they influence also the phenotype of normal surrounding keratinocytes (Kodet et al. 2013; Kučera et al. 2015). Furthermore, they can influence the phenotype of various other co-cultured epithelial cell types, e.g., breast cancer cells (Dvořánková et al. 2012). These fibroblasts also influence in vitro invasiveness of melanoma and other cancerous (e.g., glioblastoma) cells. This mechanism seems to be dependent on the production of IL-6 and IL-8 (Trylčová et al. 2015; Jobe et al. 2016).

In the context of normal epidermis, melanocytes and keratinocytes represent a functional unit requiring multiple mutual interactions of both cell types (Kondo and Hearing 2011). Such tightly regulated interaction is a prerequisite for the proper physiological functions of the epidermis, namely the melanisation and melanogenesis. The epidermal re-pigmentation after cutaneous injury also consists of several highly orchestrated events, such as keratinocyte and melanocyte proliferation, migration of both cell types into the wound site, melanin production and transfer to the neighbouring keratinocytes (Chou et al. 2013). Both epidermal and neural crest-derived stem cells exit their niche in the hair follicle and contribute to the newly reconstituted epidermal layer. This provides an excellent example of how stem cells located in the bulge region of the hair follicle cope with sudden requirements for their differentiation and also their own maintenance. Any impairment during this period (e.g., excessive and prolonged inflammatory responses) may lead to abnormal pigmentation, both hypopigmentation and hyperpigmentations are possible. However, the molecular signals responsible for these pathological responses to injury remain, in detail, unknown.

In the context of cutaneous pathology relevant for this article, keratinocytes seem to stimulate spreading of melanoma cells via deregulation of MiTF (Golan et al. 2015) resulting in the increased aggressive behaviour of melanoma cells (Cheli et al. 2011).

Melanocyte biology studies focusing on intercellular interactions have already acknowledged the importance of keratinocytes, the principal and the most numerous population of the epidermal compartment. Despite the great difference in population numbers, this interaction is certainly not unidirectional and melanocytes are not the only subject of regulation. Melanoma cells and melanocytic precursors (represented by neural crest-originated stem cells isolated from in the bulge region of the hair follicle) can influence the maintenance of low differentiation status of human keratinocytes observed in vitro and also contribute to highly aberrant epidermal architecture observed in melanoma biopsies in vivo (Kodet et al. 2015).

On the other hand, as keratinocyte–melanocyte interaction via direct cell-to-cell contact or via paracrine factors seems to be obvious, growing evidence suggests that also dermal fibroblasts modulate melanocyte behaviour, presumably in a paracrine manner. Recent evidence indicates melanocyte being active in the modulation of angiogenesis, inflammation, and fibroplasia after injury (Catania 2007; Adini et al. 2014, 2015). Similar reciprocal interaction in the case of melanoma and mCAFs seems to be likely.

As mentioned above, UV irradiation is a key factor responsible for carcinogenesis in normal melanocytes, converting them after the acquisition of a critical set of mutations in malignant melanoma cells. Notably, one of the earliest responses of viable keratinocytes to the UV-related damage is the formation of an inflammasome within their cytoplasm. Exposure to the UV light thus induces sterile inflammation associated with the production of a broad spectrum of cytokines/chemokines that influence epidermal homeostasis and can be important for melanoma cell invasion in the skin (Kim et al. 2011). In such case, UVB seems to be the relevant part of UV spectra. UVB primarily affects keratinocytes of the epidermal basal layer, leaving fibroblasts below the basement membrane relatively unaffected. This study presents data demonstrating the synergistic effect of UV-irradiated microenvironment represented by irradiated keratinocytes with either normal as well as cancer-associated fibroblasts on invasiveness of melanoma cells in 3-D collagen gels.

Materials and methods

Cell donors

Normal human dermal fibroblasts (HFs), as well as keratinocytes, were isolated from the residual tissue after mammoplasty from Department of Esthetic Surgery, 3rd Faculty of Medicine, Charles University, Prague. mCAFs

were isolated from melanoma patients (Table 1) treated at Department of Dermatovenereology, 1st Faculty of Medicine, Charles University, Prague. All tissues were acquired with the written informed consent approved by local ethical committees of abovementioned clinical centres with full respect to Declaration of Helsinki. Highly metastatic BLM melanoma cell line was kindly provided by L. van Kempen and J.H.J.M. van Krieken, Department of Pathology, Radboud University, Nijmegen Medical Centre, the Netherlands. Commercially available A2058 melanoma cells were purchased from ATCC® HTB-43™ (Teddington, UK).

Fibroblast cultivation

mCAFs and HF were isolated as described previously by tissue explant method (Trylcova et al. 2015). Briefly, the small pieces of melanoma metastasis and human dermis, respectively, were transferred to the CellBind 6-well plate (Corning, Schiphol Rijk, the Netherlands) and cultured in Dulbecco's Modified Eagle Medium (DMEM) (Biochrom) with antibiotics and 10% Foetal Bovine Serum (FBS, all Biochrom) at 37 °C and 5% CO_2. The cells outgrowing from the explants were harvested by trypsinization (0.25% trypsin and 0.02% EDTA 1:1, Biochrom) and expanded after initial confirmation of phenotype by means of immunocytochemistry. Low passage fibroblasts (below P5) of three independent strains (coded as VEM, MAM, ZAM) were used for this study.

Keratinocyte cultivation and co-culture of keratinocytes with fibroblasts

Dermo-epidermal sheets were harvested from the residual skin from aesthetic breast surgery of otherwise healthy female donors. Small pieces of tissue were cut and treated overnight in 0.3% trypsin solution at 4 °C. The epidermis was peeled off next day and the suspension of keratinocytes was prepared by careful mechanical disintegration using syringes. Obtained keratinocyte suspension was seeded on the subconfluent Mitomycin C (Sigma-Aldrich, Prague, Czech Republic) treated monolayer of 3T3 mice fibroblasts. Cultures were maintained in keratinocyte medium (Krejčí et al. 2015) at 37 °C and 5% CO_2. Low passage keratinocytes (P1, P2) were used for this study.

Consequently, using HF or mCAFs as a feeder layer, keratinocytes were cultured on these coverslips for 7 days in keratinocyte medium. The co-cultures on coverslips were used for immunocytochemical analysis.

Immunocytochemistry

HF as well as mCAFs and their co-cultures with HK were briefly fixed in paraformaldehyde, permeabilized with 0.1% Tween-20, blocked by 10% serum in PBS, and used for immunocytochemical studies according to the standard Abcam ICC/IF protocol (http://www.abcam.com/protocols/immunocytochemistry-immunofluorescence-protocol). The primary antibody dilution was according to the recommendation of the suppliers (Table 2). The specificity of the immunocytochemical reaction was tested by use of isotype controls or tissue-irrelevant antibodies instead of specific

Table 1 Characteristic of the patients from which cancer-associated fibroblasts were isolated

CAFs	Birth	Sex	Primary melanoma, year	Breslow (mm), clark	CAFs isolation from skin metastasis	Localisation of metastasis	Death
VEM	1923	Male	Back, 2010	9.3; V	2010	Left arm	2015
ZAM	1954	Male	Chest, 2009	2.3; III	2010	Chest	2011
MAM	1947	Female	Chest, 2007	2.8; IV	2010	Abdomen	2014

Table 2 Antibodies used in immunocytochemical analyses

Primary antibody	Supplier (location)	Secondary antibody/fluorochrome	Supplier (location)
Nestin/M	Merck-Millipore (Prague, Czech Republic)	Goat anti-mouse/TRITC	Sigma-Aldrich (Prague, Czech Republic)
CD 45/M	DAKO (Glostrup, Denmark)		
Vimentin/M			
Smooth muscle actin/M			
CD34/M			
Melan A (MART-1)/M	Invitrogen, ThermoFisher Scientific (Waltham, MA, USA)		
HMB-45 (Anti-Melanosome)/M			
Wide spectrum Cytokeratin/P	Abcam, (Cambridge, UK)	Swine anti-rabbit/FITC	DAKO (Glostrup, Denmark)

antibodies. Cell nuclei were counterstained with 4′,6-diamidino-2-phenylindole (DAPI, Sigma-Aldrich), mounted in Vectashield (Vector Laboratories, Peterborough, UK) and analysed using an Eclipse 90i fluorescence microscope (Nikon, Prague, Czech Republic) equipped with a ProgRes MF Cool camera (Jenoptik Optical Systems, Jena, Germany) and NIS-ElementsAR4.40.00 computer-assisted image analysis system (Laboratory Imaging, Prague, Czech Republic).

UV irradiation of keratinocytes and conditioned media preparation

Low passage keratinocytes (P2) were seeded into the CellBind 6-well plate at the density 50,000 cells/cm^2 and cultured without feeder in keratinocyte medium for 7 days. On the day 7, the subconfluent layers of keratinocytes were treated with different single doses of UVB radiation (10, 50 and 100 mJ/cm^2, respectively) using CL-1000 Ultraviolet Crosslinker (UVP, LLC Upland, Canada) with an integrated UV-B dosimetric device. The control cells were not irradiated. Conditioned media were prepared by addition of 2 ml of DMEM to each well and the cells were cultured for the next 2 days. After 24 h, conditioned media were aspirated, filtered through 0.2 µm microfilter (Corning, NY, USA), aliquoted and frozen at − 80 °C for later use. These media were labelled as 24H media.

For the study of repeated low doses of UV-B in the presence of fibroblasts, the subconfluent cultures keratinocytes were irradiated either by a single dose of 100 or by 10 mJ/cm^2 for three consecutive days. After irradiation, HF or mCAFs in the culture inserts (seeded at the density 10,000 cells/cm^2) were placed into the wells with 2 ml of fresh DMEM. The conditioned media were prepared from this experiment as described above. In a parallel experiment, keratinocytes were cultured on cover glasses under the same conditions and used for life/dead cell assay.

Detection of percentage of viable cells

To determine levels of life and dead cells in the culture, commercial staining kit Live/Dead Viability/Cytotoxicity Kit (Invitrogen, Oregon, USA) was used according to the instructions of the supplier.

Evaluation of DNA damage by single cell gel electrophoresis (comet assay) and data analysis

The single cell gel electrophoresis was performed on UVB-irradiated keratinocytes according to standard Alkaline Comet Assay guidelines (Tice et al. 2000). Briefly, the cells were irradiated as described above. The irradiated cells were embedded in low melting point agarose and poured on negatively charged glass slides at density 20,000/slide. After the cell lysis and alkaline treatment (pH 13), the electrophoresis was performed in a light protected Comet Assay Tank (Cleaver Scientific, Rugby, United Kingdom) at 25 V for 30 min in the cold room at 4 °C. The nuclei were finally counterstained with 4′,6-diamidino-2-phenylindole and imaged as described above on fluorescence microscope. The acquired images were analysed using ImageJ with bundled OpenComet plug-in (v 1.3.1) validated (Schneider et al. 2012; Gyori et al. 2014) for alkaline comet assay. The Olive moment (calculated as DNA percentage and the distance between the intensity-weighted centroids of head and tail) of at least 100 comets for each experiment was calculated. All experiments were performed in doublets. Statistical analysis was performed using Past3 package (version 3.15) (Hammer et al. 2001), the Kruskal–Wallis test for equality of medians and Mann–Whitney test with Bonferroni serial correction of p values were performed.

Spheroid invasion assay and statistical analysis

The study was performed as described in details previously (Jobe et al. 2016). Briefly, BLM and A2058 melanoma cells were cultured as spheroids in Microtissues® 3D Petri Dish® (Sigma-Aldrich) according to manufacturer's instructions. Spheroids were then embedded in Collagen R (Serva, Heidelberg, Germany) solution, containing DMEM, 5% $NaHCO_3$ and 10% FBS (Biochrom). Using a 48-well plate, one spheroid was placed per well, and collagen was polymerized. DMEM or conditioned medium was added to the wells. Images were taken immediately, and after 48 h using a Nikon-Eclipse TE2000-S (4×/0.13 PHL objective, 10×/0.13 PHL objective) (Nikon) and analysed by NIS-Elements software (Laboratory Imaging). The data were analysed with ANOVA followed by Tukey's honest significant difference test.

Microarray analysis

The cells of each fibroblast population were seeded at a density of 1000 cells/cm^2 into two 6-cm diameter Petri dishes (Corning, NY, USA) and cultured for 7 days (95–100% confluence). Culture medium was changed every 2 days and 24 h before harvest. For cell lysis, RLT buffer (Qiagen GmbH, Hilden, Germany) with 2-Mercaptoethanol (Sigma-Aldrich, Prague, Czech Republic) was used. The cell lysates (two technical replicates of each population) were collected to small Eppendorf tubes, frozen, and stored at − 80 °C.

Total RNA was isolated using RNeasy Micro Kit (Qiagen, MD, USA) according to manufacturer's protocol. Quality and concentration of RNA were measured with a NanoDrop 2000 spectrophotometer (Thermo Fisher Scientific, MA, USA). The RNA integrity was analysed by

Agilent Bioanalyzer 2100 (Agilent). Only samples with intact RNA profile were used for expression profiling analyses (RIN > 9).

Illumina HumanHT-12 v4 Expression BeadChips (Illumina, CA, USA) were used for the microarray analysis following the standard protocol. In brief, 200 ng RNA was amplified with Illumina TotalPrep RNA Amplification Kit (Ambion, TX, USA) and 750 ng of labelled RNA was hybridized on the chip according to the manufacturer's protocol. The analysis was performed in two biological replicates per group. The raw data were preprocessed using GenomeStudio software (version 1.9.0.24624; Illumina, CA, USA) and the limma package (Smyth 2006) of the Bioconductor (Gentleman et al. 2004), as described elsewhere (Mateu et al. 2016): the transcription profiles were background corrected using normal-exponential model, quantile normalized and variance stabilized using base 2 logarithmic transformation.

A moderated t test was used to detect transcripts differentially expressed between the treated samples and controls (within limma) (Smyth 2006). False discovery rate values were used to select significantly differentially transcribed genes (FDR < 0.05). The transcription data are MIAME (Minimum Information about a Microarray Experiment) compliant and have been deposited in the ArrayExpress database (Accession number E-MTAB-5973).

Results

Immunocytochemical analysis of keratinocytes and fibroblasts

Human keratinocytes from interfollicular epidermis were positive for keratins as expected (data not shown). Primary cultures of HFs and mCAFs, respectively, were negative for the leukocyte CD45 marker, endothelial marker CD34, melanocytic markers MELAN-A, HMB-45, S100 protein, tyrosinase, and epithelial keratins. All HFs, as well as mCAFs from the cutaneous metastases of melanoma from all three different donors (coded as VEM, MAM, ZAM), revealed typical spindle-shaped fibroblastoid morphology and they were positive for typical mesenchymal marker intermediate filament vimentin. The cultures prepared from one of the mCAFs (coded as ZAM) cells also contained spontaneously in high numbers the myofibroblasts positive for α-smooth muscle actin, the hallmark of CAFs (Fig. 1).

Expression profiles of HF and mCAFs

mCAFs prepared from three melanoma patients were collectively different (FDR < 0.05 and fold change two times) from normal HFs in the expression of 402 genes. While VEM and MAM mCAFs significantly differed from normal fibroblasts in 564 genes and 623 genes, respectively, ZAM mCAFs were different in outstanding 1157 genes (from

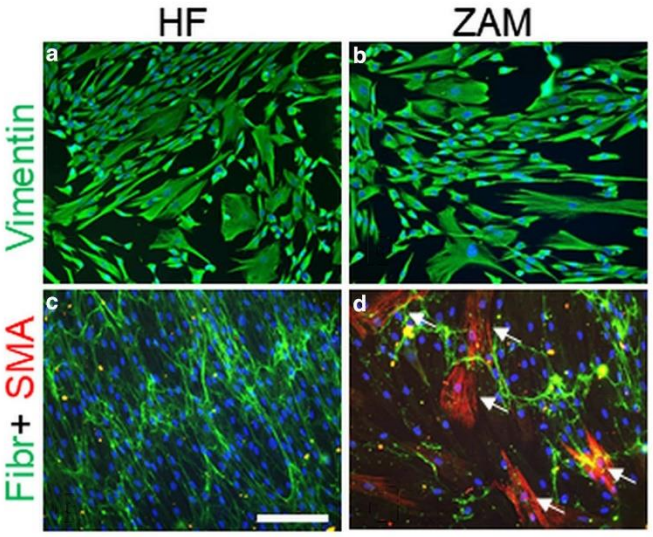

Fig. 1 Detection of vimentin (green signal, **a, b**), fibronectin (Fibr, green signal, **c, d**), and α smooth muscle actin (SMA, the red signal, **c, d**) in normal human dermal fibroblasts—HF (**a, c**) and cancer-associated fibroblasts—ZAM (**b, d**). Nuclei are counterstained with DAPI, the bar represents 100 µm

normal HFs, Fig. 2). This situation is also clearly depicted by the heat map (Fig. 3). The list of selected upregulated genes in ZAM coding extracellularly released factors (compared here to HF) with potential to influence keratinocytes and melanoma cells via paracrine interaction is shown in Table 3. Selected genes for extracellular products were also significantly upregulated in ZAM cells in comparison to mCAFs from two other donors (VEM, MAM) (Table 4). Genes coding IL6, IL8, and CXCL1 were upregulated in mCAFs from all three donors (see Tables 1, 4, respectively). Based on these indications, highly active ZAM cells were selected for further experiments as the representatives of mCAFs.

Effect of HF and ZAM on normal keratinocyte phenotype

Human keratinocytes cultured with normal HF and ZAM mCAFs formed distinct colonies. While keratinocytes cultured in the presence of HF exhibited no signal for vimentin, keratinocytes co-cultured with ZAM cells frequently coexpressed of keratins together with vimentin (Fig. 4).

Effect of keratinocyte irradiation on melanoma in vitro invasiveness in 3-D collagen gels

Keratinocytes alone stimulate invasiveness of melanoma cells almost 1.5 times in BLM and 3 times in A2058 melanoma cells using 3-D collagen migration assay. This baseline finding was compared after UV treatment of keratinocytes. Low dose UV-irradiation (10 mJ/cm^2) of keratinocytes revealed the only a very mild stimulatory effect on migration of both types of melanoma cells. More extensive UV-irradiation (50 and 100 mJ/cm^2) minimise the observed effect of keratinocytes on melanoma cells migration (Fig. 5).

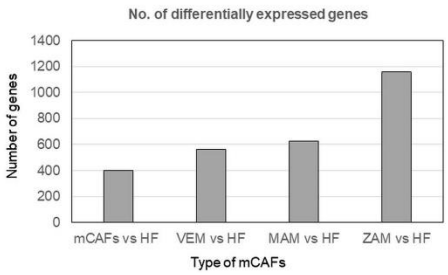

Fig. 2 The number of differentially expressed genes between cancer-associated fibroblasts (CAFs) isolated from all three donors and normal dermal fibroblasts (HF) and separately from each donor of CAF and HF

Normal HF introduced to the co-culture of keratinocytes irradiated by 3 × 10 mJ/cm^2 strongly stimulated invasiveness of BLM melanoma cells, however, it did not enhance invasiveness in A2058 cells.

When ZAM mCAFs were introduced to the co-culture system, the effect on the in vitro invasion in collagen gels was enhanced in both tested melanoma cell lines (Fig. 6).

The introduction of either HF or ZAM mCAFs to co-cultures after keratinocyte irradiation by 100 mJ/cm^2 was also effective in terms of melanoma enhanced invasiveness, but it did not reach extents observed in the case of the irradiation by 3 × 10 mJ/cm^2 (Fig. 6).

Effect of UV irradiation on DNA integrity of keratinocytes

An evident DNA damage was clearly documented in keratinocytes immediately after either 10 or 100 mJ/cm^2 UVB dose administration using Single Cell Gel Electrophoresis (Fig. 6). However, the low dose (10 mJ/cm^2) damage was readily repaired after 24 h, with or without fibroblast of any type ($p > 0.05$, no statistical significance). Keratinocytes irradiated at the high dose level (100 J/cm^2) were more seriously damaged immediately after UV irradiation ($p < 0.001$, statistical significance) and this detrimental damage could not be repaired after 24 h. Thus, single cell electrophoresis after high dose treatment could not be evaluated after 24 h in any case because only negligible numbers of keratinocytes maintained sufficient DNA and cellular integrity (Fig. 7).

Effect of HF and ZAM on normal keratinocyte: detection of life/dead cells

Non-irradiated keratinocytes, as well as keratinocytes irradiated by 3 × 10 mJ/cm^2, were practically without any signal of the presence of dead cells without and after the treatment with HF and ZAM CAFs. High-dose UVB irradiation (100 mJ/cm^2) was lethal for the majority of keratinocytes. After the introduction of either HF or ZAM to the culture of lethally irradiated keratinocytes, the cells formed clusters of shrinking cells with green cytoplasm (life cells) and red nuclei that are typical for dead cells (Fig. 8).

Discussion

The main finding of this study is the observation that even partial UV irradiation damage of tissue microenvironment supports in vitro invasion of melanoma cells on the 3D model. The compound model of tissue microenvironment consisting from insert co-culture of UV-irradiated keratinocytes and unirradiated fibroblasts allows collection of the conditioned medium after selective damage of a particular

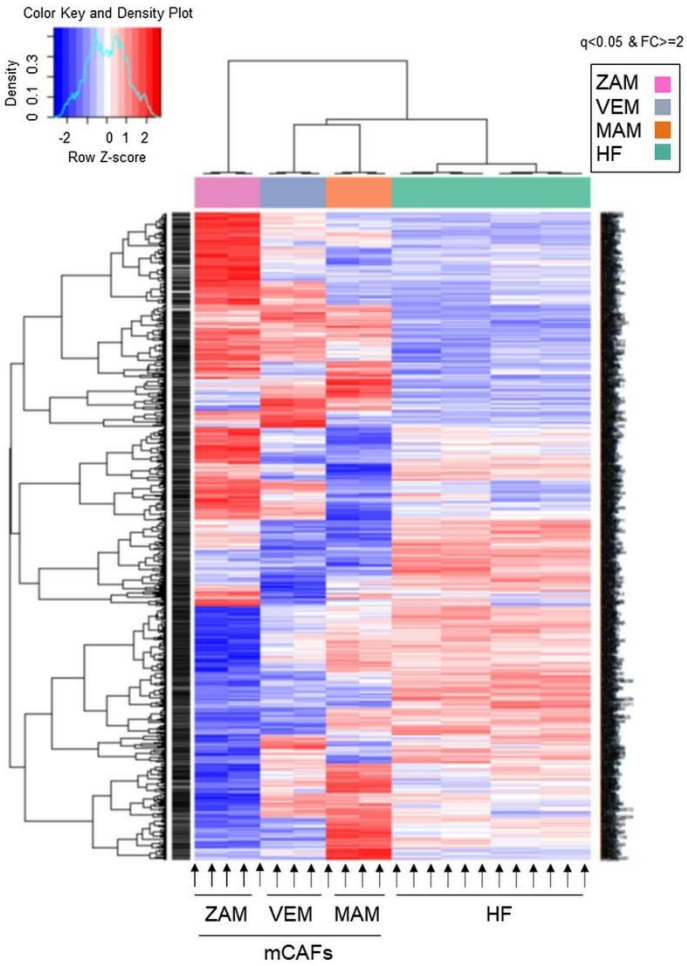

Fig. 3 Heat map demonstrates differential expression of genes in cancer-associated fibroblasts (ZAM, VEM, MAM) and normal dermal fibroblasts (HF)

component. The UVB seems to be a highly relevant component of UV light because it is causing a predominantly epidermal damage. UVB is linked to epidermal carcinogenesis. However, the selected energy of 10 mJ/cm^2 represents a low dose. It is lower than the minimal erythematous dose for fair skin (Dornelles et al. 2004). Such irradiation would not be associated with any immediate visible tissue response in vivo. However, there is a well-recognized relationship between chronic UVB-induced damage and the development of non-melanoma skin cancer. The protection mechanisms against UV-induced DNA damage have been extensively studied after subjecting cells or animal models with single acute UVB irradiation (Jackson and Bartek 2009). Until now, very little is known about how those mechanisms are influenced by chronic exposure to UVB light (Drigeard Desgarnier et al. 2017).

The dermal component of skin should be relatively unaffected by UVB irradiation, as only UVA irradiation significantly penetrates deeper into the dermis. UVA therefore potentially causes more widespread alterations in the dermis contributing to photoaging. On the other hand, acute low-level UVB irradiation upregulates matrix metalloproteinase

Table 3 Selected genes upregulated in ZAM compared to HF

Symbol	Gene name	LFC	FDR	Kerat	Melanoma
IL8	Interleukin 8	5.5	2.6e−06	+	+
ACAN	Aggrecan	4.27	3.6e−07	+	+
IL6	Interleukin 6 (interferon, beta 2)	3.87	7.5e−13	+	+
IL1B	Interleukin 1, beta	2.52	3.6e−08		
CXCL1	Chemokine (C–C–C motif) ligand 1 (melanoma growth stimulating activity, alpha)	2.49	0.0045	+	+
HBEGF	Heparin-binding EGF-like growth factor	1.74	8.5e−06	+	
BDNF	Brain-derived neurotrophic factor	1.46	5.3e−06		+
TGFB2	Transforming growth factor, beta 2	1.23	0.00017		+
IGFBP7	Insulin-like growth factor binding protein 7	1.23	0.00012	+	
GAP43	Growth associated protein 43	1.21	2.3e−05	+	
CXCL16	Chemokine (C–X–C motif) ligand 16	1.17	8.3e−05		+
BMP6	Bone morphogenetic protein 6	1.11	0.0032		
KAZALD1	Kazal-type serine peptidase inhibitor domain 1	1.03	0.016		
VEGFC	Vascular endothelial growth factor C	1.02	0.0066	+	+
CTGF	Connective tissue growth factor	0.95	0.022		+
PDGFRL	Platelet-derived growth factor receptor-like	0.93	0.055		+
LEPREL1	Leprecan-like 1	0.91	0.017		
IL17D	Interleukin 17D	0.88	0.00021		+
VEGFA	Vascular endothelial growth factor A	0.82	0.029	+	+
BMP2	Bone morphogenetic protein 2	0.73	0.028		+
LEPRE1	Leucine proline-enriched proteoglycan (leprecan) 1	0.72	0.0011		

LFC binary logarithm of the fold change in expression intensity, *FDR* false discovery rate, *Kerat* keratinocytes, *Melanoma* melanoma cells, +: genes with stimulatory effect on keratinocytes or melanoma cells according to literature data (for references see "Discussion")

Table 4 Selected genes upregulated in ZAM compared to other CAFs

Symbol	Gene name	LFC	FDR
IL8	Interleukin 8	3.87	0.00032
IL6	Interleukin 6 (interferon, beta 2)	2.61	9.8e−10
BDNF	Brain-derived neurotrophic factor	1.48	4.1e−05
HBEGF	Heparin-binding EGF-like growth factor	2.17	3.2e−07
IL1B	Interleukin 1, beta	1.95	2.7e−06
CSPG4	Chondroitin sulphate proteoglycan 4	1.77	9.1e−0.5
VEGFC	Vascular endothelial growth factor C	1.51	0.00013
KCTD10	Potassium channel tetramerisation domain containing 10	1.17	8.1e−06
TGFB2	Transforming growth factor, beta 2	1.15	0.00042
CXCL1	Chemokine (C-C-C motif) ligand 1 (melanoma growth stimulating activity, alpha)	1.06	0.42
NTF3	Neurotrophin 3	0.96	2e−05
GAP43	Growth associated protein 43	0.91	0.00094
EPS15	Epidermal growth factor receptor pathway substrate 15	0.78	0.044
CTGF	Connective tissue growth factor	0.72	0.13
BMP2	Bone morphogenetic protein 2	0.71	0.044
PDGFRL	Platelet-derived growth factor receptor-like	0.93	0.055
LEPREL1	Leprecan-like 1	0.91	0.017
VEGFA	Vascular endothelial growth factor A	0.82	0.029
BMP2	Bone morphogenetic protein 2	0.73	0.028
FGF5	FIBROBLAST growth factor 5	0.68	0.37

LFC binary logarithm of the fold change in expression intensity, *FDR* false discovery rate

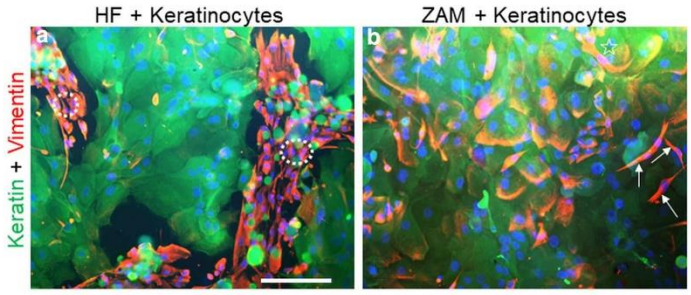

Fig. 4 Co-culture of human keratinocytes (**a, b**) with normal dermal fibroblasts (HF, **a**) and ZAM cancer-associated fibroblasts (**b**). While keratinocytes with HF exhibited only keratins (green signal, **a**), keratinocytes co-cultured with ZAM (**b**) exhibited both keratins (green signal) and vimentin (red signal). Vimentin positivity in double positive keratinocytes indicates their polarization. Vimentin-positive HFs are marked by white circles and vimentin-positive ZAM with white arrows. Nuclei are counterstained with DAPI, the bar represents 100 µm

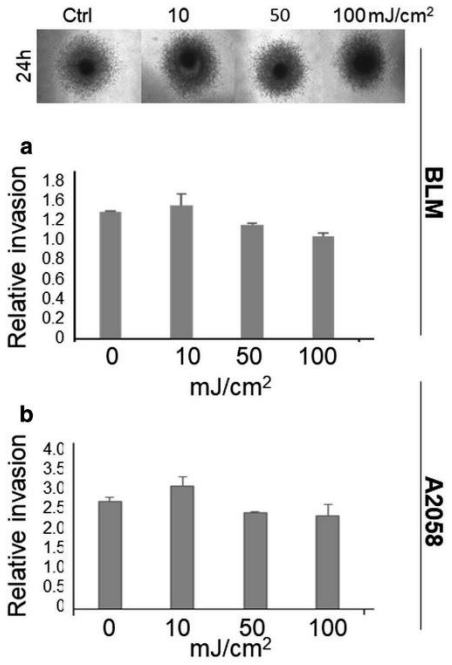

Fig. 5 Influence of UV-irradiated keratinocytes on relative invasion of BLM (**a**) and A2058 (**b**) melanoma cells. As the control, the conditioned medium from non-irradiated keratinocytes was used. The introduction of non-irradiated keratinocytes to system influences the melanoma cell invasiveness more in A2058 than in BLM cells

1 (Fisher et al. 1996) which consequently initiates collagen I fibril degradation. Ultraviolet B irradiation also suppresses procollagen I synthesis, thereby promoting further loss of collagen I fibrils (Fisher et al. 2000). Surprisingly, it was suggested that the MMPs induced by low-dose UV irradiation might be derived from the epidermis, and only to a lesser extent, from the dermis (Brennan et al. 2003; Quan et al. 2009). This clearly highlights the importance of epithelial–mesenchymal interaction in the maintenance of the epidermal structure.

Despite the increasing insight into various events in photoaging, the specific molecular pathogenesis of changes in the photodamaged dermis and their relation to various processes, such as cellular senescence, remains poorly understood. Compelling evidence about senescence in cultured cells has been gathered over the past decades. However, the senescence in living organisms is enigmatic, largely because of technical limitations relating to the identification and characterization of senescent cells in tissues and organs (Childs et al. 2015).

The autocrine and paracrine properties of senescent cells can play an important role in the contexts of ageing and age-related diseases, including cancer (Smetana et al. 2016a, b). There is convincing evidence associating senescent cells with the malignant progression of tumours. Of note, the senescence-associated secretory phenotype includes multiple pro-inflammatory cytokines, and IL-6 and IL-8 are consistently present in this repertoire (Ortiz-Montero et al. 2017).

On the other hand, the population of stromal fibroblast in malignant tumours (the CAFs) also produces a broad panel of growth factors/cytokines/chemokines broadly overlapping with the repertoire of senescence-associated secretome. As we know from our previous research (Kolář

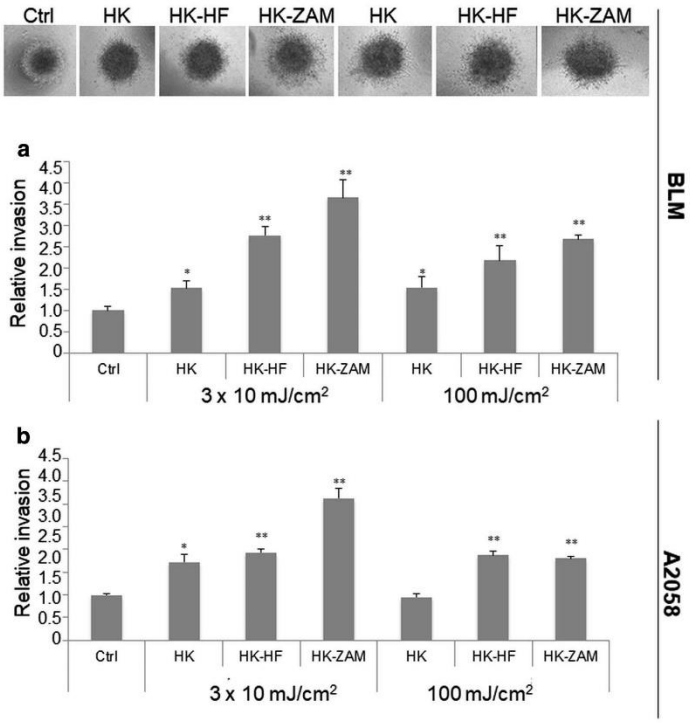

Fig. 6 Normal dermal fibroblasts (HF) and namely cancer-associated fibroblasts ZAM increased the effect of UV-irradiated keratinocytes (HK) and stimulated invasion of BLM (**a**) and A2058 (**b**) melanoma cells. Mild fractionated irradiation (3×10 mJ/cm^2) was more efficient than lethal irradiation of keratinocytes (100 mJ/cm^2)

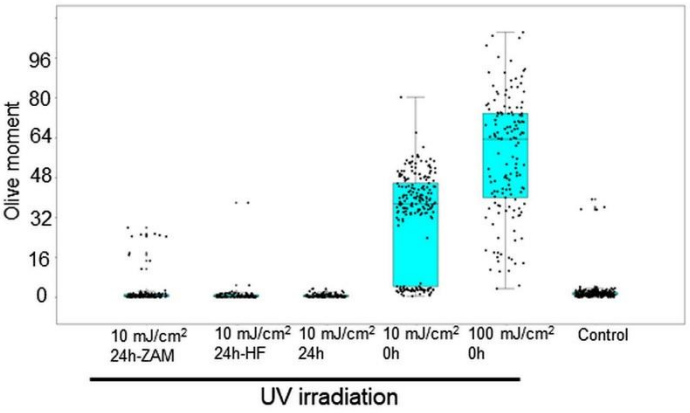

Fig. 7 Significant damage to DNA assessed by single cell gel electrophoresis (comet assay) was detected immediately after 10 and 100 mJ/cm^2 dose, respectively ($p < 0.01$). However, keratinocytes were able to repair DNA damage after 24 h in case of low dose (10 mJ/cm^2) irradiation with or without co-cultured cancer-associated fibroblasts isolated from melanoma (mCAFs) or normal fibroblasts (HF) (no significant differences, $p > 0.05$)

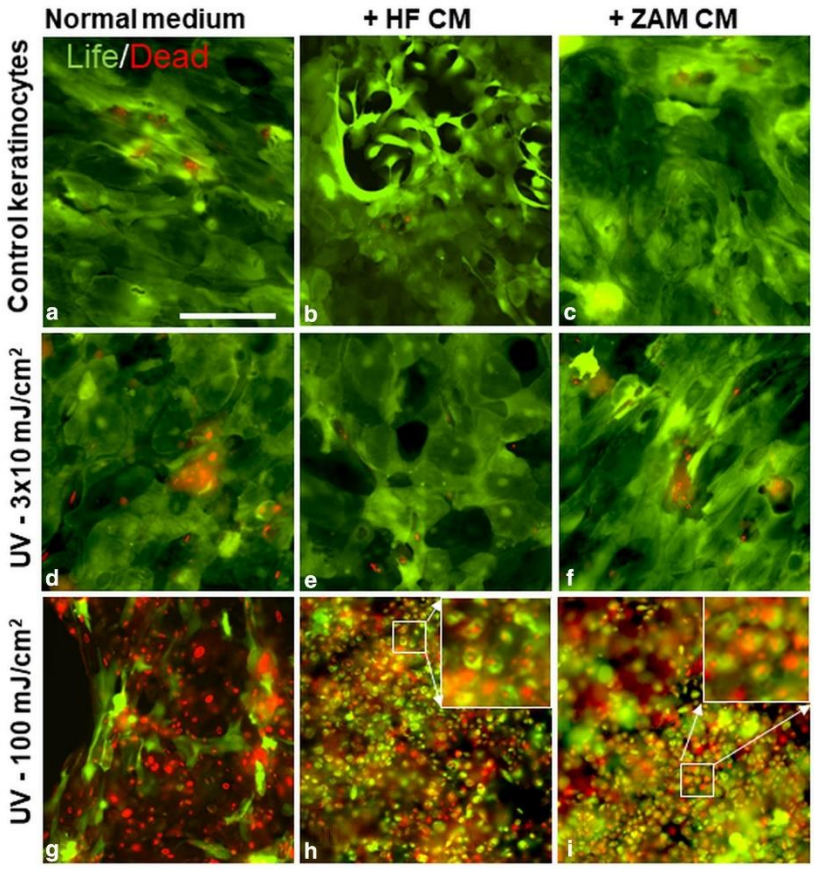

Fig. 8 Control keratinocytes (**a–c**) as well as keratinocytes after fractionated mild irradiation (3×10 mJ/cm^2) (**d–f**) exhibited the low occurrence of dead cells (red nuclei) without (**a, d**), or with normal fibroblasts (**b, e**) and with ZAM cancer-associated fibroblasts (**c, f**). High dose UV irradiation (100 mJ/cm^2) significantly increased the number of dead cells (**g**). Interestingly that introduction of HF or ZAM to the system increased a number of green cells (signal for living elements), although the number of dead nuclei was not affected (**h, i**). These green cells are very small with shrunk cytoplasm. The bar represents 100 µm

et al. 2012), IL-6, IL-8 and CXCL-1 can be produced by CAFs in a paracrine manner and these cytokines can significantly influence the maintenance of low differentiation status of keratinocytes. Besides that, IL-6 and IL-8 also potentiate invasiveness of melanoma cells in vitro (Jobe et al. 2016). The differences between the real senescence-associated secretory phenotype and its counterpart in malignant tumours are subtle, if any, and still elusive (Ghosh and Capell 2016).

Assuming that we are physiologically exposed to a repeated chronic low dose of UV radiation, it becomes crucial to understand how molecular mechanisms in skin tissue respond to these minor recurrent irradiation doses. Repeated mild UV irradiation of keratinocytes thus resembles the situation in the light-unprotected human skin. It has no detrimental effect on keratinocyte viability in contrast to high-dose (100 mJ/cm^2) with lethal effect on treated keratinocytes. However, even this low dose treatment can

cause DNA damage. Mesenchymal cells in the dermal compartment, either HF or mCAFs, respond to and interact with the UV-damaged keratinocytes via paracrine production of bioactive factors. This UV damage in keratinocytes, in fact, triggers multilateral intercellular interaction. Notably, UV-irradiated keratinocytes (and fibroblasts) secrete molecules also important for melanoma progression such as bFGF, endothelin-1, TGF-β1, TNF-α, IL-11, IL-1α, and PDGF (platelet-derived growth factor and hepatocyte growth factor) even in monoculture (Brenner et al. 2005).

Normal HF and mCAFs seem to be able to influence UV-damaged epidermal keratinocytes by the paracrine production of numerous bioactive factors that we selected from their expression profile analysis in the present study. In addition to others, aggrecan (Shafritz et al. 1994), HBEGF (Johnson and Wang 2013), IGFBP-7 (Hochberg et al. 2013), GAP-43 (Kant et al. 2015), CTGF (Barrientos et al. 2008), VEGF-C (Benke et al. 2010), PDGFRL (Kamp et al. 2003), VEGF-A (Wu et al. 2014), IL-6, IL-8 and CXCL-1 (Kolář et al. 2012) stimulate proliferation and/or migration of keratinocytes (Table 3). Moreover, factors produced by HF and mainly by mCAF (represented by strain ZAM) can also positively influence the melanoma cells. It was demonstrated for factors such as IL-6 and IL-8 (Jobe et al. 2016), aggrecan (Iida et al. 2007) and CXCL-1 (Di Cesare et al. 2007). The same effect was also observed for BDNF (Marchetti and Nicolson 1997), TGF-B2 (Zhang et al. 2009), CXCL-16 (La Porta 2012), VEGF-C (Peppicelli et al. 2014), CTGF (Finger et al. 2014), PDGFRL (Sabbatino et al. 2014), IL-17D (Zelba et al. 2014), VEGF-A (Vartanian et al. 2011), and BMP-2 (Rothhammer et al. 2005) (Table 3).

In conclusion, UV-irradiation is not only an important factor in mutagenesis. UV light represents also an important factor for melanoma in vitro invasion. The role of UV irradiation on melanoma progression can be therefore expected. The described phenomenon seems to be important in the facilitation of either radial growth in superficial melanoma or in progression to more advanced stages of disease associated vertical growth and subsequent metastasis formation. In agreement with previously published data, IL-6, IL-8, and CXCL-1 can be an attractive target for intervention in the context of chronic UV light exposure. Further analysis needs to be done to shed light on those mechanisms and their consequence for cells. A proper understanding of these mechanisms may offer a new powerful target for skin cancer prevention and therapy. The hope is that increasing precaution will be taken by all population groups to avoid harmful exposure to repeated even small UV radiation even at early ages to prevent serious adverse health outcomes including melanoma later in life.

Acknowledgements This publication is a result of the project implementation: "The equipment for metabolomic and cell analyses", registration number CZ.1.05/2.1.00/19.0400, supported by Research and Development for Innovations Operational Programme (RDIOP) co-financed by European regional development fund and the state budget of the Czech Republic. This study was also supported by the Grant Agency of the Czech Republic (Project no. 16-05534S), AZV 16-29032A, the Charles University (project of Specific University Research, GAUK 165015 and PROGRESS 28 and UNCE 23014) and by the Ministry of Education, Youth and Sports of CR within the National Sustainability Program II (Project BIOCEV-FAR reg. no. LQ1604), and by the project BIOCEV (CZ.1.05/1.1.00/02.0109). The part of the study was performed by the equipment for metabolomics and cell analyses (Grant no. CZ.1.05/2.1.00/19.0400) supported by the Research and Development for Innovations Operational Program, co-financed by the European regional development fund and the state budget of the Czech Republic.

References

Adini I, Ghosh K, Adini A, Chi ZL, Yoshimura T, Benny O, Connor KM, Rogers MS, Bazinet L, Birsner AE, Bielenberg DR, D'Amato RJ (2014) Melanocyte-secreted fibromodulin promotes an angiogenic microenvironment. J Clin Investig 124:425–436

Adini I, Adini A, Bazinet L, Watnick RS, Bielenberg DR, D'Amato RJ (2015) Melanocyte pigmentation inversely correlates with MCP-1 production and angiogenesis-inducing potential. FASEB J 29:662–670

Barrientos S, Stojadinovic O, Golinko MS, Brem H, Tomic-Canic M (2008) Growth factors and cytokines in wound healing. Wound Repair Regen 16:585–601

Benke EM, Ji Y, Patel V, Wang H, Miyazaki H, Yeudall WA (2010) VEGF-C contributes to head and neck squamous cell carcinoma growth and motility. Oral Oncol 46:e19–e24

Brash DE (2015) UV signature mutations. Photochem Photobiol 91:15–26

Brennan M, Bhatti H, Nerusu KC, Bhagavathula N, Kang S, Fisher GJ, Varani J, Voorhees JJ (2003) Matrix metalloproteinase-1 is the major collagenolytic enzyme responsible for collagen damage in UV-irradiated human skin. Photochem Photobiol 78:43–48

Brenner M, Degitz K, Besch R, Berking C (2005) Differential expression of melanoma-associated growth factors in keratinocytes and fibroblasts by ultraviolet A and ultraviolet B radiation. Br J Dermatol 153:733–739

Catania A (2007) The melanocortin system in leukocyte biology. J Leukocyte Biol 81:383–392

Cheli Y, Giuliano S, Botton T, Rocchi S, Hofman V, Hofman P, Bahadoran P, Bertolotto C, Ballotti R (2011) Mitf is the key molecular switch between mouse or human melanoma initiating cells and their differentiated progeny. Oncogene 30:2307–2318

Childs BG, Durik M, Baker DJ, van Deursen JM (2015) Cellular senescence in aging and age-related disease: from mechanisms to therapy. Nat Med 21:1424–1435

Chou WC, Takeo M, Rabbani P, Hu H, Lee W, Chung YR, Carucci J, Overbeek P, Ito M (2013) Direct migration of follicular melanocyte stem cells to the epidermis after wounding or UVB irradiation is dependent on Mc1r signaling. Nat Med 19:924–929

D'Orazio J, Jarrett S, Amaro-Ortiz A, Scott T (2013) UV Radiation and the Skin. Int J Mol Sci 14:12222–12248

Di Cesare S, Marshall JC, Logan P, Antecka E, Faingold D, Maloney SC, Burnier MN Jr (2007) Expression and migratory analysis of 5 human uveal melanoma cell lines for CXCL12, CXCL8, CXCL1, and HGF. J Carcinogen 6:2

Dornelles S, Goldim J, Cestari T (2004) Determination of the minimal erythema dose and colorimetric measurements as indicators

of skin sensitivity to UV-B radiation. Photochem Photobiol 79:540–544
Drigeard Desgarnier MC, Fournier F, Droit A, Rochette PJ (2017) Influence of a pre-stimulation with chronic low-dose UVB on stress response mechanisms in human skin fibroblasts. PLoS One 12:e0173740
Dvořánková B, Szabo P, Lacina L, Kodet O, Matoušková E, Smetana K Jr (2012) Fibroblasts prepared from different types of malignant tumors stimulate expression of luminal marker keratin 8 in the EM-G3 breast cancer cell line. Histochem Cell Biol 137:679–685
Dvořánková B, Szabo P, Kodet O, Strnad H, Kolář M, Lacina L, Krejčí E, Naňka O, Šedo A, Smetana K Jr (2017) Intercellular crosstalk in human malignant melanoma. Protoplasma 254:1143–1150
Finger EC, Cheng CF, Williams TR, Rankin EB, Bedogni B, Tachiki L, Spong S, Giaccia AJ, Powell MB (2014) CTGF is a therapeutic target for metastatic melanoma. Oncogene 33:1093–1100
Fisher GJ, Datta SC, Talwar HS, Wang ZQ, Varani J, Kang S, Voorhees JJ (1996) Molecular basis of sun-induced premature skin ageing and retinoid antagonism. Nature 379:335–339
Fisher GJ, Datta S, Wang Z, Li XY, Quan T, Chung JH, Kang S, Voorhees JJ (2000) c-Jun-dependent inhibition of cutaneous procollagen transcription following ultraviolet irradiation is reversed by all-trans retinoic acid. J Clin Investig 106:663–670
Gentleman RC, Carey VJ, Bates DM, Bolstad B, Dettling M, Dudoit S, Ellis B, Gautier L, Ge Y, Gentry J, Hornik K, Hothorn T, Huber W, Iacus S, Irizarry R, Leisch F, Li C, Maechler M, Rossini AJ, Sawitzki G, Smith C, Smyth G, Tierney L, Yang JY, Zhang J (2004) Bioconductor: open software development for computational biology and bioinformatics. Genome Biol 5:R80
Ghosh K, Capell BC (2016) The senescence-associated secretory phenotype: critical effector in skin cancer and aging. J Investig Dermatol 136:2133–2139
Golan T, Messer AR, Amitai-Lange A, Melamed Z, Ohana R, Bell RE, Kapitansky O, Lerman G, Greenberger S, Khaled M, Amar N, Albrengues J, Gaggioli C, Gonen P, Tabach Y, Sprinzak D, Shalom-Feuerstein R, Levy C (2015) Interactions of melanoma cells with distal keratinocytes trigger metastasis via notch signaling inhibition of MITF. Mol Cell 59:664–676
Gyori BM, Venkatachalam G, Thiagarajan PS, Hsu D, Clement MV (2014) OpenComet: an automated tool for comet assay image analysis. Redox Biol 2:457–465
Hammer R, Harper DAT, Ryan PD (2001) Paleontological statistics software package for education and data analysis. Palaeontol Electron 4:1–9
Hochberg M, Gilead L, Markel G, Nemlich Y, Feiler Y, Enk CD, Denichenko P, Karni R, Ingber A (2013) Insulin-like growth factor-binding protein-7 (IGFBP7) transcript: A-to-I editing events in normal and cancerous human keratinocytes. Arch Dermatol Res 305:519–528
Iida J, Wilhelmson KL, Ng J, Lee P, Morrison C, Tam E, Overall CM, McCarthy JB (2007) Cell surface chondroitin sulfate glycosaminoglycan in melanoma: role in the activation of pro-MMP-2 (progelatinase A). Biochem J 403:553–563
Jackson SP, Bartek J (2009) The DNA-damage response in human biology and disease. Nature 461:1071–1078
Jobe NP, Rösel D, Dvořánková B, Kodet O, Lacina L, Mateu R, Smetana K, Brábek J (2016) Simultaneous blocking of IL-6 and IL-8 is sufficient to fully inhibit CAF-induced human melanoma cell invasiveness. Histochem Cell Biol 146:205–217
Johnson NR, Wang Y (2013) Controlled delivery of heparin-binding EGF-like growth factor yields fast and comprehensive wound healing. J Control Release 166:124–129
Kamp H, Geilen CC, Sommer C, Blume-Peytavi U (2003) Regulation of PDGF and PDGF receptor in cultured dermal papilla cells and follicular keratinocytes of the human hair follicle. Exp Dermatol 12:662–672
Kant V, Kumar D, Kumar D, Prasad R, Gopal A, Pathak NN, Kumar P, Tandan SK (2015) Topical application of substance P promotes wound healing in streptozotocin-induced diabetic rats. Cytokine 73:144–155
Kim EJ, Kim YK, Kim JE, Kim S, Kim M-K, Park C-H, Chung JH (2011) UV Modulation of subcutaneous fat metabolism. J Investig Dermatol 131:1720–1726
Kodet O, Dvořánková B, Krejčí E, Szabo P, Dvořák P, Štork J, Krajsová I, Dundr P, Smetana K Jr, Lacina L (2013) Cultivation-dependent plasticity of melanoma phenotype. Tumour Biol 34:3345–3355
Kodet O, Lacina L, Krejčí E, Dvořánková B, Grim M, Štork J, Kodetová D, Vlček Č, Šáchová J, Kolář M, Strnad H, Smetana K Jr (2015) Melanoma cells influence the differentiation pattern of human epidermal keratinocytes. Mol Cancer 14:1
Kolář M, Szabo P, Dvořánková B, Lacina L, Gabius H-J, Strnad H, Sáchová J, Vlček C, Plzák J, Chovanec M, Cada Z, Betka J, Fík Z, Pačes J, Kovářová H, Motlík J, Jarkovská K, Smetana K Jr (2012) Upregulation of IL-6, IL-8 and CXCL-1 production in dermal fibroblasts by normal/malignant epithelial cells in vitro, immunohistochemical and transcriptomic analyses. Biol Cell 104:738–751
Kondo T, Hearing VJ (2011) Update on the regulation of mammalian melanocyte function and skin pigmentation. Expert Rev Dermatol 6:97–108
Krejčí E, Kodet O, Szabo P, Borský J, Smetana K Jr, Grim M, Dvořánková B (2015) In vitro differences of neonatal and later postnatal keratinocytes and dermal fibroblasts. Physiol Res 64:561–569
Kučera J, Dvořánková B, Smetana K Jr, Szabo P, Kodet O (2015) Fibroblasts isolated from the malignant melanoma influence phenotype of normal human keratinocytes. J Appl Biomed 13:195–198
La Porta CA (2012) CXCR6: the role of environment in tumor progression. Challenges for therapy. Stem Cell Rev 8:1282–1285
Lacina L, Plzak J, Kodet O, Szabo P, Chovanec M, Dvorankova B, Smetana K Jr (2015) Cancer microenvironment: What can we learn from the stem cell niche. Int J Mol Sci 16:24094–24110
Lacina L, Kodet O, Dvořánková B, Szabo P, Smetana K Jr (2017) Ecology of melanoma cells. Histol Histopathol. https://doi.org/10.14670/HH-11-926
Lo JA, Fisher DE (2014) The melanoma revolution: from UV carcinogenesis to a new era in therapeutics. Science 346:945–949
Marchetti D, Nicolson GL (1997) Human melanoma cell invasion: selected neurotrophin enhancement of invasion and heparanase activity. J Investig Dermatol Symp Proc 2:99–105
Mateu R, Živicová V, Drobná Krejčí E, Grim M, Strnad H, Vlček Č, Kolář M, Lacina L, Gál P, Borský J, Smetana K Jr, Dvořánková B (2016) Functional differences between neonatal and adult fibroblasts and keratinocytes. Int J Mol Med 38:1063–1074
Merkel EA, Gerami P (2017) Malignant melanoma of sun-protected sites: a review of clinical, histological, and molecular features. Lab Investig 97:630–635
Ortiz-Montero P, Londoño-Vallejo A, Vernot JP (2017) Senescence-associated IL-6 and IL-8 cytokines induce a self- and cross-reinforced senescence/inflammatory milieu strengthening tumorigenic capabilities in the MCF-7 breast cancer cell line. Cell Commun Signal 15:17
Peppicelli S, Bianchini F, Calorini L (2014) Inflammatory cytokines induce vascular endothelial growth factor-C expression in melanoma-associated macrophages and stimulate melanoma lymph node metastasis. Oncol Lett 8:1133–1138
Quan T, Qin Z, Xia W, Shao Y, Voorhees JJ, Fisher GJ (2009) Matrix-degrading metalloproteinases in photoaging. J Investig Dermatol Symp Proc 14:20–24
Rastrelli M, Tropea S, Rossi CR, Alaibac M (2014) Melanoma: epidemiology, risk factors, pathogenesis, diagnosis and classification. In Vivo 28:1005–1011

Rothhammer T, Poser I, Soncin F, Bataille F, Moser M, Bosserhoff AK (2005) Bone morphogenic proteins are overexpressed in malignant melanoma and promote cell invasion and migration. Cancer Res 65:448–456

Rünger TM (2016) Mechanisms of melanoma promotion by ultraviolet radiation. J Investig Dermatol 136:1751–1752

Sabbatino F, Wang Y, Wang X, Flaherty KT, Yu L, Pepin D, Scognamiglio G, Pepe S, Kirkwood JM, Cooper ZA, Frederick DT, Wargo JA, Ferrone S, Ferrone CR (2014) PDGFRα up-regulation mediated by sonic hedgehog pathway activation leads to BRAF inhibitor resistance in melanoma cells with BRAF mutation. Oncotarget 5:1926–1941

Schneider CA, Rasband WS, Eliceiri KW (2012) NIH Image to ImageJ: 25 years of image analysis. Nat Methods 9:671–675

Shafritz TA, Rosenberg LC, Yannas IV (1994) Specific effects of glycosaminoglycans in an analog of extracellular matrix that delays wound contraction and induces regeneration. Wound Repair Regen 2:270–276

Smetana K Jr, Dvořánková B, Lacina L (2016a) Phylogeny, regeneration, ageing and cancer: role of microenvironment and possibility of its therapeutic manipulation. Folia Biol 59:207–216

Smetana K Jr, Lacina L, Szabo P, Dvořánková B, Brož P, Šedo A (2016b) Ageing as an important risk factor for cancer. Anticancer Res 36:5009–5017

Smyth GK (2006) Linear models and empirical Bayes methods for assessing differential expression in microarray experiments. Stat Appl Genet Mol Biol 3:3

Tice RR, Agurell E, Anderson D, Burlinson B, Hartmann A, Kobayashi H, Miyamae Y, Rojas E, Ryu JC, Sasaki YF (2000) Single cell gel/comet assay: guidelines for in vitro and in vivo genetic toxicology testing. Environ Mol Mutagen 35:206–221

Trylcova J, Busek P, Smetana K Jr, Balaziova E, Dvorankova B, Mifkova A, Sedo A (2015) Effect of cancer-associated fibroblasts on the migration of glioma cells in vitro. Tumour Biol 36:5873–5879

Vartanian A, Stepanova E, Grigorieva I, Solomko E, Baryshnikov A, Lichinitser M (2011) VEGFR1 and PKCα signaling control melanoma vasculogenic mimicry in a VEGFR2 kinase-independent manner. Melanoma Res 21:91–98

Volkmer B, Greinert R (2011) UV and Children's skin. Prog Biophys Mol Biol 107:386–388

Wang JX, Fukunaga-Kalabis M, Herlyn M (2016) Crosstalk in skin: melanocytes, keratinocytes, stem cells, and melanoma. J Cell Commun Signal 10:191–196

Wu XJ, Zhu JW, Jing J, Xue D, Liu H, Zheng M, Lu ZF (2014) VEGF165 modulates proliferation, adhesion, migration and differentiation of cultured human outer root sheath cells from central hair follicle epithelium through VEGFR-2 activation in vitro. J Dermatol Sci 73:152–160

Zelba H, Weide B, Martens A, Derhovanessian E, Bailur JK, Kyzirakos C, Pflugfelder A, Eigentler TK, Di Giacomo AM, Maio M, Aarntzen EH, de Vries J, Sucker A, Schadendorf D, Büttner P, Garbe C, Pawelec G (2014) Circulating CD4+ T cells that produce IL4 or IL17 when stimulated by melan-A but not by NY-ESO-1 have negative impacts on survival of patients with stage IV melanoma. Clin Cancer Res 20:4390–4399

Zhang C, Zhang F, Tsan R, Fidler IJ (2009) Transforming growth factor-beta2 is a molecular determinant for site-specific melanoma metastasis in the brain. Cancer Res 69:828–835

PUBLIKACE II

Strnadova K, Sandera V, Dvorankova B, Kodet O, Duskova M, Smetana K, Lacina L. Skin aging: the dermal perspective. *Clin Dermatol*. 2019 Jul-Aug;37(4):326-335. **(IF: 2.458)**

Clinics in Dermatology (2019) 37, 326–335

Clinics in Dermatology

Skin aging: the dermal perspective

Karolina Strnadova, MSc[a,b,1], Vojtech Sandera, MD[d,1], Barbora Dvorankova, PhD[a,b], Ondrej Kodet, MD, PhD[a,b,c], Marketa Duskova, MD, PhD[d], Karel Smetana, MD, DSc[a,b], Lukas Lacina, MD, PhD[a,b,c,*]

[a]*Institute of Anatomy, First Faculty of Medicine, Charles University, Prague, Czech Republic*
[b]*BIOCEV, First Faculty of Medicine, Charles University, Vestec, Czech Republic*
[c]*Department of Dermatovenereology, First Faculty of Medicine, Charles University, Prague, Czech Republic*
[d]*Department of Plastic Surgery, Third Faculty of Medicine, Charles University, Prague, Czech Republic*

Abstract The world population of adults aged 60 years or more is increasing globally, and this development can impact skin disease morbidity and mortality, as well as being reflected in the health care system organization. There is substantial evidence that the burden from a remarkable number of skin nonmalignant and malignant conditions is greater in the elderly. Dermatologic research and clinical education in dermatology should focus on both challenges and opportunities created by aging. Skin aging due to intrinsic and extrinsic factors can alter significantly epidermal and dermal structure and functions. Dermal aging can be linked to a great number of complications in routine dermatologic conditions, with slow healing as an example of a severe complication in the elderly. This may be attributed to aged dermal fibroblasts modifying the tissue microenvironment via a shift in their soluble factors and extracellular matrix repertoire. This senescence-associated secretory phenotype can explain the particular proclivity of aged skin to develop malignancies.

Change in demography: global aging will affect dermatology practice

The world population of adults aged 60 or more is significantly increasing globally. More important, the population aged 60 or above is growing faster than all younger age groups. This trend was initially apparent in high-income countries. Recently, progressive aging has become apparent elsewhere. By 2050, all regions of the world except Africa will have nearly a quarter or more of their populations aged 60 or more. The number of older persons in the world is projected to be 1.4 billion in 2030, 2.1 billion in 2050, and even 3.1 billion in 2100.[1]

Globally, life expectancy at birth is projected to rise from 71 years in 2010-2015 to 77 years in 2045-2050. For example, Asia and Europe will gain approximately 6 or 7 years of life expectancy by 2045-2050, whereas the United States and Canada are expected to gain 4 to 5 years of longevity.[1]

Historically, such a remarkable increase in life expectancy was initially attributed to the successful management of various infectious diseases via the improved organization and public availability of the health care system, sanitation methods, disinfectants, vaccination, and the use of antimicrobials. Primarily, this was achieved through reduction in mortality particularly in childhood and childbirth. Later, another increment of life expectancy was achieved in adults by new

* Corresponding author.
E-mail address: lukaslacina@lf1.cuni.cz (L. Lacina).
[1]Both authors contributed equally to this work.

https://doi.org/10.1016/j.clindermatol.2019.04.005
0738-081X/

options in the treatment of noncommunicable diseases, including cardiovascular disease, metabolic disorders, and malignancies.

The lifetime risks of diseases occurring in the elderly are influenced by increased survival. This may be attributed to the higher number of survivors, where the disease incidence is peaking.[2]

How does this globally extended human life expectancy affect dermatology and health care systems in general? More specifically, how does this impact skin disease morbidity and mortality?

There is substantial evidence that the burden from a remarkable number of nonmalignant skin conditions, including psoriasis, dermatophytoses, and decubitus ulcers, is greater in the elderly.[3] This increasing burden is possible to quantify by using the disability-adjusted life year (DALY).[4] Cutaneous malignancies, including melanoma, also increase with advancing longevity.[5] An elderly population is more likely to develop, for example, skin cancer, and increased age may be a risk factor negatively influencing skin cancer outcomes.[6] Notably, the greatest skin-cancer-related DALY rates occur in individuals older than 75 years.[4]

On the basis of these data, aging—particularly skin aging—is an increasingly important topic. WHO demands that every human being "should have the opportunity to live a long and healthy life"[7] and that "everybody can experience healthy ageing."[7] Dermatologic research and clinical education in dermatology should meaningfully focus on both challenges and opportunities represented by aging. Although multiple efforts have been made to address, for example, the aging skin-related pathologies, studies of this aging-related health system costs are relatively sparse. Active screening for both melanoma and other cutaneous carcinomas is a cost-effective strategy and has been projected for a substantial reduction of 5% in skin cancer mortality during two decades.[8]

In financial terms, poor healing of, for example, decubitus ulcers costs $9.1-$11.6 billion per year in the United States. The cost of individual patient care ranges from $20,900 to $151,700 per decubitus ulcer.[9]

Aging of the epidermis: beyond the intrinsic phenomenon?

Aging is a continuous process. In general, it is very difficult to measure aging precisely, because it is perceived as a complex series of, frequently subtle, physiologic and structural changes that occur over time. These changes are represented by a broad diversity of health and functional states experienced by older people. The range of these changes in the older age group is highly individual and only loosely associated with chronologic age. This diversity is a hallmark of human older age.

Both internal and external factors can influence the onset of age-related changes. Intrinsic (chronologic) and extrinsic (environment induced) aging types are executed through different mechanisms and pathways. Their effects are synergistic for the affected individual. Different mechanisms employed can even result in different structural and functional alterations in the affected organs, including the skin.

The epidermis is a rapidly proliferating tissue. The pool of proliferating cells is located in the basal layer anchored to the basement membrane. Epidermal stem cells occupy a well-defined region of the hair follicle (the bulge region) and less clearly defined regions in interfollicular epidermis.[10] The epidermis and also its appendageal organs undergo frequent turnover to replace physiologically shed cells. In pathologic conditions, these organs also contribute to the rapid repair of externally induced wounds.

The epidermis is also a self-renewing tissue that is required throughout the whole lifespan of an organism. Cells are able to divide for only a restricted number of times, before they undergo permanent cell division arrest lasting until their death. This phenomenon is known as replicative senescence.[11] Telomere shortening acts as a mitotic clock to prevent unregulated cell proliferation.[12] This would also restrict proliferation in transit-amplifying cells and their progeny in the epidermis. Telomere shortening occurs during every normal DNA replication due to so-the called end replication problem and telomere end processing; however, there are several strategies to allow circumventing of this mechanism. This is frequently observed in cancer, including epidermal carcinomas and melanoma.[13]

Normal epidermal stem cells must stringently guide the number of mitotic divisions engaged. This is compensated by the high proliferative capacity of daughter populations (transit-amplifying cells) after asymmetric stem cell division. Low frequency of stem cell cycling is, therefore, a highly effective preventive strategy to avoid the permanent incorporation of randomly occurring genetic alterations into the genome.[14] Such a genetic mutation in self-renewing stem cells could potentially lead to devastating consequences, including tumor formation. This mechanism of cancer prevention, however, is believed to come at a cost that is senescence. A crucial question, therefore, is what controls the balance of epidermal proliferation and epidermal differentiation; however, the identity of the human epidermal stem cell has remained a matter of some controversy.[10]

Complete exhaustion of the stem cell pool has been described in a mouse model, where, for example, long-term activation of Wnt causes cell senescence and the depletion of the stem cell compartment by the persistent activation of mTOR.[15] Despite several critical differences in telomere structure, mouse models of telomerase deficiency also provided evidence that telomere shortening may be important for skin aging. Mice with critically short telomeres exhibited problems with highly proliferative tissue, including epidermal abnormalities such as poor wound healing, spontaneous ulcerative skin lesions, early hair loss, and early hair graying.[16]

There are several conditions where mutations in telomerase components result in human disease, for example, in

dyskeratosis congenita.[17] Accelerated telomere shortening leads to premature loss of tissue self-renewal capacity and untimely death, most frequently due to a fatal bone marrow failure. Common skin findings in dyskeratosis congenita include irregular pigmentation, nail dystrophy, poikiloderma with epidermal atrophy and prominent telangiectasias, and oral leukoplakia. Other cutaneous findings may include alopecia involving the scalp, eyebrows, and eyelashes with premature graying.[18] This genetic disorder, therefore, offers multiple accentuated facets of skin aging for observation; however, we have not observed a complete loss of epidermal self-renewal capacity in such patients. In addition, we also have not observed absolute loss of skin regeneration in centenarians in a clinical setting. The aged epidermis is frequently associated with multiple important structural and functional impairments. These include, for example, epidermal atrophy due to decreased cellular turnover, slow re-epithelization, weaker barrier function, lower mechanical resistance, decreased DNA repair capacity, and lower sweat and sebum production.[19]

On the contrary, the clinically relevant complete exhaustion of skin regenerative capacity is achieved by extensive exposure to radiation or chemicals, either accidental or therapeutic. These harmful external agents also trigger cellular senescence in response to DNA damage without respect to the actual extent of telomere attrition in the affected cell. It was shown that activated oncogenes are responsible for this arrest; therefore, this type of senescence was termed *oncogene-induced senescence*.[20]

There is good evidence that keratinocyte progenitors are relatively radiosensitive cells, whereas epidermal stem cells appeared to be relatively radioresistant.[21] In this study, which used radiation lower than 2 Gy, colony-forming assays showed that 82% of stem cells survived at 2 weeks, compared with only 29% for the progenitors; however, after high doses of radiation, toxicity and cell death take over the adaptive responses of the cells. This catastrophic scenario leads to depletion of the stem cell pool, which can impair skin regeneration in the long-term.[22] Dermatologists are aware of the slow healing of the so-called moist desquamation, which may occur after radiotherapy, once a cumulative dose exceeding 8 Gy was administered.[23] Less frequently, radiation therapy may sometimes lead to severe adverse effects in irradiated tissue known as radiation-induced cutaneous ulcerations, which are extremely resistant to healing.[24]

A nonhealing wound is frequently complicated by such afflictions as diabetes-induced and nondiabetic neuropathies, chronic venous insufficiency, arterial disease, nutrition deficiency, decubitus ulcers due to immobility, and so on. Successful treatment of an underlying causative disease stimulates skin healing. Chronologic aging of the epidermis and resulting poor re-epithelization seems an unlikely explanation. There might be a significant age-dependent difference in the proportion of highly clonogenic keratinocytes in human interfollicular epidermis.[25] Using a similar feeder technique, gradual age-related decrease, but not complete absence, was also confirmed by others in the case of follicular keratinocytes.[26] Keratinocyte culture methods have developed over decades and shifted to various chemically defined, low/no serum, feeder-free variants. Studies using improved cell culture methods suggest that no differences in keratinocyte doubling capacity were found among cells isolated from the skin of different body areas (thorax, breast, abdomen) or donors of different ages (here ranging from 15-58 years).[27]

The plausible explanation of these conflicting data is most likely not found in the epidermis *per se*, but it is coming from the cell culture environment. The difference in the type of feeder cells or surface coating by biomolecules, serum content, growth supplements, and so on, significantly influences the maintenance of epidermal stemness *in vitro*.[28] All these factors mimic more or less successfully the so-called tissue microenvironment. Our current incapability of reliable reconstruction of tissue microenvironment recently represents the most critical bottleneck in the broader implementation of cell-based treatment methods in clinical praxis; however, there is a steadily increasing demand for autologous adult stem-cell-based therapies or artificial organs.

One group[27] followed their expansion for more than 100 population doublings (regardless of the age of the actual donor), without reaching signs of replicative senescence in keratinocytes. Taking this possibility into account, it seems that we usually do not have a chance to meet the physical limits of epidermal proliferative capacity even in extremely aged individuals. We usually do not live long enough.

In irradiation studies,[23] the presence of, for example, fibroblast growth factor 2 (FGF2) in the irradiated microenvironment is critical for stem cell survival. Stem cell protection by its microenvironment (the so-called *niche*) is an essential factor for tissue homeostasis in the epidermis and also in other tissues. The mutual interactions between epithelial cells and their microenvironment are therefore critical.[29] It seems likely that this microenvironment could be the next therapeutic target.

Dermal fibroblasts: seemingly invisible differences

Skin is the outermost organ of the body. The barrier function is dominantly executed by epidermis as noted above. Although the primary function of the dermis is to form a protective layer, it must also cope with the environment and mechanical forces. The dermis is not a passive extracellular-matrix-rich scaffold providing mechanical support to the overlying epidermis. Dermal architecture and function depend on diverse populations of cells, predominantly on dermal fibroblasts. Minor dermal populations are represented by, for example, various cells of immune system, endothelial cells, and pericytes. Reciprocal communication via growth factors, cytokines, and chemokines across the basement membrane between the epidermis and dermis plays a key role in skin development, homeostasis, and repair.

With simple histologic methods, the dermis can be reliably distinguished as early as week 5 to 6 of human development.

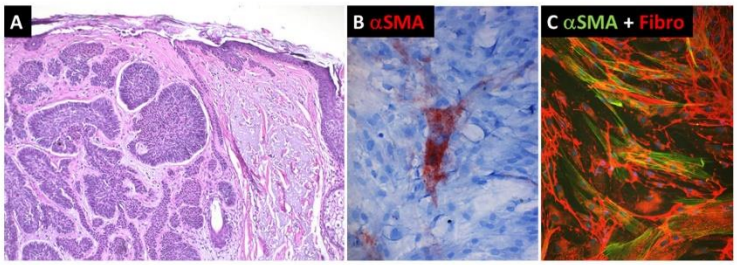

Fig. 1 **(A)** Basal cell carcinoma (on the left), surrounded by a grayish zone of heavily altered dermis (solar elastosis, on the right). **(B)** Cancer-associated fibroblasts (isolated from an elderly patient with basal cell carcinoma) in tissue culture; AEC (red) highlighted alpha-smooth muscle actin (αSMA)–positive myofibroblasts; cells are counterstained with Gill hematoxylin (blue). **(C)** Immunocytochemical analysis reveals multiple αSMA-positive cells (green) surrounded by a dense meshwork of extracellular-matrix-containing fibronectin (Fibro, red).

The dermis is derived from mesenchyme of lateral plate mesoderm (for the limbs and body wall) and also of the paraxial mesoderm (dermis of the back). Besides this purely mesodermal components, the ectomesenchyme originating from the neural crest cells forms the dermis and connective tissues of the face and neck.[30] Despite these differences in embryologic origin, the histologic arrangement of the adult dermis is otherwise uniform across the body.

Conventional histology recognizes the superficial papillary dermis and more deeply located reticular dermis with adjacent adipocyte-rich hypodermis. Dermal thickness can be variable in different body sites. This otherwise uniform dermal structure attracted the little to no attention of the researchers over decades. Such structural uniformity of the source tissue has been inappropriately extrapolated also on all fibroblasts derived from this tissue. In later years, more light has been shed on the diversity of dermal fibroblasts under physiologic and pathologic conditions.

[31] on the address of the principal cells in stroma of various tissues, collectively called fibroblasts: "*a catch-all designation that belies their diversity*."????

Fibroblasts are somewhat difficult to identify positively morphologically. In cell culture, fibroblasts are identified based on their spindle shape and loose growth pattern. This can be combined with positive immunohistochemical staining for the mesenchymal marker vimentin along with the absence of staining for epithelial cell markers (eg, keratins) or other mesenchymal cell types, such as desmin (for muscle cells), GFAP (for glial cells), CD34 (for hematopoietic cells), CD68 (for macrophages), and S100 P (neural crest-derived cells). Extensive production of representatives of the extracellular matrix such as collagen type I or III as well as of fibronectin (Figure 1C) can also be employed for *in vitro* recognition of fibroblasts. Thorough understanding of fibroblast phenotype can aid our insight into various processes significantly, not only in the skin but also in other organs; however, this approach is based on a combination of several markers and therefore has just limited applicability.[32] Also, the cell phenotype *in vitro* is frequently different from the phenotype observed in normal tissue context.[33,34]

The possibility of defining differences in fibroblasts by cell function more than by cell phenotype was noted in the context of skin tissue by e in the early 1990s.[33] In these already classic experiments, dermal papilla fibroblasts were implanted alone into footpad skin under controlled conditions in a murine model. New pelage-type follicles were induced by transdifferentiation of the footpad epidermis afterward. At this moment, the dermal compartment of the follicle, the dermal papilla, was for the first time recognized as the key signaling center. Dermal papilla fibroblasts were acknowledged for being responsible for maintaining hair growth and controlling the complex system of hair follicle cycling. It was suggested later that these dermal cells could have a great regenerative potential even outside of the hair follicle, and their role in, for example, wound healing was proposed.[35] Approximately at the same time, there was a proposal that the same epidermal organ (hair follicle) could host another pool of stem cells of different origin, the neural crest-derived stem cells.[36] The obvious need for more robust cell definition based on gene signatures shifted all these fibroblast-targeted studies inevitably to the era of transcriptomics.

Using gene microarrays in later years, fibroblasts from each body site displayed distinct and characteristic transcriptional patterns.[31] In tissue culture, adult fibroblasts maintained key features of *HOX* gene expression patterns established during embryogenesis. This observation suggests positional memory in fibroblasts. Next, these data suggest that fibroblasts at different locations in the body should be considered as distinctly differentiated cell types separable by their gene expression profiles.[31] Microarray studies have become an extensively used technique in skin research, and it has offered an excellent tool for deciphering fibroblast functional heterogeneity. It is possible to determine the typical expression profile of, for example, various skin-cancer-associated fibroblasts[37–40] or from fibroblasts activated during healing process,[41] and so on; however, all those microarray-generated data must be interpreted stringently.

Great care must be dedicated to the design of the study and appropriate control selection. It was observed that several genes defective in genetic syndromes were prominently expressed in fibroblasts originating from sites most affected in that diseases.[31] These false discoveries are worrisome. As approximately 81% of newborn boys in the United States are circumcised,[42] the residual foreskin is frequently used as a source of tissue in dermatologic research; however, the dermis and its resident fibroblasts are anatomically more heterogeneous than was previously thought.

Juvenile dermis: quick and smooth inspiration for rapid healing?

Dermal fibroblasts are highly proliferative during embryonic development. The cellularity of the dermis is much higher at this developmental stage,[43] which corresponds with the rapid growth of the body.[44] On the contrary, the adult dermal fibroblasts are typically quiescent cells[45]; however, these quiescent fibroblasts can be activated again by various external stimuli to divide in response and to maintain tissue homeostasis, if necessary.

Regeneration in adult mammals (including humans) is generally highly limited in comparison with some invertebrates and amphibians.[46] There is an indication that this loss of regenerative capacity can result from our evolutionary strategy. Due to improved obstetric care in 1970s, several anecdotal reports introduced the appealing topic of human fetal scarless healing.[47] These reports indicated that surgical incisions or even limb amputations (spontaneous, mostly due to constriction bands) in the human fetus heal rapidly and do not result in scar formation (of course without regeneration of missing limb). Notably, no acute inflammatory process and no granulation tissue formation were observed at any of the amputation sites. This was also confirmed in other mammalians.[48]

An initial hypothesis was postulated that factors present in the uterus, such as complete sterility[49] or low oxygen tension,[50] could be beneficial to, or directly responsible for, scarless healing.[48] These potential factors were extensively studied to establish a treatment method through which scarless healing could be achieved even in adults.[51] Unfortunately, later experiments and trials concluded that these factors proved to be sufficient to be meaningfully implemented into routine therapy.

Results of fetal healing are nearly indistinguishable from the uninjured tissue. It was extensively documented using robust scientific methods, for example, confocal microscopy.[52] It was assumed that these features are typical for early phases of fetal development before 24th week of gestation.[53] More recently, it was confirmed that highly favorable healing result could be achieved even in newborns within the first week of postnatal life.[54,55] These studies performed on newborns undergoing lip clef surgery highlighted the importance of the intrinsic tissue factors.

The early timing of this surgery seems to be a crucial factor. It is evident that the rate of tissue maturation/aging is rapid in this case. Of note, this excellent healing capacity is readily lost even in slightly older children. Nevertheless, such a rapid decrease of healing capacity observed in newborns within a few weeks offers acquisition of material with highly contrasting differences that could be easily studied by molecular analysis of transcriptome[56] and presumably also epigenome.[42]

What are the most critical features of fetal and newborn skin? Extracellular matrix is an obvious first target. The principal component of extracellular matrix in human dermis is collagen deposited here by dermal fibroblasts. The adult human dermis contains an excess of collagen type I,[57] whereas in rat fetal dermis content of collagen type III exceeded content of collagen type I.[58] Notably, this switch roughly coincides with the decrease of fetal-type healing capacity in the skin of newborns.[57] The adult dermis also contains, for example, more decorin. Decorin regulates collagen fibrillogenesis.[53] The 3-D arrangement of collagen bundles is therefore different in fetal dermis, as the collagen bundles are finer more reticular. There are conflicting data regarding the other components of the extracellular matrix, for example, tenascin or fibronectin expression. Differences in temporospatial expression profile were suggested.[53] One group[41] could not confirm quantitative differences in, for example, fibronectin production in fibroblast cell cultures. The extracellular matrix is also a highly dynamic structure with a variable turnover.

Various models of skin aging suggested that progressive accumulation of senescent fibrocytes in the aged dermis is leading to a subsequent reduction of collagen I production and loss of its volume, which is also associated with local overproduction of matrix metalloproteinases.[57] This turnover can be further modulated by, for example, epithelial-mesenchymal interactions during wound healing.[41] It was possible to show such enhancement via coculture methods where keratinocytes significantly enhanced the proliferative and migratory potential of the fibroblasts that was linked to changes in expression of matrix metalloproteinase MMP-2 and MMP-9.[41,59]

Another prominent component of dermal extracellular matrix is glycosaminoglycans such as hyaluronic acid. Hyaluronic acid gained a great deal of attention in dermatology and cosmetics in previous years. These molecules are extremely hydrophilic and bind an excessive amount of water. The increase in levels of glycosaminoglycans changes the rheology of the matrix toward a more pliable one. Low stiffness of the extracellular matrix is known to influence mesenchymal cell phenotype and affect cell survival; this may be also critical for the scarless healing.[60] Hyaluronic acid can also bind growth factors and cytokines form their depot and thus create temporal and spatial gradients of these molecules.[61] This might be important also in modulation of local pro-/antiinflammatory environment. Particular attention was

dedicated to the levels of growth factors, namely, TGF-β, PDGF, EGF, basic FGF, VEGF, and IL-6/IL-8/CXCL1.[56,62]

Notably, many efforts have been made to closely determine the role of, for example, transforming growth factor-beta (TGF-β) isoforms, and their receptors in the wound healing process. Their roles in scarless wound repair observed in are still not well understood.[56] TGF-β signaling is usually referred to be context dependent. It is dependent on the available amount of the TGF-β itself in various isoforms, its receptors, and also by signal duration and cytokine temporal availability and receptor internalization.

In fetal wound healing, there is a rapid induction of TGF-β, but it is in lower total levels than in adults.[63] It was suggested that fetal healing has a more rapid clearance from the wound site compared with adult wounds.[63] TGF-β is also linked to fibroblasts differentiation into the myofibroblast phenotype (Figure 1B, C). Upon injury, the fibroblasts are stimulated mechanically by inflammatory mediators to undergo this process. Examination of this phenomenon in cultured fibroblasts from newborns and adults has shown that fibroblasts can undergo this more efficiently once specific components of extracellular matrix, namely, galectin-1.[64]

Myofibroblast contraction is rather long lasting and results in a permanent tissue retraction that closes the wound. This also leads to stabilization of extracellular matrix, and it could explain the characteristic favorable tissue remodeling activity observed in the case of healing of fetal skin. This seems to be dependent on precise temporal regulation of TGF-β activity.[63] On the contrary, extended TGF-β1-mediated signaling has been implicated in diseases characterized by excessive collagen deposition, including keloids and scleroderma[65]; however, we were not able to identify quantitative differences of myofibroblasts in fibroblast cultures from various donors based on their age.[55] TGF-β1 appears as an important target to control myofibroblast activity.[66]

Similarly, conflicting data were reported by us for IL-6. It was detected on RNA and protein level in a surprisingly higher amount in fibroblasts[55] isolated from newborns compared with adult skin-derived fibroblasts. This finding was explained later by the difference in their developmental origin (trunk from mesenchyme vs face from ectomesenchyme).[56]

Aging of the dermis: wrinkled? weak? worrisome?

Dermal aging can sometimes be highly evident in routine histology. Ultraviolet radiation from natural and artificial sources is the principal environmental factor of skin damage that is accumulated by the tissues over the years of life; therefore, this damage is generally also reported as the photodamage. Structurally, complex of these changes is known as solar elastosis (or dermal elastosis, actinic elastosis; Figure 1A). There are a variety of clinical manifestations of solar elastosis. Commonly, solar elastosis manifests as yellowish, thickened, coarsely wrinkled skin. This visual aspect has a substantial impact on tissue esthetics and health. The occurrence of solar elastosis can be used as a biomarker of cutaneous photoaging.

Additional extrinsic factors corroborating this effect include other types of radiation, reactive oxygen radicals, chemical pollution, smoking, and repetitive muscle movements; in a more general sense, also lifestyle and diet can act as accelerators or intensifiers of aging signs.[67] Evaluation of the overall effect of these changes and their scoring is difficult and subjective. For purposes of comparative studies, the Beagley-Gibson grading system was developed. It evaluates skin changes and generates an individualized, objective estimate of cumulative, lifetime ultraviolet radiation (UVR) exposure.[68]

Additionally, extrinsic factors, including UV radiation, pollution, nicotine use, repetitive muscle movements, lifestyle, and diet, can act as accelerators or intensifiers of aging sign

Additional extrinsic factors, including other types of radiation, chemical pollutants (eg, released during nicotine smoking), repetitive physical stimulation (due to, e.g., movements), lifestyle, and diet, can act as accelerators or intensifiers of aging signs.

The detectable loss of elastic properties is caused by changes in elastin production, increased degradation, and modified processing. The fibroblasts are a principal group of cells in the dermis involved in the so-called elastogenesis. This process occurs predominantly in the superficial dermis, which corresponds to the natural distribution of elastin in the dermis. Elastic fibers consist of two morphologically distinct components: Microfibrils and polymerized elastin. The precursor, tropoelastin, is secreted into the extracellular space, where it becomes highly crosslinked by the activity of the copper-requiring enzyme known as lysyl oxidase.[69]

Several studies from the 1980s showed that decrease of production is associated to fibroblast aging and occurs already after approximately 30 population doublings.[70] Comparing multiple donors, a significant fall of tropoelastin production appeared in donor chronologically aged 70 years[70]; however, these tissues were from previously more sun-protected areas (from foreskins and trunk skin). Clinically notable photodamage frequently comes at much younger age. This can be explained as the real photoaging. Ultraviolet radiation can induce alternative splicing of the elastin gene, which leads to the inadequate synthesis of the proteins required for the correct assembly of elastic fibers.[71] The elastin content is estimated to be only 2% of the total dermal protein mass. Despite the relatively modest content, elastin is highly important for mechanical tissue properties.

Collagens are the main extracellular component of the dermis. Fibril-forming collagens (eg, collagen types I, III, and V) assemble into 3-D scaffolds in the dermis. This is the structural base of multiprotein networks with other matrix proteins such as the elastin fibers and nonfibrillar matrix. The nonfibrillar matrix also contributes as a visco-elastic material and prevents any motion of the network. The disorganization of collagen fibers associated with solar irradiation and aging was documented.[72] Collectively, all these components determine the mechanical behavior of the dermis and other collagen-rich tissues with clinical consequence.[68]

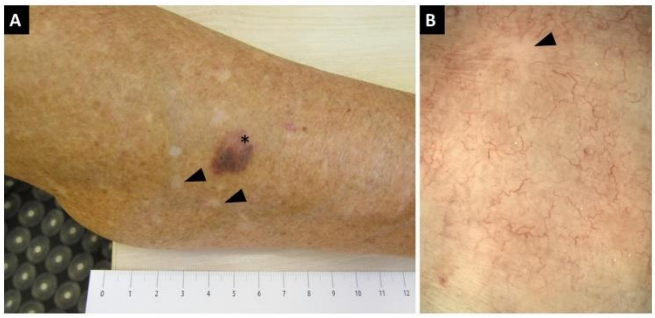

Fig. 2 Forearm of 86-year-old Caucasian woman, phototype II, with prominent signs of dermatoporosis. Stellate pseudoscars (black arrowheads **A, B**) and skin atrophy with irregularities of dermal vessels (the detailed view in dermatoscopy, **B**). Hematomas, linear skin tears, and lacerations might occur after minimal trauma in patients with dermatoporosis. Hematoma (asterisk) is not dissecting here.

In 2007, the word *dermatoporosis* was created to give an umbrella name to the chronic cutaneous fragility of aging skin.[73] The leading features of dermatoporosis include skin atrophy (both epidermal and dermal), with solar purpura and whitish scarlike changes present on the extremities of elderly patients (Figure 2). Skin lacerations and delayed healing are frequent features in dermatoporotic skin, leaving affected patients susceptible to bleeding complications and cutaneous infections.[68] The prevalence of dermatoporosis is surprisingly high as estimated recently (37.5% in French subjects aged ≥65 years; 27.5% men versus 43.9% women).[74]

All such common clinical phenomena can be linked to changed dermal architecture. The increased stiffness in aged dermis frequently reported in the literature can be attributed to the increased crosslinking between fibers, which results in increased stiffness of the whole collagen network.[75] Easier breaking is also possible due to the shortening of the fibrils in the fibers, which will then separate more easily. The degradation of proteoglycans further leads to a loss of water and impedes sliding of fibrils inside the fibers. This finally results in a more substantial increase of inner shear per fiber contributing to increased mechanical fragility.[75]

The aged dermis is obviously vulnerable; however, there are other invisible risks associated with aging. As mentioned earlier, cellular senescence occurs in culture and in the organism as a response to excessive extracellular or intracellular stress. There are several methods of senescence assessment in cultured cells and also in tissues. Senescence-associated β-galactosidase activity, detectable at pH 6.0, gained much attention in the last decades. The method based on enzyme histochemistry offers the advantages of being quantitative and relatively sensitive.[76] The interpretation of the results is sometimes problematic and it is not easy to implement, for example, in diagnostic procedures.

The senescence program drives the cells into a cell-cycle arrest, but it does not eliminate them from the tissues and leaves them viable and functional. Senescence, therefore, prevents the spread of genetic damage, but it does not lead to numeric atrophy of the tissues. Senescent cells have been shown to accumulate during the lifetime in various animals and also in humans.[76]

Once introduced, senescence leads to extensive changes in gene expression of affected cells. The repertoire of these changes is conserved. Critical differences between the transcriptome of presenescent and senescent were observed in products of genes encoding the secretory proteins. Collectively, this complex of changes constitutes to the so-called senescence-associated secretory phenotype.[77] This secretory phenotype includes several families of soluble and insoluble factors. Soluble signaling molecules include interleukins, chemokines, and growth factors (Table 1).

Next, senescence also contributes to changes of secreted proteases and secreted insoluble proteins of the extracellular matrix. In the next step, the changes of extracellular matrix can modify the effect of soluble molecules by their stabilization or sequestration as discussed earlier. All these factors of senescent cells can, therefore, modify the tissue microenvironment. So far, the senescence growth arrest has been shown to promote activities of the major tumor-suppressor cellular mechanisms.[77] Unfortunately, this is only the bright side of the story.

Epidemiologic studies have shown that markers of chronic sun exposure increase the risk of both melanoma and nonmelanoma skin cancer.[67] It is a broadly accepted idea that cumulative exposure to ultraviolet light is etiologically relevant, for example, basal cell carcinoma, squamous cell carcinoma, and malignant melanoma.[78] Ultraviolet radiation induces DNA damage, and it is responsible for the development of mutations and consecutive carcinogenesis in skin. On the other hand, ultraviolet radiation is a potent inducer of stress in the tissue and penetrates deep and reaches the dermis. Considerable attention was dedicated to environmental factors supporting the growth of the cancer cells in last years. We have accumulated evidence that tissue microenvironment is a critical factor for cancer progression. It was suggested that the so-called cancer-

Table 1 Factors extensively produced by fibroblasts with senescent phenotype, myofibroblasts, and cancer-associated fibroblasts

Category of product	Factor
Interleukins	IL-1 (a,b)
	IL-6
	IL-7
	IL-13
	IL-15
Chemokines (CXCL, CCL)	IL-8
	GRO-a (b, g)
	MCP-2
	MCP-4
	MIP-1 a
	MIP-3 a
	HCC-4
	Eotaxin-3
Other inflammation supporting factor	GM-CSE
	MIF
Growth factors	Amphiregulin
	Epiregulin
	Heregulin
	EGF
	bFGF
	HGF
	KGF(FGF7)
	VEGF
	Angiogenin
	SCF
	SDF-1
	PIGF
	NGF
	IGFBP-2 (3, 4, 6, 7)

Modified from multiple studies.[77,82,83,86]

associated fibroblast are highly biologically active population in, for example, basal cell carcinoma, squamous cell carcinoma,[37,38,79] and also in melanoma and other various types of tumors.[80,81] Cancer-associated fibroblast were suggested as clinically important modifiers of oncological therapy response.[40]

The activity of cancer-associated fibroblast is not cancer-type specific, and released molecules are secreted regularly as an important component of cancer-supporting environment.[80,82,83]

Surprisingly, we have identified that this repertoire is significantly overlapping with the repertoire of cytokines present in senescent cells. Most frequently we have detected interleukins, for example, IL-6 and IL-8. This overlap represents a double-edged sword. In this light, the protective factors of senescence become corrupted and can be engaged in tumor progression.[84] This mechanism is also attracting research attention with therapeutic potential. These principal components of cancer microenvironment also offer a potential target for future therapy.[85]

Conclusions

The association between aging and cancer seems to be more than apparent.[14] Respecting the ongoing global shift in demographics, the further increase of the epidemiclike incidence of malignant tumors in a population can be expected soon. The increased incidence of cancer will demand the attention of governmental authorities to establish an adequate economic base necessary for the expensive treatment of numerous patients.[14,46]

In this light, we should support the implementation of aging-risk-based skin cancer screening guidelines internationally. The elderly population should be the audience of such targeted screening because the essential phenotypic cancer risk factors are present in higher age. In this context, the role of cancer stroma in controlling multiple biologic properties of tumors is a prospective target for translational research with potential therapeutic outcomes.

This situation represents an excellent starting point for the development of innovations in cancer prevention and therapy.

Acknowledgments

Supported by the Grant Agency of the Czech Republic (Project No. 16-05534 S); Ministry of Health of the Czech Republic (Projects 15-28933 A and 16-29032 A); the Charles University (Project No. PROGRESS Q 28); the Ministry of Education, Youth and Sports of Czech Republic within the National Sustainability Program II (Project BIOCEV-FAR Reg. No. LQ1604), and the project BIOCEV (CZ.1.05/1.1.00/02.0109). The project "Center for Tumor Ecology—Research of the Cancer Microenvironment Supporting Cancer Growth and Spread" (Reg. No. CZ.02.1.01/0.0/0.0/16_019/0000785) is supported by the Operational Programme Research, Development and Education. The authors are also grateful for the support provided by the League Against Cancer, Prague.

References

1. World Population Prospects Volume I. 2017 Revision. Available at: https://esa.un.org/unpd/wpp/Publications/Files/WPP2017_Volume-I_Comprehensive-Tables.pdf. Accessed August 13, 2018.
2. Ebeling M, Modig K, Ahlbom A, et al. The effects of increasing longevity and changing incidence on lifetime risk differentials: a decomposition approach. *PLoS One* 2018;13, e0195307.
3. Karimkhani C, Dellavalle RP, Coffeng LE, et al. Global skin disease morbidity and mortality: an update from the Global Burden of Disease Study 2013. *JAMA Dermatol* 2017;153:406-412.
4. WHO. Metrics: Disability-Adjusted Life Year (DALY). Available at: http://www.who.int/healthinfo/global_burden_disease/metrics_daly/en/ 2014. Accessed August 9, 2018.
5. USCS Data Visualizations. Available at:https://gis.cdc.gov/Cancer/USCS/DataViz.html. Accessed August 9, 2018.
6. Buster KJ, Stevens EI, Elmets CA. Dermatologic health disparities. *Dermatol Clin* 2012;30:53-59.

7. World Report on Ageing and Health. 2015. Available at: www.who.int. Accessed August 9, 2018.
8. Pil L, Hoorens I, Vossaert K, et al. Cost-effectiveness and budget effect analysis of a population-based skin cancer screening. *JAMA Dermatol* 2017;153:147.
9. Agency for Healthcare Research & Quality. Are we ready for this change? Available at:https://www.ahrq.gov/professionals/systems/hospital/pressureulcertoolkit/putool1.html. Accessed August 9, 2018.
10. Clevers H, Watt FM. Defining adult stem cells by function, not by phenotype. *Annu Rev Biochem* 2018;87:1015-1027.
11. Hayflick L, Moorhead PS. The serial cultivation of human diploid cell strains. *Exp Cell Res* 1961;25:585-621.
12. Buckingham EM, Klingelhutz AJ. The role of telomeres in the ageing of human skin. *Exp Dermatol* 2011;20:297-302.
13. Pópulo H, Boaventura P, Vinagre J, et al. TERT promoter mutations in skin cancer: the effects of sun exposure and x-irradiation. *J Invest Dermatol* 2014;134:2251-2257.
14. Smetana K, Lacina L, Szabo P, et al. Ageing as an important risk factor for cancer. *Anticancer Res* 2016;36:5009-5017.
15. Castilho RM, Squarize CH, Chodosh LA, et al. mTOR mediates Wnt-induced epidermal stem cell exhaustion and aging. *Cell Stem Cell* 2009;5:279-289.
16. Siegl-Cachedenier I, Flores I, Klatt P, et al. Telomerase reverses epidermal hair follicle stem cell defects and loss of long-term survival associated with critically short telomeres. *J Cell Biol* 2007;179:277-290.
17. Mitchell JR, Wood E, Collins K. A telomerase component is defective in the human disease dyskeratosis congenita. *Nature* 1999;402:551-555.
18. Fernández García MS, Teruya-Feldstein J. The diagnosis and treatment of dyskeratosis congenita: a review. *J Blood Med* 2014;5:157-167.
19. Quan T. Molecular mechanisms of skin aging and age-related diseases. Available at:https://books.google.cz/books?id=j771CwAAQBAJ&dq=smetana+lacina+brož&hl=cs&source=gbs_navlinks_s. Accessed August 10, 2018.
20. Gorgoulis VG, Halazonetis TD. Oncogene-induced senescence: the bright and dark side of the response. *Curr Opin Cell Biol* 2010;22:816-827.
21. Rachidi W, Harfourche G, Lemaitre G, et al. Sensing radiosensitivity of human epidermal stem cells. *Radiother Oncol* 2007;83:267-276.
22. Barnhill RL, Cerroni L, Cook M, et al. State of the art, nomenclature, and points of consensus and controversy concerning benign melanocytic lesions: outcome of an international workshop, 2010. Available at:www.anatomicpathology.com. Accessed July 9, 2018.
23. Martin MT, Vulin A, Hendry JH. Human epidermal stem cells: role in adverse skin reactions and carcinogenesis from radiation. *Mutat Res* 2016;770:349-368.
24. Ma X, Jin Z, Li G, et al. Classification of chronic radiation-induced ulcers in the chest wall after surgery in breast cancers. *Radiat Oncol* 2017;12:135.
25. Barrandon Y, Green H. *Three Clonal Types of Keratinocyte with Different Capacities for Multiplication*,vol. 84 . 1987. Available at:http://europepmc.org/backend/ptpmcrender.fcgi?accid=PMC304638&blobtype=pdf. Accessed August 11, 2018.
26. Lecardonnel J, Deshayes N, Genty G, et al. Ageing and colony-forming efficiency of human hair follicle keratinocytes. *Exp Dermatol* 2013;22:604-606.
27. Papini S, Cecchetti D, Campani D, et al. Isolation and clonal analysis of human epidermal keratinocyte stem cells in long-term culture. *Stem Cells* 2003;21:481-494.
28. Dvořánková B, Lacina L, Smetana K. Isolation of normal fibroblasts and their cancer-associated counterparts (CAFs) for biomedical research. *Methods Mol Biol* 2019;1879:393-406.
29. Gonzales KAU, Fuchs E. Skin and its regenerative powers: an alliance between stem cells and their niche. *Dev Cell* 2017;43:387-401.
30. Sadler TW. *Langman's Medical Embryology*. Baltimore, MD: Lippincott Williams & Wilkins. 2012.
31. Chang HY, Chi J-T, Dudoit S, et al. Diversity, Topographic Differentiation, and Positional Memory in Human Fibroblasts. *Proc Natl Acad Sci U S A* 2002;99:12877-12882.
32. Goodpaster T, Legesse-Miller A, Hameed MR, et al. An immunohistochemical method for identifying fibroblasts in formalin-fixed, paraffin-embedded tissue. *J Histochem Cytochem* 2008;56:347-358.
33. Jahoda CA, Reynolds AJ. Dermal-epidermal interactions—follicle-derived cell populations in the study of hair-growth mechanisms. *J Invest Dermatol* 1993;101(Suppl):33S-38S.
34. Kodet O, Dvořánková B, Krejčí E, et al. Cultivation-dependent plasticity of melanoma phenotype. *Tumor Biol* 2013;34:3345-3355.
35. Richardson GD, Arnott EC, Whitehouse CJ, et al. Plasticity of rodent and human hair follicle dermal cells:implications for cell therapy and tissue engineering. *J Investig Dermatol Symp Proc* 2005;10:180-183.
36. Sieber-Blum M, Grim M. The adult hair follicle: Cradle for pluripotent neural crest stem cells. *Birth Defects Res C Embryo Today* 2004;72:162-172.
37. Lacina L, Smetana Jr K, Dvořánková B, et al. Stromal fibroblasts from basal cell carcinoma affect phenotype of normal keratinocytes. *Br J Dermatol* 2007;156:819-829.
38. Lacina L, Dvořánkova B, Smetana Jr K, et al. Marker profiling of normal keratinocytes identifies the stroma from squamous cell carcinoma of the oral cavity as a modulatory microenvironment in co-culture. *Int J Radiat Biol* 2007;83:837-848.
39. Dvořánková B, Szabo P, Kodet O, et al. Intercellular crosstalk in human malignant melanoma. *Protoplasma* 2017;254:1143-1150.
40. Kodet O, Dvořánková B, Bendlová B, et al. Microenvironment-driven resistance to B-Raf inhibition in a melanoma patient is accompanied by broad changes of gene methylation and expression in distal fibroblasts. *Int J Mol Med* 2018;41:2687-2703.
41. Mateu R, ivicová V, Krejí ED, et al. Functional differences between neonatal and adult fibroblasts and keratinocytes: donor age affects epithelial-mesenchymal crosstalk in vitro. *Int J Mol Med* 2016;38:1063-1074.
42. Morris BJ, Bailis SA, Wiswell TE. Circumcision rates in the United States: rising or falling? What effect might the new affirmative pediatric policy statement have? *Mayo Clin Proc* 2014;89:677-686.
43. Tan KKB, Salgado G, Connolly JE, et al. Characterization of fetal keratinocytes, showing enhanced stem cell-like properties: a potential source of cells for skin reconstruction. *Stem Cell Rep* 2014;3:324-338.
44. Coolen NA, Schouten KCWM, Middelkoop E, et al. Comparison between human fetal and adult skin. *Arch Dermatol Res* 2010;302:47-55.
45. Mitra M, Ho LD, Coller HA. An in vitro model of cellular quiescence in primary human dermal fibroblasts. *Methods Mol Biol* 2018;1686:27-47.
46. Smetana K, Dvořánková B, Lacina L. Phylogeny, regeneration, ageing and cancer: role of microenvironment and possibility of its therapeutic manipulation. *Folia Biol (Czech Republic)* 2013;59:207-216.
47. Rowlatt U. Intrauterine wound healing in a 20 week human fetus. *Virchows Arch A Pathol Anat Histol* 1979;381:353-361.
48. Adzick NS, Longaker MT. Animal models for the study of fetal tissue repair. *J Surg Res* 1991;51:216-222.
49. Frantz FW, Bettinger DA, Haynes JH, et al. Biology of fetal repair: the presence of bacteria in fetal wounds induces an adult-like healing response. *J Pediatr Surg* 1993;28:428-433. discussion 433-434.
50. Yoshida Y, Takahashi K, Okita K, et al. Hypoxia enhances the generation of induced pluripotent stem cells. *Cell Stem Cell* 2009;5:237-241.
51. Larson BJ, Longaker MT, Lorenz HP. Scarless fetal wound healing: a basic science review. *Plast Reconstr Surg* 2010;126:1172-1180.
52. Beanes SR, Hu F-Y, Soo C, et al. Confocal microscopic analysis of scarless repair in the fetal rat: defining the transition. *Plast Reconstr Surg* 2002;109:160-170.
53. Yates CC, Hebda P, Wells A. Skin wound healing and scarring: fetal wounds and regenerative restitution. *Birth Defects Res C Embryo Today* 2012;96:325-333.
54. Borský J, Tvrdek M, Kozák J, et al. Our first experience with primary lip repair in newborns with cleft lip and palate. *Acta Chir Plast* 2007;49:83-87.
55. Moslerová V, Dadáková M, Dupej J, et al. Three-dimensional assessment of facial asymmetry in preschool patients with orofacial clefts after neonatal cheiloplasty. *Int J Pediatr Otorhinolaryngol* 2018;108:40-45.

56. Živicová V, Lacina L, Mateu R, et al. Analysis of dermal fibroblasts isolated from neonatal and child cleft lip and adult skin: developmental implications on reconstructive surgery. *Int J Mol Med* 2017;40:1323-1334.
57. Mays PK, Bishop JE, Laurent GJ. Age-related changes in the proportion of types I and III collagen. *Mech Ageing Dev* 1988;45:203-212.
58. Merkel JR, DiPaolo BR, Hallock GG, et al. Type I and type III collagen content of healing wounds in fetal and adult rats. *Proc Soc Exp Biol Med* 1988;187:493-497.
59. Wang Z, Liu X, Zhang D, et al. Co-culture with human fetal epidermal keratinocytes promotes proliferation and migration of human fetal and adult dermal fibroblasts. *Mol Med Rep* 2015;11:1105-1110.
60. Alaish SM, Yager D, Diegelmann RF, et al. Biology of fetal wound healing: hyaluronate receptor expression in fetal fibroblasts. *J Pediatr Surg* 1994;29:1040-1043.
61. Skardal A, Murphy SV, Crowell K, et al. A tunable hydrogel system for long-term release of cell-secreted cytokines and bioprinted *in situ* wound cell delivery. *J Biomed Mater Res B Appl Biomater* 2017;105:1986-2000.
62. Colwell AS, Beanes SR, Soo C, et al. Increased angiogenesis and expression of vascular endothelial growth factor during scarless repair. *Plast Reconstr Surg* 2005;115:204-212.
63. Chen W, Fu X, Ge S, et al. Ontogeny of expression of transforming growth factor-β and its receptors and their possible relationship with scarless healing in human fetal skin. *Wound Repair Regen* 2005;13:68-75.
64. Dvořánková B, Szabo P, Lacina L, et al. Human galectins induce conversion of dermal fibroblasts into myofibroblasts and production of extracellular matrix: potential application in tissue engineering and wound repair. *Cells Tissues Organs* 2011;194:469-480.
65. Gilbert RWD, Vickaryous MK, Viloria-Petit AM, et al. Signalling by transforming growth factor beta isoforms in wound healing and tissue regeneration. *J Dev Biol* 2016;4:21.
66. Bochaton-Piallat M-L, Gabbiani G, Hinz B. The myofibroblast in wound healing and fibrosis: answered and unanswered questions. *F1000 Res* 2016;5. F1000 Faculty Rev-752.
67. English DR, Armstrong BK, Kricker A, et al. Reproducibility of reported measurements of sun exposure in a case-control study. *Cancer Epidemiol Biomark Prev* 1998;7:857-863.
68. Thompson MJW, Aitken DA, van der Mei IA, et al. Predictors of Beagley-Gibson skin cast grade in older adults. *Skin Res Technol* 2017;23:235-242.
69. Rosenbloom J, Abrams WR, Mecham R. Extracellular matrix 4: the elastic fiber. *FASEB J* 1993;7:1208-1218.
70. Sephel GC, Davidson JM. Elastin production in human skin fibroblast cultures and its decline with age. *J Invest Dermatol* 1986;86:279-285.
71. Schwartz E, Feinberg E, Lebwohl M, et al. Ultraviolet radiation increases tropoelastin accumulation by a post-transcriptional mechanism in dermal fibroblasts. *J Invest Dermatol* 1995;105:65-69.
72. Bai X. *Dermal Fibroblasts: Histological Perspectives, Characterization and Role in Disease.* Hauppauge, NY: Nova Science Publishers. 2013.
73. Kaya G, Saurat J-H. Dermatoporosis: a chronic cutaneous insufficiency/fragility syndrome. *Dermatology* 2007;215:284-294.
74. Saurat J-H, Mengeaud V, Georgescu V, et al. A simple self-diagnosis tool to assess the prevalence of dermatoporosis in France. *J Eur Acad Dermatol Venereol* 2017;31:1380-1386.
75. Lynch B, Bonod-Bidaud C, Ducourthial G, et al. How aging impacts skin biomechanics: a multiscale study in mice. *Sci Rep* 2017;7:13750.
76. Debacq-Chainiaux F, Erusalimsky JD, Campisi J, et al. Protocols to detect senescence-associated beta-galactosidase (SA-βgal) activity, a biomarker of senescent cells in culture and in vivo. *Nat Protoc* 2009;4:1798-1806.
77. Coppé J-P, Desprez P-Y, Krtolica A, et al. The senescence-associated secretory phenotype: the dark side of tumor suppression. *Annu Rev Pathol* 2010;5:99-118.
78. Martens MC, Seebode C, Lehmann J, et al. Photocarcinogenesis and skin cancer prevention strategies: an update. *Anticancer Res* 2018;38:1153-1158.
79. Okhovat J-P, Beaulieu D, Tsao H, et al. The first 30 years of the American Academy of Dermatology skin cancer screening program: 1985-2014. *J Am Acad Dermatol* 2018;79:884-891.e3.
80. Lacina L, Plzak J, Kodet O, et al. Cancer microenvironment: what can we learn from the stem cell niche. *Int J Mol Sci* 2015;16:24094-24110.
81. Lacina L, Kodet O, Dvořánková B, et al. Ecology of melanoma cell. *Histol Histopathol* 2018;33:247-254.
82. Strnad H, Lacina L, Kolář M, et al. Head and neck squamous cancer stromal fibroblasts produce growth factors influencing phenotype of normal human keratinocytes. *Histochem Cell Biol* 2010;133:201-211.
83. Kolář M, Szabo P, Dvořánková B, et al. Upregulation of IL-6, IL-8 and CXCL-1 production in dermal fibroblasts by normal/malignant epithelial cells in vitro: immunohistochemical and transcriptomic analyses. *Biol Cell* 2012;104:738-751.
84. Jobe NP, Živicová V, Mifková A, et al. Fibroblasts potentiate melanoma cells in vitro invasiveness induced by UV-irradiated keratinocytes. *Histochem Cell Biol* 2018;149:503-516.
85. Jobe NP, Rösel D, Dvořánková B, et al. Simultaneous blocking of IL-6 and IL-8 is sufficient to fully inhibit CAF-induced human melanoma cell invasiveness. *Histochem Cell Biol* 2016;146:205-217.
86. Baum J, Duffy HS. Fibroblasts and myofibroblasts: what are we talking about? *J Cardiovasc Pharmacol* 2011;57:376-379.

PUBLIKACE III

Kučera J, **Strnadová K**, Dvořánková B, Lacina L, Krajsová I, Štork J, Kovářová H, Skalníková HK, Vodička P, Motlík J, Dundr P, Smetana K Jr, Kodet O. Serum proteomic analysis of melanoma patients with immunohistochemical profiling of primary melanomas and cultured cells: Pilot study. *Oncol Rep.* 2019 Nov;42(5):1793-1804. **(IF: 3.417)**

Serum proteomic analysis of melanoma patients with immunohistochemical profiling of primary melanomas and cultured cells: Pilot study

JAN KUČERA[1,2*], KAROLÍNA STRNADOVÁ[2,3*], BARBORA DVOŘÁNKOVÁ[2,3], LUKÁŠ LACINA[1-3], IVANA KRAJSOVÁ[1], JIŘÍ ŠTORK[1], HANA KOVÁŘOVÁ[4], HELENA KUPCOVÁ SKALNÍKOVÁ[4], PETR VODIČKA[4], JAN MOTLÍK[4], PAVEL DUNDR[5], KAREL SMETANA Jr[2,3] and ONDŘEJ KODET[1-3]

[1]Department of Dermatovenereology, 1st Faculty of Medicine and General University Hospital; [2]Institute of Anatomy, 1st Faculty of Medicine, Charles University, Prague 128 00; [3]BIOCEV-Biotechnology and Biomedical Centre of The Czech Academy of Sciences and Charles University, 1st Faculty of Medicine, Charles University, Vestec 252 50; [4]Laboratory of Applied Proteome Analyses and Research Centre PIGMOD, Institute of Animal Physiology and Genetics, Czech Academy of Sciences, Liběchov 277 21; [5]Institute of Pathology, 1st Faculty of Medicine, Charles University, Prague 128 00, Czech Republic

Received April 14, 2019; Accepted August 7, 2019

DOI: 10.3892/or.2019.7319

Abstract. The steadily increasing incidence of malignant melanoma (MM) and its aggressive behaviour makes this tumour an attractive cancer research topic. The tumour microenvironment is being increasingly recognised as a key factor in cancer biology, with an impact on proliferation, invasion, angiogenesis and metastatic spread, as well as acquired therapy resistance. Multiple bioactive molecules playing cooperative roles promote the chronic inflammatory milieu in tumours, making inflammation a hallmark of cancer. This specific inflammatory setting is evident in the affected tissue. However, certain mediators can leak into the systemic circulation and affect the whole organism. The present study analysed the complex inflammatory response in the sera of patients with MM of various stages. Multiplexed proteomic analysis (Luminex Corporation) of 31 serum proteins was employed. These targets were observed in immunohistochemical profiles of primary tumours from the same patients. Furthermore, these proteins were analysed in MM cell lines and the principal cell population of the melanoma microenvironment, cancer-associated fibroblasts. Growth factors such as hepatocyte growth factor, granulocyte-colony stimulating factor and vascular endothelial growth factor, chemokines RANTES and interleukin (IL)-8, and cytokines IL-6, interferon-α and IL-1 receptor antagonist significantly differed in these patients compared with the healthy controls. Taken together, the results presented here depict the inflammatory landscape that is altered in melanoma patients, and highlight potentially relevant targets for therapy improvement.

Correspondence to: Dr Ondřej Kodet, Department of Dermatovenereology, 1st Faculty of Medicine and General University Hospital, Charles University, U Nemocnice 499/2, Prague 128 00, Czech Republic
E-mail: ondrej.kodet@lf1.cuni.cz

*Contributed equally

Key words: melanoma, inflammation, microenvironment, cancer-associated fibroblasts, interleukin, proteomics

Introduction

Cancer incidence is increasing worldwide (1). Malignant melanoma (MM) incidence, as well as mortality, follows this trend in almost all countries (2). MM is an aggressive skin tumour arising from melanocytes, cells involved in the protection of skin against UV-induced damage, including the genotoxic effect of irradiation on epidermal cells.

Once metastasised, MM frequently remains a fatal neoplasm with limited therapeutic options and relatively poor outcomes. There has been notable progress, predominantly in immunomodulatory therapy, in recent years, but the therapeutic response is difficult to predict (2). However, immune checkpoint-oriented therapy is also associated with a rapid increase in disease-specific healthcare costs (3).

Therefore, there is an urgent need to identify and validate informative biomarkers to improve the early selection of at-risk patients suitable for adjuvant therapy, the optimal drug choice, and possibly for disease progress monitoring (3,4).

Prognostically essential features of primary melanoma are well known and include tumour thickness [measured in mm according to Breslow staging (5)] and the presence of surface epidermal ulceration (6). These parameters are easily acquired by histologists in routine haematoxylin-eosin-stained paraffin sections and are indispensable prognostic factors in melanoma staging (6). More recently, biomarkers obtained after

immunohistochemical and molecular analysis of the tumour tissue have played a critical role in melanoma management; namely, the presence of BRAF, GTPase NRas and c-KIT mutations is predictive of response to small drug inhibitors (2,7). At present, no ideal biomarker predicting the therapeutic response in melanoma patients treated with other modern drugs, such as immune checkpoint modulators (e.g. anti-programmed cell death protein 1 or anti-cytotoxic T lymphocyte protein 4), exists (4).

In all the aforementioned cases, an invasive surgical procedure (radical excision or limited biopsy) to acquire a tissue sample is necessary.

From the perspective of a clinical oncologist, biomarkers determined from a peripheral blood sample would be extremely beneficial for a patient's regular follow-up. In case of MM, the detected molecules could include (but not be limited to) soluble proteins, melanin synthesis-related metabolites, circulating nucleic acids and/or circulating tumour cells (4,8).

In the American Joint Committee on Cancer (8th edition) staging system (6), serum lactate dehydrogenase (LDH) is the only serum biomarker that is accepted as a robust prognostic parameter for routine clinical use in melanoma patients (6). Unfortunately, LDH is not a melanoma-specific enzyme, and increased LDH is also associated with many other benign and malignant diseases (9). By contrast, the S100B protein is highly specific, and its increased levels are detected in patients with advanced melanoma. Thus, the S100B protein has a strong association with melanoma prognosis (10). Notably, the European Society of Medical Oncology, German and Swiss guidelines recommend serum S100B as the most accurate serological test for follow-up, having better specificity for progressive disease compared with LDH (11-13). However, the S100 protein did not prove to be sufficient (concerning sensitivity) for detecting tumour progression, and it cannot substitute for imaging methods [e.g. computed tomography (CT) or positron emission tomography/CT] in long-term follow-up. A plethora of other biomarkers has been advocated in the literature for MM; none of these have been broadly accepted for use in a clinical setting (6,8).

A limited percentage of cells released from a primary tumour are capable of colonising a new site. This phenomenon highlights the importance of a permissive tissue microenvironment during cancer progression and metastatic spread. This phenomenon was predicted in 1889 by Paget (14), who hypothesised that metastasis does not occur at particular body sites randomly. Cancer represents a complicated ecosystem of tumour cells and a variety of other cell types that form the tumour stroma, such as cancer-associated fibroblasts (CAFs), tumour-infiltrating leukocytes (TILs), pericytes and endothelial cells (15).

The microenvironment modifies critical aspects of tumour biology, such as tumour growth, local aggressiveness, lymphatic and metastatic spread, and resistance to therapy (16). The role of the microenvironment in MM biology has been documented at multiple levels. CAFs increase tumour cell plasticity and facilitate the maintenance of the undifferentiated status of tumour cells (17). CAFs can play a significant role in the mechanism of primary resistance to targeted therapy via the production of transforming growth factor-β (18). CAFs and other stromal cells can produce several other factors with a similar effect, such as hepatocyte growth factor (HGF), which stimulates the c-Met/PI3K/Akt signalling pathway. These factors can activate tumour cell growth in a paracrine manner, thus conferring resistance to targeted therapy (19). It is evident that the cancer microenvironment is crucial for MM growth and metastatic spread, as well as for the emergence of acquired drug resistance.

It was documented recently (20) that even a minimal number of circulating tumour cells elicit a systemic inflammatory status contributing to the promotion of tumour metastasis. These circulating tumour cells represent a clinically undetectable disease burden.

On the other hand, a recent study also demonstrated that the majority of circulating tumour cells are unable to establish a proliferatively successful metastatic clone (21). This raises several important questions regarding the timing of therapeutic intervention in cancer, including MM. It seems likely that the systemic proinflammatory response could increase the risk of consequent melanoma progression to metastatic disease, resulting in shorter survival of patients. Data describing the complexity of the inflammatory landscape in MM are limited (22). Thus, it may only be hypothesised whether therapeutic inhibition of the inflammatory response may reduce the production of cytokines contributing to the formation of premetastatic niches suitable for disease dissemination in an organism. A better understanding of the fundamental components of this inflammatory response may be important in the design of a therapeutic strategy to prevent tumour metastasis. More research on the tumour-associated systemic inflammation blockade may reveal optimal targets to prevent and treat tumour metastasis.

The present pilot study focused on comparative multiplex analysis of 31 serum proteins from 12 patients at the time of melanoma diagnosis, and during the early onset of disease, progression using Luminex technology (Luminex Corporation). It was hypothesised that the levels of these proteins could serve as biomarkers associated with the clinical progression and pathological features of the disease. These data were also compared with the immunohistochemical profiles of selected proteins in primary tumours from the same patients. MM cell lines and a model of their microenvironment *in vitro*, using melanoma-specific CAFs, were also tested.

Materials and methods

Patients. MM patients (n=12) and healthy volunteers (n=5) participated in the study after giving explicit written consent. The study was approved by the local ethics committee (Ethics Committee of the General University Hospital, Prague; no. 15/15). All tissue and blood samples were obtained strictly with the explicit informed consent of participants of the study. Samples from MM patients and healthy volunteers were collected between May 2014 and February 2015.

The patients were diagnosed with MM based on the clinical appearance of the skin lesion. Histopathological analysis verified the diagnosis of primary cutaneous MM after tumour excision. No patient had clinical evidence of metastatic disease at the time of diagnosis. Based on this favourable status, clinical follow-up was initiated. Despite radical surgery, some patients developed metastasis during the follow-up period. The

patient cohort characteristics are summarised in Table I. The healthy volunteers were three men (35, 40 and 66 years old), and two women (26 and 63 years old) without any evidence of cancer or chronic disease.

Cells. The BLM cell line was kindly provided by Dr L. van Kempen and Professor J.H.J.M. van Krieken (Department of Pathology, Radboud University, Nijmegen Medical Centre, Netherlands). The commercially available A2058 cell line and HP-Mel (HEMn) cell line was purchased from the American Type Culture Collection (ATCC® CRL-11147™ and ATCC® PCS-200-012™, respectively). MP17 melanoma cells were isolated (February 20th, 2015) from pleural ascitic fluid from a patient (74-year-old man) with tumour generalisation (Tumor-Node-Metastasis stage IV) using a previously described method (17). Culture conditions were as described in a previous study (23).

Normal primary dermal fibroblasts (acquired after breast reduction surgery, designated as HFP4 (from a 55-year-old female; localisation, chest; collected May 19th. 2014) and CAFs [two independent isolates designated as MAM (69-year-old female; localisation, chest; collected July 14th, 2014) and ZAM (48-year-old male; localisation, abdomen; collected September 9th, 2014)] from skin metastases of MM were prepared and cultured as previously described (24-26).

MP17, HFP4, MAM and ZAM cells were obtained and maintained with the informed consent of patients and the approval of the local ethical committee as indicated above. The authors confirm that mycoplasma testing was performed on all cell lines used in the present study.

Serum preparation. Venous blood was collected from MM patients (n=12) at three time intervals: i) At the time of diagnosis prior to any surgical treatment; ii) 1 month after the surgery; and iii) ~3 months after the surgery. The blood was left to clot for 30-60 min at room temperature followed by centrifugation (1,500 x g; 10 min; 4˚C). The obtained serum was immediately aliquoted to avoid later multiple freeze-thaw cycles and stored at -80˚C. Control sera were obtained from healthy individuals (n=5) under identical conditions.

Analysis of serum samples. The levels of 31 cytokines, chemokines and growth factors were analysed using Luminex xMAP® bead assays (Luminex Corporation) in the serum of MM patients and controls. The Human Cytokine Magnetic 30-Plex Panel (Thermo Fisher Scientific, Inc.) and CXCL1 Human ProcartaPlex™ Simplex kit (Thermo Fisher Scientific, Inc.) were used to quantify epidermal growth factor (EGF), eotaxin, basic fibroblast growth factor, granulocyte-colony stimulating factor (G-CSF), granulocyte-macrophage colony-stimulating factor (GM-CSF), growth regulated-α protein (also known as CXCL1), hepatocyte growth factor (HGF), interferon (IFN)-α, IFN-γ, interleukin (IL)-1β, IL-1 receptor antagonist (IL-1RA), IL-2, IL-2 receptor, IL-4, IL-5, IL-6, IL-7, IL-8, IL-10, IL-12 (p40/p70), IL-13, IL-15, IL-17, IP-10, C-C motif chemokine 1, MIG, C-C motif chemokine 3, C-C motif chemokine 4 (MIP-1β), RANTES, tumour necrosis factor-α and vascular endothelial growth factor (VEGF) levels. The manufacturer validated all antibodies used for this experiment.

Table I. Patient characteristics.

Patient no.	Sex	Age of onset, years	Location	Breslow	Ulceration	Sentinel lymph node metastasis	Clinical stage	Therapy at time of serum collection	Generalization	Mortality caused by melanoma	PFS, months	OS, months
1	F	65	Back	6.5	Yes	Not	IIC	S,N	Yes	Yes	12	14
2	M	68	Thigh	2.5	Not	Yes (N1a)	IIIB	S,N,L	Not	Not	R	55
3	F	71	Lower leg	0.3	Not	Not	IA	S,N	Not	Not	R	54
4	M	61	Back	0.8	Not	Not	IA	S,N	Not	Not	R	54
5	M	89	Toe	3.4	Yes	Not	IIB	S	Yes	Not[a]	12	43
6	M	55	Back	3.6	Not	Yes (N1a)	IIIB	S,N,L	Yes	Yes	14	16
7	M	66	Back	2.2	Yes	Yes (N1a)	IIIC	S,N,L	Yes	Yes	11	14
8	F	66	Thigh	0.5	Not	Not	IA	S,N	Not	Not	R	53
9	M	68	Back	2.0	Not	Yes	IIIB	S,N,L	Not	Not	R	50
10	F	34	Lower leg	1.7	Not	Not	IB	S,N	Not	Not	R	51
11	F	71	Toe	0.4	Not	Not	IA	S	Not	Not	R	51
12	F	68	Back	2.7	Not	Not	IIA	S,N	Not	Not	R	51

Clinical stage at the time of diagnosis was determined according to the American Joint Committee on Cancer melanoma staging guidelines (8th edition). [a]Patient with metastatic disease who died of a heart attack. F, female; M, male; S, surgical excision; N, sentinel lymph node biopsy; L, regional lymphadenectomy; R, remission; PFS, progression-free survival; OS, overall survival (updated to December 31st, 2018).

After thawing on ice, the serum samples were gently mixed, pre-cleaned via centrifugation (16,000 x g; 10 min; 4˚C), and diluted at a 1:1 ratio with Assay Diluent (in the case of the 30-plex assay) or Universal Assay Buffer (in the case of the Simplex assay) to minimize the matrix effects. The same diluent buffer was used as a blank and as a diluent for the calibration standards. The calibration curve was extended at the lower end by additional dilutions of calibration standards. Reverse pipetting was used for high accuracy in all liquid handling steps. All samples, standards and background were analysed in duplicate. The assay was performed according to the manufacturer's instructions. The fluorescence intensities of minimum 100 beads/analyte were recorded using a Luminex 200™ analyser with xPonent software build 3.1.871.0 (Luminex Corporation), adequately calibrated according to the manufacturer's instructions.

Raw data were exported from xPonent software in. csv format and processed in the R statistical environment (27) using the drLumi package (28). The median fluorescence intensity was used for standard curve fitting and quantitation of cytokine concentrations. Standard curves were fitted using 5-parameter logistic regression (SSL5) with 4-parameter logistic regression as a fall-back for occasions where the SSL5 model would not converge. The concentrations of two technical replicates of each sample were averaged before further statistical analysis.

Data analysis and statistics. Statistical analysis of the relationship between the measured protein levels and clinical features of the disease was conducted using the R statistical environment (27) and tidy verse set of packages (29). Repeated measures ANOVA was used for statistical comparisons in experiments with more than two groups. Dunnett's test was used for many-to-one group comparisons of MM melanoma samples to controls (30-32). The association between protein levels and Breslow index was evaluated using Kendall's tau correlation coefficient, and lines representing the Theil-Sen estimator of a linear relationship were used.

t-Distributed stochastic neighbour embedding (t-SNE) implemented in the R Rtsne package was used for nonlinear dimension reduction, to visualise any possible patterns in the high-dimensional cytokine concentration data (33). Analyte levels below the level of detection (missing values) were replaced by 80% of the lower limit of detection of the assay. Data for each analyte were normalized relative to mean concentration overall data points (all time points in all patients and controls) for the given analyte. Rtsne was run with the initial principal component analysis step, perplexity 12 and θ parameter 0.5 over 8,000 iterations to reduce the dimensions to 2.

Immunohistochemical analysis of paraffin sections of patient tumours and cultured cells, and microscopy. Tissue samples were fixed for 24-48 h in 4% neutral buffered formalin at room temperature and routinely processed to produce paraffin blocks. Sections (2-μm-thick) were deparaffinised and rehydrated through xylene and 98% ethanol. Afterwards, the sections were washed in PBS, and heat-induced epitope retrieval was performed in citrate buffer, pH 6.0 in an autoclave at 120˚C for 3 min, with subsequent gradual cooling to room temperature for 60 min. Non-specific binding of antibodies was inhibited using the Protein Block system (Dako; Agilent Technologies, Inc.; cat. no. X0909) followed by treatment with 3% hydrogen peroxide (in PBS; Sigma-Aldrich; Merck KGaA) for 20 min at room temperature. Sections were incubated overnight at 4˚C with biotinylated primary antibodies (manufacturer-validated summary antibody information in Table SI; the manufacturer validated all employed antibodies for use in these methods).

The following day, the sections were extensively washed and incubated with secondary (polymer horseradish peroxidase-tagged) antibody for 30 min at room temperature. 3-Amino-9-ethylcarbazol (AEC; DCS Innovative Diagnostik-Systeme) chromogen was used for visualisation of the immunohistochemical reaction, according to the manufacturer's protocol. Nuclei were counterstained with Gill's haematoxylin for 2 min at room temperature and mounted in Hydromount (National Diagnostics). Semi-quantitative analysis (0, negative; +, weakly positive; ++, moderately positive; and +++, strongly positive) of the immunohistochemistry reaction was used to express the proportion of positive staining based on inspection under an optical microscope.

The cultured cells on coverslips were briefly fixed in 2% paraformaldehyde in PBS for 5 min at room temperature and permeabilised with Triton X-100 (Sigma-Aldrich; Merck KGaA). The coverslips with cultured cells were stained according to the same protocol using identical primary antibodies and other chemicals (with the omission of antigen retrieval). Imaging was performed with a Leica microscope DM2000 equipped with camera (DFC290 HD) and software package LAS, version 4.3.0 (Leica Microsystems GmbH): Magnification, x400; calibration, 1,000 pixels/pixel; capture format, 2,048x1,536; full frame; γ=1.0; gain, 1.0; auto exposure, on; nosepiece objective magnification, 40; mag changer magnification, 1; and aperture, 0.4.

Results

Serological analysis. The present study analysed the levels of a 31-protein panel of cytokines, chemokines and growth factors in serum prepared from patients suffering from MM compared with healthy volunteers. Based on the initial hypothesis, these proteins were investigated for their ability to serve as biomarkers correlating with certain oncologically-important features of the disease. Among the analysed proteins, IL-5, IL-7 and GM-CSF were below the lower limit of detection in most of the samples and were excluded from further analyses. The levels of the remaining 28 proteins are summarised in Fig. 1 and Table SII. Data demonstrated that the levels of five studied proteins, namely IL-1RA, IL-2, IL-13, RANTES and G-CSF, were significantly different in the serum samples of healthy volunteers from the melanoma patients, according to Dunnett's test (Fig. 1). The results from the ANOVA summarised in Table SIII indicated that these five proteins were not significantly different in the serum samples of healthy volunteers compared with the melanoma patients.

It was observed that the Breslow values of primary tumours were significantly associated with the serum levels of four detected proteins, namely IL-6, IL-8, IL-13 and VEGF (Fig. 2).

The serum levels of IL-1RA, IL-13, IFNα and RANTES reflected the clinical stage of the disease at the time of MM diagnosis (Fig. 3).

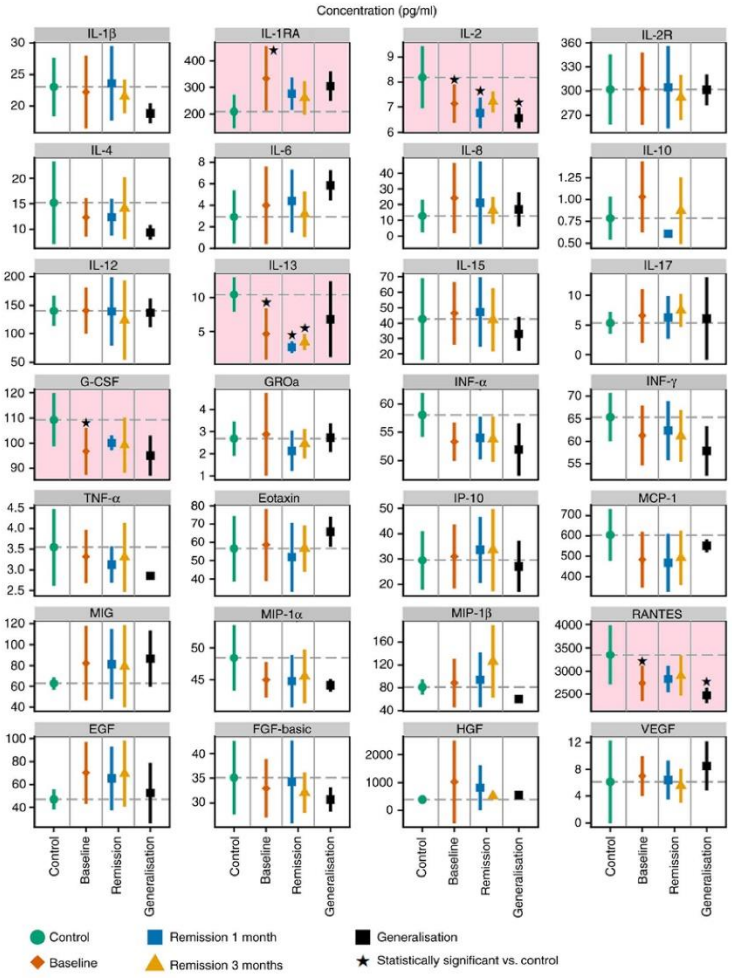

Figure 1. Levels of 28 proteins in serum samples from healthy volunteers (control; green) and patients with MM. MM patient samples were collected at the time of diagnosis (baseline; red) and again 1 month and 3 months post-surgery. Data from the two later collections are plotted separately for subsets of patients without any evidence of disease (remission; blue, yellow) and patients at the stage of MM generalisation (progression, in black). The graphs represent the mean ± SD. Statistical significance (Dunnett's one-to-many test with multiple testing correction) of comparisons between the control and patient subsets are highlighted with a pink background. *P<0.05 vs. control. IL, interleukin; G-CSF, granulocyte-colony stimulating factor; IL-1RA, IL-1 receptor antagonist; IL-2R, IL-2 receptor; GROa, C-X-C motif chemokine ligand 1; IFN, interferon; TNF, tumor necrosis factor; MCP-1, C-C motif chemokine ligand 2; MIG, C-X-C motif chemokine ligand 9; IP-10, C-X-C motif chemokine ligand 10; MIP-1α, C-C motif chemokine ligand 3; MIP-1β, C-C motif chemokine ligand 4; EGF, epidermal growth factor receptor; FGF-basic, basic fibroblast growth factor; HGF, hepatocyte growth factor; VEGF, vascular endothelial growth factor.

It is important to note that the cluster analysis demonstrated a vast extent of inter-individual differences among the tested patients and certain intra-individual level fluctuation (Fig. 4).

Analysis of primary MM lesions. To assess the contribution of the factors upregulated in MM patient sera to the MM microenvironment, immunohistochemistry of the tumours was performed in the same patients whose serum was analysed (Fig. 5). Immunohistochemical positivity for selected members of the studied protein families and their receptors in representative samples of primary tumours is illustrated in Fig. 5A-I and was quantified. Fig. 5J demonstrates the heterogeneity of primary tumours in the patients from whom the serum samples were collected. MM cells from all samples were positive for HGF, but the signal intensity

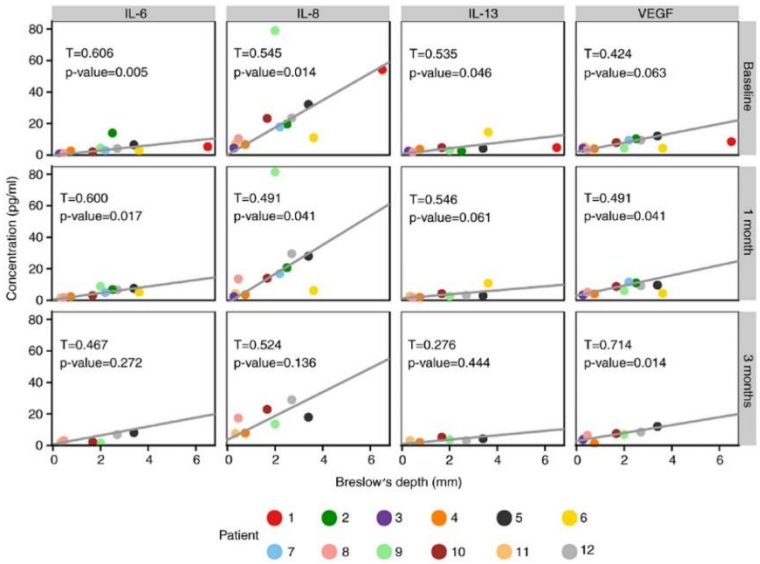

Figure 2. Correlation of Breslow values with serum levels of selected proteins. Scatterplots of values for individual MM patient at each sample collection point are presented. The lines represent the Theil-Sen estimator of a linear relationship. The non-parametric Kendall's tau correlation coefficient together with the corresponding P-value is displayed in each plot panel. IL, interleukin; VEGF, vascular endothelial growth factor.

was low. The studied tumours also widely expressed IL-6 and its receptor IL-6R, and VEGF-R1. The epidermis overlaying the MM lesions was highly positive for VEGF and VEGF-R2 in all studied samples (Fig. 5F). Macrophages widely expressed the studied markers, as demonstrated in the case of HGF (Fig. 5I).

Analysis of cultured MM cells (A2058, BLM and MP17), normal melanocytes (HP-Mel), normal dermal fibroblasts (HFP4) and CAFs (MAM and ZAM). The phenotype of melanoma cells and CAFs isolated from melanoma was analysed by studying the expression of selected factors detected in the serum of melanoma patients. The aim of this part of the study was to evaluate the production of these factors by isolated MM cells and CAFs. Data from cultured MM cells (A2058, BLM and MP17) demonstrated a similar phenotype to samples from primary MMs (Fig. 5) with several exceptions, such as high positivity for IL-8 (Fig. 6Ac, Bc and Cc) and VEGF-R2 (Fig. 6Ah, Bh and Ch). Normal melanocytes were negative for IL-6 (Fig. 6Da), IL-8 (Fig. 6Dc), CXCR1/2 (Fig. 6Dd and e), VEGF (Fig. 6Df), and the receptors VEGF-R1/R2 (Fig. 6Dg and h). As expected, these cells were highly positive for protein S100, MiTF and differentiation marker HMB45 (data not shown). Also as expected, both normal fibroblasts (HFP4) and fibroblasts isolated from the cutaneous metastases of MM (CAFs, similarly MAM or ZAM) exhibited a vimentin-rich cytoskeleton (data not shown). The signal for IL-6, IL-8, CXCR1, and CXCR2 was stronger in MM CAFs (Fig. 7Aa, c, d and e) than in normal fibroblasts (Fig. 7Ba, c, d and e).

Discussion

The present study demonstrated that the presence of a primary malignant melanoma tumour and its consequent metastatic spread is reflected by a profound change in inflammatory molecules in the serum. Similar findings for individual molecules or smaller groups have also been reported previously (34,35).

Despite the observed broad inter-individual variability, the presence of a primary tumour was associated with significantly decreased levels of IL-2, IL-13, RANTES and G-CSF, and an increase in IL-1RA detected in the patient sera.

In detail, some of these factors also significantly differed in certain clinical stages of the disease, wherein IFNα, IL-13 and RANTES were decreased significantly and IL-1RA was increased. The cohort of patients was also affected by the healing of the wound after surgery. However, no complicated courses of healing were observed in these 12 patients. An association between the Breslow index of the tumour and the serum levels of tested proteins was observed in the case of IL-6, IL-8, IL-13 and VEGF.

The low levels of IFNα in patients with melanoma seem to be important, because its anticancer effect has been well documented and recombinant IFNα is employed as a drug in cancer therapy, including adjuvant therapy for MM (36). Similar therapeutic implications are true for IL-2 (37).

Both downregulated interleukins IL-2 and IL-13 exhibit anticancer activity, with the potential for application in anticancer therapy (38-42).

RANTES is also well known as an essential inflammation-promoting chemokine. However, its role in anticancer

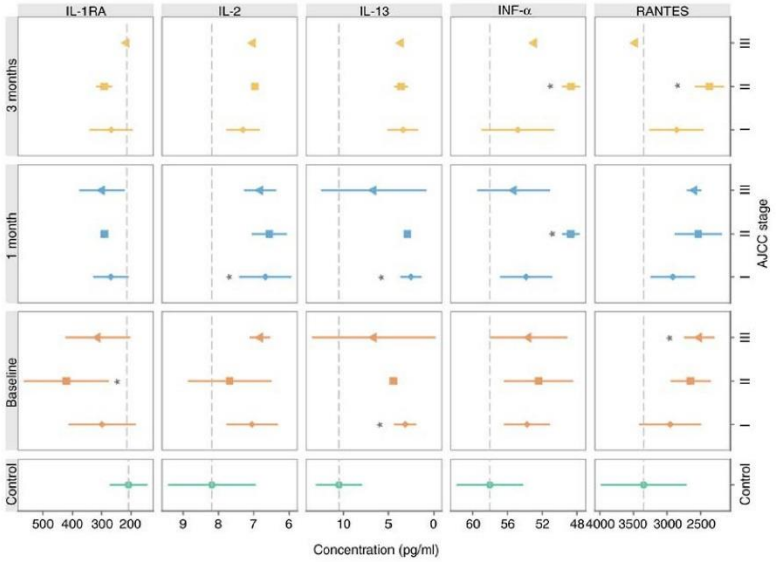

Figure 3. Relationship between selected serum proteins and clinical disease stage. Graphs represent the mean ± SD. Statistical significance (Dunnett's one-to-many test with multiple testing correction) for comparisons between the control and particular disease stages are presented. *P<0.05 vs. control. IL, interleukin; IL-1RA, IL-1 receptor antagonist; IFN, interferon.

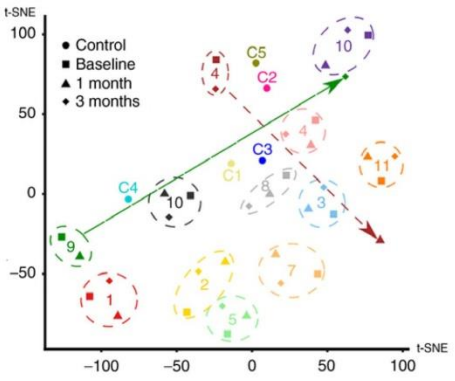

Figure 4. Cluster analysis of patients with MM. The high-dimensional dataset of 28 proteins measured for each patient was mapped onto a two-dimensional space using t-SNE. One data point for each of the controls (circles) and one data point for each patient/time-point combination (baseline, square; 1 month, triangle; 3 months, diamond) were plotted. Numbers (corresponding to Tables I and SII) were used to label the individual controls and patients. The overall variability of the dataset appeared to be mostly driven by individual differences between subjects, as data from different time points of the same patient generally clustered together (highlighted by the dashed circles). However, for a few patients, there were outlier data points (highlighted by arrows). tSNE, t-distributed stochastic neighbour embedding.

immunity/tumour facilitation requires to be further elucidated especially in melanoma (43,44).

Attention should also be paid to the cytokine IL-6 and chemokine IL-8. Both molecules exhibit a broad tumour-supporting effect (23,45). It should be noted that inflammation-supporting factors such as IL-6 and IL-8 are produced not only by MM cells and TILs, but are also provided in large quantities by CAFs (23,25,46). This is apparent from the present immunohistochemical results. The contribution of particular components of a tumour can be easily documented through immunocytochemical analysis of isolated cell populations. Therefore, it may be expected that regardless of the actual cellular origin of these factors, the protein abundance will consequently be detected in the serum (8,47-50). These facts highlight the importance of the tumour microenvironment and support the concept of cancer as a systemic disease (6,51).

In general, IL-6 and IL-8 stimulate the metastatic spread of many tumours, including MM (25,46,52), and participate in the induction of resistance to vemurafenib (18).

In the particular case of IL-6, its effect on MM seems to be stage-specific. IL-6 has an inhibitory effect in the initial stages of melanoma. However, IL-6 stimulates the growth and invasiveness of MM cells in advanced stages of the disease (53,54). In general, blocking of IL-6 production seems to be beneficial for MM patients (55) because IL-6 stimulates cancer cachexia and wasting, a severe and terminal complication of malignant disease (56-59).

Chemokine IL-8 (CXCL8) and its receptors CXCR1 and CXCR2 play a notable role in melanoma pathogenesis, particularly in melanoma progression and metastasis (60). The serum concentration of IL-8 can be correlated to the disease stage, and changes in the serum IL-8 levels could be used to

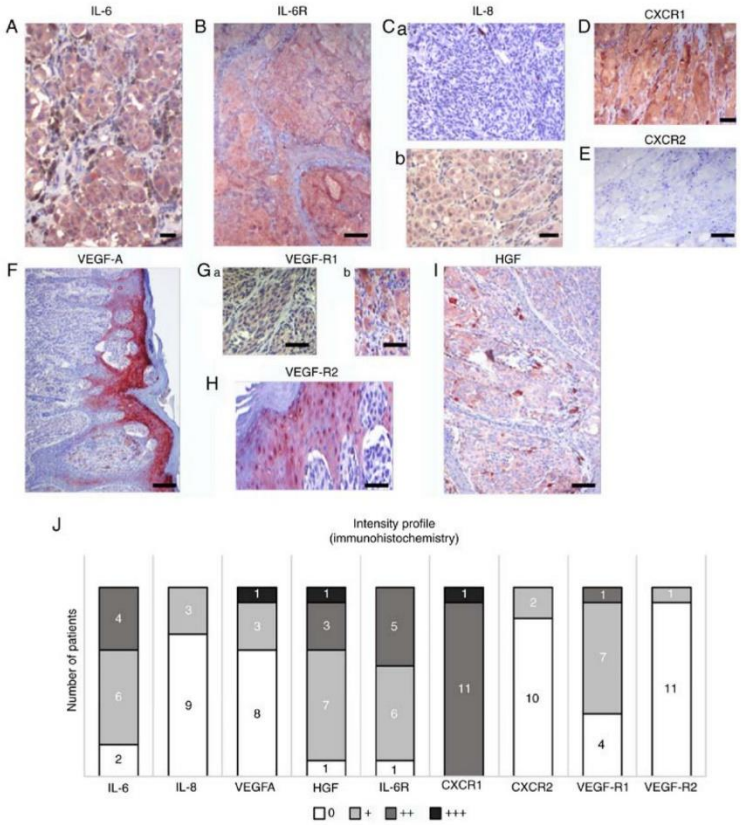

Figure 5. Characteristic samples of expression of selected protein markers in sections from primary MM in the same cohort of patients. Multiple markers were detected by immunohistochemistry in melanomas. (A) IL-6 and (B) IL-6 receptor were detected in the majority of tumours in MM cells. (C) IL-8 expression was highly variable in studied samples; representative sections are included. Differences in expression were also observed in CXCR1 and CXCR2. (D) CXCR1 with highly positive in all patients, which contrasted with (E) the low to negative CXCR2 expression. (F) Notable positivity for VEGF was observed in the epidermis overlaying the MM lesion. Expression of VEGF receptors (G) VEGF-R1 and (H) VEGF-R2 was also observed beside MM cells in the tumour microenvironment, represented by stromal macrophages and epidermis. (I) HGF was also observed in MM cells and macrophages. Scale bar, 50 μm. (J) A summary of the expression of selected markers in primary MM in the present cohort. Semi-quantitative analysis (0, +, ++, and +++) of the immunohistochemistry reaction was used to express the proportion of positive staining based on inspection under an optical microscope. The numbers of positive tumours are included on the graph. IL, interleukin; CXCR1, C-X-C motif chemokine receptor 1; HGF, hepatocyte growth factor; CXCR2, C-X-C motif chemokine receptor 2; VEGF, vascular endothelial growth factor; VEGF-AR1, VEGF-A receptor 1; VEGF-AR2, VEGF-A receptor 2; IL-6R, IL-6 receptor.

monitor and predict the clinical benefit of immune checkpoint inhibitor therapy (61).

In addition to the direct effect of IL-8 on cancer cells, this chemokine also stimulates the growth of capillaries in the tumour environment. Thus, it has a synergistic effect with VEGF (62). The correlation of serum levels of IL-8 with melanoma tumour mass has been previously described (63). Breslow's depth is generally accepted as a simple but precise prognostic factor. The present data demonstrated that the serum levels of IL-6 and IL-8 (both increased) reflect this tumour parameter.

It should be acknowledged here that surgical removal did not lead to an immediate lowering of the IL-6 and IL-8 levels. It seems likely that a sustained level of these molecules may promote another source of this cytokine, other than from a tumour itself. This can be interpreted as evidence of the systemic proinflammatory environment in the patient.

The observation of an elevated serum level of VEGF in the samples from patients with MM is unsurprising, because its cancer-stimulating effect via the support of tumour vascularisation is well known (64). Serological elevation of VEGF is associated with melanoma progression and adverse immune effects, including elevation of T_H2 cytokines (e.g., observed IL-10) and decreased of T_H1 cytokines (e.g., observed IL-2 and interferon γ). These changes result in suppression of anti-tumour immunity (65,66).

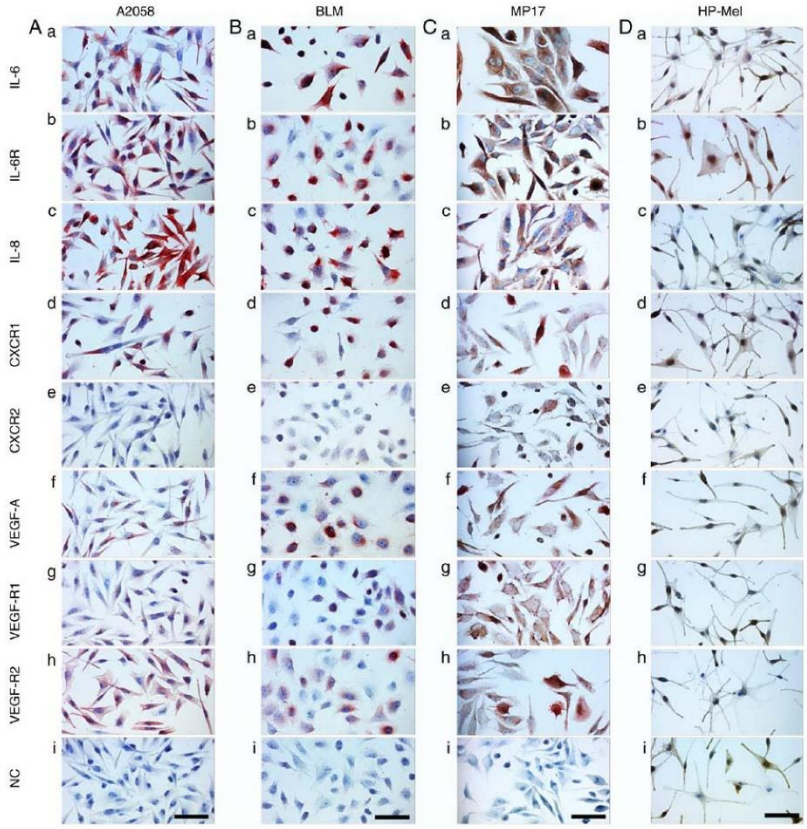

Figure 6. Detection of selected markers in MM cell lines. The detection was performed in (A) A2058, (B) BLM and (C) MP17 cells, and in (D) normal HP-Mel cells. HP-Mel are more pigmented than MM cell lines and their H_2O_2 bleaching was not as successful. Therefore, AEC substrate (red) was used for the immunocytochemical reaction detection. Generally, it was possible to note that positive staining of HP-Mel was negligible in comparison with that of MM cell lines. A positive signal for IL-6 and IL-6R was observed in HP-Mel cells. Scale bar, 100 μm. CXCR1, C-X-C motif chemokine receptor 1; CXCR2, C-X-C motif chemokine receptor 2; VEGF, vascular endothelial growth factor; VEGF-AR1, VEGF-A receptor 1; VEGF-AR2, VEGF-A receptor 2; IL-6R, IL-6 receptor; NC, normal control; HP-Mel, highly pigmented melanocyte.

Expression of CD114, a surface receptor for VEGF, has been described in association with melanoma progression (67), and it can be considered as a new marker for cancer cells originated from neural crest-derived stem cells (68).

Besides this, we observed significantly lower levels of G-CSF. G-CSF is known to stimulate formation of granulocytes, and its reduction related to cancer progression is therefore likely. Neutrophils are functionally plastic in the tumour microenvironment, and N1/N2 functional polarisation has recently been accepted. Classically activated (N1) neutrophils inhibit metastatic growth. In contrast, alternatively polarised (N2) neutrophils have been reported to facilitate colonisation of the target organ by metastasis-initiating cancer cells.

Comparative analysis of serum samples with immunohistochemical findings in primary tumours and cultured cells has shown that both MM cells and cells forming the tumour microenvironment (CAFs, TILs, keratinocytes, macrophages and pericytes) participate in the changes of serum proteins. Distinct clinical stages of MM can induce a specific pattern of serum proteins that underlines the systemic effect of the disease (18).

Immunosuppressive properties of the melanoma microenvironment are responsible for the chronic inflammatory status of the organism, thus supporting the hypothesis of cancer as a systemic disease from an early stage. However, it does not solve the question of the cause and the consequence.

Immunohistochemical analysis of IL-6, IL-8, VEGF and their receptors was performed in primary melanomas as well as in several MM cell lines and CAFs. The resulting data harmonised with the analysis of patient sera. This further demonstrated that the MM cells and stromal cells (CAFs) participated in the production of the studied factors. On the other hand, data from individual patients are highly variable, which is supported by similar evidence

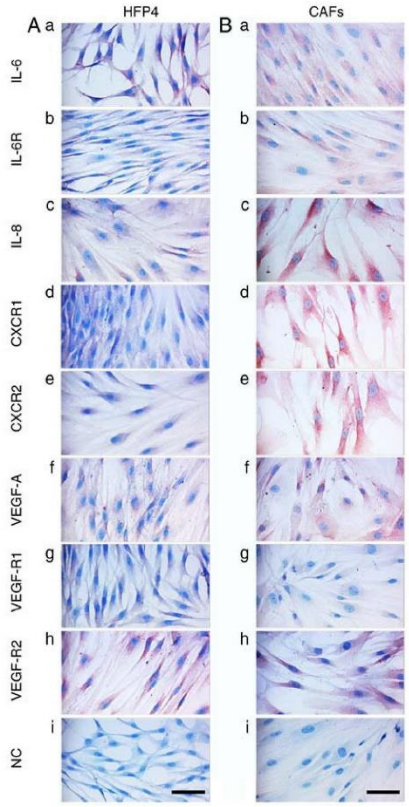

Figure 7. Detection of selected markers in normal HFP4 fibroblasts and CAFs isolated from a melanoma skin metastasis. Selected markers are visualised in primary culture of (A) normal dermal fibroblasts (HFP4) and (B) CAFs isolated from MM (MAM; ZAM data not shown). All types of fibroblasts expressed vimentin (data not shown). CAFs expressed more CXCR1 and CXCR2 than was observed in the normal fibroblasts (HFP4). Scale bar, 100 μm. CAFs, cancer-associated fibroblasts; CXCR1, C-X-C motif chemokine receptor 1; CXCR2, C-X-C motif chemokine receptor 2; VEGF, vascular endothelial growth factor; VEGF-AR1, VEGF-A receptor 1; VEGF-AR2, VEGF-A receptor 2; IL-6R, IL-6 receptor; NC, normal control.

in The Human Protein Atlas (Expression of VEGF, CXCL8, and IL-6, 2019; https://www.proteinatlas.org/ENSG00000112715-VEGFA/pathology; https://www.proteinatlas.org/ENSG00000169429-CXCL8/pathology; https://www.proteinatlas.org/ENSG00000136244-IL6/pathology). Therefore, a combination of more entries rather than a single biomarker seems to be necessary. Depression of serum levels of IL-2 and G-CSF in the serum of melanoma patients seems to have some therapeutic relevance because their participation in anticancer immunity was established and they were proposed for anticancer therapy (69).

In conclusion, the aforementioned analysis of the serum levels of growth factors VEGF and G-CSF, cytokines IL-6, IL-2, IL-1RA and IFNα, and chemokines IL-8 and RANTES reflect various aspects of tumour biology in malignant melanoma. It is necessary to acknowledge that the currently used markers, such as LDH and S100 proteins, have staging and prognostic significance, but do not reflect the exact immunopathological actions of the organism at the time of melanoma diagnosis or during the disease progression (6,51). Our data also indicated the apparent deregulation of the anti-tumour immune response, which is an essential factor for cancer progression. This sustained proinflammatory environment can significantly contribute to the clinically important phenomenon of long-lasting minimal residual disease. As noted earlier, due to the great inter-individual variability observed by us and by others, strategies based on a combination of several biomarkers or even multiplexing would be beneficial in the future. This approach can contribute to more effective therapy selection, and thus increase the therapeutic outcomes and the patient survival. This pilot study used a limited cohort of patients. Broader studies for validation of our observations are expected in the future. The present study focused on the soluble molecules detectable in human serum, and those that were significantly changed after processing using Dunnett's test. According to the ANOVA, no significant changes were observed between the control and the studied melanoma patients. This testing would require a much larger group of patients, which is planned in a continuation of this experiment. No significant changes were identified in proteins responsible for coping with oxidative stress in this study. However, there is well-established evidence that soluble molecules identified by us (e.g. IL-6) and their signalling pathways have a tight link to oxidative stress in tissues. The role of oxidative stress under pathological conditions, including in cancer biology, has been clearly established (70-72). The search for these proteins will represent the next step of our study.

Acknowledgements

Not applicable.

Funding

The manuscript represents the outcome of the project 'Centre for Tumour Ecology-Research of the Cancer Microenvironment Supporting Cancer Growth and Spread' (reg. no. CZ.02.1.01/0.0/0.0/16_019/0000785) supported by the Research, Development and Education Operational Programme. This publication is also the result of the implementation of the project: 'The equipment for metabolomic and cell analyses' (reg. no. CZ.1.05/2.1.00/19.0400), supported by the Research and Development for Innovations Operational Programme (RDIOP) co-financed by the European Regional Development Fund and the state budget of the Czech Republic. This study was supported by the Grant Agency of the Czech Republic (project no. 16-05534S), Ministry of Health of the Czech Republic (project nos. 16-29032A and 16-30954A), Charles University project PROGRESS Q 28, and by the Ministry of Education, Youth and Sports of CR within the National Sustainability Programme I (no. LO1609) and II (Project BIOCEV-FAR; reg. no. LQ1604), and by project BIOCEV (no. CZ.1.05/1.1.00/02.0109).

Availability of data and materials

The datasets used during the present study are available from the corresponding author upon reasonable request.

Authors' contributions

KSJ, LL and OK wrote the manuscript. KSJ was also head of the conception of the study. JK and PV performed the statistical analysis. JK, OK, IK and JS collected the patient samples, and HK, HKS and JM performed the proteomic analysis. LL, OK and PD conducted the histological and immunohistochemical analysis. KS, BD and LL performed the cell culture and immunocytochemistry analysis. All authors read and approved the final manuscript and agree to be accountable for all aspects of the research, in ensuring that the accuracy or integrity of any part of the work are appropriately investigated and resolved.

Ethics approval and consent to participate

The study was approved by the local ethics committee (Ethics Committee of the General University Hospital, Prague; no. 15/15). All tissue and blood samples were obtained strictly with the explicit informed consent of participants of the study.

Patient consent for publication

Not applicable.

Competing interests

The authors declare that they have no competing interests.

References

1. Global Burden of Disease Cancer Collaboration; Fitzmaurice C, Akinyemiju TF, Al Lami FH, Alam T, Alizadeh-Navaei R, Allen C, Alsharif U, Alvis-Guzman N, Amini E, *et al*: Global, regional, and national cancer incidence, mortality, years of life lost, years lived with disability, and disability-adjusted life-years for 29 cancer groups, 1990 to 2016: A systematic analysis for the global burden of disease study. JAMA Oncol 4: 1553-1568, 2018.
2. Schadendorf D, van Akkooi ACJ, Berking C, Griewank KG, Gutzmer R, Hauschild A, Stang A, Roesch A and Ugurel S: Melanoma. Lancet 392: 971-984, 2018.
3. Verma V, Sprave T, Haque W, Simone CB II, Chang JY, Welsh JW and Thomas CR Jr: A systematic review of the cost and cost-effectiveness studies of immune checkpoint inhibitors. J Immunother Cancer 6: 128, 2018.
4. Zhang M, Yang J, Hua W, Li Z, Xu Z and Qian Q: Monitoring checkpoint inhibitors: Predictive biomarkers in immunotherapy. Front Med 13: 32-44, 2019.
5. Breslow A: Thickness, cross-sectional areas and depth of invasion in the prognosis of cutaneous melanoma. Ann Surg 172: 902-908, 1970.
6. Gershenwald JE, Scolyer RA, Hess KR, Sondak VK, Long GV, Ross MI, Lazar AJ, Faries MB, Kirkwood JM, McArthur GA, *et al*: Melanoma staging: Evidence-based changes in the American Joint Committee on Cancer eighth edition cancer staging manual. CA Cancer J Clin 67: 472-492, 2017.
7. Amann VC, Ramelyte E, Thurneysen S, Pitocco R, Bentele-Jaberg N, Goldinger SM, Dummer R and Mangana J: Developments in targeted therapy in melanoma. Eur J Surg Oncol 43: 581-593, 2017.
8. Karagiannis P, Fittall M and Karagiannis SN: Evaluating biomarkers in melanoma. Front Oncol 4: 383, 2015.
9. Jurisic V, Radenkovic S and Konjevic G: The actual role of LDH as tumor marker, biochemical and clinical aspects. Adv Exp Med Biol 867: 115-124, 2015.
10. Gebhardt C, Lichtenberger R and Utikal J: Biomarker value and pitfalls of serum S100B in the follow-up of high-risk melanoma patients. J Dtsch Dermatol Ges 14: 158-164, 2016.
11. Dummer R, Hauschild A, Lindenblatt N, Pentheroudakis G and Keilholz U; ESMO Guidelines Committee: Cutaneous melanoma: ESMO clinical practice guidelines for diagnosis, treatment and follow-up. Ann Oncol 26 (Suppl 5): v126-v132, 2015.
12. Dummer R, Siano M, Hunger R, Lindenblatt N, Braun R, Michielin O, Mihic-Probst D, von Moos R, Najafi Y, Guckenberger M and Arnold A: The updated Swiss guidelines 2016 for the treatment and follow-up of cutaneous melanoma. Swiss Med Wkly 146: 14279, 2016.
13. Pflugfelder A, Kochs C, Blum A, Capellaro M, Czeschik C, Dettenborn T, Dill D, Dippel E, Eigentler T, Feyer P, *et al*: Malignant melanoma S3-guideline 'diagnosis, therapy and follow-up of melanoma.' J Dtsch Dermatol Ges 11 (Suppl 6): S1-S126, 2013 (In English, German).
14. Paget S: The distribution of secondary growths in cancer of the breast. Lancet 1: 571-573, 1889.
15. Kareva I: What can ecology teach us about cancer? Transl Oncol 4: 266-270, 2011.
16. Lacina L, Plzak J, Kodet O, Szabo P, Chovanec M, Dvorankova B and Smetana K Jr: Cancer microenvironment: What can we learn from the stem cell niche. Int J Mol Sci 16: 24094-24110, 2015.
17. Kodet O, Dvořánková B, Krejčí E, Szabo P, Dvořák P, Štork J, Krajsová I, Dundr P, Smetana K Jr and Lacina L: Cultivation-dependent plasticity of melanoma phenotype. Tumour Biol 34: 3345-3355, 2013.
18. Kodet O, Dvořánková B, Bendlova B, Sýkorová V, Krajsová I, Štork J, Kučera J, Szabo P, Strnad H, Kolář M, *et al*: Microenvironment-driven resistance to B-Raf inhibition in a melanoma patient is accompanied by broad changes of gene methylation and expression in distal fibroblasts. Int J Mol Med 41: 2687-2703, 2018.
19. Manzano JL, Layos L, Bugés C, de Los Llanos Gil M, Vila L, Martínez-Balibrea E and Martínez-Cardús A: Resistant mechanisms to BRAF inhibitors in melanoma. Ann Transl Med 4: 237, 2016.
20. Li YC, Zou JM, Luo C, Shu Y, Luo J, Qin J, Wang Y, Li D, Wang SS, Chi G, *et al*: Circulating tumor cells promote the metastatic colonization of disseminated carcinoma cells by inducing systemic inflammation. Oncotarget 8: 28418-28430, 2017.
21. Brouwer A, De Laere B, Peeters D, Peeters M, Salgado R, Dirix L and Van Laere S: Evaluation and consequences of heterogeneity in the circulating tumor cell compartment. Oncotarget 7: 48625-48643, 2016.
22. Mignogna C, Scali E, Camastra C, Presta I, Zeppa P, Barni T, Donato G, Bottoni U and Di Vito A: Innate immunity in cutaneous melanoma. Clin Exp Dermatol 42: 243-250, 2017.
23. Kodet O, Lacina L, Krejčí E, Dvořánková B, Grim M, Štork J, Kodetová D, Vlček Č, Šáchová J, Kolář M, *et al*: Melanoma cells influence the differentiation pattern of human epidermal keratinocytes. Mol Cancer 14: 1, 2015.
24. Lacina L, Smetana K Jr, Dvoránková B, Pytlík R, Kideryová L, Kucerová L, Plzáková Z, Stork J, Gabius HJ and André S: Stromal fibroblasts from basal cell carcinoma affect phenotype of normal keratinocytes. Br J Dermatol 156: 819-829, 2007.
25. Jobe NP, Živicová V, Mifková A, Rösel D, Dvořánková B, Kodet O, Strnad H, Kolář M, Šedo A, Smetana K Jr, *et al*: Fibroblasts potentiate melanoma cells in vitro invasiveness induced by UV-irradiated keratinocytes. Histochem Cell Biol 149: 503-516, 2018.
26. Dvořánková B, Lacina L and Smetana K Jr: Isolation of normal fibroblasts and their cancer-associated counterparts (CAFs) for biomedical research. Methods Mol Biol 1879: 393-406, 2019.
27. R Core Team R: A Language and Environment for Statistical Computing 2017. https://www.R-project.org/.
28. Sanz H, Aponte JJ, Harezlak J, Dong Y, Ayestaran A, Nhabomba A, Mpina M, Maurin OR, Díez-Padrisa N, Aguilar R, *et al*: drLumi: An open-source package to manage data, calibrate, and conduct quality control of multiplex bead-based immunoassays data analysis. PLoS One 12: e0187901, 2017.
29. Colin B, Clifford S, Wu P, Rathmanner S and Mengersen K: Using boosted regression trees and remotely sensed data to drive decision-making. Open J Statistics 7: 859-875, 2017.
30. Dunnett CW: A multiple comparison procedure for comparing several treatments with a control. J Am Stat Assoc 50: 1096-1121, 1955.
31. Porshneva K, Papiernik D, Psurski M, Łupicka-Słowik A, Matkowski R, Ekiert M, Nowak M, Jarosz J, Banach J, Milczarek M, *et al*: Temporal inhibition of mouse mammary gland cancer metastasis by CORM-A1 and DETA/NO combination therapy. Theranostics 9: 3918-3939, 2019.
32. Schou IM and Marschner IC: Design of clinical trials involving multiple hypothesis tests with a common control. Biom J 59: 636-657, 2017.

33. Rtsne: T-Distributed Stochastic Neighbor Embedding using a Barnes-Hut Implementation, https://cran.r-project.org/web/packages/Rtsne/index.html.
34. Muqaku B, Eisinger M, Meier SM, Tahir A, Pukrop T, Haferkamp S, Slany A, Reichle A and Gerner C: Multi-omics analysis of serum samples demonstrates reprogramming of organ functions via systemic calcium mobilization and platelet activation in metastatic melanoma. Mol Cell Proteomics 16: 86-99, 2017.
35. Weber JS, Sznol M, Sullivan RJ, Blackmon S, Boland G, Kluger HM, Halaban R, Bacchiocchi A, Ascierto PA, Capone M, *et al*: A serum protein signature associated with outcome after anti-PD-1 therapy in metastatic melanoma. Cancer Immunol Res 6: 79-86, 2018.
36. Ortiz A and Fuchs SY: Anti-metastatic functions of type 1 interferons: Foundation for the adjuvant therapy of cancer. Cytokine 89: 4-11, 2017.
37. Mizui M: Natural and modified IL-2 for the treatment of cancer and autoimmune diseases. Clin Immunol: Nov 8, 201. (Epub ahead of print). doi: 10.1016/j.clim.2018.11.002.
38. Arend WP: Interleukin 1 receptor antagonist. A new member of the interleukin 1 family. J Clin Invest 88: 1445-1451, 1991.
39. Ma HL, Whitters MJ, Jacobson BA, Donaldson DD, Collins M and Dunussi-Joannopoulos K: Tumor cells secreting IL-13 but not IL-13Ralpha2 fusion protein have reduced tumorigenicity in vivo. Int Immunol 16: 1009-1017, 2004.
40. Lavi G, Voronov E, Dinarello CA, Apte RN and Cohen S: Sustained delivery of IL-1 Ra from biodegradable microspheres reduces the number of murine B16 melanoma lung metastases. J Control Release 123: 123-130, 2007.
41. Alva A, Daniels GA, Wong MK, Kaufman HL, Morse MA, McDermott DF, Clark JI, Agarwala SS, Miletello G, Logan TF, *et al*: Contemporary experience with high-dose interleukin-2 therapy and impact on survival in patients with metastatic melanoma and metastatic renal cell carcinoma. Cancer Immunol Immunother 65: 1533-1544, 2016.
42. Buchbinder EI, Gunturi A, Perritt J, Dutcher J, Aung S, Kaufman HL, Ernstoff MS, Miletello GP, Curti BD, Daniels GA, *et al*: A retrospective analysis of High-Dose Interleukin-2 (HD IL-2) following Ipilimumab in metastatic melanoma. J Immunother Cancer 4: 52, 2016.
43. Cambien B, Richard-Fiardo P, Karimdjee BF, Martini V, Ferrua B, Pitard B, Schmid-Antomarchi H and Schmid-Alliana A: CCL5 neutralization restricts cancer growth and potentiates the targeting of PDGFRβ in colorectal carcinoma. PLoS One 6: e28842, 2011.
44. Aldinucci D and Colombatti A: The inflammatory chemokine CCL5 and cancer progression. Mediators Inflamm 2014: 292376, 2014.
45. Kolar M, Szabo P, Dvořánková B, Lacina L, Gabius HJ, Strnad H, Sáchová J, Vlček C, Plzák J, Chovanec M, *et al*: Upregulation of IL-6, IL-8 and CXCL-1 production in dermal fibroblasts by normal/malignant epithelial cells in vitro: Immunohistochemical and transcriptomic analyses. Biol Cell 104: 738-751, 2012.
46. Jobe NP, Rosel D, Dvořánková B, Kodet O, Lacina L, Mateu R, Smetana K and Brábek J: Simultaneous blocking of IL-6 and IL-8 is sufficient to fully inhibit CAF-induced human melanoma cell invasiveness. Histochem Cell Biol 146: 205-217, 2016.
47. Moretti S, Chiarugi A, Semplici F, Salvi A, De Giorgi V, Fabbri P and Mazzoli S: Serum imbalance of cytokines in melanoma patients. Melanoma Res 11: 395-399, 2001.
48. Guida M, Riccobon A, Biasco G, Ravaioli A, Casamassima A, Freschi A, Palma MD, Galligioni E, Nortilli R, Chiarion-Sileni V, *et al*: Basal level and behaviour of cytokines in a randomized outpatient trial comparing chemotherapy and biochemotherapy in metastatic melanoma. Melanoma Res 16: 317-323, 2006.
49. Yurkovetsky ZR, Kirkwood JM, Edington HD, Marrangoni AM, Velikokhatnaya L, Winans MT, Gorelik E and Lokshin AE: Multiplex analysis of serum cytokines in melanoma patients treated with interferon-alpha2b. Clin Cancer Res 13: 2422-2428, 2007.
50. Jiang H, Gebhardt C, Umansky L, Beckhove P, Schulze TJ, Utikal J and Umansky V: Elevated chronic inflammatory factors and myeloid-derived suppressor cells indicate poor prognosis in advanced melanoma patients. Int J Cancer 136: 2352-2360, 2015.
51. Mocellin S, Zavagno G and Nitti D: The prognostic value of serum S100B in patients with cutaneous melanoma: A meta-analysis. Int J Cancer 123: 2370-2376, 2008.
52. Jayatilaka H, Tyle P, Chen JJ, Kwak M, Ju J, Kim HJ, Lee JSH, Wu PH, Gilkes DM, Fan R and Wirtz D: Synergistic IL-6 and IL-8 paracrine signalling pathway infers a strategy to inhibit tumour cell migration. Nat Commun 8: 15584, 2017.
53. Lu C and Kerbel RS: Interleukin-6 undergoes transition from paracrine growth inhibitor to autocrine stimulator during human melanoma progression. J Cell Biol 120: 1281-1288, 1993.
54. Armstrong CA, Murray N, Kennedy M, Koppula SV, Tara D and Ansel JC: Melanoma-derived interleukin 6 inhibits in vivo melanoma growth. J Invest Dermatol 102: 278-284, 1994.
55. Uemura M, Trinh VA, Haymaker C, Jackson N, Kim DW, Allison JP, Sharma P, Vence L, Bernatchez C, Hwu P and Diab A: Selective inhibition of autoimmune exacerbation while preserving the anti-tumor clinical benefit using IL-6 blockade in a patient with advanced melanoma and Crohn's disease: A case report. J Hematol Oncol 9: 81, 2016.
56. Narsale AA and Carson JA: Role of interleukin-6 in cachexia: Therapeutic implications. Curr Opin Support Palliat Care 8: 321-327, 2014.
57. Belizario JE, Fontes-Oliveira CC, Borges JP, Kashiabara JA and Vannier E: Skeletal muscle wasting and renewal: A pivotal role of myokine IL-6. Springerplus 5: 619, 2016.
58. Miller A, McLeod L, Alhayyani S, Szczepny A, Watkins DN, Chen W, Enriori P, Ferlin W, Ruwanpura S and Jenkins BJ: Blockade of the IL-6 trans-signalling/STAT3 axis suppresses cachexia in Kras-induced lung adenocarcinoma. Oncogene 36: 3059-3066, 2017.
59. Pettersen K, Andersen S, Degen S, Tadini V, Grosjean J, Hatakeyama S, Tesfahun AN, Moestue S, Kim J, Nonstad U, *et al*: Cancer cachexia associates with a systemic autophagy-inducing activity mimicked by cancer cell-derived IL-6 trans-signaling. Sci Rep 7: 2046, 2017.
60. Singh S, Singh AP, Sharma B, Owen LB and Singh RK: CXCL8 and its cognate receptors in melanoma progression and metastasis. Future Oncol 6: 111-116, 2010.
61. Sanmamed MF, Perez-Gracia JL, Schalper KA, Fusco JP, Gonzalez A, Rodriguez-Ruiz ME, Oñate C, Perez G, Alfaro C, Martín-Algarra S, *et al*: Changes in serum interleukin-8 (IL-8) levels reflect and predict response to anti-PD-1 treatment in melanoma and non-small-cell lung cancer patients. Ann Oncol 28: 1988-1995, 2017.
62. Gabellini C, Gómez-Abenza E, Ibáñez-Molero S, Tupone MG, Pérez-Oliva AB, de Oliveira S, Del Bufalo D and Mulero V: Interleukin 8 mediates bcl-xL-induced enhancement of human melanoma cell dissemination and angiogenesis in a zebrafish xenograft model. Int J Cancer 142: 584-596, 2018.
63. Sanmamed MF, Carranza-Rua O, Alfaro C, Oñate C, Martín-Algarra S, Perez G, Landazuri SF, Gonzalez A, Gross S, Rodriguez I, *et al*: Serum interleukin-8 reflects tumor burden and treatment response across malignancies of multiple tissue origins. Clin Cancer Res 20: 5697-5707, 2014.
64. Jayson GC, Kerbel R, Ellis LM and Harris AL: Antiangiogenic therapy in oncology: Current status and future directions. Lancet 388: 518-529, 2016.
65. Nevala WK, Vachon CM, Leontovich AA, Scott CG, Thompson MA and Markovic SN; Melanoma Study Group of the Mayo Clinic Cancer Center: Evidence of systemic Th2-driven chronic inflammation in patients with metastatic melanoma. Clin Cancer Res 15: 1931-1939, 2009.
66. Ohm JE, Gabrilovich DI, Sempowski GD, Kisseleva E, Parman KS, Nadaf S and Carbone DP: VEGF inhibits T-cell development and may contribute to tumor-induced immune suppression. Blood 101: 4878-4886, 2003.
67. Zhang L, Agarwal S, Shohet JM and Zage PE: CD114 expression mediates melanoma tumor cell growth and treatment resistance. Anticancer Res 35: 3787-3792, 2015.
68. Zage PE, Whittle SB and Shohet JM: CD114: A new member of the neural crest-derived cancer stem cell marker family. J Cell Biochem 118: 221-231, 2017.
69. Waldmann TA: Cytokines in cancer immunotherapy. Cold Spring Harb Perspect Biol 10: pii: a028472, 2018.
70. Kumari N, Dwarakanath BS, Das A and Bhatt AN: Role of interleukin-6 in cancer progression and therapeutic resistance. Tumour Biol 37: 11553-11572, 2016.
71. Elmarakby AA and Sullivan JC: Relationship between oxidative stress and inflammatory cytokines in diabetic nephropathy. Cardiovasc Ther 30: 49-59, 2012.
72. Vallée A and Lecarpentier Y: Crosstalk between peroxisome proliferator-activated receptor gamma and the canonical WNT/β-catenin pathway in chronic inflammation and oxidative stress during carcinogenesis. Front Immunol 9: 745, 2018.

PUBLIKACE IV

Erzina M, Trelin A, Guselnikova O, Dvorankova B, **Strnadova K**, Perminova A, Ulbrich, P, Mares, D, Jerabek, V, Elashnikov, R, Svorcik, V, Lyutakov, O. Precise cancer detection via the combination of functionalized SERS surfaces and convolutional neural network with independent inputs. *Sensors and Actuators, B: Chemical*. 2020 Apr 1;308. 127660. **(IF: 7.335)**

Sensors & Actuators: B. Chemical 308 (2020) 127660

Contents lists available at ScienceDirect

Sensors and Actuators B: Chemical

journal homepage: www.elsevier.com/locate/snb

Precise cancer detection via the combination of functionalized SERS surfaces and convolutional neural network with independent inputs

M. Erzina[a,b], A. Trelin[a], O. Guselnikova[a,b], B. Dvorankova[c,*], K. Strnadova[c], A. Perminova[a], P. Ulbrich[c], D. Mares[d], V. Jerabek[d], R. Elashnikov[a], V. Svorcik[a], O. Lyutakov[a,*]

[a] Department of Solid State Engineering, University of Chemistry and Technology, 16628 Prague, Czech Republic
[b] Research School of Chemistry and Applied Biomedical Sciences, Tomsk Polytechnic University, Russian Federation
[c] Charles University in Prague, 1st Faculty of Medicine, Institute of Anatomy, 12800 Prague, Czech Republic
[d] Department of Microelectronics, Czech Technical University, Prague, Czech Republic

ARTICLE INFO

Keywords:
Cancer detection
SERS
Surface functionalization
Convolutional neural network

ABSTRACT

Combining the advanced approaches of surface functionalization and chemistry, plasmonics, surface enhanced Raman spectroscopy (SERS), and machine learning, we propose the advanced route for express and precise recognition of normal and cancer cells. Our interdisciplinary approach uses plasmonic coupling between the specific nanoparticles and underlying periodical plasmonic surface and achieves high SERS enhancement factor. The surface of gold multibranched nanoparticles (AuMs) was functionalized with different chemical groups to achieve partially selective entrapping of biomolecules from cells cultivation media and generate information-rich inputs for machine learning methods and SERS-based cells recognition. Evaluation of convolutional neural networks (CNN) training results, performed with *ad hoc* feature selection method, suggests that the grafted functional groups provide specificity to proteins, nucleic acids and lipids, responsible for cancer line identification. The dataset of SERS control spectra of normal and cancer cell's metabolites were classified by the trained CNN and perfectly distinguished with 100 % prediction accuracy.

1. Introduction

Tumour is one of the major causes of mortality in the world [1–3] and early, express, and reliable diagnosis of tumour appearance (as well as effective monitoring of potential relapse after treatment) are the indispensable measures to effectively combat tumour mortality [4,5]. It was convincingly demonstrated that there is an association between shorter time of diagnosis and more favorable outcomes [6]. Thus, it is of immense importance to develop reliable express screening and diagnostic techniques associated with biochemical changes to improve existing cancer diagnostic approaches at molecular level.

The common methods used for tumour detection include different tomography approaches, magnetic resonance imaging, ultrasound or endoscopic examination, as well as different biochemical routes in the combination with mass or optical spectroscopies [7–11]. However, their utilization is time and equipment consuming or lack of sufficient sensitivity and specificity to meet the stringent clinical demands of early tumour diagnostic. Alternatively, Raman spectroscopies could be considered as a promising diagnostic technique for tumour detection [12–16]. Raman spectroscopy was applied for diagnostics of cancer-related changes in biofluids on a molecular level as well as for analysis of cells and tissues [17–23]. The major drawback for real clinical utilization of Raman-based diagnostics is the intrinsic weakness of Raman effects. This drawback could be overcome through the utilization of surface enhanced Raman spectroscopy (SERS), which enhances Raman scattering by several orders of magnitude [24].

Usually, the SERS spectra of different (bio)samples contain the fingerprint information about the presented biomolecules (such as proteins, nucleic acids, and lipids) that can predict components changes and assist in the medical diagnosis [25–32]. On the other hand, implementation of SERS, instead of common Raman spectroscopy, significantly enhances both, the characteristic vibration bands and interference background, the latter decreasing the detection reliability. Hopefully application of an advanced algorithm for SERS data evaluation can significantly improve the effectivity of SERS based tumour diagnostics. In particular, implementation of more promising up to date data evaluation with convolutional neural network (CNN) can be considered as a very powerful tool for SERS based cancer diagnostics, according the recent global trends [33–37].

Standard statistical evaluation of SERS data allows achieving the

* Corresponding authors.
E-mail addresses: barbora.dvorankova@lf1.cuni.cz (B. Dvorankova), lyutakoo@vscht.cz (O. Lyutakov).

https://doi.org/10.1016/j.snb.2020.127660
Received 14 August 2019; Received in revised form 5 December 2019; Accepted 2 January 2020
Available online 03 January 2020

reliability of obtained results above 90 % but the application of advanced statistical methods can enhance the reliability above 95 % [34,38]. Nevertheless, an absolute degree of analysis reliability has not been still reached and thus, further advanced research in this field is strongly required. One of the most important and up to now unsolved problems in the utilization of SERS methods for analysis of real (bio) samples is the interference of peaks from a huge amount of presented molecules and related uncertainty in the manual spectra interpretation. Commonly, the surface decoration of SERS active nanostructures with specific molecules, competent to entrap selectively the targeted molecules from solution, is used to solve this task. However, with the development of the advanced design of ANN and related gigantic possibilities in the collection and interpretation of massive spectral data, this problem can be dealt in a simpler way [39]. The attempts to combine the SERS and ANN approaches, which can potentially lead to significant progress in medical diagnostics and safety fields, have started only several years ago. [40,41]. This can be illustrated by several recent works, aimed at the detection of drugs and their metabolites, as well as analysis of complex (bio)samples [42–45]. In particular, the utilization of ANN algorithms for SERS data analysis and their interpretation leads to a significant increase in analysis reliability but also make possible label-free identification of targeted molecules and compounds (for example – disease markers) without previous (bio)sample preparation [39,43–45]. In our current work, we extend SERS/ANN approach using triples of spectra as an input, each of them bringing additional information about the chemical structure of analyte. Moreover, perceptron is replaced with a convolutional network, which is able to extract specific features from the input spectra ignoring background and noise.

2. Experimental

2.1. Materials

Diethyl ether, deionized water, methanol (puriss, p.a., absolute, ≥ 99.8 % (GC)), chloroauric acid tetrahydrate ($HAuCl_4{\cdot}4H_2O$, 99.9 %), silver nitrate ($AgNO_3$,99.0 %), ascorbic acid (AA, 99.0 %), p-toluenesulfonic acid, acetic acid, tert-butyl nitrite, 4-nitroaniline, 4-aminobenzoic acid (+ 99 %), 4-aminophthalic acid (97.0 %) were purchased from Sigma-Aldrich and used without further purification. 4-aminobenzenediazonium tosylate (ADT-NH_2), 4-carboxybenzenediazonium tosylate (ADT-COOH) and 3,4-dicarboxybenzenediazonium tosylate ADT-$(COOH)_2$ were prepared according to the previously published procedure [46].

2.2. Plasmonic substrate preparation

Su-8 films were spin-coated onto freshly cleaned glass substrates and patterned using the linearly polarized excimer laser irradiation [46,47]. Gold thin films were deposited onto the patterned surface by vacuum sputtering. Gold multibranched nanoparticles (AuMs) were synthesized by the seed-mediated growth method with some modifications [32,46], by adding the Au seeds solution to $HAuCl_4$ solution. The surface of AuMs was spontaneously modified with ADT-NH_2, 4-ADT-COOH or ADT-$(COOH)_2$ according [47].

2.3. Plasmonic substrate characterization

For characterization of the SERS substrate surface the peak force AFM technique was used with Icon (Brucker) microscope. TEM images of AuMs were obtained on a JEOL JEM-1010 instrument operated at 80 kV (JEOL Ltd., Japan). The AuMs surface modification was checked using the nanoparticles precipitation on plasma-cleaned silicon substrate, drying and SERS measurements using ProRaman-L spectrometer (785 nm excitation wavelength, laser power 33 mW, 30 times measurements with 3 s accumulation time). The scanning electron microscopy and energy-dispersive X-ray spectroscopy (SEM-EDX) (LYRA3 GMU, Tescan, CR) was used to determine both, the AuMs morphology and distribution of organic elements after the AuMs surface functionalisation.

2.4. SERS EF experimental determination

For the calculation of the SERS enhancement factor (EF), the thin layer of R6G (10^{-6} M, 10^{-4} M, and 1 M solutions in methanol) was drop deposited (drop volume - 3 µl) on the prepared SERS active substrates and appropriated control surface (silicon was used as reference substrate) and measured. Calculation of SERS EF was performed according to the standard relation: $EF = \frac{I_{SERS} / C_{SERS}}{I_{RS} / C_{RS}}$, where the I_{SERS} and I_{RS} represent the Raman scattering intensities on SERS-active and reference silicon surfaces, and C_{SERS} and C_{RS} are the corresponding molar concentration of R6G in drop deposited solutions on the SERS-active and silicon surfaces.

2.5. Numerical simulation

The modelling of SERS excitation and numerical calculation of SERS EF was performed using the RSoft Photonic Component Design Suite software package. The structures were modelled in time in a fully vector spatial domain using the Finite-Difference Time-Domain (FDTD) method. Given the size of the nanoparticles in the nanometres range, the simulations were done with very fine resolution 0.1 nm to obtain precise results. The model was constructed having in mind real parameters of the materials from which the layers and nanoparticles were fabricated. The SERS EF was estimated in assumption of SERS EF ≈ (E/E_0), where E_0 is the intensity of the incident electric field and E is the plasmon enhanced intensity of electric field (estimated from numerical simulation).

2.6. Preparation of biological samples

All cell cultivations and preparations of conditioned media for further SERS analysis were carried out in the Institute of Anatomy, 1st Faculty of Medicine. There were used different types of cells, commercial cell lines and primary isolated cells. To move towards *in vivo* conditions, we isolated primary lines of dermal fibroblasts from healthy skin and cancer-associated fibroblasts from skin metastasis of malignant melanoma.

Healthy residual skin and skin melanoma metastasis were collected under approval of Local Ethics Committee of General University Hospital in Prague in accordance with the ethical standards of the Institutional and National research Committee, and according to the 1964 Helsinki declaration and its later amendments or comparable ethical standards. Single fibroblast lines were isolated from the healthy/cancer tissues [48] and cultured in Dulbecco's modified Eagle's medium (DMEM) supplemented with antibiotics (penicillin 100 U/ml and streptomycin 100 µg/ml) (both Sigma-Aldrich, Prague, Czech republic) and 10 % of fetal bovine serum (FBS) (Biosera, Nuaille, France) at 37 °C and 5 % CO_2 in a humidified incubator. In the case of melanoma cell, two commercial lines A2058 (CRL-11147, American Type Culture Collection, Manassas, USA) and G361 (CRL-1424, American Type Culture Collection, Manassas, USA) were used. As a healthy control normal human neonatal highly pigmented melanocytes (HPM) were obtained from J. Vachtenheim (Institute of Medical Biochemistry and Laboratory Medicine 1 st Faculty of Medicine, Charles University, Prague, Czech Republic) and maintained in serum free medium M254 with HMGS supplement (Gibco, USA). Single cell populations (10 biological replicates) were inoculated into 75 cm^2 culture flasks (Corning BV, Schiphol Rijk, The Netherlands) and cultured in aforementioned media till 70 % confluency. Then, the medium in all flasks was substituted either for 20 ml DMEM with 10 % of FBS or for pure DMEM. The cells were cultured for 48 h, then single culture media were collected and

Table 1
The list of (bio)samples including their characteristic.

Label of the sample	cells	characterization	origin	Serum content	No of samples
A	A2058	melanoma cells	Cell line	10 %	9
A-S	A2058	melanoma cells	Cell line	0 %	9
G	G361	melanoma cells	Cell line	10 %	9
G-S	G361	melanoma cells	Cell line	0 %	8
HPM	HPM	neonatal highly pigmented melanocytes	Cell line	10 %	9
HPM-S	HPM	neonatal highly pigmented melanocytes	Cell line	0 %	9
HF	HF	normal skin fibroblasts	Primary culture	10 %	9
HF-S	HF	normal skin fibroblasts	Primary culture	0 %	9
ZAM	ZAM	tumour associated fibroblasts	Primary culture	10 %	9
ZAM-S	ZAM	tumour associated fibroblasts	Primary culture	0 %	9
DMEM	None	pure medium - control		10 %	8
DMEM-S	None	pure medium - control		0 %	9

20 µm syringe microfilters (Corning BV, Schiphol Rijk, The Netherlands) were used to remove detritus. Single conditioned media were divided into 800 µl aliquots and froze at −80 °C. The list of samples including their characteristic is in the Table 1.

2.7. Entrapping of biomolecules expressed by the normal and tumour-associated cell lines

Before taking Raman measurements, the samples were passively thawed to room temperature (25 °C). Decorated AuMs were placed in the 0.35 µl of analyte and put in a cold, dark place for 3 h. Then the AuMs were isolated from cultivation medium, dispersed in deionized water and drop deposited on gold grating surface. After drops drying the SERS spectra were measured immediately in automatic regime. Generally, a total number of 106 specimens from normal or tumour cells cultured in the serum-free media or those with 10 % of FBS were involved in our study. 19,056 spectra were collected in total, which is shown in details in Table S1.

2.8. SERS measurements and data processing

2.8.1. Spectra measurements

SERS spectra were measured using ProRaman-L spectrometer (laser power 33 mW) with 785 nm excitation wavelength in automatic regime. The operator indicates the boundary of spot from dried drop of AuMs, deposited on Au grating surface and coupled with spectrometer motorized stage performed the subsequent SERS data collection in 10 spots from each SERS substrate. Spectra were measured 30 times, each of them with 3 s accumulation time.

2.8.2. Spectral background removal

Two algorithms were utilized in background removal problem, Asymmetric Least Squares Smoothing (ALSS) [49] and asymmetrically reweighted penalized least square smoothing [50]. After a series of experiments the ALSS algorithm was chosen for further spectra processing due to its better stability and removal quality, inspected both visually and during CNN training. Method relies on two manually tuned parameters, the smoothing penalty coefficient λ and asymmetry parameter *p*. Satisfactory results were obtained with $\lambda = 10^5$ and p = 0.01. Fine tuning of these constant was not performed, since CNN architecture is designed considering presence of background in input data.

2.8.3. Spectra normalization

MinMax normalization, a simple method to fit data into the [0,1] range was applied to each spectrum individually. For a given data vector $\vec{x}$ method defines linear transformation to normalized vector $\vec{x}_n$ as $\vec{x}_n = \frac{\vec{x} - min(\vec{x})}{max(\vec{x}) - min(\vec{x})}$

2.8.4. CNN implementation details

All further described data processing was performed in Python programming language using NumPy [51], SciPy [52] and Pandas [53] libraries. CNN was implemented with Keras framework [54] using TensorFlow backend [55] (more details are given in Results and Discussion section). The CNN model was estimated by the training on 75 % of the data set and the obtained accuracy was determined by predicting labels for the residual 25 % of the data set, which was not seen by CNN during training and comparing these predicted labels to the known ones. Since accuracy analysis was performed on another data subset than the training one, the overfitting was prevented. Classical accuracy was used as the metric, which is defined as the number of correctly classified samples divided by the total number of samples.

3. Results and discussion

3.1. Proposed experimental concept

The main experimental route for realization of our approach for rapid and reliable cancer detection is presented in the Fig. 1. We utilized several advanced concepts from different scientific areas: (i) achievement of very strong SERS enhancement factor through the plasmon coupling between the shaped gold nanoparticles and periodical noble metal surface. (ii) enhancement of selective interaction of plasmonic nanoparticles with (bio)molecules through the functionalization of metal nanoparticles surface [56,57] (nanoparticles surface functionalization modes provide several independent inputs for CNN), and (iii) utilization of advanced CNN design with several inputs.

We started from the preparation of so-called gold multibranched nanoparticles (AuMs), which contain sharp edges, where the strong enhancement of electric field intensity is realized. The surface of AuMs was further functionalized with different chemical groups and exposed to (bio)molecules from the cultivation media of normal and cancer cells (Table 1 shows a summary of used (bio)samples). Simultaneously the periodical gold grating surface was created, and the functionalized AuMs (after their interaction with (bio)sample) were deposited on the surface of gold grating with the aim to initiate plasmonic coupling between the AuMs and gold grating, which was supposed to result in huge SERS enhancement. Then the samples were subjected to SERS analysis (Table S1 provides a number of spectra taken from each pathological group) and large set of collected SERS spectra were used for CNN training and validation, with several inputs, including the mode of previous AuMs surface functionalization.

3.2. Samples characterization

The structure and properties of the pristine AuMs are presented in the Fig. 2A. As is evident from the TEM images, uniform AuMs were prepared with the 50 nm average diameter. TEM images also reveal the presence of sharp edges, which were important for significant SERS intensification. In turn, successful creation of gold grating surface was proved by AFM spectroscopy (Fig. 2B), which confirms the periodical

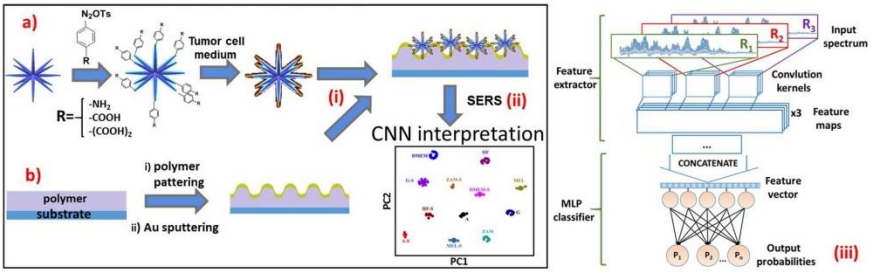

Fig. 1. Schematic representation of proposed experimental concept: a) – preparation of functional AuMs and their interaction with culture medium sample, b) – simultaneous preparation of gold grating, (i) – deposition of AuMs on the surface of gold grating, (ii) – SERS measurements, (iii) – implementation of CNN for SERS results interpretation.

grating surface, able to efficiently support the propagation of surface plasmon-polariton wave (according our previous works [24,26,46]). The AFM measurement of gold grating surface after the deposition of AuMs, presented in the Fig. 2C, indicates the apparent roughening of surface morphology with simultaneous increasing of scan amplitude. On the other hand, the surface periodicity is partially conserved, which observation suggests the relatively homogeneous coating of grating surface by the deposited AuMs.

The surface functionalization of AuMs was checked using the SEM-EDX (Fig. 3A) and Raman spectroscopy (Fig. 3B). The SEM-EDX mapping reveals apparent increase of organic elements (oxygen, carbon, nitrogen) on the surface of AuMs. Moreover, from the SEM measurements, the conservation of AuMs shape after the modification procedure is evident. The control experiments, performed using the TEM technique (Fig. S1), also confirme the conservation of AuMs shape after their grafting with organic functional groups. Raman spectroscopy, performed on the AuMs deposited on silicon substrate, indicated the main characteristic bands, corresponding to the structure of grafted organic moieties (Ar-NH_2, Ar-COOH, Ar-$(COOH)_2$). The detailed peak affiliation is given in the Table S2. In particular after the substrate correction (to remove pronounced silicon band), the pristine AuMs SERS spectrum did not show any features, SERS spectrum of AuMs-NH2 samples indicated the presence of benzene and amino characteristic vibration bands, and SERS spectra of AuMs-COOH and AuMs-$(COOH)_2$ samples showed the presence of benzene ring and carboxylic groups. Both structures, gold grating and AuMs, can provide the significant enhancement of Raman response of attached molecules in the case of coincidence of Raman excitation wavelength and plasmon absorption band.

The optical response of gold grating was characterized using the two linear polarization of transmitted light (perpendicular and parallel to grating orientation). Obtained spectra, presented in the Fig. 4A, show that absorption band is located near 780 nm. In turn, apparent polarization dependence of light absorption confirms the SPP nature of absorption band. The UV–vis spectra of pristine AuMs (Fig. 4B) indicate that the position of plasmon absorption band is also perfectly suitable for SERS excitation with 780 nm wavelength. Surface functionalization of AuMs slightly shifts the position of plasmon absorption band, but it still remains "compatible" with 780 nm SERS excitation. The impact of the deposition of AuMs, analyzed by numerical simulation is presented in Fig. 4C. As it is evident, the intensification of electric field occur even in the case of single AuMs (see Fig. 4C(I)). In turn AuMs coupling results in significant increase of the local electric field (Fig. 4C (II)). Furthermore deposition of AuMs on SPP supported gold grating surface results

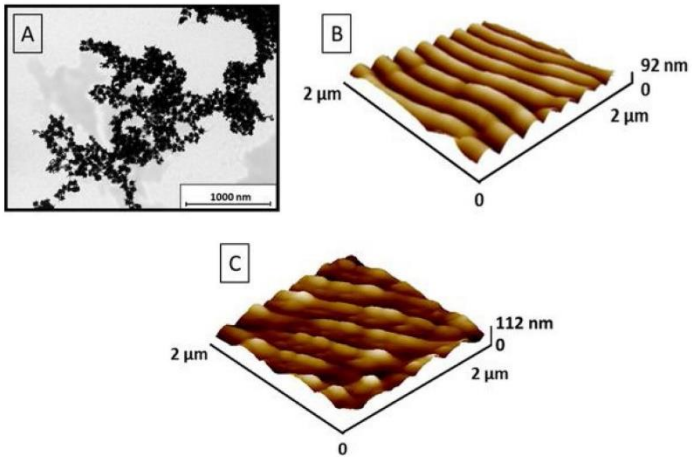

Fig. 2. (A) - TEM images of AuMs, (B) - AFM of pristine gold grating surface and (C) - AFM of gold grating surface after the deposition of AuMs.

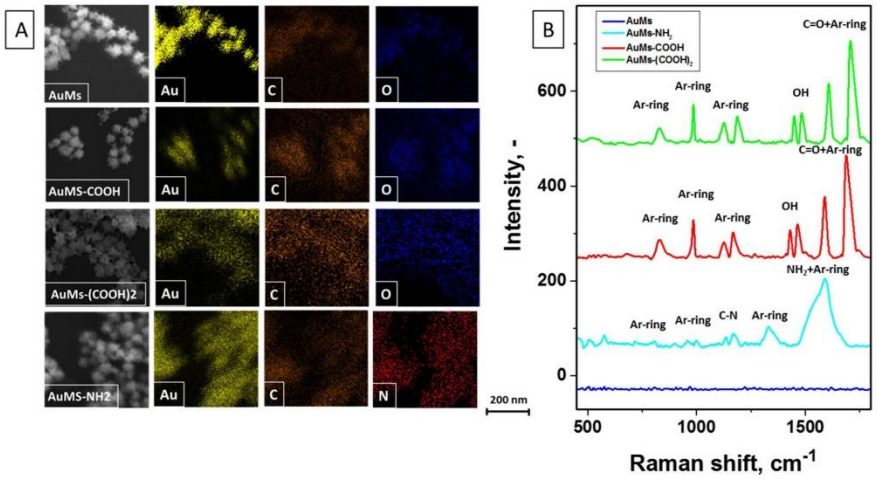

Fig. 3. Verification of AuMs surface modification procedure: (A) – results of SEM measurements with corresponding EDX mapping of elements spatial distribution, (B) – results of SERs measurements of pristine and grafted AuMs (substrate-corrected spectra).

in even higher enhancement of electric field (Fig. 4C(III)). Observed values of electric field intensity allow us to approximately estimate the SERS EF (with one order of magnitude accuracy) under assumption of its proportionality to $(E/E_0)^4$, where the E_0 is the electric field intensity of incident light (in our case equal to one), and E is the plasmon enhanced electric field intensity (see Fig. 4C). In the case of coupled gold grating and AuMs, the estimated EF is about 10^{11} (Table S3), which is sufficient for perfect enhancement of SERS signal from (bio)molecules entrapped by AuMs. Experimental verification of these results, obtained using the deposition and measurements of R6G as the model SERS analyte, is demonstrated in the Fig. S2 and corresponding Table S3. The experimental results coincide well with those of numerical simulation.

Control measurements of SERS signal from chemisorbed biphenyl-4,4′-dithiol (BPDT) molecules on non-patterned gold surface, randomly deposited AuMs array, gold grating and gold grating with drop deposited AuMs (see Fig. S3) were performed with the aim to demonstrate the impact of interactions of plasmonic coupling in the combination with periodical SPP supported surface and also the significant SERS enhancement obtained after the deposition of AuMs on the gold periodical grating. So that, proposed approach produces a superior SERS effect resulting from the plasmonic coupling between surface plasmon-polariton supported gold grating and specific metal nanoparticles with sharp edges.

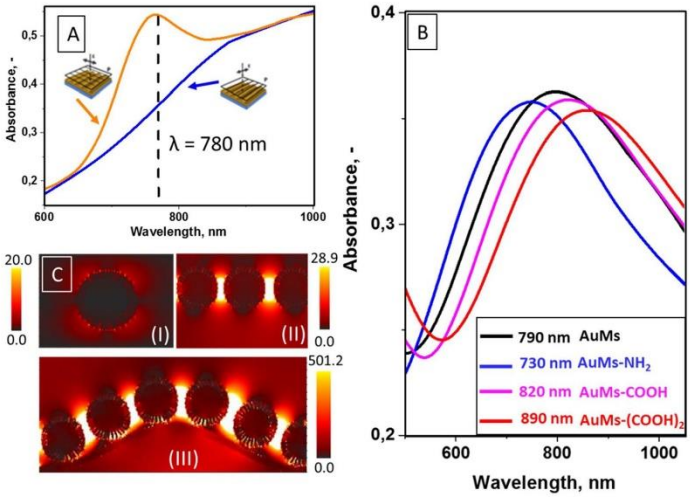

Fig. 4. (A) - UV–vis absorption spectra of the gold grating, measured in two polarization modes - perpendicular and parallel to grating orientation, (B) - UV/Vis spectra of multibranched nanoparticles and surface modified gold multibranched nanoparticles and (C) – results of numerical simulation of single AuMs (I) (AuMs arry in dielectric environment (II) and AuMs array on gold grating surface(III)).

3.3. Interaction of AuMs with (bio)samples and SERS spectra collection

The main purpose of our work was to simulate the clinical scenario where a blind patient sample will be analysed (and classified) using SERS measurements and CNN-based spectra interpretation. For this purpose, different (bio)samples were used – conditioned culture media from melanoma cell lines, melanoma associated fibroblast and normal counterparts. There were used two variants of these samples, containing the standard – 10 % or low – 0 % amounts of the fetal bovine serum (FBS), with the aim to estimate the impact of high concentration of biomolecules, uninformative about the vital activity of normal and cancer cells. The AuMs with different surface functionalization were mixed with the (bio)samples, according to the procedure described in Experimental section, gently centrifuged, dispersed in the deionized water and drop deposited on the gold grating surface. The present experimental procedure makes possible to partially selective entrap biomolecules from the normal or tumour cells cultivation media on the AuMs surface and create by subsequent SERS measurements several inputs for CNN as a function of AuMs surface functionalization. After deposition on gold grating surface, the samples were subjected to SERS measurements and the typical sets of measured Raman spectra are shown in SI (Figs. S4 – S15, the left columns). Generally, the measured SERS spectra were categorized into 13 groups, each of which corresponds to the type of (bio)sample used for the analysis (see Table S1). Each group contains three subgroups, corresponding to SERS spectra measured with AuMs functionalized by ADT-NH_2, ADT-COOH or ADT-$(COOH)_2$. Since the spectra were collected in automotive regime from randomly chosen input points, the great variation in the overall intensity as well as spectral background is evident (Figs S4 – S15 and uploaded spectra database). The overall shape of these spectra cannot be considered as informative, due to complex and interfering nature of SERS signal from immobilized (bio)molecules and uncertainty related to automatic measurement procedure.

3.4. SERS data preprocessing

In the next step, all measured spectra were subjected to preprocessing procedure, which include background removal and normalization. It should be also noted that the fine tuning of preprocessing procedure was not performed, since the proposed CNN architecture was designed to consider presence of background in input data. Results of spectral preprocessing are presented in the right columns in the Figs. S4 - S15. It could be expected, that the presented SERS spectra contain the valuable information about adsorbed biomolecules (such as proteins, nucleic acids and lipids), and predicted component changes may assist in the diagnosis of cancer. However, in all cases the biomolecules related peaks overlap and their direct identification/estimation is impossible. Thus overall and relative compositions of entrapped (bio)molecules can not be determined without further analysis, which in this case was performed using a CNN technique.

3.5. CNN structure and training

A plenty of different CNN architectures have been proposed in the last few decades and it is important to choose network architecture that optimally correspond to the structure of input data. Thus, we utilized a special kind of network – so-called convolutional neural network that was developed to process similar kind of data and previously utilized with great success in image recognition [58]. Proposed CNN perform convolution of input data with a kernel (which is tuned during CNN training), producing feature maps and describing distribution of specific features. Different kernels will correspond to different peak shapes, and the result of convolution relates to the position of this peaks. In addition, utilization of proposed CNN design allows additional background removal in analogy with well-known Sobel operator [59,60]. Precise structure of designed CNN architecture is illustrated in the Fig. S16 and Table S4. Generally, the CNN was designed to have three independent inputs, corresponding to the AuMs surface functionalization (i.e. different entrapping selectivity towards the (bio)molecules in cultivation media). Each input was processed with convolutional feature extractor, structure of which is tabulated in Table S5. The outputs of the feature extractors are concatenated to form single feature vector, which is passed to the fully-connected classifier with SoftMax activation function, giving the probability of input to belong to specific class of (bio)samples [61]. General SERS datasets were divided into training and validation in the 0.75:0.25 ratio. During the CNN training, initial convergence, determined by 1.0 validation accuracy was achieved after only 10 epochs (32 batches in epoch, batch size of 16). Due to stochastic nature of training algorithm, the process was continued until 400 epochs, which was necessary for complete convergence, as it could be seen in Fig. S17. Overall, in the end of the training process mean validation loss and validation accuracy between 10 last epochs were equal to $7.56*10^{-5}$ and 1.0 respectively, which could be considered as perfect convergence.

3.6. CNN-determined regions of interest on SERS spectra

In the next step the novel feature selection method, which has been developed specially for purposes of spectra processing and able of identification of more informative SERS spectral regions was applied to data. In particular, binary stochastic filtering [62] layers were added to the classifier after each of the CNN inputs and network was re-trained. By further analysis of filtering layer weights, the specific feature importancies were extracted, which are associated with spectral regions of interest (ROI), i.e. specific Raman shifts, corresponding to meaningful spectral changes responsible for classification of used (bio)samples and identification of the fingerprints of entrapped (bio)molecules. The obtained results are presented in the Fig. 5, where the filtering layer weights are plotted against the wavenumbers for different AuMs surface functionality. Based on the obtained images and literature data of typical (bio)molecules characteristic Raman bands position [63] we performed subsequent analysis of spectral positions of regions of interest (ROI) and attribute them to various (bio)molecules, as is also illustrated in the Fig. 5. We found that majority of ROI, involved in the spectral recognition process, could be associated with proteins, lipids, RNA, and amino-acids. Indeed, the absolute as well as relative variation of this molecules concentration in the serum was previously reported as cancer markers [64]. The variation of the ROI for each kind of surface bound moieties shows that the different functionalization is responsible for partially specific entrapping and identification of (bio)molecules. For example, the Ar-COOH functionalized surface was found to be more sensitive to RNA and proteins biomolecules in comparison with nanoparticles bearing other moieties. Ar-NH_2 and Ar-$(COOH)_2$ were found to be less specific, thus providing information about changes of lipids and amino acid as well. Summing the obtained results, presented in the Fig. 5, we can state that CNN in combination with variously functionalized AuMs was able to highlight the spectral changes related to biochemical composition in culture medium due to vital activity of normal or cancer cells.

3.7. Utilization of proposed approach for tumour detection

After the training, the performance of proposed approach was verified by validation data, which were composed of SERS spectra that have never been used for training. In this case, for better visualization, the general network output is presented in the Fig. 6 in 2-dimensional abstract space [65]. The circles defined areas of 2D space (Fig. 6) represent the characteristic for each kind of (bio)samples CNN-processed spectral features distribution. First of all, it should be noted that the characteristic areas are perfectly separated, emphasizing the fact that CNN was successfully learned to distinguish the spectral difference between the different kind of culture media. Since we utilize several

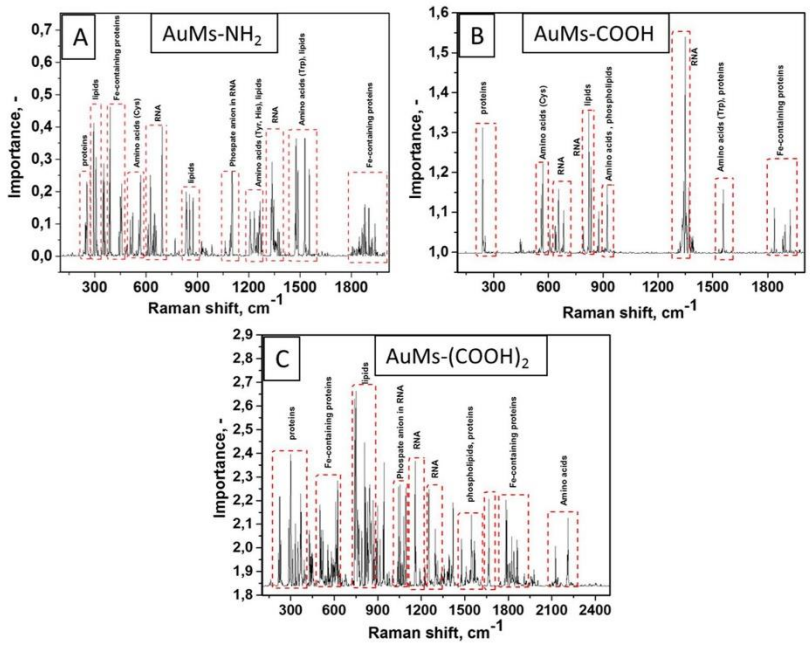

Fig. 5. CNN determined spectral regions of interest, responsible for determination of metabolic activity of tumour or normal cells, for each of three AuMs functionalization (with $-NH_2$ (A), -COOH (B) and $-(COOH)_2$ (C)). Image also provides the typical Raman response of biomolecules, which concentrations can be changed due to enormous activity of tumour cells.

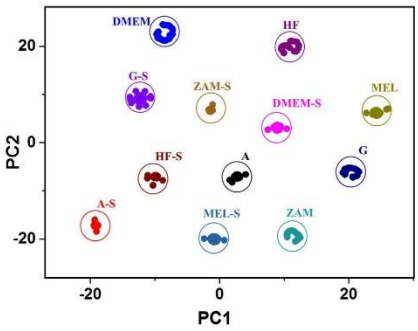

Fig. 6. The visualization of predictive ability of the proposed SERS/CNN approach: projection of the output vectors of probability (for validation dataset, consisting of SERS spectra from normal and tumours cultivation media) to the 2D space, coloured by the real class labels determined from training SERS spectra.

kinds of media, which are associated with cancer disease, applied procedure allows us to introduce the terms specificity (exact determination of which cancer cells type) and sensitivity (i.e. detection of cancer-related changes in very accurate manner). In the next step, the spectra from unknown samples were classified using the CNN and attributed to previously developed groups, depicted in the Fig. 6 by dots.

Results of CNN validation procedure indicate that all spectra, after compression to 2D space, fall exactly to "their area". So, in all cases the precise determination of melanoma-cell related spectra as well as exact determination of melanoma type was achieved within the testing set of unknown sample. Thus, we can state that in both terms, sensitivity and specificity, the 100 % accuracy was reached.

Our study demonstrates the potential of SERS and CNN with chemically provided inputs for the clinical usage, for example in rapid determination of anomalous cell activity related to tumour development. Further research will be focused on the increasing number of (bio)samples involved for the CNN training as well as introduction of additional surface functionality for enhancing of input information diversity. Indeed, taking into account that tumour is rather individual disease with a tendency to mutate over the time, obtained results cannot guarantee the absolute detection reliability in each particular case. However, the increase of (bio)sample numbers and surface functionalization specificity will lead to more effective training of CNN and compensation of the uncertain nature of diagnosis. Thus our approach could probably offer the key for truly universal tumour detection. Nevertheless, it is impossible to gather enough information for "absolute" CNN training by a single laboratory and thus large-scale collaboration would be necessary to collect sufficiently large dataset, which should be fruitful for the future interdisciplinary research between medicine, biology, chemistry and data science.

4. Conclusion

In this work, we present the advanced approach for detection of compositional changes in culture medium arising from metabolic

activity of tumour or normal cells. The approach combines several innovative techniques from the field of nanotechnology and surface chemistry, plasmonics, SERS, and machine learning. First, the specific gold nanoparticles with sharp edges were prepared and grafted with various chemical moieties to achieve partial selectivity in the biomolecules entrapping and the high plasmonic enhancement. The functionalized nanoparticles, after the interaction with (bio)samples, were deposited on the gold grating surface to achieve the plasmonic coupling and high SERS enhancement. Subsequently measured SERS spectra were used as the input for advanced CNN training and validation, while the kind of nanoparticles surface functionalization serves as additional parameters, increasing the flexibility and reliability of the method. The SERS experiments were conducted as an attempt to characterize the molecular components of medium after their interaction with normal or melanoma cells. The CNN classification results were then translated into sensitivity and specificity for each cell kind and 100 % accuracy in the discrimination of tumour and normal cell's cultivation media was achieved. We envision such approach to be useful for the preparation of a massive and reliable database that could help to make clinical decisions in a rapid and accurate manner possible.

Declaration of Competing Interest

The authors declare that they have no known competing financial interests or personal relationships that could have appeared to influence the work reported in this paper.

Acknowledgements

This work was supported by the GACR under the project 18-26170S and the project "Center for Tumor Ecology – Research of the Cancer Microenvironment Supporting Cancer Growth and Spread" (reg.n. CZ.02.1.01/0.0/0.0/16_019/0000785) supported by the Operational Programme Research, Development and Education). The research was also partly supported by CTU grant agency under the project SGS18/139/OHK3/2 T/13.

Appendix A. Supplementary data

Supplementary material related to this article can be found, in the online version, at doi:https://doi.org/10.1016/j.snb.2020.127660.

References

[1] L.A. Torre, R.L. Siegel, A. Jemal, Lung cancer statistics, in: A. Ahmad, S. Gadgeel (Eds.), Lung Cancer and Personalized Medicine: Current Knowledge and Therapies, Springer International Publishing, Cham, 2016, pp. 1–19, , https://doi.org/10.1007/978-3-319-24223-1_1.

[2] K.D. Miller, R.L. Siegel, C.C. Lin, A.B. Mariotto, J.L. Kramer, J.H. Rowland, K.D. Stein, R. Alteri, A. Jemal, Cancer treatment and survivorship statistics, 2016, CA Cancer J. Clin. 66 (2016) 271–289, https://doi.org/10.3322/caac.21349.

[3] C.A. Lieber, S.K. Majumder, D.L. Ellis, D.D. Billheimer, A. Mahadevan-Jansen, In vivo nonmelanoma skin cancer diagnosis using Raman microspectroscopy, Lasers Surg. Med. 40 (2008) 461–467, https://doi.org/10.1002/lsm.20653.

[4] Cervical Cancer, (n.d.). https://www.cancer.org/cancer/cervical-cancer.html. (Accessed 9 August 2019).

[5] R. de Bree, L. van der Putten, H. van Tinteren, J. Wedman, W.J.G. Oyen, L.M. Janssen, M.W.M. van den Brekel, E.F.I. Comans, J. Pruim, R.P. Takes, M.G.G. Hobbelink, R. Valdés Olmos, B.F.A.M. van der Laan, M. Boers, O.S. Hoekstra, C.R. Leemans, Effectiveness of an 18F-FDG-PET based strategy to optimize the diagnostic trajectory of suspected recurrent laryngeal carcinoma after radiotherapy: the RELAPS multicenter randomized trial, Radiother. Oncol. 118 (2016) 251–256, https://doi.org/10.1016/j.radonc.2015.10.010.

[6] R.D. Neal, P. Tharmanathan, B. France, N.U. Din, S. Cotton, J. Fallon-Ferguson, W. Hamilton, A. Hendry, M. Hendry, R. Lewis, U. Macleod, E.D. Mitchell, M. Pickett, T. Rai, K. Shaw, N. Stuart, M.L. Tørring, C. Wilkinson, B. Williams, N. Williams, J. Emery, Is increased time to diagnosis and treatment in symptomatic cancer associated with poorer outcomes? Systematic review, Br. J. Cancer 112 (2015) S92–S107, https://doi.org/10.1038/bjc.2015.48.

[7] C.I. Henschke, D.I. McCauley, D.F. Yankelevitz, D.P. Naidich, G. McGuinness, O.S. Miettinen, D.M. Libby, M.W. Pasmantier, J. Koizumi, N.K. Altorki, J.P. Smith, Early Lung Cancer Action Project: overall design and findings from baseline screening, Lancet 354 (1999) 99–105, https://doi.org/10.1016/S0140-6736(99)06093-6.

[8] C. Sun, J.S.H. Lee, M. Zhang, Magnetic nanoparticles in MR imaging and drug delivery, Adv. Drug Delivery Rev. 60 (2008) 1252–1265, https://doi.org/10.1016/j.addr.2008.03.018.

[9] Q.-L. Zhu, Y.-X. Jiang, J.-B. Liu, H. Liu, Q. Sun, Q. Dai, X. Chen, Real-time ultrasound elastography: its potential role in assessment of breast lesions, Ultrasound Med. Biol. 34 (2008) 1232–1238, https://doi.org/10.1016/j.ultrasmedbio.2008.01.004.

[10] J.C. Weinreb, J.O. Barentsz, P.L. Choyke, F. Cornud, M.A. Haider, K.J. Macura, D. Margolis, M.D. Schnall, F. Shtern, C.M. Tempany, H.C. Thoeny, S. Verma, PI-RADS prostate imaging – reporting and data system: 2015, version 2, Eur. Urol. 69 (2016) 16–40, https://doi.org/10.1016/j.eururo.2015.08.052.

[11] S. Maheswaran, L.V. Sequist, S. Nagrath, L. Ulkus, B. Brannigan, C.V. Collura, E. Inserra, S. Diederichs, A.J. Iafrate, D.W. Bell, S. Digumarthy, A. Muzikansky, D. Irimia, J. Settleman, R.G. Tompkins, T.J. Lynch, M. Toner, D.A. Haber, Detection of mutations in EGFR in circulating lung-cancer cells, N. Engl. J. Med. 359 (2008) 366–377, https://doi.org/10.1056/NEJMoa0800668.

[12] K. Kneipp, A.S. Haka, H. Kneipp, K. Badizadegan, N. Yoshizawa, C. Boone, K.E. Shafer-Peltier, J.T. Motz, R.R. Dasari, M.S. Feld, Surface-enhanced Raman spectroscopy in single living cells using gold nanoparticles, Appl. Spectrosc. 56 (2002) 150–154, https://doi.org/10.1366/0003702021954557.

[13] Z. Huang, A. McWilliams, H. Lui, D.I. McLean, S. Lam, H. Zeng, Near-infrared Raman spectroscopy for optical diagnosis of lung cancer, Int. J. Cancer 107 (2003) 1047–1052, https://doi.org/10.1002/ijc.11500.

[14] C.L. Zavaleta, B.R. Smith, I. Walton, W. Doering, G. Davis, B. Shojaei, M.J. Natan, S.S. Gambhir, Multiplexed imaging of surface enhanced Raman scattering nanotags in living mice using noninvasive Raman spectroscopy, PNAS 106 (2009) 13511–13516, https://doi.org/10.1073/pnas.0813327106.

[15] N. Stone, C. Kendall, J. Smith, P. Crow, H. Barr, Raman spectroscopy for identification of epithelial cancers, Faraday Discuss. 126 (2004) 141–157, https://doi.org/10.1039/B304992B.

[16] J.W. Chan, D.S. Taylor, T. Zwerdling, S.M. Lane, K. Ihara, T. Huser, Micro-Raman spectroscopy detects individual neoplastic and normal hematopoietic cells, Biophys. J. 90 (2006) 648–656, https://doi.org/10.1529/biophysj.105.066761.

[17] S.P. Singh, C. Murali Krishna, Raman spectroscopic studies of oral cancers: correlation of spectral and biochemical markers, Anal. Methods 6 (2014) 8613–8620, https://doi.org/10.1039/C4AY01615G.

[18] A. Synytsya, M. Judexova, D. Hoskovec, M. Miskovicova, L. Petruzelka, Raman spectroscopy at different excitation wavelengths (1064, 785 and 532 nm) as a tool for diagnosis of colon cancer, J. Raman Spectrosc. 45 (2014) 903–911, https://doi.org/10.1002/jrs.4581.

[19] R.E. Kast, S.C. Tucker, K. Killian, M. Trexler, K.V. Honn, G.W. Auner, Emerging technology: applications of Raman spectroscopy for prostate cancer, Cancer Metastasis Rev. 33 (2014) 673–693, https://doi.org/10.1007/s10555-013-9489-6.

[20] S. Duraipandian, W. Zheng, J. Ng, J.J.H. Low, A. Ilancheran, Z. Huang, Simultaneous fingerprint and high-wavenumber confocal Raman spectroscopy enhances early detection of cervical precancer in vivo, Anal. Chem. 84 (2012) 5913–5919, https://doi.org/10.1021/ac300394f.

[21] M. Jermyn, K. Mok, J. Mercier, J. Desroches, J. Pichette, K. Saint-Arnaud, L. Bernstein, M.-C. Guiot, K. Petrecca, F. Leblond, Intraoperative brain cancer detection with Raman spectroscopy in humans, Sci. Transl. Med. 7 (2015) 274ra19, https://doi.org/10.1126/scitranslmed.aaa2384.

[22] A. Mahadevan-Jansen, M.F. Mitchell, N. Ramanujamf, A. Malpica, S. Thomsen, U. Utzinger, R. Richards-Kortumt, Near-infrared Raman spectroscopy for in vitro detection of cervical precancers, Photochem. Photobiol. 68 (1998) 123–132, https://doi.org/10.1111/j.1751-1097.1998.tb03262.x.

[23] F.M. Lyng, E.O. Faoláin, J. Conroy, A.D. Meade, P. Knief, B. Duffy, M.B. Hunter, J.M. Byrne, P. Kelehan, H.J. Byrne, Vibrational spectroscopy for cervical cancer pathology, from biochemical analysis to diagnostic tool, Exp. Mol. Pathol. 82 (2007) 121–129, https://doi.org/10.1016/j.yexmp.2007.01.001.

[24] O. Guselnikova, P. Postnikov, M. Erzina, Y. Kalachyova, V. Švorčík, O. Lyutakov, Pretreatment-free selective and reproducible SERS-based detection of heavy metal ions on DTPA functionalized plasmonic platform, Sens. Actuators, B 253 (2017) 830–838, https://doi.org/10.1016/j.snb.2017.07.018.

[25] E.J.H. Wee, Y. Wang, S.C.-H. Tsao, M. Trau, Simple, sensitive and accurate multiplex detection of clinically important melanoma DNA mutations in circulating tumour DNA with SERS nanotags, Theranostics 6 (2016) 1506–1513, https://doi.org/10.7150/thno.15871.

[26] Y. Kalachyova, O. Guselnikova, R. Elashnikov, I. Panov, J. Žádný, V. Cirkva, J. Storch, J. Sykora, K. Zaruba, V. Švorčík, O. Lyutakov, Helicene-SPP-based chiral plasmonic hybrid structure: toward direct enantiomers SERS discrimination, ACS Appl. Mater. Interfaces 11 (2019) 1555–1562, https://doi.org/10.1021/acsami.8b15520.

[27] H. Shi, H. Wang, X. Meng, R. Chen, Y. Zhang, Y. Su, Y. He, Setting up a surface-enhanced Raman scattering database for artificial-intelligence-based label-free discrimination of tumor suppressor genes, Anal. Chem. 90 (2018) 14216–14221, https://doi.org/10.1021/acs.analchem.8b03080.

[28] C. Danciu, A. Falamas, C. Dehelean, C. Soica, H. Radeke, L. Barbu-Tudoran, F. Bojin, S.C. Pînzaru, M.F. Munteanu, A characterization of four B16 murine melanoma cell sublines molecular fingerprint and proliferation behavior, Cancer Cell Int. 13 (2013) 75, https://doi.org/10.1186/1475-2867-13-75.

[29] S.C. Pinzaru, A. Falamas, C.A. Dehelean, Molecular conformation changes along the malignancy revealed by optical nanosensors, J. Cell. Mol. Med. 17 (2013) 277–286, https://doi.org/10.1111/jcmm.12006.

[30] S.R. Hawi, W.B. Campbell, A. Kajdacsy-Balla, R. Murphy, F. Adar, K. Nithipatikom, Characterization of normal and malignant human hepatocytes by Raman microspectroscopy, Cancer Lett. 110 (1996) 35–40, https://doi.org/10.1016/S0304-3835(96)04455-2.

[31] S. Luo, C. Chen, H. Mao, S. Jin, Discrimination of premalignant lesions and cancer tissues from normal gastric tissues using Raman spectroscopy, JBO 18 (2013) 067004, , https://doi.org/10.1117/1.JBO.18.6.067004.

[32] Y. Kalachyova, A. Olshtrem, O.A. Guselnikova, P.S. Postnikov, R. Elashnikov, P. Ulbrich, S. Rimpelova, V. Švorčík, O. Lyutakov, Synthesis, characterization, and antimicrobial activity of near-IR photoactive functionalized gold multibranched nanoparticles, ChemistryOpen 6 (2017) 254–260, https://doi.org/10.1002/open.201600159.
[33] X. Li, T. Yang, S. Li, L. Jin, D. Wang, D. Guan, J. Ding, Noninvasive liver diseases detection based on serum surface enhanced Raman spectroscopy and statistical analysis, Opt. Express 23 (2015) 18361–18372, https://doi.org/10.1364/OE.23.018361.
[34] H. Chen, X. Li, N. Broderick, Y. Liu, Y. Zhou, J. Han, W. Xu, Identification and characterization of bladder cancer by low-resolution fiber-optic Raman spectroscopy, J. Biophoton. 11 (2018) e201800016, , https://doi.org/10.1002/jbio.201800016.
[35] M. Khanmohammadi, A.B. Garmarudi, K. Ghasemi, Back-propagation artificial neural network and attenuated total reflectance-fourier transform infrared spectroscopy for diagnosis of basal cell carcinoma by blood sample analysis, J. Chemometr. 23 (2009) 538–544, https://doi.org/10.1002/cem.1250.
[36] M. Jermyn, J. Desroches, J. Mercier, M.-A. Tremblay, K. St-Arnaud, M.-C. Guiot, K. Petrecca, F. Leblond, Neural networks improve brain cancer detection with Raman spectroscopy in the presence of operating room light artifacts, JBO 21 (2016) 094002, , https://doi.org/10.1117/1.JBO.21.9.094002.
[37] J. Yue, L. Liang, Y. Shen, X. Guan, J. Zhang, Z. Li, R. Deng, S. Xu, C. Liang, W. Shi, W. Xu, Investigating dynamic molecular events in melanoma cell nucleus during photodynamic therapy by SERS, Front Chem. 6 (2019), https://doi.org/10.3389/fchem.2018.00665.
[38] A. Daniel, A. Prakasarao, S. Ganesan, Near-infrared Raman spectroscopy for estimating biochemical changes associated with different pathological conditions of cervix, Spectrochim. Acta Part A: Mol. Biomol. Spectrosc. 190 (2018) 409–416, https://doi.org/10.1016/j.saa.2017.09.014.
[39] W.J. Thrift, A. Cabuslay, A.B. Laird, S. Ranjbar, A.I. Hochbaum, R. Ragan, Surface-enhanced Raman scattering-based odor compass: locating multiple chemical sources and pathogens, ACS Sens. 4 (2019) 2311–2319, https://doi.org/10.1021/acssensors.9b00809.
[40] O. Alharbi, Y. Xu, R. Goodacre, Simultaneous multiplexed quantification of nicotine and its metabolites using surface enhanced Raman scattering, Analyst 139 (2014) 4820–4827, https://doi.org/10.1039/C4AN00879K.
[41] F. Lussier, D. Missirlis, J.P. Spatz, J.-F. Masson, Machine-learning-driven surface-enhanced Raman scattering optophysiology reveals multiplexed metabolite gradients near cells, ACS Nano 13 (2019) 1403–1411, https://doi.org/10.1021/acsnano.8b07024.
[42] S. Seifert, V. Merk, J. Kneipp, Identification of aqueous pollen extracts using surface enhanced Raman scattering (SERS) and pattern recognition methods, J. Biophoton. 9 (2016) 181–189, https://doi.org/10.1002/jbio.201500176.
[43] B. Deng, X. Luo, M. Zhang, L. Ye, Y. Chen, Quantitative detection of acyclovir by surface enhanced Raman spectroscopy using a portable Raman spectrometer coupled with multivariate data analysis, Colloids Surf. B: Biointerfaces 173 (2019) 286–294, https://doi.org/10.1016/j.colsurfb.2018.09.058.
[44] N.H. Othman, L.Y. Khuan, A.R.M. Radzol, W. Mansor, Detection of NS1 from SERS Spectra of Adulterated Saliva Using ANN, (2018), https://doi.org/10.1166/asl.2018.10703.
[45] H. Shi, H. Wang, X. Meng, R. Chen, Y. Zhang, Y. Su, Y. He, Setting Up a surface-enhanced Raman scattering database for artificial-intelligence-based label-free discrimination of tumor suppressor genes, Anal. Chem. 90 (2018) 14216–14221, https://doi.org/10.1021/acs.analchem.8b03080.
[46] Y. Kalachyova, D. Mares, V. Jerabek, P. Ulbrich, L. Lapcak, V. Svorcik, O. Lyutakov, Ultrasensitive and reproducible SERS platform of coupled Ag grating with multi-branched Au nanoparticles, Phys. Chem. Chem. Phys. 19 (2017) 14761–14769, https://doi.org/10.1039/C7CP01828B.
[47] O. Guselnikova, P. Postnikov, R. Elashnikov, M. Trusova, Y. Kalachyova, M. Libansky, J. Barek, Z. Kolska, V. Švorčík, O. Lyutakov, Surface modification of Au and Ag plasmonic thin films via diazonium chemistry: evaluation of structure and properties, Colloids Surf. A: Physicochem. Eng. Asp. 516 (2017) 274–285, https://doi.org/10.1016/j.colsurfa.2016.12.040.
[48] B. Dvořánková, L. Lacina, K. Smetana, Isolation of normal fibroblasts and their cancer-associated counterparts (CAFs) for biomedical research, in: K. Turksen (Ed.), Skin Stem Cells: Methods and Protocols, Springer New York, New York, NY, 2019, pp. 393–406, , https://doi.org/10.1007/7651_2018_137.
[49] P. H C Eilers, H. F M Boelens, Baseline Correction with Asymmetric Least Squares Smoothing, Unpubl. Manuscr. (2005).
[50] S.-J. Baek, A. Park, Y.-J. Ahn, J. Choo, Baseline correction using asymmetrically reweighted penalized least squares smoothing, Analyst 140 (2015) 250–257, https://doi.org/10.1039/C4AN01061B.
[51] S. van der Walt, S.C. Colbert, G. Varoquaux, The NumPy array: a structure for efficient numerical computation, Comput. Sci. Eng. 13 (2011) 22–30, https://doi.org/10.1109/MCSE.2011.37.
[52] E. Jones, T. Oliphant, P. Peterson, SciPy: Open Source Scientific Tools for Python, (2001).
[53] W. McKinney, Data Structures for Statistical Computing in Python, (2010), p. 6.
[54] Deep Learning for Humans. Contribute to Keras-Team/Keras Development by Creating an Account on GitHub, Keras, (2019) https://github.com/keras-team/keras.
[55] M. Abadi, P. Barham, J. Chen, Z. Chen, A. Davis, J. Dean, M. Devin, S. Ghemawat, G. Irving, M. Isard, M. Kudlur, J. Levenberg, R. Monga, S. Moore, D.G. Murray, B. Steiner, P. Tucker, V. Vasudevan, P. Warden, M. Wicke, Y. Yu, X. Zheng, TensorFlow: A System for Large-Scale Machine Learning, (2016), pp. 265–283 https://www.usenix.org/conference/osdi16/technical-sessions/presentation/abadi.
[56] S.C. Pînzaru, A. Falamaș, C. Dehelean, C. Morari, M. Venter, Double amino functionalized Ag nanoparticles as SERS tags in Raman diagnostic, Croatica Chem. Acta 86 (2013) 233–244, https://doi.org/10.5562/cca2067.
[57] S. Zeng, K.-T. Yong, I. Roy, X.-Q. Dinh, X. Yu, F. Luan, A review on functionalized Gold nanoparticles for biosensing applications, Plasmonics 6 (2011) 491, https://doi.org/10.1007/s11468-011-9228-1.
[58] A. Krizhevsky, I. Sutskever, G.E. Hinton, ImageNet classification with deep convolutional neural networks, in: F. Pereira, C.J.C. Burges, L. Bottou, K.Q. Weinberger (Eds.), Advances in Neural Information Processing Systems 25, Curran Associates, Inc., 2012, pp. 1097–1105.
[59] I. Sobel, An Isotropic 3x3 Image Gradient Operator, Presentation at Stanford A.I. Project 1968, (2014).
[60] J. Liu, M. Osadchy, L. Ashton, M. Foster, C.J. Solomon, S.J. Gibson, Deep convolutional neural networks for Raman spectrum recognition: a unified solution, Analyst 142 (2017) 4067–4074, https://doi.org/10.1039/C7AN01371J.
[61] J.S. Bridle, Probabilistic Interpretation of Feedforward Classification Network Outputs, with Relationships to Statistical Pattern Recognition, (1990), pp. 227–236, https://doi.org/10.1007/978-3-642-76153-9_28.
[62] A. Trelin, A. Prochazka, Binary Stochastic Filtering: a Solution for Supervised Feature Selection and Neural Network Shape Optimization, ArXiv:1902.04510 [Cs, Stat]. (2019). http://arxiv.org/abs/1902.04510.
[63] G. Niaura, Raman spectroscopy in analysis of biomolecules, Encyclopedia of Analytical Chemistry, American Cancer Society, 2014, pp. 1–34, https://doi.org/10.1002/9780470027318.a0212.pub3.
[64] H. Lui, J. Zhao, D. McLean, H. Zeng, Real-time Raman spectroscopy for in vivo skin cancer diagnosis, Cancer Res. 72 (2012) 2491–2500, https://doi.org/10.1158/0008-5472.CAN-11-4061.
[65] L. van der Maaten, G. Hinton, Visualizing data using t-SNE, J. Mach. Learn. Res. 9 (2008) 2579–2605.

Mariia Erzina is 3rd year Ph. D. student at the University of Chemistry and Technology, Prague. The main fields of her research interest include the preparation and utilization of plasmonic nanostructures.

Andrii Trelin is a fifth-year student at the University of Chemistry and Technology, Prague. The main fields of his research interest include the application of machine learning in natural sciences, computational physics on the boundary with chemistry and semiconductors.

Guselnikova Olga received her Ph. D. in University of Chemistry and Technology Prague in 2019. Her research interests are diazonium salts, surface modification, Surface-enhanced Raman spectroscopy and smart polymers.

Barbora Dvořánková is an associated professor at the Charles University in Prague. The main fields of her research interest include the cultivation of epidermal cells and problems of wound healing.

Karolina Strnadova is 2nd year PhD student at the Charles University in Prague. The main fields of her research interest include the cultivation of normal or tumor cells.

Perminova Anastasia is 2nd year PhD student at the University of Chemistry and Technology, Prague. The main fields of her research interest include the preparation of 2D plasmonic nanostructures and their utilization for SERS analysis.

Pavel Ulbrich is an associated professor of chemistry at the University of Chemistry and Technology Prague. The main fields of his research interest include the biochemistry and TEM analysis,

David Mares is a fifth-year PhD student at the Czech Technical University, Prague. The main fields of his research interest include the numerical simulation of optical structures and devices.

Vitezslav Jerabek is an associated professor at the Czech Technical University, Prague. The main fields of his research interest include the optics and optoelectronics.

Roman Elashnikov is a fourth year Ph.D student at the University of Chemistry and Technology Prague. The main fields of his research interest include the biomaterials and SEM measurements.

Václav Švorčík is a professor of chemistry at the University of Chemistry and Technology Prague. In 1981 he graduated from the University of Chemistry and Technology Prague, four years later he obtained his doctorate in the field of macromolecular technology, he was a lecturer in material engineering in 1992 and became a professor in 2000. His research interests are biomaterials, polymers, functional materials and antibacterial materials.

Oleksiy Lyutakov received his Ph. D. in University of Chemistry and Technology Prague in 2009. His research interests are focused on surface-enhanced Raman spectroscopy, properties and applications of metal nanostructures.

PUBLIKACE V

Strnadová K, Španko M, Dvořánková B, Lacina L, Kodet O, Shbat A, Klepáček I, Smetana K Jr. Melanoma xenotransplant on the chicken chorioallantoic membrane: a complex biological model for the study of cancer cell behaviour. *Histochem Cell Biol*. 2020 Aug;154(2):177-188. **(IF: 4.304)**

Histochemistry and Cell Biology
https://doi.org/10.1007/s00418-020-01872-y

ORIGINAL PAPER

Melanoma xenotransplant on the chicken chorioallantoic membrane: a complex biological model for the study of cancer cell behaviour

Karolína Strnadová[1,2] · Michal Španko[1,3] · Barbora Dvořánková[1,2] · Lukáš Lacina[1,2,4] · Ondřej Kodet[1,2,4] · Andrej Shbat[1] · Ivo Klepáček[1] · Karel Smetana Jr.[1,2]

Accepted: 10 March 2020

Abstract
The globally increasing incidence of cancer, including melanoma, requires novel therapeutic strategies. Development of successful novel drugs is based on clear identification of the target mechanisms responsible for the disease progression. The specific cancer microenvironment represents a critically important aspect of cancer biology, which cannot be properly studied in simplistic cell culture conditions. Among other traditional options, the study of melanoma cell growth on the chicken chorioallantoic membrane offers several significant advantages. This model offers increased complexity compared to usual in silico culture models and still remains financially affordable. Using this model, we studied the growth of three established human melanoma cell lines: A2058, BLM, G361. The combination of histology, immunohistochemistry with the application of human-specific antibodies, intravascular injection of contrast material such as filtered Indian ink, Mercox solution and phosphotungstic acid, and X-ray micro-CT and live-cell monitoring was employed. Melanoma cells spread well on the chicken chorioallantoic membrane. However, invasion into the stroma of the chorioallantoic membrane and the limb primordium graft was rare. The melanoma cells also significantly influenced the architecture of the blood vessel network, resulting in the orientation of the vessels to the site of the tumour cell inoculation. The system of melanoma cell culture on the chorioallantoic membrane is suitable for the study of melanoma cell growth, particularly of rearrangement of the host vascular pattern after cancer cell implantation. The system also has promising potential for further development.

Keywords Melanoma · Cancer microenvironment · Cancer-associated fibroblasts · Melanoma invasiveness · Embryo · Chorioallantoic membrane

Introduction

The incidence of malignant melanoma is increasing worldwide at a rate faster than that of other malignant diseases. Until now, the melanoma-associated mortality has remained high in advanced stage patients, despite the enormous efforts and several new therapeutic options (Dvořánková et al. 2017). Similarly to other types of tumours, the microenvironment significantly influences the biological properties of melanoma (Lacina et al. 2015; Dvořánková et al. 2017). Some of the novel successful therapeutic strategies, namely immune checkpoint inhibitors, target the immune mechanisms in the tumour microenvironment and elicit immune clearance of the tumour. However, there are multiple other components beyond immune cells present in the tumour stroma. Their therapeutic potential has not yet been fully revealed and is worthy of scientific attention. The cellular component of the tumour microenvironment mainly

Karolína Strnadová and Michal Španko have contributed equally.

✉ Lukáš Lacina
lukas.lacina@lf1.cuni.cz

✉ Karel Smetana Jr.
karel.smetana@lf1.cuni.cz

[1] Institute of Anatomy, First Faculty of Medicine, Charles University, 12800, Prague, Czech Republic

[2] BIOCEV, First Faculty of Medicine, Charles University, 25250 Vestec, Czech Republic

[3] Department of Stomatology, First Faculty of Medicine, Charles University, 12800, Prague, Czech Republic

[4] Department of Dermatovenereology, First Faculty of Medicine, Charles University, 12808 Prague, Czech Republic

Published online: 30 March 2020

includes cancer-associated fibroblasts, as well as pericytes, endothelial cells, adipocytes, and others. Cancer-associated fibroblasts are the most numerous population, and, therefore, have attracted attention of researchers for many years. However, a significant regulatory function can be executed even by some minor population (Dvořánková et al. 2019).

The cancer microenvironment can be studied in vitro at the 2D or 3D level (Kodet et al. 2015; Jobe et al. 2016, 2018) or in vivo. The traditional cell culture methods based on separated cell types lack the complexity of the tissue microenvironment, which is an indispensable factor for cancer progression in the organism. We can enrich the standard culture model based on malignant cell lines by employing one or more stromal populations simultaneously. Their interactions may occur via direct cell-to-cell contacts or indirectly, via soluble biologically active molecules. Moreover, physiochemical features may also play a significant role in tumour biology. Tissue hypoxia is one of the traditionally extensively studied features (Gaustad et al. 2017), which can also be achieved in experimental in vitro models. However, the complexity of tissue, where multiple cell types interact simultaneously, is not reproduced entirely.

The most frequently used animal model for cancer studies is based on various highly inbred mouse strains. Compared to cell line-based research, murine models offer much higher biological complexity. Immunodeficient mouse models are particularly suitable for cancer research. However, as there is an outstanding diversity in immunodeficient mouse models, it is difficult to choose the most appropriate strain for a particular study. The selection of an immunodeficient mouse strain also brings bias to the studied experimental system. Mice are sometimes not completely reliable as models of human disease, including cancer. In addition, the achieved biological complexity is also associated with a significantly higher price (Pérez-Guijarro et al. 2017). Therefore, a simple and affordable biological model is needed for biomedical research.

It was frequently noted earlier that the chorioallantoic membrane (CAM) of the chicken embryo represents a complex structure with precisely described developmental dynamics. CAM represents a biologically relevant substrate with several cellular components, extracellular matrix and fully functional continuous blood flow. It can be used efficiently for in vitro cultures or for in vivo studies. CAM allows frequent or continuous microscopic evaluation. Finally, CAM offers straightforward interpretation by methods of histology or histochemistry. It is also reasonably cheaper than mouse models.

Ribatti (2016) reviewed various applications of CAM as an excellent tool for the study of many biologically as well as medically relevant problems. Beside traditional studies of angiogenesis, CAM was even used as an in vivo model of implantation of cancer cells, including melanoma (Ribatti 2014; Avram et al. 2017) and metastasising (Cimpean et al. 2008; Deryugina and Quigley 2008; Subauste et al. 2009).

Melanomas are tumours originating from melanocytes, the pigment-producing cells of the skin. The function of melanocytes in the skin is tightly regulated by the target tissue microenvironment. Melanocytes migrate from the neural crest to the skin during embryonic development (Shakhova 2014). Experiments in zebrafish showed that transcription factor crestin is typical of neural crest embryonic cells. Of note, crestin is also significantly activated in malignant melanoma (Kaufman et al. 2016).

When injected to the embryo, melanoma cells colonise similar body sites as the neural crest progeny (Lee et al. 2005; Bailey et al. 2012; Bailey and Kulesa 2014). Even in vitro, conditioned medium from embryonic stem cells influences the phenotype and functional properties of melanoma cells (Kodet et al. 2013). The conditioned medium can be easily used as a tissue microenvironment surrogate. These findings indicate an important effect of the embryonic microenvironment on melanoma cell biology. Furthermore, there is evidence of melanoma cell reprogramming by the embryonic microenvironment and loss of their malignant behaviour (Kasemeier-Kulesa et al. 2008; Díez-Torre et al. 2009).

In the presented study, we evaluated the growth of three melanoma cell lines in the CAM model. We mapped the remodelling of immature vessels in CAM after inoculation of melanoma cells. To study the effects of hypoxic conditions, we also grafted an isolated limb bud onto CAM before melanoma cell implantation. The spatial reorganisation of the CAM vascular pattern was visualised by injections of phosphotungstic acid (PTA), Indian ink, or synthetic resin to the CAM vessels. The melanoma cells used in this study were not chemically labelled to prevent the potential effect of chemical label on their viability and biological properties. We distinguished the grafted melanoma cells in the tissues by a species-specific antibody recognising human vimentin (Vim), enzyme expression (galactosidase), and HMB-45 marker of melanocytes.

Materials and methods

Cell culture and conditioned media preparation

Three invasive melanoma cell lines were tested. Cells of the BLM line were obtained from L. van Kempen and H. Van Krieken from the Department of Pathology, Radboud University (Nijmegen, the Netherlands). G361 and A2058 cell lines were purchased from the American Type Culture Collection. The cells were maintained in DMEM with 10% FBS (Sigma Aldrich, Prague, Czech Republic). LacZ melanoma cell lines tagging was performed according to

the manufacturer's protocol (LV-348, AMS Biotechnology (Europe) Ltd, Abingdon, U.K.) with consequent puromycin selection. As control population, normal human highly pigmented melanocytes (HPM) were obtained from J. Vachtenheim (Institute of Medical Chemistry and Laboratory Medicine, 1st Faculty of Medicine, Charles University, Prague, Czech Republic). HPM melanocytes were maintained in M254 culture medium (Thermo Fisher Scientific, Prague, Czech Republic). Human dermal fibroblasts were prepared from the skin samples of healthy donors with the donor's explicit informed consent and approval by the local ethics committee (Dvořánková et al. 2019). The same procedures were also used to prepare the chicken embryonic fibroblasts from CAM and adult chicken dermal fibroblasts (CDF), which were cultured as described earlier (Dvořánková et al. 2019). Preparation of primary cells was approved by the local ethics committees of the First and Third Faculty of Medicine, Charles University in Prague according to the Declaration of Helsinki as described for use of human material. The characterisation of cells and the cultivation procedure were described in detail by Kodet et al. (2015) and Dvořánková et al. (Jobe et al. 2016; Dvořánková et al. 2019). The conditioned media (CM) were collected from the avian fibroblast monolayers (CAM or CDF) cultured in DMEM with 10% FBS. The medium was changed in fibroblast cultures forming subconfluent layers (70%) and harvested after further 48 h of cultivation. It was filtered (0.2 µm), aliquoted, and stored (at − 80 °C) for later experimental use. All cell lines were routinely tested for Mycoplasma sp. contaminations.

Chick embryo preparation

Fertilised eggs of the Ross 308 hybrid of the chick (*Gallus gallus domestica*; Xaverov, Czech Republic) were incubated in a humidified atmosphere in an incubator at 37.5 °C for 4 days in stage 22–24 according to Hamburger and Hamilton (1992). The eggshell was decontaminated by 70% ethanol (Rugh 1948), and a manipulation window was cut to the eggshell.

In a defined cohort of embryos, the early primordium of the upper limb (HH 23–24) was transplanted to the surface of CAM outside the embryo before the application of cancer cells to mimic a hypoxic niche. After grafting, the fenestration of the eggshell was sealed by paraffin and attached sterile glass (Rugh 1948; Klepáček and Jirsa 1994) and maintained in the incubator. After day 2, the cancer cells were implanted onto the CAM surface. The melanoma cells were seeded as a concentrated suspension onto the surface of CAM in a quantity of 10^6 cells in 10 µl of PBS per embryo. Eggs were further incubated for 2–6 consecutive days. The numbers of embryos used for experimental cohorts are presented in Table 1 (total $n = 45$). All manipulations with embryos were performed using stereomicroscope SMZ 18 (Nikon, Vienna, Austria) using sterile instruments. The experimental design of this study, including both in vitro and *in ovo* studies, is summarised in Fig. 1.

Immunofluorescent and immunohistochemical detection of cancer cells in whole-mount specimens

CAM was dissected from the egg after attachment to a paper frame, which offers stabilisation of the specimen and prevents rolling. CAM was gently rinsed in PBS and briefly fixed in 4% paraformaldehyde (in PBS, pH 7.2, 5 min) and repeatedly gently washed with PBS. The specimens for immunocytochemistry were consequently permeabilised by Tween 20 (Sigma-Aldrich, Prague, Czech Republic) at concentration 0.2% in PBS. Vimentin was detected by specific antibody clone V9 (DAKO, Glostrup, Denmark) (Bohn et al. 1992). The species specificity was verified in human and chicken fibroblasts (Fig. 2a, b) with the employment of appropriate negative controls (either omission of the primary antibody or use of a tissue-irrelevant antibody of the same isotype, isotype control, ThermoFisher Scientific, Prague, Czech Republic). The chicken-reactive vimentin for avian fibroblast phenotype confirmation was mouse monoclonal antibody, clone RV202 (Abcam, Cambridge, UK).

TRITC-labelled goat anti-mouse antibody (Sigma-Aldrich, Prague, Czech Republic) was used as the second step antibody to detect vimentin. Both the first and second step antibodies were diluted as recommended by the supplier. Nuclei were counterstained with 4′,6-diamidine-2′-phenylindole dihydrochloride (DAPI) (Sigma-Aldrich, Prague, Czech Republic). Specimens were mounted as whole mounts to Vectashield (Vector Laboratories, Burlingame,

Table 1 Results of melanoma xenotransplantation on the chick embryo CAM

Cell line	No. of embryos/no. of implants	No. of embryos/invasion to CAM	No. of grafted limb buds/migration to the graft site	No. of limb buds/no. of limbs with cancer cells	No. of embryos/metastases (liver, lung, brain)
A2058	15/15	15/1	5/5	5/1	15/0
BLM	15/15	15/0	5/5	5/0	15/0
G361	15/15	15/1	5/5	5/1	15/0

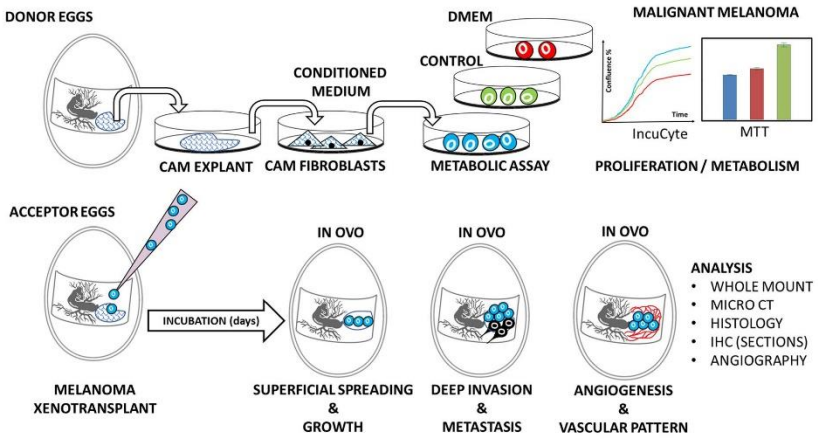

Fig. 1 Experimental workflow. The fibroblasts were isolated from CAM of donor eggs or adult avian skin. The effects of conditioned media on the growth of malignant melanoma cells was tested using the metabolic (MTT) assay and the growth was continuously monitored by microscopy (Incucyte system). Melanoma cells were grafted on the chick chorioallantoic membrane in acceptor eggs. We monitored the melanoma cell spread on the surface or invasion to the chorioallantoic membrane stroma (or into the grafted limb primordia) and changes in the vascular network surrounding the application site

CA, USA) and inspected by an Eclipse 90i microscope (Nikon, Viena, Austria) equipped with NIS-Elements AR.40.00 for data storage and analysis and with a ProgRes MF CCD camera (Jenoptik Optical Systems GmBH, Jena, Germany).

In case of X-Gal reaction for LacZ-tagged melanoma cells, the fixation was shortened to 3 min only. The visualisation was performed using a β-Gal Staining Kit (Invitrogen, Prague, Czech Republic) following the manufacturer's protocol. The documentation in the bright field was performed using a Leica DM 2000 microscope equipped with a digital camera.

Immunohistochemical detection of melanoma cells

Tissue sections (5 µm) were cut from routinely prepared FFPE blocks. Slides were deparaffinised and rehydrated. HBM-45 was selected out of melanoma markers, because this particular antibody does not require any antigen retrieval using heat treatment before staining according to the manufacturer's instructions (MA5-16712, ThermoFisher Scientific, Prague, Czech Republic). Endogenous peroxidase activity was blocked by 1% hydrogen peroxide in PBS (20 min at room temperature), and non-specific interaction of immunoglobulins was blocked by incubation in diluted 10% non-immune goat serum (20 min, room temperature). The incubation with the primary antibody (diluted 1/40 in blocking solution) was performed at 4 °C overnight. The immunohistochemical reaction was visualised using an HRP polymer kit with diaminobenzidine (Histofine Simple Stain MAX PO Multi, Nichirei, Bioscience, Tokyo Japan). The nuclei were counterstained by hematoxylin and specimens were dehydrated, cleared and mounted in synthetic mountant (Jobe et al. 2016). The imaging was performed with a Leica DM 2000 microscope equipped with a digital camera.

Again, the specificity of the reaction was tested by replacement of the specific primary antibodies by a tissue-irrelevant isotype antibody (ThermoFisher Scientific, Prague, Czech Republic).

Detection of vessels by Indian ink, PTA and resin

CAM vessels were injected with filtered Indian ink (Klepáček et al. 1999), PTA (Kokorin and Gudima 1968), or Mercox^{R} II Blue resin (Mercox-Japan Vilene, Tokyo, Japan) and processed as described elsewhere (Navarro et al. 1998; Klepáček et al. 1986). The resin/PTA-injected specimens were inspected and analysed by X-ray micro-CT using a desktop ex vivo device SkyScan1272 with a 16MPx CCD detector (Bruker, Kontich, Belgium). Each specimen was individually placed in a plastic tube with PBS and mounted on a microstage as described. The specimens were scanned in resolution 3280×4904 px without employing an X-ray filter. The data were reconstructed using program NRecon and visualised using program CTVox, both obtained from Bruker (Kolesová et al. 2018).

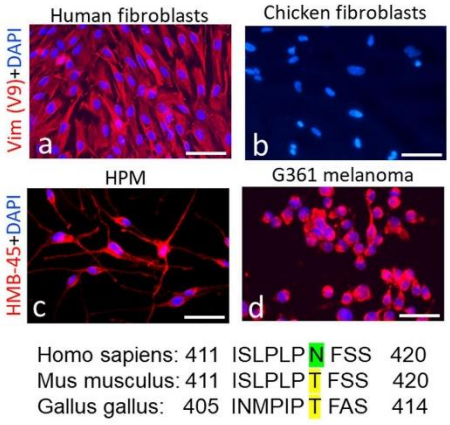

Fig. 2 Detection of human vimentin (V9 clone, red signal) in human dermal fibroblasts (**a**), and absence of V9 staining in chicken embryonic fibroblasts (**b**). Detection of melanocyte marker (HMB-45, red signal) in normal human highly pigmented melanocytes (**c**) and melanoma cells (**d**). Comparison of analogous sequences of human, murine and chicken vimentin (amino acids 411–420 and 405–414, respectively). Asparagine 417 (N) is highlighted in green in the human vimentin (the key structural motif for V9 antibody binding); in contrast, the similarity of murine and chicken vimentin (threonine 417 and 411, respectively) is highlighted in yellow. The human, murine and chicken vimentin sequences were aligned using the https://www.uniprot.org/align/ database tool and according to Kong et al. (2011) and also specifically to Tomiyama et al. (2017) for the purposes of V9 binding motif identification. The bar represents 50 µm

Testing the effect of conditioned media on the growth and metabolic properties of cancer cells

The proliferation kinetics of A2058, BLM and G361 melanoma cells was tested using the IncuCyte ZOOM Kinetic live cell imaging system (Essen BioScience, Ann Arbor, MI, USA) as described earlier (Živicová et al. 2017). The melanoma cells were seeded in low density in 96-well plates. Next day, the standard cultivation medium was replaced by the conditioned medium. The effect of conditioned media prepared from the subconfluent layers of CAM and CDF was measured and expressed as confluence (%). Cultures were screened every 2 h for approximately 9 days. The differences in proliferation were compared at the moment of exponential growth when the first averaged line (representing $n = 12$) met 50% of confluence. The data were analysed using PAST3 software (http://palaeo-electronica.org/2001_1/past/issue1_01.htm); Tukey's Honest Significant Difference test was used to detect statistical significance.

The results were further compared with the evaluation of the metabolic activity of A2058, BLM and G361 melanoma cells under the influence of conditioned media using the MTT test (Stockert et al. 2018) on the 7th day of cultivation, when the growth of the cells was stabilised.

Results

Isolation of chicken dermal and CAM fibroblasts and their effects on melanoma cell line growth

The fibroblasts from the chick chorioallantoic membrane (CAM) were successfully isolated using the explant method following the protocol published earlier by us (Kodet et al. 2013) and phenotype was determined according to our published protocol (Dvořánková et al. 2019). We also isolated chicken dermal fibroblasts (CDF) from avian skin as control cells for this experiment using otherwise identical conditions. The cells were easily expanded in DMEM with 10% FBS for experimental purposes and used before passage No. 5. The immunocytochemical staining with vimentin antibody V9 was negative in all cells of avian origin (Fig. 2). This finding contrasted with the confirmed positive result detected in human cell lines (normal human fibroblasts presented here; the data from melanoma cell lines are not presented). However, vimentin was confirmed in avian fibroblast by staining with alternative mouse monoclonal antibody RV202(data not shown). This contrast also confirms the species specificity of the immunocytochemical reaction of V9 antibody (the negative control is thus not presented here).

The fibroblast-conditioned media (CAF-CM and CDF-CM) significantly increased the proliferation kinetics of all three cancer cell lines when compared to DMEM (p value < 0.008 in all cases). However, a statistically significant difference between CDF-CM and CAM-CM was observed only in the A2058 melanoma cell line (p value 0.002). The trend observed in BLM and G361 melanoma cell line growth was similar, yet not significant (p value 0.24 and 0.15, respectively). We also measured the differences in metabolic activity of melanoma cell lines in different media using the MTT assay. Similarly, A2058 sensibly reflected the difference between CAM-CM vs CDF-CM (p value > 0.001). There was no statistically significant difference between the metabolic rate of BLM and G361 melanoma cell lines in various culture media (Fig. 3).

Observation in ovo

The results of melanoma xenotransplantation are summarised in Table 1. All cell lines used in the experiments formed distinct colonies on the surface of CAM. Colonies

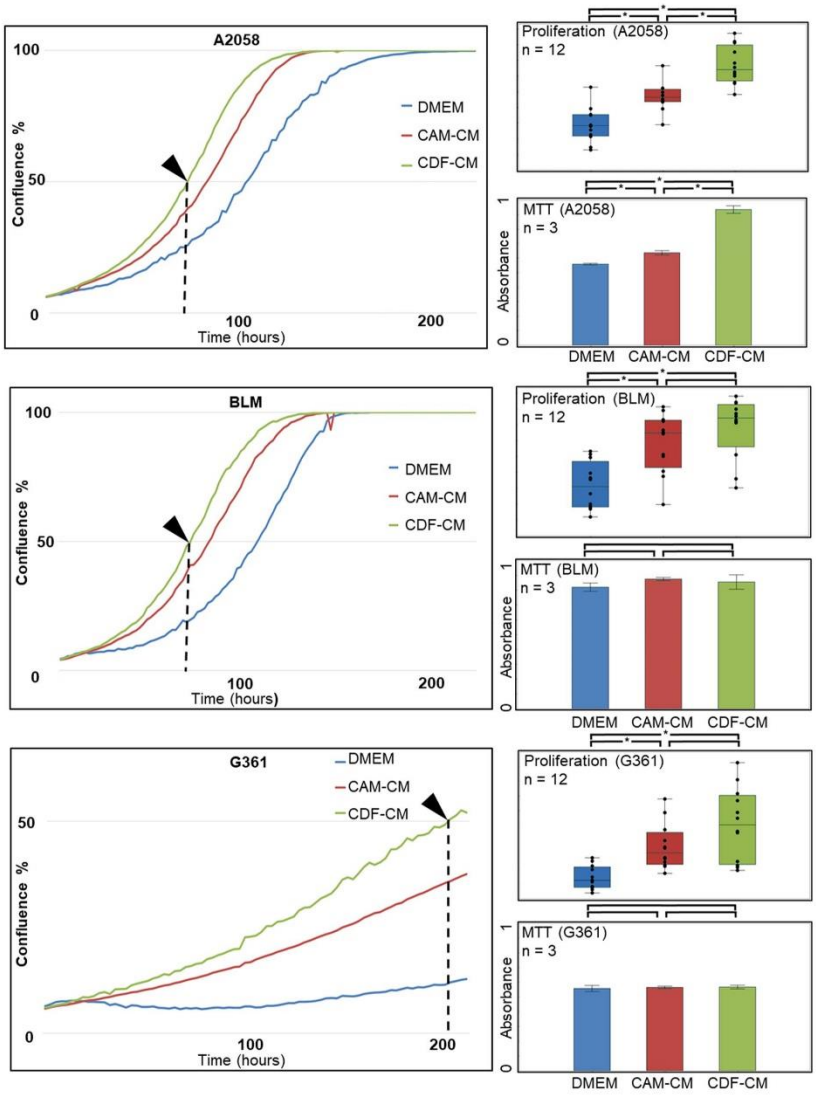

Fig. 3 Proliferation curves of A2058, BLM and G361 treated with DMEM, CAM-CM and CDF-CM, respectively. Each curve was plotted as a mean value of % confluence from independent stable reference observation points ($n = 12$) using the IncuCyte life cell analysis system. The cell proliferation was compared under different culture conditions (DMEM vs CAM-CM vs CDF-CM) at the time when the first curve met 50% confluence value (arrowhead) using the Tukey's Honest Significance test. Significant comparisons are indicated by asterisks ($p < 0.05$). The metabolic activity of cells under different culture conditions (DMEM vs CAM-CM vs CDF-CM) was evaluated using the MTT test ($n = 3$ for each condition). The significance of results was tested using the Tukey's Honest Significance test. Significant comparisons are highlighted by asterisks ($p < 0.05$)

were easy to see due to their increased opacity on CAM *in ovo* under a low-power microscope. The melanoma cells formed very small, grouped colonies at the initial stages of the experiment (day 2, Fig. 4a–d). The layer of vessels was visualised by injected Indian ink (Fig. 4a). The identity of melanoma cells was also confirmed by immunocytochemical detection of vimentin (Fig. 4b, c, red signal, Vim). This staining documented the presence of cancer cells on the surface of CAM above the vessels by accumulation of DAPI-positive nuclei. Furthermore, we performed X-ray micro-CT of the vessels injected with resin or PTA (Fig. 4d). All these methods supported the intimate relationship between the vessels and tumour cells during the initiation of melanoma growth on the CAM surface.

In later stages of the experiment (day 6), we observed more extensive opacities on the surface of CAM by the low-power microscope or even by the naked eye. These clusters were formed by the transplanted melanoma cells. This was confirmed by enzymatic X-Gal reaction on CAM whole-mount (highlighting selectively LacZ-tagged cells—Fig. 5a, bluish clusters). A similar extent of melanoma growth was confirmed by vimentin staining of untagged cells (Fig. 5b, red signal). The vascular pattern of CAM was significantly rearranged at this stage. We observed that the centripetal growth of blood vessels to the tumour site occupied by cancer cells was very well visible in specimens with resin-injected vessels (Fig. 5c). Optical visualisation of Mercox-microinjected CAM vessels demonstrated that the vessels in CAM overlaid the accumulation of tumour cells without penetration to the melanoma cell mass (Fig. 5d).

Invasion of melanoma cells into the CAM stroma was a rare event. We confirmed invasion only in two samples histologically. Vimentin staining (Fig. 6a) revealed scattered melanoma cells on the surface of CAM and also inside the CAM stroma. The second sample contained a distinct region, where tumour cells invaded from the surface into the CAM stroma and formed small clusters (Fig. 6b). Cancer cell clusters were prominent even in HE staining, and their identity was confirmed by a positive reaction for HMB-45 marker (Fig. 6c). In this case, melanoma cells were surrounded by the typical activated mesenchymal stroma of chick CAM. We did not observe the presence of any stromal elements of human origin, e.g., cancer-associated fibroblasts positive for human vimentin. The specificity of the immunohistochemical reaction was demonstrated by the negative control (Fig. 6d).

The isolated limb bud primordium (HH stages 23–24) grafted on CAM as a model of hypoxic tissue niche reshaped the vascular pattern of CAM of the acceptor eggs significantly. Under these hypoxic signals, the CAM vessels successfully penetrated the limb (Fig. 7a).

Consequently, we observed further development of the grafted limb during the experiment, confirming the viability

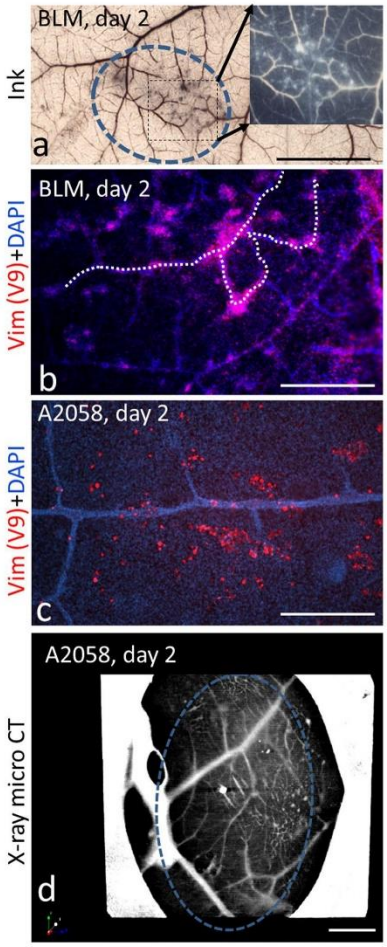

Fig. 4 Chick CAM 2 days after application of BLM (**a**, **b**) and A2058 melanoma cells (**c**, **d**) after intravascular injection of vessels by India ink in the bright and dark field (**a**). The melanoma cells are positive for human vimentin (red signal, **b**, **c**). The nuclei of melanoma cells and CAM cells are stained blue by DAPI (**b**, **c**), the white dashed line highlighted course of more prominent vessel. Similar area after injection of PTA is visualised by X-ray micro-CT in (**d**). Bar is 100 (**a**–**c**) and 500 (**d**) µm, respectively

of this tissue. Melanoma cells were attracted to the site of limb transplantation and surrounded the limb primordium in all studied samples (Fig. 7a, b—positive vimentin staining, red signal). However, the limb primordia were colonised

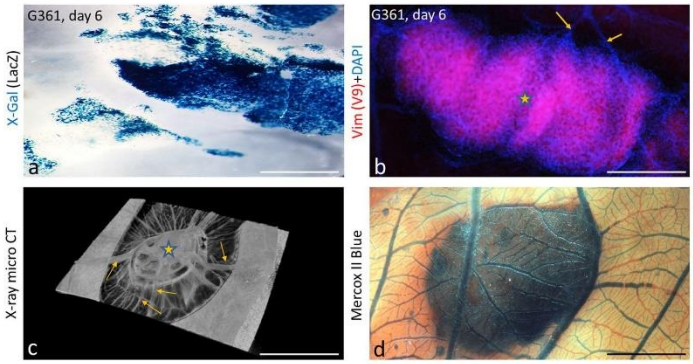

Fig. 5 Accumulation of melanoma cells on the surface of CAM 6 days after grafting (**a**—LacZ-tagged cells in bluish colour after X-Gal staining, **b**—vimentin V9-stained untagged melanoma cells in red signal (asterisk)). Chick vessels oriented to cancer cells stained blue by DAPI are marked by arrows (**b**). Similar site after injection of resin demonstrates blood vessels converging to accumulated melanoma cells (arrows, c). Inspection of a similar site by optical microscope demonstrates that blood vessels cross under the tumour inside the CAM and do not penetrate to the tumour mass (**d**). Bar is 50, 500 and 1000 µm, respectively

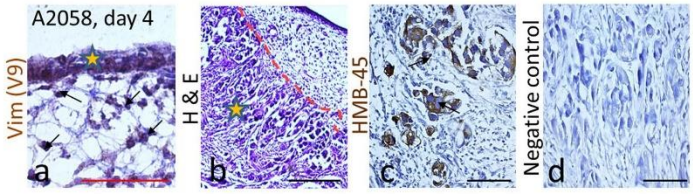

Fig. 6 Section of CAM. Melanoma cells (asterisk) are located on the CAM surface with sporadic human vimentin-positive cells in the stroma (**a**). In a single case only, we observed solid melanoma (asterisk) in the CAM stroma (**b**). These cells were positive for melanocyte marker HMB-45 (**c**). Bar is 100 and 300 µm, respectively

by melanoma cells only in two cases, in both of them in the perichondrium covering the anlage of digits (Fig. 7c). The identity of these colonising melanoma cells was confirmed by positive detection of the HMB-45 marker (negative control is presented in Fig. 7d).

We did not observe melanoma cells localised in the internal organs (liver, lung, brain) of the embryos through the interval of 5–6 days after melanoma cell transplantation by immunohostochemistry. We present the summary of all our xenotransplantation experiments in Table 1.

Discussion

This study shows that CAM in the chicken embryo offers an attractive in vivo biological substrate for the study of melanoma cell behaviour.

It is evident that any fibroblast-conditioned media used in our experiment significantly enhanced the proliferation of melanoma cells when compared to standard culture media. This observation highlights the dependence of melanoma proliferation on the microenvironmental cues represented here by fibroblast-secreted molecules (e.g., growth factors, chemokines, cytokines, etc.). The topic was recently reviewed by several authors (Lacina et al. 2018; Plzák et al. 2019; Strnadová et al. 2019). Among most likely candidates, IL-6, IL-8, CXCL-1, EGF, bFGF, HGF, and VEGFA play an essential role in cancer cell biology. We demonstrated in our previous work that IL-6 and IL-8 can influence invasiveness of melanoma cells in vitro (Jobe et al. 2018), and increased production of IL-6 by the cancer ecosystem stimulates patient cancer-dependent wasting and cachexia, as reviewed by Lacina et al. (2019). A similar trend was evident and reached

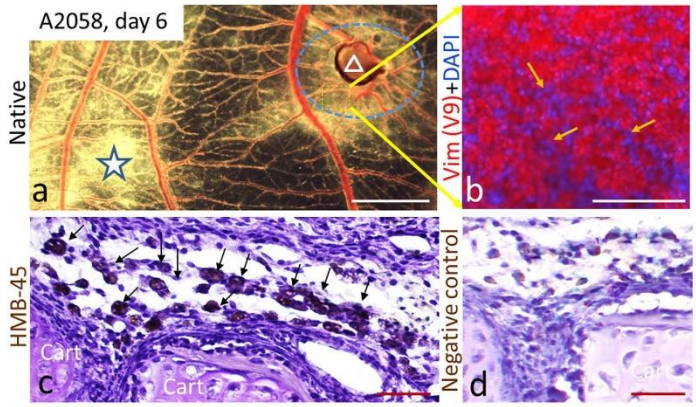

Fig. 7 Site of melanoma cell application (**a**—asterisk) and movement of melanoma cells to the grafted limb bud (**a**—triangle). When the specimen was stained as a whole-mount preparation by human vimentin (detail of the dashed quadrangle, vimentin in red signal), numerous positive cells were detected. A dense capillary network in the CAM is present at this site (**b**, yellow arrows). In the tissue section of the grafted limb primordium, the melanoma cells express specific marker HMB-45 (brown signal) in the vicinity of the cartilaginous digit primordia of the autopodial region of the limb (Cart, **c**, **d**). Bar represents 50, 100 and 1000 µm, respectively

statistical significance in all three studied cell lines. This was evident even in the case of embryonic CAM compared to pure DMEM. However, their adult CDF counterparts promoted melanoma proliferation somewhat more efficiently. This is a severe warrant to all those who use in vitro models, because employment of any complex biological material (represented here by the conditioned medium) can be potentially misleading. In such a case, a trivial comparison with pure DMEM would inevitably lead to statistically significant but biologically inappropriate conclusions.

Nevertheless, we confirmed the statistical significance of CAM vs CDF conditioned media only in the case of A2058 cell line proliferation (p value 0.002). In BLM and G361 melanoma cell lines, the trend of growth was similar, yet not statistically significant. The MTT test of metabolic activity in melanoma cells again confirmed the significant differences for A2058 melanoma in conditioned media only (p value less than 0.001). The differences observed in BLM and G361 were also insignificant.

Similarly to adult chicken fibroblasts, the chicken embryonic cells produce many factors mentioned earlier, including IL-6, IL-8, VEGFA (Xing and Schat 2000; Kosla et al. 2013), and their production can be stimulated, e.g., by heating or infection. These data can explain the stimulatory effect of both types of chicken fibroblasts on melanoma cell growth in comparison with non-conditioned media, but they are unable to elucidate the difference between both types of chicken fibroblasts.

Our data confirmed the tested melanoma cell lines as suitable candidates for further research focusing on the inhibitory effect of the embryonic microenvironment. However, the A2058 cell line is the most sensitive for further research in model embryo. This phenomenon was noted by various embryologists earlier and reviewed extensively in recent years by Kasemeier-Kulesa and Kulesa (2018). This evidence acquired with A2058 can help us to understand the switching on/off effect of the embryonic microenvironment on the phenotype and malignant behaviour of cancer cells. The embryonic microenvironment seems to be able to overdrive the tumour cell malignant potential, presumably by epigenetic mechanisms (Abbott et al. 2008). Isolated embryonic stem cells and their products can also attenuate the malignant properties of melanoma cells (Kim et al. 2011; Kodet et al. 2013). Moreover, cancer cells can enter apoptotic death after contact with specific embryonic proteins (Cucina et al. 2006). The inhibitory effect of embryonic fibroblasts on the metabolism of melanoma cells seems to be therapeutically relevant, because cell metabolism may represent a potential therapeutic target (Kroemer and Pouyssegur 2008). This proof of concept was demonstrated by the therapeutic manipulation of mitochondria in cancer cells (Kalyanaraman et al. 2018). Similar results were observed in multiple types of tumours.

Kain et al. (2014) reviewed the plausibility of CAM employment in cancer studies. The data regarding melanoma cell growth on CAM are somewhat limited. However, sparse are these data, they often support our observations

(Jayachandran et al. 2015; Avram et al. 2017). Unequivocally, we can also confirm that melanoma cells successfully adhere to CAM covering larger vessels. The tumour cell clusters consequently stimulate the centripetal growth of vessels to the engraftment site. Others have also reported stimulation of the centripetal growth of vessels to cancer cell grafting (Ribatti 2008; Nowak-Sliwinska et al. 2014, 2018). Notably, we have not detected any evident penetration of the vessels to the melanoma cell mass.

On the other hand, this oriented vessel rearrangement and growth is not tumour specific, as the limb bud grafted on CAM also stimulates this patterning. Under these hypoxic signals, CAM vessels can even penetrate to the grafted limb bud. Given by this remarkable capacity for vascular growth, CAM is, therefore, traditionally used as a suitable tool for vascular biology. These observations could indicate the sustainability of the CAM-based model for studying the melanoma neovascularisation. However, we have not detected any sign of intravascular invasion or any distant metastatic involvement in our experimental models. We assume that this should be considered with precaution if these applications are intended for melanoma research.

Local invasion is another clinically relevant aspect of melanoma that is worthy of study on the CAM model. The invasive potential of cancer cells in CAM experiments was reported with a variable rate of frequency of success. Based on our results, engrafted melanoma cells invaded into the stroma of CAM slowly and only to a minimal extent. All three cell lines used in our study revealed otherwise highly invasive behaviour in various traditional assays (e.g., in Boyden chambers). We were able to confirm the aggressive growth of tumour to CAM only in two samples. Although others do not emphasise this aspect, it seems that the invasion of tumour cells into the CAM stroma is generally rare when tumour cell suspension is used (Deryugina and Quigley 2008; Subauste et al. 2009). This invasiveness seems to be enhanced by upregulation of the histone methyltransferase EZH2 expression in cancer cells (Liu et al. 2013a, b). When minced tumour mass is transplanted to CAM instead of cell suspension, the infiltrative growth of cancer cells to the CAM stroma is more frequently observed (Ghaffari-Tabrizi-Wizsy et al. 2019). This underscores the essential role of the supportive cancer microenvironment in tumour cell invasiveness.

Of note, melanoma cells on CAM usually formed only aggregates of tumour cells without the presence of any stroma. However, when they rarely invaded the CAM, the stroma originated from the local CAM mesenchyme was well developed. Furthermore, the tissue landscape may also mechanistically enhance the melanoma cell invasion in CAM. It was proposed that the external stealth of blood vessels may serve as a possible pathway for the malignant cell migration (Lugassy and Barnhill 2007).

Finally, the solid organ metastasis after cancer cell transplantation in the chick embryo assays is believed to be exceedingly rare (Kalirai et al. 2015; Herrmann et al. 2018). Unequivocally, we confirmed no organ metastases observed by us in the embryos after application of melanoma cells to CAM in the presented study by immunohistochemical methods. On the other hand, the limb bud successfully grafted to CAM was able to attract migration of melanoma cells, which formed a distinct halo surrounding the graft. Nevertheless, only exceptional melanoma cells were detected histologically inside the grafted limb. PCR based methods might offer highly sensitive tools if detection of rare metastatic cells would be the primary target of interest (Zijlstra et al. 2002). More specifically, the ALU PCR technique (Cardeli 2011) allows highly sensitive identification of a very limited number of heterogeneous cells in the dominant cell mass (Funakoshi et al. 2017). Thus, ALU PCR can easily accompany morphological methods to detect the rare metastatic cells of human origin in the host embryo organs and tissues. This might be critical with respect to the limited duration of the CAM experiments. We believe that this combination can increase the CAM model potential in our future research.

Melanoma cells grafted to the chicken embryo reduced their malignant potential (Díez-Torre et al. 2009). The limited invasiveness of melanoma cells to CAM and the inhibitory effect of CAM fibroblasts on the melanoma cell growth corresponds with the observation that embryonic microenvironment/embryonic stem cells exhibit distinct anticancer effects on melanoma cells by inhibiting the PI3K/AKT pathway (Kim et al. 2010; Kodet et al. 2013; Liu et al. 2013a; Wang et al. 2019). Gremlin secreted by embryonic cells as an antagonist of BMP-4 may participate in the inhibition of melanoma cell proliferation (Kim et al. 2011). Similarly, noggin and its balance with BMP proteins and nodal may also be involved in the control of melanoma cell behaviour by the embryonic microenvironment (Burstyn-Cohen et al. 2004; Sinnberg et al. 2018). Finally, embryonic stem cells may exhibit tumoricidal properties based on the FAS/FASL mechanism (Li et al. 2018).

Conclusion

CAM represents an intriguing biological model for the study of several aspects of melanoma biology. This substrate allows research oriented on the study of malignant cell adhesion to the biological membrane. It can serve well for studies of both proliferation and migration to the source of chemoattractant or to the hypoxic site (inside the grafted limb bud). The CAM model is applicable in studies of neovascularization of the tumour bed. Alternatively, it can also be useful in the context of premetastatic niches formed within the microenvironment of a living organism. On the other

hand, no signs of intravascular invasion have been detected. Moreover, tumour cells are not able to extensively invade the CAM stroma and form an invasive tumour or distant metastasis. These limitations can be due to the time restrictions of the experiments (prior to embryo hatching) or to the specific non-permissive biological properties of CAM. The CAM microenvironment is, therefore, worthy of further research in the future. The invasion of melanoma cells to CAM represents a great challenge, because the understanding of this phenomenon can be of therapeutic relevance.

Acknowledgements This research was funded by the Ministry of Education, Youth and Sports of the Czech Republic, Operational Programme Research, Development and Education, project "Centre for Tumour Ecology—Research of the Cancer Microenvironment Supporting Cancer Growth and Spread" (reg. no. CZ.02.1.01/0.0/0.0/16_019/0000785), project National Sustainability Programme II (Project BIOCEV-FAR reg. no. LQ1604), and project BIOCEV (CZ.1.05/1.1.00/02.0109). Funding from the project "The Equipment for Metabolomics and Cell Analyses," reg. No. CZ.1.05/2.1.00/19.0400, supported by the Research and Development for Innovations Operational Programme (RDIOP) co-funded by the European Regional Development Fund and the state budget of the Czech Republic was also employed, along with support from Charles University (PROGRES Q28).

References

Abbott DE, Bailey CM, Postovit LM et al (2008) The epigenetic influence of tumor and embryonic microenvironments: how different are they? Cancer Microenviron 1:13–21

Avram S, Coricovac DE, Pavel IZ et al (2017) Standardization of A375 human melanoma models on chicken embryo chorioallantoic membrane and Balb/c nude mice. Oncol Rep 38:89–99

Bailey CM, Kulesa PM (2014) Dynamic interactions between cancer cells and the embryonic microenvironment regulate cell invasion and reveal EphB6 as a metastasis suppressor. Mol Cancer Res 12:1303–1313

Bailey CM, Morrison JA, Kulesa PM (2012) Melanoma revives an embryonic migration program to promote plasticity and invasion. Pigment Cell Melanoma Res 25:573–583

Bohn W, Wiegers W, Beuttenmüller M, Traub P (1992) Species-specific recognition patterns of monoclonal antibodies directed against vimentin. Exp Cell Res 201:1–7

Burstyn-Cohen T, Stanleigh J, Sela-Donenfeld D, Kalcheim C (2004) Canonical Wnt activity regulates trunk neural crest delamination linking BMP/noggin signaling with G1/S transition. Development 131:5327–5339

Cardeli M (2011) Alu PCR. Methods Mol Biol 687:221–229

Cimpean AM, Ribatti D, Raica M (2008) The chick embryo chorioallantoic membrane as a model to study tumor metastasis. Angiogenesis 11:311–319

Cucina A, Biava PM, D'Anselmi F et al (2006) Zebrafish embryo proteins induce apoptosis in human colon cancer cells ($CaCO_2$). Apoptosis 11:1617–1628

Deryugina EI, Quigley JP (2008) Chick embryo chorioallantoic membrane model systems to study and visualize human tumor cell metastasis. Histochem Cell Biol 130:1119–1130

Díez-Torre A, Andrade R, Eguizábal C et al (2009) Reprogramming of melanoma cells by embryonic microenvironments. Int J Dev Biol 53:1563–1568

Dvořánková B, Szabo P, Kodet O et al (2017) Intercellular crosstalk in human malignant melanoma. Protoplasma 254:1143–1150

Dvořánková B, Lacina L, Smetana K Jr (2019) Isolation of normal fibroblasts and their cancer-associated counterparts (CAFs) for biomedical research. Methods Mol Biol 1879:393–406

Funakoshi K, Bagheri M, Zhou M, Suzuki R, Abe H, Akashi H (2017) Highly sensitive and specific Alu-based quantification of human cells among rodent cells. Sci Rep 7:13202

Gaustad J-V, Simonsen TG, Andersen LMK, Rofstad EK (2017) Vascular abnormalities and development of hypoxia in microscopic melanoma xenografts. J Transl Med 15(1):241

Ghaffari-Tabrizi-Wizsy N, Passegger CA, Nebel L, Krismer F, Herzer-Schneidhofer G, Schwach G, Pfragner R (2019) The avian chorioallantoic membrane as an alternative tool to study medullary thyroid cancer. Endocr Connect EC-180431.R1

Hamburger V, Hamilton HL (1992) A series of normal stages in the development of the chick embryo. 1951. Dev Dyn 195:231–272

Herrmann A, Taylor A, Murray P et al (2018) Magnetic resonance imaging for characterization of a chick embryo model of cancer cell metastases. Mol Imaging 17:1536012118809585

Jayachandran A, McKeown SJ, Woods BL et al (2015) Embryonic chicken transplantation is a promising model for studying the invasive behavior of melanoma cells. Front Oncol 5:36

Jobe NP, Rösel D, Dvořánková B et al (2016) Simultaneous blocking of IL-6 and IL-8 is sufficient to fully inhibit CAF-induced human melanoma cell invasiveness. Histochem Cell Biol 146:205–217

Jobe NP, Živicová V, Mifková A et al (2018) Fibroblasts potentiate melanoma cells in vitro invasiveness induced by UV-irradiated keratinocytes. Histochem Cell Biol 149:503–516

Kain KH, Miller JW, Jones-Paris CR et al (2014) The chick embryo as an expanding experimental model for cancer and cardiovascular research. Dev Dyn 243:216–228

Kalirai H, Shahidipour H, Coupland SE et al (2015) Use of the chick embryo model in uveal melanoma. Ocul Oncol Pathol 1:133–140

Kalyanaraman B, Cheng G, Hardy M et al (2018) A review of the basics of mitochondrial bioenergetics, metabolism, and related signaling pathways in cancer cells: therapeutic targeting of tumor mitochondria with lipophilic cationic compounds. Redox Biol 14:316–327

Kasemeier-Kulesa JC, Kulesa PM (2018) The convergent roles of CD271/p75 in neural crest-derived melanoma plasticity. Dev Biol 444:S352–S355

Kasemeier-Kulesa JC, Teddy JM, Postovit LM et al (2008) Reprogramming multipotent tumor cells with the embryonic neural crest microenvironment. Dev Dyn 237:2657–2666

Kaufman CK, Mosimann C, Fan ZP et al (2016) A zebrafish melanoma model reveals emergence of neural crest identity during melanoma initiation. Science 29:351

Kim EY, Jeon K, Park HY et al (2010) Differences between cellular and molecular profiles of induced pluripotent stem cells generated from mouse embryonic fibroblasts. Cell Reprogram 12:627–639

Kim MO, Kim SH, Oi NZ et al (2011) Embryonic stem-cell-preconditioned microenvironment induces loss of cancer cell properties in human melanoma cells. Pigment Cell Melanoma Res 24:922–931

Klepáček I, Jirsa M (1994) Vascular pattern in the chorioallantoic membrane (CAM) after laser/photosenzitive compound treatment. I. Macroscopical findings. Folia Biol (Praha) 40:141–147

Klepáček I, Seichert V, Stingl J (1986) Ultrastructure of the peripheral vascular network of the wing of the chick embryo between the second and eight day of incubation (HH Stages 18-31). Folia Morphol (Praha) 34:346–351

Klepáček I, Peterka M, Jirsa M (1999) The embryotoxicity of PDT sensitizers (Mesoporphyrin IX, Protoporphyrin IX) before and after light irradiation in chicken embryo. In Berger J (ed) Cells. KOPP České Budějovice pp 78–79

Kodet O, Dvořánková B, Krejčí E et al (2013) Cultivation-dependent plasticity of melanoma phenotype. Tumour Biol 34:3345–3355
Kodet O, Lacina L, Krejčí E et al (2015) Melanoma cells influence the differentiation pattern of human epidermal keratinocytes. Mol Cancer 14:1
Kokorin IN, Gudima OS (1968) An electron microscopic study of D. sibiricus contrasted with phosphowolframic acid. Zh Mikrobiol Epidemiol Immunobiol 45:5–8 **(in Russian)**
Kolesová H, Bartoš M, Hsieh WC et al (2018) Novel approaches to study coronary vasculature development in mice. Dev Dyn 247:1018–1027
Kong BW, Lee JY, Bottje WG et al (2011) Genome-wide differential gene expression in immortalized DF-1 chicken embryo fibroblast cell line. BMC Genom 12:571
Kosla J, Dvorak M, Cermak V (2013) Molecular analysis of the TGF-beta controlled gene expression program in chicken embryo dermal myofibroblasts. Gene 513:90–100
Kroemer G, Pouyssegur J (2008) Tumor cell metabolism: cancer's Achilles' heel. Cancer Cell 13:472–482
Lacina L, Plzak J, Kodet O et al (2015) Cancer microenvironment: what can we learn from the stem cell niche. Int J Mol Sci 16:24094–24110
Lacina L, Kodet O, Dvořánková B, Szabo P, Smetana K (2018) Ecology of melanoma cells. Histol Histoathol 33:247–254
Lacina L, Brábek J, Král V, Kodet O, Smetana K Jr (2019) Interleukin-6: a molecule with complex biological impact in cancer. Histol Histopathol 34:125–136
Lee LM, Seftor EA, Bonde G et al (2005) The fate of human malignant melanoma cells transplanted into zebrafish embryos: assessment of migration and cell division in the absence of tumor formation. Dev Dyn 233:1560–1570
Li Y, Fan Y, Xu J et al (2018) Genome-wide RNA-Seq identifies Fas/FasL-mediated tumoricidal activity of embryonic stem cells. Int J Cancer 142:1829–1841
Liu J, Huang Z, Yang L et al (2013a) Embryonic stem cells modulate the cancer-permissive microenvironment of human uveal melanoma. Theranostics 9:4764–4778
Liu M, Scanlon CS, Banerjee R et al (2013b) The histone methyltransferase EZH2 mediates tumor progression on the chick chorioallantoic membrane assay, a novel model of head and neck squamous cell carcinoma. Transl Oncol 6:273–281
Lugassy C, Barnhill RL (2007) Angiotropic melanoma and extravascular migratory metastasis: a review. Adv Anat Pathol 14:195–201
Navarro M, Carretero A, Canut L et al (1998) Injection technique and scanning electron microscopic study of the arterial pattern of the 20 gestation days (G20) rat fetus. Lab Anim 32:95–105
Nowak-Sliwinska P, Segura T, Iruela-Arispe ML (2014) The chicken chorioallantoic membrane model in biology, medicine and bioengineering. Angiogenesis 17:779–804
Nowak-Sliwinska P, Alitalo K, Allen E et al (2018) Consensus guidelines for the use and interpretation of angiogenesis assays. Angiogenesis 21:425–532
Pérez-Guijarro E, Day CP, Merlino G et al (2017) Genetically engineered mouse models of melanoma. Cancer 123(S11):2089–2103
Plzák J, Bouček J, Bandúrová V et al (2019) The head and neck squamous cell carcinoma microenvironment as a potential target for cancer therapy. Cancers 11:440
Ribatti D (2008) Chick embryo chorioallantoic membrane as a useful tool to study angiogenesis. Int Rev Cell Mol Biol 270:181–224
Ribatti D (2014) The chick embryo chorioallantoic membrane as a model for tumor biology. Exp Cell Res 328:314–324
Ribatti D (2016) The chick embryo chorioallantoic membrane (CAM). A multifaceted experimental model. Mech Dev 141:70–77
Rugh R (1948) Experimental embryology. A manual of techniques and procedures. Burgess Publishing Comp, Minneapolis
Shakhova O (2014) Neural crest stem cells in melanoma development. Curr Opin Oncol 26:215–221
Sinnberg T, Levesque MP, Krochmann J et al (2018) Wnt-signaling enhances neural crest migration of melanoma cells and induces an invasive phenotype. Mol Cancer 17:59
Stockert JC, Horobin RW, Colombo LL et al (2018) Tetrazolium salts and formazan products in cell biology: viability assessment, fluorescence imaging, and labeling perspectives. Acta Histochem 120:159–167
Strnadova K, Sandera V, Dvorankova B et al (2019) Skin aging: the dermal perspective. Clin Dermatol 37:326–335
Subauste MC, Kupriyanova TA, Conn EM et al (2009) Evaluation of metastatic and angiogenic potentials of human colon carcinoma cells in chick embryo model systems. Clin Exp Metastasis 26:1033–1047
Tomiyama L, Kamino H, Fukamachi H, Urano T (2017) Precise epitope determination of the anti-vimentin monoclonal antibody V9. Mol Med Rep 16(4):3917–3921
Wang C, Wang X, Liu J et al (2019) Embryonic stem cell microenvironment suppresses the malignancy of cutaneous melanoma cells by down-regulating PI3K/AKT pathway. Cancer Med 8:4265–4277
Xing Z, Schat KA (2000) Expression of cytokine genes in Marek's disease virus-infected chickens and chicken embryo fibroblast cultures. Immunology 100:70–76
Zijlstra A, Mellor R, Panzarella G et al (2002) A quantitative analysis of rate-limiting steps in the metastatic cascade using human-specific real-time polymerase chain reaction. Cancer Res 62:7083–7092
Živicová V, Lacina L, Mateu R et al (2017) Analysis of dermal fibroblasts isolated from neonatal and child cleft lip and adult skin: developmental implications on reconstructive surgery. Int J Mol Med 40:1323–1334

PUBLIKACE VI

Kodet O, Kučera J, **Strnadová K**, Dvořánková B, Štork J, Lacina L, Smetana K Jr. Cutaneous melanoma dissemination is dependent on the malignant cell properties and factors of intercellular crosstalk in the cancer microenvironment (Review). *Int J Oncol*. 2020 Sep;57(3):619-630. **(IF: 5.65)**

Cutaneous melanoma dissemination is dependent on the malignant cell properties and factors of intercellular crosstalk in the cancer microenvironment (Review)

ONDŘEJ KODET[1-3], JAN KUČERA[1,2], KAROLÍNA STRNADOVÁ[1,3], BARBORA DVOŘÁNKOVÁ[1,3], JIŘÍ ŠTORK[2], LUKÁŠ LACINA[1-3] and KAREL SMETANA Jr[1,3]

[1]Institute of Anatomy, First Faculty of Medicine, Charles University, 128 00 Prague 2; [2]Department of Dermatovenereology, First Faculty of Medicine, Charles University and General University Hospital, 120 00 Prague; [3]Biotechnology and Biomedicine Center of the Academy of Sciences and Charles University in Vestec (BIOCEV), First Faculty of Medicine, Charles University, 252 50 Vestec, Czech Republic

Received December 29, 2019; Accepted June 15, 2020

DOI: 10.3892/ijo.2020.5090

Abstract. The incidence of cutaneous malignant melanoma has been steadily increasing worldwide for several decades. This phenomenon seems to follow the trend observed in many types of malignancies caused by multiple significant factors, including ageing. Despite the progress in cutaneous malignant melanoma therapeutic options, the curability of advanced disease after metastasis represents a serious challenge for further research. In this review, we summarise data on the microenvironment of cutaneous malignant melanoma with emphasis on intercellular signalling during the disease progression. Malignant melanocytes with features of neural crest stem cells interact with non-malignant populations within this microenvironment. We focus on representative bioactive factors regulating this intercellular crosstalk. We describe the possible key factors and signalling cascades responsible for the high complexity of the melanoma microenvironment and its premetastatic niches. Furthermore, we present the concept of melanoma early becoming a systemic disease. This systemic effect is presented as a background for the new horizons in the therapy of cutaneous melanoma.

Correspondence to: Professor Karel Smetana Jr or Dr Lukáš Lacina, Institute of Anatomy, First Faculty of Medicine, Charles University, U Nemocnice 3, 128 00 Prague 2, Czech Republic
E-mail: karel.smetana@lf1.cuni.cz
E-mail: lukas.lacina@lf1.cuni.cz

Abbreviations: CAFs, cancer-associated fibroblasts; CMM, cutaneous malignant melanoma; EMT, epithelial to mesenchymal transition; NC, neural crest; SCs, stem cells; SMA, smooth muscle actin

Key words: melanoma, cancer microenvironment, cancer-associated fibroblast, cytokine, chemokine, growth factor

Contents

1. Introduction

Similarly to other malignant diseases, the incidence of cutaneous malignant melanoma (CMM) is increasing worldwide (1). This increased incidence seems to be influenced by many factors, including ageing of the population, behavioural habits, and climatic and environmental changes. Formation of CMM is associated with the main genetic drivers such as BRAF, NF1 and NRAS mutations, also usually associated with chronic skin sun damage (2). Aberrant activation of the RAS/BRAF/MEK/ERK signalling pathway causes uncontrolled proliferation of malignant cells in the majority of CMM (3). Melanoma causes most of the skin cancer-related deaths. The patient overall survival at five years depends on the thickness of the primary melanoma. CMM is also known for its remarkable ability to metastasise. Despite the new therapeutic options, the curability of advanced-stage melanoma is still limited. These recent therapeutic approaches modulate the immune response of the organism (e.g., via application of anti-CTLA-4 and anti-PD-1 antibodies) or target proliferation in specifically mutated melanomas (e.g., by application of BRAF or MEK inhibitors). In order to establish novel targeted melanoma therapies, it is

of fundamental importance to understand the mechanisms activated in the permissive tumour microenvironment. In particular, interactions between melanoma cells and the tissue microenvironment play key roles in the disease progression. This article summarises data on the multifaceted roles of CMM microenvironment in tumour spreading. This concept may be extended to the intravasation of bioactive molecules participating in the melanoma cell crosstalk with non-malignant cells forming the CMM microenvironment. These molecules also participate in premetastatic niche formation. Finally, their role in patient wasting is also widely discussed. The concept of CMM microenvironment as a complex system suitable for therapeutic targeting is introduced in this article.

2. Cutaneous malignant melanoma (CMM) disseminates extensively in the organism of the patient

The critical feature associated with melanoma is its enormous capability to spread and form lymph node or distant visceral metastases (Fig. 1). Almost any tissue in the patient's body can host metastatic cells, and even a small and thin primary tumour can metastasise to the entire body, leading to the death of the patient (1). Metastatic spread is a complex multistep process, as was noted almost 200 years ago by surgeon Stephen Paget, who coined the 'seed and soil' hypothesis (4). Surprisingly, cutaneous melanoma can spread to different organs without any particular predilection, and thus differs from, e.g., uveal melanoma of similar histogenesis. However, the first predictive site of metastatic disease is a lymph node. The presence of tumour cells in this lymph node is generally investigated in melanoma patients with tumours thicker than 1 mm. This procedure is routinely called sentinel lymph node biopsy. The presence of melanoma cells in the lymph node is a powerful predictor of melanoma recurrence, but not of survival, in the melanoma patients (5). VEGF-C, which is involved in lymphangiogenesis and promotes increased lymphatic vessel density, can also play a role in lymph node metastasis (6).

CMM metastasis to the lungs and brain and other visceral organs. In the case of visceral melanoma metastasis, the most predictive localisations are the lungs and pleura (7). Lung metastases are also the most frequent metastases in mouse models of metastatic melanoma (8). In these mouse models using the B16 model of melanoma, chloride channel accessory 2 (CLCA2), an extracellular protein expressed predominantly in the lung, was identified as a factor mediating interactions with α6β4-integrin, which is expressed by tumour cells (9). Brain metastases are associated with poor prognosis. Historically, melanoma patients with brain metastases have had dismal outcomes and very limited treatment options. Systemic treatment with BRAF inhibitors and immunotherapy offers therapeutic responses in up to 55-58% of patients (10). The actual mechanism of brain metastases is not clear, but mouse models point to some factors that play a role in this process. The original model suggested a role of transferrin receptors and their interaction with their ligand, transferrin, mediating metastases of melanoma cells to the brain. Another study highlighted the importance of neurotrophins and neurotrophin receptors in the process of brain-specific melanoma metastases (11).

Other common sites for melanoma metastases are the liver (up to 20% of patients), bones (11-17%), or skin and subcutaneous tissue (12).

CMM metastasis to the skin. Skin metastasis represents haematogenous dissemination of melanoma cells. Specific interactions between chemokines C-C motif chemokine receptor 10 (CCR10) and C-C motif chemokine ligand 27 (CCL27) have been determined as crucial factors in melanoma metastasis to the skin (13). CCL27 is a chemokine expressed in the epidermis by normal keratinocytes. In addition, high expression in supratumoral epidermis is associated with more prolonged melanoma-specific survival (14). Presumably, CCL27 interacts with the chemokine receptor CCR10, which is expressed in melanoma cells. Experiments with blocking antibodies to CCL27 showed inhibition of development of skin metastasis in a mouse model (15).

CMM metastasis and somatic mutations. Despite that, no specific biomarker with predictive potential to determine the metastatic site exists to date. In melanoma, there is also an observed lack of association between the site of visceral or lymph node metastasis and either the clinicopathological variant or location of the primary tumour (16). The dependence on the presence of somatic mutations has been reported. One study suggested that BRAF mutation is associated with lymph node metastasis as the first metastasis and sentinel lymph node positivity. BRAF and NRAS mutations were associated with different metastatic patterns, with metastases more frequently affecting the central nervous system and the liver. NRAS-mutated tumours formed lung metastases (17). This highlights an earlier-unexpected internal heterogeneity of the group of tumours nowadays collectively called melanoma. Although intense visceral organ-specific surveillance may be initiated in patients with tumours harbouring these somatic mutations, this does not necessarily lead to a decrease in mortality. It is not easy to understand this metastatic potency of CMM, which represents the main, frequently fatal, complication in the treatment of patients. The complexity of these mechanisms is also shown by the concept of pre-malignant melanocyte dissemination, suggesting that benign melanocytes may exist at disseminated sites in the body and may be capable of undergoing malignant progression. It is not uncommon to find benign melanocytic nevi in the lymph node during sentinel lymph node biopsy or in non-melanoma patients (up to 7% of patients) (18). These findings support the hypothesis mentioned above. It is also critically important to identify the mechanisms driving the metastatic behaviour.

CMM cells are similar to neural crest-originated stem cells. CMM cells arise after malignant transformation from pigment-producing cells called melanocytes. Melanocytes originate from the embryonic neuroectoderm structure called the neural crest (NC). NC cells are multipotent stem cells derived from the neuroectoderm that delaminate from the neural tube in early vertebrate development (in the 4th week) and migrate throughout the developing embryo. Consequently, NC cells differentiate into various cell lineages, including melanocytes (19).

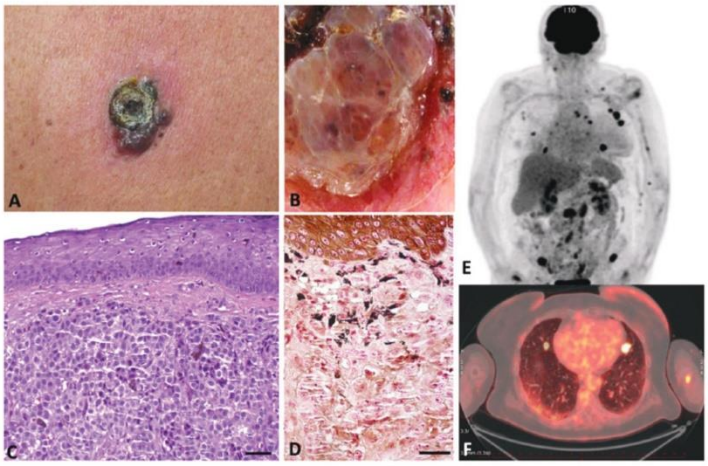

Figure 1. This figure presents the extensive capability of melanoma to form lymphatic/distant metastases in all tissues in the patient's body documented at a single patient level. (A) Primary cutaneous melanoma (Breslow thickness 6 mm) with clinical apparent ulceration in a 69-year-old female, and (B) dermoscopy of this primary cutaneous melanoma with atypical black dots, dotted vessels and erythema in regression areas. (C) The same primary tumour stained with H&E, magnification, x200. (D) After staining with Fontana-Masson (melanin), dark black granules of melanin in melanoma are visualised; magnification, x400. (E) PET-CT scan shows generalisation of the tumour to the lung, bones, lymph nodes, and soft tissue. (F) Horizontal section of PET-CT scan demonstrates metastasis in the lung and left humerus. The images were kindly provided by the Department of Dermatovenereology, First Faculty of Medicine, Charles University with explicit informed consent.

NC cells are unique because of their remarkably broad differentiation potential (Table I) (20-22). Once they have reached the final tissue niche in the skin, NC cells differentiate to melanocytes by a cascade of events controlled by transcription factors such as microphthalmia-associated transcription factor (MITF) and sex-determining region Y-box 10 (Sox10). This process occurs during the prenatal period of human development (23,24). The signalling molecules and transcription factors that are required for NC cell specification, migration and differentiation form a highly orchestrated gene regulatory network. Every individual signalling molecule has either individual or combinatorial roles in transcriptional regulation (25). The precise understanding of this mechanism seems to be critically important because similar pathways are activated in malignancy, and they could control the biological properties of malignant CMM cells (26). The signalling pathways regulating epithelial to mesenchymal transition (EMT) can be triggered by transcription factors that are active in both NC development and cancer progression (27).

Interestingly, both melanoblasts and NC cells also reside in the bulge region of the hair follicle in the outer root sheath. In this highly specialised niche, NC cells retain their multipotency during adult life. NC cells can be isolated and expanded *in vitro* with the remarkable features of highly multipotent stem cells (SCs). It is possible to differentiate NC cells to various specialised cell types such as melanocytes, adipocytes, osteoblasts, chondroblasts, smooth muscle cells, neurons, and Schwann cells (28). The NC cell phenotype is defined by expression of multiple markers, and NC cell identification cannot be based on a single molecule. Of note, there is a significant overlap with the marker profile of CMM [Table II based on (29-37)]. This highlights the low differentiation frequently observed in melanoma, where many cells typically have properties of stem cells (37). These cancer-initiating cells of CMM have an indispensable role in CMM resistance to therapy, progression and generalisation (38).

The life-long postnatal presence of NC cells in hair follicles raises important questions regarding the maintenance of their multipotency and regulation of their normal behaviour within this niche. There is strong evidence that the microenvironment is a critical condition of this steady-state. The signalling cues within the proper microenvironment, via both extrinsic and intrinsic factors, orchestrate the interplay necessary for healthy tissue dynamics. The importance of the normal tissue microenvironment was highlighted in several studies using transplantation of malignant cells to animal embryos. In experiments performed in the early chicken embryo, labelled CMM cells were injected into the region of the neural tube. It was demonstrated that melanoma cells migrate to the same regions as the autologous embryonic NC cells (39). Similar experiments performed later in zebrafish embryos supported these findings. Both the embryonic NC cells and the cells of CMM in zebrafish express specific protein crestin, which is absent in normal melanocytes (40).

Taking into account the low differentiation status of NC cells and their natural migratory activity, the similarity of CMM and NC cells can also explain the highly metastatic behaviour observed in melanoma in the clinic.

Circulating CMM cells in disease dissemination. Similarly to other types of malignant tumours, cells of CMM can also be detected in the circulation. These circulating melanoma

Table I. Examples of cells originated from neural crest cells.

Cell type	Specification
Peripheral neurons	Sensory, sympathetic + parasympathetic ganglia
Glial cells	Schwann cells
Merkel cells	Mechanoreceptor function
Parafollicular cells	Production of calcitonin
Adrenal medullar cells	Chromaffin cells
Osteoblasts/odontoblasts	Facial skeleton
Chondroblasts	Facial skeleton
Myoblasts	Striated/smooth-facial region
Dental pulp cells	Multipotent stem cell potential
Fibroblast/mesenchymal cells	Facial region
Cornea	Stromal cells
Melanocytes	All parts of the body

Table II. Comparison of markers of hair follicle NC SCs and CMM cells.

Factor	NC SCs	CMM cells
BMP4[a]	+	+
SNAIL[a]	+	+
SLUG[a]	+	+
SOX9[a]	+	+
TWIST[a]	+	+
MITF[b]	+	+
Desmin[c]	+	+/-
Calponin[c]	+	+/-
β-III tubulin[d]	+	+

[a]NC marker, [b]melanocyte progenitor marker, [c]smooth muscle differentiation marker, [d]neuronal marker. NC, neural crest; SCs, stem cells; CMM, cutaneous malignant melanoma; BMP3, bone morphogenetic protein 3; SOX9, SRY-box transcription factor 9; MITF, microphthalmia-associated transcription factor. Based on Person *et al* (29), Stasiak *et al* (30), Yang *et al* (31), Lee *et al* (32), Tudrej *et al* (33), Iwakami *et al* (34), Goding and Arnheiter (35), Campbell *et al* (36), Krejčí and Grim (37).

cells harbour the functional properties of cells of the primary tumour, including their SC-like properties (41,42). These cells leave the primary tumour and penetrate the vessels and use them as a highway for dissemination through the patient's body to target the organ/tissue where they form metastases. Using an identical vascular path, the normal adult tissue SCs can migrate in order to facilitate body repair processes during wound healing (43,44). From this point of view and based on histological/molecular similarity, cancer again resembles wound healing. With a certain hyperbole, cancer can be seen as a distorted cascade of wound repair events (45). These data can also predict the great invasive metastatic potential of CMM.

3. The microenvironment of CMM participates in the control of its invasive potential

Melanoma is a complex ecosystem. Malignant cells define the type of tumour. However, there are other non-cancerous populations forming the tumour stroma. It is the interaction of both components of this microenvironment that finally defines the biological behaviour of the tumour. It is truly applicable to solid tumours in general, and CMM is no exception (46-48). Concerning CMM, the cancer microenvironment is formed by cancer-associated fibroblasts (CAFs) and several types of leukocytes, as comprehensively reviewed by Lacina *et al* (49) (Fig. 2A).

The origin of CAFs is not fully understood. Local normal dermal fibroblasts, attracted mesenchymal SCs and pericytes are frequently mentioned as source cell populations from which CAFs are recruited (50). However, the transition of cancer cells to CAFs cannot be entirely excluded, although its likeliness is not very high. This fact is difficult to prove in the experimental model (51).

Treg lymphocytes, tumour-associated macrophages and myeloid-derived immunosuppressive cells stimulating the CMM progression, as well as NK cells, macrophages and CD8-positive T lymphocytes, are attracted to the CMM site. Interestingly, CAFs stimulate the activity of immune cells supporting melanoma cells and inhibit the cancer-suppressing cells (52,53).

Unlike in other epidermal tumours, keratinocytes are also an important component of the CMM microenvironment. Melanoma cells can stimulate surrounding keratinocytes (54). On the other hand, keratinocytes control growth and differentiation of melanocytes and potentiate the invasiveness of melanoma cells during early progression as observed in a reconstructed skin model (55).

Role of intercellular contact. Cell-cell adhesion molecules (cadherins) and cell-extracellular matrix adhesion proteins (integrins) play a critical role in the regulation of cancer invasion and metastasis. Many members of the cadherin superfamily play an important role in cancer biology. However, the most significant explanation is seen in the E-/N-cadherin switch, and its role in epithelial to mesenchymal transition (EMT), in cancer progression. N-cadherin expression in CMM cells helps cancer cells to interact with fibroblasts and extracellular matrix and stimulates the invasive potential of melanoma cells and their proliferation, but also activation of PI3/AKT, mTOR, and ERK kinase. Inhibition of N-cadherin represents an interesting possibility, with potential clinical use (56).

Intercellular contacts of normal melanocytes, or malignant melanoma cells, respectively, and their non-cancerous neighbours within the tissue environment influence their properties mutually (62). Keratinocytes reduce expression of N-cadherin not only via cell-cell contacts, but also via cell-derived extracellular matrix and conditioned medium with calcium regulators (57). These findings support the importance of the balance in communications between melanoma cells and non-cancerous cells in the melanoma microenvironment.

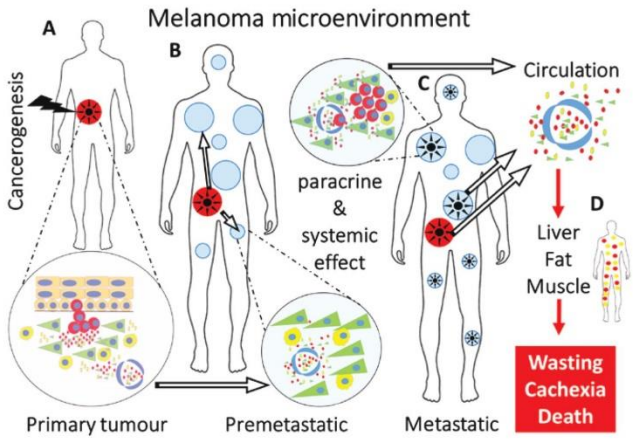

Figure 2. The figure demonstrates the paracrine and systemic effect of CMM during progression. (A) Once initiated, the tumour growths and via paracrine signalling influences surrounding non-cancerous tissues (detail in the pink-filled circle). This paracrine interaction strengthens the malignant potential of CMM. However, signalling molecules diffuse and also leak to the circulation via capillaries. (B) Exposed to the released cytokines, chemokines and growth factors, the normal distant tissues become activated and form premetastatic niches (detail in the blue-filled circle). This is an early systemic effect of the primary tumour. (C) In some of these niches, the metastasising malignant cells will harbour and initiate a metastatic tumour (detail in the blue-filled circle). The concentration of circulating bioactive molecules is further enhanced by their production in metastases. This represents a later systemic effect typical of generalised malignancies. (D) Circulating bioactive molecules induce physical and functional organ changes. This consequently results in wasting, cachexia and death. CMM, cutaneous malignant melanoma.

Integrins β1 and β3, as adhesion cell-extracellular matrix proteins, are differentially expressed during the transformation of melanoma radial growth to the vertical invasion (58,59). The differentiation status of melanoma cells and the ability to invade the surrounding tissue also highlights this impact. For example, the expression of connexin-43 in CMM cells indicates the ability of CMM cells to metastasise (52,60,61). Expression of desmoglein-2, which participates in the contacts with keratinocytes, has an inhibitory effect on CMM cell migration.

On the other hand, the expression of desmoglein-2 promotes the vasculogenic mimicry of CMM cells, which is associated with a poor outcome of patients (62,63). Furthermore, in melanoma cells that do not express β3 integrins, β1 integrins instead play a role in promoting their transendothelial migration by binding to vascular cell adhesion molecule 1 (VCAM-1) (64). Integrins also play an important role in connecting the extracellular matrix with the melanocyte and melanoma cell cytoskeleton. Cytoskeletal rearrangements, such as the increase of the overall contractility, impact cell mechanical properties and cell deformability. These changes may then potentiate prometastatic phenotypes of melanoma cells. Expression of αvβ3 integrin increases elasticity in human melanoma cells in adherent and non-adherent conditions (65). Intercellular contacts and molecules play an important role in the mechanisms of targeted therapy. Targeting of the CMM cell surface receptor Notch-dependent pathway improves the activity of Erk inhibitors in BRAF-V600E mutated tumours. Further, it can be combined with inhibition of ERBB3 to suppress melanoma cell growth (63). On the other hand, Notch expression in CAFs reduces the growth and migration potential of melanoma cells (66).

Role of paracrine signalling in communication across the CMM microenvironment. The paracrine mode of signalling between cancerous and non-cancerous cells in CMM has been extensively studied (Fig. 2B and C). For example, CAFs, keratinocytes and infiltrating immune cells produce a variety of growth factors/cytokines/chemokines that significantly influence the biological properties of malignant CMM cells (67,68) (Table III). Interestingly, many of these factors are also associated with skin ageing. Collectively, these bioactive molecules are called the senescence-associated secretome (69). As expected, chemokines attract inflammatory cells to the tumour site. However, they also have multiple other functions (70). CMM cells express receptors for CXCL1 and interleukin (IL)8, and these factors enhance their invasiveness (71,72). Antagonists of CXCR1/2 receptors have a well-documented inhibitory effect on migration of CMM cells (73). The IL8 chemokine also stimulates vascularisation of CMM (74,75), and in general, its high expression indicates poor prognosis of CMM patients (76).

Expression of chemokine CXCL16 seems to participate in the malignant transformation of a melanocytic nevus to CMM (77). Activation of CXCR6 recognising this chemokine induces SC-like properties in CMM cells and initiates their migration (78).

IL1β is predominantly produced by macrophages. It participates in the progression of CMM in collaboration with IL8 and caspase recruitment domain family member 8 (CARD8) (79).

IL6 is a crucial factor initiating the immune response. IL6 has a multifaceted role in cancer progression (80). While the initial stage of CMM growth can be inhibited by IL6 (81), the more advanced stages are associated with production of

Table III. Examples of factors produced by CAFs, Kerat and melanoma cells in CMM.

Symbol	Gene name	CAFs	Kerat	CMM cells
IL8	Interleukin 8	+	+	+
CXCL1	Chemokine (C-X-C motif) ligand 1 (melanoma growth stimulating activity α)	+	-	-
CXCL16	Chemokine (C-X-C motif) ligand 16	+	-	+
IL1B	Interleukin 1β	+	-	-
IL6	Interleukin 6	+	+	+
IL17D	Interleukin 17D	+	-	+
ACAN	Aggrecan	+	+	+
HBEGF	Heparin-binding EGF-like growth factor	+	+	-
BDNF	Brain-derived neurotrophic factor	-	-	+
TGFB2	Transforming growth factor, β2	-	-	+
IGFBP7	Insulin-like growth factor binding protein-7	+	+	-
GAP43	Growth associated protein 43	+	+	-
BMP2	Bone morphogenetic protein 2	+	-	+
BMP6	Bone morphogenetic protein 6	+	-	-
VEGFA	Vascular endothelial factor A	+	+	+
VEGFC	Vascular endothelial factor C	+	+	+
CTGF	Connective tissue growth factor	+	-	+
PDGFRL	Platelet-derived growth factor receptor-like	+	-	+
LEPRE1	Leucine proline-enriched proteoglycan (Leprecan)	+	-	-
LEPREL1	Leprecan-like 1	+	-	+
KAZALD1	Kazal-type serine peptidase inhibitor domain 1	+	-	-

CAFs, cancer-associated fibroblasts; CMM, cutaneous malignant melanoma; Kerat, keratinocytes. Based on Kodet *et al* (54), Jobe *et al* (67).

this interleukin (82,83). IL6, frequently in cooperation with IL8, exhibits an additive effect on WNT5A in the stimulation of CMM cell invasiveness (67,84). IL6 induces Twist and N-cadherin expression in CMM angiogenesis in a mechanism dependent on the p50 subunit of nuclear factor κB (85).

In general, IL17D (IL27) has an anti-tumoral effect in CMM (86), where it participates in generating tumour-specific cytotoxic T cells (87). The effect of IL17D on CMM cells seems to be TRAIL-dependent (88). On the other hand, it is also known as a potent inducer of the production of IL6 and IL8 in endothelial cells. It is highly expressed in the initial stages of CMM (89), stimulating the CMM growth and tumour vascularisation.

Glycoprotein aggrecan is produced by cells of the CMM, CAFs and keratinocytes. It is usually secreted during the process of chondroblast differentiation, and it has an inhibitory effect on CMM progression (90). A similar anti-CMM effect is produced by insulin-like growth factor-binding protein 7 (IGFBP-7), namely in BRAF-mutated V600E-positive dysplastic nevi (91). On the other hand, heparin-binding EGF-like growth factor has a stimulatory impact on CMM growth (92). The same result was described in the case of another growth factor, neurotrophin (93,94). miRNA-328 controls production of TGF-β2, and attenuation of its expression has a strong inhibitory effect on CMM cell proliferation (95). VEGFA and VEGFC are generally responsible for the activation of CMM neovascularisation by blood/lymphatic vessels that support the CMM growth and progression. Connective tissue growth factor has a synergistic effect on VEGFA and stimulates the tumour site neovascularisation (96).

As mentioned earlier, CAFs do not support tumour growth and metastases exclusively. CAFs are also implicated in the acquisition of resistance to the targeted therapy in BRAF-mutated melanomas. Under the influence of BRAF inhibitors, CAFs secrete factors that contribute to CMM cell survival and melanoma resistance. CAFs release factors such as hepatocyte growth factor (HGF) and neuregulin 1 (NRG1), which can trigger alternative cascades in MAP kinase signalling (97,98).

The short overview in Table III demonstrates the complexity of signalling between CMM cells and non-cancerous cells, where intercellular contacts, cytokines, chemokines, and growth factors with both the stimulatory and inhibitory effect influence the tumour growth and generalisation.

Concluding this paragraph, paracrine signalling represents a critical aspect in the control of biological properties of CMM. In addition to the crosstalk between melanoma cells, this process includes an exchange of information between CMM cells and non-malignant cells of the microenvironment.

Role of exosomes. In addition to paracrine signalling via soluble products, exosomes represent another tool of CMM cell communication with non-cancerous partners within the microenvironment. All affected cell populations of the cancer microenvironment produce these bodies. Exosomes thus influence CMM cell biological properties (99).

Exosomes stimulate CMM cell metastasis via support of the epithelial-mesenchymal transition. Exosomes influence vascularisation of the lymph node in order to prepare the vascular bed for the metastasising (100,101). Exosomes significantly participate in the regulation of local invasiveness and also in the entrance of melanoma cells to the target organs (102). This effect is frequently associated with the presence of miRNAs in CMM-derived exosomes. It was confirmed both *in vitro* and *in vivo* in clinical material (103). Exosomes exert a robust immunosuppressive effect on the cancer microenvironment, where they inhibit IL2-dependent proliferation of CD8-positive T lymphocytes (104). Moreover, CMM exosomal miRNA-125b-5p induces a tumour-promoting phenotype in macrophages (105). These changes can induce a mixed M1, and M2 tumour-promoting macrophage activation included production of CCL22, IL-12B, IL-1β, IL-6, i-NOS, and TNF-α (106). These data highlight exosomes as a critically important component of the CMM microenvironment significantly participating in its biological properties, with the ability to stimulate the immune response of the melanoma microenvironment.

4. Differences in serum proteins between CMM patients and healthy individuals

Serological biomarkers represent a diverse group of biomolecules with importance in diagnosis, staging, and monitoring the therapeutic response. Serum lactate dehydrogenase (LDH) is the only serum biomarker that has been accepted as a prognostic biomarker for routine clinical use in melanoma patients with a predictive therapeutic outcome and has been implemented in the American Joint Committee on Cancer (8th edition) staging system (107). Routinely used S100B (S100 calcium binding protein B) protein is highly specific for melanoma patients. Its increased levels can be detected in patients with advanced melanoma during melanoma prognosis (108). Another serological protein is MIA (melanoma inhibitory activity), which interacts with extracellular matrix proteins. Its expression can also be detected in normal tissue such as cartilage. In pathological processes, its overexpression is observed in breast cancer or colorectal cancer, in addition to melanoma (109).

Introduction of a new treatment strategy for advanced melanoma leads to the search for new biomarkers to improve both prognostic and predictive outcome. Likely, the high intensity of molecular exchange between cancer cells and other members of the microenvironment via cytokines, chemokines and growth factors can lead to leakage out from the tumour microenvironment, and mediators can be consequently detected in systemic circulations in the serum (110,111) (Fig. 2A-D). Therapy by monoclonal antibodies targeting immune checkpoint inhibitors is one of the most potent treatments of CMM patients. Measurement of current concentrations and dynamics of these mediators in the serum can have the potential of liquid biopsy. Indeed, the serum protein signature even reflects the efficiency of anti-PD-1 therapy of CMM patients and can be substantial for therapeutic indications (112).

Similarly to other types of tumours, an elevated serum level of IL6 in CMM has been observed (111), which has reached some prognostic validity (113). Serum elevation of IL6 sensibly reflected the tumour burden and indicated a relapse of the disease or insensitivity to tumour therapy in several studies (114-116).

A similar finding was observed in the case of serum levels of IL8 (71,117,118). Interestingly, the levels of IL6, IL8, and VEGFA correlated with the level of Breslow index at the time of diagnosis (117,119). Moreover, the amount of VEGFA also depended on the stage of the disease (120). As IL8 also supports CMM neovascularisation, it is not surprising that the elevation of the serum level of both IL8 and VEGFA correlates with the progression of the disease and poor survival of CMM patients (121). Proteins of the TGF-β family are also elevated in the sera of CMM patients, and the prognostic relevance of these factors has been proposed (122). Elevated concentration of factors with immunomodulatory activity such as IL6 and/IL10 influence the presence of self-renewal tumour-initiating (stem) cells in CMM (123).

Serum protein imbalance influences premetastatic niche formation. Based on the selected examples, it is possible to demonstrate the systemic effect of CMM. The serum/plasma of CMM patients contains numerous bioactive proteins and exosomes that are transported to the distant parts of the patient's body through the vessels (Fig. 2B-D). These factors participate in the preparation of a premetastatic niche suitable for cancer cell homing and metastasis formation (124). Under the influence of CMM-derived exosomes, the dermal fibroblasts reprogram their metabolism significantly (125). The distant dermal fibroblasts from CMM patients at the stage of metastatic tumour dissemination differ from the normal dermal fibroblasts from healthy donors. The phenotype of distant dermal fibroblasts, as well as the expression profile and methylation profile of gene promoters, is shifted closer to CAFs (126). Due to this activation, it is possible to hypothesise that the tissue microenvironment in the distant body parts is influenced by the released bioactive factors from the melanoma microenvironment. It is, therefore, likely that melanoma becomes a systemic disease very early. If so, it is the signalling in the primary tumour that already prepares the rest of the organism to host CMM cells and facilitate metastases (114) (Fig. 2B).

5. Intravasation and extravasation of CMM cells and their inhibition via migrastatics

In recent years, the term 'migrastatics' has been introduced for drugs interfering with all modes of cancer cell invasion (115). Migrastatics inhibit local invasion and consequent metastasis. This group of drugs was recently established to define and distinguish them from conventional cytostatic drugs that traditionally target cell proliferation. Malignant melanoma, therefore, seems to be a tempting disease for validation of this concept.

Endothelial cells of capillaries are also an important structure of the cancer microenvironment. Migrating CMM cells adhere to the capillary endothelium, intercalate between endothelial cells, and migrate throughout the vessels in both directions. From the endothelial cell perspective, this process is not passive. Endothelial cells actively participate in extravasation, where the role of N-cadherin has been broadly

investigated (117). It seems to be also controlled by CD146, which cooperates with VEGFA. CD146 is also elevated in the patients' serum/plasma (127).

On the other hand, VE-cadherin expressed on the surface of endothelial cells prevents the migration of cancer cells through the endothelium of capillaries. VE-cadherin must, therefore, be eliminated from the site of malignant cell migration (128). P-selectin has an essential role in the recruitment of inflammatory cells to the site of inflammation, so-called homing.

P-selectin expression on endothelial cells is under the control of the local microenvironment. Expression of this molecule on endothelial cells and blood platelets seems to be a prerequisite for successful metastasising of CMM cells to the target tissue (129,130). P-selectin expression on the surface of endothelial cells is induced by STAT3 activation (129). IL6 is available in the serum of CMM patients, and it is known as a potent activator of STAT3. The observation that capsular polysaccharides from E. coli attenuate adhesion of CMM cells to the endothelium via P-selectin demonstrates the specificity of this interaction (130). Endogenous lectin galectin-3 locally accumulates in inflamed tissues, including endothelium. This lectin also enhances invasion of CMM cells, e.g., to the lungs (131). These examples show that an imbalance in serum proteins can participate in the process of extravasation of CMM cells to the target tissue and metastasising.

Therefore, the combination of migrastatics with other groups of traditional oncologic drugs may be possible. Beyond that, we suggest that directed therapy (biologics, small-molecule receptor-associated kinase inhibitors) against the most prominent inflammatory cytokines, namely IL6, could bring highly desirable synergism. However, it seems evident that inhibition of the IL6 signalling axis is not sufficient and must, therefore, be accompanied by simultaneous blockade of other proteins/receptors such as IL8, VEGFA and MFGE8 (48,132). The therapeutic blockade of IL6, in combination with checkpoint inhibitor anti-PD1, represents an interesting possibility of overcoming some immunological mechanisms of resistance. IL6 blockade upregulated expression of PD-L1 on melanoma cells in a mouse model and may sensitise melanoma to this treatment (133). These findings underscore the importance of the IL6-PD1/PD-L1 crosstalk in the tumour microenvironment of melanoma.

The local microenvironment and its control by bioactive factors can be a highly relevant target in the prevention of the deadly complication of malignant disease (Fig. 2D).

6. Cancer-associated wasting and cachexia as a terminal complication of CMM; clinically relevant complications are also associated with factors of intercellular crosstalk

Advanced stages of cancer, including CMM, are associated with metastasising, which in the case of CMM has a character of extensive generalisation. The increasing burden of tumour cells generates an imbalance in growth factors, cytokines and chemokines, among which IL6 seems to have the leading position (80). This stage of the disease is usually terminated by cancer-associated cachexia (CAC), which affects approximately 16 patients per 100,000 individuals (134) (Fig. 2D). CAC is a highly complex and multifaceted catabolic process (135). IL6, in cooperation with TNFα and IL1β influences the metabolism of striated muscle fibres, adipocytes and hepatocytes (136,137). The level of the mentioned factors in the serum can even predict the onset of CAC and survival of cancer patients (138). The terminal stage of cancer is also associated with decreased food intake in cancer patients, which is called anorexia (139). IL6 seems to be linked to the control of food intake, where it inhibits the appetite and participates in the development of anorexia (140). TNFα and IL6 can cross the blood-brain barrier (141). TNFα, IL1 and IL6 can interact with hypothalamic neurons and affect the serotoninergic metabolism, which can be reflected by decreased food intake (142). Patients with advanced cancer frequently suffer from depression that seems to be associated with elevation of IL6, IL10 and TNFα (143). On the other hand, the serum levels of IL6 (and also IL8) are significantly elevated in tumour-free patients with bipolar disease, but not with major depressive disorder (144). This section demonstrates that factors produced by the cancer ecosystem have a strong systemic effect by which they influence the metabolic functions of cancer patients, resulting in wasting and death.

7. Conclusion

CMM, similarly to the majority of cancers, can be characterised as a genetic abnormality and a regulation failure in which cancer cells employ predestined pathophysiological pathways that are normally activated in the course of organism growth, tissue regeneration and repair. This deregulation is typically associated with accumulation of mutations acquired during the ageing of the individual.

The progression of CMM from tumour initiation to the systemic effect on the patient's metabolism is organised according to a quite uniform scenario (Fig. 2A-D). The intercellular crosstalk within this ecosystem is mediated either directly by intercellular contacts, or indirectly by paracrine secretion of numerous active molecules. This interconnection strengthens the malignant potential of cancer cells, and it can inhibit the anticancer immune response or protect malignant cells from the harmful effect of oncological therapy. A plethora of bioactive factors are transported via vessels and significantly influence even the distant tissue. Collectively, these factors prepare a suitable microenvironment for the malignant cell extravasation and metastasising, the premetastatic niche. The increasing mass of CMM cells in the body of patients generates a cancer-induced profile of inflammatory mediators in the patients' serum. The systemic availability of these bioactive molecules triggers mental disorders, depression, and mental anorexia-associated problems with food intake. Wasting leads to cancer cachexia and death. Based on this scenario, it is evident that besides the conventional anticancer therapy, it would be necessary to influence the migration of CMM cells and their metastasising - the concept of migrastatics (115). Because the CMM microenvironment stimulates malignant cell invasiveness (145), targeting both cancerous and non-cancerous cells of the tumour ecosystem and their products seems to be a promising approach. IL6 and its signalling pathway influence CMM cell growth and migration, but it can also

positively affect the entire patient metabolism and mental status (82). Therefore, targeting the IL6/IL6R/STAT3 axis as a new therapeutic modality was enthusiastically expected, but, unfortunately, the reality did not meet this expectation (146). The progress in the detection of clinically relevant markers using a robust omics approach that includes stromal factors can be translated into personalised therapy of CMM (147). For example, a combination of blocking the anti-IL6 axis with drugs blocking other signalling pathways seems to be promising for future trials (48). It can be hypothesised that the progress in diagnostics and therapy covering the complex ecosystem of melanoma can bring some benefit to CMM patients.

Acknowledgements

Authors are grateful to Dr Šárka Takáčová for her assistance in English language editing of this revised version.

Funding

The project 'Centre for Tumour Ecology-Research of the Cancer Microenvironment Supporting Cancer Growth and Spread' (reg. no. CZ.02.1.01/0.0/0.0/16_019/0000785) is supported by the Operational Programme 'Research, Development and Education'. Additional support was received from the Ministry of Education, Youth and Sports of CR within the National Sustainability Programme II (Project BIOCEV-FAR, reg. no. LQ1604), project BIOCEV (CZ.1.05/1.1.00/02.0109), grant no. CZ.1.05/2.1.00/19.0400 supported by the Research and Development for Innovations Operational Programme, co-financed by the European Regional Development Fund and the state budget of the Czech Republic, from the Grant Agency of the Czech Republic, project no. 19-05048S and from Charles University project PROGRES Q28.

Availability of data and materials

All data and information are supported by relevant references.

Authors' contributions

Conceptualisation, data collection and manuscript preparation were carried out by KSm, OK and LL. Manuscript preparation was conducted by JK, JŠ, KSt and BD.

Ethics approval and consent to participate

Not applicable.

Patient consent for publication

The images in Fig. 1 were kindly provided by the Department of Dermatovenereology, First Faculty of Medicine, Charles University with explicit informed consent.

Competing interests

The authors declare no competing interests.

References

1. Sacchetto L, Zanetti R, Comber H, Bouchardy C, Brewster DH, Broganelli P, Chirlaque MD, Coza D, Galceran J, Gavin A, *et al*: Trends in incidence of thick, thin and in situ melanoma in Europe. Eur J Cancer 92: 108-118, 2018.
2. Rabbie R, Ferguson P, Molina-Aguilar C, Adams DJ and Robles-Espinoza CD: Melanoma subtypes: Genomic profiles, prognostic molecular markers and therapeutic possibilities. J Pathol 247: 539-551, 2019.
3. Lorentzen HF: Targeted therapy for malignant melanoma. Curr Opin Pharmacol 46: 116-121, 2019.
4. Paget S: The distribution of secondary growths in cancer of the breast. Lancet 133: 571-573, 1889.
5. Faries MB, Thompson JF, Cochran AJ, Andtbacka RH, Mozzillo N, Zager JS, Jahkola T, Bowles TL, Testori A, Beitsch PD, *et al*: Completion dissection or observation for sentinel-node metastasis in melanoma. N Engl J Med 376: 2211-2222, 2017.
6. Nathanson SD: Insights into the mechanisms of lymph node metastasis. Cancer 98: 413-423, 2003.
7. Barth A, Wanek LA and Morton DL: Prognostic factors in 1,521 melanoma patients with distant metastases. J Am Coll Surg 181: 193-201, 1995.
8. Damsky WE Jr and Bosenberg M: Mouse melanoma models and cell lines. Pigment Cell Melanoma Res 23: 853-859, 2010.
9. Abdel-Ghany M, Cheng HC, Elble RC and Pauli BU: The breast cancer β 4 integrin and endothelial human CLCA2 mediate lung metastasis. J Biol Chem 276: 25438-25446, 2001.
10. Tawbi HA, Boutros C, Kok D, Robert C and McArthur G: New era in the management of melanoma brain metastases. Am Soc Clin Oncol Educ Book 38: 741-750, 2018.
11. Menter DG, Herrmann JL and Nicolson GL: The role of trophic factors and autocrine/paracrine growth factors in brain metastasis. Clin Exp Metastasis 13: 67-88, 1995.
12. Balch CM, Houghton AN, Sober AJ and Soong S: Cutaneous Melanoma, 4th Edition. Dermatologic Surg 31: 1715-1715, 2005.
13. Murakami T, Cardones AR and Hwang ST: Chemokine receptors and melanoma metastasis. J Dermatol Sci 36: 71-78, 2004.
14. Martinez-Rodriguez M, Thompson AK and Monteagudo C: High CCL27 immunoreactivity in 'supratumoral' epidermis correlates with better prognosis in patients with cutaneous malignant melanoma. J Clin Pathol 70: 15-19, 2017.
15. Ben-Baruch A: Organ selectivity in metastasis: Regulation by chemokines and their receptors. Clin Exp Metastasis 25: 345-356, 2008.
16. Marcoval J, Ferreres JR, Martín C, Gómez S, Penín RM, Ochoa de Olza M and Fabra A: Patterns of Visceral Metastasis in Cutaneous Melanoma: A Descriptive Study. Actas Dermosifiliog 104: 593-597, 2013.
17. Adler NR, Wolfe R, Kelly JW, Haydon A, McArthur GA, McLean CA and Mar VJ: Tumour mutation status and sites of metastasis in patients with cutaneous melanoma. Br J Cancer 117: 1026-1035, 2017.
18. Holt JB, Sangueza OP, Levine EA, Shen P, Bergman S, Geisinger KR and Creager AJ: Nodal melanocytic nevi in sentinel lymph nodes. Correlation with melanoma-associated cutaneous nevi. Am J Clin Pathol 121: 58-63, 2004.
19. Ji Y, Hao H, Reynolds K, McMahon M and Zhou CJ: Wnt signaling in neural crest ontogenesis and oncogenesis. Cells 8: 1173, 2019.
20. Lim J, Thiery JP, Kassem Y, Kalcheim C, Moens CB, Burden SJ and Granato M: Epithelial-mesenchymal transitions: Insights from development. Development 139: 3471-3486, 2012.
21. Mayor R and Theveneau E: The neural crest. Development 140: 2247-2251, 2013.
22. Hall BK: The neural crest and neural crest cells: Discovery and significance for theories of embryonic organization. J Biosci 33: 781-793, 2008.
23. Mort RL, Jackson IJ and Patton EE: The melanocyte lineage in development and disease. Development 142: 620-632, 2015.
24. Duband JL, Monier F, Delannet M and Newgreen D: Epithelium-mesenchyme transition during neural crest development. Acta Anat (Basel) 154: 63-78, 1995.
25. Vega-Lopez GA, Cerrizuela S and Aybar MJ: Trunk neural crest cells: Formation, migration and beyond. Int J Dev Biol 61: 5-15, 2017.
26. Larribère L and Utikal J: Stem cell-derived models of neural crest are essential to understand melanoma progression and therapy resistance. Front Mol Neurosci 12: 111, 2019.

27. Gallik KL, Treffy RW, Nacke LM, Ahsan K, Rocha M, Green-Saxena A and Saxena A: Neural crest and cancer: Divergent travelers on similar paths. Mech Dev 148: 89-99, 2017.
28. Sieber-Blum M and Grim M: The adult hair follicle: Cradle for pluripotent neural crest stem cells. Birth Defects Res C Embryo Today 72: 162-172, 2004.
29. Person F, Wilczak W, Hube-Magg C, Burdelski C, Möller-Koop C, Simon R, Noriega M, Sauter G, Steurer S, Burdak-Rothkamm S, *et al*: Prevalence of βIII-tubulin (TUBB3) expression in human normal tissues and cancers. Tumour Biol 39: 1010428317712166, 2017.
30. Stasiak M, Boncela J, Perreau C, Karamanou K, Chatron-Colliet A, Proult I, Przygodzka P, Chakravarti S, Maquart FX, Kowalska MA, *et al*: Lumican inhibits SNAIL-induced melanoma cell migration specifically by blocking MMP-14 activity. PLoS One 11: e0150226, 2016.
31. Yang X, Liang R, Liu C, Liu JA, Cheung MPL, Liu X, Man OY, Guan XY, Lung HL and Cheung M: SOX9 is a dose-dependent metastatic fate determinant in melanoma. J Exp Clin Cancer Res 38: 17, 2019.
32. Lee H, Torres FX, McLean SA, Chen R and Lee MW: Immunophenotypic heterogeneity of primary sinonasal melanoma with aberrant expression of neuroendocrine markers and calponin. Appl Immunohistochem Mol Morphol 19: 48-53, 2011.
33. Tudrej KB, Czepielewska E and Kozłowska-Wojciechowska M: SOX10-MITF pathway activity in melanoma cells. Arch Med Sci 13: 1493-1503, 2017.
34. Iwakami Y, Yokoyama S, Watanabe K and Hayakawa Y: STAM-binding protein regulates melanoma metastasis through SLUG stabilization. Biochem Biophys Res Commun 507: 484-488, 2018.
35. Goding CR and Arnheiter H: MITF-the first 25 years. Genes Dev 33: 983-1007, 2019.
36. Campbell K, Kumarapeli AR, Gokden N, Cox RM, Hutchins L and Gardner JM: Metastatic melanoma with dedifferentiation and extensive rhabdomyosarcomatous heterologous component. J Cutan Pathol 45: 360-364, 2018.
37. Krejčí E and Grim M: Isolation and characterization of neural crest stem cells from adult human hair follicles. Folia Biol (Praha) 56: 149-157, 2010.
38. Marzagalli M, Raimondi M, Fontana F, Montagnani Marelli M, Moretti RM and Limonta P: Cellular and molecular biology of cancer stem cells in melanoma: Possible therapeutic implications. Semin Cancer Biol 59: 221-235, 2019.
39. Kasemeier-Kulesa JC, Teddy JM, Postovit LM, Seftor EA, Seftor REB, Hendrix MJC and Kulesa PM: Reprogramming multipotent tumor cells with the embryonic neural crest microenvironment. Dev Dyn 237: 2657-2666, 2008.
40. Kaufman CK, Mosimann C, Fan ZP, Yang S, Thomas AJ, Ablain J, Tan JL, Fogley RD, van Rooijen E, Hagedorn EJ, *et al*: A zebrafish melanoma model reveals emergence of neural crest identity during melanoma initiation. Science 351: aad2197, 2016.
41. Agnoletto C, Corrà F, Minotti L, Baldassari F, Crudele F, Cook WJJ, Di Leva G, d'Adamo AP, Gasparini P and Volinia S: Heterogeneity in circulating tumor cells: The relevance of the stem-cell subset. Cancers (Basel) 11: 11, 2019.
42. Gkountela S and Aceto N: Stem-like features of cancer cells on their way to metastasis. Biol Direct 11: 33, 2016.
43. Empringham B, Chiang KY and Krueger J: Collection of hematopoietic stem cells and immune effector cells in small children. Transfus Apheresis Sci 57: 614-618, 2018.
44. Feehan J, Nurgali K, Apostolopoulos V, Al Saedi A and Duque G: Circulating osteogenic precursor cells: Building bone from blood. EBioMedicine 39: 603-611, 2019.
45. Ratajczak MZ, Bujko K, Mack A, Kucia M and Ratajczak J: Cancer from the perspective of stem cells and misappropriated tissue regeneration mechanisms. Leukemia 32: 2519-2526, 2018.
46. Lacina L, Plzak J, Kodet O, Szabo P, Chovanec M, Dvorankova B and Smetana K Jr: Cancer microenvironment: What can we learn from the stem cell niche. Int J Mol Sci 16: 24094-24110, 2015.
47. Hill BS, Pelagalli A, Passaro N and Zannetti A: Tumor-educated mesenchymal stem cells promote pro-metastatic phenotype. Oncotarget 8: 73296-73311, 2017.
48. Plzák J, Bouček J, Bandúrová V, Kolář M, Hradilová M, Szabo P, Lacina L, Chovanec M and Smetana K Jr: The head and neck squamous cell carcinoma microenvironment as a potential target for cancer therapy. Cancers (Basel) 11: 11, 2019.
49. Lacina L, Kodet O, Dvořánková B, Szabo P and Smetana K Jr: Ecology of melanoma cell. Histol Histopathol 33: 247-254, 2018.
50. Preisner F, Leimer U, Sandmann S, Zoernig I, Germann G and Koellensperger E: Impact of human adipose tissue-derived stem cells on malignant melanoma cells in an in vitro co-culture model. Stem Cell Rev Rep 14: 125-140, 2018.
51. Dvořánková B, Smetana K Jr, Říhová B, Kučera J, Mateu R and Szabo P: Cancer-associated fibroblasts are not formed from cancer cells by epithelial-to-mesenchymal transition in nu/nu mice. Histochem Cell Biol 143: 463-469, 2015.
52. Inada M, Takita M, Yokoyama S, Watanabe K, Tominari T, Matsumoto C, Hirata M, Maru Y, Maruyama T, Sugimoto Y, *et al*: Direct melanoma cell contact induces stromal cell autocrine prostaglandin E2-EP4 receptor signaling that drives tumor growth, angiogenesis, and metastasis. J Biol Chem 290: 29781-29793, 2015.
53. Ziani L, Safta-Saadoun TB, Gourbeix J, Cavalcanti A, Robert C, Favre G, Chouaib S and Thiery J: Melanoma-associated fibroblasts decrease tumor cell susceptibility to NK cell-mediated killing through matrix-metalloproteinases secretion. Oncotarget 8: 19780-19794, 2017.
54. Kodet O, Lacina L, Krejčí E, Dvořánková B, Grim M, Štork J, Kodetová D, Vlček Č, Šáchová J, Kolář M, *et al*: Melanoma cells influence the differentiation pattern of human epidermal keratinocytes. Mol Cancer 14: 1, 2015.
55. Van Kilsdonk JWJ, Bergers M, Van Kempen LCLT, Schalkwijk J and Swart GWM: Keratinocytes drive melanoma invasion in a reconstructed skin model. Melanoma Res 20: 372-380, 2010.
56. Ciołczyk-Wierzbicka D and Laidler P: The inhibition of invasion of human melanoma cells through N-cadherin knock-down. Med Oncol 35: 42, 2018.
57. Chung H, Jung H, Jho EH, Multhaupt HAB, Couchman JR and Oh ES: Keratinocytes negatively regulate the N-cadherin levels of melanoma cells via contact-mediated calcium regulation. Biochem Biophys Res Commun 503: 615-620, 2018.
58. Nikkola J, Vihinen P, Vlaykova T, Hahka-Kemppinen M, Heino J and Pyrhönen S: Integrin chains β1 and alphav as prognostic factors in human metastatic melanoma. Melanoma Res 14: 29-37, 2004.
59. Van Belle PA, Elenitsas R, Satyamoorthy K, Wolfe JT, Guerry D IV, Schuchter L, Van Belle TJ, Albelda S, Tahin P, Herlyn M, *et al*: Progression-related expression of β3 integrin in melanomas and nevi. Hum Pathol 30: 562-567, 1999.
60. Li G, Satyamoorthy K, Meier F, Berking C, Bogenrieder T and Herlyn M: Function and regulation of melanoma-stromal fibroblast interactions: When seeds meet soil. Oncogene 22: 3162-3171, 2003.
61. Brandner JM and Haass NK: Melanoma's connections to the tumour microenvironment. Pathology 45: 443-452, 2013.
62. Peitsch WK, Doerflinger Y, Fischer-Colbrie R, Huck V, Bauer AT, Utikal J, Goerdt S and Schneider SW: Desmoglein 2 depletion leads to increased migration and upregulation of the chemoattractant secretoneurin in melanoma cells. PLoS One 9: e89491, 2014.
63. Tan LY, Mintoff C, Johan MZ, Ebert BW, Fedele C, Zhang YF, Szeto P, Sheppard KE, McArthur GA, Foster-Smith E, *et al*: Desmoglein 2 promotes vasculogenic mimicry in melanoma and is associated with poor clinical outcome. Oncotarget 7: 46492-46508, 2016.
64. Klemke M, Weschenfelder T, Konstandin MH and Samstag Y: High affinity interaction of integrin α4β1 (VLA-4) and vascular cell adhesion molecule 1 (VCAM-1) enhances migration of human melanoma cells across activated endothelial cell layers. J Cell Physiol 212: 368-374, 2007.
65. Lacaria L, Lange JR, Goldmann WH, Rico F and Alonso JL: αvβ3 integrin expression increases elasticity in human melanoma cells. Biochem Biophys Res Commun 525: 836-840, 2020.
66. Bedogni B: Notch signaling in melanoma: Interacting pathways and stromal influences that enhance Notch targeting. Pigment Cell Melanoma Res 27: 162-168, 2014.
67. Jobe NP, Rösel D, Dvořánková B, Kodet O, Lacina L, Mateu R, Smetana K and Brábek J: Simultaneous blocking of IL-6 and IL-8 is sufficient to fully inhibit CAF-induced human melanoma cell invasiveness. Histochem Cell Biol 146: 205-217, 2016.
68. Jobe NP, Živicová V, Mifková A, Rösel D, Dvořánková B, Kodet O, Strnad H, Kolář M, Šedo A, Smetana K Jr, *et al*: Fibroblasts potentiate melanoma cells in vitro invasiveness induced by UV-irradiated keratinocytes. Histochem Cell Biol 149: 503-516, 2018.
69. Strnadova K, Sandera V, Dvorankova B, Kodet O, Duskova M, Smetana K and Lacina L: Skin aging: The dermal perspective. Clin Dermatol 37: 326-335, 2019.

70. Payne AS and Cornelius LA: The role of chemokines in melanoma tumor growth and metastasis. J Invest Dermatol 118: 915-922, 2002.
71. Gebhardt C, Averbeck M, Viertel A, Kauer F, Saalbach A, Anderegg U and Simon JC: Ultraviolet-B irradiation enhances melanoma cell motility via induction of autocrine interleukin 8 secretion. Exp Dermatol 16: 636-643, 2007.
72. Araki K, Shimura T, Yajima T, Tsutsumi S, Suzuki H, Okada K, Kobayashi T, Raz A and Kuwano H: Phosphoglucose isomerase/autocrine motility factor promotes melanoma cell migration through ERK activation dependent on autocrine production of interleukin-8. J Biol Chem 284: 32305-32311, 2009.
73. Kemp DM, Pidich A, Larijani M, Jonas R, Lash E, Sato T, Terai M, De Pizzol M, Allegretti M, Igoucheva O, *et al*: Ladarixin, a dual CXCR1/2 inhibitor, attenuates experimental melanomas harboring different molecular defects by affecting malignant cells and tumor microenvironment. Oncotarget 8: 14428-14442, 2017.
74. Brennecke S, Deichmann M, Naeher H and Kurzen H: Decline in angiogenic factors, such as interleukin-8, indicates response to chemotherapy of metastatic melanoma. Melanoma Res 15: 515-522, 2005.
75. Gabellini C, Trisciuoglio D, Desideri M, Candiloro A, Ragazzoni Y, Orlandi A, Zupi G and Del Bufalo D: Functional activity of CXCL8 receptors, CXCR1 and CXCR2, on human malignant melanoma progression. Eur J Cancer 45: 2618-2627, 2009.
76. Nürnberg W, Tobias D, Otto F, Henz BM and Schadendorf D: Expression of interleukin-8 detected by in situ hybridization correlates with worse prognosis in primary cutaneous melanoma. J Pathol 189: 546-551, 1999.
77. Ortega-Bernal D, La Rosa CHG, Arechaga-Ocampo E, Alvarez-Avitia MA, Moreno NS and Rangel-Escareño C: A meta-analysis of transcriptome datasets characterizes malignant transformation from melanocytes and nevi to melanoma. Oncol Lett 16: 1899-1911, 2018.
78. Adamski V, Mentlein R, Lucius R, Synowitz M, Held-Feindt J and Hattermann K: The chemokine receptor CXCR6 evokes reverse signaling via the transmembrane chemokine CXCL16. Int J Mol Sci 18: 18, 2017.
79. da Silva WC, Oshiro TM, de Sá DC, Franco DDGS, Festa Neto C and Pontillo A: Genotyping and differential expression analysis of inflammasome genes in sporadic malignant melanoma reveal novel contribution of CARD8, IL1B and IL18 in melanoma susceptibility and progression. Cancer Genet 209: 474-480, 2016.
80. Lacina L, Brábek J, Král V, Kodet O and Smetana K Jr: Interleukin-6: A molecule with complex biological impact in cancer. Histol Histopathol 34: 125-136, 2019.
81. Armstrong CA, Murray N, Kennedy M, Koppula SV, Tara D and Ansel JC: Melanoma-derived interleukin 6 inhibits in vivo melanoma growth. J Invest Dermatol 102: 278-284, 1994.
82. Lu C and Kerbel RS: Interleukin-6 undergoes transition from paracrine growth inhibitor to autocrine stimulator during human melanoma progression. J Cell Biol 120: 1281-1288, 1993.
83. Elias EG, Hasskamp JH and Sharma BK: Cytokines and growth factors expressed by human cutaneous melanoma. Cancers (Basel) 2: 794-808, 2010.
84. Linnskog R, Jönsson G, Axelsson L, Prasad CP and Andersson T: Interleukin-6 drives melanoma cell motility through p38α-MAPK-dependent up-regulation of WNT5A expression. Mol Oncol 8: 1365-1378, 2014.
85. Karst AM, Gao K, Nelson CC and Li G: Nuclear factor kappa B subunit p50 promotes melanoma angiogenesis by upregulating interleukin-6 expression. Int J Cancer 124: 494-501, 2009.
86. Nagai H, Oniki S, Fujiwara S, Xu M, Mizoguchi I, Yoshimoto T and Nishigori C: Antitumor activities of interleukin-27 on melanoma. Endocr Metab Immune Disord Drug Targets 10: 41-46, 2010.
87. Shinozaki Y, Wang S, Miyazaki Y, Miyazaki K, Yamada H, Yoshikai Y, Hara H and Yoshida H: Tumor-specific cytotoxic T cell generation and dendritic cell function are differentially regulated by interleukin 27 during development of anti-tumor immunity. Int J Cancer 124: 1372-1378, 2009.
88. Chiba Y, Mizoguchi I, Mitobe K, Higuchi K, Nagai H, Nishigori C, Mizuguchi J and Yoshimoto T: IL-27 enhances the expression of TRAIL and TLR3 in human melanomas and inhibits their tumor growth in cooperation with a TLR3 agonist poly(I:C) partly in a TRAIL-dependent manner. PLoS One 8: e76159, 2013.
89. Bisevac JP, Stanojevic I, Mijuskovic Z, Banovic T, Djukic M and Vojvodic D: High interleukin 27 production is associated with early clinical stage and localized disease in patients with melanoma. J Med Biochem 35: 443-450, 2016.
90. Onoue K, Kusubashi H, Sato Y, Wakitani S and Takagi M: Quantitative correlation between production rate of melanoma inhibitory activity and aggrecan gene expression level during differentiation from mesenchymal stem cells to chondrocytes and redifferentiation of chondrocytes. J Biosci Bioeng 111: 594-596, 2011.
91. Decarlo K, Yang S, Emley A, Wajapeyee N, Green M and Mahalingam M: Oncogenic BRAF-positive dysplastic nevi and the tumor suppressor IGFBP7 - challenging the concept of dysplastic nevi as precursor lesions? Hum Pathol 41: 886-894, 2010.
92. Yotsumoto F, Yagi H, Suzuki SO, Oki E, Tsujioka H, Hachisuga T, Sonoda K, Kawarabayashi T, Mekada E and Miyamoto S: Validation of HB-EGF and amphiregulin as targets for human cancer therapy. Biochem Biophys Res Commun 365: 555-561, 2008.
93. Marchetti D and Nicolson GL: Neurotrophin stimulation of human melanoma cell invasion: Selected enhancement of heparanase activity and heparanase degradation of specific heparan sulfate subpopulations. Adv Enzyme Regul 37: 111-134, 1997.
94. Antunes LCM, Cartell A, de Farias CB, Bakos RM, Roesler R and Schwartsmann G: Tropomyosin-related kinase receptor and neurotrophin expression in cutaneous melanoma is associated with a poor prognosis and decreased survival. Oncology 97: 26-37, 2019.
95. Li JR, Wang JQ, Gong Q, Fang RH and Guo YL: MicroRNA-328 inhibits proliferation of human melanoma cells by targeting TGFβ2. Asian Pac J Cancer Prev 16: 1575-1579, 2015.
96. Hutchenreuther J, Vincent K, Norley C, Racanelli M, Gruber SB, Johnson TM, Fullen DR, Raskin L, Perbal B, Holdsworth DW, *et al*: Activation of cancer-associated fibroblasts is required for tumor neovascularization in a murine model of melanoma. Matrix Biol 74: 52-61, 2018.
97. Straussman R, Morikawa T, Shee K, Barzily-Rokni M, Qian ZR, Du J, Davis A, Mongare MM, Gould J, Frederick DT, *et al*: Tumour micro-environment elicits innate resistance to RAF inhibitors through HGF secretion. Nature 487: 500-504, 2012.
98. Capparelli C, Rosenbaum S, Berger AC and Aplin AE: Fibroblast-derived neuregulin 1 promotes compensatory ErbB3 receptor signaling in mutant BRAF melanoma. J Biol Chem 290: 24267-24277, 2015.
99. Ruivo CF, Adem B, Silva M and Melo SA: The biology of cancer exosomes: Insights and new perspectives. Cancer Res 77: 6480-6488, 2017.
100. Hood JL: Melanoma exosome induction of endothelial cell GM-CSF in pre-metastatic lymph nodes may result in different M1 and M2 macrophage mediated angiogenic processes. Med Hypotheses 94: 118-122, 2016.
101. Xiao D, Barry S, Kmetz D, Egger M, Pan J, Rai SN, Qu J, McMasters KM and Hao H: Melanoma cell-derived exosomes promote epithelial-mesenchymal transition in primary melanocytes through paracrine/autocrine signaling in the tumor microenvironment. Cancer Lett 376: 318-327, 2016.
102. Gowda R, Robertson BM, Iyer S, Barry J, Dinavahi SS and Robertson GP: The role of exosomes in metastasis and progression of melanoma. Cancer Treat Rev 85: 101975, 2020.
103. Gajos-Michniewicz A and Czyz M: Role of mirnas in melanoma metastasis. Cancers (Basel) 11: 11, 2019.
104. Clayton A, Mitchell JP, Court J, Mason MD and Tabi Z: Human tumor-derived exosomes selectively impair lymphocyte responses to interleukin-2. Cancer Res 67: 7458-7466, 2007.
105. Gerloff D, Lützkendorf J, Moritz RKC, Wersig T, Mäder K, Müller LP and Sunderkötter C: Melanoma-derived exosomal mir-125b-5p educates tumor associated macrophages (TAMs) by targeting lysosomal acid lipase A (LIPA). Cancers (Basel) 12: 12, 2020.
106. Bardi GT, Smith MA and Hood JL: Melanoma exosomes promote mixed M1 and M2 macrophage polarization. Cytokine 105: 63-72, 2018.
107. Gershenwald JE and Scolyer RA: Melanoma Staging: American Joint Committee on Cancer (AJCC) 8th Edition and Beyond. Ann Surg Oncol 25: 2105-2110, 2018.
108. Michielin O, van Akkooi ACJ, Ascierto PA, Dummer R and Keilholz U; ESMO Guidelines Committee. Electronic address: clinicalguidelines@esmo.org: Cutaneous melanoma: ESMO Clinical Practice Guidelines for diagnosis, treatment and follow-up. Ann Oncol 30: 1884-1901, 2019.
109. Riechers A and Bosserhoff AK: Melanoma inhibitory activity in melanoma diagnostics and therapy - a small protein is looming large. Exp Dermatol 23: 12-14, 2014.

110. Forgber M, Trefzer U, Sterry W and Walden P: Proteome serological determination of tumor-associated antigens in melanoma. PLoS One 4: e5199, 2009.
111. Muqaku B, Eisinger M, Meier SM, Tahir A, Pukrop T, Haferkamp S, Slany A, Reichle A and Gerner C: Multi-omics analysis of serum samples demonstrates reprogramming of organ functions via systemic calcium mobilization and platelet activation in metastatic melanoma. Mol Cell Proteomics 16: 86-99, 2017.
112. Weber JS, Sznol M, Sullivan RJ, Blackmon S, Boland G, Kluger HM, Halaban R, Bacchiocchi A, Ascierto PA, Capone M, *et al*: A serum protein signature associated with outcome after anti-PD-1 therapy in metastatic melanoma. Cancer Immunol Res 6: 79-86, 2018.
113. Hoejberg L, Bastholt L, Johansen JS, Christensen IJ, Gehl J and Schmidt H: Serum interleukin-6 as a prognostic biomarker in patients with metastatic melanoma. Melanoma Res 22: 287-293, 2012.
114. Correa D, Somoza RA, Lin P, Schiemann WP and Caplan AI: Mesenchymal stem cells regulate melanoma cancer cells extravasation to bone and liver at their perivascular niche. Int J Cancer 138: 417-427, 2016.
115. Gandalovičová A, Rosel D, Fernandes M, Veselý P, Heneberg P, Čermák V, Petruželka L, Kumar S, Sanz-Moreno V and Brábek J: Migrastatics-anti-metastatic and anti-invasion Drugs: Promises and challenges. Trends Cancer 3: 391-406, 2017.
116. Herman H, Fazakas C, Haskó J, Molnár K, Mészáros Á, Nyúl-Tóth Á, Szabó G, Erdélyi F, Ardelean A, Hermenean A, *et al*: Paracellular and transcellular migration of metastatic cells through the cerebral endothelium. J Cell Mol Med 23: 2619-2631, 2019.
117. Kucera R, Topolcan O, Treskova I, Kinkorova J, Windrichova J, Fuchsova R, Svobodova S, Treska V, Babuska V, Novak J, *et al*: Evaluation of IL-2, IL-6, IL-8 and IL-10 in malignant melanoma diagnostics. Anticancer Res 35: 3537-3541, 2015.
118. Sanmamed MF, Carranza-Rua O, Alfaro C, Oñate C, Martín-Algarra S, Perez G, Landazuri SF, Gonzalez A, Gross S, Rodriguez I, *et al*: Serum interleukin-8 reflects tumor burden and treatment response across malignancies of multiple tissue origins. Clin Cancer Res 20: 5697-5707, 2014.
119. Kučera J, Strnadová K, Dvořánková B, Lacina L, Krajsová I, Štork J, Kovářová H, Skalníková HK, Vodička P, Motlík J, *et al*: Serum proteomic analysis of melanoma patients with immunohistochemical profiling of primary melanomas and cultured cells: Pilot study. Oncol Rep 42: 1793-1804, 2019.
120. Pelletier F, Bermont L, Puzenat E, Blanc D, Cairey-Remonnay S, Mougin C, Laurent R, Humbert P and Aubin F: Circulating vascular endothelial growth factor in cutaneous malignant melanoma. Br J Dermatol 152: 685-689, 2005.
121. Ugurel S, Rappl G, Tilgen W and Reinhold U: Increased serum concentration of angiogenic factors in malignant melanoma patients correlates with tumor progression and survival. J Clin Oncol 19: 577-583, 2001.
122. Krasagakis K, Thölke D, Farthmann B, Eberle J, Mansmann U and Orfanos CE: Elevated plasma levels of transforming growth factor (TGF)-β1 and TGF-β2 in patients with disseminated malignant melanoma. Br J Cancer 77: 1492-1494, 1998.
123. Tuccitto A, Tazzari M, Beretta V, Rini F, Miranda C, Greco A, Santinami M, Patuzzo R, Vergani B, Villa A, *et al*: Immunomodulatory factors control the fate of melanoma tumor initiating cells. Stem Cells 34: 2449-2460, 2016.
124. Tung KH, Ernstoff MS, Allen C and Shu S: A Review of exosomes and their role in the tumor microenvironment and host-tumor 'macroenvironment'. J Immunol Sci 3: 4-8, 2019.
125. Shu S, Yang Y, Allen CL, Maguire O, Minderman H, Sen A, Ciesielski MJ, Collins KA, Bush PJ, Singh P, *et al*: Metabolic reprogramming of stromal fibroblasts by melanoma exosome microRNA favours a pre-metastatic microenvironment. Sci Rep 8: 12905, 2018.
126. Kodet O, Dvořánková B, Bendlová B, Sýkorová V, Krajsová I, Štork J, Kučera J, Szabo P, Strnad H, Kolář M, *et al*: Microenvironment driven resistance to B Raf inhibition in a melanoma patient is accompanied by broad changes of gene methylation and expression in distal fibroblasts. Int J Mol Med 41: 2687-2703, 2018.
127. Jouve N, Bachelier R, Despoix N, Blin MG, Matinzadeh MK, Poitevin S, Aurrand-Lions M, Fallague K, Bardin N, Blot-Chabaud M, *et al*: CD146 mediates VEGF-induced melanoma cell extravasation through FAK activation. Int J Cancer 137: 50-60, 2015.
128. Hamilla SM, Stroka KM and Aranda-Espinoza H: VE-cadherin-independent cancer cell incorporation into the vascular endothelium precedes transmigration. PLoS One 9: e109748, 2014.
129. Kim KJ, Kwon SH, Yun JH, Jeong HS, Kim HR, Lee EH, Ye SK and Cho CH: STAT3 activation in endothelial cells is important for tumor metastasis via increased cell adhesion molecule expression. Oncogene 36: 5445-5459, 2017.
130. Borgenström M, Wärri A, Hiilesvuo K, Käkönen R, Käkönen S, Nissinen L, Pihlavisto M, Marjamäki A, Vlodavsky I, Naggi A, *et al*: O-sulfated bacterial polysaccharides with low anticoagulant activity inhibit metastasis. Semin Thromb Hemost 33: 547-556, 2007.
131. Dange MC, Srinivasan N, More SK, Bane SM, Upadhya A, Ingle AD, Gude RP, Mukhopadhyaya R and Kalraiya RD: Galectin-3 expressed on different lung compartments promotes organ specific metastasis by facilitating arrest, extravasation and organ colonization via high affinity ligands on melanoma cells. Clin Exp Metastasis 31: 661-673, 2014.
132. Desch A, Strozyk EA, Bauer AT, Huck V, Niemeyer V, Wieland T and Schneider SW: Highly invasive melanoma cells activate the vascular endothelium via an MMP-2/integrin αvβ5-induced secretion of VEGF-A. Am J Pathol 181: 693-705, 2012.
133. Tsukamoto H, Fujieda K, Miyashita A, Fukushima S, Ikeda T, Kubo Y, Senju S, Ihn H, Nishimura Y and Oshiumi H: Combined blockade of IL6 and PD-1/PD-L1 signaling abrogates mutual regulation of their immunosuppressive effects in the tumor microenvironment. Cancer Res 78: 5011-5022, 2018.
134. Anker MS, Holcomb R, Muscaritoli M, von Haehling S, Haverkamp W, Jatoi A, Morley JE, Strasser F, Landmesser U, Coats AJS, *et al*: Orphan disease status of cancer cachexia in the USA and in the European Union: A systematic review. J Cachexia Sarcopenia Muscle 10: 22-34, 2019.
135. Loumaye A and Thissen JP: Biomarkers of cancer cachexia. Clin Biochem 50: 1281-1288, 2017.
136. Weidle UH, Klostermann S, Eggle D and Krüger A: Interleukin 6/interleukin 6 receptor interaction and its role as a therapeutic target for treatment of cachexia and cancer. Cancer Genomics Proteomics 7: 287-302, 2010.
137. Zimmers TA, Fishel ML and Bonetto A: STAT3 in the systemic inflammation of cancer cachexia. Semin Cell Dev Biol 54: 28-41, 2016.
138. Cehreli R, Yavuzsen T, Ates H, Akman T, Ellidokuz H and Oztop I: Can inflammatory and nutritional serum markers predict chemotherapy outcomes and survival in advanced stage nonsmall cell lung cancer patients? BioMed Res Int 2019: 1648072, 2019.
139. Johannes CM and Musser ML: Anorexia and the cancer patient. Vet Clin North Am Small Anim Pract 49: 837-854, 2019.
140. Pisetsky DS, Trace SE, Brownley KA, Hamer RM, Zucker NL, Roux-Lombard P, Dayer JM and Bulik CM: The expression of cytokines and chemokines in the blood of patients with severe weight loss from anorexia nervosa: An exploratory study. Cytokine 69: 110-115, 2014.
141. Rochfort KD and Cummins PM: The blood-brain barrier endothelium: A target for pro-inflammatory cytokines. Biochem Soc Trans 43: 702-706, 2015.
142. Dwarkasing JT, Witkamp RF, Boekschoten MV, Ter Laak MC, Heins MS and van Norren K: Increased hypothalamic serotonin turnover in inflammation-induced anorexia. BMC Neurosci 17: 26, 2016.
143. Liu WJ, Wang XD, Wu W and Huang X: Relationship between depression and blood cytokine levels in lung cancer patients. Med Sci (Paris) 34 Focus issue F1: 113-115, 2018.
144. Lu YR, Rao YB, Mou YJ, Chen Y, Lou HF, Zhang Y, Zhang DX, Xie HY, Hu LW and Fang P: High concentrations of serum interleukin-6 and interleukin-8 in patients with bipolar disorder. Medicine (Baltimore) 98: e14419, 2019.
145. Ju RJ, Stehbens SJ and Haass NK: The role of melanoma cell-stroma interaction in cell motility, invasion, and metastasis. Front Med (Lausanne) 5: 307, 2018.
146. Johnson DE, O'Keefe RA and Grandis JR: Targeting the IL-6/JAK/STAT3 signalling axis in cancer. Nat Rev Clin Oncol 15: 234-248, 2018.
147. Donnelly D III, Aung PP and Jour G: The '-OMICS' facet of melanoma: Heterogeneity of genomic, proteomic and metabolomic biomarkers. Semin Cancer Biol 59: 165-174, 2019.

PUBLIKACE VII

Brábek J, Jakubek M, Vellieux F, Novotný J, Kolář M, Lacina L, Szabo P, **Strnadová K**, Rösel D, Dvořánková B, Smetana K Jr. Interleukin-6: Molecule in the Intersection of Cancer, Ageing and COVID-19. *Int J Mol Sci*. 2020 Oct 26;21(21):7937. **(IF: 5.923)**

International Journal of
Molecular Sciences

MDPI

Review

Interleukin-6: Molecule in the Intersection of Cancer, Ageing and COVID-19

Jan Brábek [1,2,3], Milan Jakubek [3,4,5,6], Fréderic Vellieux [3,5], Jiří Novotný [3,7], Michal Kolář [3,7], Lukáš Lacina [3,5,8,9], Pavol Szabo [8], Karolína Strnadová [3,5,8], Daniel Rösel [1,2,3], Barbora Dvořánková [3,5,8] and Karel Smetana, Jr. [3,5,8,*]

1 Department of Cell Biology, Faculty of Science, Charles University, 120 00 Prague 2, Czech Republic; jan.brabek@natur.cuni.cz (J.B.); Daniel.Rosel@natur.cuni.cz (D.R.)
2 BIOCEV, Faculty of Science, Charles University, 252 50 Vestec, Czech Republic
3 Centre for Tumour Ecology, First Faculty of Medicine, Charles University, 120 00 Prague 2, Czech Republic; Milan.Jakubek@lf1.cuni.cz (M.J.); Frederic.Vellieux@lf1.cuni.cz (F.V.); Jiri.Novotny@img.cas.cz (J.N.); Michal.Kolar@img.cas.cz (M.K.); Lukas.Lacina@lf1.cuni.cz (L.L.); Karolina.Strnadova@lf1.cuni.cz (K.S.); Barbora.Dvorankova@lf1.cuni.cz (B.D.)
4 Department of Paediatrics and Adolescent Medicine, First Faculty of Medicine, Charles University and General University Hospital, 120 00 Prague, Czech Republic
5 BIOCEV, First Faculty of Medicine, Charles University, 252 50 Vestec, Czech Republic
6 Department of Analytical Chemistry, University of Chemistry and Technology Prague, 166 28 Praha 6, Czech Republic
7 Laboratory of Genomics and Bioinformatics, Institute of Molecular Genetics, Czech Academy of Sciences, 140 00 Prague 4, Czech Republic
8 Institute of Anatomy, Fist Faculty of Medicine, Charles University, 120 00 Prague 2, Czech Republic; szabopavol@gmail.com
9 Department of Dermatovenereology, First Faculty of Medicine, Charles University and General University Hospital, 120 00 Prague 2, Czech Republic
* Correspondence: Karel.Smetana@lf1.cuni.cz; Tel.: +420-224-965-873

Received: 4 October 2020; Accepted: 21 October 2020; Published: 26 October 2020

Abstract: Interleukin-6 (IL-6) is a cytokine with multifaceted effects playing a remarkable role in the initiation of the immune response. The increased level of this cytokine in the elderly seems to be associated with the chronic inflammatory setting of the microenvironment in aged individuals. IL-6 also represents one of the main signals in communication between cancer cells and their non-malignant neighbours within the tumour niche. IL-6 also participates in the development of a premetastatic niche and in the adjustment of the metabolism in terminal-stage patients suffering from a malignant disease. IL-6 is a fundamental factor of the cytokine storm in patients with severe COVID-19, where it is responsible for the fatal outcome of the disease. A better understanding of the role of IL-6 under physiological as well as pathological conditions and the preparation of new strategies for the therapeutic control of the IL-6 axis may help to manage the problems associated with the elderly, cancer, and serious viral infections.

Keywords: tumour microenvironment; cancer ecosystem; ageing; COVID-19; IL-6; cytokine storm; cytokine; cancer-associated fibroblasts

1. Introduction

Interleukin-6 (IL-6) is a bioactive protein known under numerous synonyms (Table 1). It is a cytokine of a pro-inflammatory nature, and it can be produced by various cell types of the immune system as well as by some nonimmune cells, including fibroblasts. Regarding the anatomical distribution

of Il-6, it was identified in the lungs, urinary bladder, adipose tissue, muscles, vermiform appendix, etc. (The Human Protein Atlas, [1]).

Table 1. Synonyms for interleukin-6 (IL-6).

Name	Author
Interferon β-2	Zilberstein et al., 1986 [2]
26K factor	Haegeman et al., 1986 [3]
B-cell stimulatory factor	Hirano et al., 1985 [4]
Hybridoma growth factor	Brakenhoff et al., 1987 [5]
Plasmacytoma growth factor	Nordan et al., 1987 [6]
Hepatocyte stimulatory factor	Gauldie et al., 1987 [7]
Haematopoietic factor	Ikebuchi et al., 1987 [8]
Cytotoxic T-cell differentiation factor	Takai et al., 1988 [9]

The main cell types acting as producers of IL-6 are shortlisted in Table 2.

Table 2. Examples of cells producing IL-6.

Type of cell	Author
Keratinocyte	Groeger and Meyle, 2019 [10]
Enterocyte	Pritts et al., 2002 [11]
Urothelium	Uehling et al., 1999 [12]
Hepatocyte	Schmidt-Arras and Rose-John, 2016 [13]
Pneumocyte and bronchial epithelial cell	Cheung, 2005 [14]
Smooth muscle	Kyotani et al., 2019 [15]
Skeletal muscle	Barbalho et al., 2020 [16]
Osteoblast	Kovács et al., 2019 [17]
Adipocyte	Xie et al., 2019 [18]
Macrophage	Shapouri-Moghaddam et al., 2018 [19]
Neuron	Shapouri-Moghaddam et al., 2018 [19]

IL-6 is recognised by its transmembrane receptor (IL-6R), which forms a complex with glycoprotein 130 (gp130). This receptor has tyrosine kinase activity and activates signal transducer and activator of transcription 3 (STAT3) via phosphorylation. On the other hand, the extracellular portion of IL-6R can be cleaved from the intramembranous domain of the receptor by membrane protease ADAM-17. Soluble IL-6R without tyrosine kinase activity interacts with gp130 outside the cell and forms a complex of IL-6, soluble IL-6R and gp130, which is docked back to the cell membrane [20]. This arrangement of the IL-6–IL-6R axis can be functionally variable when the actual function of IL-6 signalling is dependent on the type of cell and the type of interacting receptor. While the interaction of IL-6 with transmembrane IL-6R and gp130 participates in anti-inflammatory pro-cancerogenic signalling, the interaction of IL-6 with soluble IL-6R and gp130 stimulates inflammation [20].

In this review, we aim to highlight the molecular similarity between apparently distinct phenomena and their mechanisms such as physiological ageing, formation of the cancer niche ecosystem and severe inflammatory conditions, including viral infections such as COVID-19. In all of them, we can invariably observe deregulation of the IL-6–IL-6R axis. Therefore, our more in-depth insight into the IL-6 function in the context of ageing, tumourigenesis and infections may bring new therapeutic strategies for the treatment of age-related disorders, cancer and transmissible, e.g., viral, diseases.

2. Physiological Functions of IL-6

The family of IL-6-related proteins consists of members with remarkable and distinct biological activities that are structurally similar to IL-6, such as IL-11, IL-31, cardiotrophin-1, ciliary neurotrophic factor (CNTF), cardiotrophin-like cytokine (CLC), granulocyte colony-stimulating factor (G-CSF), leptin, leukaemia inhibitory factor (LIF), neuropoietin, and oncostatin [21]. This cytokine family

is defined by sharing common IL-6 family signalling receptor gp130 more than by any structural homology of its members. It is therefore not surprising that the IL-6 family cytokines not only display partially overlapping, but also, more significantly, very different biological activities [22].

IL-6 knockout mice are available for research purposes [23]. Interestingly, their embryonic and foetal development is not hampered, and knockout animals do not have any apparent developmental abnormalities. On the other hand, these mouse strains were highly susceptible to several pathogens, and they failed to generate acute-phase responses [24].

IL-6 contributes to the host defence by stimulation of the acute phase immune response, including elevation of body temperature [25]. In this context, IL-6 positively influences the maturation of B lymphocytes and cytotoxic T lymphocytes [26,27]. In the same motion, IL-6 deficiency in an experimental model leads to protection against triggering autoimmune encephalomyelitis [28]

IL-6 also belongs to the family of myokines such as IL-8, IL-15, irisin, myostatin, fibroblast growth factor (FGF)21, leukemia inhibitory factor (LIF), brain-derived neurotrophic factor (BDNF), and insulin like growth factor-1 (IGF-1) that influence the function of skeletal muscle with metabolic impacts on the whole organism [16], namely by interaction with adipocytes and factors produced by these cells [29]. In knockout mice, surviving animals had reduced age-related obesity development [30].

The role of IL-6 in the bone metabolism was also confirmed by the stimulation of osteoclast activity [31]. This is in good agreement with the observed protection against the bone loss after ovariectomy in a mouse knockout model [32].

These few examples demonstrate the complex and multifaceted role of IL-6 both in physiological and pathological conditions in the human body.

3. IL-6 and Ageing

3.1. "Inflammaging" as a Developmentally Controlled Process

In the last seventy years, the life expectancy of citizens dramatically increased in many countries across the world. In a number of developed countries, it now reaches around 80 years of age. This represents an increase in life expectancy from the beginning of the 20th century by approximately 30 years. Unfortunately, this trend is associated with numerous age-related phenomena such as cardiovascular diseases, cognitive function impairment, sarcopoenia, metabolic disorders, cachexia, and also an increased incidence of cancer [33]. "Adding years to life and life to years" [34] has become an appealing manifesto of health care-providing authorities in recent times. It urges in-depth insights into the mechanisms typical of healthy longevity.

Even in the absence of any disease, chronologically aged cells differ from juvenile cells. Bioinformatic analysis of events associated with the ageing of tissues and organs in otherwise healthy seniors highlighted specific developmentally regulated mechanisms. Surprisingly, age-induced changes are typical of inflammation [35]. This finding correlates well with an increasing number of neutrophils—cells of innate immunity. On the other hand, lymphocytes—the principal cells of adaptive immunity—are significantly reduced during ageing [36]. One of the typical humoral markers of inflammation, namely in the early stage, is IL-6. The serum concentration of IL-6 increases during ageing, and it is independent of ethnicity [36–38]. The moderately elevated serum concentration of IL-6 in aged people plays a significant role in functional impairment, including low locomotion, cognitive and mental functions, and depression [39]. The highly elevated level of this cytokine can even predict increased mortality in very old individuals [40]. On the other hand, a low level of IL-6 representing lower "inflammaging" was typical of successful centenarians [41].

Ageing in itself is not a disease [42]. However, it is a condition that allows or induces the emergence of some diseases. Even healthy senescent tissue, devoid of clinically apparent disease, exerts some alarming molecular features. This might be exemplified by the study of the expression profiles of the dermal fibroblasts isolated from very old donors. These fibroblasts demonstrated a remarkable similarity to cancer-associated fibroblasts (CAFs), including a high expression of mRNA encoding

IL-6 [43]. Indeed, transcriptional profiling of facial dermal fibroblasts from children, healthy adults, photodamaged dermal fibroblasts of patients suffering from basal cell carcinoma, and CAFs directly from basal and cutaneous squamous cell carcinomas revealed striking similarities in the expression of downstream components of the IL-6 signalling pathway [44] between aged fibroblasts and CAFs. Notably, Janus kinase 2 (JAK2) and signal transducer and activator of transcription 3 (STAT3) displayed a clear rising trend from very low activity in child fibroblasts, through to intermediate activity in photoaged dermal fibroblasts, and then to elevated activity in CAFs (Figure 1), indicating an increasing degree of "inflammaging"

As stated above, ageing is not a disease. However, ageing and disease are frequently tightly associated. As noted by the WHO, health shall not be understood as an absence of disease [34]. Hence, the tie of ageing and disease is sometimes so close that it is obviously challenging at this level to draw a sharp demarcation line separating "healthy yet aged tissue" from already precancerous or even cancerous tissue.

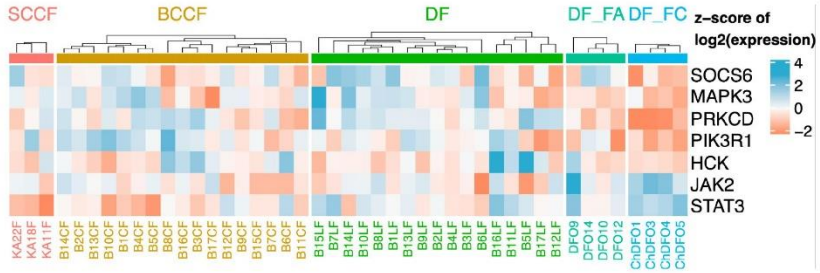

Figure 1. Multiple genes of the interleukin-6 (IL-6) signalling pathway display gradual changes in transcription activity, differing among facial dermal fibroblasts from children (DF_FC), healthy adults (DF_FA), photodamaged dermal fibroblasts (DF) of patients suffering from basal cell carcinoma, and cancer-associated fibroblasts (CAFs) from basal cell carcinomas (BCCF) and cutaneous squamous cell carcinomas (SCCF).

Our understanding of "inflammaging" and the significance of elevated IL-6, C-reactive protein (CRP) and tumour necrosis factor (TNF)-α concentrations is not yet complete. The role of a developmentally programmed genetic process is hypothesised. Still, other processes, such as chronic viral infection (cytomegalovirus), a high volume of visceral fat, altered gut permeability, ineffective immune response in the elderly and the accumulation of senescent cells in the body may also be responsible for "inflammaging" [45]

3.2. Non-Steroid Anti-Inflammatory Drugs as "Inflammaging" Therapy in Ageing

Upon broadly accepted medical advice, the aged population frequently uses low-dose acetylsalicylic acid (ASA). It acts as prevention of thromboembolism and cardiovascular diseases, mainly because of its anticlotting effect. It was observed in many studies that this prophylactic application also has a significant anti-cancer effect, at least for cancer of the prostate, lung, colorectum, ovary, uterus, and stomach [46–48]. ASA is a member of the non-steroid anti-inflammatory drug family. The molecular mechanism of ASA activity is well known, and it is explained by irreversible acetylation of cyclooxygenase (COX) enzymes, resulting in the anti-inflammatory effect. It seems that the anti-cancer effect of non-steroid anti-inflammatory drugs is not strictly dependent on the abovementioned molecular mechanism. It was confirmed that other non-steroid anti-inflammatory drugs affecting other molecular mechanisms are also beneficial in cancer prevention, as exemplified in breast cancer [49,50]. ASA and other non-steroid anti-inflammatory drugs can successfully reduce "inflammaging" in the tissue/organ microenvironment. Such inhibition can adversely impact the cancer

ecosystem and thus consequently inhibit the probability of successful cancer initiation and growth in this niche. In the context of this article, it should be mentioned that these substances reduce the actual levels of IL-6 and TNF-α, factors known for their supporting role in tumour growth and spread, as discussed above [49,50]. Moreover, ASA has a direct effect on the production of IL-6 by adipocytes, and so it has an indirect effect on cancer [51]. ASA also stimulates apoptosis in cancer cells [52]. Its effect on blood platelets has also demonstrated the role of non-steroid antirheumatic drugs in cancer. The anti-platelet activity of low doses of ASA in combination with COX in suppressing tumourigenesis was clearly established [53]. However, ASA and other non-steroid anti-inflammatory drugs display side effects, namely in the gastrointestinal system, where they induce gastric erosions, ulcerations, and bleeding. According to the U.S. Preventive Services Task Force Recommendation [54], the risk of bleeding is minimal after low-dose use, and the benefits, including colorectal cancer prevention, prevail. The data about ASA and other non-steroid anti-inflammatory drugs in cancer prevention by modulation of the cancer microenvironment may be an inspiration for the development of novel preventive strategies for cancer incidence reduction in the elderly.

3.3. Summary of the Role in IL-6 in Ageing

Ageing is associated with a proclivity to inflammation. At the cellular level, accumulating evidence shows that senescent cells may have deleterious effects on the tissue microenvironment [55]. The elevation of IL-6 notably accompanies this developmental programme of ageing. Apart from its orderly physiological functions, the IL-6 cytokine plays a fundamental role in the intercellular communication between various cells across tissues harbouring a potentially cancerogenic mutational burden. IL-6 acts as a key messenger between cancerous and non-cancerous cell populations at the tumour site. It strengthens their local interactions, but it also has a prominent systemic effect after leakage to the circulation. Terminal stages of disease in the elderly and malignant diseases share outstanding similarities. Both in ageing-related and cancer-induced cachexia, IL-6 alone, or in combination with other factors, plays a critical role [56]. Evidence suggests that long-term prophylactic systemic therapy by recently available non-steroid anti-inflammatory drugs in the elderly can be beneficial for these individuals. Apart from improved cardiovascular outcomes, this therapy can lead to a reduction in the incidence of malignant tumours in aged patients. However, even this therapy should be carefully individualised. It was revealed in recent years that the ASA effects on several condition outcomes, including cancer, also showed interactions particularly with body mass [57]. Therefore, the simplistic "one-dose-fits-all" strategy of prevention is unlikely to be optimal.

4. IL-6 and Chronic Inflammatory Diseases

Human pathology and clinical medicine describe a plethora of chronic inflammatory systemic diseases [58]. In recent years, many of these conditions have been classified as autoimmune disorders, namely rheumatoid arthritis, systemic lupus erythematosus, and multiple sclerosis, and should be associated with tumour formation. In agreement with the topic of this article, participation of chronic inflammation in experimentally induced inflammatory bowel disease induces tissue fibrosis, which promotes cancer in the treated animals [59]. Because of the critical role of IL-6 in the control of inflammation, it is not surprising that this cytokine is essential in the chronic, frequently autoimmune inflammations listed above. Notably, in rheumatoid arthritis, the blocking of the IL-6–IL-6R axis can be successfully controlled in clinical practice, for example, by tocilizumab [60]. However important, all these conditions originating from the immune cell aggression against the organism, in principle, represent very different issues that are relatively remote to the scope of our review. Therefore, we decided not to follow this aspect and focus primarily on the oncological and developmental implications.

5. Cancer and IL-6

5.1. Cancer as a Complex Tissue/Organ

The incidence of malignant tumours in humans is significantly increasing. This phenomenon seems to be associated with population ageing in developed countries, where it is traditionally attributed to advanced medical care. We may expect that each third or even every other citizen is at risk of encountering cancer in the course of his or her life [61]. Therefore, all knowledge improving our understanding of cancer biology is critically important because it can establish a basis for new therapeutic strategies. The scientific interest, as well as therapeutic efforts, have primarily focused on cancer cells. This population is usually widely genetically altered [62] because of the attenuation of the gene repair machinery in the elderly [63]. This concept was successful many times and allowed for even highly efficient, personalised treatment, as exemplified in everyday practice on the case of, e.g., BRAF-mutated melanoma. However, a tumour is a complex tissue and contains highly important yet non-cancerous components, usually described as the stroma. In a broader view, the tumour can be described using the terminology and principles of classical ecology. This approach allows for the identification of some previously neglected functional interactions. In this concept, the tumour cells reside in a suitable niche that can support them via nutrients and oxygen, and that also provides protection against predators such as anti-cancer immunity [64]. In parallel, it is known that normal adult stem cells also require a similar specific environment for their life-long stemness maintenance [65]. This suggests an intriguing similarity between some aspects of cancer and regenerative biology. It is not surprising that cancer was tentatively compared to chronic wounds [66], and remarkable similarities between the wound repair mechanisms and cancer were indeed identified based on the molecular architecture of the healing process [67].

Except for cancer cells, the cancer ecosystem contains cancer-associated fibroblasts (CAFs) and infiltrating immune cells ((natural killer (NK) cells, Treg lymphocytes, CD8+ T lymphocytes, tumour-associated macrophages, myeloid-derived immunosuppressive cells, etc. [68]) (Figure 2). From this point of view, a tumour, for example, cancer of the breast, can be seen as a parallel of a specific organ. It requires highly orchestrated regulation that improves the tumour growth and consequently allows its spread [43]. It is critically important to identify individual components of the tumour, but it is even more important to be able to identify all the interactions that they are undergoing.

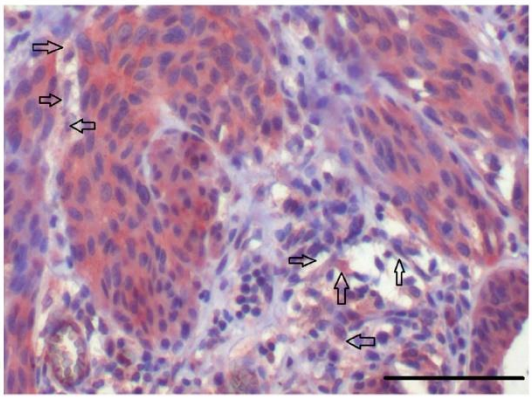

Figure 2. Positive immunohistochemical detection of IL-6 in human cutaneous malignant melanoma. Nests of melanoma cells are highly positive for IL-6 (in brown). Stromal cells, including representatives of CAFs (arrows), are also somewhat positive in this staining. The bar is 100 μm.

5.2. CAFs as Producers of IL-6

The cancer ecosystem is quite uniform in different types of tumours. Apart from the cancer cells and immune cells, it contains large numbers of fibroblasts, the CAFs. These cells seem to be important in the control of coordination of the whole cancer ecosystem [69–71]. However, these cells differ from normal tissue fibroblasts in many aspects. Functionally, CAFs are highly activated, and they frequently express α-smooth muscle actin in the majority of tumours (Figure 3A). No unique or universal marker of CAFs has been described thus far. CAFs express several characteristic proteins such as fibroblast-activating protein (FAP), tenascin-C, periostin, Thy-1, podoplanin, and caveolin-1 [72]. In practice, we usually have to rely on a combination of several markers. Therefore, distinguishing them exactly from normal fibroblasts, namely in tissue sections, is not simple. In research practice, several markers should be detected to estimate their quantity and activity.

The origin of CAFs is not entirely clear. It is most likely that CAFs are formed from the local mesenchyme, namely fibroblasts. Similarly, their origin in other mesenchymal cell populations, e.g., adipocytes, pericytes, or endothelial cells, was also hypothesised [71].

Alternatively, CAFs may originate from the bone marrow mesenchymal stem cells chemoattracted to the tumour site, which is less likely via epithelial-to-mesenchymal transition [73,74].

It is known that CAFs are formed from their precursors by factors such as transforming growth factor β (TGF-β)1/3, inflammatory signals such as IL-6, and proteins such as platelet-derived growth factor (PDGF), FGF and galectin-1. The damage to DNA by previous chemo/actinotherapy and reactive oxygen species (ROS) can also enhance CAF formation [71,75,76].

CAFs are not a homogeneous population, and they can be further stratified to several subgroups. Such clustering would slightly differ according to the type of tumours and the stage of the disease. However, it can be concluded that part of CAFs usually produce the extracellular matrix (Figure 3) and others secrete bioactive proteins that influence the biological properties of cancer cells [72]. CAFs are frequently characterised by their senescence-associated secretory phenotype (SASP) [55,77]. This feature is also seen in aged fibroblasts [78]. Despite a general similarity in the expression of SASP components [79], several genes of the SASP signature differ in their expression between CAFs from cutaneous squamous cell carcinoma, basal cell carcinoma, and photodamaged facial fibroblasts of the same patient (Figure 3D).

CAFs from basal or squamous cell carcinoma (all from the head and neck) are bioactive in normal epithelial cells, where they control their low differentiation status [69,70]. Interestingly, CAFs from the basal cell carcinoma, squamous cell carcinoma, breast cancer, and melanoma significantly influenced the phenotype of the breast cancer cell line to the more aggressive appearance close to the breast cancer stem cells [80], which underlines the non-specific character of the crosstalk between the cancer cells and CAFs within the cancer ecosystem. CAFs prepared from malignant cutaneous melanoma significantly improve in vitro migration of glioblastoma cells [81]. However, CAFs are also able to influence the phenotype of fibroblasts in their vicinity, which consequently acquire the phenotype and differentiation plasticity of mesenchymal stem cells [82]. This observation may help to explain the observation of ectopic cartilage or bone in the stroma of some soft tissue tumours or even in epithelial cancers, e.g., pilomatrixoma. Notably, in some cancers, it is accepted as a marker of poor prognosis.

Modern, robust genomic procedures can gently trace transcriptional differences between normal fibroblasts and CAFs. The latter usually present upregulated expression of IL-6 (frequently accompanied by upregulation of IL-8) [20,83]. Very similar findings were confirmed across several types of tumours (Figure 2, Table 3), indicating a general role of IL-6 in cancer biology.

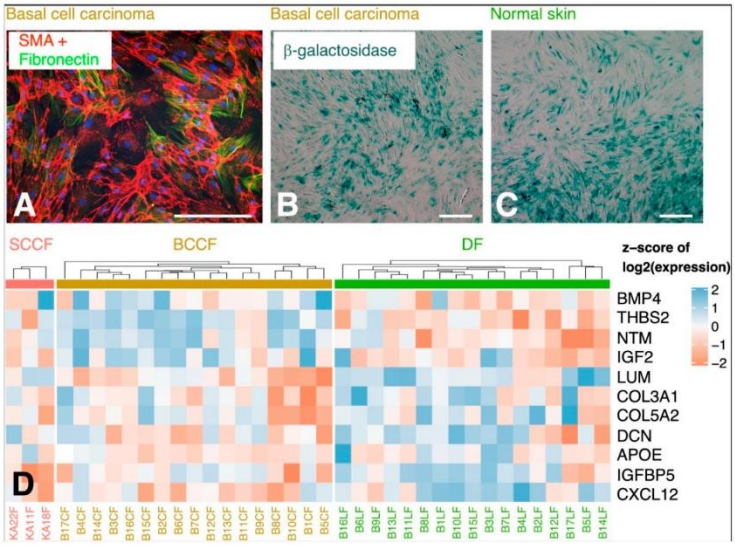

Figure 3. Cultured cancer-associated fibroblasts from basal cell carcinoma and normal skin. Part of fibroblasts isolated from the tumour exhibit α-smooth muscle actin (SMA; green signal). All cells produce fibronectin (red signal). Nuclei were counterstained with 4′,6-diamidino-2-phenylindole (DAPI; blue signal) (**A**). Cultured normal dermal fibroblasts (DF) from the face of an aged donor (**B**) and CAFs from basal cell carcinoma (BCCF) from the face of the same donor (**C**) contain a very high proportion of senescent fibroblasts positive for senescence-associated acid β-galactosidase. The bar is 100 μm. While the senescent phenotype is present in both fibroblast groups, the cells differ in gene expression of several senescence-associated secretory phenotype (SASP) markers (**D**). The same genes are strongly expressed in CAFs from cutaneous squamous cell carcinoma (SCCF).

Table 3. Examples of production of IL-6 by CAFs in different types of cancer and its effect on cancer.

Type of Cell	Effect on Tumour Growth and Spreading	Author
Prostate	+	Heneberg, 2016 [84]
Adenocarcinoma of pancreas	+	Heneberg, 2016 [84]
Liver	+	Li et al., 2019 [85]
Colorectal	+	Nagasaki et al., 2014 [86]
Stomach	+	Wu et al., 2017 [87]
Lung	+	Wang et al., 2017 [88]
Head and neck squamous cell carcinoma	+	Plzák et al., 2019 [83]
Basal cell carcinoma of skin	+	Omland et al., 2017 [89]
Squamous cell carcinoma of skin	+	Depner et al., 2014 [90]
Cutaneous malignant melanoma	+	Jobe et al., 2018 [91]
Urinary bladder	+	Goulet et al., 2019 [92]

5.3. Local and Systemic Effect of IL-6 in Cancer Progression

Factors of paracrine signalling participating in the crosstalk between cancerous and non-malignant cells of the cancer ecosystem profoundly influence the biological behaviour of the tumour [20]. Abundant production of IL-6 by CAFs and other cell types (e.g., adipocytes in breast cancer) in different types of tumours indicates the importance of this factor in cancer cell biology. IL-6 stimulates cancer

cell proliferation [93] and epithelial-to-mesenchymal transition [92]. The experimental blockade of IL-6 with the simultaneous inhibition of IL-8 significantly attenuated the invasiveness of cancer cells in vitro [94,95]. The activation of STAT3, JAK/STAT, mTOR, sonic hedgehog and nuclear factor κ B (NFκB) signalling is important for the IL-6 effect on cancer cells and supports the metastatic spreading of malignant disease [96]. The role of IL-6 in cooperation with IL-8 in neovascularisation and thus in the progression of cancer was also confirmed [97]. As demonstrated in Figure 2 and extensively discussed by Lacina and co-workers [20], cancer cells, including the cells of CMM, also produce IL-6. The combination of the paracrine and autocrine routes of production of this cytokine and their complex regulation influencing the CMM cell biology must therefore be expected.

Factors of the intercellular crosstalk from the cancer site can also cross the capillary wall and thus enter systemic blood circulation. Consequently, these bioactive molecules can be detected in the blood serum of cancer patients [98]. This observation suggests that these molecules might serve as biomarkers and can be potentially used to estimate the progression of the disease. However, problems might come from the specificity of these findings. Moreover, the general health status of the patients must be carefully reflected, because, for example, even a mild respiratory infection before the examination can completely change the serum profile. These factors, produced by the cancer ecosystem and transported by circulation, seem to participate in shaping the premetastatic tissue landscape, a safe niche serving as a suitable cradle for cancer cell homing and later development of metastases, as was demonstrated in the case of breast cancer and malignant melanoma [99,100].

Finally, high concentrations of IL-6, IL-10 and TNF-α in the serum can even predict the mortality of patients with an advanced stage of malignant disease [101].

Cancer patients frequently die in the terminal, therapy-refractive stage of the disease due to cancer cachexia and wasting. This process seems to be strongly influenced by IL-6 and TNF-α, which affect adipocytes, hepatocytes and striated muscle fibres, where both factors induce skeletal muscle atrophy, lipolysis, the "browning" of white adipocytes and ketogenesis in the liver [20,102,103]. It seems that there is a direct association between the high level of IL-6 produced by the malignant tissue, low skeletal muscle mass, and the survival of the patient [104]. In addition to these severe metabolic problems, IL-6 can cross the blood–brain barrier, where it is recognised by groups of hypothalamic and hippocampal neurons controlling food intake and causing depression [105,106]. A high level of IL-6 even correlates with an increased risk of suicide [107]. The combination of metabolic and central nervous system-related issues seems to be fatal in the terminal stage of the disease when anti-cancer therapy has failed.

5.4. Summary of the Role of IL-6 and Cancer

IL-6 represents an important factor of intercellular communication in the cancer cell niche. It also participates in cancer progression, including formation of the premetastatic niche and the process of metastatic dissemination itself. IL-6 has a remarkable systemic effect, culminating, by the failure of metabolism, in severe psychological and mental problems, and finally leading to the death of the cancer patient.

6. COVID-19

6.1. Covid-19 and IL-6

In contrast to the slow rate of progression of ageing and cancer, the course of acute infectious diseases is associated with an uncontrolled and excessive flare of inflammation. Surprisingly, many molecular players of these clinically distinct conditions remain identical. This offers a useful insight into the regulation of the involved mechanisms.

COVID-19 is a transmissible respiratory disease caused by coronavirus SARS-CoV-2. The majority of infected persons are, fortunately, asymptomatic, or their symptoms are only mild. Unfortunately, some of the patients develop severe pneumonia accompanied by a risk of damage to other organs

such as the liver, heart, digestive system, brain, etc. This severe progression leads to acute respiratory distress syndrome (ARDS), and the illness may result in the failure of respiration and the death of the patient [108,109].

COVID-19 is usually accompanied by an elevation of numerous bioactive factors such as IL-1β, TNF-α, IL-2, IL-7, IL-8, IL-9, IL-17 G-CSF, interferon (IFN)-γ, XXC-10, CCL-2 CCL-3, CCL-4, and especially IL-6, which is produced predominantly by macrophages [110,111]. The severe and frequently fatal character of the disease is characterised by a high level of IL-6 and CRP in the blood or plasma of the patients [112–115]. IL-6, in collaboration with other factors, influences the endothelial cells of lung capillaries, increasing their permeability for serum proteins and improving the transmigration of inflammatory cells [116]. Interestingly, similar findings were noted in earlier serious coronavirus outbreaks, severe acute respiratory syndrome (SARS) and middle east respiratory syndrome (MERS). Both conditions were associated with a severe complication: cytokine storm [117]. This finding demonstrates similarity across serious coronaviral infections. Another well-known respiratory infection, influenza, underlines the role of IL-6 in late immune problems in the patients suffering from these infections. This immune dysregulation can be described as cytokine storm/cytokine released syndrome, where cells such as Tregs, decreasing the level of inflammation, are also reduced. The leading role of IL-6 in this process was also demonstrated in COVID-19. To be characterised as causal for cytokine storm, it should meet the following criteria: 1. rapid and extensive viral replication; 2. infection of airways or alveolar cells; 3. delayed IFN-γ response; 4. monocyte–macrophage and neutrophil accumulation [117]. These conditions are sufficiently accomplished in the COVID-19 disease.

6.2. Summary of the Role of IL-6 in COVID-19

IL-6 plays a fundamental role in the advanced stage of COVID-19, where it is associated with the initiation and progression of cytokine storm, which frequently has fatal consequences for the infected person.

7. Targeting the IL-6/IL-6R/gp130-Dependent Signalling

As exemplified above, IL-6 signalling is very important in ageing-related disorders, cancer, and severe viral diseases such as SARS, MERS and COVID-19. From this aspect, therapeutic targeting of the IL-6-dependent axis may be vitally important for the treatment of these diseases. The IL-6 pathway-regulating agents can be classified, concerning the biotechnology of their manufacturing, as antibodies and small-molecule inhibitors.

7.1. Antibodies

The prominent representatives of antibodies targeted to IL-6, IL-6R and gp130 are summarised in Table 4. These antibodies are predominantly used for therapy in autoimmune diseases such as rheumatoid/psoriatic arthritis, but their employment as therapeutics for certain tumours is also approved (Table 4). The in vitro anti-migratory effect of some of these antibodies such as tocilizumab suggests the possible employment of IL-6–IL-6R targeting as in migrastatic drugs [118,119] (Figure 4). Unfortunately, the therapeutic effect of migrastatics in anti-cancer treatment is much lower than previously anticipated [120,121]. Perhaps migrastatics in combination with the targeting of other signalling cascades could be more promising. The combination of anti-IL-6 and anti-IL-8 targeting seems to be useful [94,95]. The combination of in vitro and bioinformatic approaches demonstrated that a simultaneous blockade of bascular endothelial growth factor A (VEGF-A) and milk fat globule epidermal growth factor –E8 (MFGE-8) signalling could offer satisfactory results [83]. As summarised by Johnson and co-workers [121], the combination of targeting the IL-6 axis with therapy influencing immune checkpoints can be introduced into clinical practice.

Table 4. Examples of antibodies designed to target IL-6, IL-6R and gp130.

Antibody	Target	Main Application	Producer
Siltuximab *	IL-6	Renal + prostate cancer Castleman's disease COVID-19	EUSA Pharma
Sirukumab +	IL-6	Rheumatoid arthritis COVID-19	Janssen Biotech
Olokizumab +	IL-6	Rheumatoid arthritis	R-Pharm Group
Clazakizumab +	IL-6	Psoriatic arthritis COVID-19	Bristol Myers Squibb and Alder Biopharmaceuticals
Elsilimomab +	IL-6	Lymphoma Myeloma	Diaclone
Tocilizumab *	IL-6R	Rheumatoid arthritis Multiple myeloma Prostate cancer COVID-19	Hoffmann-La Roche and Chugai
Sarilumab *	Gp130	Rheumatoid arthritis	Regeneron Pharmaceuticals and Sanofi

* used in clinical practice, + experimental or under clinical trial.

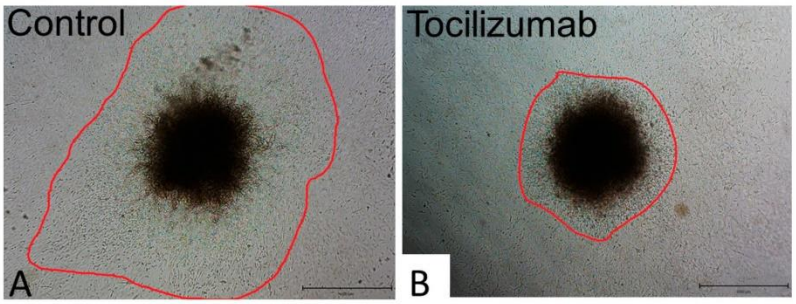

Figure 4. Migration of G361 melanoma cells from spheroids. G361 melanoma cells migrate from the heterogeneous spheres constructed from G361 melanoma cells and juvenile fibroblasts in 3D collagen gels without (**A**) and after tocilizumab application (**B**). Migration of melanoma cells was strongly reduced by the therapeutic humanised monoclonal antibody. Bar is 1 mm.

New data have also demonstrated that antibodies targeting IL-6/IL-6R/gp130 such as tocilizumab, siltuximab and clazakizumab could be employed for the therapy of COVID-19 [122–125], as was also recommended by the National Institute of Health (NIH COVID-19 Treatment Guidelines, 2020) [126]. The testing of other therapeutic antibodies influencing IL-6 signalling for the treatment of COVID-19 can be expected.

7.2. Natural and Synthetic Small Molecules as IL-6 Receptor Complex Inhibitors

7.2.1. Oestrogen Analogues—Experimental Drugs for Inhibition of IL-6 Signalling

An interesting molecule with a documented potential to block IL-6R is a synthetic analogue of oestrogens, bazedoxifene. This clinically available drug was designed and later approved for the therapy of postmenopausal osteoporosis [127]. Another substance with a very similar structure was prepared for the same purpose: raloxifene [128] (Figure 5). These therapeutics are also able to interact with gp130 and thus inhibit docking of IL-6 to its receptor [129,130]. Because of their low price and minimal adverse effects, these substances were tested for the therapy of some malignant tumours such

as rhabdomyosarcoma [129], head and neck cancer [131], adenocarcinoma of the pancreas [132,133], colorectal cancer [134], and hepatocellular carcinoma [135]. They were also proposed for the treatment of cytokine storm in patients suffering from COVID-19 [136–138]. Moreover, bazedoxifene also reduces the replication of SARS-CoV-2 in susceptive cells [139].

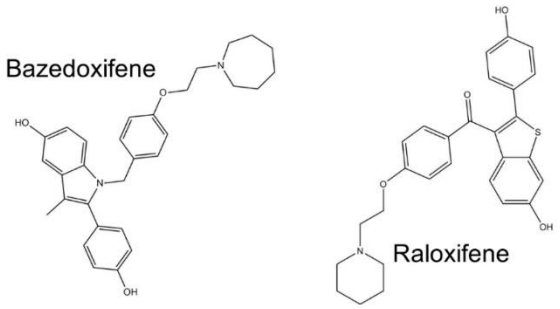

Figure 5. Structure of synthetic oestrogen analogues bazedoxifene and raloxifene.

7.2.2. Other Small Molecules—Experimental Drugs

Recently, it was demonstrated that targeting the IL-6 receptor by monoclonal antibodies is a promising therapy for a number of diseases associated with increased inflammation. However, monoclonal antibodies have some limitations (high cost, invasive route of administration, and appreciable rate of immunogenicity) to their clinical benefit [140]. Therefore, the development of low-molecular weight inhibitors is highly demanded for their superiority in oral absorption, low toxicity, and low antigenicity. Despite the immense importance of this task and the invested efforts, the IL-6 axis-influencing compounds are only few [141–149].

For example, natural compounds (madindolines A and B) (Figure 6) produced by Streptomyces sp. displayed vigorous inhibition activity against the growth rate of IL-6-dependent cell lines [141,145]. It was observed that the addition of higher IL-6 levels repressed this phenomenon, and the growth rate of IL-6-independent lines was not affected, implying that these compounds could target the IL-6 receptor complex. However, subsequent studies showed that the effect of madindoline is based on its binding to gp130 [142]. Madindoline A did not affect osteoclast formation controlled by the heterodimer type of gp130 (LIF-induced) or cAMP (IL-1), but, in this case, the homodimer types of gp130 (induced by IL-6 and Il-11) were found to be significantly efficient.

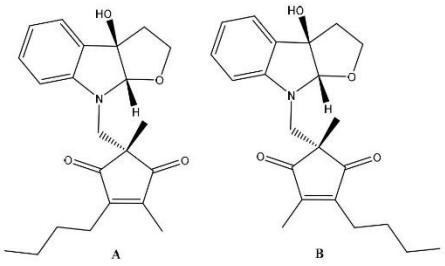

Figure 6. Madindoline regioisomers (**A**) and (**B**).

In the C3H-HeJ mouse model (lipopolysaccharide-insensitive), secretion of serum amyloid induced by IL-6 was inhibited by madindoline A in a dose-dependent manner. However, the secretion of serum amyloid induced by lipopolysaccharide-sensitive C3H-HeN mice) was not reduced by

madindoline A [144]. These facts also ignited the development of a novel synthetic madindoline analogue. For example, Yamamoto and co-workers [146] prepared a library of candidate structures and tested their effect on the growth of 7TDI cells (IL-6-dependent cell line). These authors proposed that hydrophobic substitution by acyl chains can sometimes improve madindoline inhibition activity.

A promising therapeutic application of madindoline analogues such as MDL-101 (Figure 7) for the treatment of neurodegenerative diseases was also demonstrated by Aqel et al. [147]. These compounds can also interfere via IL-17 production (induced by STAT 3 signalling) in myelin-specific CD4 T lymphocytes in a dose-dependent manner.

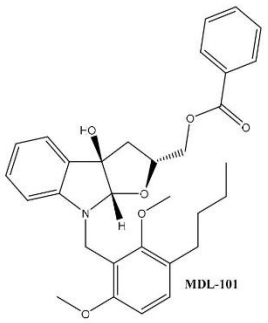

Figure 7. MDL-101 derivative of madindoline.

Other compounds targeting the IL-6 receptor are bufadienolide derivatives. These natural anti-cancer compounds are isolated from a Chinese toad skin extract—the Ch'an Su drug [150]. It contains active components such as 20S,21-epoxy-resibufogenin-3-formate (ERBF, Figure 8) [142]. This compound did not affect IL-2-, IL-3- and IL-5-dependent cell growth. However, in the case of IL-6-dependent cell lines, the effect of this molecule was notable. In a co-culture of osteoblasts and bone marrow cells, similar to madindoline A, the repression of IL-6 induced osteoblast formation. The effect of substances such as LIF and 1-25(OH)2D3 vitamin was not compromised. Enomoto and colleagues [143] demonstrated that the mechanism of its effect on the IL-6 signalling axis is based on the blockade of IL-6 interaction with its receptor. This finding is substantial because ERBF could treat pathologies such as cancer cachexia, which is associated with IL-6 overactivity. This was demonstrated in an experimental model of colon cancer-induced cachexia. ERBF markedly inhibited body weight loss, but, unfortunately, did not affect tumour growth.

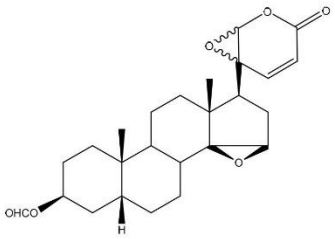

Figure 8. 20S,21-Epoxy-resibufogenin-3-formate (ERBF) inhibitor.

The relationship between the structure of bufadienolide derivatives and their inhibition activity was studied using IL-6-dependent and independent MH-60 cell lines [143]. Both epoxides at the C-14, C-15 and C-20, C-21 positions in the structure are required to exhibit the inhibitory activity, and the

C-16 position must be unsubstituted. The introduction of aliphatic organic acid in the C-3 position increased the inhibition activity in IL-6-dependent cells. This inhibition activity decreased according to the increase in the carbon chains of fatty acids at the C-3 position, such as propionate, butyrate and isobutyrate, whereas a carbonyl group at the C-3 position exhibited cytotoxic activity for both types of MH-60 cells. The above facts inspired Kino et al. [145] to study the effects of bufadienolide derivatives such as TB-2-081 (3-O-formyl-20R,21 epoxyresibufogenin) on the IL-6 signalling in the hepatocyte cell lines. As expected, the authors observed a reduced expression of IL-6-controlled genes (e.g., α1-antichymotrypsin, α1-acid glycoprotein, α2-macroglobulin, and β-fibrinogen) and low secretion of C-reactive protein. Nevertheless, because IL-11-induced α1-antichymotrypsin expression was also repressed, this implies that the effect of the tested compounds is based on the inhibition of gp130 and not directly on the level of IL-6R.

Another interesting inhibitor targeting gp130, LMT-28 (Figure 9), was designed by Hong and co-workers [148]. It interacts with gp130 and subsequently reduces the affinity of the receptor complex for the binding of available IL-6. In agreement with this mechanistic explanation, this leads to a reduction in STAT3 phosphorylation, stimulated by IL-6 in permissive cells. This observation was further confirmed in a mouse model.

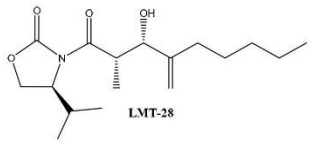

Figure 9. LMT-28 inhibitor.

In general terms, certain structural motives (e.g., bufadienolide and madindoline derivatives) are suitable for targeting IL-6 receptors and the suppression of IL-6 pathway signalling activity. They were shown to display low toxicity. Consequent studies performed in vitro and in vivo offered some therapeutic potential, for example, for the treatment of inflammatory, neurodegenerative, and also oncological diseases. Their biological effects are summarised in Supplementary Table S1. Nevertheless, to progress towards their clinical application, and a more in-depth understanding of the relationship between their molecular structure and biological effect must first be achieved. Notably, it is crucial to improve their in vivo delivery to suitable cells.

Other examples of synthetic/natural small-molecule inhibitors that affect IL-6 production, docking and signalling, including the description of the molecular mechanism, are excellently provided in a recent review by Kaur and co-workers [151].

As an example, we show the efficiency of the experimental substance TBMS47, developed in our laboratory. The substance was designed to be active in micromolar concentrations, such as is requested of modern low-molecular weight anticancer drugs [152]. However, the therapeutic concentration in clinics could has not yet been estimated. TBMS47 recognises the biding site of IL-6R that blocks the interaction between IL-6 and IL-6R. In vitro application of this molecule has a significant effect on the growth of melanoma cells, and the effect is concentration dependent (Figure 10).

Until now, numerous studies focused on the association of the chemical structure of the inhibitor and its biological effect. However, several essential issues still remain open. For example, the inhibition effect of ERBF is dependent on the blocking of the interaction of IL-6 with its receptor. Other bufadienolide derivatives (e.g., TB-2-081)—against expectation—inhibit the interaction of gp130 with the complex of IL-6 and IL-6R [145]. It is well known that some types of cancer are associated with the mutation of proteins of the IL-6 axis that can significantly influence IL-6 signalling [13,153,154]. The strict requirement to employ a distinct inhibitor to receive a correct biological response is still valid. Robust and mechanistically clear studies of the IL-6 signalling cascade and its specific inhibition are highly desirable before clinical application of the novel inhibitors.

In the case of small molecules, low solubility remains one of the greatest issues. In particular, poorly soluble ones suffer from insufficient selectivity for the target organs and tissues, and their half-life in the blood is short. Currently, numerous suitable drug delivery systems for these types of compounds are being developed or are already available, for example, cyclodextrins, silica nanoparticles, and liposomes [155–157]. Notably, these systems can be successfully used for drug transport across the blood–brain barrier. This can significantly enhance the therapeutic potential of these small IL-6 receptor inhibitors for the treatment of brain tumours or neurological diseases.

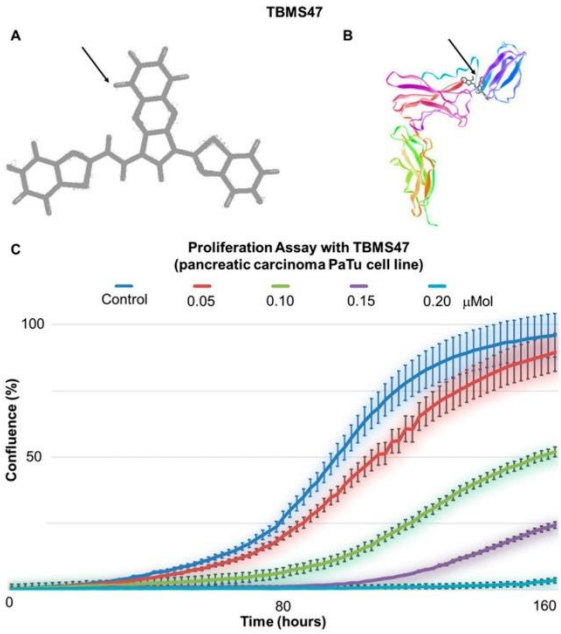

Figure 10. Inhibitor TBMS47 (**A**—structure, **B**—model). Chemical structure of experimental substance TBMS47 (arrow) was designed to interact with IL-6R and its docking to the binding site of IL-6R recognizing IL-6. (**C**) TBMS47 inhibits in vitro proliferation of PaTu cells from pancreatic adenocarcinoma (represented here as Confluence %) in a concentration-dependent manner measured using Incucyte instrumentation (each line represents six technical replicates; error bars represent standard deviation of six wells).

8. Direct Targeting of CAFs

In the case of malignant tumours with a prominent role in CAFs, therapy targeting different molecules in these cells is in the phase of clinical trials, as summarised in a recent review by Sahai and co-workers [71]. Suitable targets are FGF receptor (FGFR), hedgehog, TGF-β, CXC-chemokine receptor 4 (CXCR-4), RHO kinase (ROCK), focal adhesion kinase (FAK), lysyl oxidase-like 2 (LOXL-2), connective tissue growth factor (GTF), hyaluronic acid, and FAP. The targeting of CAFs using a synthetic antibody analogue (iBody) directed to FAP by a sensitive substrate appears to be rather promising [158,159]. Despite the prominent role of IL-6 in tumour biology, this aspect of stromal biology seems to have been somewhat neglected until now. Nevertheless, it is too early to evaluate the therapeutic relevance of these approaches and determine their position among other recently available treatment options.

9. Concluding Remarks

IL-6 is a multifaceted cytokine with a remarkable role in the initiation of inflammation and immune response. On the other hand, the failure of regulation and increased levels of this cytokine in a patient's body are influenced by ageing, cancer progression and fatal complications of serious viral infections. The high level of IL-6 and abnormal activation of the IL-6–IL-6R axis are associated with the severe progression of disease and may be responsible for the failure of therapy and, eventually, fatal complications. A detailed understanding of the biology of IL-6, the IL-6R receptor and its signalling axis can bring new information essential for the amelioration of the problems of ageing and offer an efficient therapy for malignancies and viral infections. A panel of therapeutic antibodies influencing IL-6 signalling is available, but their use has various biological and economic limitations. Another potential modality is represented by the class of small-molecule inhibitors. Nevertheless, in-depth knowledge of the biology of IL-6 signalling along with the precise determination of the relationship between the inhibitor's chemical structure and the IL-6–IL-6R complex are prerequisites for its rapid addition to the therapeutic arsenal.

Supplementary Materials: Supplementary materials can be found at http://www.mdpi.com/1422-0067/21/21/7937/s1.

Author Contributions: Conceptualisation: K.S.J., J.B., M.J., M.K. and L.L.; data collection: M.J., K.S.J., K.S., L.L., P.S., B.D., M.J., F.V., M.K., J.N. and J.B., writing—original draft preparation: D.R., K.S.J., L.L., M.J., M.K. and J.B.; funding acquisition: K.S.J. All authors have read and agreed to the published version of the manuscript.

Funding: This research was funded by the project "Centre for Tumour Ecology—Research of the Cancer Microenvironment Supporting Cancer Growth and Spread" (No. CZ.02.1.01/0.0/0.0/16_019/0000785), supported by the Operational Programme "Research, Development and Education" of the European Regional Development Fund (ERDF), BIOCEV (No. CZ.1.05/1.1.00/02.0109), "The Equipment for Metabolomics and Cell Analyses" (No. CZ.1.05/2.1.00/19.0400) and by Charles University in Prague (PROGRES Q28).

Acknowledgments: The authors are grateful to Šárka Takáčová for the language revision of the manuscript.

Conflicts of Interest: The authors declare no conflict of interest.

Abbreviations

ASA	Acetylsalicylic acid
ARDS	Acute respiratory distress syndrome
BCC	Basal cell carcinoma
BCCF	Basal cell carcinoma-associated fibroblasts
BDDF	Brain-derived neurotrophic factor
CNTF	Ciliary neurotrophic factor
CAFs	Cancer-associated fibroblasts
CLC	Cardiotrophin-like cytokine
COX	Cyclooxygenase
CRP	C-reactive protein
CXCR-4	CXC-chemokine receptor 4
DAPI	4′,6-Diamidino-2-phenylindole
DF	Dermal fibroblast
ERBF	20S,21-Epoxy-resibufogenin-3-formate
FAK	Focal adhesion kinase
FAP	Fibroblast-activating protein
FGF	Fibroblast growth factor
FGFR	Fibroblast growth factor receptor
GTF	Connective tissue growth factor
G-CSF	Granulocyte colony-stimulating factor
Gp130	Glycoprotein 130

IFN	Interferon
IGF-1	Insulin growth factor-1
IL	Interleukin
IL-6R	Receptor for IL-6
LIF	Leukaemia inhibitory factor
LOXL-2	Lysyl oxidase-like 2
MFGE8	Milk fat globule epiderma drowth factor E8
MERS	Middle east respiratory syndrome
NFκB	Nuclear factor κ B
NK cells	Nature killer cells
PDGF	Platelet-derived growth factor
ROCK	RHO kinase
ROS	Reactive oxygen species
SARS	Severe acute respiratory syndrome
SASP	Senescence-associated secretory phenotype
SCC	Squamous cell carcinoma
SCCF	Squamous cell carcinoma-associated fibroblasts
sHH	Sonic hedgehog
SMA	α-Smooth muscle actin
Treg	Regulatory T lymphocytes
TGF-β	Transforming growth factor β
TNF	Tumour necrosis factor
VEGFA	Vascular endothelial growth factor A

References

1. Tissue Expression of IL6—Summary—The Human Protein Atlas. Available online: https://www.proteinatlas.org/ENSG00000136244-IL6/tissue (accessed on 21 September 2020).
2. Zilberstein, A.; Ruggieri, R.; Korn, J.H.; Revel, M. Structure and expression of cDNA and genes for human interferon-beta-2, a distinct species inducible by growth-stimulatory cytokines. *EMBO J.* **1986**, *5*, 2529–2537. [CrossRef]
3. Haegeman, G.; Content, J.; Volckaert, G.; Derynck, R.; Tavernier, J.; Fiers, W. Structural analysis of the sequence coding for an inducible 26-kDa protein in human fibroblasts. *Eur. J. Biochem.* **1986**, *159*, 625–632. [CrossRef] [PubMed]
4. Hirano, T.; Taga, T.; Nakano, N.; Yasukawa, K.; Kashiwamura, S.; Shimizu, K.; Nakajima, K.; Pyun, K.H.; Kishimoto, T. Purification to homogeneity and characterization of human B-cell differentiation factor (BCDF or BSFp-2). *Proc. Natl. Acad. Sci. USA* **1985**, *82*, 5490–5494. [CrossRef] [PubMed]
5. Brakenhoff, J.P.; de Groot, E.R.; Evers, R.F.; Pannekoek, H.; Aarden, L.A. Molecular cloning and expression of hybridoma growth factor in Escherichia coli. *J. Immunol.* **1987**, *139*, 4116–4121. [PubMed]
6. Nordan, R.P.; Pumphrey, J.G.; Rudikoff, S. Purification and NH2-terminal sequence of a plasmacytoma growth factor derived from the murine macrophage cell line P388D1. *J. Immunol.* **1987**, *139*, 813–817. [PubMed]
7. Gauldie, J.; Richards, C.; Harnish, D.; Lansdorp, P.; Baumann, H. Interferon beta 2/B-cell stimulatory factor type 2 shares identity with monocyte-derived hepatocyte-stimulating factor and regulates the major acute phase protein response in liver cells. *Proc. Natl. Acad. Sci. USA* **1987**, *84*, 7251–7255. [CrossRef]
8. Ikebuchi, K.; Wong, G.G.; Clark, S.C.; Ihle, J.N.; Hirai, Y.; Ogawa, M. Interleukin 6 enhancement of interleukin 3-dependent proliferation of multipotential hemopoietic progenitors. *Proc. Natl. Acad. Sci. USA* **1987**, *84*, 9035–9039. [CrossRef]
9. Takai, Y.; Wong, G.G.; Clark, S.C.; Burakoff, S.J.; Herrmann, S.H. B cell stimulatory factor-2 is involved in the differentiation of cytotoxic T lymphocytes. *J. Immunol.* **1988**, *140*, 140.
10. Groeger, S.; Meyle, J. Oral mucosal epithelial cells. *Front. Immunol.* **2019**, *10*, 208. [CrossRef]
11. Pritts, T.; Hungness, E.; Wang, Q.; Robb, B.; Hershko, D.; Hasselgren, P.O. Mucosal and enterocyte IL-6 production during sepsis and endotoxemia—Role of transcription factors and regulation by the stress response. *Am. J. Surg.* **2002**, *183*, 372–383. [CrossRef]

12. Uehling, D.T.; Brooke Johnson, D.; Hopkins, W.J. The urinary tract response to entry of pathogens. *World J. Urol.* **1999**, *17*, 351–358. [CrossRef] [PubMed]
13. Schmidt-Arras, D.; Rose-John, S. IL-6 pathway in the liver: From physiopathology to therapy. *J. Hepatol.* **2016**, *64*, 1403–1415. [CrossRef] [PubMed]
14. Cheung, C.Y.; Poon, L.L.M.; Ng, I.H.Y.; Luk, W.; Sia, S.-F.; Wu, M.H.S.; Chan, K.-H.; Yuen, K.-Y.; Gordon, S.; Guan, Y.; et al. Cytokine Responses in Severe Acute Respiratory Syndrome Coronavirus-Infected Macrophages In Vitro: Possible Relevance to Pathogenesis. *J. Virol.* **2005**, *79*, 7819–7826. [CrossRef]
15. Kyotani, Y.; Takasawa, S.; Yoshizumi, M. Proliferative pathways of vascular smooth muscle cells in response to intermittent hypoxia. *Int. J. Mol. Sci.* **2019**, *20*, 2706. [CrossRef] [PubMed]
16. Barbalho, S.; Vieira Prado Neto, E.; de Alvares Goulart, R.; Bechara, M.; Federighi Baisi Chagas, E.; Audi, M.; Guissoni Campos, L.; Landgraf Guiger, E.; Leoni Buchain, R.; Buchain, D.; et al. Myokines: A descriptive review. *J. Sports Med. Phys. Fit.* **2020**. [CrossRef]
17. Kovács, B.; Vajda, E.; Nagy, E.E. Regulatory effects and interactions of the Wnt and OPG-RANKL-RANK signaling at the bone-cartilage interface in osteoarthritis. *Int. J. Mol. Sci.* **2019**, *20*, 4653. [CrossRef] [PubMed]
18. Xie, C.; Chen, Q. Adipokines: New Therapeutic Target for Osteoarthritis? *Curr. Rheumatol. Rep.* **2019**, *21*, 71. [CrossRef] [PubMed]
19. Shapouri-Moghaddam, A.; Mohammadian, S.; Vazini, H.; Taghadosi, M.; Esmaeili, S.A.; Mardani, F.; Seifi, B.; Mohammadi, A.; Afshari, J.T.; Sahebkar, A. Macrophage plasticity, polarization, and function in health and disease. *J. Cell. Physiol.* **2018**, *233*, 6425–6440. [CrossRef]
20. Lacina, L.; Brábek, J.; Král, V.; Kodet, O.; Smetana, K. Interleukin-6: A molecule with complex biological impact in cancer. *Histol. Histopathol.* **2019**, *34*, 125–136.
21. Unver, N.; McAllister, F. IL-6 family cytokines: Key inflammatory mediators as biomarkers and potential therapeutic targets. *Cytokine Growth Factor Rev.* **2018**, *41*, 10–17. [CrossRef]
22. Rose-John, S. Interleukin-6 Family Cytokines. *Cold Spring Harb. Perspect. Biol.* **2018**, *10*, a028415. [CrossRef] [PubMed]
23. Kopf, M.; Baumann, H.; Freer, G.; Freudenberg, M.; Lamers, M.; Kishimoto, T.; Zinkernagel, R.; Bluethmann, H.; Köhler, G. Impaired immune and acute-phase responses in interleukin-6-deficient mice. *Nature* **1994**, *368*, 339–342. [CrossRef] [PubMed]
24. Ramsay, A.J.; Kopf, M. IL-6 Gene Knockout Mice. In *Cytokine Knockouts. Contemporary Immunology*; Durum, S.K., Muegge, K., Eds.; Humana Press: Totowa, NJ, USA, 1998; pp. 227–236. [CrossRef]
25. Tanaka, T.; Narazaki, M.; Kishimoto, T. Il-6 in inflammation, Immunity, And disease. *Cold Spring Harb. Perspect. Biol.* **2014**, *6*, a016295. [CrossRef] [PubMed]
26. Takatsuki, F.; Okano, A.; Suzuki, C.; Chieda, R.; Takahara, Y.; Hirano, T.; Kishimoto, T.; Hamuro, J.; Akiyama, Y. Human recombinant IL-6/B cell stimulatory factor 2 augments murine antigen-specific antibody responses in vitro and in vivo. *J. Immunol.* **1988**, *141*, 3072–3077.
27. Luger, T.A.; Krutmann, J.; Kirnbauer, R.; Urbanski, A.; Schwarz, T.; Klappacher, G.; Köck, A.; Micksche, M.; Malejczyk, J.; Schauer, E. IFN-beta 2/IL-6 augments the activity of human natural killer cells. *J. Immunol.* **1989**, *143*, 1206–1209.
28. Mendel, I.; Katz, A.; Kozak, N.; Ben-Nun, A.; Revel, M. Interleukin-6 functions in autoimmune encephalomyelitis: A study in gene-targeted mice. *Eur. J. Immunol.* **1998**, *28*, 1727–1737. [CrossRef]
29. Rodríguez, A.; Becerril, S.; Ezquerro, S.; Méndez-Giménez, L.; Frühbeck, G. Crosstalk between adipokines and myokines in fat browning. *Acta Physiol.* **2017**, *219*, 362–381. [CrossRef]
30. Wallenius, V.; Wallenius, K.; Ahrén, B.; Rudling, M.; Carlsten, H.; Dickson, S.L.; Ohlsson, C.; Jansson, J.O. Interleukin-6-deficient mice develop mature-onset obesity. *Nat. Med.* **2002**, *8*, 75–79. [CrossRef]
31. Tamura, T.; Udagawa, N.; Takahashi, N.; Miyaura, C.; Tanaka, S.; Yamada, Y.; Koishihara, Y.; Ohsugi, Y.; Kumaki, K.; Taga, T.; et al. Soluble interleukin-6 receptor triggers osteoclast formation by interleukin 6. *Proc. Natl. Acad. Sci. USA* **1993**, *90*, 11924–11928. [CrossRef]
32. Poli, V.; Balena, R.; Fattori, E.; Markatos, A.; Yamamoto, M.; Tanaka, H.; Ciliberto, G.; Rodan, G.A.; Costantini, F. Interleukin-6 deficient mice are protected from bone loss caused by estrogen depletion. *EMBO J.* **1994**, *13*, 1189–1196. [CrossRef]
33. Ahmad, S.I. *Aging: Exploring a Complex Phenomenon*; CRC Press: Boca Raton, FL, USA, 2017; ISBN 1315283875.
34. World Health Organization. *World Report on Ageing And Health*; World Health Organization: Geneva, Switzerland, 2015.

35. Feltes, B.C.; De Faria Poloni, J.; Bonatto, D. The developmental aging and origins of health and disease hypotheses explained by different protein networks. *Biogerontology* **2011**, *12*, 293–308. [CrossRef] [PubMed]
36. Valiathan, R.; Ashman, M.; Asthana, D. Effects of Ageing on the Immune System: Infants to Elderly. *Scand. J. Immunol.* **2016**, *83*, 255–266. [CrossRef] [PubMed]
37. Puzianowska-Kuźnicka, M.; Owczarz, M.; Wieczorowska-Tobis, K.; Nadrowski, P.; Chudek, J.; Slusarczyk, P.; Skalska, A.; Jonas, M.; Franek, E.; Mossakowska, M. Interleukin-6 and C-reactive protein, successful aging, and mortality: The PolSenior study. *Immun. Ageing* **2016**, *13*, 1–12. [CrossRef] [PubMed]
38. Torres, K.C.L.; de Rezende, V.B.; Lima-Silva, M.L.; de Santos, L.J.S.; Costa, C.G.; de Mambrini, J.V.M.; Peixoto, S.V.; Tarazona-Santos, E.; Martins Filho, O.A.; Lima-Costa, M.F.; et al. Immune senescence and biomarkers profile of Bambuí aged population-based cohort. *Exp. Gerontol.* **2018**, *103*, 47–56. [CrossRef]
39. Adriaensen, W.; Matheï, C.; Van Pottelbergh, G.; Vaes, B.; Legrand, D.; Wallemacq, P.; Degryse, J.M. Significance of serum immune markers in identification of global functional impairment in the oldest old: Cross-sectional results from the BELFRAIL study. *Age (Omaha)* **2014**, *36*, 457–467. [CrossRef]
40. Adriaensen, W.; Matheï, C.; Vaes, B.; van Pottelbergh, G.; Wallemacq, P.; Degryse, J.M. Interleukin-6 as a first-rated serum inflammatory marker to predict mortality and hospitalization in the oldest old: A regression and CART approach in the BELFRAIL study. *Exp. Gerontol.* **2015**, *69*, 53–61. [CrossRef]
41. Franceschi, C.; Capri, M.; Monti, D.; Giunta, S.; Olivieri, F.; Sevini, F.; Panourgia, M.P.; Invidia, L.; Celani, L.; Scurti, M.; et al. Inflammaging and anti-inflammaging: A systemic perspective on aging and longevity emerged from studies in humans. *Mech. Ageing Dev.* **2007**, *128*, 92–105. [CrossRef]
42. Rattan, S.I.S. Aging is not a disease: Implications for intervention. *Aging Dis.* **2014**, *5*, 196–202. [CrossRef]
43. Strnadova, K.; Sandera, V.; Dvorankova, B.; Kodet, O.; Duskova, M.; Smetana, K.; Lacina, L. Skin aging: The dermal perspective. *Clin. Dermatol.* **2019**, *37*, 326–335. [CrossRef]
44. Schrell, U.M.H.; Koch, U.; Marschalek, R.; Schrauzer, T.; Anders, M.; Adams, E.; Fahlbusch, R. Formation of autocrine loops in human cerebral meningioma tissue by leukemia inhibitor factor, interleukin-6, and oncostatin M: Inhibition of meningioma cell growth in vitro by recombinant oncostatin M. *Neurosurg. Focus* **2008**, *2*, E9. [CrossRef]
45. Chambers, E.S.; Akbar, A.N. Can blocking inflammation enhance immunity during aging? *J. Allergy Clin. Immunol.* **2020**, *145*, 1323–1331. [CrossRef]
46. Win, T.T.; Aye, S.N.; Fern, J.L.C.; Fei, C.O. Aspirin and reducing risk of gastric cancer: Systematic review and meta-analysis of the observational studies. *J. Gastrointest. Liver Dis.* **2020**, *29*, 191–198. [CrossRef] [PubMed]
47. Wang, Y.; Zhao, J.; Chen, X.; Zhang, F.; Li, X. Aspirin use and endometrial cancer risk: A meta-analysis and systematic review. *Ann. Transl. Med.* **2020**, *8*, 461. [CrossRef] [PubMed]
48. Fiala, C.; Pasic, M.D. Aspirin: Bitter pill or miracle drug? *Clin. Biochem.* **2020**, *85*, 1–4. [CrossRef]
49. Zhang, Y.; Kong, W.; Jiang, J. Prevention and treatment of cancer targeting chronic inflammation: Research progress, potential agents, clinical studies and mechanisms. *Sci. China Life Sci.* **2017**, *60*, 601–616. [CrossRef] [PubMed]
50. Kast, R.E. Melanoma inhibition by cyclooxygenase inhibitors: Role of interleukin-6 suppression, a putative mechanism of action, and clinical implications. *Med. Oncol.* **2007**, *24*, 1–6. [CrossRef]
51. Hsieh, C.C.; Chiu, H.H.; Wang, C.H.; Kuo, C.H. Aspirin modifies inflammatory mediators and metabolomic profiles and contributes to the suppression of obesity-associated breast cancer cell growth. *Int. J. Mol. Sci.* **2020**, *21*, 4652. [CrossRef]
52. Tian, Y.; Ye, Y.; Gao, W.; Chen, H.; Song, T.; Wang, D.; Mao, X.; Ren, C. Aspirin promotes apoptosis in a murine model of colorectal cancer by mechanisms involving downregulation of IL-6-STAT3 signaling pathway. *Int. J. Colorectal. Dis.* **2011**, *26*, 13–22. [CrossRef]
53. Patrignani, P.; Patrono, C. Aspirin and Cancer. *J. Am. Coll. Cardiol.* **2016**, *68*, 967–976. [CrossRef]
54. Bibbins-Domingo, K.; Grossman, D.C.; Curry, S.J.; Davidson, K.W.; Epling, J.W.; García, F.A.R.; Gillman, M.; Harper, D.M.; Kemper, A.R.; Krist, A.H.; et al. Aspirin use for the primary prevention of cardiovascular disease and colorectal cancer: U.S. preventive services task force recommendation statement. *Ann. Intern. Med.* **2016**, *164*, 836–845. [CrossRef]
55. Coppé, J.-P.; Patil, C.K.; Rodier, F.; Sun, Y.; Muñoz, D.P.; Goldstein, J.; Nelson, P.S.; Desprez, P.-Y.; Campisi, J. Senescence-Associated Secretory Phenotypes Reveal Cell-Nonautonomous Functions of Oncogenic RAS and the p53 Tumor Suppressor. *PLoS Biol.* **2008**, *6*, e301. [CrossRef] [PubMed]

56. Hubbard, R.E.; O'Mahony, M.S.; Calver, B.L.; Woodhouse, K.W. Nutrition, inflammation, and leptin levels in aging and frailty. *J. Am. Geriatr. Soc.* **2008**, *56*, 279–284. [CrossRef] [PubMed]
57. Rothwell, P.M.; Cook, N.R.; Gaziano, J.M.; Price, J.F.; Belch, J.F.F.; Roncaglioni, M.C.; Morimoto, T.; Mehta, Z. Effects of aspirin on risks of vascular events and cancer according to bodyweight and dose: Analysis of individual patient data from randomised trials. *Lancet* **2018**, *392*, 387–399. [CrossRef]
58. Straub, R.H.; Schradin, C. Chronic inflammatory systemic diseases—An evolutionary trade-off between acutely beneficial but chronically harmful programs. *Evol. Med. Public Health* **2016**, *2016*, 37–51. [CrossRef]
59. Sacco, A.; Bruno, A.; Contursi, A.; Dovizio, M.; Tacconelli, S.; Ricciotti, E.; Guillem-Llobat, P.; Salvatore, T.; Di Francesco, L.; Fullone, R.; et al. Platelet-Specific Deletion of Cyclooxygenase-1 Ameliorates Dextran Sulfate Sodium-Induced Colitis in Mice s. *J. Pharmacol. Exp. Ther. J. Pharmacol. Exp. Ther* **2019**, *370*, 416–426. [CrossRef]
60. Pandolfi, F.; Franza, L.; Carusi, V.; Altamura, S.; Andriollo, G.; Nucera, E. Interleukin-6 in rheumatoid arthritis. *Int. J. Mol. Sci.* **2020**, *21*, 1–12. [CrossRef]
61. Smetana, K.; Lacina, L.; Szabo, P.; Dvořánková, B.; Broż, P.; Šedo, A. Ageing as an important risk factor for cancer. *Anticancer Res.* **2016**, *36*, 5009–5017. [CrossRef]
62. Moraes, M.C.S. DNA repair mechanisms protect our genome from carcinogenesis. *Front. Biosci.* **2012**, *17*, 1362. [CrossRef]
63. Edifizi, D.; Schumacher, B. Genome instability in development and aging: Insights from nucleotide excision repair in humans, mice, and worms. *Biomolecules* **2015**, *5*, 1855–1869. [CrossRef]
64. Kareva, I. What can ecology teach us about cancer? *Transl. Oncol.* **2011**, *4*, 266–270. [CrossRef]
65. Birbrair, A. Stem cell microenvironments and beyond. In *Advances in Experimental Medicine and Biology*; Springer New York LLC: New York, NY, USA, 2017; Volume 1041, pp. 1–3.
66. Flier, J.S.; Underhill, L.H.; Dvorak, H.F. Tumors: Wounds That Do Not Heal. *N. Engl. J. Med.* **1986**, *315*, 1650–1659. [CrossRef] [PubMed]
67. Smetana, K.; Szabo, P.; Gál, P.; André, S.; Gabius, H.J.; Kodet, O.; Dvořánková, B. Emerging role of tissue lectins as microenvironmental effectors in tumors and wounds. *Histol. Histopathol.* **2015**, *30*, 293–309. [PubMed]
68. Lacina, L.; Kodet, O.; Dvořánková, B.; Szabo, P.; Smetana, K. Ecology of melanoma cell. *Histol. Histopathol.* **2018**, *33*, 247–254. [PubMed]
69. Lacina, L.; Smetana, K.; Dvořánková, B.; Pytlík, R.; Kideryová, L.; Kučerová, L.; Plzáková, Z.; Štork, J.; Gabius, H.J.; André, S. Stromal fibroblasts from basal cell carcinoma affect phenotype of normal keratinocytes. *Br. J. Dermatol.* **2007**, *156*, 819–829. [CrossRef]
70. Lacina, L.; Dvořánkova, B.; Smetana Jr., K.; Chovanec, M.; Plzák, J.; Tachezy, R.; Kideryovă, L.; Kučerová, L.; Čada, Z.; Bouček, J.; et al. Marker profiling of normal keratinocytes identifies the stroma from squamous cell carcinoma of the oral cavity as a modulatory microenvironment in co-culture. *Int. J. Radiat. Biol.* **2007**, *83*, 837–848. [CrossRef]
71. Sahai, E.; Astsaturov, I.; Cukierman, E.; DeNardo, D.G.; Egeblad, M.; Evans, R.M.; Fearon, D.; Greten, F.R.; Hingorani, S.R.; Hunter, T.; et al. A framework for advancing our understanding of cancer-associated fibroblasts. *Nat. Rev. Cancer* **2020**, *20*, 174–186. [CrossRef]
72. Kanzaki, R.; Pietras, K. Heterogeneity of cancer-associated fibroblasts: Opportunities for precision medicine. *Cancer Sci.* **2020**, *111*, 2708–2717. [CrossRef]
73. Dvořánková, B.; Smetana, K.; Říhová, B.; Kučera, J.; Mateu, R.; Szabo, P. Cancer-associated fibroblasts are not formed from cancer cells by epithelial-to-mesenchymal transition in nu/nu mice. *Histochem. Cell Biol.* **2015**, *143*, 463–469. [CrossRef]
74. Hill, B.S.; Pelagalli, A.; Passaro, N.; Zannetti, A. Tumor-Educated mesenchymal stem cells promote Pro-Metastatic phenotype. *Oncotarget* **2017**, *8*, 73296–73311. [CrossRef]
75. Barcellos-Hoff, M.H.; Ravani, S.A. Irradiated Mammary Gland Stroma Promotes the Expression of Tumorigenic Potential by Unirradiated Epithelial Cells 1. *Cancer Res.* **2000**, *60*, 1254–1260.
76. Dvořánková, B.; Szabo, P.; Lacina, L.; Gal, P.; Uhrova, J.; Zima, T.; Kaltner, H.; André, S.; Gabius, H.-J.; Sykova, E.; et al. Human galectins induce conversion of dermal fibroblasts into myofibroblasts and production of extracellular matrix: Potential application in tissue engineering and wound repair. *Cells Tissues Organs* **2011**, *194*, 469–480. [CrossRef] [PubMed]

77. Acosta, J.C.; Banito, A.; Wuestefeld, T.; Georgilis, A.; Janich, P.; Morton, J.P.; Athineos, D.; Kang, T.W.; Lasitschka, F.; Andrulis, M.; et al. A complex secretory program orchestrated by the inflammasome controls paracrine senescence. *Nat. Cell Biol.* **2013**, *15*, 978–990. [CrossRef] [PubMed]
78. Lewis, D.A.; Travers, J.B.; Machado, C.; Somani, A.K.; Spandau, D.F. Reversing the aging stromal phenotype prevents carcinoma initiation. *Aging (Albany. NY)* **2011**, *3*, 407–416. [CrossRef] [PubMed]
79. Hernandez-Segura, A.; de Jong, T.V.; Melov, S.; Guryev, V.; Campisi, J.; Demaria, M. Unmasking Transcriptional Heterogeneity in Senescent Cells. *Curr. Biol.* **2017**, *27*, 2652–2660. [CrossRef]
80. Dvořánková, B.; Szabo, P.; Lacina, L.; Kodet, O.; Matouškové, E.; Smetana, K. Fibroblasts prepared from different types of malignant tumors stimulate expression of luminal marker keratin 8 in the EM-G3 breast cancer cell line. *Histochem. Cell Biol.* **2012**, *137*, 679–685. [CrossRef]
81. Trylcova, J.; Busek, P.; Smetana, K.; Balaziova, E.; Dvorankova, B.; Mifkova, A.; Sedo, A. Effect of cancer-associated fibroblasts on the migration of glioma cells in vitro. *Tumor Biol.* **2015**, *36*, 5873–5879. [CrossRef]
82. Szabó, P.; Kolář, M.; Dvořánková, B.; Lacina, L.; Štork, J.; Vlček, Č.; Strnad, H.; Tvrdek, M.; Smetana, K. Mouse 3T3 fibroblasts under the influence of fibroblasts isolated from stroma of human basal cell carcinoma acquire properties of multipotent stem cells. *Biol. Cell* **2011**, *103*, 233–248. [CrossRef]
83. Plzák, J.; Bouček, J.; Bandúrová, V.; Kolář, M.; Hradilová, M.; Szabo, P.; Lacina, L.; Chovanec, M.; Smetana, K. The head and neck squamous cell carcinoma microenvironment as a potential target for cancer therapy. *Cancers* **2019**, *11*, 440. [CrossRef]
84. Heneberg, P. Paracrine tumor signaling induces transdifferentiation of surrounding fibroblasts. *Crit. Rev. Oncol. Hematol.* **2016**, *97*, 303–311. [CrossRef]
85. Li, Y.; Wang, R.; Xiong, S.; Wang, X.; Zhao, Z.; Bai, S.; Wang, Y.; Zhao, Y.; Cheng, B. Cancer-associated fibroblasts promote the stemness of CD24 + liver cells via paracrine signaling. *J. Mol. Med.* **2019**, *97*, 243–255. [CrossRef]
86. Nagasaki, T.; Hara, M.; Nakanishi, H.; Takahashi, H.; Sato, M.; Takeyama, H. Interleukin-6 released by colon cancer-associated fibroblasts is critical for tumour angiogenesis: Anti-interleukin-6 receptor antibody suppressed angiogenesis and inhibited tumour-stroma interaction. *Br. J. Cancer* **2014**, *110*, 469–478. [CrossRef] [PubMed]
87. Wu, X.; Tao, P.; Zhou, Q.; Li, J.; Yu, Z.; Wang, X.; Li, J.; Li, C.; Yan, M.; Zhu, Z.; et al. IL-6 secreted by cancer-associated fibroblasts promotes epithelial-mesenchymal transition and metastasis of gastric cancer via JAK2/STAT3 signaling pathway. *Oncotarget* **2017**, *8*, 20741–20750. [CrossRef] [PubMed]
88. Wang, L.; Cao, L.; Wang, H.; Liu, B.; Zhang, Q.; Meng, Z.; Wu, X.; Zhou, Q.; Xu, K. Cancer-associated fibroblasts enhance metastatic potential of lung cancer cells through IL-6/STAT3 signaling pathway. *Oncotarget* **2017**, *8*, 76116–76128. [CrossRef] [PubMed]
89. Omland, S.H.; Wettergren, E.E.; Mourier, T.; Hansen, A.J.; Asplund, M.; Mollerup, S.; Robert, R. Cancer associated fibroblasts (CAFs) are activated in cutaneous basal cell carcinoma and in the peritumoural skin. *BMC Cancer* **2017**, *17*, 675. [CrossRef]
90. Depner, S.; Lederle, W.; Gutschalk, C.; Linde, N.; Zajonz, A.; Mueller, M.M. Cell type specific interleukin-6 induced responses in tumor keratinocytes and stromal fibroblasts are essential for invasive growth. *Int. J. Cancer* **2014**, *135*, 551–562. [CrossRef]
91. Jobe, N.P.; Živicová, V.; Mifková, A.; Rösel, D.; Dvořánková, B.; Kodet, O.; Strnad, H.; Kolář, M.; Šedo, A.; Smetana, K.; et al. Fibroblasts potentiate melanoma cells in vitro invasiveness induced by UV-irradiated keratinocytes. *Histochem. Cell Biol.* **2018**, *149*, 503–516. [CrossRef]
92. Goulet, C.R.; Champagne, A.; Bernard, G.; Vandal, D.; Chabaud, S.; Pouliot, F.; Bolduc, S. Cancer-associated fibroblasts induce epithelial-mesenchymal transition of bladder cancer cells through paracrine IL-6 signalling. *BMC Cancer* **2019**, *19*, 1–13. [CrossRef]
93. Gyamfi, J.; Eom, M.; Koo, J.S.; Choi, J. Multifaceted Roles of Interleukin-6 in Adipocyte—Breast Cancer Cell Interaction. *Transl. Oncol.* **2018**, *11*, 275–285. [CrossRef]
94. Jobe, N.P.; Rösel, D.; Dvořánková, B.; Kodet, O.; Lacina, L.; Mateu, R.; Smetana, K.; Brábek, J. Simultaneous blocking of IL-6 and IL-8 is sufficient to fully inhibit CAF-induced human melanoma cell invasiveness. *Histochem. Cell Biol.* **2016**, *146*, 205–217. [CrossRef]

95. Jayatilaka, H.; Tyle, P.; Chen, J.J.; Kwak, M.; Ju, J.; Kim, H.J.; Lee, J.S.H.; Wu, P.H.; Gilkes, D.M.; Fan, R.; et al. Synergistic IL-6 and IL-8 paracrine signalling pathway infers a strategy to inhibit tumour cell migration. *Nat. Commun.* **2017**, *8*, 15584. [CrossRef]
96. Von Ahrens, D.; Bhagat, T.D.; Nagrath, D.; Maitra, A.; Verma, A. The role of stromal cancer-associated fibroblasts in pancreatic cancer. *J. Hematol. Oncol.* **2017**, *10*, 1–8. [CrossRef] [PubMed]
97. Middleton, K.; Jones, J.; Lwin, Z.; Coward, J.I.G. Interleukin-6: An angiogenic target in solid tumours. *Crit. Rev. Oncol. Hematol.* **2014**, *89*, 129–139. [CrossRef] [PubMed]
98. Kučera, J.; Strnadová, K.; Dvořánková, B.; Lacina, L.; Krajsová, I.; Štork, J.; Kovářová, H.; Skalníková, H.K.H.K.; Vodička, P.; Motlík, J.; et al. Serum proteomic analysis of melanoma patients with immunohistochemical profiling of primary melanomas and cultured cells: Pilot study. *Oncol. Rep.* **2019**, *42*, 1793–1804. [CrossRef] [PubMed]
99. Kodet, O.; Dvořánková, B.; Bendlová, B.; Sýkorová, V.; Krajsová, I.; Štork, J.; Kučera, J.; Szabo, P.; Strnad, H.; Kolář, M.; et al. Microenvironment-driven resistance to B-Raf inhibition in a melanoma patient is accompanied by broad changes of gene methylation and expression in distal fibroblasts. *Int. J. Mol. Med.* **2018**, *41*, 2687–2703. [CrossRef]
100. Kolb, A.D.; Shupp, A.B.; Mukhopadhyay, D.; Marini, F.C.; Bussard, K.M. Osteoblasts are "educated" by crosstalk with metastatic breast cancer cells in the bone tumor microenvironment. *Breast Cancer Res.* **2019**, *21*, 31. [CrossRef]
101. Stoll, J.R.; Vaidya, T.S.; Mori, S.; Dusza, S.W.; Lacouture, M.E.; Markova, A. Association of interleukin-6 and tumor necrosis factor-α with mortality in hospitalized patients with cancer. *J. Am. Acad. Dermatol.* **2020**. [CrossRef]
102. White, J.P. IL-6, cancer and cachexia: Metabolic dysfunction creates the perfect storm. *Transl. Cancer Res.* **2017**, *6*, S280–S285. [CrossRef]
103. Shinsyu, A.; Bamba, S.; Kurihara, M.; Matsumoto, H.; Sonoda, A.; Inatomi, O.; Andoh, A.; Takebayashi, K.; Kojima, M.; Iida, H.; et al. Inflammatory cytokines, appetite-regulating hormones, and energy metabolism in patients with gastrointestinal cancer. *Oncol. Lett.* **2020**, *20*, 1469–1479. [CrossRef]
104. Kays, J.K.; Koniaris, L.G.; Cooper, C.A.; Pili, R.; Jiang, G.; Liu, Y.; Zimmers, T.A. The combination of low skeletal muscle mass and high tumor interleukin-6 associates with decreased survival in clear cell renal cell carcinoma. *Cancers* **2020**, *12*, 1605. [CrossRef]
105. Dwarkasing, J.T.; Witkamp, R.F.; Boekschoten, M.V.; Ter Laak, M.C.; Heins, M.S.; van Norren, K. Increased hypothalamic serotonin turnover in inflammation-induced anorexia. *BMC Neurosci.* **2016**, *17*, 26. [CrossRef]
106. Shimura, Y.; Kurosawa, H.; Tsuchiya, M.; Sawa, M.; Kaneko, H.; Liu, L.; Makino, Y.; Nojiri, H.; Iwase, Y.; Kaneko, K.; et al. Serum interleukin 6 levels are associated with depressive state of the patients with knee osteoarthritis irrespective of disease severity. *Clin. Rheumatol.* **2017**, *36*, 2781–2787. [CrossRef] [PubMed]
107. Keaton, S.A.; Madaj, Z.B.; Heilman, P.; Smart, L.A.; Grit, J.; Gibbons, R.; Postolache, T.T.; Roaten, K.; Achtyes, E.D.; Brundin, L. An inflammatory profile linked to increased suicide risk. *J. Affect. Disord.* **2019**, *247*, 57–65. [CrossRef]
108. Pormohammad, A.; Ghorbani, S.; Baradaran, B.; Khatami, A.J.; Turner, R.; Mansournia, M.A.; Kyriacou, D.N.; Idrovo, J.P.; Bahr, N.C. Clinical characteristics, laboratory findings, radiographic signs and outcomes of 61,742 patients with confirmed COVID-19 infection: A systematic review and meta-analysis. *Microb. Pathog.* **2020**, *147*, 104390. [CrossRef] [PubMed]
109. He, J.; Guo, Y.; Mao, R.; Zhang, J. Proportion of asymptomatic coronavirus disease 2019: A systematic review and meta-analysis. *J. Med. Virol.* **2020**. [CrossRef]
110. Bonam, S.R.; Kaveri, S.V.; Sakuntabhai, A.; Gilardin, L.; Bayry, J. Adjunct Immunotherapies for the Management of Severely Ill COVID-19 Patients. *Cell Reports Med.* **2020**, *1*, 100016. [CrossRef]
111. Paces, J.; Strizova, Z.; Smrz, D.; Cerny, J. COVID-19 and the immune system. *Physiol. Res.* **2020**, *69*, 379–388. [CrossRef]
112. Han, H.; Ma, Q.; Li, C.; Liu, R.; Zhao, L.; Wang, W.; Zhang, P.; Liu, X.; Gao, G.; Liu, F.; et al. Profiling serum cytokines in COVID-19 patients reveals IL-6 and IL-10 are disease severity predictors. *Emerg. Microbes Infect.* **2020**, *9*, 1123–1130. [CrossRef]
113. Herold, T.; Jurinovic, V.; Arnreich, C.; Hellmuth, J.C.; Bergwelt-Baildon, M.; Klein, M.; Weinberger, T. *Level of IL-6 Predicts Respiratory Failure in Hospitalized Symptomatic COVID-19 Patients*; Cold Spring Harbor Laboratory Press: Long Island, NY, USA, 2020.

114. Liu, W.-J.; Wang, X.-D.; Wu, W.; Huang, X. Relationship between depression and blood cytokine levels in lung cancer patients. *Médecine/Sciences* **2018**, *34*, 113–115. [CrossRef]
115. Ulhaq, Z.S.; Soraya, G.V. Interleukin-6 as a potential biomarker of COVID-19 progression. *Med. Mal. Infect.* **2020**, *50*, 382–383. [CrossRef]
116. Polidoro, R.B.; Hagan, R.S.; de Santis Santiago, R.; Schmidt, N.W. Overview: Systemic Inflammatory Response Derived From Lung Injury Caused by SARS-CoV-2 Infection Explains Severe Outcomes in COVID-19. *Front. Immunol.* **2020**, *11*, 1626. [CrossRef]
117. Channappanavar, R.; Perlman, S. Pathogenic human coronavirus infections: Causes and consequences of cytokine storm and immunopathology. *Semin. Immunopathol.* **2017**, *39*, 529–539. [CrossRef]
118. Gandalovičová, A.; Rosel, D.; Fernandes, M.; Veselý, P.; Heneberg, P.; Čermák, V.; Petruželka, L.; Kumar, S.; Sanz-Moreno, V.; Brábek, J. Migrastatics—Anti-metastatic and Anti-invasion Drugs: Promises and Challenges. *Trends Cancer* **2017**, *3*, 391–406. [CrossRef] [PubMed]
119. Rosel, D.; Fernandes, M.; Sanz-Moreno, V.; Brábek, J. Migrastatics: Redirecting R&D in Solid Cancer Towards Metastasis? *Trends Cancer* **2019**, *5*, 755–756. [PubMed]
120. Fulciniti, M.; Hideshima, T.; Vermot-Desroches, C.; Pozzi, S.; Nanjappa, P.; Shen, Z.; Patel, N.; Smith, E.S.; Wang, W.; Prabhala, R.; et al. A high-affinity fully human anti-IL-6 mAb, 1339, for the treatment of multiple myeloma. *Clin. Cancer Res.* **2009**, *15*, 7144–7152. [CrossRef]
121. Johnson, D.E.; O'Keefe, R.A.; Grandis, J.R. Targeting the IL-6/JAK/STAT3 signalling axis in cancer. *Nat. Rev. Clin. Oncol.* **2018**, *15*, 234–248. [CrossRef]
122. Vaidya, G.; Czer, L.S.C.; Kobashigawa, J.; Kittleson, M.; Patel, J.; Chang, D.; Kransdorf, E.; Shikhare, A.; Tran, H.; Vo, A.; et al. Successful Treatment of Severe COVID-19 Pneumonia With Clazakizumab in a Heart Transplant Recipient: A Case Report. *Transplant. Proc.* **2020**. [CrossRef]
123. Moreno-Pérez, O.; Andres, M.; Leon-Ramirez, J.M.; Sánchez-Payá, J.; Rodríguez, J.C.; Sánchez, R.; García-Sevila, R.; Boix, V.; Gil, J.; Merino, E. Experience with tocilizumab in severe COVID-19 pneumonia after 80 days of follow-up: A retrospective cohort study. *J. Autoimmun.* **2020**, *114*, 102523. [CrossRef] [PubMed]
124. Palanques-Pastor, T.; López-Briz, E.; Poveda Andrés, J.L. Involvement of interleukin 6 in SARS-CoV-2 infection: Siltuximab as a therapeutic option against COVID-19. *Eur. J. Hosp. Pharm.* **2020**, *27*, 297–298. [CrossRef]
125. Tomasiewicz, K.; Piekarska, A.; Stempkowska-Rejek, J.; Serafińska, S.; Gawkowska, A.; Parczewski, M.; Ściągorska-Olsen, J.; Łapiński, T.W.; Zarębska-Michaluk, D.; Kowalska, J.D.; et al. Tocilizumab for patients with severe COVID-19: A retrospective, multi-centre study. *Expert Rev. Anti Infect. Ther.* **2020**, *1*, 1–8. [CrossRef]
126. Coronavirus Disease 2019 (COVID-19) Treatment Guidelines. Available online: https://www.covid19treatmentguidelines.nih.gov/ (accessed on 25 September 2020).
127. Gennari, L.; Merlotti, D.; De Paola, V.; Martini, G.; Nuti, R. Bazedoxifene for the prevention of postmenopausal osteoporosis. *Ther. Clin. Risk Manag.* **2008**, *4*, 1229–1242. [CrossRef]
128. Quintanilla Rodriguez, B.S.; Correa, R. *Raloxifene*; StatPearls Publishing: Treasure Island, FL, USA, 2020.
129. Xiao, H.; Bid, H.K.; Chen, X.; Wu, X.; Wei, J.; Bian, Y.; Zhao, C.; Li, H.; Li, C.; Lin, J. Repositioning Bazedoxifene as a novel IL-6/GP130 signaling antagonist for human rhabdomyosarcoma therapy. *PLoS ONE* **2017**, *12*, e0180297. [CrossRef]
130. Song, D.; Yu, W.; Ren, Y.; Zhu, J.; Wan, C.; Cai, G.; Guo, J.; Zhang, W.; Kong, L. Discovery of bazedoxifene analogues targeting glycoprotein 130. *Eur. J. Med. Chem.* **2020**, *199*, 112375. [CrossRef] [PubMed]
131. Yadav, A.; Kumar, B.; Teknos, T.N.; Kumar, P. Bazedoxifene enhances the anti-tumor effects of cisplatin and radiation treatment by blocking IL-6 signaling in head and neck cancer. *Oncotarget* **2017**, *8*, 66912–66924. [CrossRef] [PubMed]
132. Wu, X.; Cao, Y.; Xiao, H.; Li, C.; Lin, J. Bazedoxifene as a novel GP130 inhibitor for pancreatic cancer therapy. *Mol. Cancer Ther.* **2016**, *15*, 2609–2619. [CrossRef]
133. Chen, X.; Tian, J.; Su, G.H.; Lin, J. Blocking IL-6/GP130 Signaling Inhibits Cell Viability/Proliferation, Glycolysis, and Colony Forming Activity in Human Pancreatic Cancer Cells. *Curr. Cancer Drug Targets* **2018**, *19*, 417–427. [CrossRef] [PubMed]
134. Wei, J.; Ma, L.; Lai, Y.H.; Zhang, R.; Li, H.; Li, C.; Lin, J. Bazedoxifene as a novel GP130 inhibitor for Colon Cancer therapy. *J. Exp. Clin. Cancer Res.* **2019**, *38*, 1–13. [CrossRef] [PubMed]

135. Ma, H.; Yan, D.; Wang, Y.; Shi, W.; Liu, T.; Zhao, C.; Huo, S.; Duan, J.; Tao, J.; Zhai, M.; et al. Bazedoxifene exhibits growth suppressive activity by targeting interleukin-6/glycoprotein 130/signal transducer and activator of transcription 3 signaling in hepatocellular carcinoma. *Cancer Sci.* **2019**, *110*, 950–961. [CrossRef]
136. Existing Osteoporosis Drug Shows Potential for Treating COVID-19|News|CORDIS|European Commission. Available online: https://cordis.europa.eu/article/id/421499-existing-osteoporosis-drug-shows-potential-for-treating-covid-19 (accessed on 20 September 2020).
137. Smetana, K.; Rosel, D.; BrÁbek, J. Raloxifene and Bazedoxifene Could Be Promising Candidates for Preventing the COVID-19 Related Cytokine Storm, ARDS and Mortality. *In Vivo* **2020**, *34*, 3027–3028. [CrossRef]
138. Smetana, K.; Smetana, K.; Brábek, J.; Brábek, J. Role of interleukin-6 in lung complications in patients with COVID-19: Therapeutic implications. *In Vivo (Brooklyn)* **2020**, *34*, 1589–1592. [CrossRef]
139. Jeon, S.; Ko, M.; Lee, J.; Choi, I.; Byun, S.Y.; Park, S.; Shum, D.; Kim, S. Identification of antiviral drug candidates against SARS-CoV-2 from FDA-approved drugs. *Antimicrob. Agents Chemother.* **2020**, *64*, 64. [CrossRef]
140. Protein Scaffolds—BioProcess InternationalBioProcess International. Available online: https://bioprocessintl.com/upstream-processing/expression-platforms/protein-scaffolds-339588/ (accessed on 21 September 2020).
141. Hayashi, M.; Kim, Y.P.; Takamatsu, S.; Enomoto, A.; Shinose, M.; Takahashi, Y.; Tanaka, H.; Komiyama, K.; Omura, S. Madindoline, a novel inhibitor of IL-6 activity from Streptomyces sp. K93-0711. I. Taxonomy, fermentation, isolation and biological activities. *J. Antibiot. (Tokyo)* **1996**, *49*, 1091–1095. [CrossRef] [PubMed]
142. Hayashi, M.; Rho, M.C.; Enomoto, A.; Fukami, A.; Kim, Y.P.; Kikuchi, Y.; Sunazuka, T.; Hirose, T.; Komiyama, K.; Omura, S. Suppression of bone resorption by madindoline a, a novel nonpeptide antagonist to gp130. *Proc. Natl. Acad. Sci. USA* **2002**, *99*, 14728–14733. [CrossRef]
143. Enomoto, A.; Rho, M.-C.; Fukami, A.; Hiraku, O.; Komiyama, K.; Hayashi, M. Suppression of cancer cachexia by 20S,21-epoxy-resibufogenin-3-acetate—A novel nonpeptide IL-6 receptor antagonist. *Biochem. Biophys. Res. Commun.* **2004**, *323*, 1096–1102. [CrossRef] [PubMed]
144. Saleh, A.Z.M.; Kevin, L.G.; Billings, S.; van Vranken, D.L.; Krolewski, J.J. Binding of Madindoline A to the Extracellular Domain of gp130†. *Biochemistry* **2005**, *44*, 10822–10827. [CrossRef] [PubMed]
145. Kino, T.; Boos, T.L.; Sulima, A.; Siegel, E.M.; Gold, P.W.; Rice, K.C.; Chrousos, G.P. 3-O-Formyl-20R,21-epoxyresibufogenin suppresses IL-6–type cytokine actions by targeting the glycoprotein 130 subunit: Potential clinical implications. *J. Allergy Clin. Immunol.* **2007**, *120*, 437–444. [CrossRef] [PubMed]
146. Yamamoto, D.; Sunazuka, T.; Hirose, T.; Kojima, N.; Kaji, E.; Omura, S. Design, synthesis, and biological activities of madindoline analogues. *Bioorganic Med. Chem. Lett.* **2006**, *16*, 2807–2811. [CrossRef] [PubMed]
147. Aqel, S.I.; Kraus, E.E.; Jena, N.; Kumari, V.; Granitto, M.C.; Mao, L.; Farinas, M.F.; Zhao, E.Y.; Perottino, G.; Pei, W.; et al. Novel small molecule IL-6 inhibitor suppresses autoreactive Th17 development and promotes T reg development. *Clin. Exp. Immunol.* **2019**, *196*, 215–225. [CrossRef]
148. Hong, S.-S.; Choi, J.H.; Lee, S.Y.; Park, Y.-H.; Park, K.-Y.; Lee, J.Y.; Kim, J.; Gajulapati, V.; Goo, J.-I.; Singh, S.; et al. A Novel Small-Molecule Inhibitor Targeting the IL-6 Receptor β Subunit, Glycoprotein 130. *J. Immunol.* **2015**, *195*, 237–245. [CrossRef]
149. Wang, J.; Qiao, C.; Xiao, H.; Lin, Z.; Li, Y.; Zhang, J.; Shen, B.; Fu, T.; Feng, J. Structure-based virtual screening and characterization of a novel IL-6 antagonistic compound from synthetic compound database. *Drug Des. Dev. Ther.* **2016**, *10*, 4091–4100. [CrossRef]
150. Kamano, Y.; Nogawa, T.; Yamashita, A.; Hayashi, M.; Inoue, M.; Drašar, P.; Pettit, G.R. Isolation and structure of a 20,21-epoxybufenolide series from "Ch'an Su. " *J. Nat. Prod.* **2002**, *65*, 1001–1005. [CrossRef]
151. Kaur, S.; Bansal, Y.; Kumar, R.; Bansal, G. A panoramic review of IL-6: Structure, pathophysiological roles and inhibitors. *Bioorganic Med. Chem.* **2020**, *28*, 115327. [CrossRef] [PubMed]
152. Liston, D.R.; Davis, M. Clinically relevant concentrations of anticancer drugs: A guide for nonclinical studies. *Clin. Cancer Res.* **2017**, *23*, 3489–3498. [CrossRef] [PubMed]
153. Rodriguez, C.; Theillet, C.; Portier, M.; Bataille, R.; Klein, B. Molecular analysis of the IL-6 receptor in human multiple myeloma, an IL-6-related disease. *FEBS Lett.* **1994**, *341*, 156–161. [CrossRef]
154. Stephens, O.W.; Zhang, Q.; Qu, P.; Zhou, Y.; Chavan, S.; Tian, E.; Williams, D.R.; Epstein, J.; Barlogie, B.; Shaughnessy, J.D. An intermediate-risk multiple myeloma subgroup is defined by sIL-6r: Levels synergistically increase with incidence of SNP rs2228145 and 1q21 amplification. *Blood* **2012**, *119*, 503–512. [CrossRef]

155. Buchwald, P.; Bodor, N. Brain-Targeting Chemical Delivery Systems and Their Cyclodextrin-Based Formulations in Light of the Contributions of Marcus E. Brewster. *J. Pharm. Sci.* **2016**, *105*, 2589–2600. [CrossRef]
156. Nigro, A.; Pellegrino, M.; Greco, M.; Comandè, A.; Sisci, D.; Pasqua, L.; Leggio, A.; Morelli, C. Dealing with skin and blood-brain barriers: The unconventional challenges of mesoporous silica nanoparticles. *Pharmaceutics* **2018**, *10*, 250. [CrossRef] [PubMed]
157. Lin, E.Y.; Chen, Y.S.; Li, Y.S.; Chen, S.R.; Lee, C.H.; Huang, M.H.; Chuang, H.M.; Harn, H.J.; Yang, H.H.; Lin, S.Z.; et al. Liposome Consolidated with Cyclodextrin Provides Prolonged Drug Retention Resulting in Increased Drug Bioavailability in Brain. *Int. J. Mol. Sci.* **2020**, *21*, 4408. [CrossRef]
158. Dvořáková, P.; Bušek, P.; Knedlík, T.; Schimer, J.; Etrych, T.; Kostka, L.; Stollinová Šromová, L.; Šubr, V.; Šácha, P.; Šedo, A.; et al. Inhibitor-Decorated Polymer Conjugates Targeting Fibroblast Activation Protein. *J. Med. Chem.* **2017**, *60*, 8385–8393. [CrossRef]
159. Šimková, A.; Bušek, P.; Šedo, A.; Konvalinka, J. Molecular recognition of fibroblast activation protein for diagnostic and therapeutic applications. *Biochim. Biophys. Acta-Proteins Proteom.* **2020**, *1868*, 140409. [CrossRef]

PUBLIKACE VIII

Novotný J, **Strnadová K**, Dvořánková B, Kocourková Š, Jakša R, Dundr P, Pačes V, Smetana K Jr, Kolář M, Lacina L. Single-Cell RNA Sequencing Unravels Heterogeneity of the Stromal Niche in Cutaneous Melanoma Heterogeneous Spheroids. *Cancers* (Basel). 2020 Nov 10;12(11):3324. **(IF: 6.639)**

cancers

MDPI

Article

Single-Cell RNA Sequencing Unravels Heterogeneity of the Stromal Niche in Cutaneous Melanoma Heterogeneous Spheroids

Jiří Novotný [1,2,†], Karolína Strnadová [3,4,†], Barbora Dvořánková [3,4], Šárka Kocourková [1], Radek Jakša [5], Pavel Dundr [5], Václav Pačes [1], Karel Smetana Jr [3,4], Michal Kolář [1,*] and Lukáš Lacina [3,4,6,*]

[1] Laboratory of Genomics and Bioinformatics, Institute of Molecular Genetics of the Czech Academy of Sciences, 142 20 Prague, Czech Republic; jiri.novotny@img.cas.cz (J.N.); sarka.kocourkova@img.cas.cz (Š.K.); vaclav.paces@img.cas.cz (V.P.)

[2] Department of Informatics and Chemistry, Faculty of Chemical Technology, University of Chemistry and Technology, 160 00 Prague, Czech Republic

[3] Institute of Anatomy, First Faculty of Medicine, Charles University, 128 00 Prague, Czech Republic; karolina.strnadova@lf1.cuni.cz (K.S.); barbora.dvorankova@lf1.cuni.cz (B.D.); karel.smetana@lf1.cuni.cz (K.S.J.)

[4] BIOCEV, First Faculty of Medicine, Charles University, Vestec 25250, Czech Republic

[5] Institute of Pathology, First Faculty of Medicine, Charles University, 128 00 Prague, Czech Republic; radek.jaksa@vfn.cz (R.J.); pavel.dundr@lf1.cuni.cz (P.D.)

[6] Department of Dermatovenereology, First Faculty of Medicine, Charles University and General University Hospital, 128 00 Prague, Czech Republic

* Correspondence: michal.kolar@img.cas.cz (M.K.); lukas.lacina@lf1.cuni.cz (L.L.); Tel.: +420-241063412 (M.K.); +420-224965756 (L.L.)

† These authors contributed equally.

Received: 15 September 2020; Accepted: 08 November 2020; Published: 10 November 2020

Simple Summary: Cutaneous malignant melanoma is one of the most dangerous forms of skin cancer affecting humans. Frequently, it is linked to DNA damage due to ultraviolet radiation. Photoageing along with chronological ageing are therefore critically important factors in melanoma biology. The tissue microenvironment is also heavily affected by induced senescence. There is growing evidence that senescent dermal fibroblasts can consequently promote tumour progression. We focused on the analysis of microenvironmental factors represented in melanoma heterogeneous spheroids by either photodamaged or normal dermal fibroblasts. Our effort was primarily focused on the determination of the functional diversity of fibroblasts in heterogeneous spheroids. Therefore, we analysed these 3D models by single-cell RNA sequencing and advanced bioinformatic analysis. We aimed to map the fibroblast diversity resulting from previously acquired damage caused by exposure to extrinsic and intrinsic stimuli. Using this robust methodology, we highlighted molecules that could become important for the control of melanoma cell–cancer-associated fibroblast interaction as an essential part of the tumour microenvironment.

Abstract: Heterogeneous spheroids have recently acquired a prominent position in melanoma research because they incorporate microenvironmental cues relevant for melanoma. In this study, we focused on the analysis of microenvironmental factors introduced in melanoma heterogeneous spheroids by different dermal fibroblasts. We aimed to map the fibroblast diversity resulting from previously acquired damage caused by exposure to extrinsic and intrinsic stimuli. To construct heterogeneous melanoma spheroids, we used normal dermal fibroblasts from the sun-protected skin of a juvenile donor. We compared them to the fibroblasts from the sun-exposed photodamaged skin of an adult donor. Further, we analysed the spheroids by single-cell RNA sequencing. To validate transcriptional data, we also compared the immunohistochemical analysis of heterogeneous spheroids to melanoma biopsies. We have distinguished three functional clusters in primary human fibroblasts from melanoma spheroids. These clusters differed in the expression of

(a) extracellular matrix-related genes, (b) pro-inflammatory factors, and (c) TGFβ signalling superfamily. We observed a broader deregulation of gene transcription in previously photodamaged cells. We have confirmed that pro-inflammatory cytokine IL-6 significantly enhances melanoma invasion to the extracellular matrix in our model. This supports the opinion that the aspects of ageing are essential for reliable melanoma 3D modelling in vitro.

Keywords: melanoma; spheroids; fibroblasts; subpopulation; heterogeneity; Interleukin-6; cytokine; senescence-associated secretory phenotype; extracellular matrix; single-cell sequencing

1. Introduction

Cutaneous malignant melanoma is one of the most dangerous forms of skin cancer in humans. This life-threatening solid tumour can be linked to the DNA damage due to ultraviolet radiation from natural and artificial sources [1]. Epidemiological studies have identified that intermittent sunburns leading to inflammation constitute a significant risk factor in the development of malignant cutaneous diseases. The sunburn injury depends on the absorbed UV dose, UV wavelength applied, and finally also on the skin phototype. Similar to other types of tumours, the melanoma incidence is increasing with age because of the reduction of gene repair machinery in post-reproductive life [2–4]. This highlights the importance of chronological ageing in cancer research.

The formation of dipyrimidine photoproducts by direct absorption of UV energy in DNA can lead to the so-called UV signature mutations [5]. UV exposure also causes generation of reactive species through various pathways. Oxidative DNA damage may also, to some extent, play a role in photocarcinogenesis [6]. Genotoxic effects of skin irradiation can combine in epidermal cells, and thus contribute to cancer initiation and progression [7]. In a deeper layer, skin photoageing is caused by the repeated exposure of the dermis predominantly to UVA radiation. There is also evidence that repeated UVA irradiation of fibroblasts alters functions in photoaged skin, and it is an essential factor of deeper cancer invasion [8].

Regardless of the mechanism of senescence induction, senescent cells do accumulate in the organism with age [2]. This may also lead to deleterious effects. Impaired cellular functions may contribute to tissue structure degeneration and functional impairment, with the consequent onset of various inflammatory disorders and many other age-associated pathologies. Surprisingly, this list would also include cancer. In contrast to what was mentioned above, this makes senescence a double-edged sword [9,10].

The definition of senescence remains primarily functional. Senescent cells can be, to a certain extent, also characterised by morphological changes, and these changes are distinct in cell cultures [11]. However, the pathological identification of individual senescent cells in complex tissues remains somewhat troublesome [12]. Although it was previously believed that fibroblasts are homogeneous and mostly quiescent cells, it has become increasingly recognised that numerous fibroblast subtypes with unique functions and morphologies exist [13]. Importantly, senescent cells broadly alter their gene expression. Therefore, single-cell transcriptome analysis seems to be of crucial importance in this research. Compared to normal juvenile cells, senescence results in a pro-inflammatory secretory phenotype occurring without any usual pro-inflammatory stimulus. It is known as the senescence-associated secretory phenotype (SASP).

There is evidence that senescent dermal fibroblasts can promote tumour progression by activating their SASP [14]. This phenotype is triggered in the dermis by either extrinsic stimuli (oxidative stress, UV-related DNA damage), or intrinsic factors of chronological ageing. Fibroblasts are consequently switched into pro-inflammatory cells, acquiring the ability to affect adjacent cells of the local microenvironment [15]. Senescent fibroblasts produce numerous factors, e.g., cytokines, chemokines, growth factors or extracellular matrix proteins [9]. Besides dermal fibroblasts and their secreted factors, the tissue microenvironment consists of the extracellular matrix, endothelial and immune cells, and the network of blood and lymphatic vessels. These elements in the deep inner skin

layer collectively form a complex niche beneficial for tumour initiation and spreading. This can, e.g., drive melanoma cells to relocate from the epidermis into the dermis. The dermal fibroblasts accidentally surrounding a malignant tumour are exposed to massive intercellular signalling and alter their phenotypic profile. These initially innocent bystanders are converted into cancer-associated fibroblasts (CAFs), which are conducive to cancer growth and metastasis [16–18]. The cancer cells form, along with their noncancerous partners (also including CAFs and immune cells), a complex ecosystem [19,20] whose understanding is fundamental for the development of new procedures of anticancer therapy.

In earlier years, the in vitro methods of cancer research investigating, e.g., the effect of anticancer drugs were limited to the study of individual cell lines in culture dishes. This concept was somewhat misleading, because it completely neglected the important biological aspect of intercellular interactions [20,21]. Later, the crosstalk between various cells was extensively investigated, again primarily using 2D monolayer cultures that were in physical contact or separated by porous membranes [22–24]. To some extent, these simplistic models introduced the microenvironment. However, they were far from the complexity of real tumours, and that is why they are recently being abandoned. In the recent decade, research is focusing on 3D cultures or organotypic modelling. This helps to acquire higher complexity and brings more relevant data closer to in vivo conditions. It was exemplified on the study of apoptosis of melanoma cells in 3D culture by tumour necrosis factor α-related apoptosis-inducing ligand (TRAIL) [25]. Data from 3D cultures can more closely mimic the clinical setting, and this justifies their employment [26]. This trend was seen in melanoma and can be confirmed by data from multiple other types of tumours [27].

Employment of other cell types can further increase the complexity of the acquired model. These heterogeneous spheroids are an intermediate stage between non-complex 2D cultures and in vivo animal models [28–30]. The addition of dermal fibroblasts achieves the goal of making in vitro melanoma heterogeneous spheroids better resemble the melanoma tumour. Fibroblasts represent structural and metabolic support and provide the microenvironmental cues occurring in human malignant melanoma [31]. However, several critical questions must be addressed. For instance, are human dermal fibroblasts in standard cultures a homogenous population? As noted earlier, there is an unexpected natural heterogeneity of the mesenchymal populations of the dermis in the tissues [32]. Is it maintained in the cultures, and for how long? If so, should we also take ageing into account in these models [33]?

Therefore, we focused on the analysis of microenvironmental factors represented in melanoma heterogeneous spheroids by different fibroblasts. We focused on characterisation of the functional diversity of these fibroblasts in heterogeneous spheroids consisting of melanoma cells and fibroblasts. Our interest was predominantly oriented on characterisation of the functional features of dermal fibroblasts in 3D coculture with melanoma cells with respect to the fibroblast donor's age and previous skin UV exposure. The biologically relevant variables were represented by employment of either primary human dermal fibroblasts from the sun-protected skin of a juvenile donor or fibroblasts from the sun-exposed photodamaged skin of an adult donor. The spheroids were analysed by single-cell RNA sequencing and advanced bioinformatic analysis. Using this robust methodology, we focused on molecules that could be potential therapeutic targets in the melanoma microenvironment. We used the BRAF mutated melanoma cell line. The effect of BRAF treatment was not tested and our results did not address the effect of this therapy on the fibroblast heterogeneity.

2. Results

2.1. Description of Heterogeneous Spheres Formed from the Melanoma Cells and Fibroblasts

Compact heterogeneous spheres were formed from suspensions of melanoma cells (cell line G361) and multiple primary human dermal fibroblasts (Figure 1a).

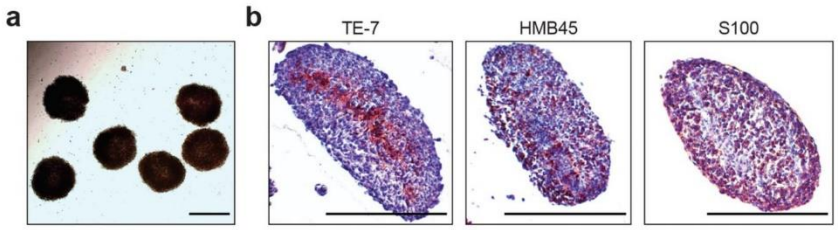

Figure 1. Melanoma heterogeneous spheroids (**a**) of typical regular morphology harvested for experiments. Spheroids display consistent localisation of melanoma cells on the periphery and fibroblasts in their core. The spheroids show structural inhomogeneity with fibroblasts marked by TE-7 antibody in their core and melanoma cells on their periphery visualised by HMB45 and S100 markers (**b**). The bar denotes 1000 μm.

Surprisingly, we observed a uniform structural pattern in our spheres, which was revealed by immunohistochemistry (Figure 1b). Invariably, fibroblasts occupied the core of the spheres. The mantle zone of the sphere was predominantly formed by melanoma cells. We detected fibroblasts by specific TE-7 antibody. We also detected melanocyte markers such as HMB45, tyrosinase and protein S100 in melanoma. These markers were also observed in cells of the peripheral zone in spheroids (Figure 1, antibodies in Supplementary Table S1). For closer analysis by scRNA-seq, we used spheres from juvenile dermal fibroblasts (JDF, isolated from a child sun-protected skin) and adult fibroblasts from the skin, revealing clinically extensive signs of photoageing due to previous UV irradiation (PDF).

2.2. *scRNA-seq Comparative Analysis of Fibroblasts and Melanoma Cells*

After the dissociation of spheres to single-cell suspensions, we were able to separate individual fibroblasts from G361 melanoma cells using scRNA-seq (Supplementary Figure S1). We identified fibroblasts clearly by expression of fibroblast-activating protein (*FAP*), a widely used marker of fibroblasts. Melanoma cells were identified by expression of marker MELAN-A (*MLANA*). Expression of these markers at the mRNA level could also be confirmed at the protein level by immunohistochemistry in sections of spheroids. Moreover, the relevance of these markers was also supported by findings in human samples of melanoma and its lymph node metastases from 10 patients (Supplementary Figure S1a, with detailed information regarding tumours in Supplementary Table S1).

We could further demonstrate the reliability of the scRNA-seq procedure by examples of several other typical melanoma proteins in human tumours and transcripts in spheroids (heatmap shown in Supplementary Figure S2) and also by a known CDKN2A mutation present in the G361 melanoma cell line (Supplementary Figure S3).

The genes for markers melanogenesis tyrosinase (*TYR*) and transcription factor MiTF (*MITF*), which are specific for melanoma cells, were observed predominantly in the pool of melanoma cells (Supplementary Figures S4 and S5). *CDH1* (E-cadherin) and *CDH2* (N-cadherin) were also dominant in the melanoma cell pool. This observation corresponded to the weak but specific signal from clinical samples (Supplementary Figure S6). On the other hand, cells producing the extracellular matrix (for example *COL1A2*) and expressing an active gene for a protein participating in collagen metabolism such as *LOX*, were particularly enriched in fibroblast cells (Supplementary Figures S4 and S5). As expected, mRNA transcripts for intermediate filament vimentin (*VIM*) were strongly transcribed in both cell types, i.e., in fibroblasts and melanoma cells (Supplementary Figures S4 and S5) and also in clinical samples (Supplementary Figure S6). While we observed significant differences between melanoma cells and both types of fibroblasts (heatmap in Supplementary Figure S2), we analysed these cell populations separately for further stratification.

2.3. Bioinformatic Analysis of Primary Dermal Fibroblasts (JDF vs PDF) Dissociated from Spheres

Analysis of scRNA-seq data revealed three different clusters of fibroblasts in both spheroid types (Figure 2). The clustering was similar in JDF and PDF spheroids, yet the cell groups were more notably separated in the PDF sample. The clusters differed in the expression of genes with well-described cellular functions: the first one was enriched in genes encoding inflammatory factors such as cytokines and chemokines (e.g., *CXCL8*) and depleted in genes responsible for production of the extracellular matrix (ECM). Thus, we denote the cluster as ECM$^-$. The second cluster was enriched in *ID* genes responsible for differentiation/dedifferentiation processes that are included in the transforming growth factor β (TGF-β) signalling family cascade. We call this cluster ID$^+$. The last cluster was enriched in ECM transcripts such as *COL1A1*, and thus we denote it ECM$^+$.

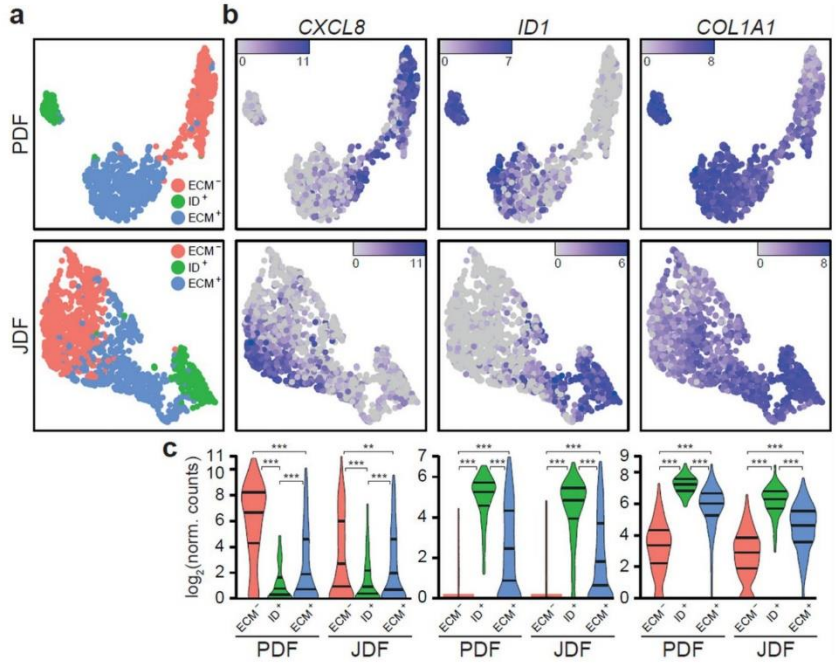

Figure 2. Fibroblasts in JDF and PDF spheroids split into three phenotypically distinct clusters. (**a**) The clusters are defined by specific gene expression signatures and separate well in the UMAP visualisation. (**b**) ECM- cells produce various cytokines and interleukins (*CXCL8*), ID+ cells are identified by strong expression of ID genes (*ID1*), and ECM+ cells by marked expression of ECM components (*COL1A1*). (**c**) The clusters are equivalent in JDF and PDF spheroids and display statistically significant differences in expression of their marker genes (** $p < 0.01$; *** $p < 0.001$, Mann-Whitney U test).

Gene expression differences between the clusters were to a large extent similar in JDF and PDF (Venn diagrams in Supplementary Figure S7). However, we observed some significant differences (Figures 3 and 4 and heatmaps in Supplementary Figures S8 and S9). Comparison of the ECM$^-$ to ID$^+$ clusters (Figure 3 and Supplementary Table S2) revealed downregulation of genes associated with focal adhesion (KEGG hsa04510), ECM receptor interaction (hsa04512), and TGF-β signalling pathways (hsa04350) in both JDF and PDF. However, we observed a strong upregulation of genes

associated with cytokine-cytokine receptor interaction (hsa04060), Nod-like receptor (hsa04621), and Toll-like receptor (hsa04620) signalling pathways in PDF only with prominent upregulation of the *CXCL8*, *IL6*, *IL1A*, and *LIF* genes (Figure 3). Furthermore, the downregulation of the genes in the oxidative phosphorylation (hsa00190) pathway was detected.

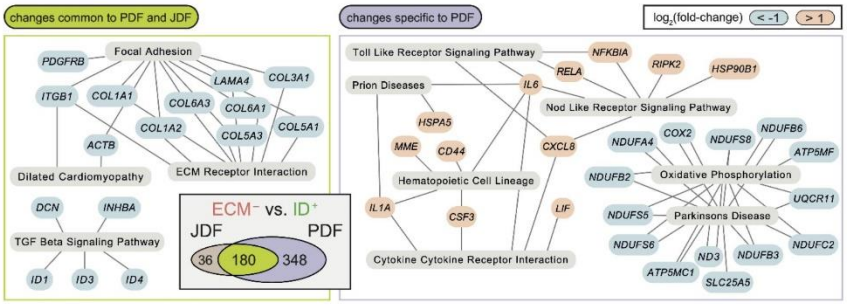

Figure 3. The differences between the ECM⁻ and ID⁺ fibroblast clusters are largely replicated in PDF and JDF spheroids, with distinct features present in PDF fibroblasts. Changes common to both samples (left) are enriched in genes downregulated in ECM⁻ clusters and participating in several KEGG pathways related to the extracellular matrix and TGF-β signalling. Changes specific to PDF spheroids (right) include hyperactivation of genes participating in cytokine signalling in the ECM⁻ cluster. No KEGG pathway enrichment specific to the JDF sample was observed. The Venn diagram (inset) displays a significant overlap ($p < 10^{-6}$, Fisher's exact test) of differentially expressed genes (false discovery rate FDR < 0.05, at least two-fold change in gene expression) in the comparison of the ECM⁻ and ID⁺ fibroblast clusters in JDF and PDF samples.

Similarly, we saw common differences in the comparison of ECM⁻ to ECM⁺ clusters (Figure 4): the TGF-β signalling pathway was significantly enriched for downregulated genes (*ID1*, *INHBA*, and *DCN*) in both JDF and PDF. In PDF, we observed a further enrichment of downregulated genes in the ECM receptor signalling pathway and focal adhesion, including several collagen types (e.g., *COL1A1*, *COL4A1*). We observed only marginal differences in the activity of the signalling pathways in the comparison of ID⁺ and ECM⁺ clusters.

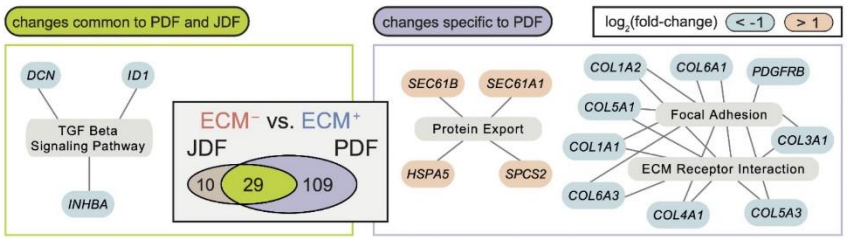

Figure 4. The differences between the ECM⁻ and ID⁺ fibroblast clusters are largely replicated in PDF and JDF spheroids with distinct features present in PDF fibroblasts. Changes common to both samples (left) are enriched in genes downregulated in ECM⁻ clusters and participating in several KEGG pathways related to extracellular matrix and TGF-β signalling. Changes specific to PDF spheroids (right) include hyperactivation of genes participating in cytokine signalling in the ECM⁻ cluster. No KEGG pathway enrichment specific to the JDF sample was observed. The Venn diagram (inset) displays a significant overlap ($p < 10^{-6}$, Fisher's exact test) of differentially expressed genes (false discovery rate FDR < 0.05, at least two-fold change in gene expression) in the comparison of the ECM⁻ and ID⁺ fibroblast clusters in JDF and PDF samples.

These results indicated that the differences between fibroblasts caused by photoageing in PDF concentrate in the ECM⁻ clusters. To validate the hypothesis, we aggregated the scRNA-seq data from PDF and JDF using library size standardisation and compared ECM⁻ (ID⁺, ECM⁺ respectively) clusters between PDF and JDF spheroids. In all comparisons, we detected tens of differentially expressed genes (Supplementary Table S3 and Supplementary Figure S7 for their expression profile in aggregated data). Both ECM⁺ and ECM⁻ clusters displayed common upregulation of several genes in PDF (*TNFAIP6*, *TFPI2*, *ACKR3*, *DCN*, and *CTHRC1*). Specific changes in ECM⁻ clusters included upregulation of the genes linked to the TNF signalling pathway (hsa04668; *IL6*, *CCL20*, *CCL5*, *LIF*, *PTGS2*, and *MMP9*). These genes are often overexpressed in senescent cells. Changes between the ECM⁺ clusters involved upregulation of periostin *POSTN*, fibromodulin *FMOD*, and the gene coding for fibroblast activation protein *FAP*. Surprisingly, we observed the activation of the *LRRC15* (leucine-rich repeat containing 15) gene in ECM⁺ PDF fibroblasts, while no expression of *LRRC15* was detected in ECM⁺ JDF fibroblasts (Figure 5).

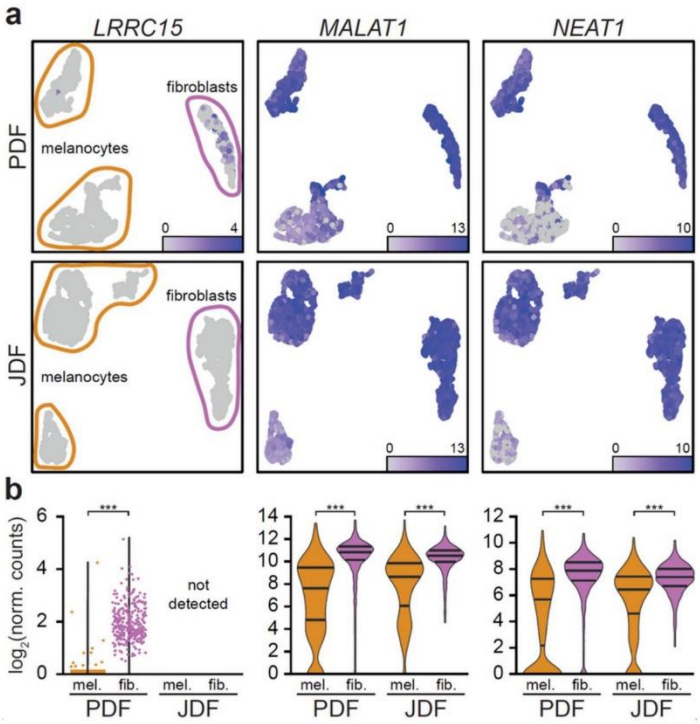

Figure 5. Expression of *MALAT1* and *NEAT1* distinguishes two melanoma cell clusters in each spheroid type. In UMAP projection of the data (**a**), LRRC15 (left) is expressed only in the ECM+ cluster of PDF (top) fibroblasts. *MALAT1* (centre), and *NEAT1* (right) display expression predominantly in the upper cluster of melanoma cells both in PDF (top) and JDF (bottom). (**b**) The expression intensities of the genes are different in fibroblasts and melanoma cells, with markedly bimodal distribution in melanoma cells (*** $p < 0.001$, Mann-Whitney U test).

CTHRC1 (collagen triple helix repeat containing 1) was upregulated in all PDF clusters compared to JDF, see Supplementary Table S3 and Supplementary Figure S7. We also observed

downregulation of specific genes in ECM⁻ PDF fibroblasts (*RHOB*), in ECM⁺ PDF fibroblasts (*PGF* and *GAL*) and in ID⁺ PDF fibroblasts (*DUSP2* and *IGFBP2*) compared to their JDF counterparts. In all PDF clusters, we detected downregulation of the *MGP* gene, see Supplementary Figure S7.

In summary, while we found scattered changes in gene expression between PDF and JDF spheroids in ECM⁺ and ID⁺ clusters with the upregulation of genes coding for inflammation-supporting factors in the fibroblasts prepared from adult UV-irradiated skin, ECM⁻ clusters also displayed distinct upregulation of the TNF signalling pathway.

2.4. Bioinformatic Analysis of Melanoma Cells Isolated from Spheres Containing both Types of Fibroblasts

Using bioinformatic analysis of scRNA-seq data, we divided G361 melanoma cells from heterogeneous spheres to two clusters. In this case, we did not observe principally different transcriptional profiles. Instead, these clusters differed in transcriptional activity with one cluster more active than the other. The more active cells exhibited higher expression of *NEAT1*, *MALAT1* (Figure 5), *SERPINE2*, and *IGFBP3* genes. They also displayed a higher expression of *CDH1* and *CDH2* genes (Supplementary Figures S4 and S5).

2.5. Expression of Pro-Inflammatory Cytokines in Spheroid Components

As we observed the expression of pro-inflammatory cytokines in specific clusters of fibroblasts, we examined whether these factors were also expressed by melanoma cells. We observed that *CXCL1* was predominantly produced by the melanoma cells, while *IL6* and *LIF* were expressed mainly by the fibroblasts and *CXCL8* by both cell types (Figure 6a,b).

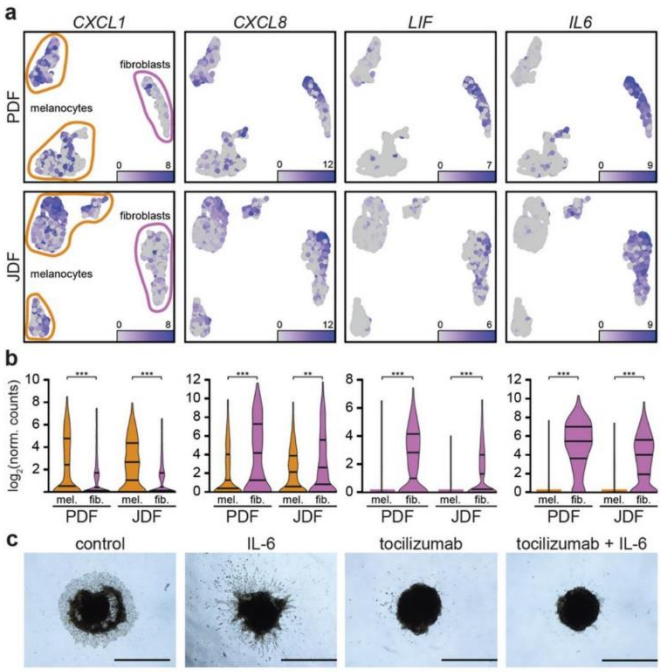

Figure 6. Expression of inflammation-related genes in different components of the PDF and JDF spheroids. In UMAP projection of the data (**a**), chemokine *CXCL1* (left) and interleukin *CXCL8* (centre left) are expressed both in melanoma cells and fibroblasts in PDF (top) and JDF (middle) spheroids.

LIF (centre right) and interleukin *IL6* (right) are predominantly expressed in fibroblasts. The observed differences in gene expression are statistically significant (** $p < 0.01$; *** $p < 0.001$, Mann-Whitney U test). (**b**) The migratory behaviour of cells in a heterogenous spheroid is strongly stimulated by IL-6 and diminished upon tocilizumab treatment (**c**). Bar denotes 1000 µm.

2.6. Spheroid Viability, Invasion to the Extracellular Matrix and Pharmacological Blockade of the IL-6 Receptor

The spheroids retained high viability of cells, as evidenced by trypan blue supravital staining performed after enzymatic digestion prior to RNA analysis (not shown). Moreover, both types of cells from the digested spheres were able to be read here and continue proliferation in 2D.

After embedding to the collagen matrix, heterogeneous spheroids presented clear cellular outgrowths as a sign of invasion. We observed a migration of individual fibroblasts followed by melanoma cells (Figure 6c, JDF presented here, similar PDF not shown). Their remarkably distinct morphology can easily distinguish these cell types. In controls with complete culture medium (DMEM 10% FBS), we observed the tightly packed invasive front of G361 melanoma cells. The invasive potential was remarkably enhanced by addition of exogenous IL-6 to the culture medium. The G361 invasion was more irregular and formed massive tentacular outgrowths in the full thickness of the collagen layer. We also observed individual G361 cell migration. The addition of tocilizumab to the culture medium significantly restricted the outgrowth of melanoma cells to the collagen gel. The rescue experiment where tocilizumab was applied simultaneously with IL-6 did not differ significantly from the earlier one. Invariably, the viability of spheroids even after ten days in the collagen matrix was confirmed by MTT test (Supplementary Figure S11). This suggested the sustained metabolic activity of spheroids in all experiments.

3. Discussion

As evidenced by our data, heterogeneous spheres containing fibroblasts and melanoma cells can be analysed by the scRNA-seq technique. This approach represents a very promising tool for deeper study of the cancer microenvironment organisation and function. scRNA-seq gives a unique chance to identify even a minor population within a seemingly homogeneous pool of stromal fibroblasts and reveal their regulatory function. Bioinformatic analysis allows shedding light on the combinations of well-established markers and identifying the previously unknown activity of a subset of genes in a defined population. It can facilitate study of the changes associated with the intercellular crosstalk in tumours in 3D.

In our experiments, both JDF and PDF fibroblasts from photodamaged skin exhibited marker of activated fibroblasts *FAP* (fibroblast activations protein) in heterogeneous spheroids with G361 melanoma cells. FAP is a cell-surface serine protease that acts on the extracellular matrix components and some other substrates. FAP is highly upregulated in a wide variety of cancers and it is often used as a marker for pro-tumorigenic stroma [34].

Fibroblasts were, according to their expression profile, assigned into three clusters. This observation shows that they do not represent the homogeneous population and that they can be distinguished according to their effect on the cancer cell. This also indicates a high complexity of the melanoma ecosystem.

Fibroblasts of the ECM$^+$ cluster produced ECM, e.g., different types of collagen. This cluster represents an older paradigmatic view of fibroblasts as cells continuously contributing to the formation of scaffolds of ECM in both normal tissues and tumours. Notably, we observed activation of *LRRC15* in the ECM$^+$ cluster of PDF fibroblasts. LRRC15 was described as a membrane-bound protein on stromal fibroblasts in many solid tumours (e.g., breast, head and neck, lung, pancreatic). The LRRC15 expression was induced by TGF-β on activated fibroblasts (αSMA$^+$) and on mesenchymal stem cells [35]. In our case, LRRC15 was surprisingly detected in photodamaged, yet normal primary fibroblasts. This finding highlights the loose definition of CAFs and the contemporary lack of their specific markers [36–39].

When compared to other fibroblasts clusters, the ECM$^-$ cluster cells displayed upregulated genes for production of inflammation-promoting factors, namely *IL6*, *CXCL8*, and *TGFβ*.

The signal was much stronger in the cells of the ECM$^-$ cluster of the PDF population, which also overexpressed several other genes linked to the pro-inflammatory TNF signalling pathway (*IL6*, *CCL20*, *CCL5*, *LIF*).

These molecules have a potent regulatory effect and can promote tumorigenesis. Notably, there is an obvious overlap with molecules representing the senescence-associated secretory phenotype. Because of the prominent role of IL-6, we studied the effect of clinically approved antibody tocilizumab directed against the complex of IL-6 receptor with gp130 on the migration of cells from the spheres transferred to adhesive conditions. While both types of fibroblasts and melanoma cells can migrate out of the spheroids, the application of tocilizumab remarkably inhibited migration of melanoma cells (Figure 6c).

IL-8 seems to be another dominant player that we observed in the ECM$^-$ cluster phenotype. IL-8 is also activated in senescent cells. In stress conditions, IL-8 confers chemotherapeutic resistance on cancer cells [40]. IL-8 signalling promotes angiogenic responses, proliferation, and survival of cancer cells, and potentiates their migration. Therefore, inhibiting the effects of IL-8 signalling may be a significant therapeutic intervention in targeting the tumour microenvironment. However, IL-8 targeting has reached rather modest clinical attention so far [41].

Chronic inflammation is a hallmark of senescence and represents a very important condition for initiation and progression of practically all types of malignant diseases, including melanoma. Beside immune cells, CAFs produce numerous factors that stimulate tumour growth [42]. Among factors that enhance cancer growth and spreading, both IL-6 and IL-8 play a fundamental role not only in cutaneous but also in uveal melanoma [15,43–46]. This observation can demonstrate how the model conditions can mimic the microenvironment. Further, employment of the presented system based on fibroblasts is important in the design and testing of potential new anticancer approaches.

It was observed in pancreatic cancer that IL-1 induces LIF expression and downstream JAK/STAT activation to generate inflammatory CAFs [47]. Moreover, TGF-β was suggested to antagonise this process by downregulating IL-1R1 expression and promoting differentiation into myofibroblasts. Therefore, it was suggested that distinct CAF subtypes are characterised by either myofibroblastic or inflammatory phenotypes.

TGF-β itself can have both tumour-suppressive (at an early stage) and tumour-promoting effects (at the late stage of carcinogenesis). TGF-β directly promotes the oncogenic potential of tumour cells and enhances tumour cell invasion and migration. This is achieved by driving epithelial-to-mesenchymal transition (EMT), a hallmark of cancer [48].

The ID$^+$ cluster is also related to TGF-β in a broader sense. However, it must be seen independently from the previous one. Fibroblasts of this cluster had a prominent activity of *ID* (Inhibitor of Differentiation) genes. Members of the broad TGF-β family of ligands include the TGF-βs, activins, NODAL, BMPs, and GDFs. These molecules share pleiotropic effects on cell behaviour ranging from germ layer specification and patterning in embryonic development to tissue homeostasis and regeneration in adults [49].

The best characterised signalling pathway downstream of TGF- β is through SMAD2 and SMAD3 via their phosphorylation. However, there is also non-canonical signalling induced by TGF-β, which depends on SMAD1/5 phosphorylation. This somewhat surprising alternative was explained in recent years by a new paradigm for receptor activation where TGFBR1 phosphorylates and activates ACVR1 [50]. Primary early transcriptional targets of this axis are the *ID* genes typical of this cluster of our fibroblasts.

A similar extent of fibroblast heterogeneity was also observed by other authors, who confirmed the polarisation of normal dermal fibroblasts to those producing ECM and fibroblasts producing pro-inflammatory factors. Of note, the particular composition of the proposed clusters was age-dependent [51,52]. This was also demonstrated in our study, comparing JDF and PDF.

A heterogeneous population of CAFs was also observed in tumours, such as breast and prostate [53,54]. Production of collagen by CAFs and its elongation is even able to influence the prognosis of patients in many types of cancers [55].

Our model of heterogeneous spheroids demonstrated differences between fibroblasts prepared from a young person and an adult donor after chronic UV exposure, which is not surprising [2,52]. The population of PDF after years of UV chronic injury of donor skin seems to be more heterogeneous, which may be influenced by accumulated UV-dependent damage. Induction of a senescence-associated secretory phenotype may stimulate cancer growth to a greater extent than factors released from the young individual not damaged by irradiation. Such interpretation is supported by a classical study [56] that demonstrated the effect of the irradiation of fibroblasts on mammary gland cancer formation in animal experiments.

It is also noteworthy that we used JDF and PDF fibroblasts after significant in vitro quantity expansion (at passage 5). This is a generally accepted maximum passage number when working with early primary isolates, including fibroblasts. The clonal selection occurring in-vitro and its potential implications have long been discussed [56]. This phenomenon may have significant consequences for reliable disease modelling at a larger scale [57], because the natural cellular diversity seen in the tissue can be easily lost. This would lead to the underrepresentation of specific phenotypes in the models. Based on our observation, a certain diversity in fibroblast clustering remained preserved even in the earlier passages (no. 5). The mechanisms underlying the maintenance of their diversity remain unknown. Of note, we have earlier observed sustained biological activity in various cancer-associated fibroblast cultures even of significantly higher passages [31,58,59].

In melanoma cells, we identified two clusters in both types of spheres. We used the well-characterised cell line G361 for our melanoma 3D model. These cells have been immortalised and maintained in vitro for a substantially long time. The reason for clustering is, therefore, unlikely to represent any natural heterogeneity observed in tumours [60,61]. Melanoma is an aggressive disease, frequently adopting a more de-differentiated phenotype close to stemness and also similar to neural crest stem cells [62,63]. This low differentiation status is typical of many malignant melanoma cell lines. Emerging evidence indicates that both quiescent (out of cell cycle and in a lower metabolic state) and active (in cell cycle and not able to retain DNA labels) stem cell subpopulations may coexist, as described in several tissues [64,65].

As mentioned above, we observe a division of G361 cells into two clusters. The transcriptionally more active cluster of G361 in our spheroids exhibited an upregulation of *NEAT1*, *MALAT1* (also known as *NEAT2*), *SERPINE2*, and *IGFBP3* genes. Both *NEAT1* and *MALAT1* genes are affiliated with the lncRNA class. Recent studies have demonstrated implication of long noncoding RNAs (lncRNAs) in a variety of physiological and pathological processes. These genes are important for nuclear organisation because of their role in stabilisation of nuclear bodies and splicing of pre-mRNA. They stimulate migration of both types, i.e., cutaneous and uveal melanoma [66–69]. Their role in chemoresistance of cancer cells to therapeutics is discussed [70]. Therefore, their targeting by small inhibitors was recently proposed in the literature [71].

Mechanistically, it was suggested that the MALAT1-protein complex facilitates dephosphorylation of pSmad2/3 by providing the interaction niche for pSMAD2/3 and their specific phosphatase PPM1A, thus regulating TGF-β/SMAD signalling [72].

Similarly, the activity of *SERPINE2* stimulates the melanoma metastatic behaviour [73]. On the other hand, the role of the *IGFBP3* gene in cancer is not entirely understood, because both melanoma-supporting and inhibiting effect was shown concerning this factor [74,75]. The activity of genes encoding E- and N-cadherins (*CDH1*, *CDH2*) was detected in melanoma cells prepared from the spheroids. The presence of N-cadherin in these cells seems to biologically relevant because the switch of the expression of E-cadherin to N-cadherin enhances migration of cancer cells and stimulates cancer spreading [76]. This result harmonises well with the activity of noncoding transcripts *MALAT1* and *NEAT1*.

We demonstrated that spheroids constructed from melanoma cells and fibroblasts in combination with single-cell sequencing represent a suitable model for melanoma research that can be employed for the study of the interaction of fibroblasts with melanoma cells.

Our study confirmed that dermal fibroblasts are not homogeneous but instead comprise multiple discrete subpopulations with extensive variations confirmed by our scRNA-seq data. Since fibroblasts are the predominant cell type in dermal tissue, the regulation of their behaviour is likely to be important in tissue physiology and pathology. We believe that these variations documented by scRNA-seq are relevant to our understanding of skin biology and their involvement in dermatological diseases, including melanoma. We hypothesize that more in-depth knowledge of fibroblast heterogeneity represents an important benefit and can impact on the development of new approaches to therapy. As fibroblasts are the most ubiquitous cells found in the dermis and various other tissues, therapeutic targeting of this cell type, in general, seems to be a risky and unrealistic goal for future therapy. It is more likely that the targeting of a discrete population with distinct protumorigenic behaviour would be more plausible and could be associated with a clinical benefit.

In the nearest future, it must also be verified how these heterogeneous models could be subjected to various external stimuli, including pharmacological treatment with, e.g., BRAF and MEK inhibitors. We believe that our presented findings would allow us to interpret these models realistically and overcome the current limitations of our study.

4. Materials and Methods

4.1. Cell isolation and Culture

Skin specimens were obtained during the routine surgery at the Department of Dermatology (n = 10), Charles University, Prague. The samples of residual skin were collected under the Local Ethics Committee approval in accordance with the ethical standards of the Institutional and National Research Committee, and according to the 1964 Helsinki declaration and its later amendments or comparable ethical standards. Informed consent from individual participants and/or representatives was obtained.

The fibroblasts were isolated from skin explants according to a protocol published earlier by us and immunophenotyped [77]. Briefly, fibroblasts were expanded in Dulbecco's Modified Eagle's Medium (DMEM), supplemented with 10% foetal bovine serum (both from Biosera, Nuaille, France) with antibiotics (penicillin 100 IU/mL, streptomycin 100 μg/mL and gentamycin 100 μg/mL, all Sigma Aldrich, Prague, Czech Republic) (FBS, Biosera, Nuaille, France). For the scRNA-seq study, two isolates of fibroblasts were used. PDF (photoaged dermal fibroblasts) were isolated from the heavily photodamaged skin of a 55-year-old male. JDF (juvenile dermal fibroblasts) were isolated from the sun-protected skin of a 3-year-old boy. In both cases, the skin samples were clinically normal and devoid of any clinical signs of skin disease. For this experiment, we used early passages before P4-5. The cells were well and fast growing and were devoid of β-galactosidase reaction (at pH = 6, less than 1% subconfluent cells). The cell line of cutaneous malignant melanoma G-361 harbouring BRAF mutation (heterozygous for BRAF p.Val600Glu—c.1799T > A), was used for our study[78,79]. Cell authentication was performed before the experiment according to ISO/IEC 17025. The cells were maintained in Mc Coy's Medium (Biosera, Nuaille, France) supplemented with antibiotics and 10% FBS. For further experiments with fibroblasts, G361 was grown in DMEM as above. All cells were routinely screened for mycoplasma infection.

4.2. Preparation of Heterogeneous Spheres

The spheroids were prepared by the hanging drop method [80]. Briefly, fibroblasts were mixed in suspension with G-361 cells in a 1:1 ratio in complete culture medium. Individual drops (25 μl each) containing 50,000 cells were placed on the inner non-adhesive side of a 100 mm Petri dish lid (Corning Life Sciences, Tewksbury, MA, USA). Then, the Petri dish bottom part was filled with 15 mL of Dulbecco's Phosphate-Buffered Saline (PBS, Biosera, Nuaille, France). The lid with drops was gently reverted and placed on the top. The hanging drops (approximately 50 per lid) were kept

undisturbed in the incubator (37 °C, 5% CO_2) for 60 h. Using a Pasteur pipette, the spheres were collected and moved to a new, sterile, bacteriological, non-adherent Petri dish with DMEM with 10% FBS and kept floating for an additional 48 h in the incubator.

4.3. Immunohistochemistry

The spheroids were collected and gently rinsed in PBS, and the fixation and embedding followed the AMeX technology described elsewhere [81]. The human melanoma samples were fixed in 10% neutral buffered formalin and routinely processed in paraffin blocks (FFPE). The FFPE samples were sectioned (5 μm) and attached on positively charged X-tra adhesive slides (Leica, Bretton, UK). Heat-induced epitope retrieval was performed in DAKO Envision Flex buffer with endogenous peroxidase quenching using 1% hydrogen peroxide. Primary antibody incubation was performed overnight at 4 °C. The antibodies and immunohistochemical detection kit are listed in Supplementary Table S1. The photodocumentation was performed with a Leica DM2000 microscope using LASx software.

4.4. Single-cell RNA Sequencing

For scRNA-seq analysis, 50 spheroids of each type (G-361 + PDF and G-361 + JDF, respectively) were used. The spheroids were collected and washed twice with PBS followed once by 0.02% EDTA solution. To prepare a single-cell suspension, we used a 1:1 mixture of 0.25% trypsin and 0.02% EDTA solution (all Sigma Aldrich, Prague, Czech Republic) at room temperature for approximately 10 min with gentle agitation. The viability of cells was assessed by trypan blue and counted in an automated TC20 cell counter (BioRad, Prague, Czech Rep.). Both samples had cell viability above 80%. Single-cell RNA-seq libraries were prepared using the Chromium controller instrument and Chromium next gem single-cell 3' reagent kit (version 3.1) according to the manufacturer's protocol (both 10× Genomics, Pleasanton, CA, USA) targeting at 4000 cells per sample. The quality and quantity of the resulting cDNA and libraries was determined using Agilent 2100 Bioanalyzer (Agilent, Santa Clara, CA, USA). The libraries were sequenced in two runs of NextSeq 500 sequencer using NextSeq 500/550 high output kit v2.5 (75 cycles) (both Illumina, San Diego, CA, USA) according to the manufacturer's protocol.

4.5. Bioinformatic Analysis of scRNA-seq Data

Raw sequencing data were processed by CellRanger software v3.1.0 (10× Genomics, Pleasanton, CA, USA). The resulting raw feature barcode matrices were analysed in the R/Bioconductor statistical environment [82,83]. Empty droplets containing only ambient RNA were removed using DropletUtils [84]. Subsequently, dead or damaged cells were filtered out, resulting in 3908 and 4507 cells in the PDF and JDF sample, respectively. Features expressed in less than 5% of cells were removed from the analysis, giving a total number of 11,818 and 10,965 detected features in the PDF and JDF sample, respectively. The data were normalised, $\log_2$-transformed, and highly variable genes (HVGs) were detected. HVGs were used for the principal component analysis, which was used for the dimensionality reduction using Uniform manifold approximation and projection (UMAP) [85]. Single-cell consensus clustering (SC3) [86] was performed. The selected number of clusters was in accordance with the UMAP embedding of the cells.

Cluster marker genes were detected by the Mann–Whitney U test. The marker genes were required to be statistically significant (false discovery rate (FDR) < 0.05) and to have at least two-fold change in expression intensity between the clusters. The marker genes were subsequently used in the gene set enrichment analysis [87] of KEGG pathways [88]. The normalised enrichment score (NES) was used to account for differences in the gene set sizes. The thresholds for significantly enriched pathways were FDR < 0.005 and $|NES| > 2.25$. For analysis of the aggregated fibroblast dataset, the data of fibroblast subgroups within each sample were corrected for sequencing depth, integrated by mutual-nearest-neighbour algorithm, and clustered using SC3.

For the full description of bioinformatic analysis, see Appendix A [82–97].

4.6. Migration of Melanoma Cells from the Spheroids and Viability Assessment

To test the extracellular matrix invasion, we first coated the plates with a thin layer of 1% low melting point agarose (Promega, Madison, WI, USA). Next, we transferred the spheroids (6 per 10 cm2 well) onto agarose and overlaid them with freshly neutralised 2 mg/mL pre-cooled solution of collagen-1 (Gibco, Thermo Fisher, Waltham, MA, USA) following the manufacturer's protocol. After collagen polymerisation (approximately 5 min at 37 °C), the complete culture medium was gently added dropwise. The culture medium was changed every 48 h afterwards. To stimulate ECM invasion, we supplemented the culture medium with human recombinant IL-6 (Sigma Aldrich, Prague, Czech Republic) at a final concentration of 10 ng/mL [98]. To block the IL-6 signalling cascade, we used monoclonal antibody tocilizumab (Roche, Grenzah-Wyhlen, Germany) at a final concentration of 10 ug/mL [98]. For the rescue experiment, we used the combination of IL-6 and tocilizumab simultaneously. DMEM + 10% FBS-treated spheroids were used as a control. The spheroids were maintained at 37 °C, 5% CO_2 in a humidified incubator. Photos of migrating cells were taken every 24 h using a phase-contrast microscope. At day 10, we performed the final spheroid viability assessment using the MTT test. The medium was supplemented with MTT (3-(4,5-dimethylthiazol-2-yl)-2,5-diphenyl tetrazolium bromide (Sigma Aldrich, Prague, Czech Republic) at a final concentration of 1 mg/mL for 60 min, and insoluble formazan production in cells was assessed microscopically.

5. Conclusions

Heterogeneous spheroids combining cancer cells and other cell populations forming the cancer ecosystem (as exemplified here on fibroblasts) represent a highly relevant and still affordable model for cancer research. The combination with scRNA-seq allows deciphering the complex interactions in the heterogeneous spheroids. scRNA-seq is an excellent tool to understand the intercellular interactions in cancer under defined conditions significantly closer to the real situation than conventional cell cultures. Extrinsic and intrinsic stimuli shape the tissue microenvironment and can contribute to the establishment of a cancer-promoting niche. Fibroblasts are critical players in establishing the pro-inflammatory environment surrounding tumour cells. We have demonstrated that fibroblasts are functionally heterogeneous in spheroids. This aspect of their heterogeneity should be carefully investigated in the future. Based on our findings, targeting distinct subpopulations within the cancer microenvironment seems to be a plausible approach to the development of novel anticancer therapeutics.

Supplementary Materials: The following are available online at www.mdpi.com/2072-6694/12/11/3324/s1, **Supplementary Figure S1:** Single-cell RNA-seq profiling separates melanoma cell from fibroblasts. (a) Markers of fibroblasts (FAP) and melanoma cells (melan-A) distinguish cellular types in the tumour microenvironment. Bar denotes 100 μm. M denotes malignant melanoma cells, S denotes surrounding stroma, yellow arrowheads show FAP-positive stromal fibroblasts (in red). (b) Identical markers used to identify clusters of fibroblasts (*FAP*) and melanoma cells (*MLANA*) in UMAP visualisation of the scRNA-seq data. (c) There is virtually no expression of *FAP* in melanoma cells and *MLANA* in fibroblasts (*** $p < 0.001$, Mann-Whitney U test). **Supplementary Figure S2:** Clusters of melanoma cells and fibroblasts identified in scRNA-seq data express typical lineage markers. In the heatmap, expression intensity of the top fifteen specific genes for each cluster are plotted in the PDF (top) and JDF spheroid (bottom). **Supplementary Figure S3:** Read coverage for the *CDKN2A* gene. The melanoma cell line G361 is characterised by truncating deletion of the *CDKN2A* gene at its 3' end, which leads to translational failure. Position on chromosome 9 is shown in (a). Separate coverage tracks are shown for melanoma and fibroblast cells within PDF and JDF samples (b). The gene model for the *CDKN2A* gene is given in (c). **Supplementary Figure S4:** Expression intensity of selected markers in the PDF spheroid. Melanoma markers (tyrosinase *TYR* and *MITF*) are expressed in melanoma cells (two left clusters). Cadherins *CDH1* and *CDH2* show complementary activity in the active melanoma cell cluster in the UMAP projection. Vimentin (*VIM*) is expressed in both cell populations. Fibroblast markers collagen *COL1A2*, lysyl oxidase (*LOX*), podoplanin (*PDPN*), and *S100A4* are expressed predominantly in the right cell cluster, which consists of fibroblast cells. **Supplementary Figure S5:** Expression intensity of selected markers in the JDF spheroid. Melanoma markers (tyrosinase *TYR* and *MITF*) are expressed in melanoma cells (two left clusters). Cadherins *CDH1* and *CDH2* show complementary activity in the active melanoma cell cluster in the UMAP projection. Vimentin (*VIM*) is

expressed in both cell populations. Fibroblast markers collagen *COL1A2*, lysyl oxidase (*LOX*), podoplanin (*PDPN*), and *S100A4* are expressed predominantly in the right cell cluster, which consists of fibroblast cells. The small upper cluster displays markers of both fibroblasts and melanoma cells and most probably consists of cell duplets. It was disregarded in all present analyses. **Supplementary Figure S6:** Immunohistochemical analysis of melanoma primary tumours and metastases. Tyrosinase was highly positive in primary tumours and metastases, the stroma was negative. E-cadherin and N-cadherin staining was of weak-to-moderate intensity in melanoma cells as well. The vimentin signal was strong both in tumour cells and in stromal fibroblasts. Podoplanin was negative in either melanoma cells or stromal fibroblasts. **Supplementary Figure S7:** Venn diagrams displaying overlap of the upregulated (left) and downregulated (right) genes in ECM^- (or ID^+ and ECM^+) fibroblast clusters across JDF and PDF spheroids. Only genes with statistically significant (false discovery rate FDR < 0.05) and at least two-fold change in gene expression are shown. See Additional Table S3 for details. **Supplementary Figure S8**: Heatmap of expression intensities of the markers of three fibroblast clusters identified in the JDF spheroid. ECM^-, ID^+, and ECM^+ clusters are clearly identified by expression of chemokines, ID genes, and components of extracellular matrix, respectively. **Supplementary Figure S9**: Heatmap of expression intensities of the markers of three fibroblast clusters identified in the PDF spheroid. ECM^-, ID^+, and ECM^+ clusters are clearly identified by expression of chemokines, ID genes, and components of extracellular matrix, respectively. **Supplementary Figure S10:** Differences in expression between ECM^- and ID^+ (left), ECM^- and ECM^+ (centre), and ID^+ and ECM^+ (right) are largely similar in PDF (top) and JDF spheroids (bottom). The Venn diagrams display overlap of differentially expressed genes (false discovery rate FDR < 0.05, at least two-fold change in gene expression) in each comparison. **Supplementary Figure S11:** The migratory behaviour of cells in a heterogenous spheroid in 3D gels is strongly stimulated by IL-6 and diminished upon tocilizumab treatment. However, these differences were remarkable; all spheroids invariably retained good viability as visualised by formation of the purple-blue formazan product in MTT test after 10 days of the experiment. Bar denotes 200 μm. **Supplementary Table S1:** Antibodies used in the study and tumour sample-related details. **Supplementary Table S2**: Differentially expressed genes (DEG) between identified fibroblast clusters within JDF and PDF spheroids. Only DEG with statistically significant (false discovery rate FDR < 0.05) and at least two-fold change in gene expression are given. **Supplementary Table S3:** Differentially expressed genes (DEG) between identified fibroblast clusters across JDF and PDF spheroids. Only DEG with statistically significant (false discovery rate FDR < 0.05) and at least two-fold change in gene expression are given. The data were standardised by library size normalisation. **The dataset supporting the conclusions of this article is available in the ArrayExpress repository, [E-MTAB-9216, https://www.ebi.ac.uk/arrayexpress/experiments/ E-MTAB-9216]**.

Author Contributions: Conceptualisation, K.S.J. M.K., and L.L.; data curation, J.N. and K.S.; formal analysis, V.P.; funding acquisition, B.D., K.S.J., and V.P.; investigation, J.N. K.S., B.D. Š.K., and L.L.; methodology, J.N., B.D., M.K., and L.L.; Project administration, B.D.; resources, K.S.J. and M.K.; software, J.N. and M.K.; supervision, K.S.J., M.K., and L.L.; Validation, B.D., R.J., and P.D.; visualization, J.N., R.J., and K.S.J.; Writing—original draft, K.S. and J.N; writing—review & editing, K.S.J., M.K., and L.L. All authors have read and agreed to the published version of the manuscript.

Funding: This research was funded by the Operational Programme Research, Development and Education under the project "Center for Tumor Ecology—Research of the Cancer Microenvironment Supporting Cancer Growth and Spread" (reg. No. CZ.02.1.01/0.0/0.0/16_019/0000785), by the Research and Development for Innovations Operational Programme under project no. CZ.1.05/2.1.00/19.0400 (co-financed by the European Regional Development Fund and the state budget of the Czech Republic) and the Charles University programme Q28, Czech Science Foundation, project no. 19-05048S. This work was also supported by ELIXIR CZ research infrastructure project (MEYS Grant No: LM2018131) including access to computing and storage facilities.

Acknowledgments: Authors are grateful to Šárka Takáčová, who performed the language editing.

Conflicts of Interest: "The authors declare no conflict of interest."

Appendix A. Supplementary Details of Bioinformatic Analysis of scRNA-seq Data

Appendix A.1. Preprocessing of Raw Data

Raw sequencing data were processed by CellRanger software v3.1.0 (10× Genomics, Pleasanton, CA, USA). The resulting raw feature barcode matrices were analysed in the R/Bioconductor statistical environment. Empty droplets containing only ambient RNA were detected using the DropletUtils package. Subsequently, dead or damaged cells were filtered out: filtering of PDF cells was based on

median absolute deviation (MAD) of the following cell metrics: total read counts, number of detected features, and percentage of mitochondrial and ribosomal features. A value was considered an outlier if it was more than three MADs from the median (downwards for total read counts and number of detected features, and upwards for percentage of mitochondrial and ribosomal features). Filtering based on MAD resulted in 3908 cells in the PDF sample. MAD filtering with the same threshold was not suitable for the JDF sample. After investigation of cell metrics (data not shown), several per cell filtering thresholds were chosen: minimum and maximum unique molecule counts of 1000 and 50,000, respectively, minimum of 1000 features detected, maximum of 20 % of mitochondrial features, and minimum of 10% of ribosomal features. After the application of these rules, 4507 JDF cells remained. Features expressed in less than 5% of cells were filtered out, giving a total number of 11,818 and 1965 detected features for PDF and JDF samples, respectively.

Appendix A.2. Data Normalisation

Cell-specific biases were normalised using the deconvolution strategy for scaling normalisation implemented in the computeSumFactors function from the scran package. Normalised expression values were calculated using the logNormCounts method from the scater package. The expression values can be interpreted as log2-transformed normalised counts and can be used for clustering or dimensionality reduction.

Appendix A.3. Selection of Highly Variable Genes (HVGs)

To identify HVGs, the squared coefficient of variation (CV2) for each gene was computed within scran and a minimal CV2 value of 1.5 was used as the threshold. This resulted in 2054 and 712 HVGs found in the PDF and JDF samples, respectively.

Appendix A.4. Dimensionality Reduction

Prior to downstream analysis, principal component analysis (PCA) was performed using HVGs. Based on the elbow plots, the first six and eight principal components (PC) were chosen for PDF and JDF samples, respectively, as the ones explaining most of the variance in the data. The selected PCs were used for the dimensionality reduction using the uniform manifold approximation and projection (UMAP) method implemented in scatter.

Appendix A.5. Cell Clustering

Single-cell consensus clustering (SC3) was performed with a different number of cell target clusters. Based on the subsequent analysis of cluster marker genes, two clusters were chosen as appropriate to distinguish between melanocytes and fibroblasts. The selected number of clusters was in accordance with the UMAP embedding of the cells.

Appendix A.6. Cluster Marker Genes and Gene Set Enrichment Analysis (GSEA)

Cluster marker genes between melanocyte and fibroblast clusters were detected by the Mann–Whitney U test implemented in the FindAllMarkers function from Seurat v3 package. The marker genes were required to be statistically significant (false discovery rate (FDR) < 0.05) and to have at least two-fold change in expression. The marker genes were subsequently used in GSEA (53) on KEGG pathways using the clusterProfiler package. The normalised enrichment score (NES) was used to account for differences in the gene set sizes. The thresholds for significantly enriched pathways were FDR < 0.005 and $|NES| > 2.25$.

Appendix A.7. Division of Data to Melanocyte and Fibroblast Subgroups

According to the UMAP embedding, the cells were divided to melanocyte and fibroblast subgroups. Data normalisation, HVG selection, dimensionality reduction, cell clustering, cluster

marker genes, and GSEA were repeated in the independent subgroups. In the case of SC3 clustering, two and three clusters were selected as appropriate for melanocyte and fibroblast cells, respectively.

Appendix A.8. Aggregation of Fibroblast Subgroups of the PDF and JDF Samples

The data of fibroblast subgroups within each sample were corrected for sequencing depth by the multiBatchNorm function from the batchelor package. The corrected data were integrated by the mutual-nearest-neighbour algorithm implemented in the fastMNN function from the same package, and SC3 was used for clustering. In this case, three target clusters yielded inappropriate results, with one of the clusters being split in parts (data not shown). Thus, four target clusters were chosen, where one of the clusters contained a low number of cells and was disregarded. The obtained cell-cluster assignments were used together with the data corrected for sequencing depth for the computation of cluster marker genes and GSEA.

References

1. Kalia, S.; Kwong, Y.K.K. Relationship between sun safety behaviours and modifiable lifestyle cancer risk factors and vitamin D levels. *Photodermatol. Photoimmunol. Photomed.* **2019**, *35*, 429–435, doi:10.1111/phpp.12494.
2. Strnadova, K.; Sandera, V.; Dvorankova, B.; Kodet, O.; Duskova, M.; Smetana, K.; Lacina, L. Skin aging: The dermal perspective. *Clin. Dermatol.* **2019**, *37*, 326–335, doi:10.1016/j.clindermatol.2019.04.005.
3. Smetana, K.; Dvořánková, B.; Lacina, L.; Szabo, P.; Brož, B.; Šedo, A. Cancer: The Price for Longevity; In *Aging Exploring a Complex Phenomenon*, Ahmad, S.I. ed. CRC Press: Boca Raton, FL, USA, 2017; pp. 237–245, ISBN 9781315283883.
4. Apalla, Z.; Lallas, A.; Sotiriou, E.; Lazaridou, E.; Ioannides, D. Epidemiological trends in skin cancer. *Dermatol. Pract. Concept.* **2017**, *7*, doi:10.5826/dpc.0702a01.
5. Brash, D.E. UV signature mutations. *Photochem. Photobiol.* **2015**, *91*, 15–26.
6. Melis, J.P.M.; Van Steeg, H.; Luijten, M. Oxidative DNA damage and nucleotide excision repair. *Antioxid. Redox Signal.* **2013**, *18*, 2409–2419.
7. Sarkar, S.; Gaddameedhi, S. Solar UV-induced DNA damage response: Melanocytes story in transformation to environmental melanomagenesis. *Environ. Mol. Mutagen.* **2020**, 1–16, doi:10.1002/em.22370.
8. Chang, H.Y.; Sneddon, J.B.; Alizadeh, A.A.; Sood, R.; West, R.B.; Montgomery, K.; Chi, J.T.; Van De Rijn, M.; Botstein, D.; Brown, P.O. Gene expression signature of fibroblast serum response predicts human cancer progression: Similarities between tumors and wounds. *PLoS Biol.* **2004**, *2*, doi:10.1371/journal.pbio.0020007.
9. Coppé, J.-P.; Desprez, P.-Y.; Krtolica, A.; Campisi, J. The senescence-associated secretory phenotype: The dark side of tumor suppression. *Annu. Rev. Pathol.* **2010**, *5*, 99–118, doi:10.1146/annurev-pathol-121808-102144.
10. Campisi, J. Senescent cells, tumor suppression, and organismal aging: Good citizens, bad neighbors. *Cell* **2005**, *120*, 513–522.
11. Dimri, G.P.; Lee, X.; Basile, G.; Acosta, M.; Scott, G.; Roskelley, C.; Medrano, E.E.; Linskens, M.; Rubelj, I.; Pereira-Smith, O.; et al. A biomarker that identifies senescent human cells in culture and in aging skin in vivo. *Proc. Natl. Acad. Sci. USA* **1995**, *92*, 9363–9367.
12. Debacq-Chainiaux, F.; Erusalimsky, J.D.; Campisi, J.; Toussaint, O. Protocols to detect senescence-associated beta-galactosidase (SA-βgal) activity, a biomarker of senescent cells in culture and in vivo. *Nat. Protoc.* **2009**, *4*, 1798–1806, doi:10.1038/nprot.2009.191.
13. Griffin, M.F.; desJardins-Park, H.E.; Mascharak, S.; Borrelli, M.R.; Longaker, M.T. Understanding the impact of fibroblast heterogeneity on skin fibrosis. *DMM Dis. Model. Mech.* **2020**, *13*, doi:10.1242/dmm.044164.
14. Fujita, K. P53 isoforms in cellular senescence-and ageing-associated biological and physiological functions. *Int. J. Mol. Sci.* **2019**, *20*, 6023, doi:10.3390/ijms20236023.
15. Jobe, N.P.N.P.; Živicová, V.; Mifková, A.; Rösel, D.; Dvořánková, B.; Kodet, O.; Strnad, H.; Kolář, M.; Šedo, A.; Smetana, K.; et al. Fibroblasts potentiate melanoma cells in vitro invasiveness induced by UV-irradiated keratinocytes. *Histochem. Cell Biol.* **2018**, *149*, 503–516, doi:10.1007/s00418-018-1650-4.

16. Marsh, T.; Pietras, K.; McAllister, S.S. Fibroblasts as architects of cancer pathogenesis. *Biochim. Biophys. Acta Mol. Basis Dis.* **2013**, *1832*, 1070–1078, doi:10.1016/j.bbadis.2012.10.013.
17. Lacina, L.; Plzak, J.; Kodet, O.; Szabo, P.; Chovanec, M.; Dvorankova, B.; Smetana, K. Cancer microenvironment: What can we learn from the stem cell niche. *Int J Mol Sci.* **2015**; *16*, 24094–24110, doi:10.3390/ijms161024094
18. Plaks, V.; Kong, N.; Werb, Z. The Cancer Stem Cell Niche: How Essential is the Niche in Regulating Stemness of Tumor Cells? *Cell Stem Cell* **2016**, *16*, 225–238, doi:10.1016/j.stem.2015.02.015.
19. Lacina, L.; Kodet, O.; Dvořánková, B.; Szabo, P.; Smetana, K. Ecology of melanoma cell. *Histol Histopathol.* **2018**, *33*, 247–254, doi: 10.14670/HH-11-926
20. Kodet, O.; Dvořánková, B.; Bendlová, B.; Sýkorová, V.; Krajsová, I.; Štork, J.; Kučera, J.; Szabo, P.; Strnad, H.; Kolář, M.; et al. Microenvironment-driven resistance to B-Raf inhibition in a melanoma patient is accompanied by broad changes of gene methylation and expression in distal fibroblasts. *Int. J. Mol. Med.* **2018**, *41*, 2687–2703, doi:10.3892/ijmm.2018.3448.
21. Krejčí, E.; Dvořánková, B.; Szabo, P.; Naňka, O.; Strnad, H.; Kodet, O.; Lacina, L.; Kolář, M.; Smetana, K. Fibroblasts as drivers of healing and cancer progression: from in vitro experiments to clinics. In *Molecular Mechanisms of Skin Aging and Age-Related Diseases*, Quan, T. ed. CRC Press: Boca Raton, FL, USA, 2016; pp. 121–137, ISBN 9781498704656.
22. Konieczkowski, D.J.; Johannessen, C.M.; Abudayyeh, O.; Kim, J.W.; Cooper, Z.A.; Piris, A.; Frederick, D.T.; Barzily-Rokni, M.; Straussman, R.; Haq, R.; et al. A melanoma cell state distinction influences sensitivity to MAPK pathway inhibitors. *Cancer Discov.* **2014**, *4*, 816–827, doi:10.1158/2159-8290.CD-13-0424.
23. Yang, H.; Higgins, B.; Kolinsky, K.; Packman, K.; Go, Z.; Iyer, R.; Kolis, S.; Zhao, S.; Lee, R.; Grippo, J.F.; et al. RG7204 (PLX4032), a selective BRAFV600E inhibitor, displays potent antitumor activity in preclinical melanoma models. *Cancer Res.* **2010**, *70*, 5518–5527, doi:10.1158/0008-5472.CAN-10-0646.
24. Kawakami, T.; Soma, Y.; Kawa, Y.; Ito, M.; Yamasaki, E.; Watabe, H.; Hosaka, E.; Yajima, K.; Ohsumi, K.; Mizoguchi, M. Transforming growth factor beta1 regulates melanocyte proliferation and differentiation in mouse neural crest cells via stem cell factor/KIT signaling. *J. Investig. Dermatol.* **2002**, *118*, 471–478.
25. Eberle, J. Countering TRAIL resistance in melanoma. *Cancers* **2019**, *11*, 656, doi:10.3390/cancers11050656.
26. Vörsmann, H.; Groeber, F.; Walles, H.; Busch, S.; Beissert, S.; Walczak, H.; Kulms, D. Development of a human three-dimensional organotypic skin-melanoma spheroid model for in vitro drug testing. *Cell Death Dis.* **2013**, *4*, doi:10.1038/cddis.2013.249.
27. Chang, T.T.; Hughes-Fulford, M. Monolayer and spheroid culture of human liver hepatocellular carcinoma cell line cells demonstrate distinct global gene expression patterns and functional phenotypes. *Tissue Eng. Part. A* **2009**, *15*, 559–567, doi:10.1089/ten.tea.2007.0434.
28. Beaumont, K.; Mohana-Kumaran, N.; Haass, N. Modeling Melanoma In Vitro and In Vivo. *Healthcare* **2013**, *2*, 27–46, doi:10.3390/healthcare2010027.
29. Lazzari, G.; Couvreur, P.; Mura, S. Multicellular tumor spheroids: A relevant 3D model for the: In vitro preclinical investigation of polymer nanomedicines. *Polym. Chem.* **2017**, *8*, 4947–4969, doi:10.1039/c7py00559h.
30. Marconi, A.; Quadri, M.; Saltari, A.; Pincelli, C. Progress in melanoma modelling in vitro. *Exp. Dermatol.* **2018**, *27*, 578–586, doi:10.1111/exd.13670.
31. Dvořánková, B.; Szabo, P.; Kodet, O.; Strnad, H.; Kolář, M.; Lacina, L.; Krejčí, E.; Naňka, O.; Šedo, A.; Smetana, K. Intercellular crosstalk in human malignant melanoma. *Protoplasma*. **2017**, *254*, 1143–1150. doi: 10.1007/s00709-016-1038-z.
32. Lynch, M.D.; Watt, F.M. Fibroblast heterogeneity: Implications for human disease. *J. Clin. Investig.* **2018**, *128*, 26–35, doi:10.1172/JCI93555.
33. Živicová, V.; Lacina, L.; Mateu, R.; Smetana, K.; Kavková, R.; Krejcí, E.D.; Grim, M.; Kvasilová, A.; Borský, J.; Strnad, H.; et al. Analysis of dermal fibroblasts isolated from neonatal and child cleft lip and adult skin: Developmental implications on reconstructive surgery. *Int. J. Mol. Med.* **2017**, *40*, doi:10.3892/ijmm.2017.3128.
34. Puré, E.; Blomberg, R. Pro-tumorigenic roles of fibroblast activation protein in cancer: Back to the basics. *Oncogene* **2018**, *37*, 4343–4357.
35. Purcell, J.W.; Tanlimco, S.G.; Hickson, J.; Fox, M.; Sho, M.; Durkin, L.; Uziel, T.; Powers, R.; Foster, K.; McGonigal, T.; et al. LRRC15 is a novel mesenchymal protein and stromal target for antibody–drug conjugates. *Cancer Res.* **2018**, *78*, 4059–4072, doi:10.1158/0008-5472.CAN-18-0327.

36. Tlsty, T.D. Stromal cells can contribute oncogenic signals. *Semin. Cancer Biol.* **2001**, *11*, 97–104, doi:10.1006/scbi.2000.0361.
37. Lo, A.; Wang, L.C.S.; Scholler, J.; Monslow, J.; Avery, D.; Newick, K.; O'Brien, S.; Evans, R.A.; Bajor, D.J.; Clendenin, C.; et al. Tumor-promoting desmoplasia is disrupted by depleting FAP-expressing stromal cells. *Cancer Res.* **2015**, *75*, 2800–2810, doi:10.1158/0008-5472.CAN-14-3041.
38. Sahai, E.; Astsaturov, I.; Cukierman, E.; DeNardo, D.G.; Egeblad, M.; Evans, R.M.; Fearon, D.; Greten, F.R.; Hingorani, S.R.; Hunter, T.; et al. A framework for advancing our understanding of cancer-associated fibroblasts. *Nat. Rev. Cancer* **2020**, *20*, 174–186.
39. Baum, J.; Duffy, H.S. Fibroblasts and myofibroblasts: What are we talking about? *J. Cardiovasc. Pharmacol.* **2011**, *57*, 376–379, doi:10.1097/FJC.0b013e3182116e39.
40. Waugh, D.J.J.; Wilson, C. The interleukin-8 pathway in cancer. *Clin. Cancer Res.* **2008**, *14*, 6735–6741.
41. Wen, J.; Zhao, Z.; Huang, L.; Wang, L.; Miao, Y.; Wu, J. IL-8 promotes cell migration through regulating EMT by activating the Wnt/β-catenin pathway in ovarian cancer. *J. Cell. Mol. Med.* **2020**, *24*, 1588–1598, doi:10.1111/jcmm.14848.
42. Chiavarina, B.; Turtoi, A. Collaborative and Defensive Fibroblasts in Tumor Progression and Therapy Resistance. *Curr. Med. Chem.* **2017**, *24*, doi:10.2174/0929867324666170428104311.
43. Jobe, N.P.N.P.; Rösel, D.; Dvořánková, B.; Kodet, O.; Lacina, L.; Mateu, R.; Smetana, K.; Brábek, J. Simultaneous blocking of IL-6 and IL-8 is sufficient to fully inhibit CAF-induced human melanoma cell invasiveness. *Histochem. Cell Biol.* **2016**, *146*, 205–217, doi:10.1007/s00418-016-1433-8.
44. Kučera, J.; Strnadová, K.; Dvořánková, B.; Lacina, L.; Krajsová, I.; Štork, J.; Kovářová, H.; Skalníková, H.K.H.K.; Vodička, P.; Motlík, J.; et al. Serum proteomic analysis of melanoma patients with immunohistochemical profiling of primary melanomas and cultured cells: Pilot study. *Oncol. Rep.* **2019**, *42*, 1793–1804, doi:10.3892/or.2019.7319.
45. Lacina, L.; Brábek, J.; Král, V.; Kodet, O.; Smetana, K. Interleukin-6: A molecule with complex biological impact in cancer. *Histol. Histopathol.* **2019**, *34*, 125–136.
46. Tabib, T.; Morse, C.; Wang, T.; Chen, W.; Lafyatis, R. SFRP2/DPP4 and FMO1/LSP1 Define Major Fibroblast Populations in Human Skin. *J. Investig. Dermatol.* **2018**, *138*, 802–810, doi:10.1016/j.jid.2017.09.045.
47. Biffi, G. IL1-induced JAK/STAT signaling is antagonized by TGFbeta to shape CAF heterogeneity in pancreatic ductal adenocarcinoma. *Cancer Discov.* **2019**, *9*, 282–301.
48. Massagué, J. TGFβ signalling in context. *Nat. Rev. Mol. Cell Biol.* **2012**, *13*, 616–630.
49. Morikawa, M.; Derynck, R.; Miyazono, K. TGF- β and the TGF-β family: Context-dependent roles in cell and tissue physiology. *Cold Spring Harb. Perspect. Biol.* **2016**, *8*, a021873.
50. Ramachandran, A.; Vizán, P.; Das, D.; Chakravarty, P.; Vogt, J.; Rogers, K.W.; Müller, P.; Hinck, A.P.; Sapkota, G.P.; Hill, C.S. TGF-β uses a novel mode of receptor activation to phosphorylate SMAD1/5 and induce epithelial-to-mesenchymal transition. *Elife* **2018**, *7*, doi:10.7554/eLife.31756.
51. Vorstandlechner, V.; Laggner, M.; Kalinina, P.; Haslik, W.; Radtke, C.; Shaw, L.; Lichtenberger, B.M.; Tschachler, E.; Ankersmit, H.J.; Mildner, M. Deciphering the functional heterogeneity of skin fibroblasts using single-cell RNA sequencing. *FASEB J.* **2020**, *34*, 3677–3692, doi:10.1096/fj.201902001RR.
52. Solé-Boldo, L.; Raddatz, G.; Schütz, S.; Mallm, J.P.; Rippe, K.; Lonsdorf, A.S.; Rodríguez-Paredes, M.; Lyko, F. Single-cell transcriptomes of the human skin reveal age-related loss of fibroblast priming. *Commun. Biol.* **2020**, *3*, doi:10.1038/s42003-020-0922-4.
53. Bartoschek, M.; Oskolkov, N.; Bocci, M.; Lövrot, J.; Larsson, C.; Sommarin, M.; Madsen, C.D.; Lindgren, D.; Pekar, G.; Karlsson, G.; et al. Spatially and functionally distinct subclasses of breast cancer-associated fibroblasts revealed by single cell RNA sequencing. *Nat. Commun.* **2018**, *9*, doi:10.1038/s41467-018-07582-3.
54. Vickman, R.E.; Broman, M.M.; Lanman, N.A.; Franco, O.E.; Sudyanti, P.A.G.; Ni, Y.; Ji, Y.; Helfand, B.T.; Petkewicz, J.; Paterakos, M.C.; et al. Heterogeneity of human prostate carcinoma-associated fibroblasts implicates a role for subpopulations in myeloid cell recruitment. *Prostate* **2020**, *80*, 173–185, doi:10.1002/pros.23929.
55. Hanley, C.J.; Noble, F.; Ward, M.; Bullock, M.; Drifka, C.; Mellone, M.; Manousopoulou, A.; Johnston, H.E.; Hayden, A.; Thirdborough, S.; et al. A subset of myofibroblastic cancer-associated fibroblasts regulate collagen fiber elongation, which is prognostic in multiple cancers. *Oncotarget* **2016**, *7*, 6159–6174, doi:10.18632/oncotarget.6740.
56. Barcellos-Hoff, M.H.; Ravani, S.A. Irradiated mammary gland stroma promotes the expression of tumorigenic potential by unirradiated epithelial cells. *Cancer Res.* **2000**, *60*, 1254–1260.

57. Tuveson, D.; Clevers, H. Cancer modeling meets human organoid technology. *Science* **2019**, *364*, 952–955.
58. Lacina, L.; Smetana K., Jr.; Dvořánková, B.; Pytlík, R.; Kideryová, L.; Kučerová, L.; Plzáková, Z.; Štork, J.; Gabius, H.-J.; André, S. Stromal fibroblasts from basal cell carcinoma affect phenotype of normal keratinocytes. *Br. J. Dermatol.* **2007**, *156*, 819–829, doi:10.1111/j.1365-2133.2006.07728.x.
59. Strnad, H.; Lacina, L.; Kolář, M.; Čada, Z.; Vlček, C.; Dvořánková, B.; Betka, J.; Plzák, J.; Chovanec, M.; Šáchova, J.; et al. Head and neck squamous cancer stromal fibroblasts produce growth factors influencing phenotype of normal human keratinocytes. *Histochem. Cell Biol.* **2010**, *133*, 201–211, doi:10.1007/s00418-009-0661-6.
60. Fattore, L.; Ruggiero, C.F.; Liguoro, D.; Mancini, R.; Ciliberto, G. Single cell analysis to dissect molecular heterogeneity and disease evolution in metastatic melanoma. *Cell Death Dis.* **2019**, *10*, 1–12.
61. Grzywa, T.M.; Paskal, W.; Włodarski, P.K. Intratumor and Intertumor Heterogeneity in Melanoma. *Transl. Oncol.* **2017**, *10*, 956–975.
62. Faião-Flores, F.; Smalley, K.S.M. Get with the Program! Stemness and Reprogramming in Melanoma Metastasis. *J. Investig. Dermatol.* **2018**, *138*, 10–13.
63. Heppt, M.V.; Wang, J.X.; Hristova, D.M.; Wei, Z.; Li, L.; Evans, B.; Beqiri, M.; Zaman, S.; Zhang, J.; Irmler, M.; et al. MSX1-Induced Neural Crest-Like Reprogramming Promotes Melanoma Progression. *J. Investig. Dermatol.* **2018**, *138*, 141–149, doi:10.1016/j.jid.2017.05.038.
64. Li, N.; Clevers, H. Coexistence of quiescent and active adult stem cells in mammals. *Science* **2010**, *327*, 542–545.
65. Clevers, H.; Watt, F.M. Defining Adult Stem Cells by Function, Not by Phenotype. *Annu. Rev. Biochem.* **2018**, *87*, doi:10.1146/annurev-biochem-062917-012341.
66. Merta, L.; Gandalovičová, A.; Čermák, V.; Dibus, M.; Gutschner, T.; Diederichs, S.; Rösel, D.; Brábek, J. Increased Level of Long Non-Coding RNA MALAT1 is a Common Feature of Amoeboid Invasion. *Cancers* **2020**, *12*, 1136, doi:10.3390/cancers12051136.
67. Ding, F.; Lai, J.; Gao, Y.; Wang, G.; Shang, J.; Zhang, D.; Zheng, S. NEAT1/miR-23a-3p/KLF3: A novel regulatory axis in melanoma cancer progression. *Cancer Cell Int.* **2019**, *19*, doi:10.1186/s12935-019-0927-6.
68. Wu, S.; Chen, H.; Zuo, L.; Jiang, H.; Yan, H. Suppression of long noncoding RNA MALAT1 inhibits the development of uveal melanoma via microRNA-608-mediated inhibition of HOXC4. *Am. J. Physiol. Cell Physiol.* **2020**, *318*, C903–C912, doi:10.1152/ajpcell.00262.2019.
69. Zou, J.X.; Ge, T.W. Long non-coding RNA NEAT1 promotes tumor development and metastasis through targeting miR-224-5p in malignant melanoma. *Eur. Rev. Med. Pharmacol. Sci.* **2020**, *24*, 1302–1308, doi:10.26355/eurrev_202002_20187.
70. Kessler, S.M.; Hosseini, K.; Khamis Hussein, U.; Kim, K.M.; List, M.; Schultheiß, C.S.; Schulz, M.H.; Laggai, S.; Jang, K.Y.; Kiemer, A.K.; et al. Cellular Physiology and Biochemistry Cellular Physiology and Biochemistry Original Paper Hepatocellular Carcinoma and Nuclear Paraspeckles: Induction in Chemoresistance and Prediction for Poor Survival The expression of transcript Cellular Physiology and Biochemistry Cellular Physiology and Biochemistry. *Cell. Physiol. Biochem.* **2019**, *52*, 787–801, doi:10.33594/000000055.
71. Abulwerdi, F.A.; Xu, W.; Ageeli, A.A.; Yonkunas, M.J.; Arun, G.; Nam, H.; Schneekloth, J.S.; Dayie, T.K.; Spector, D.; Baird, N.; et al. Selective Small-Molecule Targeting of a Triple Helix Encoded by the Long Noncoding RNA, MALAT1. *ACS Chem. Biol.* **2019**, doi:10.1021/acschembio.8b00807.
72. Zhang, J.; Han, C.; Song, K.; Chen, W.; Ungerleider, N.; Yao, L.; Ma, W.; Wu, T. The long-noncoding RNA MALAT1 regulates TGF-β/Smad signaling through formation of a lncRNA-protein complex with Smads, SETD2 and PPM1A in hepatic cells. *PLoS ONE* **2020**, *15*, doi:10.1371/journal.pone.0228160.
73. Wu, Q.W. Serpine2, a potential novel target for combating melanoma metastasis. *Am. J. Transl. Res.* **2016**, *8*, 1985–1997.
74. Naspi, A.; Zingariello, M.; Sancillo, L.; Panasiti, V.; Polinari, D.; Martella, M.; Rosa Alba, R.; Londei, P. IGFBP-3 inhibits Wnt signaling in metastatic melanoma cells. *Mol. Carcinog.* **2017**, *56*, 681–693, doi:10.1002/mc.22525.
75. Murekatete, B.; Shokoohmand, A.; McGovern, J.; Mohanty, L.; Meinert, C.; Hollier, B.G.; Zippelius, A.; Upton, Z.; Kashyap, A.S. Targeting Insulin-Like Growth Factor-I and Extracellular Matrix Interactions in Melanoma Progression. *Sci. Rep.* **2018**, *8*, doi:10.1038/s41598-017-19073-4.
76. Casal, J.I.; Bartolomé, R.A. Beyond N-cadherin, relevance of cadherins 5, 6 and 17 in cancer progression and metastasis. *Int. J. Mol. Sci.* **2019**, *20*, 3373, doi:10.3390/ijms20133373.

77. Dvořánková, B.; Lacina, L.; Smetana, K. Isolation of normal fibroblasts and their cancer-associated counterparts (CAFs) for biomedical research. In *Methods in Molecular Biology*, Turksen, K. ed. Humana Press: New York, NY, USA, 2018; Volume 1879, pp. 393–406, ISBN 978-1-4939-8869-3.
78. Li, Y.; Cheng, H.S.; Chng, W.J.; Tergaonkar, V.; Cleaver, J.E. Activation of mutant TERT promoter by RAS-ERK signaling is a key step in malignant progression of BRAF-mutant human melanomas. *Proc. Natl. Acad. Sci. USA* **2016**, *113*, 14402–14407, doi:10.1073/pnas.1611106113.
79. Sasaki, Y.; Niu, C.; Makino, R.; Kudo, C.; Sun, C.; Watanabe, H.; Matsunaga, J.; Takahashi, K.; Tagami, H.; Aiba, S.; et al. BRAF point mutations in primary melanoma show different prevalence by subtype. *J. Investig. Dermatol.* **2004**, *123*, 177–183, doi:10.1111/j.0022-202X.2004.22722.x.
80. Alhaque, S.; Themis, M.; Rashidi, H. Three-dimensional cell culture: From evolution to revolution. *Philos. Trans. R. Soc. B Biol. Sci.* **2018**, *373*, 20170216
81. Sato, Y.; Mukai, K.; Watanabe, S.; Goto, M.; Shimosato, Y. The AMeX method: A simplified technique of tissue processing and paraffin embedding with improved preservation of antigens for immunostaining. *Am. J. Pathol.* **1986**, *125*, 431–435.
82. Huber, W.; Carey, V.J.; Gentleman, R.; Anders, S.; Carlson, M.; Carvalho, B.S.; Bravo, H.C.; Davis, S.; Gatto, L.; Girke, T.; et al. Orchestrating high-throughput genomic analysis with Bioconductor. *Nat. Methods* **2015**, *12*, 115–121, doi:10.1038/nmeth.3252.
83. R: The R Project for Statistical Computing. Available online: https://www.r-project.org/ (accessed on 14 June 2020).
84. Lun, A.T.L.; Riesenfeld, S.; Andrews, T.; Dao, T.P.; Gomes, T.; Marioni, J.C. EmptyDrops: Distinguishing cells from empty droplets in droplet-based single-cell RNA sequencing data. *Genome Biol.* **2019**, *20*, 63, doi:10.1186/s13059-019-1662-y.
85. Mcinnes, L.; Healy, J.; Saul, N.; Großberger, L. UMAP: Uniform Manifold Approximation and Projection. *Softw. Rev. Repos. Arch.* **2018**, doi:10.21105/joss.00861.
86. Kiselev, V.Y.; Kirschner, K.; Schaub, M.T.; Andrews, T.; Yiu, A.; Chandra, T.; Natarajan, K.N.; Reik, W.; Barahona, M.; Green, A.R.; et al. SC3: Consensus clustering of single-cell RNA-seq data. *Nat. Methods* **2017**, *14*, 483–486, doi:10.1038/nmeth.4236.
87. Subramanian, A.; Tamayo, P.; Mootha, V.K.; Mukherjee, S.; Ebert, B.L.; Gillette, M.A.; Paulovich, A.; Pomeroy, S.L.; Golub, T.R.; Lander, E.S.; et al. Gene set enrichment analysis: A knowledge-based approach for interpreting genome-wide expression profiles. *Proc. Natl. Acad. Sci. USA* **2005**, *102*, 15545–15550, doi:10.1073/pnas.0506580102.
88. KEGG: Kyoto Encyclopedia of Genes and Genomes. Available online: https://www.kegg.jp/ (accessed on 13 Jun 2020).
89. Lun, A.T.L.; Bach, K.; Marioni, J.C. Pooling across cells to normalize single-cell RNA sequencing data with many zero counts. *Genome Biol.* **2016**, *17*, 75, doi:10.1186/s13059-016-0947-7.
90. Lun, A.T.L.; McCarthy, D.J.; Marioni, J.C. A step-by-step workflow for low-level analysis of single-cell RNA-seq data with Bioconductor. *F1000Research* **2016**, *5*, 2122, doi:10.12688/f1000research.9501.2.
91. Mccarthy, D.J.; Campbell, K.R.; Lun, A.T.L.; Wills, Q.F. Scater: Pre-processing, quality control, normalization and visualization of single-cell RNA-seq data in R. *Bioinformatics* **2017**, *33*, 1179–1186, doi:10.1093/bioinformatics/btw777.
92. Using Scran to Analyze Single-cell RNA-seq Data. Available online: https://bioconductor.org/packages/release/bioc/vignettes/scran/inst/doc/scran.html (accessed on 14 Jun 2020).
93. Butler, A.; Hoffman, P.; Smibert, P.; Papalexi, E.; Satija, R. Integrating single-cell transcriptomic data across different conditions, technologies, and species. *Nat. Biotechnol.* **2018**, *36*, 411–420, doi:10.1038/nbt.4096.
94. Stuart, T.; Butler, A.; Hoffman, P.; Hafemeister, C.; Papalexi, E.; Mauck, W.M.; Hao, Y.; Stoeckius, M.; Smibert, P.; Satija, R. Comprehensive Integration of Single-Cell Data. *Cell* **2019**, *177*, 1888–1902.e21, doi:10.1016/j.cell.2019.05.031.
95. Yu, G.; Wang, L.G.; Han, Y.; He, Q.Y. ClusterProfiler: An R package for comparing biological themes among gene clusters. *Omi. A J. Integr. Biol.* **2012**, *16*, 284–287, doi:10.1089/omi.2011.0118.
96. Haghverdi, L.; Lun, A.T.L.; Morgan, M.D.; Marioni, J.C. Batch effects in single-cell RNA-sequencing data are corrected by matching mutual nearest neighbors. *Nat. Biotechnol.* **2018**, *36*, 421–427, doi:10.1038/nbt.4091.

97. Kuleshov, M.V.; Jones, M.R.; Rouillard, A.D.; Fernandez, N.F.; Duan, Q.; Wang, Z.; Koplev, S.; Jenkins, S.L.; Jagodnik, K.M.; Lachmann, A.; et al. *Enrichr: A Comprehensive Gene Set Enrichment Analysis Web Server 2016 Update*; 2016; Volume 44.
98. Lokau, J.; Kleinegger, F.; Garbers, Y.; Waetzig, G.H.; Grötzinger, J.; Rose-John, S.; Haybaeck, J.; Garbers, C. Tocilizumab does not block interleukin-6 (IL-6) signaling in murine cells. *PLoS ONE* **2020**, *15*, doi:10.1371/journal.pone.0232612.

PUBLIKACE IX

Strnadová K, Pfeiferová L, Přikryl P, Dvořánková B, Vlčák E, Frýdlová J, Vokurka M, Novotný J, Šáchová J, Hradilová M, Brábek J, Šmigová J, Rösel D, Smetana K Jr., Kolář M, Lacina L. Exosomes produced by melanoma cells significantly influence the biological properties of normal and cancer-associated fibroblasts. *Histochem Cell Biol.* 2022;157(2):153–172. **(IF: 4.304)**

Histochemistry and Cell Biology
https://doi.org/10.1007/s00418-021-02052-2

ORIGINAL PAPER

Exosomes produced by melanoma cells significantly influence the biological properties of normal and cancer-associated fibroblasts

Karolína Strnadová[1,2] · Lucie Pfeiferová[3,8] · Petr Přikryl[4] · Barbora Dvořánková[1,2] · Erik Vlčák[5] · Jana Frýdlová[4] · Martin Vokurka[4] · Jiří Novotný[3,8] · Jana Šáchová[3] · Miluše Hradilová[3] · Jan Brábek[6] · Jana Šmigová[6] · Daniel Rösel[6] · Karel Smetana Jr.[1,2] · Michal Kolář[3,8] · Lukáš Lacina[1,2,7]

Accepted: 5 November 2021

Abstract
The incidence of cutaneous malignant melanoma is increasing worldwide. While the treatment of initial stages of the disease is simple, the advanced disease frequently remains fatal despite novel therapeutic options . This requires identification of novel therapeutic targets in melanoma. Similarly to other types of tumours, the cancer microenvironment plays a prominent role and determines the biological properties of melanoma. Importantly, melanoma cell-produced exosomes represent an important tool of intercellular communication within this cancer ecosystem. We have focused on potential differences in the activity of exosomes produced by melanoma cells towards melanoma-associated fibroblasts and normal dermal fibroblasts. Cancer-associated fibroblasts were activated by the melanoma cell-produced exosomes significantly more than their normal counterparts, as assessed by increased transcription of genes for inflammation-supporting cytokines and chemokines, namely IL-6 or IL-8. We have observed that the response is dependent on the duration of the stimulus via exosomes and also on the quantity of exosomes. Our study demonstrates that melanoma-produced exosomes significantly stimulate the tumour-promoting proinflammatory activity of cancer-associated fibroblasts. This may represent a potential new target of oncologic therapy .

Keywords Melanoma · Cancer-associated fibroblasts · Exosomes · IL-6 · IL-8 · Proinflammatory cytokine

Introduction

Cancer incidence has reached a pandemic-like extent in numerous developed countries worldwide. The explanation for this phenomenon is not straightforward: numerous factors ranging from environmental pollution and food

Karolína Strnadová, Lucie Pfeiferová and Petr Přikryl have contributed equally.

✉ Michal Kolář
michal.kolar@img.cas.cz

✉ Lukáš Lacina
lukas.lacina@lf1.cuni.cz

[1] Institute of Anatomy, 1st Faculty of Medicine, Charles University, 128 00 Prague 2, Czech Republic

[2] BIOCEV, 1st Faculty of Medicine, Charles University, 25250 Vestec, Czech Republic

[3] Laboratory of Genomics and Bioinformatics, Institute of Molecular Genetics of the Czech Academy of Sciences, 142 20 Prague 4, Czech Republic

[4] Institute of Pathological Physiology, 1st Faculty of Medicine, Charles University, 128 00 Praha, Czech Republic

[5] Electron Microscopy Core Facility, Institute of Molecular Genetics of the Czech Academy of Sciences, 142 20 Prague 4, Czech Republic

[6] BIOCEV, Faculty of Sciences, Charles University, 25250 Vestec, Czech Republic

[7] Department of Dermatovenereology, 1st Faculty of Medicine, Charles University and General University Hospital, 120 00 Prague 2, Czech Republic

[8] Department of Informatics and Chemistry, Faculty of Chemical Technology, University of Chemistry and Technology, Prague, Czech Republic

Published online: 27 November 2021

contamination, through excessive caloric intake to civilisation-associated stressful lifestyle seem to contribute to this trend. Another critical factor is ageing of the population (Smetana et al. 2016). Cutaneous malignant melanoma (CMM) follows the trend of other cancers. Moreover, climate and lifestyle changes represent another important contribution to the increasing incidence of CMM, as tumour initiation and progression is strongly facilitated by ultraviolet (UV) irradiation (Jobe et al. 2018).

Despite remarkable progress in CMM-targeted therapy and immunotherapy, the metastatic disease represents a therapeutic challenge and leaves patients with an uncertain prognosis (Smetana et al. 2020). From this perspective, identification of new therapeutic targets is critical to manage CMM successfully (Brustugun et al. 2014). Similarly to other types of tumours, CMM is not only composed of cancer cells, but also contains other cell types. The tumour forms a malignant organ that evolves in the patient's body (Alberts et al. 2002; Egeblad et al. 2010). Among non-cancerous cells forming the cancer ecosystem within the tumour niche, one has to emphasise the prominent role of different subtypes of immune cells and also cancer-associated fibroblasts (CAFs) (Lacina et al. 2015; Falcone et al. 2020). These non-malignant cells can substantially influence the biological properties of cancer cells, resulting in their locally aggressive growth and increased migratory potential leading to metastatic spread (Kodet et al. 2020). The cells shaping the landscape of the tumour microenvironment must be precisely coordinated, similarly to cell populations forming a normal organ. Cancer cells and the surrounding stromal elements communicate by their mutual intercellular contacts, in an autocrine and paracrine signalling manner. It necessitates production of bioactive agents that include extracellular matrix molecules, growth factors, cytokines and chemokines, frequently with properties supporting chronic inflammation. A distinct position in the regulation of the cancer ecosystem is held by IL-6 and IL-8 (Jobe et al. 2016; Brábek et al. 2020).

The role of extracellular vesicles, including exosomes, as versatile communication tools mediating intercellular interactions is well accepted (Zebrowska et al. 2020), and they represent a significant component of the tumour microenvironment in cancer biology. The activity of exosomes depends on their cargo. It is formed by bioactive proteins (e.g., PD-L1, IL-6, IL-10, TNF-α, TGF-β1) and a broad range of microRNAs or mRNAs that can control the functional properties of targeted cells (Zebrowska et al. 2020). As expected, these substances were also detected in biological fluids of melanoma patients (Pfeffer et al. 2015; Kučera et al. 2019). All cell populations forming the tumour ecosystem secrete extracellular vesicles, and their activity is broad. Exosomes, via their cargo, can modulate functions of cancer stem cells, cancer-associated fibroblasts, immune cells, and endothelium.

Interestingly, exosomes deliver cargoes that can both be of cancer-supporting and cancer-inhibiting nature (Cavallari et al. 2020). The melanoma-produced exosomes promote proinflammatory signalling important for tumour local progression and metastasis (Gener Lahav et al. 2019; Kodet et al. 2020). Moreover, exosomes can suppress the antitumoural activity of infiltrating CD8 + T lymphocytes (Shu et al. 2020). Further, melanoma-derived exosomes have a distinct role in the transformation of fibroblasts to cancer-associated fibroblasts (la Shu et al. 2018; Hu and Hu 2019). All these findings have highlighted the prominent role of exosomes in the tumour microenvironment. Therefore, exosomes are in the focus of interest of clinical oncology and represent a potential therapeutic target in anticancer research.

We need to understand the contribution of exosomes in the progression of malignant melanoma within the tumour microenvironment and in the course of metastatic spread in the organism. In this study, we aimed to demonstrate in vitro the different effect of melanoma-produced exosomes on the functional properties of normal dermal fibroblasts and cancer-associated fibroblasts isolated from CMM (mCAFs). This knowledge could be critically important for deeper insight into the mechanisms supporting local progression and metastatic spread to remote body sites. It also opens further discussion on whether exosomes in the tissue microenvironment and circulating in body fluids could serve as biomarkers for melanoma diagnosis and disease prognosis.

Material and methods

Cell culture for exosome isolation

Authenticated melanoma cell line G361 (CRL-1424, ATCC, Manassas, VA, USA) was chosen as an efficient exosome producer. The cells were routinely maintained in McCoy's 5A medium (BioConcept, Allschwil, Switzerland) with antibiotics (100 × concentrated penicillin and streptomycin) and with 10% of foetal bovine serum (FBS, both Biosera, Nuaille, France). Six million G361 cells were inoculated to each of eight 150-cm^2 flasks (Corning, Glendale, AZ, USA) in McCoy's 5A medium with 10% FBS for 24 h. For exosome harvesting, we replaced the medium using 35 ml of Dulbecco's modified Eagles medium (DMEM, Biosera, Nuaille, France) with 5% exosome-depleted foetal bovine serum (EDS, A27208-01, Thermo Fisher Scientific, Waltham, MA, USA). We kept the flasks for the next 72 h in a humidified incubator (37 °C, 5% CO_2). From eight 150-cm^2 flasks, we collected a total of 280 ml of conditioned growth medium for exosome isolation.

Other tested melanoma cell lines, A2058 (CRL-11147, ATCC, Manassas, VA, USA) and BLM (a generous gift provided by Prof. JHJM van Krieken, Radboud University, Nijmegen, Netherlands) (Quax et al. 1991) were maintained in DMEM supplemented by 10% FBS and used as above. All experiments were performed in three independent replicates.

To test the non-specific effect of extracellular vesicles (unrelated to melanoma) as an additional control for some of our experiments, we also isolated exosomes from FBS used for cell culture.

Exosome isolation and characterisation

Exosome isolation by density gradient ultracentrifugation

Exosomes were isolated by cushioned-density gradient ultracentrifugation as previously described by Li et al. with partial modifications (Li et al. 2018). This protocol maximises exosome recovery and allows for better preservation of their physical integrity and biological activity. Briefly, the conditioned medium was centrifuged at 300×*g* for 10 min at 4 °C to pellet cells and debris. The supernatant was then centrifuged at 2000×*g* for 15 min at 4 °C, transferred to new tubes, centrifuged for 30 min at 10,000×*g* at 4 °C and filtered through a 0.22 µm Steriflip-GP sterile filter (Merck Millipore, Burlington, MA, USA). Then, six aliquots of 28 ml of this cleared conditioned media (CM) were underlain with 2 ml of 60% OptiPrep density gradient medium (Alere Technologies AS, Oslo, Norway) and concentrated in ultracentrifuge tubes using cushioned ultracentrifugation at 140,000×*g* for 3 h with an SW 28 Ti swinging-bucket rotor in an Optima XPN 80 ultracentrifuge (Beckman-Coulter, Brea, CA, USA). Two ml of Optiprep and 1 ml of supernatant above the cushion were aspirated from the bottom by a blunt-point needle to obtain 3 ml of cushioned concentrate per tube. Concentrates were placed to the bottom of the tubes below a discontinuous gradient composed of the top 3 ml of 5%, then 3 ml of 10%, and 3 ml of 20% Optiprep solution. The ultracentrifuge tubes with the gradient were then spun at 140,000×*g* for 18 h at 4 °C using an SW 28.1 Ti swinging-bucket rotor. After centrifugation, the tube content was divided into 12 1 ml fractions and collected starting from the top of the tube. Individual fractions nos. 6, 7 and 8, containing purified exosomes, from the six tubes were pooled together, diluted with filtered phosphate-buffered saline (PBS) and re-centrifuged again at 140,000×*g* for 2 h at 4 °C. Finally, these washed and concentrated fractions were resuspended in 50 µl of PBS, combined, filled to a volume of 200 µl in a protein LoBind tube (Eppendorf, Hamburg, Germany) and stored at 4 °C or −80 °C. Buoyant densities of the gradient fractions were estimated by measuring the absorbance at 340 nm using a multi-well plate reader. Contamination of fractions with non-exosomal proteins was monitored using the Qubit Protein Assay Kit and a Qubit 2.0 fluorometer (Thermo Fisher Scientific, Waltham, MA, USA) (Li et al. 2018). Exosomes present in fractions 6–8 were confirmed by western blot, transmission electron microscopy and nanoparticle tracking analysis.

Detection of exosome protein concentration

For the purposes of experiment normalisation, the quantity of exosomes was determined as the total protein concentration using a Pierce BCA Protein Assay Kit (23,225 Thermo Fisher Scientific, Waltham, MA, USA). Briefly, exosomes were disrupted using 25% Triton X-100 in PBS (25 µl exosome suspension and 1 µl Triton) by agitation on a shaker (300 RPM) at room temperature for 15 min. Then, the sample was processed following the manufacturer's instructions. Absorbance was measured at 562 nm using a SpectraMax iD3 (Molecular Devices, San Jose, CA, USA), and the concentration of total protein was extrapolated from the calibration curve. For cell culture applications, we used exosomes in a quantity corresponding to 10 µg/ml of total protein diluted in culture medium (unless otherwise specified).

Exosome characterisation by SDS-PAGE and western blot analysis

Exosomal fractions were supplemented with a protease inhibitor cocktail and lysed for at least 15 min in RIPA buffer. We followed by adding 4 × Laemmli sample buffer (Bio-Rad, Hercules, CA, USA) and boiling at 95 °C for 5 min. Proteins (2 µg per well) were loaded to 12% SDS polyacrylamide gel and electrophoresed at 125 V for 70 min. Separated proteins were transferred from gels onto 0.45 µm PVDF membranes at 20 V for 60 min. The membranes were blocked in 5% skim milk in TBS containing 0.1% Tween 20 for 1 h and probed overnight at 4 °C in blocking solution containing primary antibodies against classical exosome markers CD9, CD63 and CD81 (all Thermo Fisher Scientific, Waltham, MA, USA—see Supplementary Table 1). Then, the membranes were washed five times for 5 min in TBS-Tween buffer and incubated at room temperature for 1 h with HRP-conjugated secondary antibody. Probed membranes were then washed five times in TBS-Tween buffer. Chemiluminescent detection using LumiGLO Reagent (Cell Signaling Technology) was performed in the ChemiDoc MP Imaging System (Bio-Rad, Hercules, CA, USA).

Exosome characterisation by nanoparticle tracking analysis (NTA)

The size and concentration of extracellular vesicles were analysed by NTA using the NanoSight NS300 instrument (Malvern Panalytical, Malvern, Great Britain). To achieve

a concentration range of $10^8 - 10^9$ particles per ml, isolated exosome fractions were diluted in PBS filtered through a 0.1 µm Stericup filter. Each sample was analysed with a optimised auto-setup camera level and a detection threshold value of 5. Five replicate video recordings of 180-s duration per fraction were collected. Statistical analysis and graph plotting of resulted data was performed with NanoSight NTA software version 3.2.

Electron microscopy of exosomes

Ultrathin sections of collagen-embedded exosomes and their electron microscopic analysis

Melanoma-derived exosomes were mixed with neutralised rat tail collagen-1 (2 mg/ml; Advanced BioMatrix, San Diego, CA, USA) to reach the final exosome protein concentration of 10 µg/ml and cast into a cap of a 0.5 ml Eppendorf tube. The polymerised collagen block with embedded exosomes was removed and fixed using 2.5% glutaraldehyde in 0.1 M Sörensen's sodium–potassium phosphate buffer (SB) with adjusted pH 7.2–7.4 (all Thermo Fisher Scientific, Waltham, MA, USA). After several gentle washes in SB, samples were postfixed with 1% osmium tetroxide in SB for 2 h at room temperature. Samples were then dehydrated in a series of acetone (Lach-Ner, Neratovice, Czech Republic) with increasing concentration and embedded in Epon-Durcupan resin (Sigma-Aldrich, St. Louis, MO, USA). After polymerisation for 72 h at 60 °C, resin blocks with embedded samples were cut into 80 nm ultrathin sections using a Ultramicrotome Leica EM UC6 (Leica Microsystems, Wetzlar, Germany) with a diamond knife (Diatome, Biel, Switzerland) and mounted on 200 mesh size copper grids. Sections were examined in a JEOL JEM-1400Flash transmission electron microscope operated at 80 kV equipped with a Matataki Flash sCMOS camera (JEOL, Akishima, Tokyo, Japan).

Negative staining of isolated exosomes

Undiluted suspensions were applied to glow-discharged 400 mesh size copper grids with thin formvar/carbon film and allowed to absorb for 20 min. Excess was blotted away with filter paper, and the absorbed sample was fixed in a drop of 1% formaldehyde (all Thermo Fisher Scientific, Waltham, MA, USA) for 20 min. Grids were then quickly washed in double-distilled water and negatively stained with 2% methylcellulose (Sigma-Aldrich, St. Louis, MO, USA) and 0.4% uranyl acetate (Honeywell, Charlotte, NC, USA) for 10 min. Excess solution was blotted away, and grids were air-dried. Samples were examined in a JEOL JEM-1400Flash transmission electron microscope operated at 80 kV equipped with a Matataki Flash sCMOS camera (JEOL, Akishima, Tokyo, Japan).

Establishment of fibroblast cell lines

Fibroblasts were isolated as published elsewhere (Dvořánková et al. 2019). For this purpose, we used two different fibroblast types, mCAFs and human dermal fibroblasts (HDFs); two biological replicates of each type were used in all experiments. Briefly, these fibroblasts were isolated earlier from the residual tissue from the operation, and both samples were of the dermal origin from the trunk region. Tissues were collected after local ethics committee approval following the ethical standards of the Institutional and National Research Committee and according to the 1964 Helsinki Declaration and its later amendments or comparable ethical standards. The patient's informed consent was obtained.

Transcriptome analysis

Transcriptome analysis after 24 h of cultivation

Cell suspensions were inoculated in DMEM + 10% foetal bovine serum and cultured for 24 h. The next day, the medium was replaced by DMEM + 10% EDS without/with G361-derived exosomes. The cells were cultured for an additional 24 h. Cells were washed in PBS and digested in 0.25% trypsin + EDTA solution (1:1) (all Sigma-Aldrich, St. Louis, MO, USA) at room temperature. The viability of cells was assessed by trypan blue and counted in an automated TC20 cell counter (Bio-Rad, Hercules, CA, USA). Both samples had cell viability above 99%.

Single-cell RNA-seq libraries were prepared using a Chromium controller instrument and Chromium Next Gem single-cell 3' reagent kit (version 3.1) according to the manufacturer's protocol (both 10 × Genomics, Pleasanton, CA, USA) targeting at 4000 cells per sample. The quality and quantity of the resulting cDNA and libraries were determined using an Agilent 2100 Bioanalyzer (Agilent Technologies, Santa Clara, CA, USA). The libraries were sequenced in two runs of a NextSeq 500 sequencer using a NextSeq 500/550 high output kit v2.5 (75 cycles) (both Illumina, San Diego, CA, USA) according to the manufacturer's protocol.

Raw sequencing data were processed by CellRanger software v. 4.0.0 (10 × Genomics, Pleasanton, CA, USA). The resulting raw feature barcode matrices were analysed in the R/Bioconductor statistical environment (R Core Team 2020). Empty droplets containing only ambient RNA were removed using DropletUtils (Lun et al. 2018). Subsequently, dead or damaged cells were filtered out, and features expressed in less than 5% of cells were removed from the barcode matrix, resulting in 4207, 3955, 2390 and 3098 cells

in the HDFs control, HDF EXO G361, mCAFs control and mCAFs EXO G361 sample, respectively, and, in the same sample order, 11,832, 11,796, 11,860 and 11,918 features. The data were normalised, log2-transformed, and features within each sample were averaged to produce pseudo-bulk expression values. Heatmaps were produced by the ComplexHeatmap package (Gu et al. 2016).

All transcriptomic data were deposited in the ArrayExpress database (http://www.ebi.ac.uk/arrayexpress) under accessions E-MTAB-10278 and E-MTAB-10290.

Transcriptome analysis after 72 h of cultivation

Both fibroblast types (mCAFs and HDFs) were inoculated in DMEM with 10% FBS at the density of 3500 cells/cm^2 in 6-well plates. After 24 h, culture medium was changed for: (a) DMEM with 10% exosome-depleted serum (EDS, Gibco/ Thermo Fisher Scientific, Waltham, MA, USA) (control); (b) DMEM with 10% EDS + G361-derived exosomes; and (c) DMEM with 10% EDS + exosomes from FBS (also 10 µg/ml), and the cells were cultured for 72 h. Then, the cells were washed twice with PBS, and the cell lysates were harvested by 350 µl buffer RLT (Qiagen GmbH, Hilden, Germany) and 2-mercaptoethanol (Sigma-Aldrich, St. Louis, MO, USA; Merck KGaA, Darmstadt, Germany), immediately frozen and stored at −80 °C. Total RNA was isolated from 180 µl of the cell lysate according to the RNeasy Micro Kit (Qiagen GmbH, Hilden, Germany) manufacturer's protocol, including treatment by DNase I. The quantity and quality of isolated RNA were measured by a NanoDrop ND-1000 (Thermo Fisher Scientific, Waltham, MA, USA) and Agilent 2100 Bioanalyzer (Agilent Technologies, Santa Clara, CA, USA). The RNA integrity number (RIN) ranged between 8.6 and 10. For the sequencing library construction, a KAPA mRNA HyperPrep kit with poly(A) mRNA selection (Roche, Basel, Switzerland) was used, starting with 1 µg of total RNA. Libraries were sequenced on a NextSeq 500 platform (Illumina, San Diego, CA, USA) using the 75-bp single-end configuration. The sequencing yielded an average of 30 million reads per sample.

Technical quality control and gene quantification were done using the nf-core/rnaseq v2.0 bioinformatics pipeline (Ewels et al. 2020), with HISAT2 mapping (Kim et al. 2015) and featureCounts read counting (Liao et al. 2014). GRCh38 (Ensembl assembly version 95) was chosen as the reference genome (Yates et al. 2020). Genes expressed in a single sample only were discarded. The DESeq2 (v1.30.1) (Love et al. 2014) Bioconductor (v3.12) R package was used to identify differentially expressed genes. Significant changes in gene expression were defined by two-fold change and false discovery rate (FDR) < 0.1. Shrunken log-fold change estimates were used (adaptive shrinkage estimator; Stephens 2017). The gene set enrichment analysis was performed in Gene Ontology terms (Ashburner et al. 2000) using the goseq package (Young et al. 2010). The mevalonate pathway was visualised using PathView software (Luo and Brouwer 2013).

Proteomic analysis of cultured medium and ELISA

For proteomic analysis, mCAFs and HDFs (3 500 cells/cm^2) were cultured in (a) DMEM with 10% EDS (control) or (b) DMEM with 10% EDS + G361-derived exosomes. After 72 h, we collected the conditioned culture media for proteomic analysis using a Proteome Profiler Human XL Cytokine Array (R&D Systems, Minneapolis, MN, USA). Briefly, we used the membrane-based antibody array for parallel determination of the relative levels of selected human cytokines and chemokines according to the manufacturer's instructions. Freshly prepared conditioned media were centrifuged to remove the debris and incubated overnight with the Proteome Profiler™ Human XL Cytokine Array membrane. The membranes were washed to remove unbound analytes, followed by incubation with a cocktail of biotinylated detection antibodies. Streptavidin-HRP and chemiluminescent detection reagents provided by the manufacturer were then applied. Finally, the signal produced at each capture spot corresponding to the amount of protein bound was detected using a C-DiGit Blot Scanner and analysed using the Image Studio software (LI-COR Biosciences GmbH, Bad Homburg, Germany).

Quantification of IL-6 and CXCL-8 was performed according to protocol using the AssayMax™ Human IL-6 ELISA Kit and AssayMax™ Human Interleukin 8 (IL-8) ELISA Kit (both BioVendor, Brno, Czech Republic).

Cell culture of mCAFs and HDFs influenced by G361-derived exosomes

Evaluation of the effect of exosomes on cell proliferation and MTT assay

Using the iCELLigence instrument (Agilent Technologies, Santa Clara, CA, USA), we studied the growth of fibroblasts influenced by exosomes. Briefly, we seeded 5000 fibroblasts in DMEM with 10% EDS to each well (0.7 cm^2) in a plate compatible with iCELLigence (two biological replicates of each, three technical experiments per run). Then, we added the suspension of exosomes. To determine efficient exosome concentration, we used a scale of concentrations (data obtained with 3 µg/ml and 10 µg/ml are presented). We used Dulbecco's PBS (BioConcept, Allschwil, Switzerland) for control experiments. The final volume of the culture medium was equalised to 450 µl in each well. We monitored the cell proliferation for the next 96 h. Finally, we evaluated the viability of cells by MTT in the wells (Mosmann 1983).

Evaluation of the effect of exosomes on HDF and mCAF adhesion and migration (velocity) in 2D and 3D

Cell adhesion area measurement was performed by monitoring electrical impedance (cell index value) in real time using the xCELLigence RTCA System (Agilent Technologies, Santa Clara, CA, USA). Cells were incubated in DMEM with 10% EDS + G361-derived exosomes on a rotator for 4 h at 37 °C and then seeded into a pre-treated xCELLigence plate (Hamidi et al. 2017). Cell adhesion was monitored every 2 min for the first 30 min and every 5 min for the next 90 min. Further, measurement was performed every 15 min for the next 11 h.

Cell migration was studied using time-lapse microscopy of cells seeded in glass-bottom Ibidi 8-well plates (Ibidi GmbH, Gräfelfing, Germany) coated with fibronectin. Cells were incubated with G361-derived exosomes for 8 h and afterwards recorded at 15-min intervals for 13 h. The images were captured as tile scans using a Leica Thunder system (Leica Microsystems, Wetzlar, Germany) equipped with an LAS-X Navigator software module. Data analysis was done using ImageJ/Fiji in three consecutive sets of steps (data not shown). First, the collected series of images were stitched using the Stitching plug-in of ImageJ/Fiji. Second, the stitched imaged were processed for cell visualisation using the Edge Finder Tool, background suppression and binary masking. Third, cell tracking was performed at 16 time points with ~ 55 cells using the TrackMate plug-in of ImageJ/Fiji. All experiments were performed in parallel with a control (DMEM with 10% EDS) and exosome-treated (DMEM with 10% EDS and exosomes) mCAFs and HDFs. The step-by-step summary of this protocol is presented in Supplementary Fig. 5 with minimal and maximal velocity assessment.

The mobility of HDFs and mCAFs treated with exosomes was also evaluated using a 3D spheroid assay. 3D fibroblast spheroids were formed of ~ 700 cells an in agarose mould for 72 h. The spheroids were embedded into rat tail collagen (1 mg/ml) and covered with DMEM + 10% EDS with or without G361-derived exosomes. The images were captured at time 0, 24 and 48 h using a Leica Thunder system. The spheroid area was outlined using the Threshold or Edge Finder tool of ImageJ/Fiji. The invasion index was calculated as a normalised ratio of the spheroid area of interest to the starting spheroid area. The normalisation was done to the average spheroid area of control cells measured at time 0 h.

Statistical significance was evaluated using GraphPad Prism software (version 8.0.0 for Windows, GraphPad Software, San Diego, CA, USA, www.graphpad.com) by a two-tailed Student's t test after ascertaining normality of the data (p value ≤ 0.05).

Evaluation of the effect of G361-derived exosomes on 3D melanoma spheroid invasion

Heterogeneous spheroids were prepared from melanoma cell line G361 with HDFs or mCAFs using the hanging drop method (Novotný et al. 2020). Briefly, mixed-cell spheroids were formed of 50,000 cells in a 1:1 ratio. Drops of mixed-cell suspension (each 25 µl) were placed on the inner side of a 100 mm Petri dish lid for 48 h, while the bottom of the dish was filled with 15 ml of PBS (Biosera, Nuaille, France). Afterwards, spheroids were gently transferred by a Pasteur pipette to non-adhesive Petri dishes with complete culture medium for an additional 24 h. To test the invasion, heterogeneous spheroids were transferred onto 1% low-melting-point agarose-coated dishes (Promega, Madison, WI, USA) and covered with neutralised collagen-1 from rat tails (2 mg/ml; Advanced BioMatrix, CA, USA) with or without G361-derived exosomes. For optimal stability during the extended experiment, the polymerised collagen was overlaid with 1% low-melting-point agarose. Finally, it was gently overlaid with DMEM + 10% EDS. The culture medium was changed every 48 h for 1 week. The endpoint images were captured after 144 h using an Olympus IX71 (Olympus, Shinjuku, Japan). The spheroid area was outlined using the Threshold and Edge Finder plug-in of ImageJ/Fiji. The invasion index was calculated as a normalised ratio of the spheroid of interest to the final outgrowth area to the initial spheroid area. Statistical significance was tested as above.

Immunocytochemistry

Fibroblasts were seeded in the µ-Slide 8 Well system (Ibidi GmbH, Gräfelfing, Germany) at a density of 10,000/cm^2 in DMEM + 10% EDS with or without G361-derived exosomes. Cells were fixed in 2% paraformaldehyde and permeabilised by TBS with 0.2% Tween. Endogenous peroxidase was blocked by incubation with 3% hydrogen peroxide in TBS at room temperature for 20 min. To block non-specific protein binding and primary antibody dilution, we used Universal IHC Blocking/Diluent (Leica, Wetzlar, Germany). After overnight incubation at 4 °C, the slides were washed, and the immunohistochemical reaction was developed using Histofine High Stain™ HRP (MULTI) and AEC substrate (both Nichirei Biosciences Inc, Tokyo, Japan). Slides were counterstained in Gill's haematoxylin and mounted in Hydromount. Negative controls were performed using isotype control antibodies (Thermo Fisher Scientific, Waltham, MA, USA). The imaging was performed using the Leica DM2000 system (Leica Microsystems, Wetzlar, Germany) equipped with the LAS software. Primary antibodies were validated by producers and provided proof of validation on the technical specifications. All antibodies are listed in Supplementary Table 1.

Results

Characterisation of melanoma-derived exosomes

Using cushioned-density gradient ultracentrifugation, we achieved high-quality exosome purification (Fig. 1). This procedure resulted in elimination of non-exosomal vesicles and also protein contaminants (Supplementary Figure 1), meaning around 90% of total proteins (Li et al. 2018). The exosome production was studied in three malignant melanoma cell lines: A2058, BLM and G361. Surprisingly, only the G361 melanoma line cells produced exosomes in amounts sufficient for further analysis and subsequent experiments (Fig. 1a). Therefore, G361-derived exosomes were characterised and complied with the size distribution and morphological criteria typical of exosomes by NTA and electron microscopy (Fig. 1b). Exosomes were dominantly present in density gradient fractions nos. 6–8 (Supplementary Figure 1a) having an expected exosome density of 1.08–1.13 g/cm^3 (Brennan et al. 2020). All exosomes from studied cell lines exhibited surface protein markers CD9, CD63 and CD81 (Supplementary Figure 1b). Based on these observations, we confirmed that vesicles produced by G361 meet the criteria for being recognised as exosomes, and thus, we employed them for further experiments with HDFs and mCAFs. The quantity of exosomes produced by G361 is also followed proportionally by increased total protein concentration (Supplementary Figure 1c). We have not detected any significant residual contamination in commercially exosome-depleted serum (Supplementary Fig. 1a, lane 1). Therefore, we conclude that the observed effects can be attributed to G361-produced exosomes in our models.

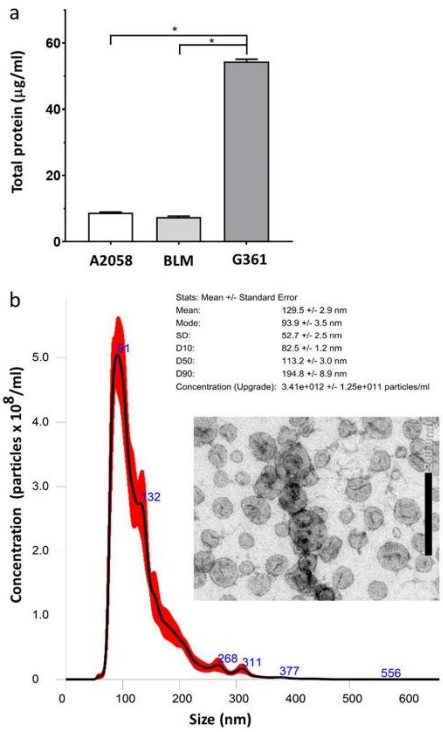

Fig. 1 Characterisation of exosomes according to total protein detection, size and electron microscopy. **a** The graph shows that only G361 cells produced a sufficient quantity of exosomes; data represent quantification of three independent isolation experiments with A2058, BLM and G361 melanoma cell lines, respectively; error bars represent standard deviations of observed values; statistical significance calculated by non-parametric Tukey's honest significance test (p value ≤ 0.05 was regarded as statistically significant). **b** Exosomes produced by G361 cells were homogenous concerning their size and morphology. Inset represents electron microscopic image presenting purified extracellular vesicles of usual exosomal size and morphology

Effect of G361-derived exosomes on HDF and mCAF adhesion, proliferation and velocity in 2D and 3D

The RTCA iCELLigence™ instrument uses non-invasive electrical impedance monitoring to quantify attachment quality in a label-free, real-time manner. As fibroblast seeding density was identical, the measured values reflect the physical interaction of adherent cells with the surface of the electrode, primarily via surface receptors.

Generally, the adhesive properties of mCAFs were lower than those of HDFs. In both fibroblast types, the addition of exosomes flattened the adhesion curves, suggesting decreased cell adhesion and spreading. This effect was more prominent in HDFs than in mCAFs, and the difference was statistically significant at the endpoint (Fig. 2). Moreover, the exosome-treated cells did not reach the maximum cell indices of control cells before reaching the curve plateau stage. This suggested that the lower adhesion of exosome-treated cells is not only a temporary post-seeding issue, but is persistent and cannot be rescued by subsequent exchange of media without exosomes (data not shown).

Once the cells are adjusted to their new environment, their proliferation can start again. The proliferation activity of fibroblasts is usually low within the initial 24 h after subculture. Starting day 2, changes of electrical impedance can reflect the increasing number of cells in culture wells. Similarly to the above-mentioned, the extent of proliferation of fibroblasts treated by exosomes was lower than that in the non-treated controls. This phenomenon was dependent on the concentration of applied exosomes (Fig. 3). Based

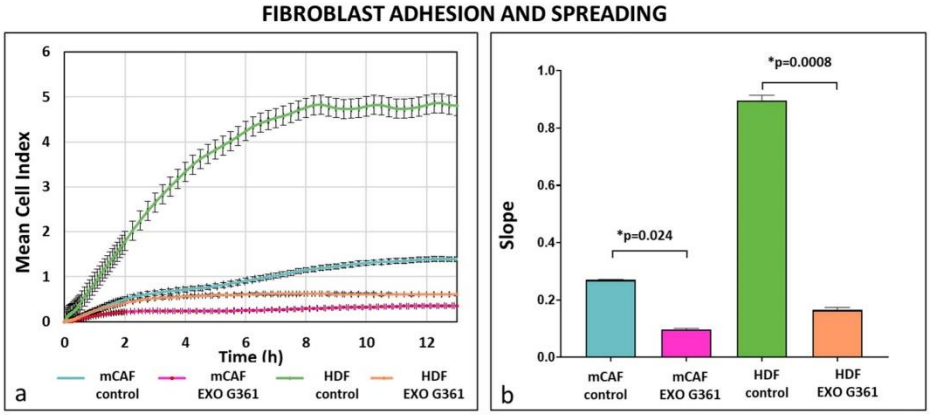

Fig. 2 Exosomes decrease cell adhesion and spreading. **a** The graph shows cell adhesion as a mean cell index. Time point 0 represents the point of cell addition onto the xCELLigence plate. Before that, the cells were treated for 4 h with melanoma exosomes or with the medium without exosomes. **b** The rate of cell growth was determined by calculating the slope of the line between two given time points using xCelligence software. *p* values indicate statistical significance calculated by a two-tailed Student's *t* test

on that, we decided to use a concentration of 10 µg/ml of exosomes as a reference in our experiments.

Evaluation of the effect of exosomes on the velocity of the migration of both types of fibroblasts demonstrated no significant effect on mCAFs. However, we observed a significant increase in the velocity of HDFs (Fig. 4). This observation in 2D can be somewhat extended by results observed in 3D. In the collagen gel, application of G361-derived exosomes significantly increased the normalised invasion index of both types of fibroblasts, i.e., mCAFs and HDFs, in the 3D collagen gel (Fig. 5).

Effect of exosomes on the invasion from composite melanoma spheroids in 3D collagen gels

For a long-term experiment maintained for 1 week, we mixed G361 melanoma cells with HDFs and mCAFs, respectively, to form heterogeneous spheroids as a more reliable 3D model of melanoma (Fig. 6a). These spheroids invaded collagen (Fig. 6b) and remained viable for 1 week (MTT test-based images not presented). To mimic the exosome-enriched microenvironment, the spheroids were embedded into collagen gels containing G361-derived exosomes (Fig. 6c). Indeed, the collagen gel casting procedure did not adversely impact the exosomes (Fig. 6c, arrow). Both cell types, i.e., melanoma cells as well as fibroblasts, migrated readily from composite spheroids (highlighted in green) to the collagen gel. These two invading cell types could be easily distinguished based on their cytological characteristics (Fig. 7a). Fibroblasts formed sparse outgrowths of predominantly individual cells (similar as presented in Fig. 5). Melanoma cells migrated mostly in densely packed outgrowths (highlighted in orange). G361-derived exosomes lowered invasion of melanoma cells from HDF-containing spheroids. Reversely, exosomes facilitated melanoma cell migration in the case of mCAF-containing spheroids. However intriguing, these differences were not statistically significant. Of note, we also observed a statistically significant difference between the extent of invasion from mCAF- and HDF-containing spheroids, respectively.

Influence of exosomes on the HDF and mCAF transcriptome

In our previous work (Novotný et al. 2020), we observed three distinct subpopulations in otherwise homogeneous cultures of fibroblasts (HDFs and mCAFs) exposed to melanoma cells in a 3D model. Therefore, we have decided to use single-cell RNA sequencing to study potentially diverse effects of exosomes on different fibroblast subpopulations of HDFs and mCAFs. Surprisingly, the effect of G361 exosomes on the transcriptome of HDFs and mCAFs was not rapid, and we observed only modest changes at 24 h after stimulation by exosomes (Fig. 7a). However, 72 h after exosome application, notable changes in gene expression were observed in fibroblasts (Fig. 8b). The results were also compared with application of exosomes

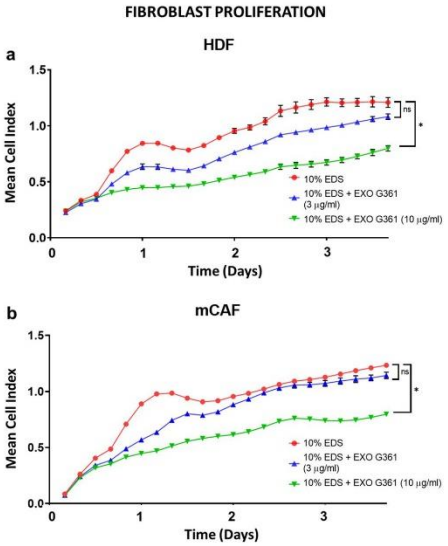

Fig. 3 Exosomes decrease fibroblast proliferation. **a** The graph shows cell proliferation (90 h) of HDF as a mean cell index. **b** The graph shows mCAF proliferation (90 h) as a mean cell index. Time point 0 represents the point of cell addition onto the iCELLigence plate with exosomes (3 µg/ml blue, 10 µg/ml green) or without exosomes in DMEM + 10% EDS (red). Statistical significance (at the endpoint) was tested by Dunn's post hoc multiple comparison test with Bonferroni correction (significant comparison with p value < 0.05 indicated by asterisk)

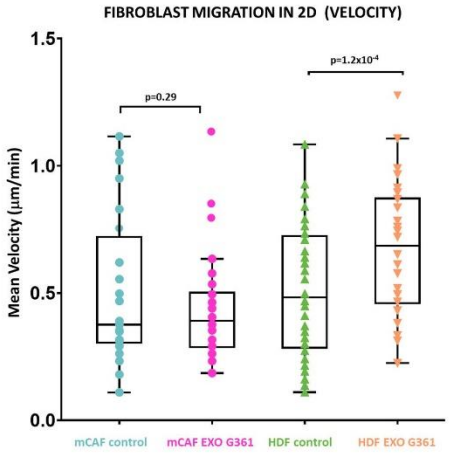

Fig. 4 Exosomes increase the speed of cell migration in 2D. The box plot graph shows the cell speed differences between untreated and exosome-treated cells. p values indicate statistical significance calculated by a two-tailed Student's t test

isolated from the normal foetal bovine serum, which resulted in a weaker effect in both HDFs and mCAFs (Supplementary Figure 2).

In transcriptomic analysis, we have primarily focused on three important aspects potentially related to our above-mentioned findings. We have summarised in Supplementary Table 2 differentially regulated genes in KEGG pathways for (a) focal adhesion, (b) cell migration and (c) cell proliferation. We have highlighted genes which were significantly deregulated in both HDF and mCAF fibroblasts.

Exosomes influenced organisation of extracellular matrix in both types of fibroblasts. We have observed discordant deregulation of tenascin C (*TNC*) where mCAF increased expression after exosome stimulation. Similar effect was observed for integrin alpha-8 (*ITGA8*). We have also observed a significant increase of podoplanin (*PDPN*) in mCAFs.

In contrast to HDFs, exosomes significantly influenced the inflammatory response and cytokine-mediated signalling pathways and cholesterol synthesis in mCAFs (Fig. 8a, b). Exosomes also significantly stimulated mevalonate pathways in CAFs (Supplementary Figure 3).

Previously, we have demonstrated (Novotný et al. 2020) that cancer-associated fibroblasts differ from normal cells by excessive expression of IL-6, CXCL-8 and their receptors. Upon this ground, we focused our interest on these proteins in the experiment of 24-h exosome exposure to HDFs and mCAFs. Employing immunocytochemistry, we detected no presence of IL-6 in all cultured fibroblasts before and after G361 exosome treatment (Fig. 9a–d). A low but specific signal of IL-6R was present in cultured cells except for non-treated HDFs (Fig. 9e–h). Only insignificant differences were observed in the IL-6R gene on a mRNA level (not shown). CXCL-8 was not detected (Fig. 9i–l). Both receptors CXCR1 and CXCR2 (Fig. 9m–t) were low to negative in all cultured fibroblasts. This is in good agreement with the absence of IL-6, CXCL-8, CXCR1 and CXCR2 at the mRNA level before and after G361 exosome treatment.

Our further interest was focused on detailed analysis of the influence of both types of exosomes, i.e., from foetal bovine serum and G361 melanoma cells, on both HDFs and mCAFs after 72 h of treatment. We present here representatives of interleukins (Fig. 10a), matrix metalloproteinases (Fig. 10b), chemokines (Fig. 10c) and extracellular matrix molecules (Fig. 10d). Interestingly, the effect of exosomes on the activity of some genes such as *IL1A, IL6, MMP3*, *CCL5*, *CXCL8* or *TNC* is different in HDFs and mCAFs. On the other hand, it is similar in the case of *MMP11* and

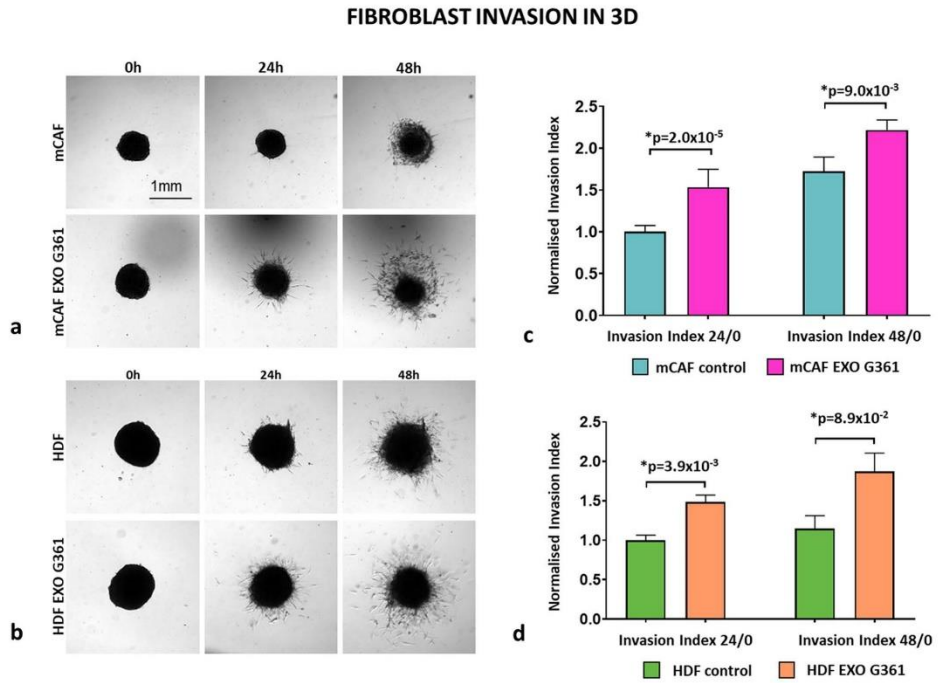

Fig. 5 Exosomes enhance cell invasion in 3D. **a** 3D fibroblast spheroids formed of mCAF cells were treated with or without exosomes and imaged at time points 0, 24 and 48 h. The bar indicates 1 mm. **b** 3D fibroblast spheroids formed of HDF cells were treated with or without exosomes and imaged at time points 0, 24 and 48 h. **c** Bar graphs show the mean invasion index of mCAF cells at time points 24 and 48 h. **d** Bar graphs show the mean invasion index of HDF cells at time points 24 and 48 h. The *p* values in (**c**) and (**d**) indicate statistical significance calculated by two-tailed Student's *t* test

COL1A1. To support the validity of these mRNA profiles, we have tested protein levels of IL-6 and CXCL8 released in fibroblasts -conditioned media by ELISA (Fig. 9u–v). We observed initially high IL-6 in mCAFs-conditioned media and further increase upon exosome stimulation. The IL-6 level in HDF control was initially lower, and differences induced by exosomes were subtle. In mCAFs, CXCL8 followed a similar trend. Of note, we also detected the effect of exosomes isolated from FBS, but these were not so potent as in the case of G361-derived exosomes (Fig. 10a–d).

Using the Proteome Profiler XL kit, we analysed supernatants prepared from fibroblast cell cultures with or without G361-derived exosomes for secretion of 105 cytokines. Selected data are presented in a bar graph (Fig. 11a). The IL1RL1 protein was present only in the non-treated HDFs and G361 exosome-treated mCAFs. On the other hand, thrombospondin-1 was present in the G361 exosome-treated HDFs and non-treated mCAFs. Dickkopf-1 was observed in both types of fibroblasts, and it was downregulated by exosomes in HDFs and upregulated by application of exosomes in mCAFs. The same and pronounced trend was also observed in the expression of angiogenin. Application of exosomes strongly increased the presence of IL-6 and CXCL-8, especially in mCAFs (Fig. 11a). The expression of both IL1R1 and thrombospondin-1 was also compared at the mRNA level. We observed a very similar trend in the activity of the *THSD1* gene for both types of fibroblasts, corresponding well to proteomic results. There was a partial similarity in the case of *1L1RL1* gene in HDFs (Fig. 11b).

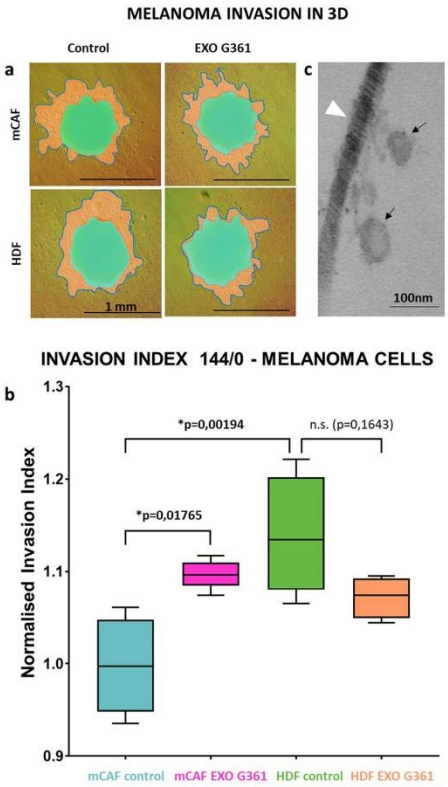

Fig. 6 Exosomes enhance melanoma cell invasion in 3D. **a** 3D mixed spheroids formed of G-361 melanoma cells with fibroblasts (mCAFs and HDFs, respectively) were embedded in 3D collagen gel with or without exosomes and imaged at time points 0 h (green mask) and 144 h (orange mask with outline). **b** Box and whisker graphs show the mean invasion of G-361 cells at time point 144 h. **c** Electron microscopy of collagen gel with embedded exosomes (black arrow) and collagen fibril (white arrowhead). The bar in (**a**) indicates 1 mm and in (**c**) 100 nm. The *p* values in (**b**) indicate statistical significance calculated by non-parametric Tukey's honest significance test (p value ≤ 0.05 was regarded as statistically significant)

Discussion

We isolated extracellular vesicles produced by melanoma cells, which meet the criteria of exosomes (Théry et al. 2006; Xu et al. 2015). It was observed earlier that melanoma cell lines produce exosomes (Lazar et al. 2015); however, their cargo and function may vary significantly. In our experiments, only one melanoma cell line, G361, produced exosomes in sufficient quantity, despite its lower migratory and invasive capability in comparison to cell line A2058 (Kim et al. 2017).

Of note, G361 was established from a primary malignant melanoma of a 31-year-old male Caucasian (Peebles et al. 1978). G-361 thus represents a model potentially more sensitive to microenvironmental cues (Preisner et al. 2018) than other commonly used melanoma cell lines, which frequently originate from metastatic lesions. It was hypothesised (Hsu et al. 2000) that loss of microenvironmental dominance over early melanoma cells correlates with downregulation of adhesive molecules and results consequently in increased invasiveness of the tumour. In contrast, cells from metastatic lesions are highly invasive and already less sensitive to the influence of the microenvironment. Exosomes can represent such microenvironmental stimuli.

Exosomes secreted by malignant cells are an integral part of the tumour microenvironment. They can interact with collagen fibres, the most abundant ECM molecules in the dermis, and likely with numerous other ECM molecules. It was hypothesised earlier by others (Vlodavsky et al. 1990) that ECM provides a storage depot for biologically active agents that are stabilised, protected and gradually released. The exosome cargo can provide a persistent mode of action compared to the same molecules in a fluid phase. It can lead to stable tuning of the microenvironment facilitating cancer progression.

The interaction of exosomes with ECM was described in many cancer types and other pathological conditions (Buzás et al. 2018; Xu et al. 2019). In our experiments, G361-derived exosomes immobilised in high concentration to collagen non-significantly suppressed migration of cancer cells from spheroids containing normal fibroblasts. However, in the context of the highly permissive microenvironment represented here by mCAFs in composite spheroids, exosomes revealed an opposite trend.

Application of these exosomes to 2D culture of HDFs or mCAFs inhibited their adhesion and proliferation in a concentration-dependent manner. Similarly, umbilical cord stem cell-derived or oral epithelial cell-derived exosomes have an inhibitory effect on fibroblast proliferation (Sjöqvist et al. 2019; Yao et al. 2020). Regarding mobility, exosomes were not able to influence the velocity of mCAFs, but they stimulated the migration of HDFs. Ovarian- or prostate cancer-derived exosomes also reduce adhesion and stimulate the velocity of fibroblast migration (McAtee et al. 2019; Lee et al. 2020).

However, in the 3D system in collagen gel, we observed that exosomes positively influenced cell migration of both HDFs and mCAFs. These differences between 2D and 3D cultures are well known (Duval et al. 2017). We must highlight here that collagen gels do not represent a complex architecture of dermal extracellular matrix. This model

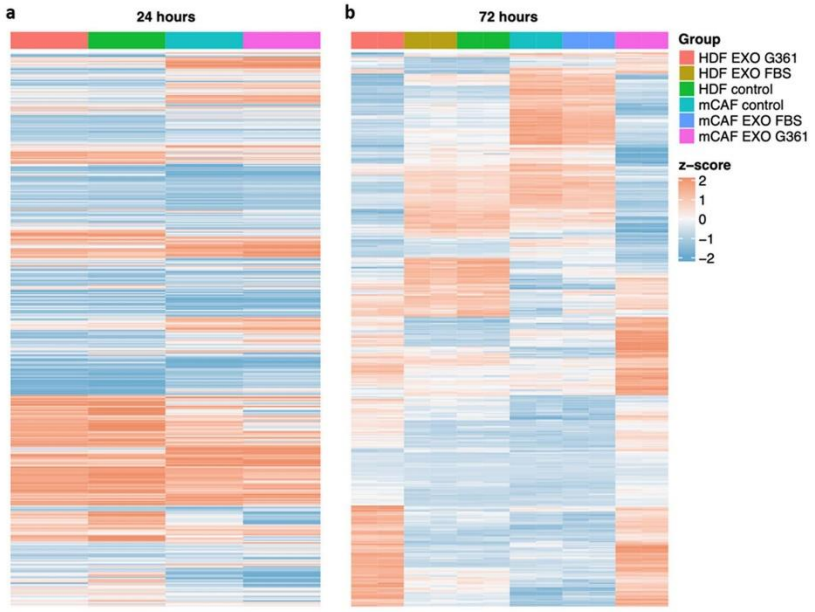

Fig. 7 G-361-derived exosomes influenced the fibroblast transcriptome. **a** The heatmap presents the transcriptomic profile of HDFs and mCAFs 24 h after exosome stimulation. **b** The heatmap presents the transcriptomic profile of HDFs and mCAFs 72 h after exosome stimulation

can be in fact much closer to the stochastic arrangement observed during early wound healing. This migration-enhancing effect of exosomes seems to be particularly important, because fibroblasts can lead to tumour cell invasion (Liu et al. 2019). Inhibition of the motility of fibroblasts and their adhesion to tumour cells can be achieved by application of INFγ. Of note, fibroblasts modified by DNA present in exosomes from uveal melanoma acquire properties of cancer cells, and they proliferate more and migrate more readily after application of cancer-derived exosomes (Tsering et al. 2020). Our observations harmonise well with these findings and indicate broad activity of cancer cell-derived exosomes on both normal and cancer-associated fibroblasts. We must acknowledge here that this effect is not uniform and highlights the functional diversity of fibroblasts under normal (Rodemann and Rennekampff 2011) and pathological (Bu et al. 2020) conditions. Such diversity can be documented by genes deregulated discordantly in comparison of HDF and mCAF after stimulation (Supplementary Table 2).

As fibroblast seeding density was identical in RTCA experiments, the measured values reflect the physical interaction of adherent cells with the surface of the electrode, primarily via surface receptors like integrins. Various cells can significantly differ in the types and numbers of these surface receptors. We have observed changes in expression of various integrins (*ITGA2*, *ITGA7*, *ITGA10*) in both fibroblast types in the same direction. Of note, *ITGA8* was deregulated discordantly and was increased in mCAFs in response to exosome stimulation. Identical trend was observed for *TNC*—it is known that this integrin is the receptor for tenascin.

The physical adherence of a cell can also be significantly modified by the environment and surface physiochemical features, e.g., substrate stiffness. Due to these factors, even cells of equal physical volume can spread to different extents and thus occupy an area of unequal size. There is no generally accepted precise timing that would allow us to separate the initial cell adhesion from consecutive cell spreading to achieve optimal surface attachment. This can also lad to differences in activity of focal-adhesin kinase (FAK) signalling pathways. One of these discordantly deregulated genes is *PDPN*. *PDPN* is known for induction of major reorganisation of the actin

a) mCAF EXO G361 vs. mCAF control

TOP 10 GO terms (mCAF EXO G361 vs. mCAF control)

Accesion GO	Description	Overlap/ Size	Odds Ratio	pValue
GO:0030198	extracellular matrix organization	68/233	5.59	1.45E-17
GO:0006954	inflammatory response	73/303	4.61	7.51E-17
GO:0019221	cytokine-mediated signaling pathway	56/228	4.7	1.94E-13
GO:0006695	cholesterol biosynthetic process	21/38	10.6	2.66E-13
GO:0045540	regulation of cholesterol biosynthetic process	19/33	11	1.18E-12
GO:0007155	cell adhesion	85/407	4	2.45E-11
GO:0001525	angiogenesis	53/224	4.53	4.35E-11
GO:0030199	collagen fibril organization	23/47	9.37	8.17E-11
GO:0006955	immune response	49/224	4.19	1.15E-10
GO:0071222	cellular response to lipopolysaccharide	33/127	4.97	1.09E-09

b) HDF EXO G361 vs. HDF control

TOP 10 GO terms (HDF EXO G361 vs. HDF control)

Accesion GO	Description	Overlap/ Size	Odds Ratio	pValue
GO:0030198	extracellular matrix organization	44/233	8.06	2.71E-16
GO:0030199	collagen fibril organization	17/47	15.4	7.36E-12
GO:0007155	cell adhesion	51/407	5.35	1.82E-11
GO:0030335	positive regulation of cell migration	35/222	6.73	2.60E-11
GO:0045766	positive regulation of angiogenesis	25/126	8.47	5.11E-11
GO:0030324	lung development	19/78	10.4	9.36E-10
GO:0007267	cell-cell signaling	25/159	6.71	2.36E-08
GO:0006695	cholesterol biosynthetic process	12/38	13.5	4.27E-08
GO:0045540	regulation of cholesterol biosynthetic process	11/33	14.2	9.40E-08
GO:0008284	positive regulation of cell population proliferation	42/410	4.37	2.80E-07

Fig. 8 Comparison of the influence of G-361-derived exosomes on HDFs and mCAFs. The results of gene set enrichment analysis indicate that the G-361-derived exosomes influence extracellular matrix organisation in mCAFs (**a**) and HDFs (**b**). The exosomes also influence the inflammatory response and cytokine-mediated signalling pathway in mCAFs (**a**). The top ten GO terms for **a** and **b** are presented in tables below (based on *p* value)

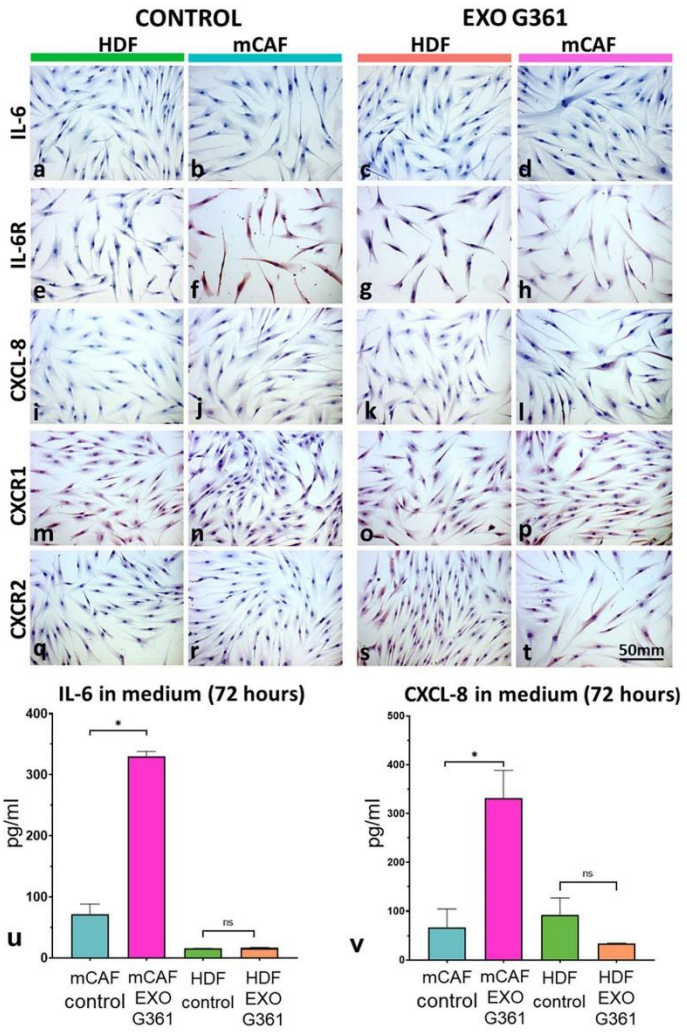

Fig. 9 Immunocytochemical analysis of HDFs and mCAFs treated for 24 h with exosomes in culture medium. **a–d** IL-6 was not detected in cells; **e–h** low–medium signal of IL-6R in fibroblasts; **i–l**) detection of CXCL-8 (negative); **m–p**: detection of CXCR1 (low–negative); **q–t** CXCR2 (low–negative). Bar represents 50 µm. **u** IL-6 was detected in conditioned media after 72 h (pg/ml) by ELISA. **v** CXCL-8 was detected in conditioned media after 72 h (pg/ml) by ELISA. Error bars represent standard deviation (two independent experiments, three technical replicates for each. *p* values indicate statistical significance calculated by a two-tailed Student's *t* test

cytoskeleton, increased motility and decreased cell adhesion in tumours (Martín-Villar et al. 2005).

Histologic observations of desmoplastic reaction surrounding proliferating tumour buds were initially understood as a response of the host tissue against invasive cancer cells. It was taken as a thick tissue barrier against cancer invasion and potential metastasis. To initiate this fibroplasia, paracrine signalling across the tissue microenvironment is necessary, and it should facilitate alterations of cell proliferation and differentiation. Exosomes are an efficient tool for this information exchange across the niche. Indeed, HDFs in the G361 exosome-enriched environment slowed down melanoma cell invasion in our experiments. The naïve fibroblast population in real tissue, represented here by HDFs in spheroids, once stimulated by exosomes possibly acts as a

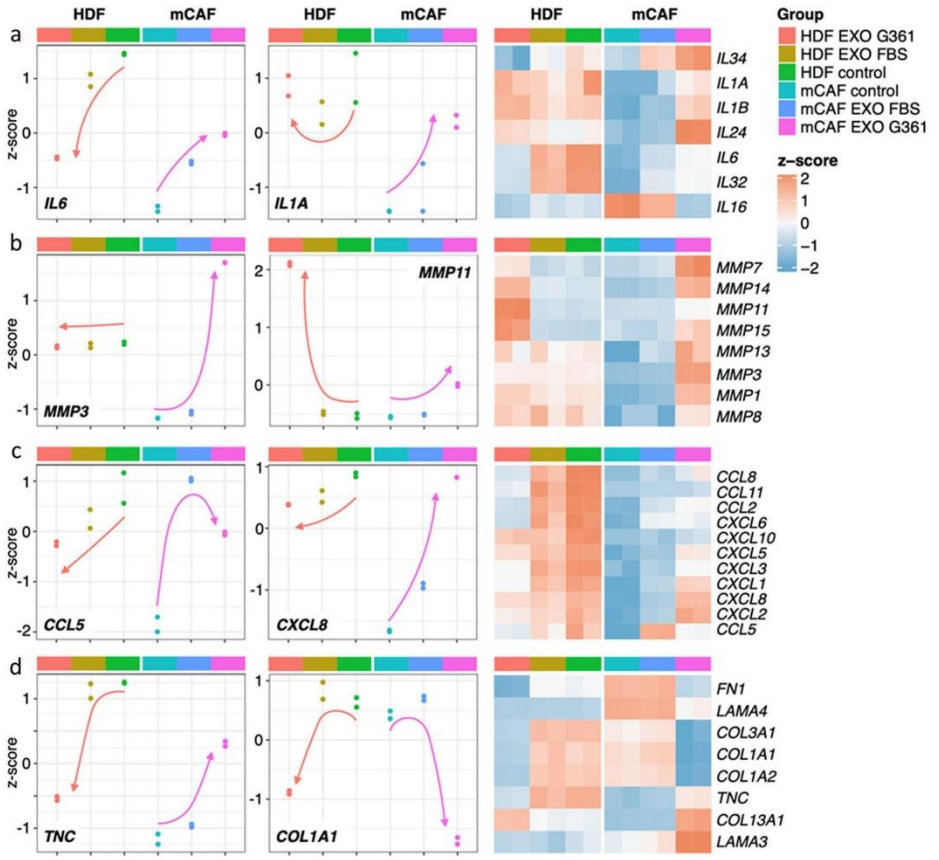

Fig. 10 Transcriptional changes in HDFs and mCAFs after 72 h of exosomal stimulation (G361-derived vs FBS-derived exosomes). Panel **a** presents global changes with emphasis on interleukins, **b** represents matrix metalloproteinases, **c** represents chemokines and **d** represents extracellular matrix molecules. The overall trend is indicated by the orange (HDFs) or purple arrow (mCAFs)

defensive mechanism to insulate the tumour (Schäfer and Werner 2008). However, this is just a temporary advantage. In an extended time frame, the exosomes can also contribute to fibroblast recruitment and their transformation into myofibroblasts, e.g., by TFG-β-dependent mechanisms described in detail by others (Webber et al. 2010). It was suggested recently that α8β1 integrin enhances cellular contractility and TGFβ activity in liver fibrosis (Nishimichi et al. 2021). Similar can be expected in cancer. Hence, the defender can be easily corrupted and become a cancer abettor (Fiori et al. 2019).

G361-derived exosomes significantly influenced transcription profiles of both normal HDFs and mCAFs. Interestingly, the effect of exosomes observed on the HDF and mCAF transcriptomes was not the same. For example, the activity of genes for cytokines/chemokines such as *IL1*, *IL6*, *IL24*, *IL32*, *IL34*, *CCL2*, *CCL5*, *CCL8*, *CCL11*, *CXCL1*, *CXCL2*, *CXCL3*, *CXCL5*, *CXCL6*, *CXCL8* and *CXCL10* was upregulated in mCAFs and not affected/downregulated in HDFs. It suggests that mCAFs under exosomal stimuli shift the microenvironment to a chronic proinflammatory setting typical of cancer. On the other hand, the activity of genes for

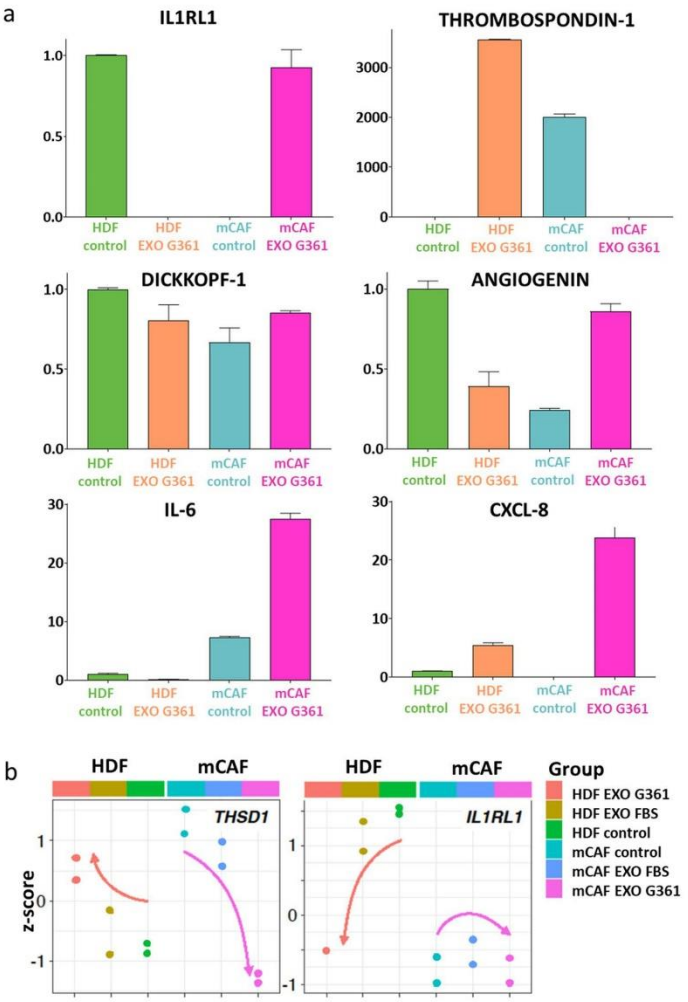

Fig. 11 Panel **a** presents bar graphs representing changes in selected proteins in fibroblast-conditioned media after 72 h of stimulation by G-361 exosomes (detected in the Proteome Profiler Human XL Cytokine Array). Data represent an average of two capture spots for a particular analyte, and for purposes of comparison were normalised to the HDF level; error bar represents standard deviation. **b** The expression of both IL1R1 and thrombospondin-1 was also compared at the mRNA level, and a very similar trend was shown in the activity of *THSD1* gene for both types of fibroblasts and in the case of *1L1RL1* gene for HDFs. The overall trend is indicated by the orange (HDFs) or purple arrow (mCAFs)

matrix metalloproteinases *MMP1*, *MMP3*, *MMP7*, *MMP8*, *MMP11*, *MMP13*, *MMP14* and *MMP15* was upregulated in mCAFs, and in the case of *MMP7*, *MMP11*, *MMP14* and *MMP15*, also in HDFs. It highlights the potential of the tumour microenvironment for dynamic structural changes allowing tumour invasion. Concerning the genes encoding production of extracellular matrix proteins, activation of genes for tenascin-C (*TNC*) or laminins (*LAM3, LAM4*) was observed after the application of exosomes to mCAFs. The activity of genes encoding collagen type 1 (*COL1A1*, *COL1A2*) and collagen type 3 (*COL3A1*) was reduced in both mCAFs and HDFs. These data have demonstrated that G361-derived exosomes enhance the remarkable properties of cancer-associated fibroblasts in mCAFs.

In closer detail, CAFs are not functionally uniform either. CAFs represent a heterogeneous population where distinct subpopulations differ in production of ECM and secretion of bioactive cytokines/chemokines/growth factors, as was

demonstrated for example in melanoma, urothelial carcinoma or adenocarcinoma of the pancreas (Lin et al. 2020; Tsering et al. 2020; Novotný et al. 2020). Inflammation-supporting factors, predominantly IL-6 secreted by CAFs, enhance the aggressiveness of tumours, including cutaneous malignant melanoma. A biologically relevant increase in cancer cell proliferation and metastasis formation was observed in many types of malignant tumours due to the CAF activity (Lacina et al. 2019; Plzák et al. 2019; Kodet et al. 2020; Brábek et al. 2020). A similar tumour-promoting effect can be assigned to activation of the gene for ECM protein tenascin-C. This ECM protein is rich in the microenvironment of many types of tumours, including malignant cutaneous melanoma, where it seems to be associated with cancer cell survival and invasion (Grahovac et al. 2013; Shao et al. 2015).

The effect of exosomes on activation of matrix metalloproteinases also stimulated cancer cell invasiveness by degradation of ECM proteins. The exosome-activated mCAFs upregulate the activity of genes for MMP-1, MMP-2, MMP-7, MMP-8, MMP-13 and MMP-14 that are associated with cancer growth and progression. Part of them (MMP-1, MMP-2, MMP-7 and MMP-13) also participate in inflammatory processes under the control of IL-1, IL-6 and CXCL-8 that are upregulated in mCAFs treated with exosomes (Cabral-Pacheco et al. 2020). The functional link of MMP with IL-1, IL-6 and CXCL-8 in mCAFs is shown in Supplementary Figure 4. This orchestration supports the role of exosomes in inflammation and of its mediators in the progression of cutaneous malignant melanoma.

Two proteins, IL1RL1 and thrombospondin-1, are expressed differentially with or without exosome application in both HDFs and mCAFs. IL1RL1, the receptor for IL-33, is present in non-stimulated HDFs and exosome-stimulated mCAF. Its role in cancer progression is highly probable (Zhou et al. 2020). Thrombospondin is up/down-regulated in different tumours (Wang et al. 2020). In cutaneous melanoma, thrombospondin seems to be a marker of poor prognosis stimulating tumour vascularisation (Trotter et al. 2003). The stimulation of angiogenin in mCAF after exosome application can also be associated with tumour vascularisation (Gorain et al. 2019). Dickkopf-1 is a Wnt inhibitor. It is strongly expressed in both HDFs and mCAFs. The interpretation of this finding is complicated because its role as tumour-promoting and tumour-inhibiting factor was described (Li et al. 2020). Since the knockdown of Dickkopf-1 has a suppressive role in apoptosis induced by the combination of temsirolimus and temozolomide in vitro, it should be hypothesised that its role in cutaneous melanoma is tumour suppressing (Niessner et al. 2017).

The upregulation of the mevalonate pathway in exosome-stimulated mCAFs may be associated with RHO-GTPases and actin cytoskeleton biology that may influence mCAF formation and function. It was suggested that in fibroblast-led collective invasion of tumour cells, leading and following cells differ in activity and roles of RhoGTPases (Gaggioli et al. 2007). The proposed employment of statins in the therapeutic manipulations of the tumour ecosystem harmonises with this observation (Emelyanova et al. 2019; Ji et al. 2020; Yu et al. 2021).

Based on these data, it can be concluded that exosomes derived from G361 melanoma cells have a stimulatory effect on mCAF prepared from human cutaneous melanoma. It might be understood that fibroblasts turn into CAFs in the niche of the tumour microenvironment by the process of gradual and slow recruitment. This paradigm can also be extended to other tumour-supporting populations, including macrophages (Gok Yavuz et al. 2019).

Exosomes produced by cancer cells contribute to the co-evolution of cancer cells with their microenvironment during cancer formation and propagation (Valcz et al. 2020). Hu and Hu observed that exosomes prepared from melanoma cells re-programme NIH/3T3 to CAFs (Hu and Hu 2019). However, it must be highlighted in this context that 3T3 cells were established from mouse embryonic tissue (Todaro and Geen 1963), and they greatly differ from normal adult dermal fibroblasts. In the broader view of the whole organism, melanoma-derived exosomes are released to body fluids and thus influence distant fibroblasts to develop a premetastatic microenvironment (la Shu et al. 2018). This positive systemic effect of melanoma cell-derived exosomes should be reflected by tumour biology research in the nearest future. Because CAFs are very important players in information transfer in the tumour microenvironment, their therapeutic targeting may be beneficial for patient therapy in the future.

Supplementary Information The online version contains supplementary material available at https://doi.org/10.1007/s00418-021-02052-2.

Author contributions Conceptualization: KS, MK, LL; Investigation: KS, LP, PP, JF; JŠ, MH; LL; Visualisation: EV, LL; JN; LP; Data curation: JN; LP; JŠ; Formal Analysis: DR, MK; Methodology: PP; BD; JB; MK; Supervision: MV. The first draft of the manuscript was written by KS, MK and LL, and all authors commented on previous versions of the manuscript. All authors read and approved the final manuscript.

Funding The work was supported by the Czech Science Foundation project No. 19-05048S, Operational Programme "Research, Development and Education" (project CZ.02.1.01/0.0/0.0/16_019/0000785 "Centre for Tumour Ecology—Research of the Cancer Microenvironment Supporting Cancer Growth and Spread"), and Charles University programme PROGRESS Q28. We thank the Electron Microscopy Core Facility, IMG CAS, supported by MEYS CR (LM2018129) and ERDF (CZ.02.1.01/0.0/0.0/18_046/0016045 and CZ.02.1.01/0.0/0.0/16_013/0001775) for technical support. This work was also generously supported by the League Against Cancer Prague grant (LPR Praha). The authors are grateful to Dr Takáčová for professional English style and grammar revisions.

Data availability All transcriptomic data has been deposited in the ArrayExpress database (http://www.ebi.ac.uk/arrayexpress) under accessions E-MTAB-10278 and E-MTAB-10290.

Code availability Not applicable.

Declarations

Conflict of interest All authors declare no conflicting/competing interests.

Ethical approval Tissues for fibroblast isolations were collected after local ethics committee approval following the ethical standards of the Institutional and National Research Committee and according to the 1964 Helsinki Declaration and its later amendments or comparable ethical standards. The patient's informed consent was obtained.

Consent to participate Not applicable.

Consent for publication Not applicable.

References:

Alberts B, Johnson A, Lewis J, et al (2002) Cancer as a Microevolutionary Process. Available from: https://www.ncbi.nlm.nih.gov/books/NBK26891/. Accessed 01 June 2021

Ashburner M, Ball CA, Blake JA et al (2000) Gene ontology: tool for the unification of biology. Nat Genet 25:25–29

Brábek J, Jakubek M, Vellieux F et al (2020) Interleukin-6: molecule in the intersection of cancer, ageing and COVID-19. Int J Mol Sci 21:1–25

Brennan K, Martin K, FitzGerald SP et al (2020) A comparison of methods for the isolation and separation of extracellular vesicles from protein and lipid particles in human serum. Sci Rep. https://doi.org/10.1038/s41598-020-57497-7

Brustugun OT, Møller B, Helland Å (2014) Years of life lost as a measure of cancer burden on a national level. Br J Cancer 111:1014–1020. https://doi.org/10.1038/bjc.2014.364

Bu L, Baba H, Yasuda T et al (2020) Functional diversity of cancer-associated fibroblasts in modulating drug resistance. Cancer Sci 111:3468–3477. https://doi.org/10.1111/cas.14578

Buzás EI, Tóth E, Sódar BW, Szabó-Taylor K (2018) Molecular interactions at the surface of extracellular vesicles. Semin Immunopathol 40:453–464

Cabral-Pacheco GA, Garza-Veloz I, Castruita-De la Rosa C et al (2020) The roles of matrix metalloproteinases and their inhibitors in human diseases. Int J Mol Sci 21:9739. https://doi.org/10.3390/ijms21249739

Cavallari C, Camussi G, Brizzi MF (2020) Extracellular vesicles in the tumour microenvironment: eclectic supervisors. Int J Mol Sci 21:1–21

Duval K, Grover H, Han LH et al (2017) Modeling physiological events in 2D vs. 3D cell culture. Physiology 32:266–277

Dvořánková B, Lacina L, Smetana K (2019) Isolation of normal fibroblasts and their cancer-associated counterparts (CAFs) for biomedical research. In: Turksen K (ed) Skin stem cells: methods and protocols. Springer, New York, pp 393–406

Egeblad M, Nakasone ES, Werb Z (2010) Tumors as organs: complex tissues that interface with the entire organism. Dev Cell 18:884–901

Emelyanova L, Sra A, Schmuck EG et al (2019) Impact of statins on cellular respiration and de-differentiation of myofibroblasts in human failing hearts. ESC Heart Fail 6:1027–1040. https://doi.org/10.1002/ehf2.12509

Ewels PA, Peltzer A, Fillinger S et al (2020) The nf-core framework for community-curated bioinformatics pipelines. Nat Biotechnol 38:276–278. https://doi.org/10.1038/s41587-020-0439-x

Falcone I, Conciatori F, Bazzichetto C et al (2020) Tumor microenvironment: Implications in melanoma resistance to targeted therapy and immunotherapy. Cancers 12:1–26

Fiori ME, di Franco S, Villanova L et al (2019) Cancer-associated fibroblasts as abettors of tumor progression at the crossroads of EMT and therapy resistance. Mol Cancer. https://doi.org/10.1186/s12943-019-0994-2

Gaggioli C, Hooper S, Hidalgo-Carcedo C et al (2007) Fibroblast-led collective invasion of carcinoma cells with differing roles for RhoGTPases in leading and following cells. Nat Cell Biol. https://doi.org/10.1038/ncb1658

Gener Lahav T, Adler O, Zait Y et al (2019) Melanoma-derived extracellular vesicles instigate proinflammatory signaling in the metastatic microenvironment. Int J Cancer 145:2521–2534. https://doi.org/10.1002/ijc.32521

Gok Yavuz B, Gunaydin G, Gedik ME et al (2019) Cancer associated fibroblasts sculpt tumour microenvironment by recruiting monocytes and inducing immunosuppressive PD-1 + TAMs. Sci Rep 9:1–15. https://doi.org/10.1038/s41598-019-39553-z

Gorain B, Choudhury H, Yee GS, Bhattamisra SK (2019) Adenosine receptors as novel targets for the treatment of various cancers. Curr Pharm Des 25:2828–2841. https://doi.org/10.2174/1381612825666190716102037

Grahovac J, Becker D, Wells A (2013) Melanoma cell invasiveness is promoted at least in part by the epidermal growth factor-like repeats of tenascin-C. J Invest Dermatol 133:210–220. https://doi.org/10.1038/jid.2012.263

Gu Z, Eils R, Schlesner M (2016) Complex heatmaps reveal patterns and correlations in multidimensional genomic data. Bioinformatics 32:2847–2849. https://doi.org/10.1093/bioinformatics/btw313

Hamidi H, Lilja J, Ivaska J (2017) Using xCELLigence RTCA instrument to measure cell adhesion. Bio-Protocol. https://doi.org/10.21769/bioprotoc.2646

Hsu M-Y, Meier FE, Nesbit M et al (2000) E-cadherin expression in melanoma cells restores keratinocyte-mediated growth control and down-regulates expression of invasion-related adhesion receptors. Am J Pathol 156:1515–1525. https://doi.org/10.1016/S0002-9440(10)65023-7

Hu T, Hu J (2019) Melanoma-derived exosomes induce reprogramming fibroblasts into cancer-associated fibroblasts via Gm26809 delivery. Cell Cycle 18:3085–3094. https://doi.org/10.1080/15384101.2019.1669380

Ji L, Liu C, Yuan Y et al (2020) Key roles of Rho GTPases, YAP, and Mutant P53 in anti-neoplastic effects of statins. Fundam Clin Pharmacol 34:4–10. https://doi.org/10.1111/fcp.12495

Jobe NP, Rösel D, Dvořánková B et al (2016) Simultaneous blocking of IL-6 and IL-8 is sufficient to fully inhibit CAF-induced human melanoma cell invasiveness. Histochem Cell Biol. https://doi.org/10.1007/s00418-016-1433-8

Jobe NP, Živicová V, Mifková A et al (2018) Fibroblasts potentiate melanoma cells in vitro invasiveness induced by UV-irradiated keratinocytes. Histochem Cell Biol. https://doi.org/10.1007/s00418-018-1650-4

Kim D, Langmead B, Salzberg SL (2015) HISAT: a fast spliced aligner with low memory requirements. Nat Methods 12:357–360. https://doi.org/10.1038/nmeth.3317

Kim HY, Lee H, Kim SH et al (2017) Discovery of potential biomarkers in human melanoma cells with different metastatic potential by metabolic and lipidomic profiling. Sci Rep 7:1–14. https://doi.org/10.1038/s41598-017-08433-9

Kodet O, Kučera J, Strnadová K et al (2020) Cutaneous melanoma dissemination is dependent on the malignant cell properties and factors of intercellular crosstalk in the cancer microenvironment (review). Int J Oncol 57:619–630. https://doi.org/10.3892/ijo.2020.5090

Kučera J, Strnadová K, Dvořánková B et al (2019) Serum proteomic analysis of melanoma patients with immunohistochemical profiling of primary melanomas and cultured cells: pilot study. Oncol Rep. https://doi.org/10.3892/or.2019.7319

la Shu S, Yang Y, Allen CL et al (2018) Metabolic reprogramming of stromal fibroblasts by melanoma exosome microRNA favours a pre-metastatic microenvironment. Sci Rep. https://doi.org/10.1038/s41598-018-31323-7

la Shu S, Matsuzaki J, Want MY et al (2020) An immunosuppressive effect of melanoma-derived exosomes on NY-ESO-1 antigen-specific human CD8+ T cells is dependent on IL-10 and independent of BRAFV600E mutation in melanoma cell lines. Immunol Investig 49:744–757. https://doi.org/10.1080/08820139.2020.1803353

Lacina L, Plzak J, Kodet O et al (2015) Cancer microenvironment: what can we learn from the stem cell niche. Int J Mol Sci. https://doi.org/10.3390/ijms161024094

Lacina L, Brábek J, Král V et al (2019) Interleukin-6: a molecule with complex biological impact in cancer. Histol Histopathol. https://doi.org/10.14670/HH-18-033

Lazar I, Clement E, Ducoux-Petit M et al (2015) Proteome characterization of melanoma exosomes reveals a specific signature for metastatic cell lines. Pigment Cell Melanoma Res 28:464–475. https://doi.org/10.1111/pcmr.12380

Lee AH, Ghosh D, Quach N et al (2020) Ovarian cancer exosomes trigger differential biophysical response in tumor-derived fibroblasts. Sci Rep 10:1–16. https://doi.org/10.1038/s41598-020-65628-3

Li K, Wong DK, Hong KY, Raffai RL (2018) Cushioned-density gradient ultracentrifugation (C-DGUC): a refined and high performance method for the, isolation, characterization, and use of exosomes. Methods Mol Biol. https://doi.org/10.1007/978-1-4939-7652-2_7

Li J, Gao Y, Yue W (2020) The clinical diagnostic and prognostic value of dickkopf-1 in cancer. Cancer Manag Res 12:4253–4260. https://doi.org/10.2147/CMAR.S254596

Liao Y, Smyth GK, Shi W (2014) featureCounts: an efficient general purpose program for assigning sequence reads to genomic features. Bioinformatics 30:923–930. https://doi.org/10.1093/bioinformatics/btt656

Lin W, Noel P, Borazanci EH et al (2020) Single-cell transcriptome analysis of tumor and stromal compartments of pancreatic ductal adenocarcinoma primary tumors and metastatic lesions. Genome Med. https://doi.org/10.1186/s13073-020-00776-9

Liu X, Zhu L, Wang R et al (2019) IFNγ inhibits fibroblast-leading tumor cell invasion through downregulating N-cadherin. Biochem Biophys Res Commun 512:544–551. https://doi.org/10.1016/j.bbrc.2019.03.136

Love MI, Huber W, Anders S (2014) Moderated estimation of fold change and dispersion for RNA-seq data with DESeq2. Genome Biol 15:550. https://doi.org/10.1186/s13059-014-0550-8

Lun ATL, Riesenfeld S, Andrews T et al (2018) Distinguishing cells from empty droplets in droplet-based single-cell RNA sequencing data. bioRxiv. https://doi.org/10.1101/234872

Luo W, Brouwer C (2013) Pathview: an R/Bioconductor package for pathway-based data integration and visualization. Bioinformatics 29:1830–1831. https://doi.org/10.1093/bioinformatics/btt285

Martín-Villar E, Scholl FG, Gamallo C et al (2005) Characterization of human PA2.26 antigen (T1α-2, podoplanin), a small membrane mucin induced in oral squamous cell carcinomas. Int J Cancer. https://doi.org/10.1002/ijc.20656

McAtee CO, Booth C, Elowsky C et al (2019) Prostate tumor cell exosomes containing hyaluronidase Hyal1 stimulate prostate stromal cell motility by engagement of FAK-mediated integrin signaling. Matrix Biol 78–79:165–179. https://doi.org/10.1016/j.matbio.2018.05.002

Mosmann T (1983) Rapid colorimetric assay for cellular growth and survival: application to proliferation and cytotoxicity assays. J Immunol Methods 65:55–63. https://doi.org/10.1016/0022-1759(83)90303-4

Niessner H, Kosnopfel C, Sinnberg T et al (2017) Combined activity of temozolomide and the mTOR inhibitor temsirolimus in metastatic melanoma involves DKK1. Exp Dermatol 26:598–606. https://doi.org/10.1111/exd.13372

Nishimichi N, Tsujino K, Kanno K et al (2021) Induced hepatic stellate cell integrin, α8β1, enhances cellular contractility and TGFβ activity in liver fibrosis. J Pathol. https://doi.org/10.1002/path.5618

Novotný J, Strnadová K, Dvořánková B et al (2020) Single-cell RNA sequencing unravels heterogeneity of the stromal niche in cutaneous melanoma heterogeneous spheroids. Cancers 12:1–22. https://doi.org/10.3390/cancers12113324

Peebles PT, Trisch T, Papageorge AG (1978) 727 isolation of four unusual pediatric solid tumor cell lines. Pediatr Res 12:485–485. https://doi.org/10.1203/00006450-197804001-00732

Pfeffer S, Grossmann K, Cassidy P et al (2015) Detection of exosomal miRNAs in the plasma of melanoma patients. J Clin Med 4:2012–2027. https://doi.org/10.3390/jcm4121957

Plzák J, Bouček J, Bandúrová V et al (2019) The head and neck squamous cell carcinoma microenvironment as a potential target for cancer therapy. Cancers. https://doi.org/10.3390/cancers11040440

Preisner F, Leimer U, Sandmann S et al (2018) Impact of human adipose tissue-derived stem cells on malignant melanoma cells in an in vitro co-culture model. Stem Cell Rev 14:125–140. https://doi.org/10.1007/s12015-017-9772-y

Quax PHA, van Muijen GNP, Weening-Verhoeff EJD et al (1991) Metastatic behavior of human melanoma cell lines in nude mice correlates with urokinase-type plasminogen activator, its type-1 inhibitor, and urokinase-mediated matrix degradation. J Cell Biol 115:191–199. https://doi.org/10.1083/jcb.115.1.191

R Core Team (2020) The R Project for Statistical Computing, Vienna, Austria. In: https://www.R-project.org/. Accessed 01 June 2021

Rodemann HP, Rennekampff H-O (2011) Functional diversity of fibroblasts. Tumor-associated fibroblasts and their matrix. Springer, Dordrecht, pp 23–36

Schäfer M, Werner S (2008) Cancer as an overhealing wound: an old hypothesis revisited. Nat Rev Mol Cell Biol 9:628–638

Shao H, Kirkwood JM, Wells A (2015) Tenascin-C signaling in melanoma. Cell Adh Migr 9:125–130

Sjöqvist S, Ishikawa T, Shimura D et al (2019) Exosomes derived from clinical-grade oral mucosal epithelial cell sheets promote wound healing. J Extracell Vesicles. https://doi.org/10.1080/20013078.2019.1565264

Smetana K, Lacina L, Szabo P et al (2016) Ageing as an important risk factor for cancer. Anticancer Res. https://doi.org/10.21873/anticanres.11069

Smetana K, Lacina L, Kodet O (2020) Targeted therapies for melanoma. Cancers 12:1–4

Stephens M (2017) False discovery rates: a new deal. Biostatistics 18:275–294. https://doi.org/10.1093/biostatistics/kxw041

Théry C, Amigorena S, Raposo G, Clayton A (2006) Isolation and characterization of exosomes from cell culture supernatants and biological fluids. Curr Protoc Cell Biol. https://doi.org/10.1002/0471143030.cb0322s30

Todaro GJ, Green H (1963) Quantitative studies of the growth of mouse embryo cells in culture and their development into established linesJ. Cell Biol 17:299–313. https://doi.org/10.1083/jcb.17.2.299

Trotter MJ, Colwell R, Tron VA (2003) Thrombospondin-1 and cutaneous melanoma. J Cutan Med Surg 7:136–141

Tsering T, Laskaris A, Abdouh M et al (2020) Uveal melanoma-derived extracellular vesicles display transforming potential and carry protein cargo involved in metastatic niche preparation. Cancers 12:1–25. https://doi.org/10.3390/cancers12102923

Valcz G, Buzás EI, Sebestyén A et al (2020) Extracellular vesicle-based communication may contribute to the co-evolution of cancer stem cells and cancer-associated fibroblasts in anti-cancer therapy. Cancers 12:2324. https://doi.org/10.3390/cancers12082324

Vlodavsky I, Korner G, Ishai-Michaeli R et al (1990) Extracellular matrix-resident growth factors and enzymes: possible involvement in tumor metastasis and angiogenesis. Cancer Metastasis Rev 9:203–226. https://doi.org/10.1007/BF00046361

Wang P, Zeng Z, Lin C et al (2020) Thrombospondin-1 as a potential therapeutic target: multiple roles in cancers. Curr Pharm Des 26:2116–2136. https://doi.org/10.2174/1381612826666200128091506

Webber J, Steadman R, Mason MD et al (2010) Cancer exosomes trigger fibroblast to myofibroblast differentiation. Cancer Res 70:9621–9630. https://doi.org/10.1158/0008-5472.CAN-10-1722

Xu R, Greening DW, Rai A et al (2015) Highly-purified exosomes and shed microvesicles isolated from the human colon cancer cell line LIM1863 by sequential centrifugal ultrafiltration are biochemically and functionally distinct. Methods 87:11–25. https://doi.org/10.1016/j.ymeth.2015.04.008

Xu S, Xu H, Wang W et al (2019) The role of collagen in cancer: from bench to bedside. J Transl Med. https://doi.org/10.1186/s12967-019-2058-1

Yao Z, Li J, Wang X et al (2020) Microrna-21-3p engineered umbilical cord stem cell-derived exosomes inhibit tendon adhesion. J Inflamm Res 13:303–316. https://doi.org/10.2147/JIR.S254879

Yates AD, Achuthan P, Akanni W et al (2020) Ensembl 2020. Nucleic Acids Res 48:D682–D688. https://doi.org/10.1093/nar/gkz966

Young MD, Wakefield MJ, Smyth GK, Oshlack A (2010) Gene ontology analysis for RNA-seq: accounting for selection bias. Genome Biol. https://doi.org/10.1186/gb-2010-11-2-r14

Yu WY, Hill ST, Chan ER et al (2021) Computational drug repositioning identifies statins as modifiers of prognostic genetic expression signatures and metastatic behavior in melanoma. J Invest Dermatol. https://doi.org/10.1016/j.jid.2020.12.015

Zebrowska A, Widlak P, Whiteside T, Pietrowska M (2020) Signaling of tumor-derived sev impacts melanoma progression. Int J Mol Sci 21:1–21

Zhou Q, Wu X, Wang X et al (2020) The reciprocal interaction between tumor cells and activated fibroblasts mediated by TNF-α/IL-33/ST2L signaling promotes gastric cancer metastasis. Oncogene 39:1414–1428. https://doi.org/10.1038/s41388-019-1078-x